ASSESSMENT OF CONSOLIDATION SETTLEMENTS IN KARACABEY SOFT CLAYS: ESTIMATED AND MONITORED BEHAVIOUR

A THESIS SUBMITTED TO
THE GRADUATE SCHOOL OF NATURAL AND APPLIED SCIENCES
OF
MIDDLE EAST TECHNICAL UNIVERSITY

BY

GÖZDE ÇELİK

IN PARTIAL FULFILLMENT OF THE REQUIREMENTS
FOR
THE DEGREE OF DOCTOR OF PHILOSOPHY
IN
GEOLOGICAL ENGINEERING

SEPTEMBER 2020

Approval of the thesis:

ASSESSMENT OF CONSOLIDATION SETTLEMENTS IN KARACABEY SOFT CLAYS: ESTIMATED AND MONITORED BEHAVIOUR

submitted by **GÖZDE ÇELİK** in partial fulfillment of the requirements for the degree of **Doctor of Philosophy in Geological Engineering, Middle East Technical University** by,

Prof. Dr. Halil Kalıpçılar
Dean, Graduate School of **Natural and Applied Sciences** ________________

Prof. Dr. Erdin Bozkurt
Head of the Department, **Geological Engineering** ________________

Prof. Dr. Tamer Topal
Supervisor, **Geological Engineering Dept., METU** ________________

Prof. Dr. Ahmet Orhan Erol
Co-Supervisor, **Civil Engineering Dept., METU** ________________

Examining Committee Members:

Prof. Dr. Nurkan Karahanoğlu
Geological Engineering Dept., METU ________________

Prof. Dr. Tamer Topal
Geological Engineering Dept., METU ________________

Prof. Dr. Kemal Önder Çetin
Civil Engineering Dept., METU ________________

Prof. Dr. Sami Oğuzhan Akbaş
Civil Engineering Dept., Gazi University ________________

Assoc. Prof. Dr. Müge Akın
Civil Engineering Dept., Abdullah Gül University ________________

Date: 02.09.2020

I hereby declare that all information in this document has been obtained and presented in accordance with academic rules and ethical conduct. I also declare that, as required by these rules and conduct, I have fully cited and referenced all material and results that are not original to this work.

Name, Last name : Gözde Çelik

Signature :

ABSTRACT

ASSESSMENT OF CONSOLIDATION SETTLEMENTS IN KARACABEY SOFT CLAYS: ESTIMATED AND MONITORED BEHAVIOUR

Çelik, Gözde
Doctor of Philosophy, Geological Engineering
Supervisor : Prof. Dr. Tamer Topal
Co-Supervisor: Prof. Dr. Ahmet Orhan Erol

September 2020, 360 pages

Settlement of highway embankments constructed over clayey soft soils is a major problem encountered in maintaining highway facilities. Accurate estimation of consolidation settlement amounts and times has been a challenge for engineers in practice.

In this study, field settlement measurements of 26 stations between 600 and 750 days of durations in Karacabey NC clays and comparison of these measured magnitudes of settlements with calculated settlements from oedometer tests are assessed. The correlation between predicted settlements using oedometer test data and observed settlements in the field is proposed. Stroud approaches are compared with the coefficients of volume compressibility back calculated and their trend is presented. The relationship between tip resistance (q_c) of cone penetration test and constrained modulus is investigated.

The magnitudes of final settlements are estimated by using Asaoka and Horn's extrapolation methods including 70% of the monitored settlement data.

Furthermore, time data versus field settlement are used to predict the primary consolidation amounts. Equations providing correction factors to the magnitudes of settlements, calculated by oedometer results, are formed to estimate the magnitudes of settlements that would occur in the field. Karacabey clays exhibit typical secondary consolidation behaviors. Tertiary consolidation behaviors are also observed in 11 of total 26 stations. C_s/C_c and C_t/C_c ranges are recommended for engineering practices to predict the secondary and tertiary consolidation settlements. In addition, the relationship between the compression index (C_c) and the secondary and tertiary consolidation coefficients (C_s-C_t) is investigated, and relations, in which laboratory data and idealized geological profile geometry are evaluated as numerical parameters, are proposed. Studies have shown that there is a nonlinear relationship rather than a linear one between independent variables and targeted dependent variables, and iterative non-linear regression analysis are performed to drive the assumed equation model.

Keywords: consolidation settlement prediction, clay, tertiary consolidation, soft soils, Karacabey

ÖZ

KARACABEY YUMUŞAK KİLLERİNDEKİ KONSOLİDASYON OTURMALARININ DEĞERLENDİRİLMESİ: TAHMİN EDİLEN VE GÖZLEMLENEN DAVRANIŞI

Çelik, Gözde
Doktora, Jeoloji Mühendisliği
Tez Yöneticisi: Prof. Dr. Tamer Topal
Ortak Tez Yöneticisi: Prof. Dr. Ahmet Orhan Erol

Eylül 2020, 360 sayfa

Yumuşak killi zeminler üzerinde inşa edilen karayolu dolgularının oturması, karayolu olanaklarının korunmasında karşılaşılan önemli bir problemdir. Konsolidasyon oturma miktarlarının ve zamanlarının doğru tahmin edilmesi, pratikte mühendisler için zorluk teşkil etmektedir.

Bu çalışmada, 26 istasyona ait Karacabey normal konsolide killerdeki 600 ile 750 gün arasındaki saha oturma ölçümlerinin, ödometre deneyi sonuçlarından hesaplanan oturma miktarlarının karşılaştırılması değerlendirilmiştir. Ödometre deneyi sonuçları kullanılarak öngörülen oturma miktarları ile sahada gözlemlenen oturma miktarları arasındaki bağıntı önerilmiştir. Stroud yaklaşımları ile geri analizlerden elde edilen hacimsel sıkışma katsayısı arasındaki eğilim sunulmuştur. Konik penetrasyon deneyinden elde edilen koni uç direnci (q_c) ve ödometrik modül arasındaki ilişki araştırılmıştır.

Asaoka ve Horn ekstrapolasyon yöntemlerinden, gözlemlenen oturma verisinin %70’i kullanılarak nihai oturma miktarı tahmin edilmiştir. Ayrıca, oturma

miktarına karşın karekök zaman ve oturma miktarına karşın logaritmik zaman grafikleri birincil oturma miktarlarını tahmin etmek için kullanılmıştır. Ödometre sonuçları ile hesaplanan oturma miktarlarına düzeltme faktörü sağlayan denklemler oluşturularak, sahada meydana gelecek oturma miktarlarının tahmin edilmesi sağlanmıştır.

Karacabey killeri tipik ikincil oturma davranışı göstermektedir. 26 istasyonun 11'inde üçüncül oturma davranışları gözlemlenmiştir. Mühendislik uygulamalarında ikincil ve üçüncül oturmaların tahmin edilmesi için C_s/C_c ve C_t/C_c aralıkları önerilmiştir. Ek olarak, sıkışma indisi değerleri (C_c) ile ikincil ve üçüncül sıkışma katsayıları (C_s-C_t) arasındaki ilişki araştırılmış olup, laboratuvar verileri ile idealize jeolojik profil geometrisinin sayısal parametre olarak değerlendirildiği bağıntılar önerilmiştir. Gerçekleştirilen çalışmalar, bağımsız değişkenler ile hedeflenen bağımlı değişkenler arasında doğrusal bir ilişkinden ziyade doğrusal olmayan bir ilişki olduğunu göstermiş ve varsayılan denklem modelini çözmek için iterative doğrusal olmayan regresyon analizleri gerçekleştirilmiştir.

Anahtar Kelimeler: konsolidasyon oturma tahmini, kil, üçüncül konsolidasyon, zayıf zeminler, Karacabey

To my mother, the strongest woman I know…

ACKNOWLEDGMENTS

I would like to express my sincere thanks to my supervisor Prof. Dr. Tamer Topal for his guidance, advice, criticism and insight throughout the research and writing process of this thesis. He had given me a great chance to continue my research with him and this had provided me to improve my abilities in engineering and to gain an insight into bringing solutions to engineering problems. His never-ending motivation, unlimited assistance and patience made this study possible.

I would like to express my sincere gratitude to my co-supervisor Prof. Dr. Ahmet Orhan Erol for his generosity in sharing his knowledge, his invaluable guidance and motivation throughout my studies. I feel very lucky to have an opportunity to work with Prof. Erol who has expertise and great experience on the subject. His wisdom and ambition helped me to find my path through the difficulties of the research.

I would like to express my special thanks to Prof. Dr. Kemal Önder Çetin for his positive approach, confidence and constructive suggestions throughout this research period. His insightful remarks, unlimited assistance and tolerance helped me succeed in this study.

I would further like to thank to Prof. Dr. Nurkan Karahanoğlu for his inestimable guidance, support and suggestions throughout this study.

I would like to address my sincere gratitude to all the jury members, whom kindly accepted to review my thesis. It was definitely their guidance, criticism and suggestions throughout the research that made this thesis complete.

I would like to thank to Mr. Yüksel Domaniç for his invaluable support, positive approach and confidence throughout the study.

I would like to express my thanks to Mr. Haluk. G. Ulusoy for his support, positive approach and encouragement.

I would like to extend my gratitude to Mr. Abidin Akbulut and Mr. İ. Yavuz Oktay for supporting me and supplying data for this study.

Never to be forgotten are my dearest friends; Ekin Eren, Zeren Güder Oflas, Bade Güven Kardeş and Oğuz Baysal, whose friendship and supports are invaluable for me.

I would like to sincerely thank to my colleagues at Yüksel Domaniç Eng. and all of my friends for their continuous support and help during this study.

I also would like to convey my deepest thanks to my parents Sevgi-Abdullah Çelik, my brother Mehmet Bersel Çelik and my grandmother Sebahat Çelik for their invaluable support, encouragement and motivation. Also, I would like to give special thanks to my niece, my little love Valen Nil Çelik, for her sweetness. I would also like to commemorate my dear late grandmother who has raised me, Sebiha Baydar. She always trusted me, supported my education and kept being with me as long as she could.

Last, but not the least, sincere appreciations of mine go to Dr. Kemal Arman Domaniç, for his technical supports, encouragements and trust in me in every way. He was always generous to share his ideas troughout my studies and to give feedbacks in this study. During this long and laborious period of research, I occasionally had hard time of studying on my thesis. I was able to overcome these difficulties with the support of this accomplished colleague who had been available for my technical questions with patience at all times.

TABLE OF CONTENTS

LIST OF TABLES

TABLES

LIST OF FIGURES

FIGURES

LIST OF SYMBOLS

SYMBOLS

a	:	width of a band-shaped drain cross-section
b	:	thickness of a band-shaped drain cross-section
b^*	:	length which characterized the size of the loaded area
C_c	:	primary compression index
C_s, C_α	:	secondary compression index
C_t	:	tertiary compression index
c_h	:	coefficient of horizontal consolidation
c_v	:	coefficient of vertical consolidation
c_u	:	undrained shear strength
CPT	:	cone penetration test
D'	:	drain constraint modulus
d_e	:	diameter of the influence zone in a unit cell
d_w	:	equivalent drain diameter
e	:	void ratio
e_0	:	initial void ratio
F(n)	:	drain spacing factor
H_0	:	thickness of compressible layer

PI, I_p	:	plasticity index
K	:	ratio of horizontal to vertical effective stress
LI	:	liquidity index
LL	:	liquid limit
k	:	coefficient of permeability
m_v	:	coefficient of volume compressibility
n	:	load intensity ratio
N_{60}	:	corrected SPT value for 60% hammer efficiency
OCR	:	over consolidation ratio
PI	:	plasticity index
PVD	:	prefabricated vertical drain
q	:	vertical stress applied over loaded area
q_c	:	CPT cone resistance
r_s	:	smear zone radius
S	:	spacing of prefabricated vertical drain
S_f	:	ultimate settlement value
S_i	:	immediate settlement value
S_p	:	primary settlement value
S_s	:	secondary settlement value

S_t	:	tertiary settlement value
S_o/S_p	:	ratio of observed settlement from instrumented test embankments to predicted settlement from oedometer test data
SPT	:	standard penetration test
t	:	time
t_f	:	total settlement time
T_v	:	time factor for vertical consolidation
T_h	:	time factor for radial consolidation
u	:	excess pore pressure
U	:	average consolidation ratio
U_v	:	average vertical consolidation ratio
U_r	:	average radial consolidation ratio
w	:	water content
w_N	:	natural water content
v^*	:	settlement speed
z	:	thickness of compressible soil / depth from top of the compressible layer
z_d	:	depth of influence of stress
α_m	:	coefficient of correlation for tip resistance

β_1	:	slope of a straight line on the curve that represents the settlements according to time
γ_w	:	unit weight of water
γ'	:	effective unit weight of soil
ε	:	normal strain
λ	:	ratio of sand thickness to clay thickness
μ	:	friction coefficient
$\Delta\sigma$	:	increase in vertical stress
Δt	:	time interval
Δu	:	increase in excess pore-water pressure
σ'_0	:	effective vertical normal stress
σ_c	:	preconsolidation pressure
σ'_1	:	effective total normal stress
ϕ'	:	effective internal friction angle
ψ	:	ratio of length of road platform to total clay thickness

CHAPTER 1

INTRODUCTION

For engineering approaches, soil is defined as the uncemented aggregate of mineral grains and decayed organic matter (solid particles) with liquid and gas in the empty spaces between the soil particles (Das, 2008). When a soil is loaded, deformation will occur due to stress changes. The total vertical deformation resulting from the load is called settlement. In general, the soil settlement caused by load may be divided into three broad categories with respect to mode of occurrences; immediate settlement, primary consolidation settlement and secondary consolidation settlement. The uniform settlement and differential settlement are the settlement types classified according to uniformity. Soils have both elastic and plastic deformation. If this deformation is retained when the load is released, it is said to have plastic deformation and consolidation settlement falls in this category. Conversely, settlement due to elastic compression of soil is usually reversible and immediate settlement is calculated by elastic theory.

Evaluation of expected settlements depends on the consolidation parameters obtained from laboratory and field tests. Consolidation parameters have inaccuracies resulting from sample disturbance, sample size, experiment errors and engineering approaches. Furthermore, both the magnitude of loading and the deformation characteristics of the subsoil exhibit variations, which results in non-uniform settlement of the subsoil. The non-uniform settlements result in unevenness of the road and this cause to decrease in traffic safety and driving comfort.

1.1 Problem Statement

The term clay is used as a rock term and also particle size term. As a rock term, it implies a natural earthy and fine-grained material which develops plasticity when mixed with a limited amount of water. As a particle size term, clay fraction is composed of particles having diameter less than 4μm (1/256 mm) according to Wentworth scale. The estimation of consolidation settlements of embankments constructed on clayey, compressible soils is a critical issue for engineering projects. Accurate estimation of settlements renders possible tight optimization of design and construction schedule. If settlements continue past the expected duration, construction cost and deadline may be adversely affected. If settlements continue after paving, structural performance may be reduced to such a level that, early renewal of pavement would be required.

In order to make a reasonable estimation for consolidation magnitude and rate in analytical calculations, consolidation parameters should be assigned correctly. The oedometer test or empirical approaches can be used to obtain consolidation parameters. However, in laboratory tests, small homogeneous samples which only consist of clay are used while in reality, the soil profile consists of sand lenses and these lenses lead to quicker dissipation of pore water pressure and so result in quicker settlement. Back analysis from test embankment gives the most reasonable consolidation parameters when compared to laboratory tests, so that future estimations on consolidation become easier.

1.2 Research Objectives

The main objectives of this study are;

- To check the compatibilities of soil compressibility parameters obtained from field tests empirically, from oedometer tests and from test embankments,

- To check the applicability of Skempton-Bjerrum correction factors, which are defined in ranges, in consolidation calculations,
- To evaluate the applicability of semi-empirical methods available in literature (Asaoka's method, Horn's method) to predict the final settlement by using monitoring results,
- To present the secondary and tertiary behaviors of Karacabey clay,
- To recommend C_s/C_c and C_t/C_c ranges for engineering practices,
- To obtain non linear correlation between independent variables; SPT N, PI, w_N, LL and dependent variables $m_{v(field)}/m_{v(stroud)}$,
- To obtain a correlation between cone tip resistance (q_c) and α_m,
- To obtain correlation between independent variable; LI and dependent variables which is the ratio of Primary and Tertiary Consolidation Coefficients (C_t/C_c),
- To obtain an equation that defines the relationship between independent variables (w_N, LL, λ, ψ) and dependent variables S_o/S_p (the ratio of field settlement to predicted settlement).

1.3 Scope

The scope of this study can be expressed as analytical calculation of consolidation settlements for 26 test embankments constructed in Bursa-Susurluk Section between Km: 139+100 ve Km: 160+000 of Gebze-İzmir Highway Project. And then, the amounts and the rates of consolidation measured by settlement plates directly in the field are presented. Observed settlements are divided into three phases; namely primary, secondary and tertiary on settlement vs. time curves. Asaoka's and Horn's Methods are used to predict the final magnitudes of settlements using 70% of the monitored data and calculated data are compared with observed data. Finally, the comparisons of the consolidation magnitudes of settlements calculated from oedometer tests, predicted from observational methods and measured in field directly are presented and non linear correlations are obtained between independent variables (PI, LL, LI, SPT N, w_N, λ, ψ) and dependent variables (S_o/S_p, C_t/C_c, $m_{v(field)}$ /m $_{(stroud)}$).

Literature survey is an important part of research work. The literature review for consolidation theory and observational methods (graphical and semi-empirical methods) and multi variable regression analysis are included in this study. The information about the soil profile under embankments, compressibility parameters obtained from laboratory tests and field measurements are also provided in the content of the thesis study.

1.4 Location and Accessibility

The study area is located in Karacabey Plain of Bursa and approximately 4.7 km NW of Ulubat Lake. The route takes place between the longitudes N40º14’02 and N40º05’31 and the latitudes E28º25’08 and E28º16’28 (Google Earth Software, 2019). The study area is presented in Figure 1.1:

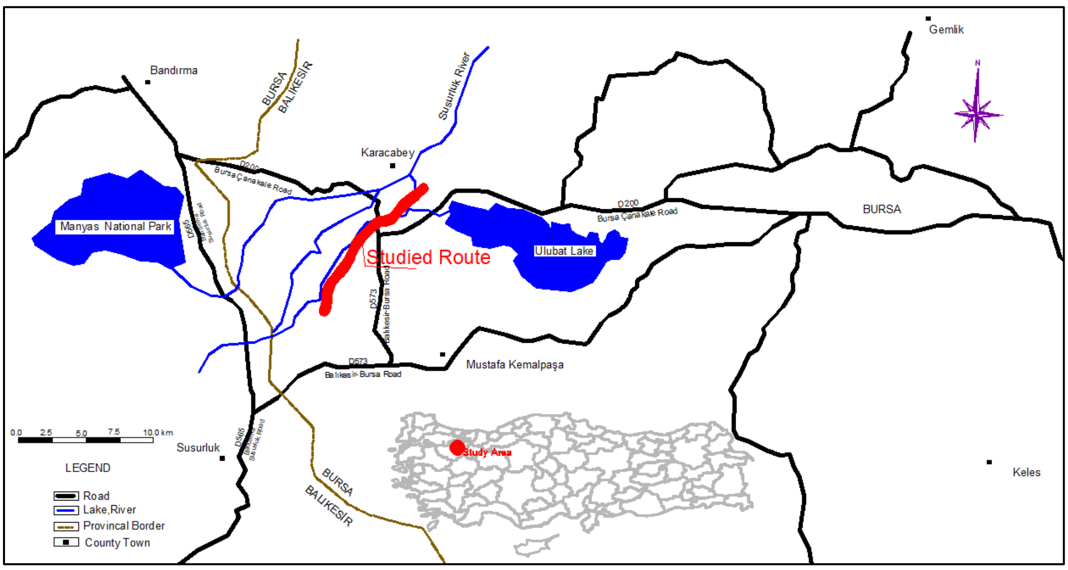

Figure 1.1. Location map of the study area

D200 Bursa-Çanakkale main road is used to access the start of study route. After reaching Karacabey district, Karacabey Road is taken to North. On the division from main road to Taşlık Village, Taşlık Village Road starts. Accession to the study area is obtained after moving 3.3 km on Taşlık Village Road to the East.

1.5 Methodology

In order to succeed the purpose of this study, several stages were considered. As a first stage; literature survey about geology of Bursa-Susurluk Region, determination of physical and mechanical properties of soils, calculation methods about consolidation settlements were reviewed.

Second stage of the study comprised detailed site investigations perfomed in order to obtain geological and geotechnical information about study area. Site investigation involved drilling of boreholes and cone penetration tests to identify subsurface structures, construct idealized soil profiles, obtain disturbed and undisturbed soil samples and evaluate strength parameters.

In the third stage of the study, laboratory tests were performed. The laboratory test program had the content of sieve analysis, Atterberg limits, unified soil classification, moisture content, natural unit weight, consolidation test, triaxial compressive strength test.

Following the third stage, consolidation settlement calculations and then evaluations of data obtained from settlement plates were performed.

Comparisons of theoretical consolidation behaviors with the observed ones were utilized in the final stage of the study.

CHAPTER 2

LITERATURE REVIEW ON SOIL CONSOLIDATION

In order to understand the behavior of soils, it will be beneficial to give information about some terms and definitions. The settlement is defined as the total vertical deformation at soil surface resulting from the load. The rate of decrease in volume due to unit load is defined as compressibility. When a saturated soil is loaded externally, the water is squeezed out of the soil and the soil shrinks over a long time depending on the permeability of the soil and this phenomena is called consolidation. Some addition statements should also be given to explain the relationship between water and soil, which are swelling and shrinkage. Swelling is volume expansion of the soil due to increase in water content and shrinkage is volume contraction of the soil due to reduction in water content. Immediate settlement, primary consolidation, secondary consolidation and tertiary consolidation are the types of settlements caused by load application. Their definitions are given below.

Immediate settlement: This settlement occurs more or less simultaneously with the applied loads (Murthy, 2002).

Primary consolidation: It is the result of volume change in saturated cohesive soils because of the expulsion of water that occupies in void spaces (Das, 2008).

Secondary consolidation: After all excess pore pressures have dissipated, continuous settlement may exist, and this is known as secondary settlement, secondary consolidation or creep (Murthy, 2002).

Tertiary consolidation: At secondary consolidation phase, when the rate of settlement in e-log t curve increases, it is called tertiary consolidation (den Haan, 1994).

The general shape of the plot of deformation of the soil specimen versus time for a given load increment is given in Figure 2.1.

In order to calculate the total settlement S_{max} of the cohesive soil, due to structural loading, the four components of the settlement are added together:

$$S_{max} = s_i + s_c + s_s + s_t \qquad \text{(Eq. 2.1)}$$

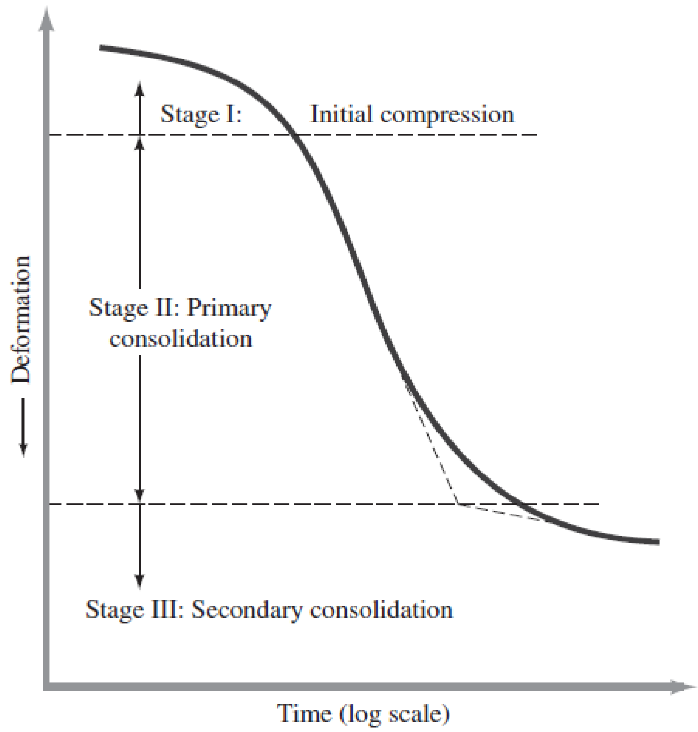

Figure 2.1. Time – Deformation plot during consolidation for a given load increment (Das, 2008)

2.1 Consolidation Settlement

The increase in pore water pressure takes place when a saturated soil is subjected to stress increase. Since the sandy soils are highly permeable, drainage occurs by the increase of the pore water pressure immediately. The immediate settlement takes place in sandy soils because of rapid drainage of the water. However, clayey soils have low hydraulic conductivity and drainage of pore water is time dependent (Das, 2008).

The behavior of soil during one-dimensional consolidation or swelling can be determined by oedometer test. The one-dimensional consolidation testing procedure was first suggested by Terzaghi (1925). For this test, the test specimen is placed into two porous stones, one at the top and the other at the bottom. The load is applied on the specimen usually for 24 hours and compression is measured by a micrometer dial gauge (Figure 2.2). The specimen is kept in water during the test and the load is doubled for each period. For doubling the pressure, measurements are continued (Das, 2008).

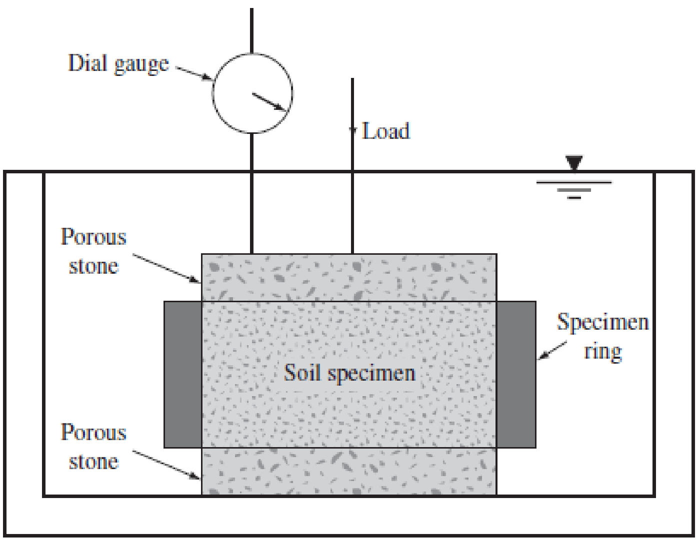

Figure 2.2. Consolidometer (Das, 2008)

The coefficient of volume compressibility or the compression index is required to predict the consolidation settlement of a saturated clay layer. These definitions are given below.

The coefficient of volume compressibility (m_v): It is defined as the volume change per unit volume per unit increase in effective stress. The coefficient of volume compressibility is not constant; it depends on the stress range where it is calculated.

$$m_v = \frac{1}{1+e_0}\left(\frac{e_0-e_1}{\sigma_1'-\sigma_0'}\right) = \frac{1}{H_0}\left(\frac{H_0-H_1}{\sigma_1'-\sigma_0'}\right) \text{ (Craig, 2004)} \qquad \text{(Eq. 2.2)}$$

The compression index (C_c): It is the slope of the linear portion of e-log σ' plot and it is dimensionless.

$$C_c = \frac{e_0-e_1}{\log\left(\sigma_1'/\sigma_0'\right)} \text{ (Craig, 2004)} \qquad \text{(Eq. 2.3)}$$

A typical void ratio-effective stress graph with recompression and expansion is presented in Figure 2.3.

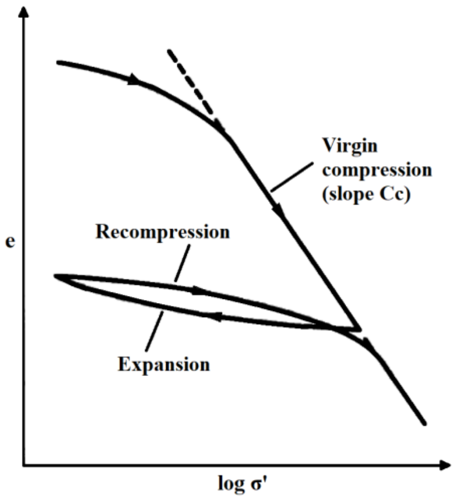

Figure 2.3. Void ratio-effective stress relationship (Craig, 2004)

The coefficient of volume compressibility (m_v) can be obtained empirically by using SPT N and plasticity index values. A relation is proposed by Stroud (1974) as presented in Figure 2.4:

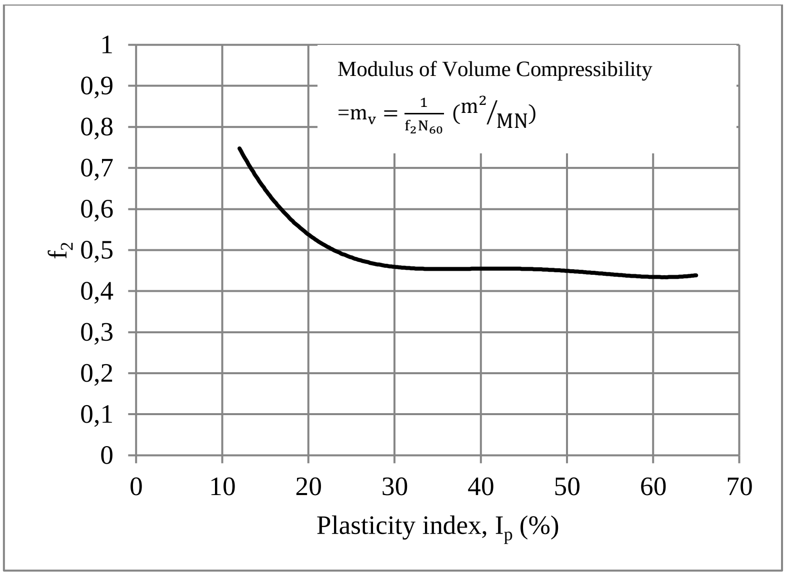

Figure 2.4. Modulus of volume compressibility from SPT N and plasticity index (Stroud, 1974)

The coefficient of volume compressibility can be assigned by using cone penetration test data by equation (2.3) presented below and Table 2.1 presents the coefficients of α_m.

$$M = \frac{1}{m_v} = \alpha_m q_c \text{ (Sanglerat, 1972)} \qquad \text{(Eq. 2.4)}$$

Table 2.1 The coefficients of α_m (Sanglerat, 1972)

q_c intervals		α_m values	Soil type
q_c<0.7 MN/m2		$3<\alpha_m<8$	
0.7 MN/m^2<q_c<2.0 MN/m^2		$2<\alpha_m<5$	Clay of low plasticity (CL)
q_c>2.0 MN/m^2		$1<\alpha_m<2.5$	
q_c>2.0 MN/m^2		$3<\alpha_m<6$	Silts of low plasticity (ML)
q_c<2.0 MN/m^2		$1<\alpha_m<3$	
q_c<2.0 MN/m^2		$2<\alpha_m<6$	Highly plastic silts and clays (MH, CH)
q_c<1.2 MN/m^2		$2<\alpha_m<8$	Organic silts (OL)
q_c<0.7 MN/m^2			
	50<w<100	$1.5<\alpha_m<4$	Peat and organic clay (P_t, OH)
	100<w<200	$1.0<\alpha_m<1.5$	
	w>200	$0.4<\alpha_m<1.0$	

w: water content (%)

The settlement of the layer of thickness H is calculated using the coefficient of volume compressibility (m_v) by;

$$S_c = \int_0^H m_v \, \Delta\sigma' dz \text{ (Craig, 2004)} \qquad \text{(Eq. 2.5)}$$

If m_v and $\Delta\sigma'$ are assumed to be constant with depth, it is obtained as;

$$S_c = m_v \Delta\sigma' H \text{ (Craig, 2004)} \qquad \text{(Eq. 2.6)}$$

The settlement of the layer of thickness H is can also be calculated using the Compression Index (C_c) for normally consolidated clays by;

$$S_p = \frac{C_c H}{1+e_0} log\left(\frac{\sigma_0' + \Delta\sigma'}{\sigma_0'}\right) \text{ (Das,2008)} \qquad \text{(Eq. 2.7)}$$

In overconsolidated clays for $\sigma_0' + \Delta\sigma' \leq \sigma_c'$;

$$S_p = \frac{C_s H}{1+e_0} log\left(\frac{\sigma_0' + \Delta\sigma'}{\sigma_0'}\right) \text{ (Das, 2008)} \qquad \text{(Eq. 2.8)}$$

In overconsolidated clays for $\sigma_0' + \Delta\sigma' > \sigma_c'$;

$$S_p = \frac{C_s H}{1+e_0} log\left(\frac{\sigma_c'}{\sigma_0'}\right) + \frac{C_c H}{1+e_0} log\left(\frac{\sigma_0' + \Delta\sigma'}{\sigma_c'}\right) \text{ (Das,2008)} \qquad \text{(Eq. 2.9)}$$

In the geologic history, the soil at some depth is subjected to maximum effective past pressure. Two basic definitions are arisen based on the geologic history. If the present effective overburden pressure is the maximum pressure that the soil has been subjected to in the past, the soil is defined as *normally consolidated*. If the present effective overburden pressure is less than that the soil has experienced in the past, the soil is defined as *overconsolidated*. The maximum past pressure is called *preconsolidation pressure* (Das, 2008) and overconsolidation ratio of a soil can be defined as;

$$OCR = \frac{\sigma_c'}{\sigma'} \qquad \text{(Eq. 2.10)}$$

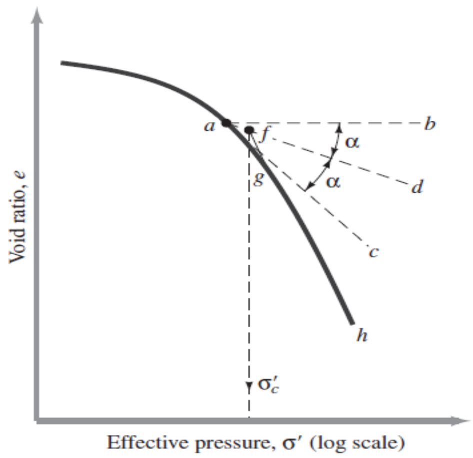

Figure 2.5. Graphic procedure for determining preconsolidation pressure (Das, 2008)

In order to estimate the degree of consolidation of a clay layer at some time t after the load application, the rate of dissipation is needed and the coefficient of consolidation (c_v) is the parameter that controls the rate of consolidation.

Terzaghi derived the following equation for a vertical drainage condition;

$$\frac{\partial(\Delta u)}{\partial t} = c_v \frac{\partial^2(\Delta u)}{\partial z^2} \qquad \text{(Eq. 2.11)}$$

in which;

$$c_v = \frac{k}{m_v \gamma_w} \quad \text{(Eq. 2.12)}$$

where;

u: excess pore pressure

z: depth from top of the compressible layer

t: time from the instantaneous application of a total stress increment

c_v: coefficient of consolidation in vertical direction

k: coefficient of permeability

γ_w: unit weight of water

In order to determine coefficient of consolidation (c_v), Casagrande's Log Time Method and Taylor's Root Time Method are proposed.

Casagrande's Log Time Method

In Casagrande's Log Time Method, the dial gauge readings in the oedometer test against the logarithmic time in minutes are plotted. In this plot, the first point a_s which corresponds to U (%) equals to zero is determined. Then the second point a_{100} which corresponds to U (%) equals to 100 is determined. The point U (%) equals to 50 can be placed between U (%)=0 and U (%)= 100 and the corresponding time t_{50} obtained (Craig, 1997) (Figure 2.6).

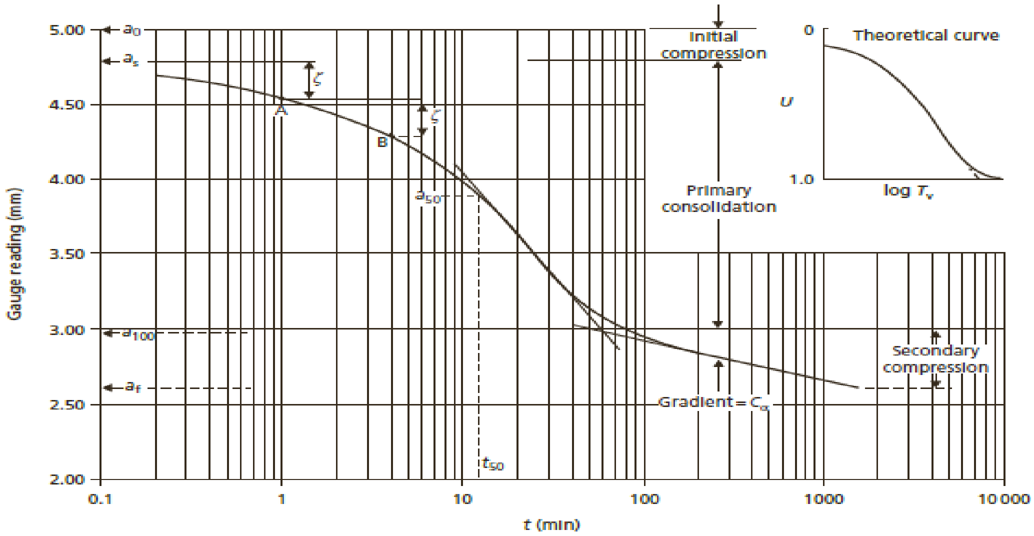

Figure 2.6. Casagrande's Log of Time Method (Craig, 1997)

The value of T_v corresponding to U= 50% is 0.196 and the coefficient of consolidation can be calculated by;

$$c_v = \frac{0.196d^2}{t_{50}} \qquad \text{(Eq. 2.13)}$$

d can be taken as the half of the average thickness of the specimen for the particular pressure increment.

Taylor's Square Root of Time Method

In Taylor's Log Time Method, the dial gauge readings are plotted against the square root of time as presented in Figure 2.7. The early part of the plot is approximately a straight line which is extended in both directions as shown by dashed line. Another straight line is drawn such that the abscissa is 1.15 times larger than the previous line. The intersection of the second line with the laboratory curve defines the 90% consolidation point (Sivakugan and Das, 2010). The value of T_v corresponding to U= 90% is 0.848 and the coefficient of consolidation is given by;

$$c_v = \frac{0.848d^2}{t_{90}} \quad \text{(Eq. 2.14)}$$

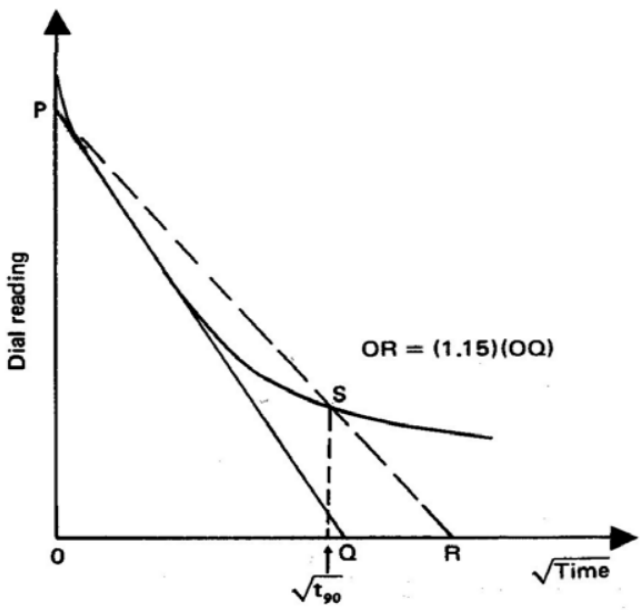

Figure 2.7. Taylor's Square Root of Time Method (Sivakugan and Das, 2010)

2.2 Secondary Consolidation

The origins of the term secondary compression most probably lie in North America in the 1930s. In the 1st ICSMFE, Gray and Keverling Buisman both refer to the term as being widespread use there (Den Haan, 1994).

Basic laws describing the behavior of ideal continuum do not account for the structural rearrangement of the material and there is a need for a fundamental theory which describes the mechanistic behavior of particulate materials and for structural changes (Erol, 1977).

One of the main models for explaining creep behavior is the Rate Process Theory. This theory was developed in the area of Physical Chemistry and was originally intended for assessing the speed at which chemical reactions occur (Alexandre, 2006).

Gibson and Lo (1961) used a rheologic model composed of a spring series with a combination of a spring and dashpod. In the model, the effective stress is applied to the top of the primary spring with a resulting instantaneous compression of that primary spring (compressibility= “a”) (Figure 2.8). For a linearly elastic body (the spring is then called a Hookean element), the compressibility of the primary spring becomes m_v if we define compressibility using total height, or a_v if we use the height of solids. The load in the primary spring is also transferred to the secondary spring and dashpot (a Kelvin body). Instantaneously, the load is entirely carried in the dashpot because it is incompressible. However, fluid escapes from the dashpot and it compresses, thus causing the secondary spring to compress, and thus take load. When the secondary spring takes load, that amount of load is removed from the dashpot, when then compresses more slowly. Thus, the load is gradually transferred from the dashpot to the spring and, at time infinity; the entire load is in the spring. Secondary compression is then the compression of the Kelvin body.

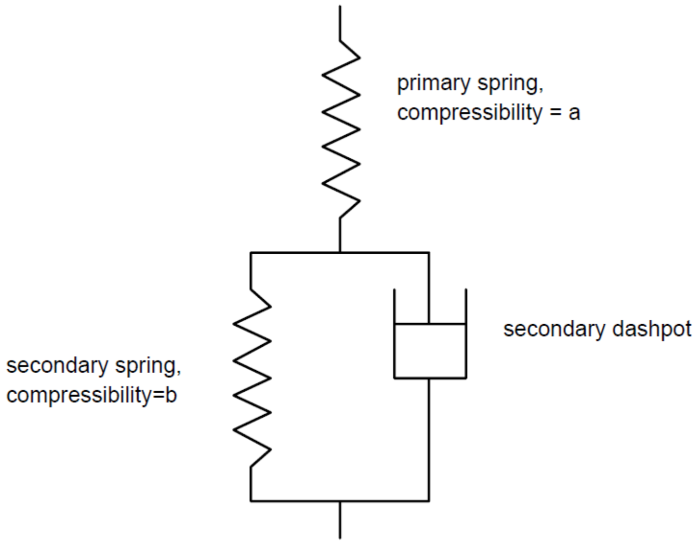

Figure 2.8. Secondary Consolidation Model (Gibson and Lo, 1961)

Other models for assessing creep include visco-elastic, visco-plastic or visco-elasto-plastic models combined with or not with the Rate Process Theory. A few models were described by Murayama and Shibata (1958, 1961, 1964), Mesri et al. (1981), Adachi and Okano (1974), Sekiguski (1984) and Kutter and Sathialingam (1992) and Martins (1992). Since detailed formulations of these models are available in literature, they are not given in the content of this study.

For large values of time, the time-dependent strain, ε (t) is written as (Edil, 1997);

$$\varepsilon(t) = \Delta\sigma \left[a + b(1 - e^{-(\lambda/b)t}\right] \qquad \text{(Eq. 2.15)}$$

where Δσ = stress increment, t= time, a= primary compressibility, b= secondary compressibility, and λ/b= rate factor for secondary compression

Secondary consolidation occurs in saturated cohesive soils as a result of rearrangement of soil particles under nearly constant effective stress. The most evidence of secondary compression is the settlement that occurs after the conclusion of primary consolidation. According to Buisman (1936), the relationship between deformation and the logarithm of time is essentially linear in the secondary compression stage. Furthermore, he pointed out that creeping of clays never ends.

Examination of data from numerous laboratory tests indicates that the secondary settlement may range from less than 10% of the total settlement to essentially 100% (Olson, 1989).

Sas and Malinowska (2006) stated that the staged construction on organic soils caused acceleration of consolidation and reduced long-lasting secondary settlement. Furthermore, the surcharging significantly influenced the acceleration of secondary settlements which received about 20-30% of the total settlements which had to be considered in the settlement calculations.

Figure 2.9 shows a typical relationship between void ratio and the logarithmic time in the one dimensional creep test. The S-shaped is observed in the curve and it can be divided into two parts; the main consolidation stage and the secondary consolidation stage.

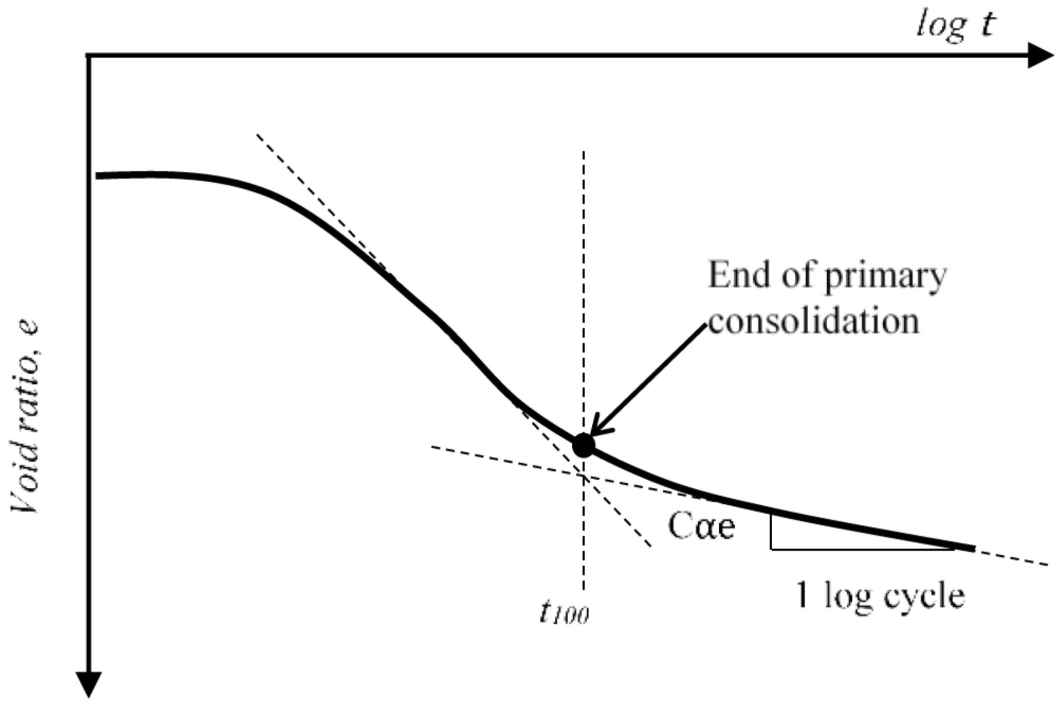

Figure 2.9. Identification of secondary compression coefficient (Zhao, 2017)

2.2.1 Causes of Secondary Compression

Secondary effects probably result from different mechanisms in different soils. Some simple mechanisms include (Olson, 1989):

Soils have void spaces of widely differing sizes. In some soils, water may drain from the larger voids in accord with primary theory and then water may more slowly squeeze out of smaller voids, producing a secondary effect.

In organic soils containing plant matter, water may similarly squeeze out of the voids in accord with primary theory and then water may squeeze slowly out of the individual plant cells, through the cell walls, at a slow rate, producing a secondary effect.

Some clay particles may be surrounded by water that is adsorbed onto the surfaces by local electrical effects. This adsorbed water may grade imperceptibly outwards into normal liquid water. As particles are pressed more closely together during primary consolidation, there would be expected to be a viscous resistance to volume change developed, which might produce apparent secondary effects.

Some case histories of settlement of wide embankments involve a shallow highly compressible soil and deeper less compressible soils. Apparent secondary settlement may actually represent delayed primary consolidation of the relatively incompressible soil which cannot drain until the overlaying, more compressible layer, has consolidated somewhat.

In the case of some organic soils, the hydraulic conductivity of the soil decreases by more than an order of magnitude during consolidation under a given load. Consolidation naturally proceeds more rapidly initially but then at a decreasing rate because of the reduction in hydraulic conductivity, thus producing an apparent secondary effect.

Highly non-linear stress-strain curves can produce settlement-time behavior that looks like primary consolidation followed by secondary consolidation.

In the secondary consolidation stage, the slope of the void ratio versus logarithmic time is defined as the secondary consolidation coefficient:

$C_\alpha = -\frac{\Delta e}{\Delta log t}$ (Zhao, 2019) (Eq. 2.16)

Secondary consolidation settlement can be calculated as;

$$S_s = \frac{C_\alpha}{1+e_p} H_0(\Delta logt) \text{ (Duncan and Buchignani, 1976)} \qquad \text{(Eq. 2.17)}$$

C_α: Secondary consolidation index

e_p: void ratio at end of primary consolidation

H_0: Thickness of the compressible layer

$$\Delta logt = \frac{t_{sc}}{t_p} \qquad \text{(Eq. 2.18)}$$

t_p: time of start of secondary consolidation

t_{sc}: time for secondary consolidation calculation

$\frac{C_\alpha}{1+e_p}$: Modified secondary consolidation index

According to the long term (140 days) creep tests, conducted by Leroueil et al. (1985) on Batiscan clay under different vertical stresses, showed a general non linear strain-time behavior as presented in Figure 2.10 and following conclusions are obtained:

Type I corresponds to the overconsolidated soil, the vertical stress is less than the preconsolidation stress, no significant cross-point is between the primary consolidation and secondary consolidation.

Type II corresponds to a normally consolidated sample which the vertical consolidation pressure is close to the preconsolidation stress, and the slope of σ_v-log t during secondary compression is significantly larger that of type I.

Type III is a normally consolidated sample and vertical consolidation pressure is much higher than the preconsolidation pressure, and the slope of σ_v-log t curve is gradually reduced.

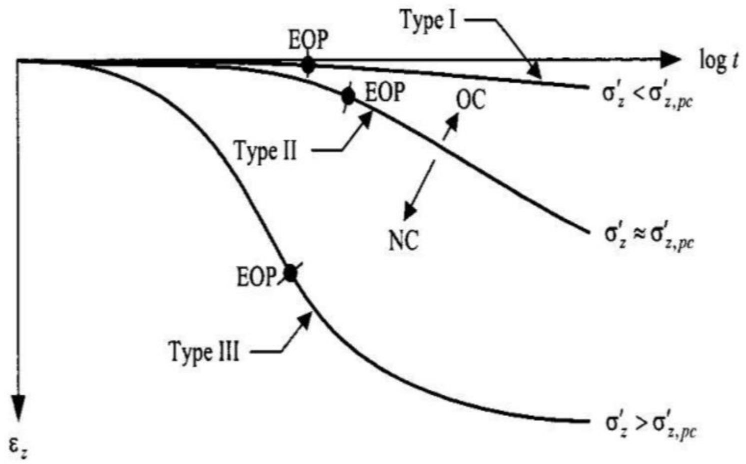

Figure 2.10. Types of strain versus time relations (Leroueil et al., 1985)

The creep characteristics of clay in one dimensional test are described by parameter of secondary compression coefficient (C_α). According to previous investigations, C_α depends on type of soil, consolidation stress, overconsolidation, stress duration, remoulding, shear stress and temperature.

Type of soil

Secondary consolidation may be defined as the mechanism of continuation of volume change, which is initiated from primary consolidation. This mechanism includes deformation of individual particles and the relative movements of individual particles with respect to each other. Therefore, in normally consolidated clays where contact stresses are relatively high, the rate of secondary consolidation will be higher than for overconsolidated soils where contact stresses are lower (Buri, 1978).

Sridharan and Jayadeva (1982) showed that the compressibility of pure clays under external load not only depended on the negative charges and crystallite structure of clay minerals but also on the ion concentration, cation valency, dielectric constant and temperature of the pore fluid.

Stress dependency

The relationship between rate of secondary consolidation and consolidation stress is not clear. Haefeli and Schaad (1948) stated that there was no relationship between S_α and consolidation stress, Newland and Allely (1960) indicated C_α was independent of consolidation stress, Wahls (1962) indicated C_α decreased with stress, Ladd and Preston (1965) indicated that for one soil C_α increased slightly with consolidation stress while for another soil it decreased substantially with consolidation stress, Horn and Lambe (1964) concluded that ε_α was independent of consolidation stress, Adams (1965) concluded that ε_α increased considerably with consolidation stress and Goldberg (1965) indicated that ε_α increased with magnitude of load. According to study of Mesri (1973), for normally consolidated clays, C_α decreased with consolidation stress. According to study conducted by Mesri and Godlewski (1977), C_α increased gradually with increase of σ'_z for natural undisturbed soil. Leroueil et al. (1985) stated that C_α was associated with vertical stress. Fodil et al. (1997) found that C_α increased with the increase of σ'_z.

Sridharan and Rao (1982) reported that the secondary compression coefficient decreases with increase in effective stress (or strength).

Al-Shamrani (1998) conducted series of one dimensional consolidation tests on Sabkha soil and it was concluded that C_α was strongly depend on effective stresss.

According to Bjerrum (1972), C_α was related to the preconsolidation pressure. Experimental results on remolded Kaolin and Shanghai clay showed that C_α depends not only on the applied stress but also on preconsolidation pressure (Ladd and Preston, 1965; Tavenas et al., 1978; Graham et al., 1983; Lansivaara and Nordal, 2000; Augustesen et al., 2004).

Tripathy et al. (2010) showed that a vertical pressure increase was more effective in reducing the water content and the void ratio for the bentonite studied. Mineralogy and the physico-chemical interactions between the clay particles and the pore fluid have a significant influence on the volume change behavior of clays due to an increase in vertical pressure.

According to study presented by Das (2015), C_α decreased with increase in stress but increased with increase in plasticity index.

Time dependency

According to the studies of Mesri and Godlewski (1977), Feda (1992), Wu et al. (2011), it was concluded that both C_α and C_c changed with time. Fox et al. (1992) revealed long-duration odometer tests on Middleton peat, which showed the important contribution of creep to total settlement. This study indicated that C_α was not constant but increased in time under constant effective stress.

Mesri and Vardhanabhuti (2005) conducted a large volume of reliable measurements of one-dimensional settlement. They observed in the laboratory and in the field for a wide variety of natural soil deposits. They determined that secondary compression index $C\alpha = \Delta e/\Delta \log t$ (therefore, also $\Delta S/\Delta \log t$) might remain constant, decreased, or increased with time.

Remoulding

Remoulding generally decreases the rate of secondary consolidation and also more secondary consolidation occurs in undisturbed samples than remoulded soils (Keene, 1964).

Shear Stress

According to Taylor (1942), greater secondary consolidation occurs in one dimensional compression than in three-dimensional compressions (Ladd and Preston, 1965).

Temperature

Simons (1965) noted that compressibility depended on the strength of the bonds at the points of contact, which was reduced with an increase in the testing temperature. Habibagahi (1969) conducted the studies on inorganic and organic clays and concluded that the coefficient of secondary consolidation for normally consolidated and over consolidated specimens were independent of testing temperature. According to studies by Gray (1936) and Lo (1961), the secondary compression curve increases as the temperature increases.

If determination of secondary consolidation from laboratory tests is not practical, C_α/C_c can be obtained from Table 2.2 presented below:

Table 2.2 Values of C_α/C_c for natural soils (modified from Mesri and Godlewski, 1977)

Organic Silts	0.035-0.06
Amorphous and fibrous peat	0.035-0.085
Canadian muskeg	0.09-0.10
Lada clay (Canada)	0.03-0.06
Postglacial Swedish clay	0.05-0.07
Soft blue clay (Vicrotria, B.C.)	0.026
Organic clays and silts	0.04-0.06
Sensitive clay, Portland, Maine	0.025-0.055
San Francisco Bay mud	0.04-0.06
New Liskeard (Canada) varved clay	0.03-0.06
Mexico City clay	0.03-0.035
Hudson River silt	0.03-0.06
New Haven organic clay silt	0.04-0.075

Mesri (1973) investigated the importance of secondary or delayed compression and noted that the coefficient of secondary compression was a powerful tool to explain the secondary consolidation. He classified the soil based on Secondary compressibility as presented in Table 2.3.

Table 2.3 Classification of soils based on secondary compressibility (Mesri, 1973)

Coefficient of secondary compression (C_α) as a percentage	Secondary compressibility
<0.2	Very low
0.4	Low
0.8	Medium
1.6	High
3.2	Very high
>6.4	Exteremly high

2.3 Tertiary Consolidation

The clayey soils consist of the two major components which are, fabric characterizing the geometrical arrangement of mineral particles and void spaces, and particle interactions, describing the bonding mechanism and nature of shear resistance. Changes in both components are result of creep deformation (Erol, 1977).

At the first International Conference on Soil Mechanics and Foundation Engineering in 1936 at Harvard University, Cambridge, MA., A.S. Keverling Buisman presented a theory for creep of fine-grained soft soils. The statement of him that creeping of clays never ends was severely questioned at first not only by Terzaghi but also internationally. Meanwhile this theory has been accepted and confirmed by test results showing long term creep but also transition to tertiary creep (Brandl, 2018).

Tertiary compression is defined as the steepening up part of the strain- log *t* curve at a higher stress level (Den Haan, 1994). According to Edil (1997), tertiary compression refers to a decreasing strain rate however changing at an increasing rate. As presented in Figure 2.11, secondary creep should be considered as a transition zone between primary and tertiary creep and tertiary creep eventually ends in a creep rupture (Lacasse and Berre, 2005). Creep rupture refers to failure which occurs at the end of the tertiary creep (Singh and Mitchell, 1969). It occurs mostly due to re-structuring of the clayey particles (Dey, 2019).

Primary creep is always present, tertiary creep is observed only for stress levels close to failure stresses, whereas secondary creep is seldom observed (Hicher, 1985; Flavigny, 1987).

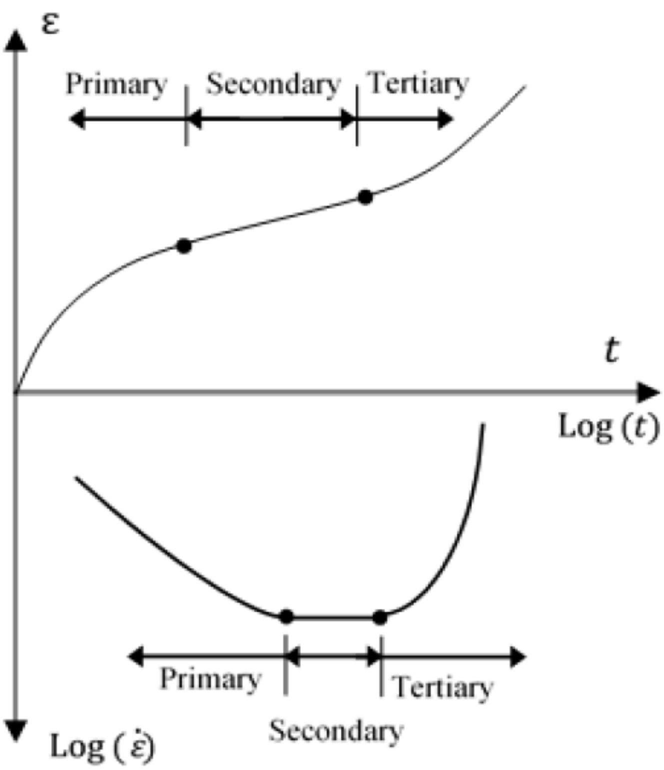

Figure 2.11. Definition of primary, secondary and tertiary creep
(Sheahan, 1995; Mitchell, 2003)

According to Yılmaz and Sağlamer (2001), secondary and tertiary compressibility characteristics of Samsun Blue Clay were investigated by comparing six one-dimensional test results with collected data of in-situ consolidation behavior of the blue clay. Furthermore, microfabric structures of the soft clay in undisturbed phase and during primary, secondary and tertiary compression phases were investigated. They pointed out that the observed in-situ secondary and tertiary compression ratios were approximately 2 to 4 times greater than the ones determined in the laboratory and tertiary compression took place because of breaking down the frame of organic matters during long term compression as a result of their study.

A highway junction on highly compressible soils with locally organic inclusions was designed in 1971-1972. Some samples were taken and investigated in the laboratory. Several of them were left in the oedometers for observation from 1971 and 2013 for creep tests. According to this study performed in 42 years, secondary creep occurred linearly with logarithm of time until one year, followed by a transition period to tertiary creep. However, even after 42 years no final value was reached in oedometer test, indicating viscous behavior and on-going rearrangements of the soil micro-structure (Brandl, 2018).

According to study presented by Gofar (2006), the primary consolidation was dominant in the compression of the peat, but the consolidation occurs in a relatively short time as compared to clay. Secondary compression, even though less significant than the primary consolidation in term of magnitude, could be very important in term of the design life of a structure. Tertiary compression was observed from the test results, but may not be very significant in term of the design life of the structure.

A study presented by Sing et al. (2018) about preloading simulations of both untreated and stabilized Klang peats using standard oedometer consolidation apparatus. Ordinary Portland cement, ground granulated blast furnace slag and siliceous sand were used to stabilize the soil. As the consolidation pressure increased, the rate of tertiary compression for both untreated and stabilized Klang peats approached its rate of secondary compression, indicating that the tertiary component of the soils merged with its secondary component at high consolidation pressure.

Consolidation behavior of peats were studied by Dhowian and Edil (1980) by four peat samples, covering a wide range of fiber contents which were subjected to one-dimensional consolidation tests. According to this study, tertiary compression was defined when the rate of secondary compression increased with the logarithm of time and the presence of a two-level structure, involving macropores and micropores were suggested. In this study, they stated that the rate of tertiary compression depended primarily on void ratio and peat type had the second importance.

According to the study presented by Jose et al. (1988), it was stated that the tertiary compression component was more than the secondary compression component in most cases and it decreased with the load increment ratio. For smaller load increment ratio, the influence of tertiary component was significant and for load increment ratio less than one, tertiary component came up to 35-45% of the total load.

2.4 Calculation of Stress Distribution

Prediction of vertical stress at any point in soil mass due to external loading is of great significance for the prediction of settlements of embankments or many other structures. When a load is applied to soil surface, the vertical stresses increase. In fill designs, the depth of influence needs to be assessed to determine the depth of clay that contributes the consolidation settlement. The variation of vertical stress with depth can be predicted by using linear, homogeneous, isotropic elastic theory. Such theory predicts the depth of influence of typical foundation loads but it overpredicts the depth of influence of more extensive surcharge loads. Some uncompacted waste fills have been treated and the depth of influence of the surcharge has been much smaller than that predicted by elastic theory (Charles, Burford, Watts, 1986).

A study about vertical stress increment is presented by Charles (1996) for two loading situations which are surcharge and footing load. In both cases, a load is applied which results in vertical stress (q) at the surface of the ground. The increase in vertical stress due to the surface loading has been calculated using elastic theory and using the principle of superposition. As a result, the relationships between stress increment and overburden pressure (γz) are very different. The stress increment due to surface load is much larger than the overburden pressure for the footing, whereas for the surcharge, the stress increment is much smaller than the overburden pressure.

Loading situations can be characterized by a load intensity ratio "n" which is introduced as;

$$n = \frac{q}{\gamma b^*} \qquad \text{(Eq. 2.19)}$$

where;

q: vertical stress applied over the loaded area

γ: effective unit weight of the loaded soil (the bulk unit weight if there is no water-table within the fill or the submerged unit weight if the water-table is at groud level)

b^*: the length which characterized the size of the loaded area (for a square loaded area, b^* is simply the length of a side of the square)

Typical values of n found in various types of loading situation on granular soils are shown in Figure 2.12. With field plate tests and test footings, n is likely to be smaller. For low-rise foundations, values of n are typically between 2-10 and it is smaller than this for the high-rise buildings (Charles, 1996).

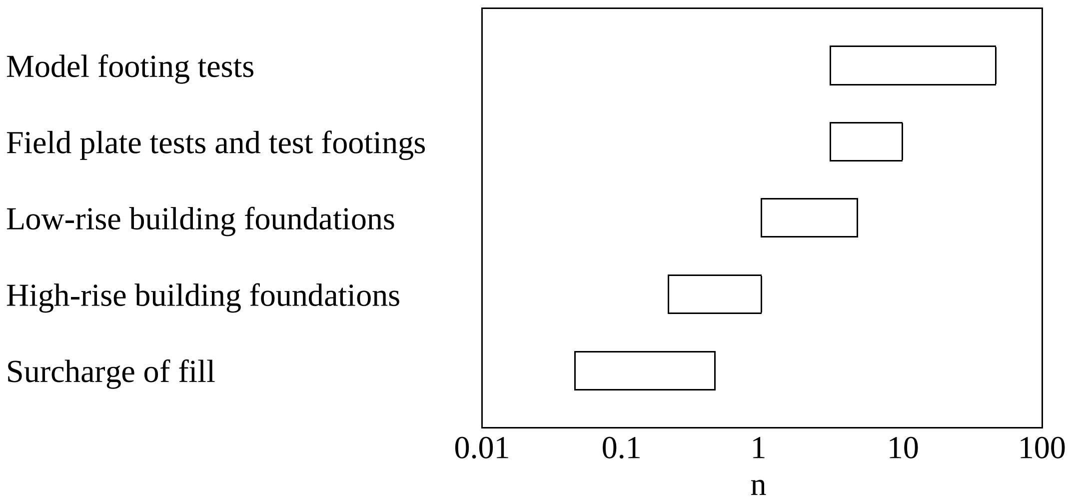

Figure 2.12. Load intensity ratio n for various loading situations (Charles, 1996)

Since shear strength usually increases as the effective stress increases, at same depth ratio the shear strength will be much larger for the surcharge than for the footing. The analysis has predicted that with a surcharge where n is small, the increase in shear strength with depth will have a significant effect and elastic theory will over-predict the depth of influence. In 1910, first Marston initiated a study of the loads on underground conduits for determining the magnitude of the loads (Spangler, 1948). Some of the limitations of this model have been discussed by Handy (1985). In a study of pressures in silos, Blight (1986) participated in this type of theory to Janssen (1895).

In the Marston Type analysis of the settlement of a loaded area, the following assumptions are made (Charles, 1996):

The additional vertical stress due to the surface loading decreases with depth due to the mobilization of shear stress over a right cylinder formed by a surface vertically below the perimeter of the loaded area.

At any particular depth the vertical stress and vertical strain are uniform within the area vertically below the loaded area.

The settlement is due solely to one-dimensional compression of the fill immediately below the area.

The shear strength is related to the vertical effective stress σ_v using Marston approach:

$$\tau = \mu K \sigma_v \qquad \text{(Eq. 2.20)}$$

where;

K: the ratio of horizontal to vertical effective stress

$$K = 1 - sin\phi' \qquad \text{(Eq. 2.21)}$$

μ: a friction coefficient

$$\mu = \frac{tan\emptyset\prime(1 - sin\emptyset')}{K} \qquad \text{(Eq. 2.22)}$$

$\sigma_v = \gamma z$ (Eq. 2.23)

b*=2b (for a strip footing)

f=4μK (Eq. 2.24)

The total depth of influence zd of the surface:

$$\frac{z_d}{b^*} = \frac{1}{f} ln \left[\frac{1-nf}{1-(\frac{z_d f}{b^*})} \right]$$ (Eq. 2.25)

The increase in stress at depth z:

$$\sigma_v - \gamma z = \frac{q}{nf} \left\{ 1 - \left[(1-nf) \exp\left(\frac{-zf}{b^*}\right) \right] \right\} - \gamma z$$ (Eq. 2.26)

Therefore;

$$n = \frac{1}{f} (1 - \left\{ \left[1 - (\frac{z_d f}{b^*}) \right] \exp(\frac{z_d f}{b^*}) \right\})$$ (Eq. 2.27)

The analysis conducted by Charles (1996), with a footing where n is large, it is predicted that the variation of vertical stress with depth from the Marston Type analysis is more similar to that predicted by elastic theory. For footings with n= 10, a ratio of z_e/b^*= 1 is predicted. Also with a surcharge where n is small, the increase in shear strength with depth will have a significant effect and elastic theory will over-predict the depth of influence. For surcharges with n= 0.1, a ratio of z_e/b^*= 0.2 is predicted.

2.5 Prediction of Soil Settlements by Graphical and Semi-Empirical Methods

The final settlement prediction is very significant fact in geotechnical applications. Since completion of the final settlement is theoretically infinite, it is not practical to observe the final settlement in practice. In order to estimate the final settlement, some practical methods are used in literatures which are Asaoka's Method and Horn's Method.

2.5.1 Asaoka's Method

This method was developed by Asoaka in (1978) to predict the ultimate settlement from past observations. The procedure consists of plotting settlement data points taken at regular intervals after the load is added. Each settlement data point at time *n* (S_i) is plotted against the settlement point at time *n-1* (S_{i-1}). The plot of the observed data points on S_i *vs.* S_{i-1} is intersected with line y=x as presented in Figure 2.13. The intersection point means that the settlement was completed and the obtained value was the final settlement due to applied load.

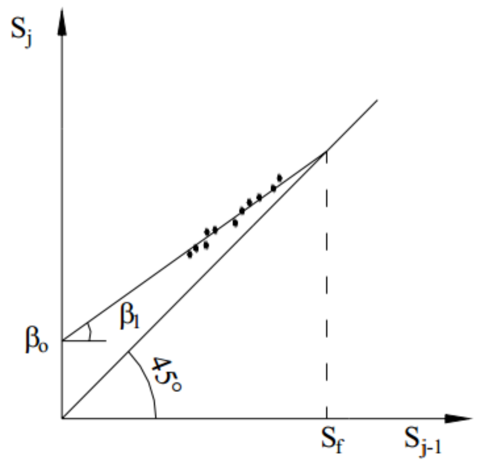

Figure 2.13. Graphical presentation of Asaoka's Method (Asaoka, 1978)

The coefficient of consolidation (c_v) is derived by Asaoka (1978) as follows;

$$c_v = -\frac{D^2 \ln\beta_1}{2\Delta t} \quad \text{; one-way drainage} \qquad \text{(Eq. 2.28)}$$

$$c_v = -\frac{D^2 \ln\beta_1}{6\Delta t} \quad \text{; two-way drainage} \qquad \text{(Eq. 2.29)}$$

Magnan et al. (1983) has proposed a method for estimating c_r based on the solution proposed by Asaoka (1978). This method is presented with Eq. 2.30.

$$c_r = -\frac{d_e^2 F(n)}{8\Delta t} ln\beta_1 = C\frac{d_e^2}{8} F(n) \qquad \text{(Eq. 2.30)}$$

where;

$$F(n) = \frac{n^2}{n^2-1}\ln(n) - \frac{3n^2-1}{4n^2} \qquad \text{(Eq. 2.31)}$$

Δt: time interval

d_e: diameter of the influence zone of each drain

n: ratio of the d_e to the drain diameter d_w

F(n): drain spacing factor

β_1: the slope of a straight line on the curve that represents the settlements according to time

C: coefficient denoted by ($-\ln\beta_1/\Delta t$)

2.5.2 Horn's Method

This method was proposed by Horn in 1983 to predict the ultimate settlement by evaluation of the observed time vs. settlement curves. From time-settlement curves the settlement speed (v*) can be calculated as presented in Figure 2.14:

$$v^* = \frac{ds}{dt} \qquad \text{(Eq. 2.32)}$$

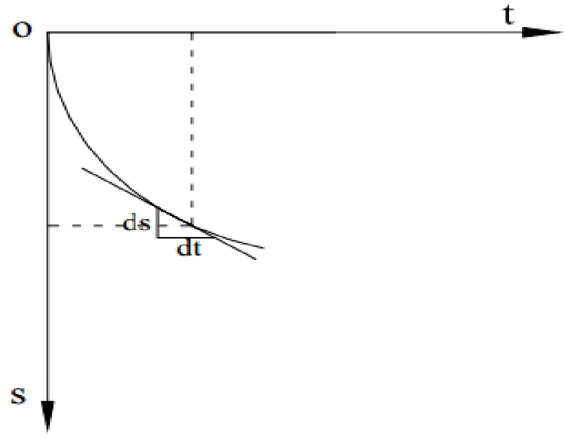

Figure 2.14. Time-Settlement diagram (Horn, 1983)

In order to estimate ultimate settlement, total settlement time (t_f) must be known. The Horn's method (1983) evaluates the rate of settlement curve, t-v* that runs against zero with a straight line. The value of the time at zero speed where v=0 gives the total settlement time, t_f. The time vs. velocity diagram is presented in Figure 2.15:

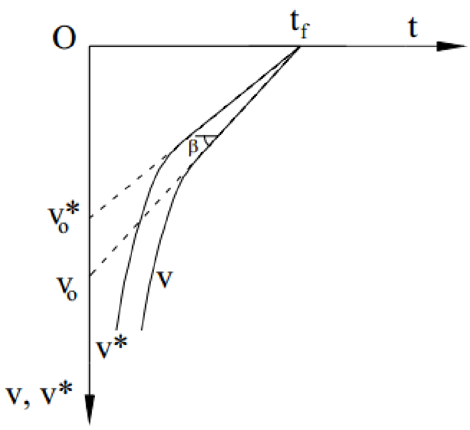

Figure 2.15. Time (t) vs. settlement velocity (v) relationship (Horn, 1983)

The ultimate settlement value (S_f) can be considered by drawing time/settlement (t/s) versus time (t) graph as presented in Figure 2.16:

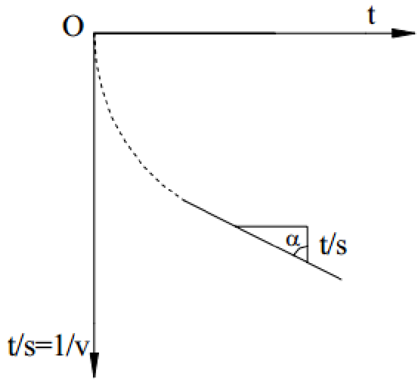

Figure 2.16. Graphical presentation of t vs. t/s relationship (Horn, 1983)

$$S_f = \frac{t}{t/s} = tan\alpha \qquad \text{(Eq. 2.33)}$$

The coefficient of consolidation value is calculated by the following formula (Horn, 1983):

$$c_v = \frac{D^2}{t_f} \qquad \text{: one-way drainage} \qquad \text{(Eq. 2.34)}$$

$$c_v = \frac{D^2}{4t_f} \qquad \text{: two-way drainage} \qquad \text{(Eq. 2.35)}$$

2.6 Previous Studies About Comparisons of Predicted and Observed Settlements

In order to plan an effective study period, it is required to obtain background information on the previous studies. In literature, to evaluate and solve inaccuracies in settlement calculations, field settlement monitoring is conducted by settlement plates in different places and compared with calculated settlements based on laboratory and field tests to check the compatibility.

According to the study conducted by Bergado et al. (1992), excellent agreements were attained in the predicted rate and amount of settlements using back-analyzed parameters by the methods of Asaoka (1978). Another study was presented as a thesis study by Gündüz (2010) and the following results were obtained; the finite element model of Plaxis gave fairly good results in all cases. According to the study presented by Salem and El-Sherbiny (2013), it seems that the measured settlements were within the range of settlements estimated based on laboratory and field tests. Moreover, it was observed that measured and calculated settlements followed similar settlement rates. Li (2014) proposed that the calculated settlement results were very close to the observed ones. A case study on soil settlements induced by preloading and vertical drains was presented by Cascone and Biondi (2013) and a general fair agreement was obtained for measured and expected settlement from this study.

Bergado et al. (2002) proposed a case study about prefabricated vertical drains in soft Bankok clay and they concluded that degree of consolidation estimated from the pore-pressure dissipation measurements agreed with those obtained from the settlement measurements. Lo et al. (2008) studied long-term performance of wide embankment on soft clay improved with prefabricated vertical drains and the predicted pore-water pressure showed reasonable agreement with measured values. According to the study conducted by Karim and Lo (2013) about estimation of hydraulic conductivity of soils improved with vertical drains, the field observations closely matched the analytical calculations.

Dalgıç and Şimşek (2002) studied the Anatolian Motorway between Ankara-İstanbul and they concluded that predicted settlement quantities were found reliable and comparable to field measurements and significant differences were observed between calculated and measured rate of settlement. Liu conducted a study about settlement prediction of embankments with stage construction on soft ground in 2003 and he concluded that Asaoka method might be successfully used to make settlement predictions according to the observational results. However, the ratio of $c_{v(field)}/c_{v(lab)}$= 6-12 was acquired as a result of his study. Saowapakpiboon presented a study about measured and predicted performances of prefabricated vertical drains in 2009, he obtained that c_h values of specimens in laboratory tests were nearly half of the values obtained from field test data. However, surface settlement prediction performed by Asoaka (1978) method yielded very good consistency with field data. Hadewych (2010) presented a study about settlement measurements and concluded that calculated settlement fit the observed settlement. On the other hand, the time for completion of the settlement in the field was less than the calculated one. Quang and Giao and Quang (2014) presented a study about improvement of soft clay by vacuum preloading. According to their studies, there was a good agreement between calculated and predicted settlements. Furthermore, in that study the ratio of c_h(field)/c_h(lab) was obtained as 2.0.

Moh et al. (1998) presented another study and they concluded that the field settlement data were much higher than designed total settlement, and waiting period was longer. Back-calculation of consolidation parameters from field measurements was achieved by Cao et al. (2001) and they obtained that the compression index was generally larger than that of measured in the laboratory, and the coefficient of consolidation back-calculated was larger than the values calculated from pore pressure measurement. According to study conducted by Shen et al. (2005) about analysis of field performance of embankments on soft clay deposit with and without PVD (prefabricated vertical drain) improvement, it was concluded that the settlement amount and rate of measured values were greater than the calculated values. Back analyses of compressibility parameters of PVD improved soft ground in Southern Vietnam were carried out by Long (2006) and the back calculated values of c_h were about 4 to 6 times of the average c_v values obtained from conventional oedometer tests and the secondary compression ratios (C_α) were about 1.5 times that of laboratory tests.

Chung presented a study in 2009 for predicting the settlement rate of a ground area that incorporates prefabricated vertical drains. According to the results of two documented case studies, he concluded that estimated coefficients of radial consolidation were larger than the values obtained from oedometer tests and for two cases, c_v values obtained from field were very close to the results of standard oedometer tests. Tedjakusuma performed a study in 2012 about the application of prefabricated vertical drain in soil improvement. Their study contained comparisons of the preliminary consolidation parameters and final parameters obtained from the pilot test embankment after soil improvement. From back-analysis, it was concluded that horizontal and vertical consolidation coefficients for marine clay is 1.5.

Comparison of field measurements and predicted performance beneath full scale embankments was achieved by Indraratna and Sathananthan (2003) and they stated that the calculated settlement amount and rate were greater than the measured values. According to a study completed by Geiser and Commend (2012) in Switzerland, it was concluded that the predictions obtained by Plaxis model overestimates the settlements by factors of 2-3. Furthermore, the area of influence of the settlements was also overestimated. A project was conducted by Wetzel (2014) to compare the theoretical and actual time dependent settlement induced by fill settlement, and it was concluded that the predicted settlements were more than the actual measured settlements. Bhosle and Vaishampayan (2009) presented a case study for ground improvement using PVD with preloading and they obtained that the consolidation settlements obtained theoretically from laboratory test results were much higher than predicted by Asoaka and Hyperbolic Method. Kemp (2013) studied on the consolidation behavior of alluvial soft clay and according to his study, back-analyzed coefficient of consolidation of the clay was higher while the compression ratio was lower than the original design estimate.

CHAPTER 3

SITE DESCRIPTION OF THE INSTRUMENTED EMBANKMENT SECTIONS

Bursa-Susurluk Section takes place between Km: 104+535 and Km: 178+927 in Gebze-İzmir Highway Project and the interval of Km: 137+800 and Km: 176+060 is defined as Karacabey Plain according to State Hydraulic Works. In the Karacabey Plain, the flood plain is located between Km: 139+100 and Km: 144+360 according to State Hydraulic Works. At the Karacabey Plain, the embankment with maximum height of 11.0 m and with 27° embankment slope is designed on thick alluvial deposit. Prefabricated vertical drain installation and embankment construction in the Karacabey Plain are shown in Figures 3.1 and 3.2.

Figure 3.1. Prefabricated vertical drain installation in the Karacabey Plain

Figure 3.2. Embankment construction on the Karacabey Plain

Karacabey Plain was formed during Middle-Late Miocene with the control of extensional tectonics. Under the control of this tectonism, alluvial fan systems were formed from north to south in Marmara Sea as presented in Figure 3.3. Depending on this tectonism, Facies A was formed near the source with high energy and defined as sandstone, blocky gravels with reverse gradataion (Özdoğan et al., 2000).

When river moved away from source and because of the topography, the energy of river decreased, the size of material decreased and river transferred to meandering river characteristic. As a result of this, flood plains and oxbow lakes were formed (Facies B). Lithofacies C and D were formed from lacustrine deposits (Özdoğan et al., 2000).

The views for meandering river and flood plan characteristics of Susurluk River is presented in Figures 3.4 and 3.5.

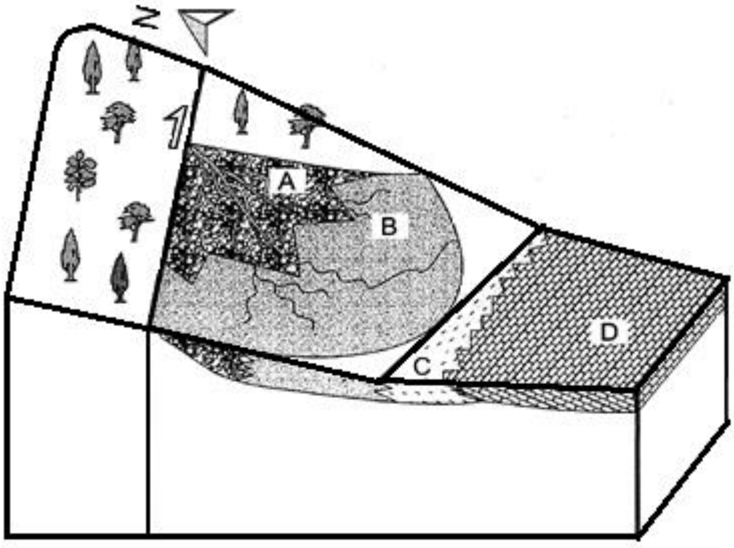

Figure 3.3. Depositional episodes at the Middle-Late Miocene (Özdoğan et al., 2000)

Figure 3.4. Meandering river characteristic view of Susurluk river

Figure 3.5. Flood plain view of Karacabey Plain

The geological map of the study area is presented in Figure 3.6. The geological formation in the study area is defined as alluvium which consists of clay, silt, sand and gravel. The units of clay, silt, sand and gravel are formed due to young river beds.

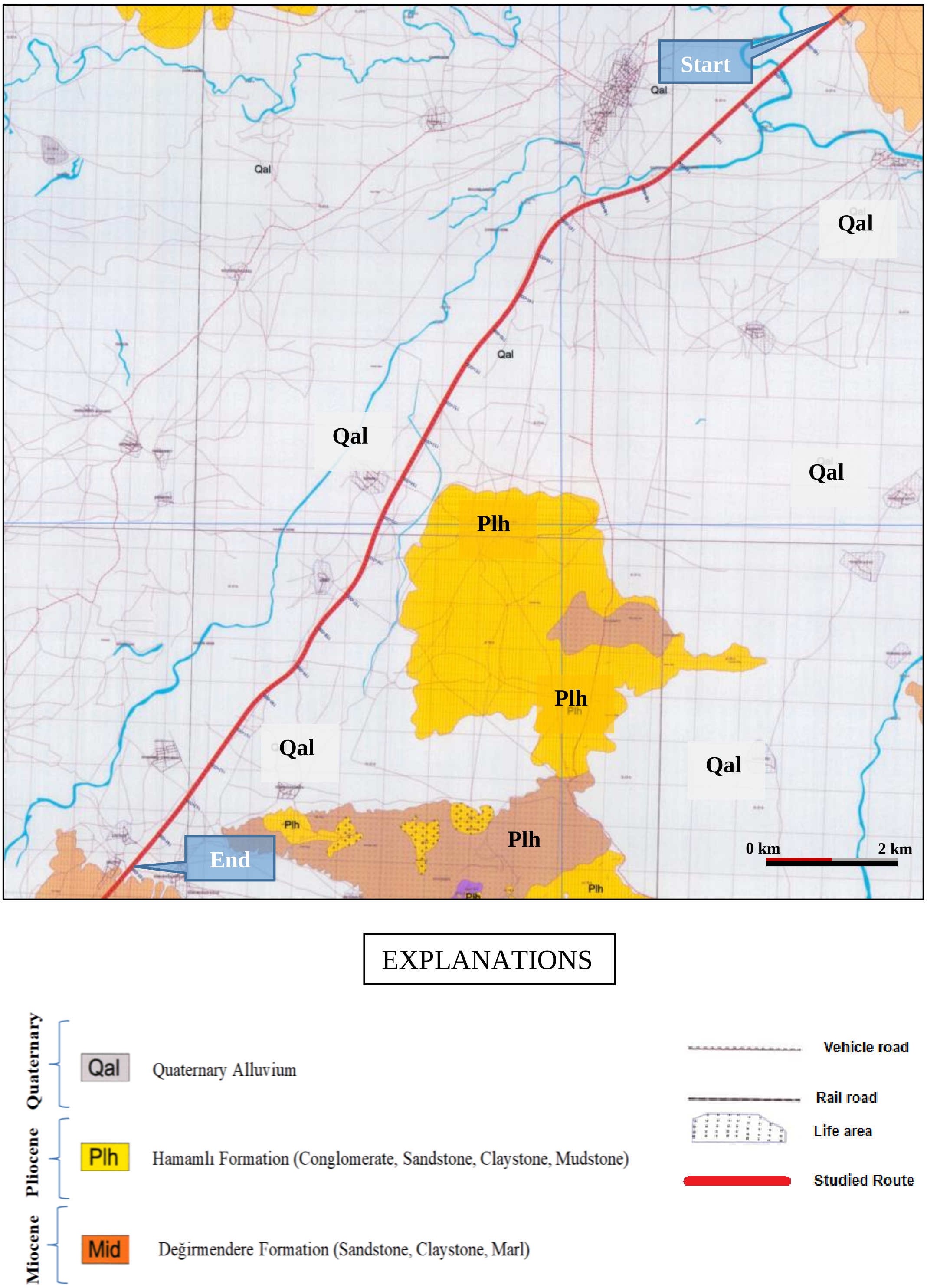

Figure 3.6. Geological map of the study area (MTA, 2008)

As a part of this study, 26 different embankment sections were evaluated. Existing site conditions of the instrumented test embankments including geological conditions, site investigation and laboratory test results are presented in this part of the thesis.

3.1 KM: 139+764 Section

The soil profile of the embankment at Km: 139+764 is characterized by 24.45 m deep borehole (BSSK 447) and BS-CPT-01 cone penetration test. The laboratory test results and SPT N graphs are presented in Appendix A and B, consolidation settlement calculations are presented in Appendix C. The soil profile consists of the layers layers shown in Table 3.1.

Table 3.1 A typical soil profile at Km: 139+764 section of the study area

Depth (m)	Soil Profile	SPT N (av.)	q_c (av.) (MPa)	PI (av.) (%)	w_N (av.) (%)	c_u (kPa)
-1.8	Medium-Stiff Clay (CH)	6	0.52	47	35	
-19	Medium-Stiff Clay (CH-CL)	10	0.93	45	40	58
-23.9	Stiff Clay (CH)	24	1.00	51	25	
-44.11	Stiff Silt (MH)	25	2.61	46	29	

The geological longitudinal section of embankment is presented in Figure 3.7. SPT results of BSSK-447 borehole and cone resistance values of BS-CPT-1 results for clay layers are presented in Figure 3.8. According to the geological longitudinal section, the embankment with 8.0-9.0 m in height is planned to be constructed on clayey soil with a thickness of more than 40.0 m, and also sand layers are defined in clay layer with a thickness of less than 1.0 m. From surface down to a depth of 1.8 m, SPT N value is obtained as 6 whereas q_c value is obtained as 0.52 MPa in average, which indicates “soft clay”. From depth of 1.8 m to 19.0 m, SPT N value is obtained as 10 whereas q_c value is obtained 0.93 MPa in average, which indicates “medium-stiff clay”. From depth of 19.0 m, SPT N values are greater than 24 whereas q_c values are greater than 1.5 MPa in average, which is the indicator of “Stiff Clay”. When the values of SPT N and q_c are compared, they both point out similar stiffness and also strength values for the clay units defined in the specified depth of intervals. The graph of In-Situ Settlement (m) vs. Time (day) behavior measured in the embankment for surface and deep settlement is presented in Figure 3.9. The last measured settlement from surface settlement plate is 167.3 cm and from deep settlement plate at depth of 24.0 m is 69.1 cm under embankment load with a maximum height of 8.8 m after 730 days of measurement.

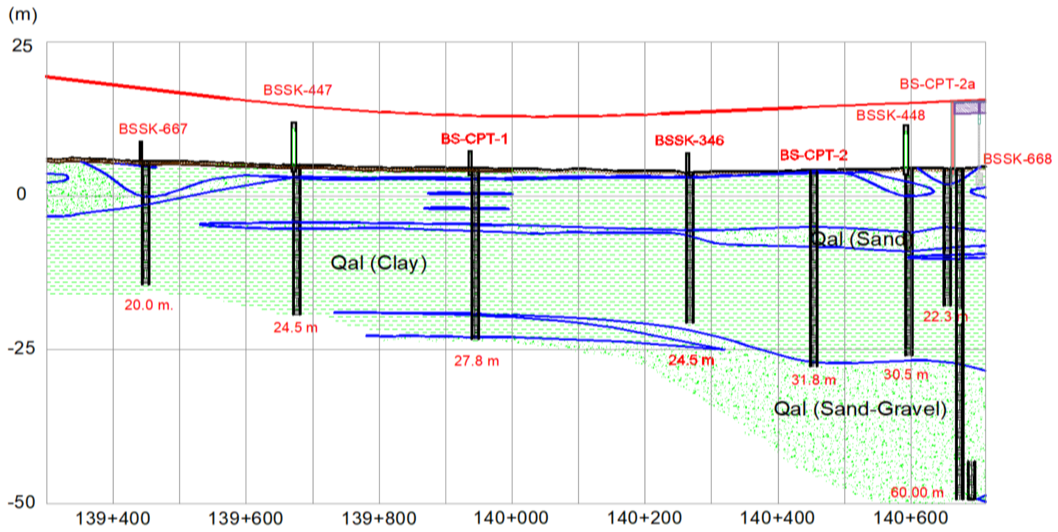

Figure 3.7. The longitudinal geological section of Km: 139+764

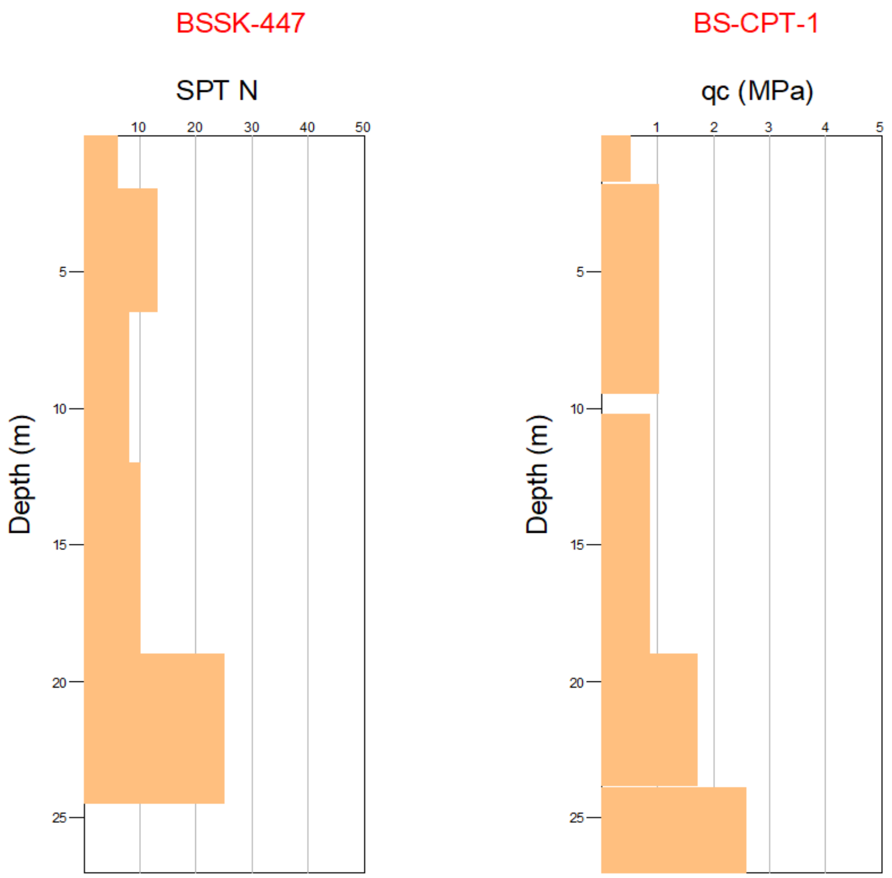

Figure 3.8. SPT N vs. Depth (m) and q_c (MPa) vs. Depth (m) graphs for clay layers

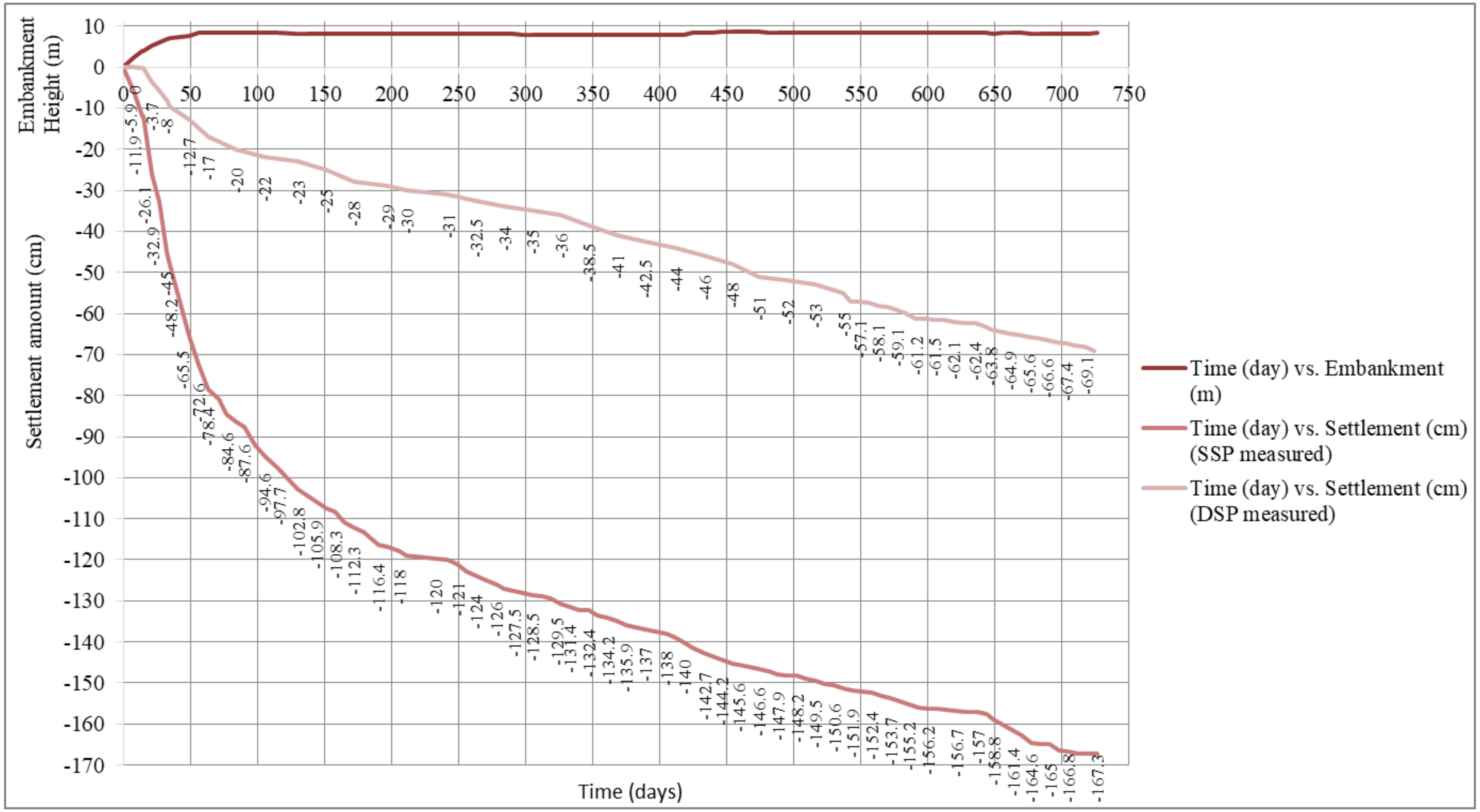

Figure 3.9. In situ Settlement (cm) vs. Time (day) behavior measured in embankment for surface and deep settlement

3.2 KM: 139+860 Section

The soil profile of the embankment at Km: 139+860 is characterized by 24.45 m deep borehole (BSSK 447) and BS-CPT-01 cone penetration test. The laboratory test results and SPT N graphs are presented in Appendix A and B, consolidation settlement calculations are presented in Appendix C. The soil profile consists of the layers shown in Table 3.2:

Table 3.2 A typical soil profile at Km: 139+860 section of the study area

Depth (m)	Soil Profile	SPT N (av.)	q_c (av.) (MPa)	PI (av.) (%)	w_N (av.) (%)	c_u (kPa)
-1.80	Soft Clay (CH)	6	0.52	47	35	
-19.00	Medium-Stiff Clay (CH-CL)	10	0.93	45	40	58
-23.90	Stiff Clay (CH)	24	1.00	51	25	
-44.11	Stiff Silt (MH)	25	2.61	46	29	

The geological longitudinal section of embankment is presented in Figure 3.10. SPT results of BSSK-447 borehole and cone resistance values of BS-CPT-1 results for clay layers are presented in Figure 3.11. According to the geological longitudinal section, the embankment with 8.0-9.0 m in height is planned to be constructed on clayey soil with a thickness of more than 40.0 m, and also sand layers are defined in clay layer with a thickness of less than 1.0 m. Till to depth of 1.8 m, SPT N value is obtained as 6 whereas q_c value is obtained as 0.52 MPa in average, which indicates "soft clay". From depth of 1.8 m to 19.0 m, SPT N value is obtained as 10 whereas q_c value is obtained 0.93 MPa in average, which indicates “medium-stiff clay”. From depth of 19.0 m, SPT N values are greater than 24 whereas q_c values are greater than 1.5 MPa in average, which is the indicator of “Stiff Clay”. When the values of SPT N and q_c are compared, they both point out similar stiffness and also strength values for clay units defined in specified depth of intervals. The graph of In-Situ Settlement (m) vs. Time (day) behavior measured in the embankment for surface and deep settlement is presented in Figure 3.12. The last measured settlement from surface settlement plate is 190.2 cm and from deep settlement plate at depth of 24.0 m is 90.0 cm under embankment load with a maximum height of 8.8 m after 860 days of measurement.

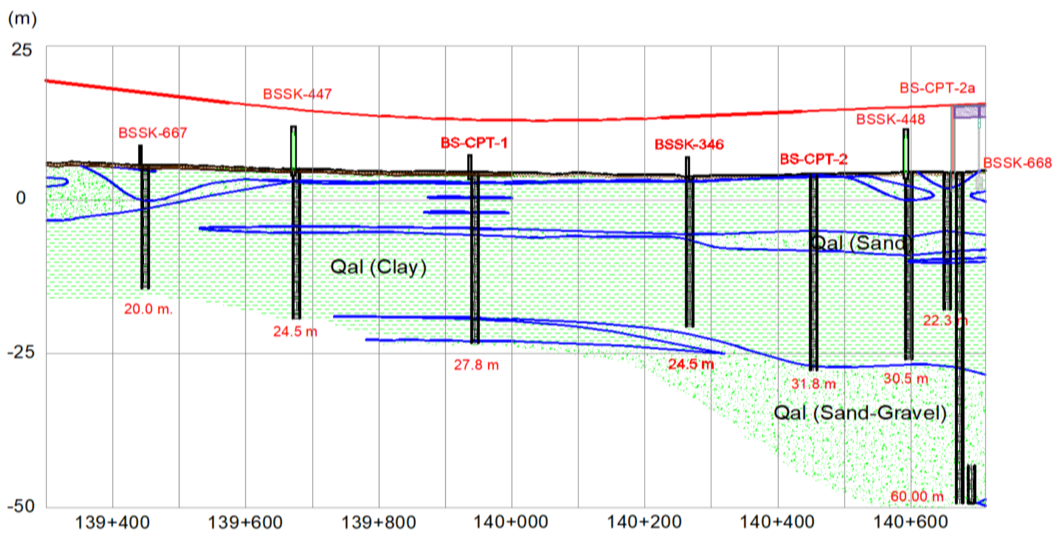

Figure 3.10. The longitudinal geological section of Km: 139+860

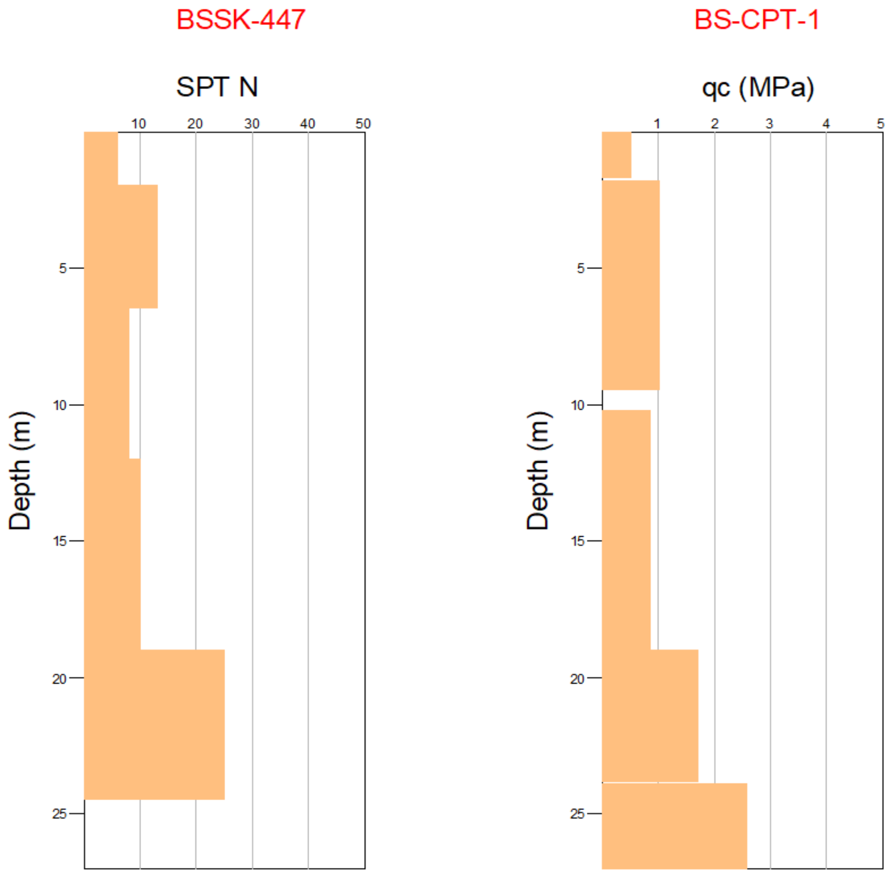

Figure 3.11. SPT N vs. Depth (m) and q_c (MPa) vs. Depth (m) graphs for clay layers

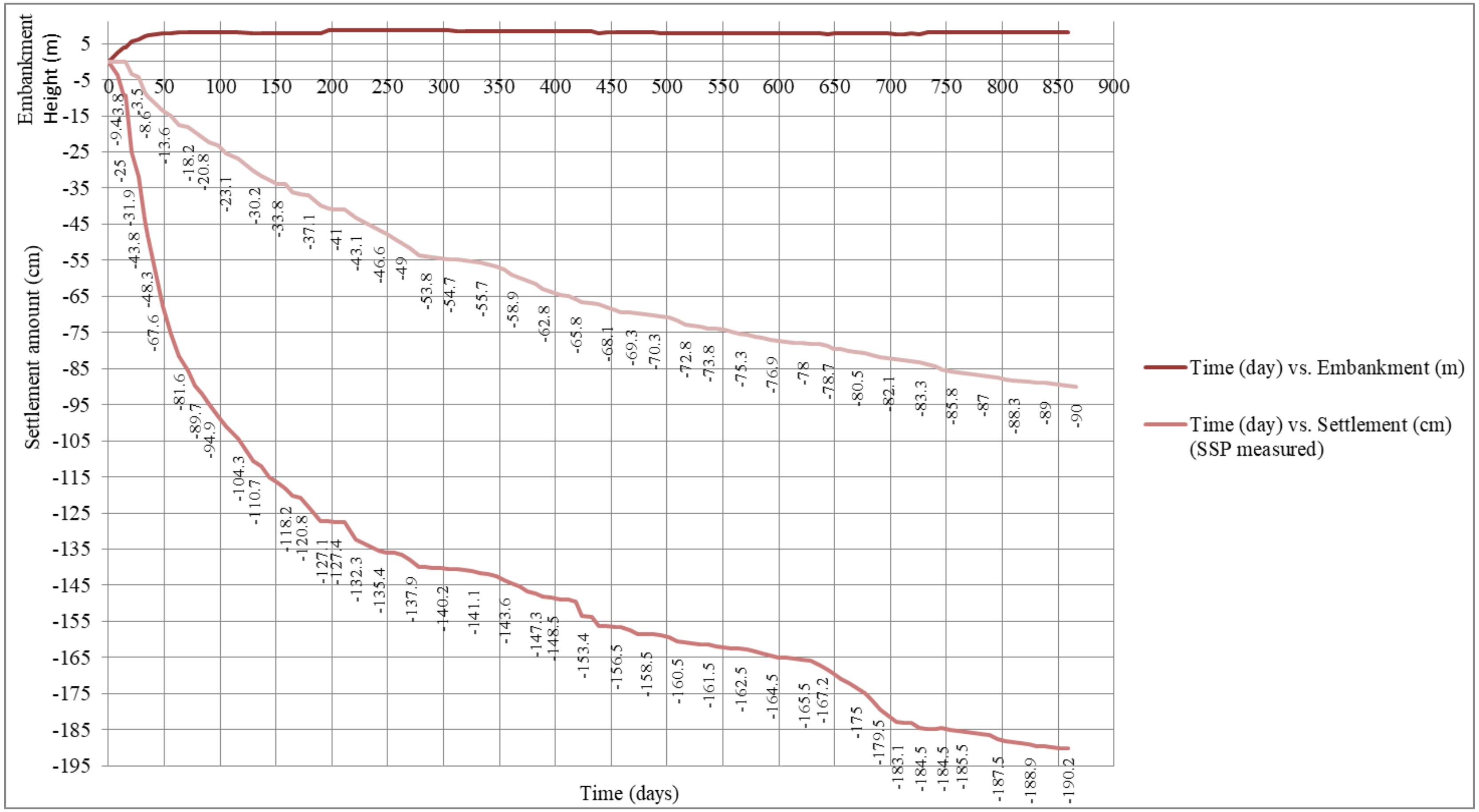

Figure 3.12. In situ Settlement (cm) vs. Time (day) behavior measured in embankment for surface and deep settlement

3.3 KM: 140+592 Section

The soil profile of the embankment at Km: 140+592 is characterized by 24.45 m deep borehole (BSSK 447) and BS-CPT-01 cone penetration test. The laboratory test results and SPT N graphs are presented in Appendix A and B, consolidation settlement calculations are presented in Appendix C. The soil profile consists of the layers shown in Table 3.3:

Table 3.3 A typical soil profile at Km: 140+592 section of the study area

Depth (m)	Soil Profile		SPT N (av.)	q_c (av.) (MPa)	PI (av.) (%)	w_N (av.) (%)	c_u (kPa)
-1.80	Soft Clay (CH)		6	0.52	47	35	
-19.00	Medium-Stiff Clay (CH-CL)		10	0.93	45	40	52
-23.90	Stiff Clay (CH)		24	1.00	51	25	44
-42.00	Stiff Silt (MH)		25	2.61	46	29	

The geological longitudinal section of embankment is presented in Figure 3.13. SPT results of BSSK-447 borehole and cone resistance values of BS-CPT-1 results for clay layers are presented in Figure 3.14. According to the geological longitudinal section, the embankment with 8.0-9.0 m in height is planned to be constructed on clayey soil with a thickness of more than 40.0 m, and also sand layers are defined in clay layer with a thickness of less than 1.0 m. Till to depth of 1.8 m, SPT N value is obtained as 6 whereas q_c value is obtained as 0.52 MPa in average, which indicates "soft clay". From depth of 1.8 m to 19.0 m, SPT N value is obtained as 10 whereas q_c value is obtained 0.93 MPa in average, which indicates “medium-stiff clay”. From depth of 19.0 m, SPT N values are greater than 24 whereas q_c values are greater than 1.5 MPa in average, which is the indicator of “Stiff Clay”. When the values of SPT N and q_c are compared, they both point out similar stiffness and also strength values for clay units defined in specified depth of intervals. The graph of In-Situ Settlement (m) vs. Time (day) behavior measured in the embankment for surface settlement plate is presented in Figure 3.15. The last measured settlement from surface settlement plate is 116.6 cm under embankment load with a maximum height of 9.1 m after 835 days of measurement.

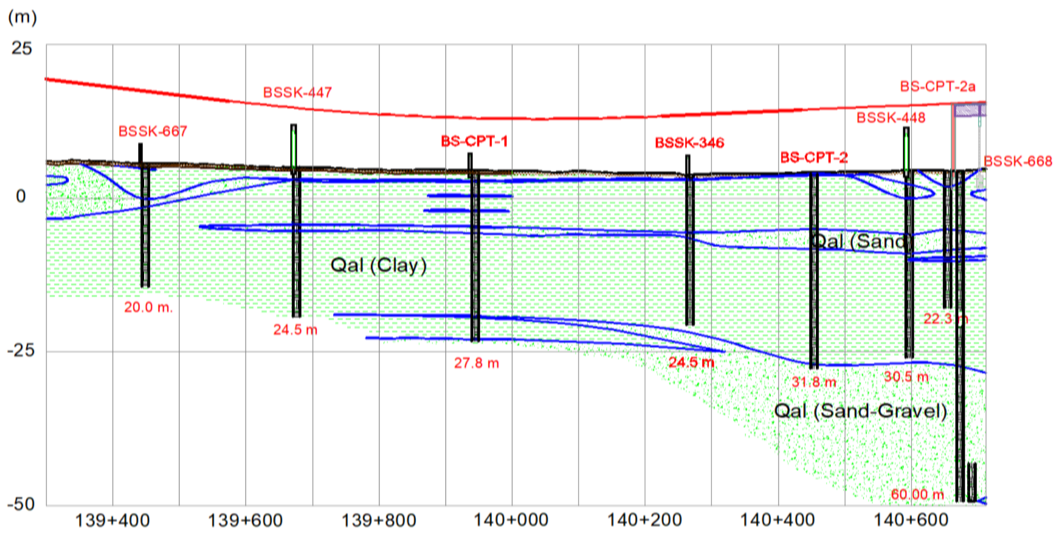

Figure 3.13. The longitudinal geological section of Km: 140+592

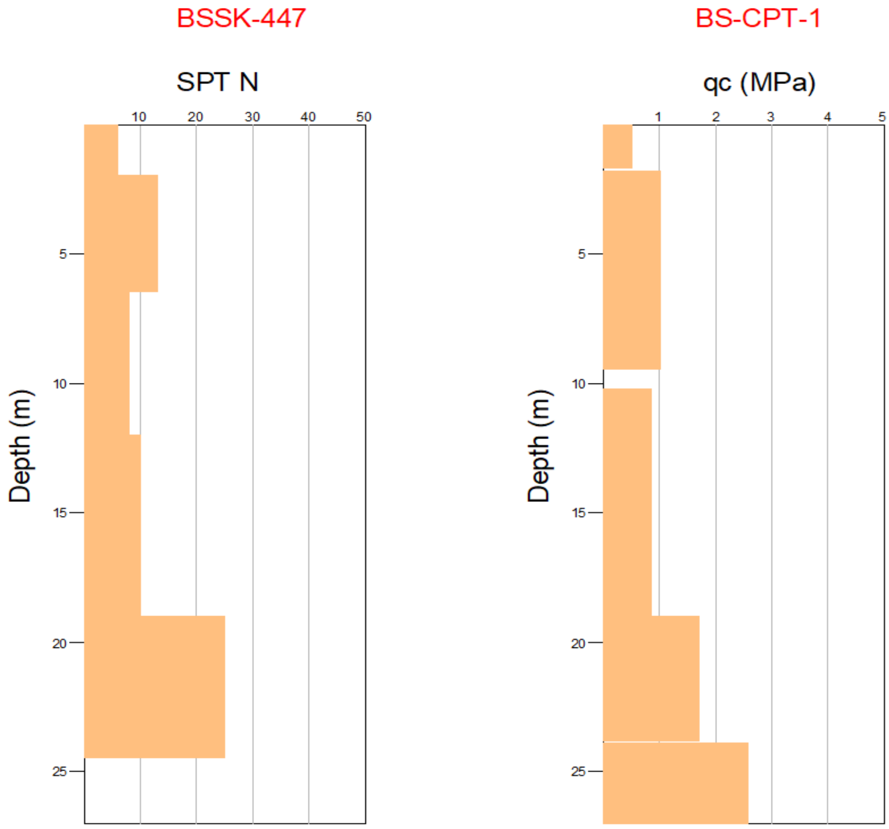

Figure 3.14. SPT N vs. Depth (m) and q_c (MPa) vs. Depth (m) graphs for clay layers

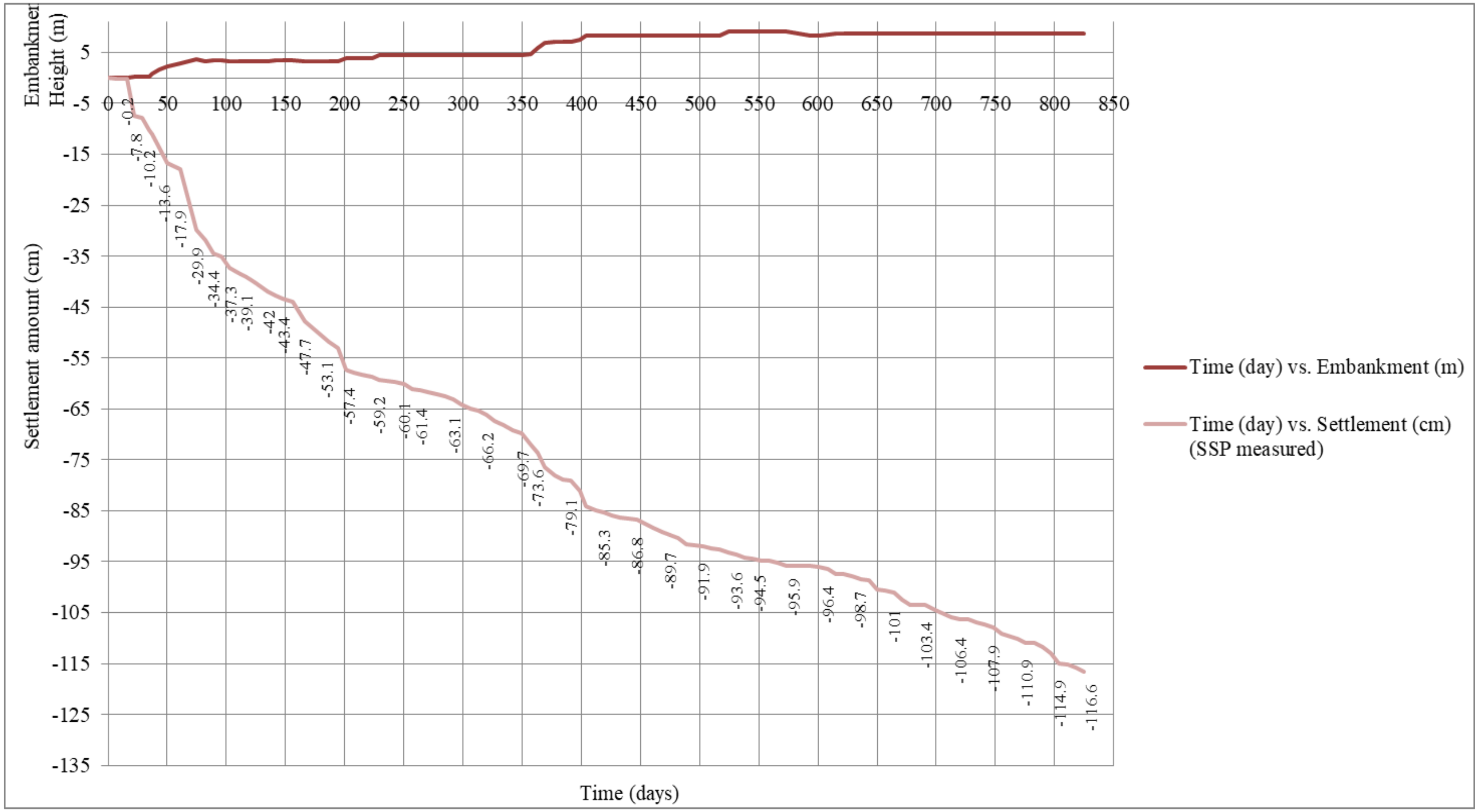

Figure 3.15. In situ Settlement (cm) vs. Time (day) behavior measured in embankment for surface settlement

3.4 KM: 141+680 Section

The soil profile of the embankment at Km: 141+667 is characterized by 15.45 m deep borehole (BSSK 451) and BS-CPT-04 cone penetration test. The laboratory test results and SPT N graphs are presented in Appendix A and B, consolidation settlement calculations are presented in Appendix C. The soil profile consists of the layers shown in Table 3.4:

Table 3.4 A typical soil profile at Km: 141+680 section of the study area

Depth (m)	Soil Profile	SPT N (av.)	q_c (av.) (MPa)	f_s (av.) (kPa)	PI (av.) (%)	w_N (av.) (%)	c_u (kPa)
-2.50	Medium-Stiff Clay (CH)	9	1.08		55	34	
-9.00	Stiff Clay (CH)	18	1.36		46	33	
-15.50	Very Dense Sand (SP-SM)	40	5.49	33.98			
-46.34	Stiff Clay-Silt (CH-ML)	18	1.16		55	22	

The geological longitudinal section of embankment is presented in Figure 3.16. SPT results of BSSK-451 borehole and cone resistance values of BS-CPT-4 results for clay layers are presented in Figure 3.17. According to the geological longitudinal section, the embankment with 10.3 m in height is planned to be constructed on clayey soil with a thickness of more than 40.0 m. Till to depth of 2.5 m, SPT N value is obtained as 9 whereas q_c value is obtained as 1.08 MPa in average, which indicates "medium-stiff clay". From depth of 2.5 m to 9.0 m, SPT N value is obtained as 18 whereas q_c value is obtained 1.36 MPa in average, which indicates "stiff clay". From depth 9.0 m to 15.5 m, sand layer is defined according to borehole and it is ended at 15.5 m depth. According to BS-CPT-4, clay layers are defined in depth of intervals 8.6 m and 8.8 m, 10.1 m and 10.6 m, 11.1 m and 12.92 m with qc value of 0.85 MPa in average. These thin clay layers are defined as “medium-stiff clay”. From depth of 15.5 m, clay layer with qc value 1.15 MPa in average is obtained and it is defined as “stiff clay”. When the values of SPT N and q_c are compared, they both point out similar stiffness and also strength values for clay units defined in specified depth of intervals. The graph of In-Situ Settlement (m) vs. Time (day) behavior measured in the embankment for surface settlement plate is presented in Figure 3.18. The last measured settlement from surface settlement plate is 181.19 cm under embankment load with a maximum height of 10.259 m after 800 days of measurement.

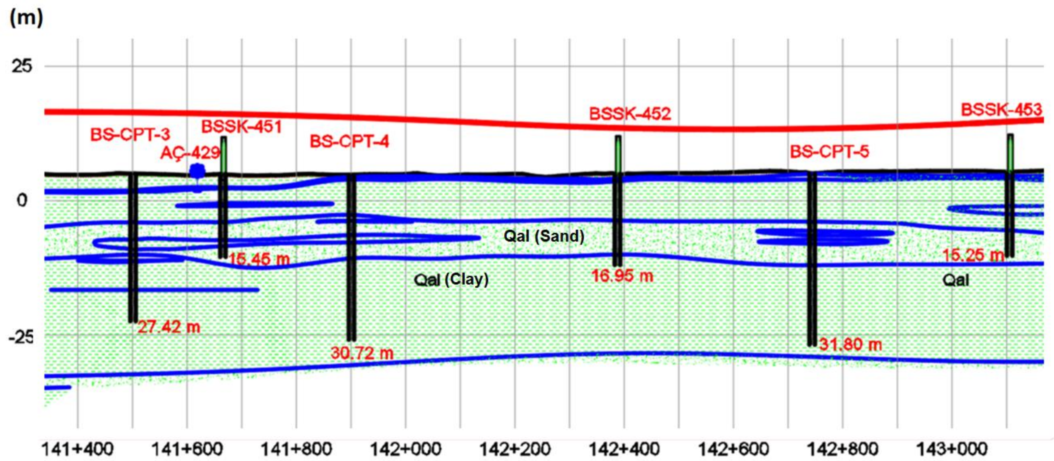

Figure 3.16. The longitudinal geological section of Km: 141+680

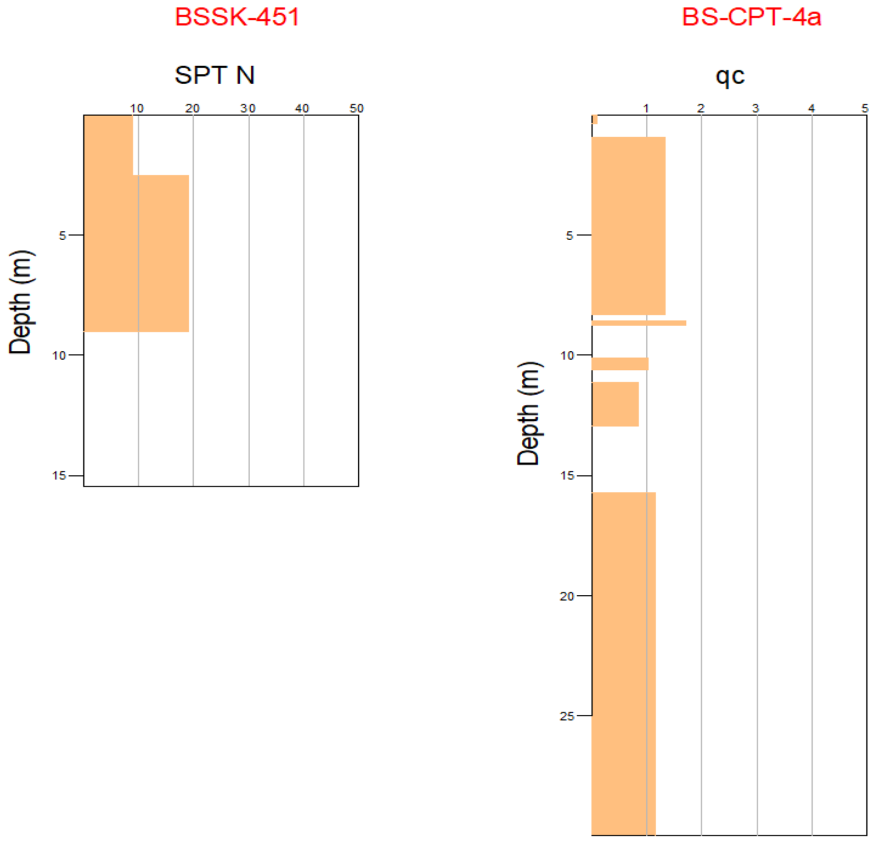

Figure 3.17. SPT N vs. Depth (m) and q_c (MPa) vs. Depth (m) graphs for clay layers

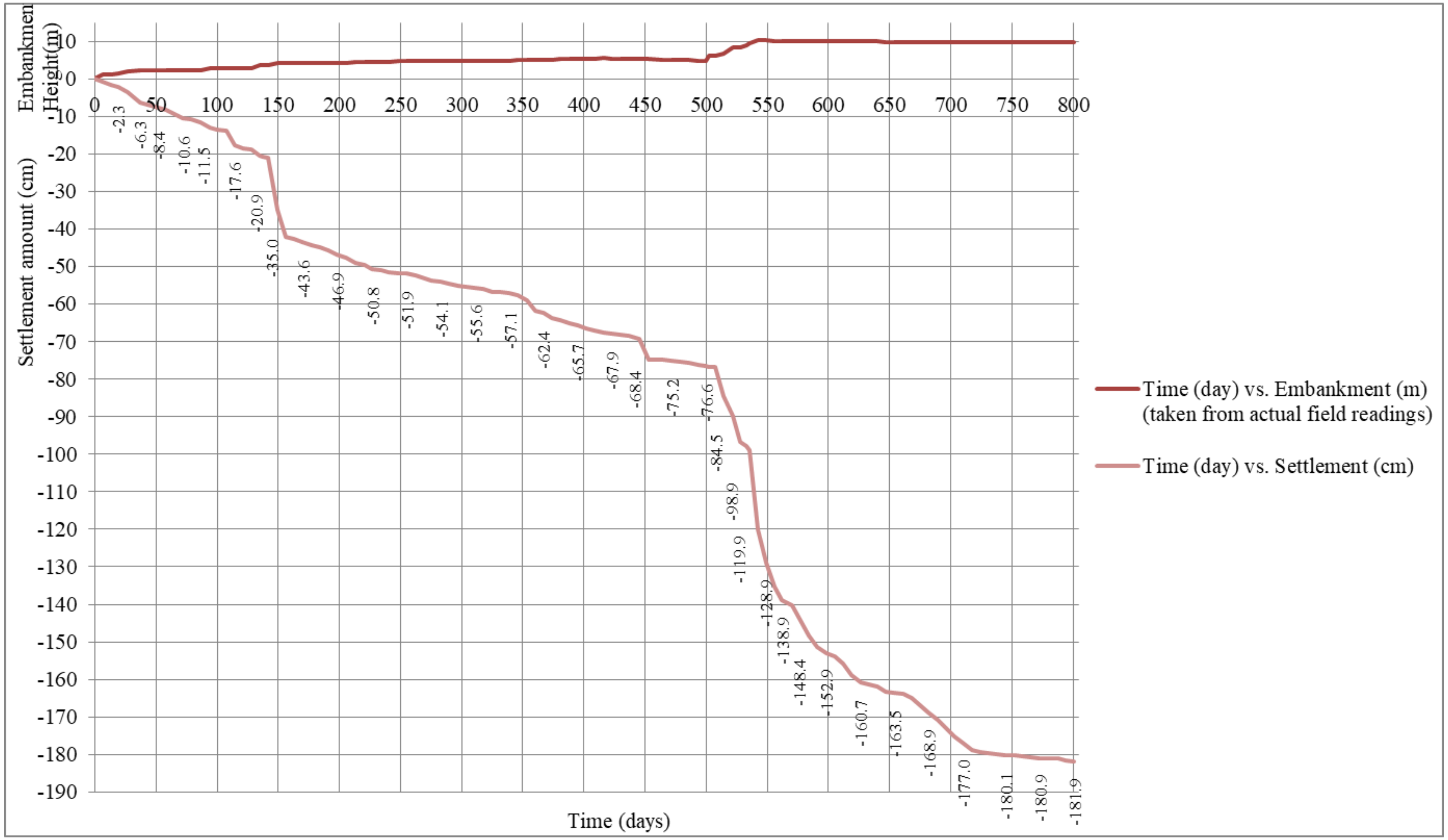

Figure 3.18. In situ Settlement (cm) vs. Time (day) behavior measured in embankment for surface settlement

3.5 KM: 142+000 Section

The soil profile of the embankment at Km: 142+000 is characterized by 16.95 m deep borehole (BSSK 452) and BS-CPT-04 cone penetration test. The laboratory test results and SPT N graphs are presented in Appendix A and B, consolidation settlement calculations are presented in Appendix C. The soil profile consists of the layers shown in Table 3.5:

Table 3.5 A typical soil profile at Km: 142+000 section of the study area

Depth (m)	Soil Profile		SPT N (av.)	q_c (av.) (MPa)	f_s (av.) (kPa)	PI (av.) (%)	w_N (av.) (%)	c_u (kPa)
-9.00	Stiff Clay (CH)		15	1.29		47	33	
-15.00	Medium Dense Sand (SM)		21	5.49	33.98	NP	30	
-46.28	Stiff Clay- Silt (CH-ML)		24	1.16		13	22	

The geological longitudinal section of embankment is presented in Figure 3.19. SPT results of BSSK-452 borehole and cone resistance values of BS-CPT-4 results for clay layers are presented in Figure 3.20. According to the geological longitudinal section, the embankment with 9.97 m in height is planned to be constructed on clayey soil with a thickness of more than 40.0 m, and also sand layers are defined at depth of 9.0 m and 15.0 m. Till to depth of 9.0 m, SPT N value is obtained as 15 whereas q_c value is obtained as 1.29 MPa in average, which indicates “stiff clay”. According to BS-CPT-4, clay layers are defined in depth of intervals 8.6 m and 8.8 m, 10.1 m and 10.6 m, 11.1 m and 12.92 m with q_c value of 0.85 MPa in average. These thin clay layers are defined as “medium-stiff clay”.

From depth of 15.0 m, SPT N value is obtained as 24 whereas q_c value is obtained 1.16 MPa in average, which indicates "stiff clay". When the values of SPT N and q_c are compared, they both point out similar stiffness and also strength values for clay units defined in specified depth of intervals. The graph of In-Situ Settlement (m) vs. Time (day) behavior measured in embankment for surface settlement plate is presented in Figure 3.21. The last measured settlement from surface settlement plate is 125.8 cm under embankment load with a maximum height of 9.97 m after 850 days of measurement.

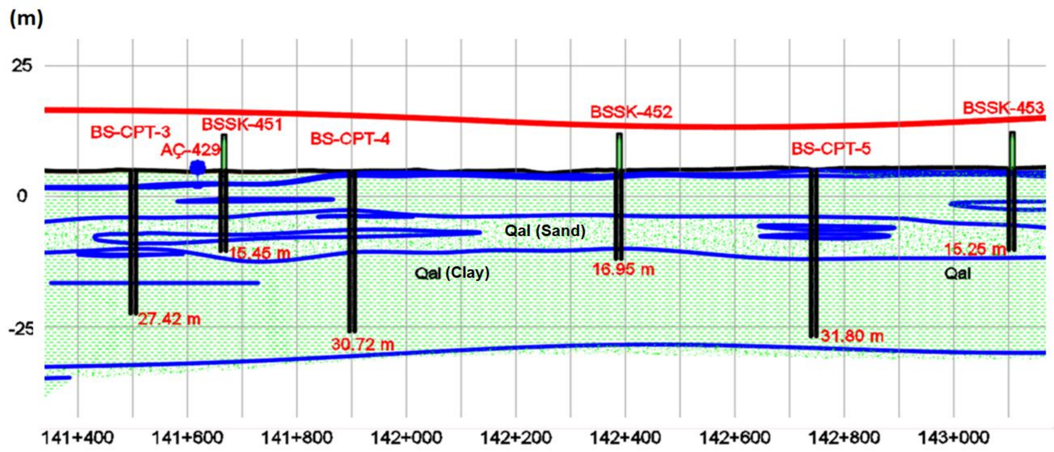

Figure 3.19. The longitudinal geological section of Km: 142+000

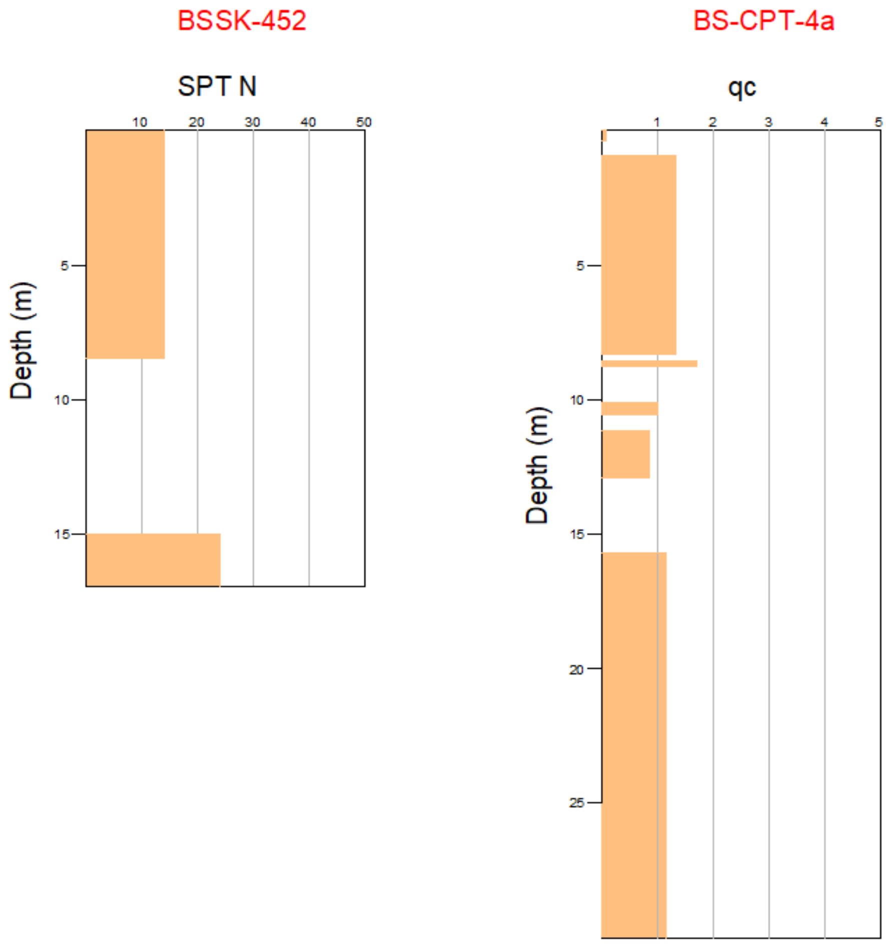

Figure 3.20. SPT N vs. Depth (m) and q_c (MPa) vs. Depth (m) graphs for clay layers

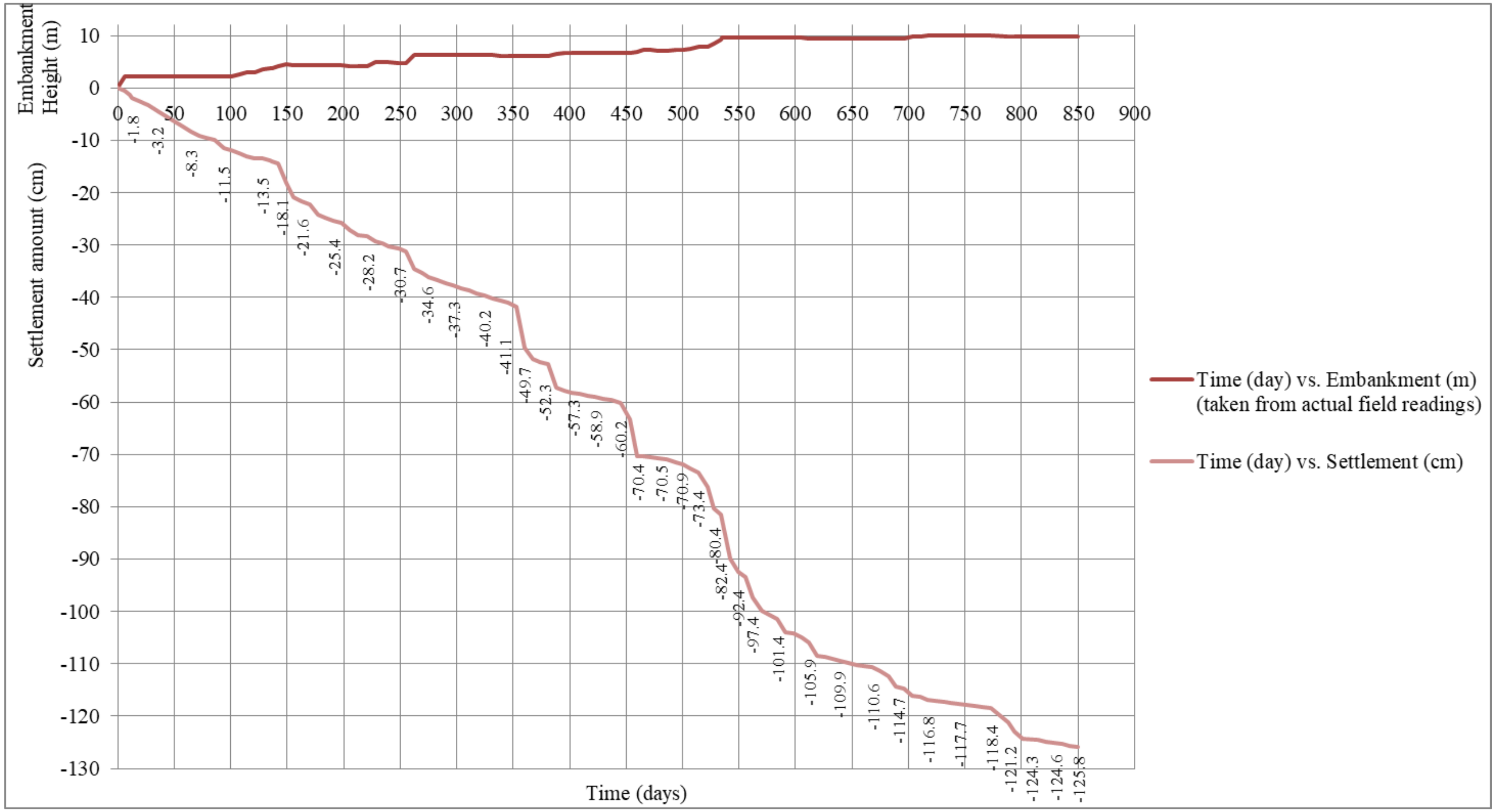

Figure 3.21. In situ Settlement (cm) vs. Time (day) behavior measured in embankment for surface settlement

3.6 KM: 142+400 Section

The soil profile of the embankment at Km: 142+400 is characterized by 16.95 m deep borehole (BSSK 452) and BS-CPT-04 cone penetration test. The laboratory test results and SPT N graphs are presented in Appendix A and B, consolidation settlement calculations are presented in Appendix C. The soil profile consists of the layers shown in Table 3.6:

Table 3.6 A typical soil profile at Km: 142+400 section of the study area

Depth (m)	Soil Profile		SPT N (av.)	q_c (av.) (MPa)	f_s (av.) (kPa)	PI (av.) (%)	w_N (av.) (%)	c_u (kPa)
-9.00	Stiff Clay (CH)		15	1.29		47	33	
-15.00	Medium Dense Sand (SM)		21	5.49	33.98	NP	30	
-42.69	Stiff Clay- Silt (CH-ML)		24	1.16		13	22	

The geological longitudinal section of embankment is presented in Figure 3.22. SPT results of BSSK-452 borehole and cone resistance values of BS-CPT-4 results for clay layers are presented in Figure 3.23. According to the geological longitudinal section, the embankment with 8.09 m in height is planned to be constructed on clayey soil with a thickness of more than 40.0 m, and also sand layers are defined at depth of 9.0 m and 15.0 m. Till to depth of 9.0 m, SPT N value is obtained as 15 whereas q_c value is obtained as 1.29 MPa in average, which indicates “stiff clay”. According to BS-CPT-4, clay layers are defined in depth of intervals 8.6 m and 8.8 m, 10.1 m and 10.6 m, 11.1 m and 12.92 m with q_c value of 0.85 MPa in average. These thin clay layers are defined as “medium-stiff clay”.

From depth of 15.0 m, SPT N value is obtained as 24 whereas q_c value is obtained 1.16 MPa in average, which indicates “stiff clay”. When the values of SPT N and q_c are compared, they both point out similar stiffness and also strength values for clay units defined in specified depth of intervals. The graph of In-Situ Settlement (m) vs. Time (day) behavior measured in embankment for surface settlement plate is presented in Figure 3.24. The last measured settlement from surface settlement plate is 105.8 cm under embankment load with a maximum height of 8.09 m after 760 days of measurement.

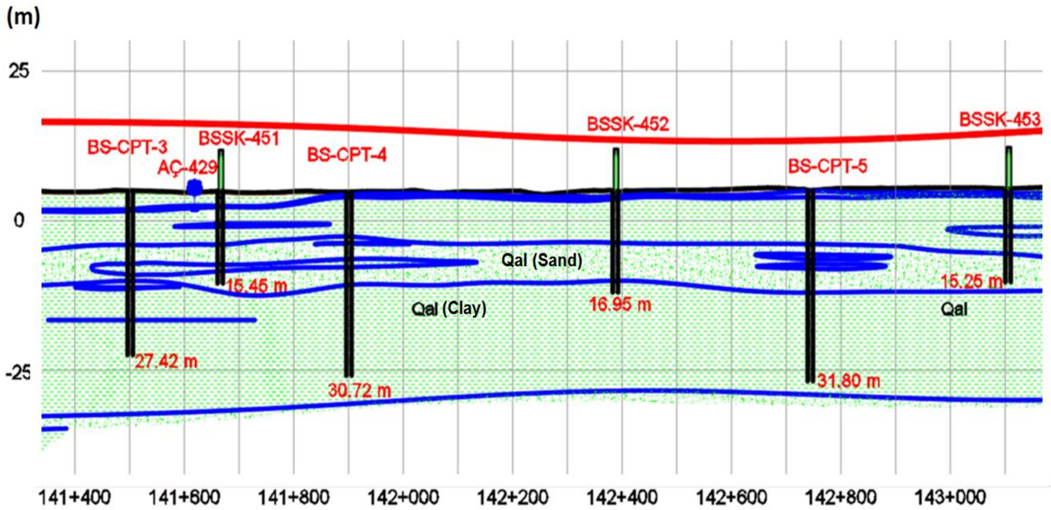

Figure 3.22. The longitudinal geological section of Km: 142+400

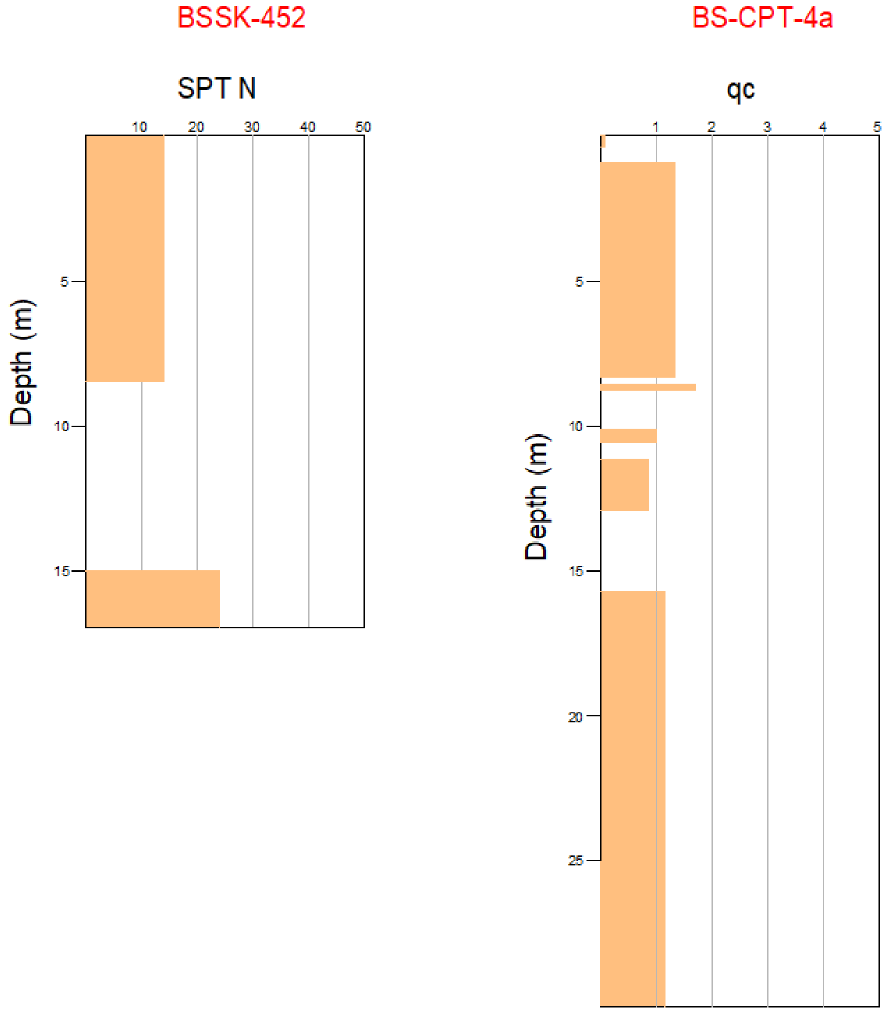

Figure 3.23. SPT N vs. Depth (m) and q_c (MPa) vs. Depth (m) graphs for clay layers

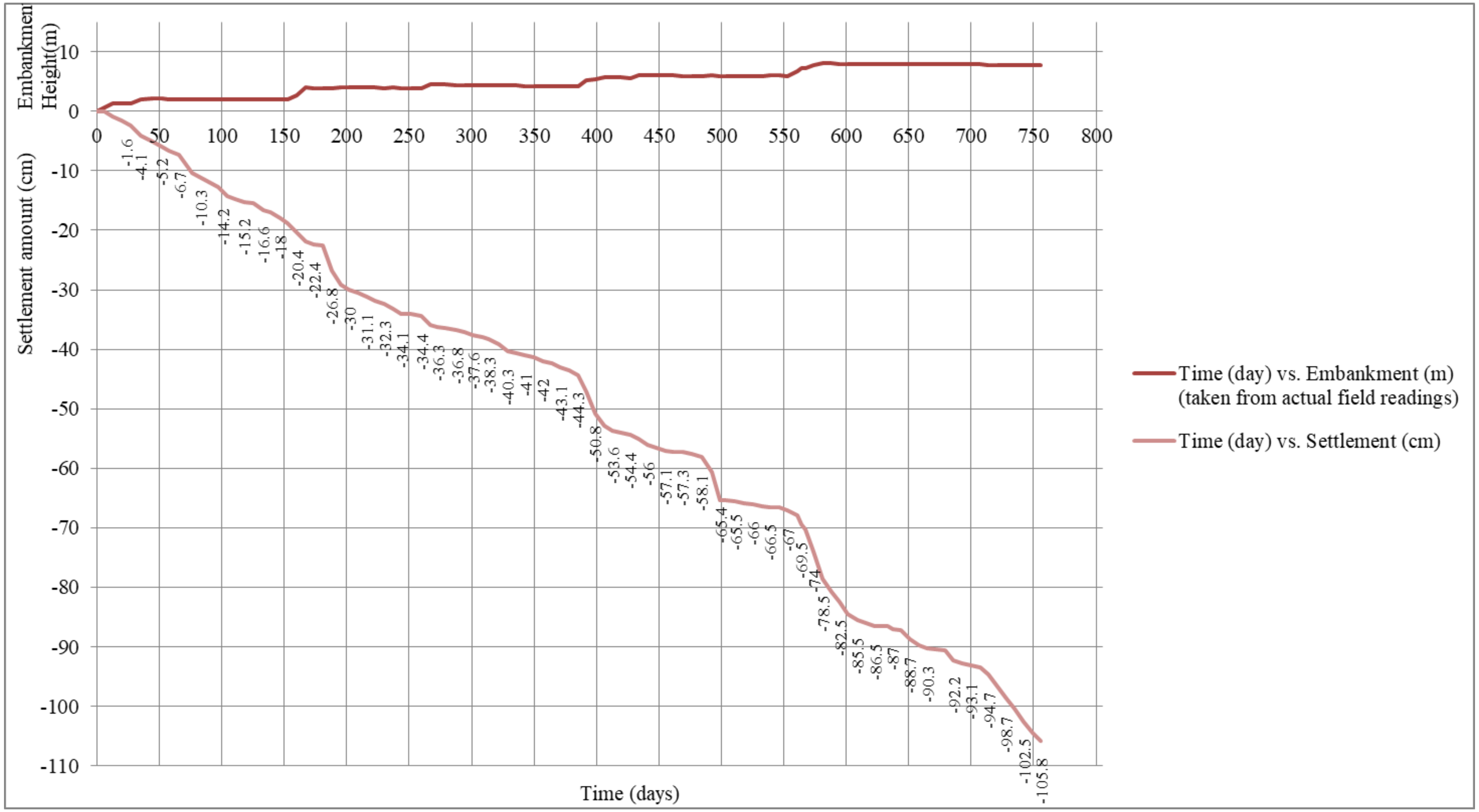

Figure 3.24. In situ Settlement (cm) vs. Time (day) behavior measured in embankment for surface settlement

3.7 KM: 143+107 Section

The soil profile of the embankment at Km: 143+107 is characterized by 31.80 m deep CPT (BSSK CPT-5) and 15.25 m deep borehole log (BSSK-453) The laboratory test results and SPT N graphs are presented in Appendix A and B, consolidation settlement calculations are presented in Appendix C. The soil profile consists of the layers shown in Table 3.7:

Table 3.7 A typical soil profile at Km: 143+107 section of the study area

Depth (m)	Soil Profile	SPT N (av.)	q_c (av.) (MPa)	f_s (av.) (kPa)	PI (av.) (%)	w_N (av.) (%)	c_u (kPa)
-6.50	Stiff Clay (CH)	14	1.20		48	30	
-7.50	Sand		3.37	44.98			
-14.00	Stiff Clay (CH)	17	1.03		55	28	
-17.00	Medium Dense Sand	28	7.05	51.30			
-43.42	Stiff Clay (CH-CL)		1.12				

The geological longitudinal section of embankment is presented in Figure 3.25. SPT results of BSSK-453 borehole and cone resistance values of BS-CPT-5 results for clay layers are presented in Figure 3.26. According to the geological longitudinal section, the embankment with 8.448 m in height is planned to be constructed on clayey soil with a thickness of more than 40.0 m, and also sand layers are defined at depths of 6.5 m - 7.5 m and 14.0 m – 17.0 m. Till to depth of 6.5 m, SPT N value is obtained as 14 whereas q_c value is obtained as 1.20 MPa in average, which indicates “stiff clay”. From depth of 7.5 m to 14.0 m, the average values of SPT N is obtained as 17 which indicates “stiff clay” whereas average value of q_c is obtained 1.03 MPa which indicates “medium-stiff clay”. From depth of 17.0 m, q_c values are 1.12 MPa in average, which is the indicator of “Stiff Clay”. When the values of SPT N and qc are compared, they both point out similar stiffness and strength values for clay units defined in specified depth of intervals. The graph of In-Situ Settlement (m) vs. Time (day) behavior measured in the embankment for surface settlement plate is presented in Figure 3.27. The last measured settlement from surface settlement plate is 127 cm under embankment load with a maximum height of 8.448 m after 740 days of measurement.

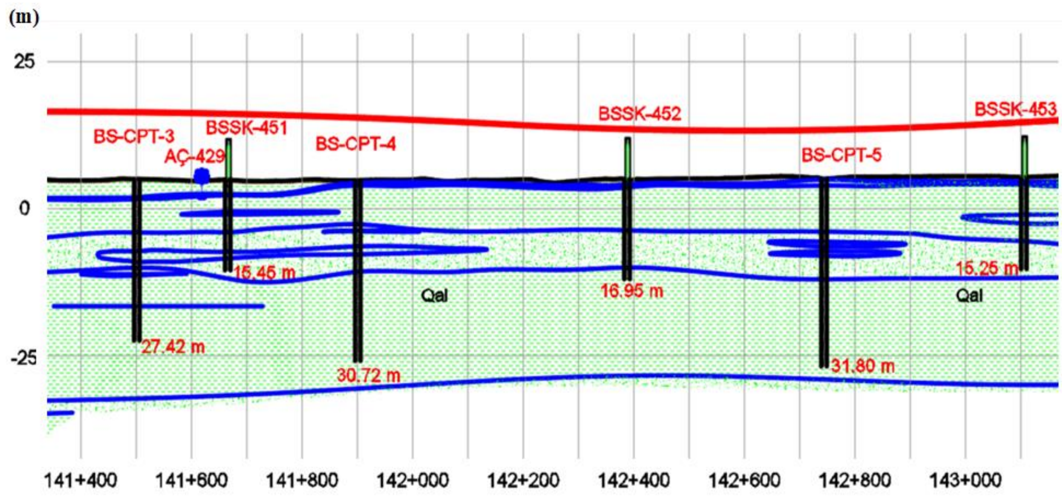

Figure 3.25. The longitudinal geological section of Km: 143+107

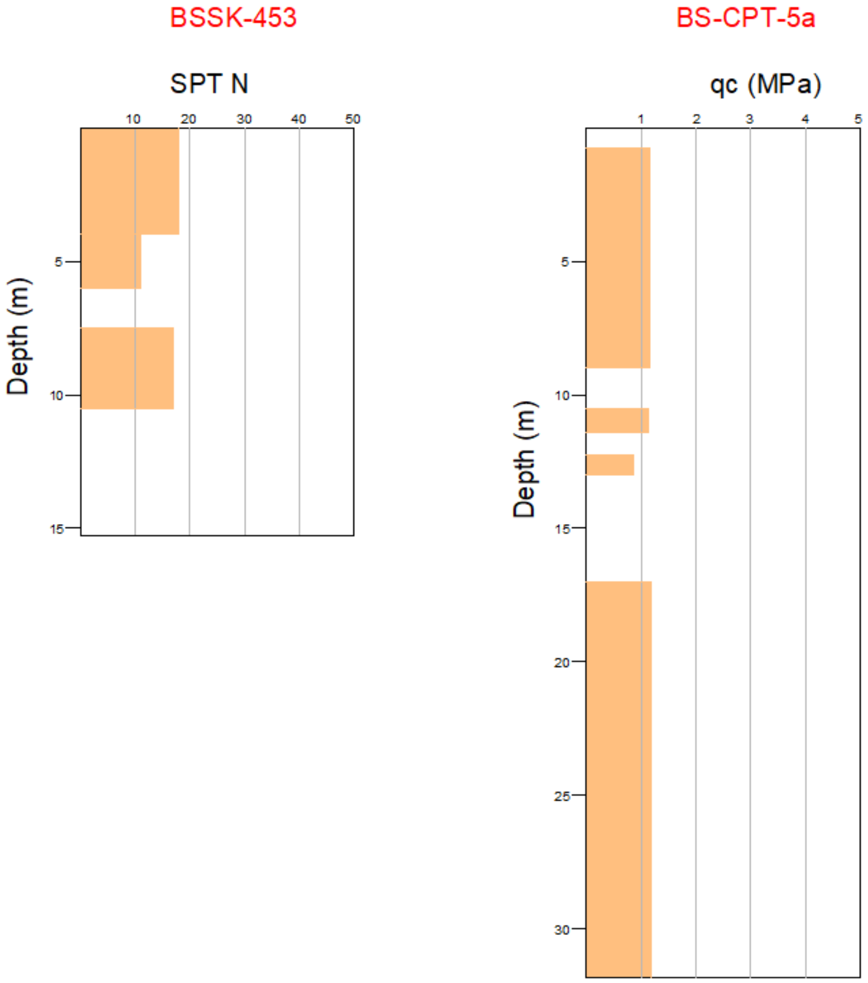

Figure 3.26. SPT N vs. Depth (m) and q_c (MPa) vs. Depth (m) graphs for clay layers

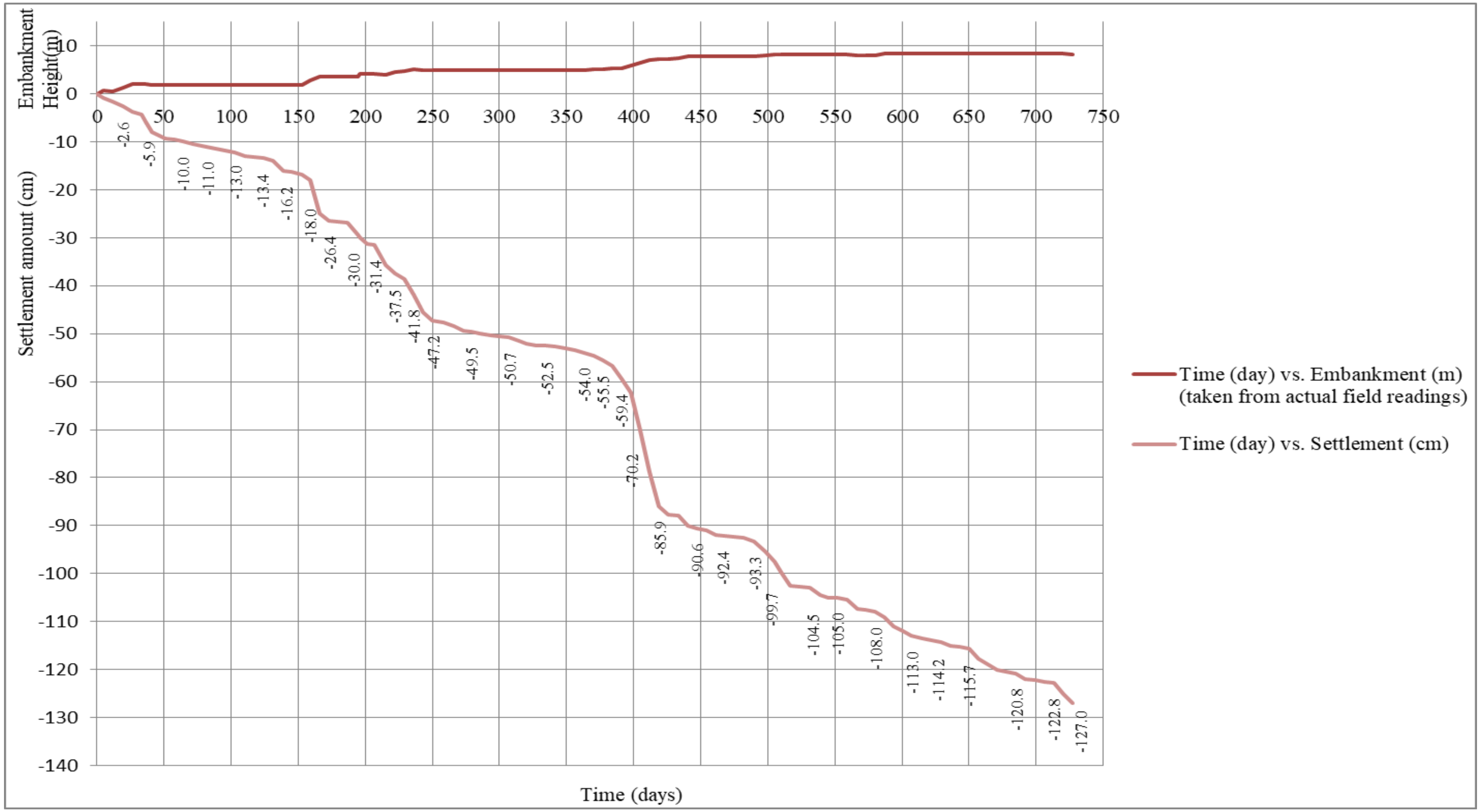

Figure 3.27. In situ Settlement (cm) vs. Time (day) behavior measured in embankment for surface settlement

3.8 KM: 144+000 Section

The soil profile of the embankment at Km: 144+000 is characterized by 28.68 m deep CPT (BSSK CPT-6) and 15.45 m deep borehole log (BSSK-454) The laboratory test results and SPT N graphs are presented in Appendix A and B, consolidation settlement calculations are presented in Appendix C. The soil profile consists of the layers shown in Table 3.8:

Table 3.8 A typical soil profile at Km: 144+000 section of the study area

Depth (m)	Soil Profile		SPT N (av.)	q_c (av.) (MPa)	f_s (av.) (kPa)	PI (av.) (%)	w_N (av.) (%)	c_u (kPa)
-6.50	Stiff Clay (CH)		14	1.19		40	31	101
-7.50	Sand			3.37	44.98			
-14.00	Stiff Clay (CH)		24	1.03		35	36	
-17.00	Medium Dense Sand		28	7.05	51.30			
-46.30	Stiff Clay (CH-CL)			1.15				

The geological longitudinal section of embankment is presented in Figure 3.28. SPT results of BSSK-454 borehole and cone resistance values of BS-CPT-6 results for clay layers are presented in Figure 3.29. According to the geological longitudinal section, the embankment with 9.98 m in height is planned to be constructed on clayey soil with a thickness of more than 40.0 m, and also sand layers are defined at depths of 6.5 m – 7.5 m and 14.0 m – 17.0 m. Till to depth of

6.5 m, SPT N value is obtained as 14 whereas q_c value is obtained as 1.19 MPa in average, which indicates "stiff clay". From depth of 7.5 m to 14.0 m, average value of SPT N is obtained as 24 which indicates "stiff clay" whereas average value of q_c is obtained 1.03 MPa which indicates "medium-stiff clay". From depth of 17.0 m, q_c values are 1.15 MPa in average, which is the indicator of "Stiff Clay". When the values of SPT N and q_c are compared, they both point out similar stiffness and also strength values for clay units defined in specified depth of intervals. The graph of In-Situ Settlement (m) vs. Time (day) behavior measured in the embankment for surface settlement plate is presented in Figure 3.30. The last measured settlement from surface settlement plate is 155.4 cm under embankment load with a maximum height of 9.98 m after 950 days of measurement.

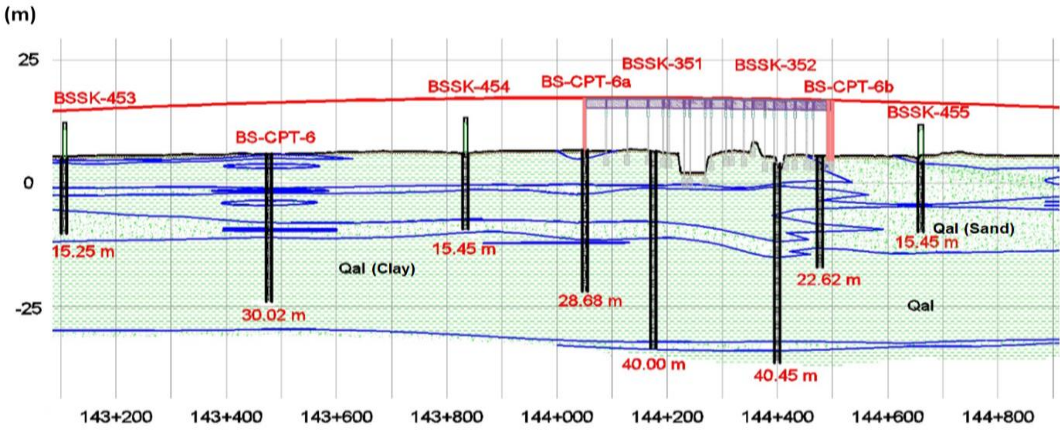

Figure 3.28. The longitudinal geological section of Km: 144+000

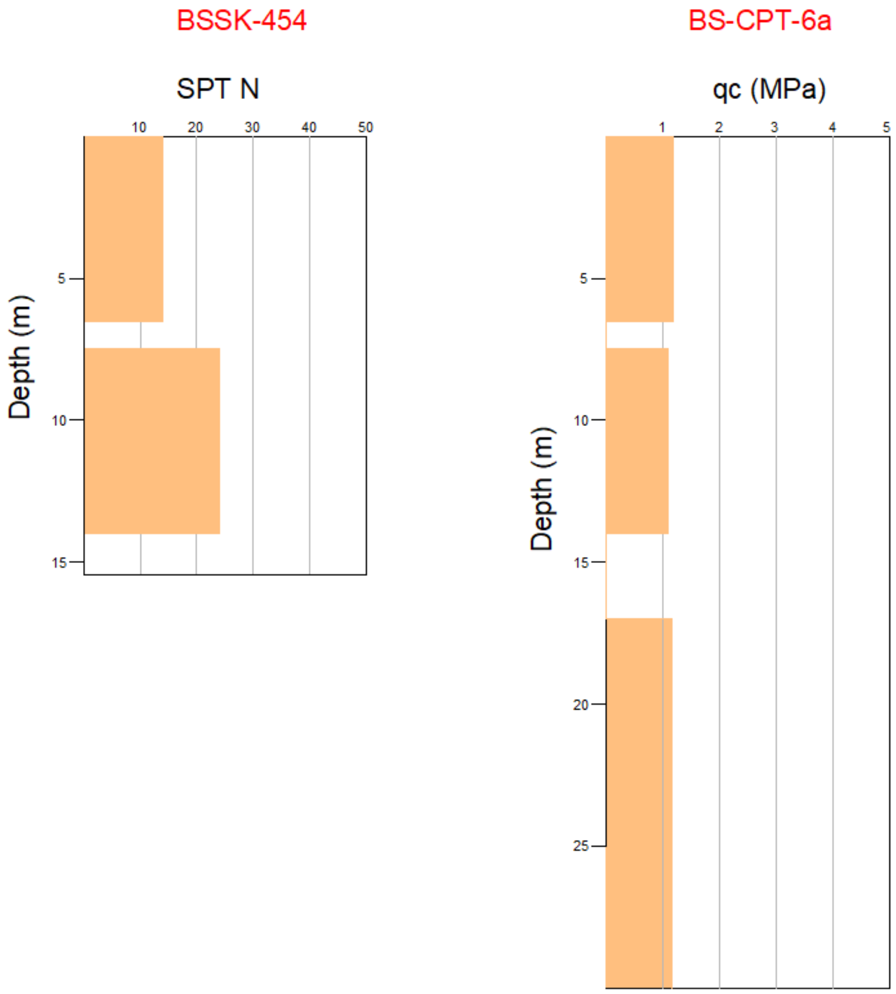

Figure 3.29. SPT N vs. Depth (m) and q_c (MPa) vs. Depth (m) graphs for clay layers

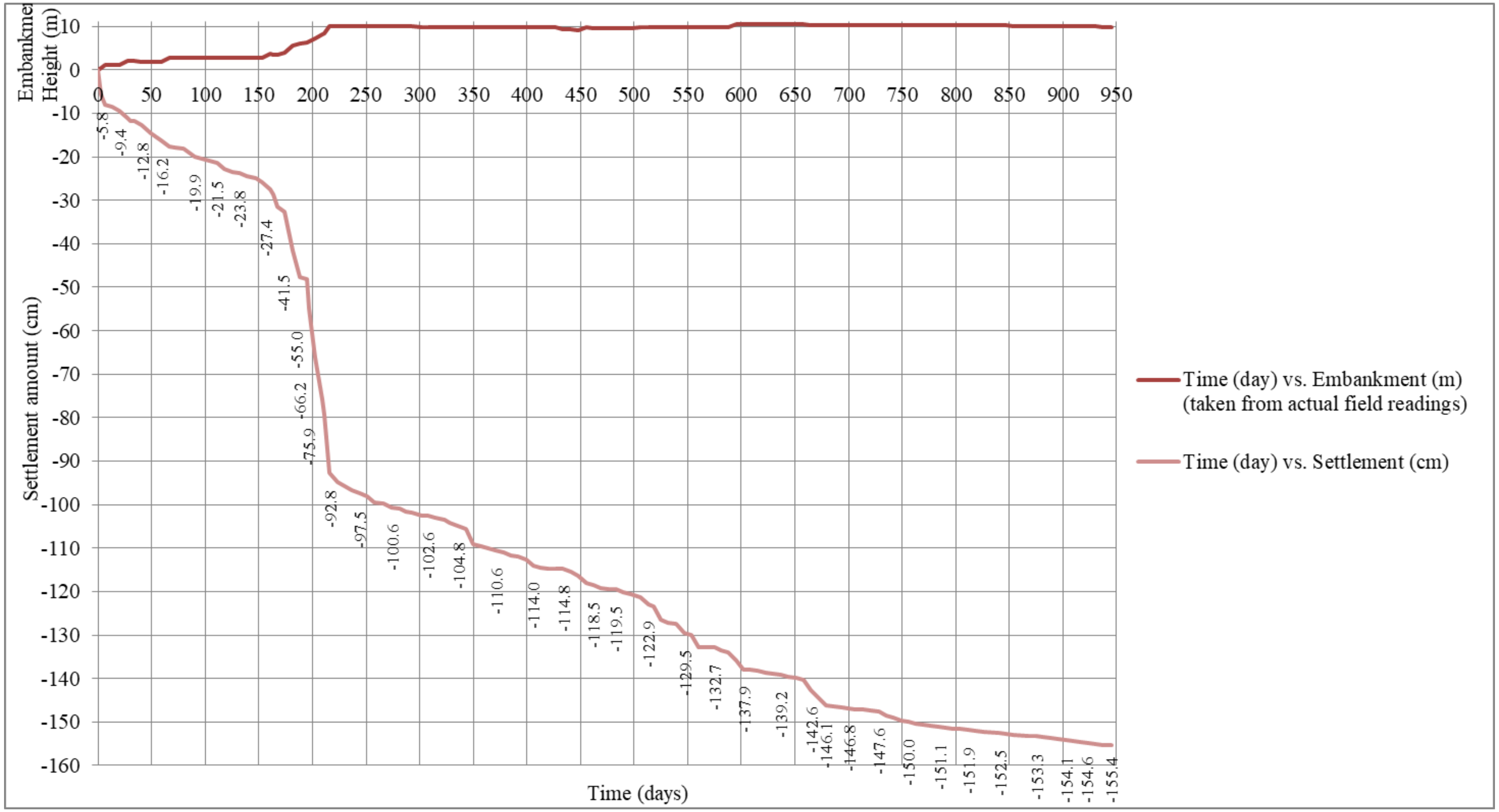

Figure 3.30. In situ Settlement (cm) vs. Time (day) behavior measured in embankment for surface settlement

3.9 KM: 145+000 Section

The soil profile of the embankment at Km: 145+000 is characterized by 15.45 m deep borehole (BSSK 456) and BS-CPT-07 cone penetration test. The laboratory test results and SPT N graphs are presented in Appendix A and B, consolidation settlement calculations are presented in Appendix C. The soil profile consists of the layers shown in Table 3.9:

Table 3.9 A typical soil profile at Km: 145+000 section of the study area

Depth (m)	Soil Profile	SPT N (av.)	q_c (av.) (MPa)	f_s (av.) (kPa)	PI (av.) (%)	w_N (av.) (%)	c_u (kPa)
-11.00	Stiff Clay (CL-CH)	17	1.32		44	31	
-18.00	Medium Dense Sand	27	8.52	40.52			
-42.51	Stiff Clay		1.42				

The geological longitudinal section of embankment is presented in Figure 3.31. SPT results of BSSK-456 borehole and cone resistance values of BS-CPT-7 results for clay layers are presented in Figure 3.32. According to the geological longitudinal section, the embankment with 9.97 m in height is planned to be constructed on clayey soil with a thickness of more than 40.0 m, and also sand layers are defined at depth of 11.0 m and 18.0 m. Till to depth of 11.0 m, SPT N value is obtained as 17 whereas q_c value is obtained as 1.32 MPa in average, which indicates “stiff clay”. Also, sand layers are defiend in depths of intervals 1.68 m and 2.18 m, 2.62 m and 2.92 m, 3.52 m and 3.64 m, 6.66 m and 7.36 m, 7.5 m and 9.24 m according to cone penetration test. From depth of 18.0 m, q_c value is obtained 1.36 MPa in average, which indicates “stiff clay”. The graph of In-Situ Settlement (m) vs. Time (day) behavior measured in the embankment for surface settlement plate is presented in Figure 3.33. The last measured settlement from surface settlement plate is 116.8 cm under embankment load with a maximum height of 9.97 m after 850 days of measurement.

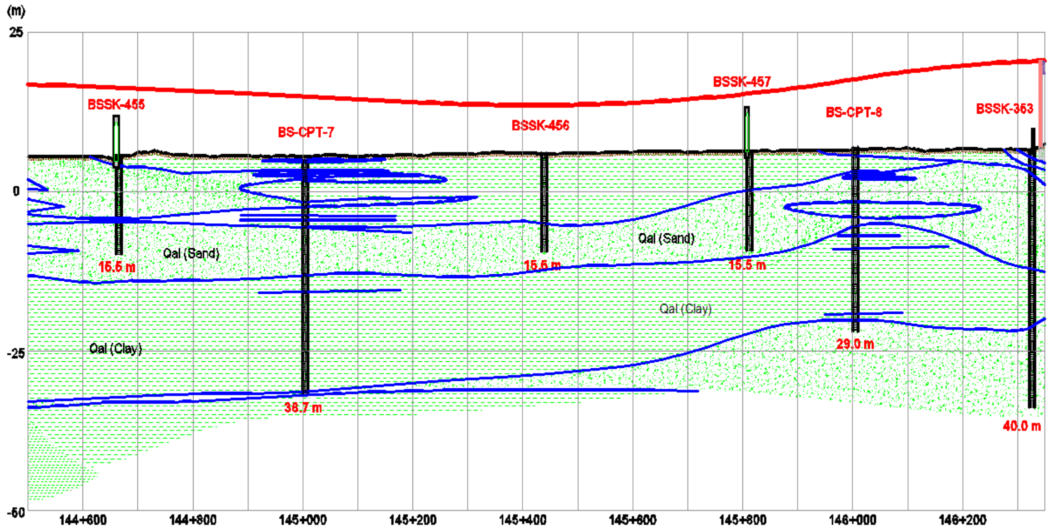

Figure 3.31. The longitudinal geological section of Km: 145+000

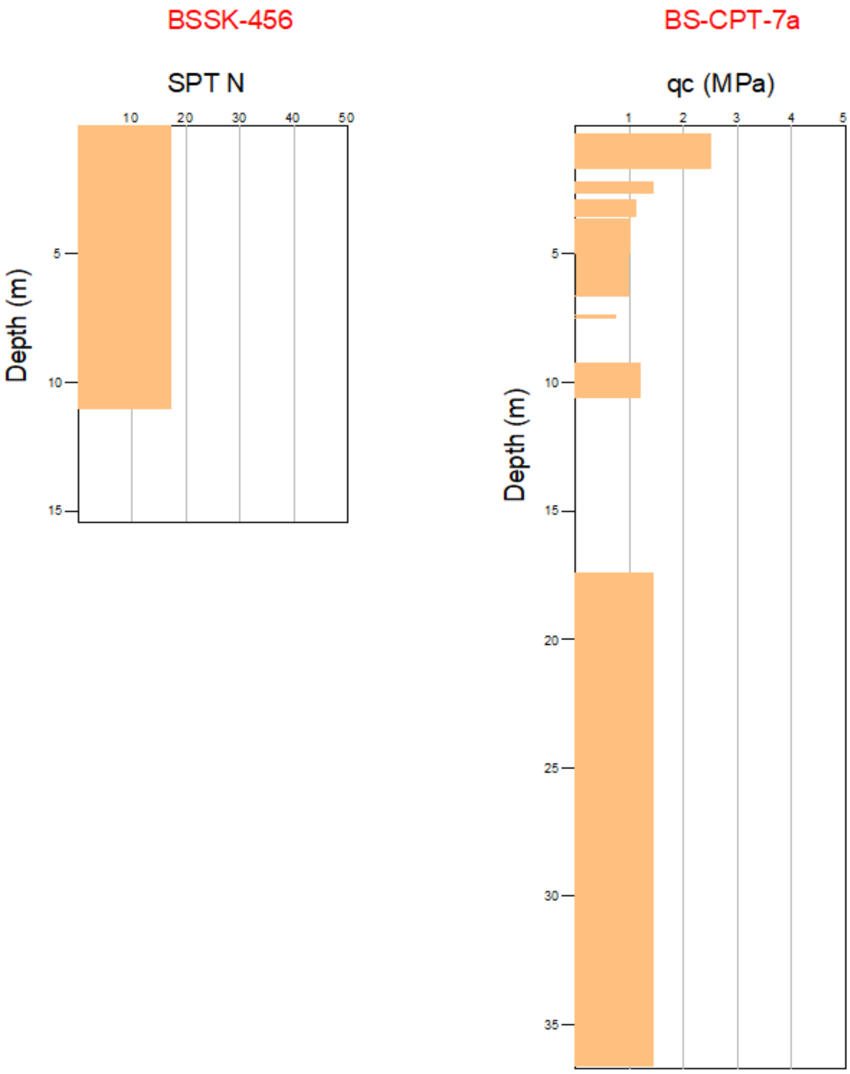

Figure 3.32. SPT N vs. Depth (m) and q_c (MPa) vs. Depth (m) graphs for clay layers

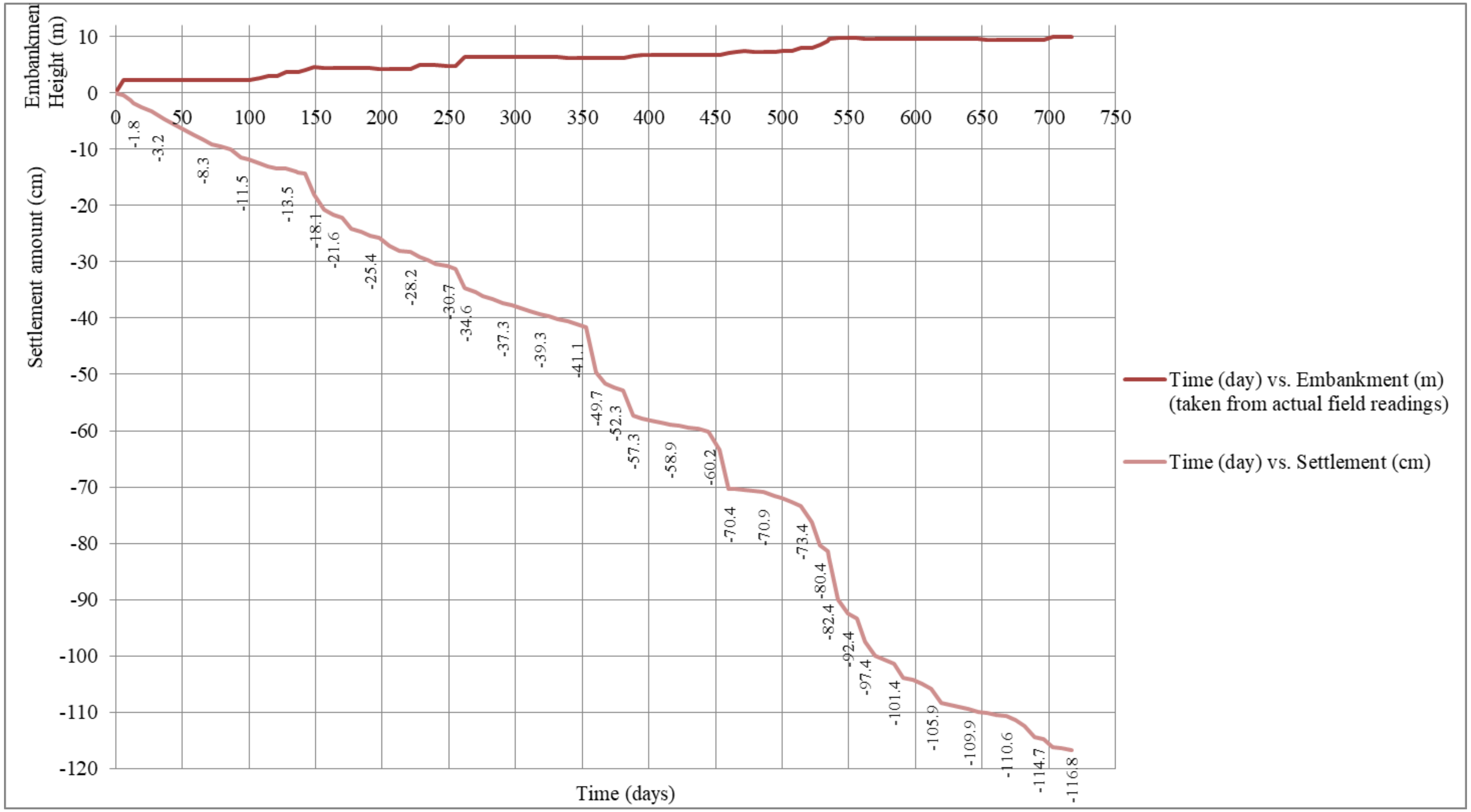

Figure 3.33. In situ Settlement (cm) vs. Time (day) behavior measured in embankment for surface settlement

3.10 KM: 146+210 Section

The soil profile of the embankment at Km: 146+210 is characterized by 15.45 m deep borehole (BSSK 457) and BS-CPT-08 cone penetration test. The laboratory test results and SPT N graphs are presented in Appendix A and B, consolidation settlement calculations are presented in Appendix C. The soil profile consists of the layers shown in Table 3.10:

Table 3.10 A typical soil profile at Km: 146+210 section of the study area

Depth (m)	Soil Profile	SPT N (av.)	q_c (av.) (MPa)	f_s (av.) (kPa)	PI (av.) (%)	w_N (av.) (%)	c_u (kPa)
-4.00	Stiff Clay (CL-CH)	14	1.37		29	35	
-9.00	Sand (SM-SP-SW)	36	7.48	36.14	NP	19	
-27.00	Medium-Stiff Clay (CH-CL)		1.09				

The geological longitudinal section of embankment is presented in Figure 3.34. SPT results of BSSK-457 borehole and cone resistance values of BS-CPT-8 results for clay layers are presented in Figure 3.35. According to the geological longitudinal section, the embankment with 12.18 m in height is planned to be constructed on clayey soil with a thickness of more than 35.0 m, and also sand layers are defined at depth of 4.0 m and 9.0 m. Till to depth of 4.0 m, SPT N value is obtained as 14 whereas q_c value is obtained as 1.37 MPa in average, which indicates "stiff clay". From depth of 9.0 m, q_c value is obtained 1.09 MPa in average, which indicates "medium-stiff clay". When the values of SPT N and q_c are compared in the first layer, they both point out similar stiffness and also strength values for clay units defined in specified depth of intervals. The graph of In-Situ Settlement (m) vs. Time (day) behavior measured in the embankment for surface settlement plate is presented in Figure 3.36. The last measured settlement from surface settlement plate is 108.8 cm under embankment load with a maximum height of 12.18 m after 460 days of measurement.

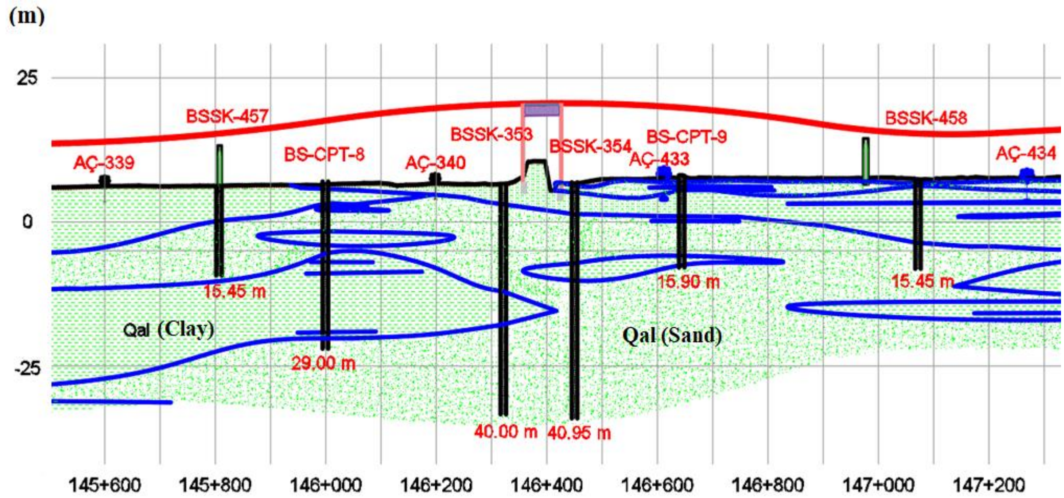

Figure 3.34. The longitudinal geological section of Km: 146+210

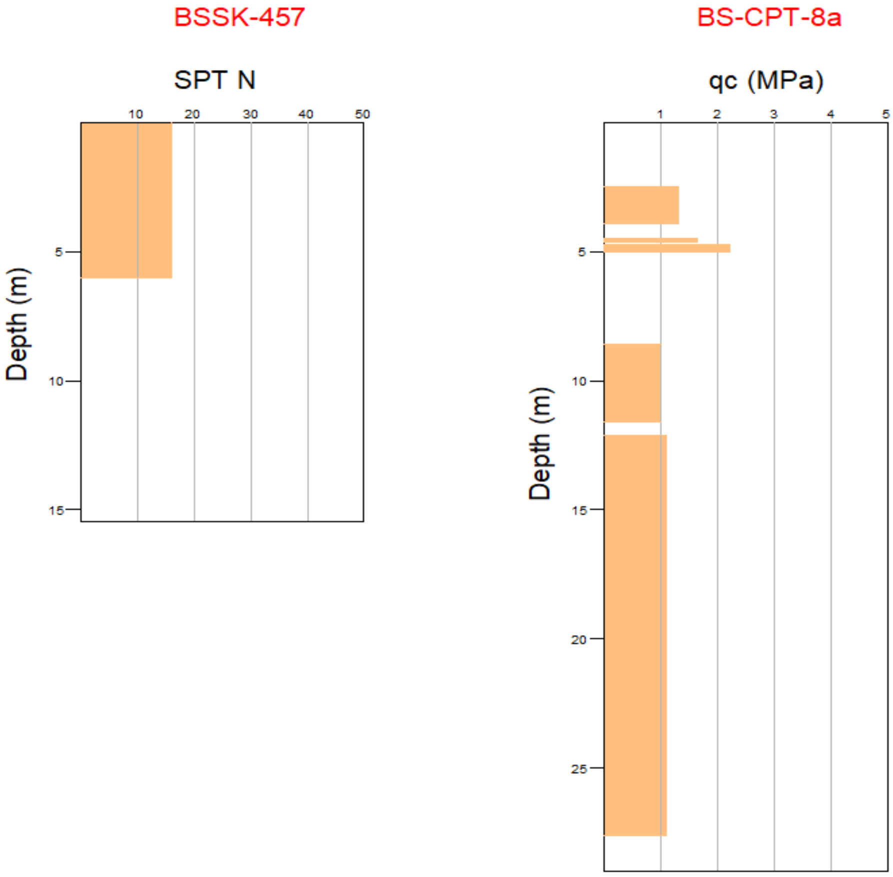

Figure 3.35. SPT N vs. Depth (m) and q_c (MPa) vs. Depth (m) graphs for clay layers

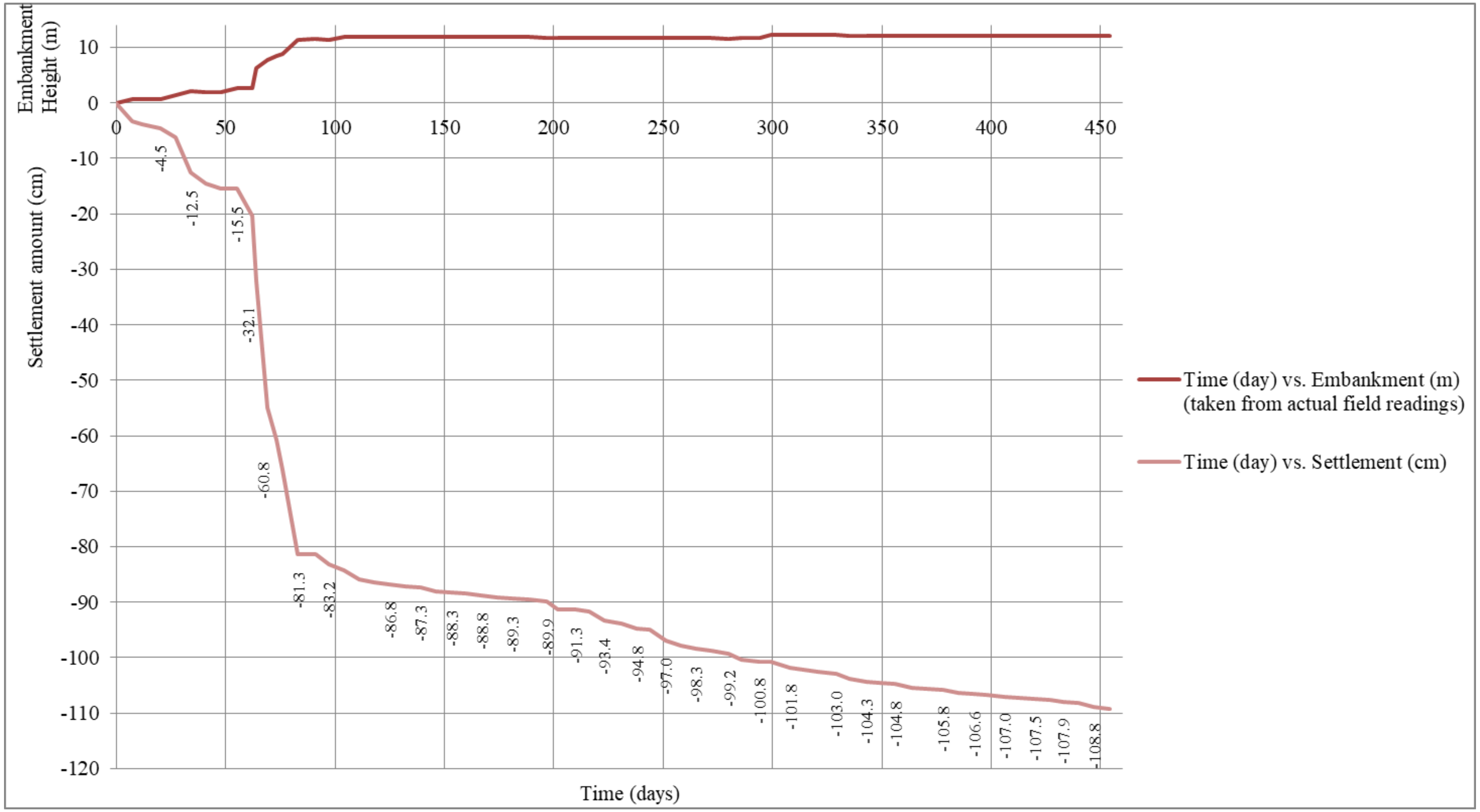

Figure 3.36. In situ Settlement (cm) vs. Time (day) behavior measured in embankment for surface settlement

3.11 KM: 147+000 Section

The soil profile of the embankment at Km: 147+000 is characterized by 15.45 m deep borehole (BSSK 458) and BS-CPT-10 cone penetration test. The laboratory test results and SPT N graphs are presented in Appendix A and B, consolidation settlement calculations are presented in Appendix C. The soil profile consists of the layers shown in Table 3.11:

Table 3.11 A typical soil profile at Km: 147+000 section of the study area

Depth (m)	Soil Profile	SPT N (av.)	q_c (av.) (MPa)	f_s (av.) (kPa)	PI (av.) (%)	w_N (av.) (%)	c_u (kPa)
-4.50	Medium-Stiff Clay (CL)	9	0.99		29	38	
-13.00	Stiff Clay (CH-CL)	18	1.32		30	35	
-15.50	Medium Dense Sand	24	5.77	41.50			
-21.00	Medium-Stiff Clay		1.03				
-22.00	Sand		3.02	11.59			
-41.78	Very Stiff Clay		2.77				

The geological longitudinal section of embankment is presented in Figure 3.37. SPT results of BSSK-458 borehole and cone resistance values of BS-CPT-10 results for clay layers are presented in Figure 3.38. According to the geological longitudinal section, the embankment with 8.1 m in height is planned to be constructed on clayey soil with a thickness of more than 40.0 m, and also sand layers are defined at depths of 13.0 m - 15.5 m and 21.0 m – 22.0 m. Till to depth of 4.5 m, SPT N value is obtained as 9 whereas q_c value is obtained as 0.99 MPa in average, which indicates "medium-stiff clay". From depth of 4.5 m to 13.0 m, SPT N value is obtained as 18 whereas q_c value is obtained 1.32 MPa in average, which indicates "stiff clay". In the depth interval of 15.5 m and 21.0 m, q_c value is obtained 1.03 MPa in average and clay is defined as "Medium-stiff clay". From depth of 22.0 m, q_c value is obtained 2.77 MPa in average, which indicates "very stiff clay". When the values of SPT N and q_c are compared, they both point out similar stiffness and also strength values for clay units defined in specified depth of intervals. The graph of In-Situ Settlement (m) vs. Time (day) behavior measured in the embankment for surface is presented in Figure 3.39. The last measured settlement from surface settlement plate is 98 cm under embankment load with a maximum height of 8.1 m after 720 days of measurement.

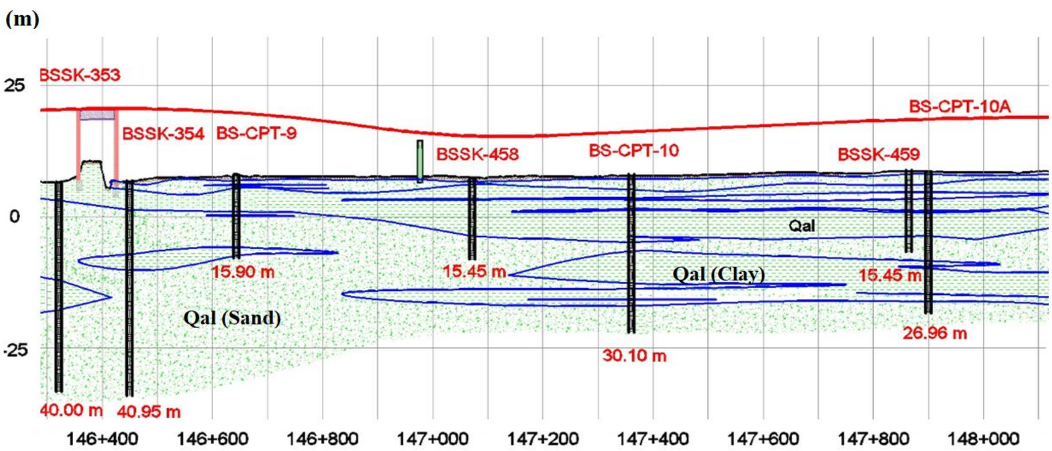

Figure 3.37. The longitudinal geological section of Km: 147+000

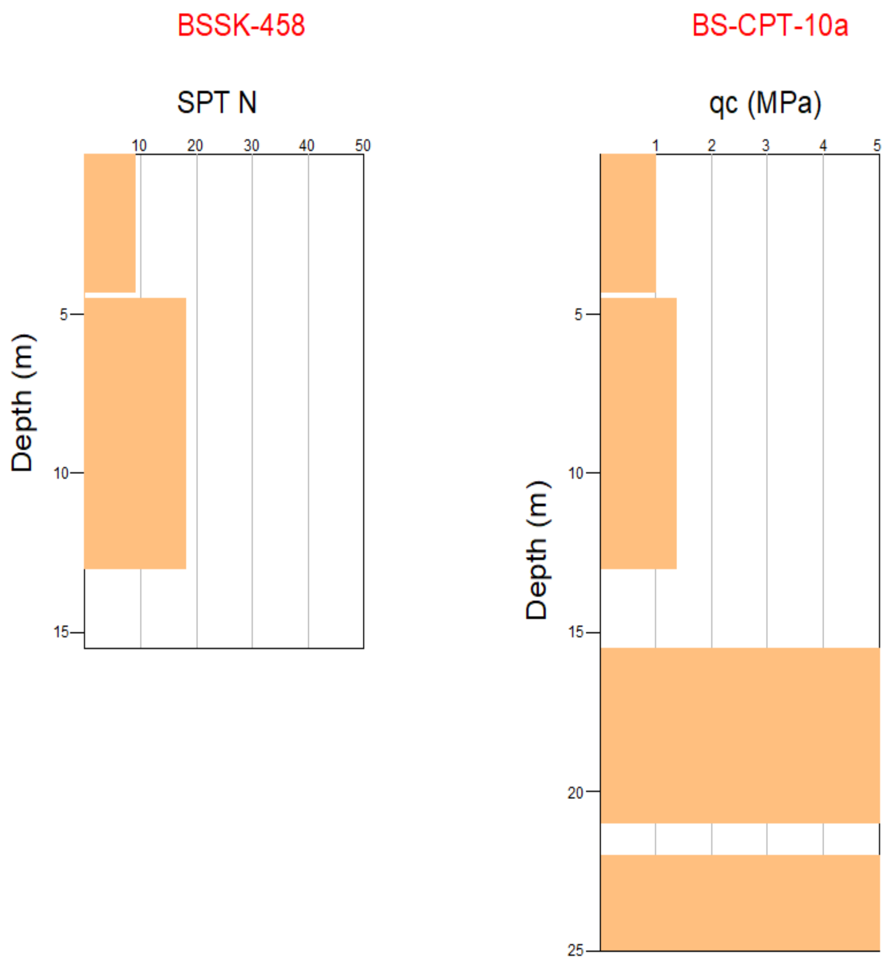

Figure 3.38. SPT N vs. Depth (m) and q_c (MPa) vs. Depth (m) graphs for clay layers

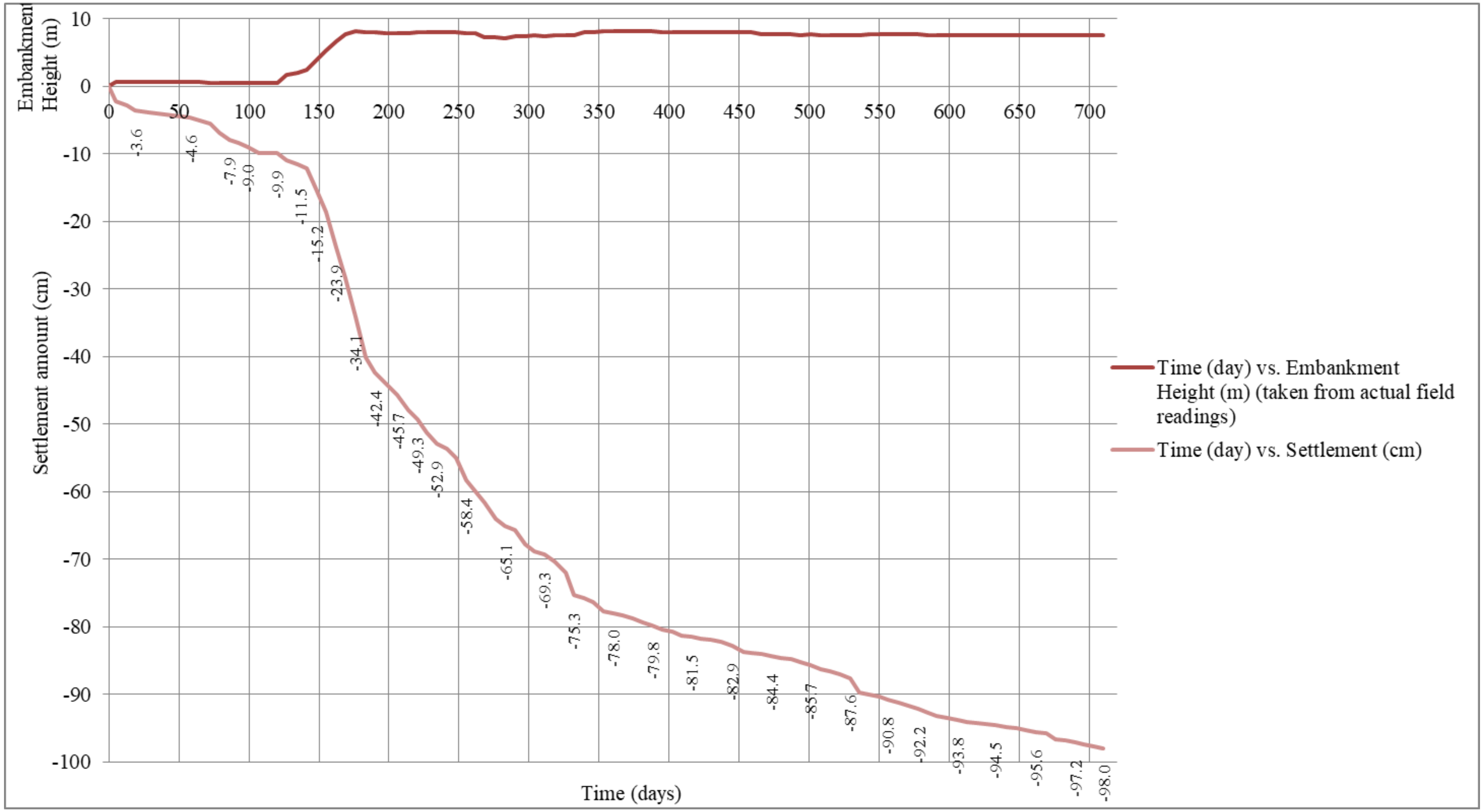

Figure 3.39. In situ Settlement (cm) vs. Time (day) behavior measured in embankment for surface settlement

3.12 KM: 149+000 Section

The soil profile of the embankment at Km: 149+000 is characterized by 16.95 m deep borehole (BSSK 461) and BS-CPT-11 cone penetration test. The laboratory test results and SPT N graphs are presented in Appendix A and B, consolidation settlement calculations are presented in Appendix C. The soil profile consists of the layers shown in Table 3.12:

Table 3.12 A typical soil profile at Km: 149+000 section of the study area

Depth (m)	Soil Profile	SPT N (av.)	q_c (av.) (MPa)	f_s (av.) (kPa)	PI (av.) (%)	w_N (av.) (%)	c_u (kPa)
-4.80	Soft Clay (CL-CH)	6	1.04		26	26	
-8.00	Sand (SC)	9	5.75	32.61			
-14.00	Stiff Clay (CH-CL)	22	1.24		35	33	
-15.80	Medium Dense Sand		8.32	45.58			
-27.20	Stiff Clay (CH)	26	1.25		31	33	132
-30.50	MediumDense Sand		1.28	35.43			
-41.99	Stiff Clay (CH-CL)		1.59				

The geological longitudinal section of embankment is presented in Figure 3.40. SPT results of BSSK-461 borehole and cone resistance values of BS-CPT-11 results for clay layers are presented in Figure 3.41. According to the geological longitudinal section, the embankment with 8.2 m in height is planned to be constructed on clayey soil with a thickness of more than 40.0 m, and also sand layers are defined at depths of 4.8 m – 8.0 m, 14.0 m – 15.8 m and 27.2 m – 30.5 m. Till to depth of 4.8 m, SPT N value is obtained as 6 whereas q_c value is obtained as 1.04 MPa in average. According to SPT N values, it is defined as “soft clay”. On the other hand, if q_c values are considered, it is defined as “medium-stiff clay”. From depth of 8.0 m to 14.0 m, SPT N value is obtained as 22 whereas q_c value is obtained 1.24 MPa in average, which indicates “stiff clay”. In the depths of 15.8 m and 27.2 m, SPT N value is obtained as 26, q_c value is obtained 1.25 MPa in average and clay is defined as “stiff clay”. From depth of 30.5 m, q_c value is obtained 1.59 MPa in average, which indicates “stiff clay”. When the values of SPT N and q_c are compared, they both point out similar stiffness and also strength values for clay units defined in specified depth of intervals. The graph of In-Situ Settlement (m) vs. Time (day) behavior measured in embankment for surface settlement plate is presented in Figure 3.42. The last measured settlement from surface settlement plate is 96.0 cm under embankment load with a maximum height of 8.2 m after 600 days of measurement.

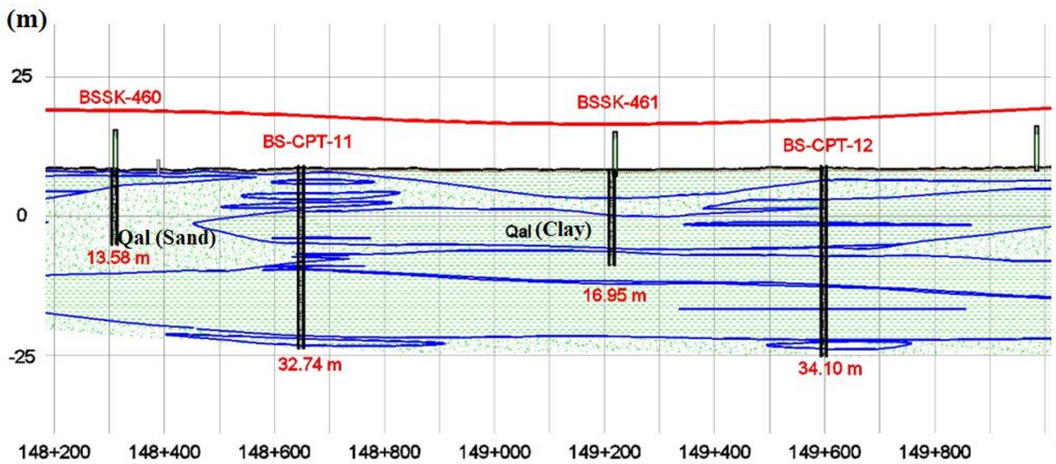

Figure 3.40. The longitudinal geological section of Km: 149+000

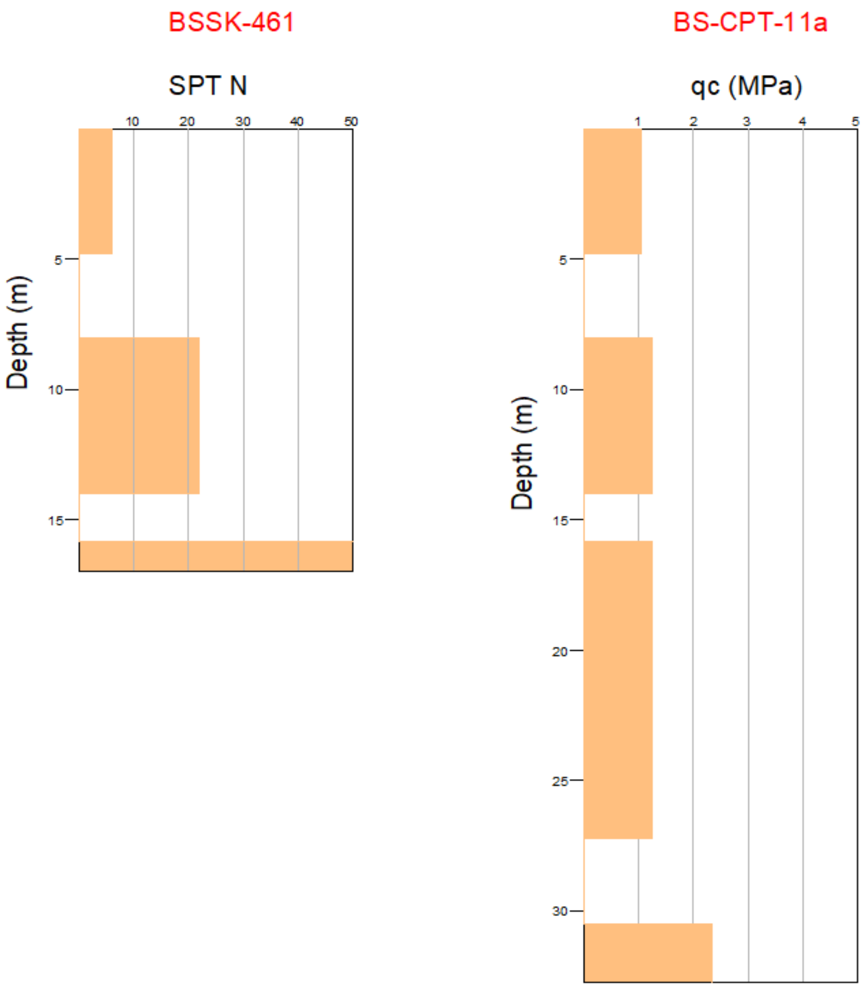

Figure 3.41. SPT N vs. Depth (m) and q_c (MPa) vs. Depth (m) graphs for clay layers

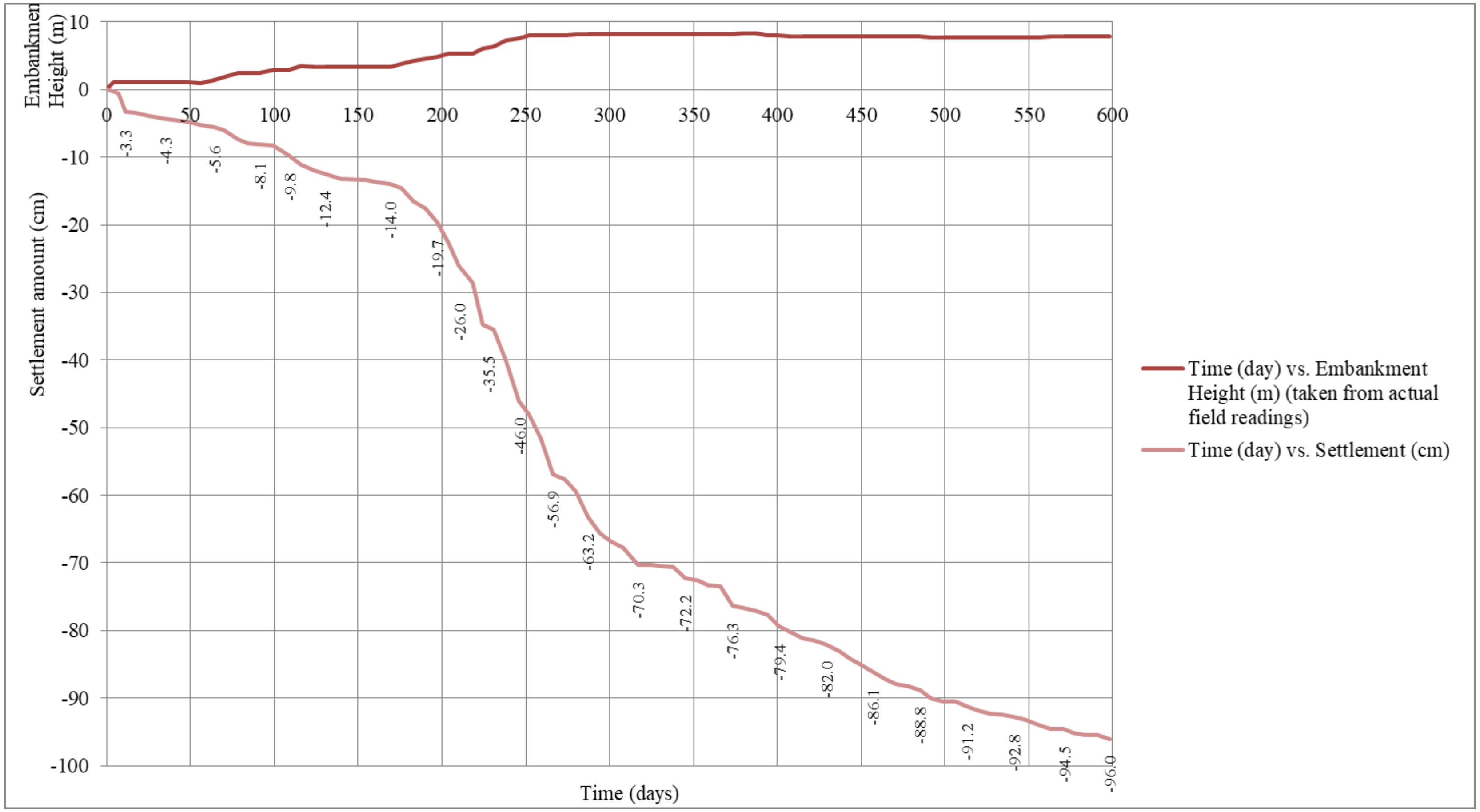

Figure 3.42. In situ Settlement (cm) vs. Time (day) behavior measured in embankment for surface settlement

3.13 KM: 150+000 Section

The soil profile of the embankment at Km: 150+000 is characterized by 20.0 m deep borehole (BSSK 685A) and BS-CPT-13 cone penetration test. The laboratory test results and SPT N graphs are presented in Appendix A and B, consolidation settlement calculations are presented in Appendix C. The soil profile consists of the layers shown in Table 3.13:

Table 3.13 A typical soil profile at Km: 150+000 section of the study area

Depth (m)	Soil Profile		SPT N (av.)	q_c (av.) (MPa)	f_s (av.) (kPa)	PI (av.) (%)	w_N (av.) (%)	c_u (kPa)
-3.00	Soft Clay (CL)		5	1.27		18	18	
-5.00	Sand (SM)		16	1.96	16.80			
-11.00	Stiff Clay (CH)		16	1.48		30	29	
-18.00	Sand		42	15.60	47.80			
-45.30	Medium-Stiff Clay (CL)		12	1.70		15	28	106

The geological longitudinal section of embankment is presented in Figure 3.43. SPT results of BSSK-685 borehole and cone resistance values of BS-CPT-13 results for clay layers are presented in Figure 3.44. According to the geological longitudinal section, the embankment with 9.88 m in height is planned to be constructed on clayey soil with a thickness of more than 40.0 m and also sand layers are defined at depths of 3.0 m – 5.0 m and 11.0 m – 18.0 m. Till to depth of 3.0 m, SPT N value is obtained as 5 whereas q_c value is obtained as 1.24 MPa in average. According to SPT N values, it is defined as “soft clay”. On the other hand, if q_c values are considered, it is defined as “medium-stiff clay”. From depth of 5.0 m to 11.0 m, SPT N value is obtained as 16 whereas q_c value is obtained 1.48 MPa in average, which indicates “stiff clay”. From depth of 18.0 m, SPT N value is obtained as 12 whereas q_c value is obtained 1.7 MPa in average, which indicates “medium-stiff clay”. When the values of SPT N and q_c are compared, they both point out similar stiffness and also strength values for clay units defined in specified depth of intervals. The graph of In-Situ Settlement (m) vs. Time (day) behavior measured in the embankment for surface settlement plate is presented in Figure 3.45. The last measured settlement from surface settlement plate is 106.7 cm under embankment load with a maximum height of 9.88 m after 600 days of measurement.

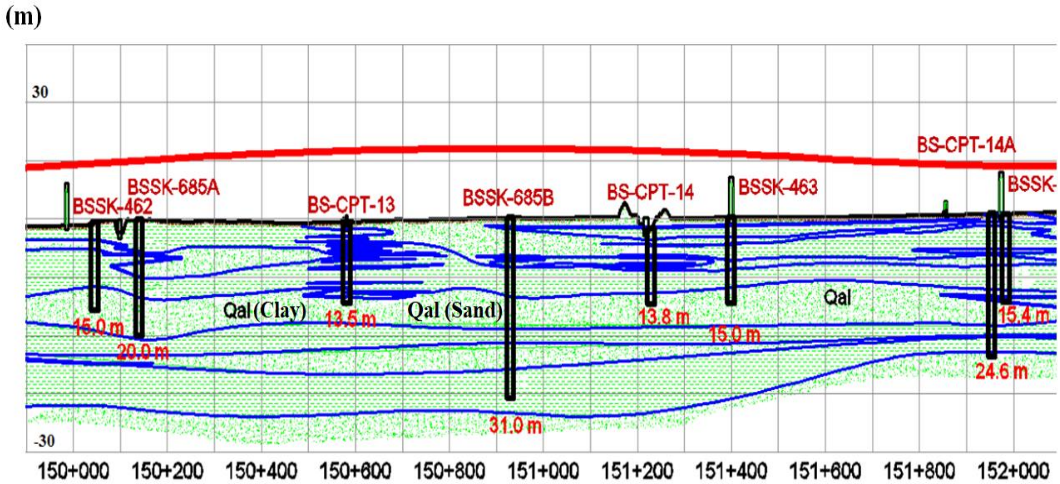

Figure 3.43. The longitudinal geological section of Km: 150+000

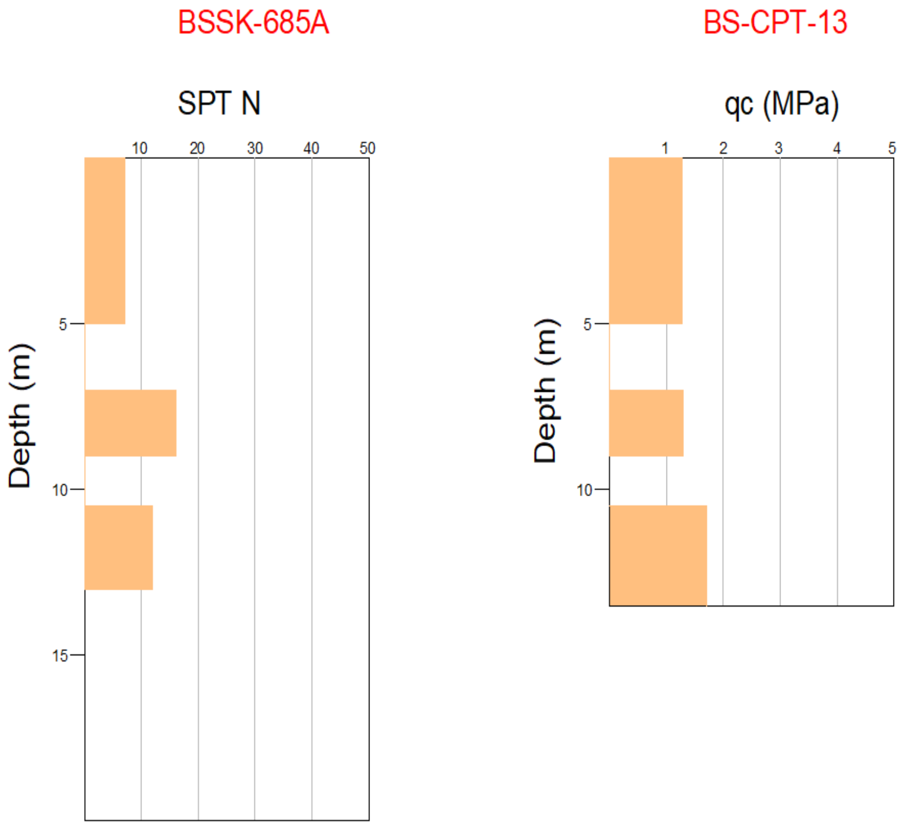

Figure 3.44. SPT N vs. Depth (m) and q_c (MPa) vs. Depth (m) graphs for clay layers

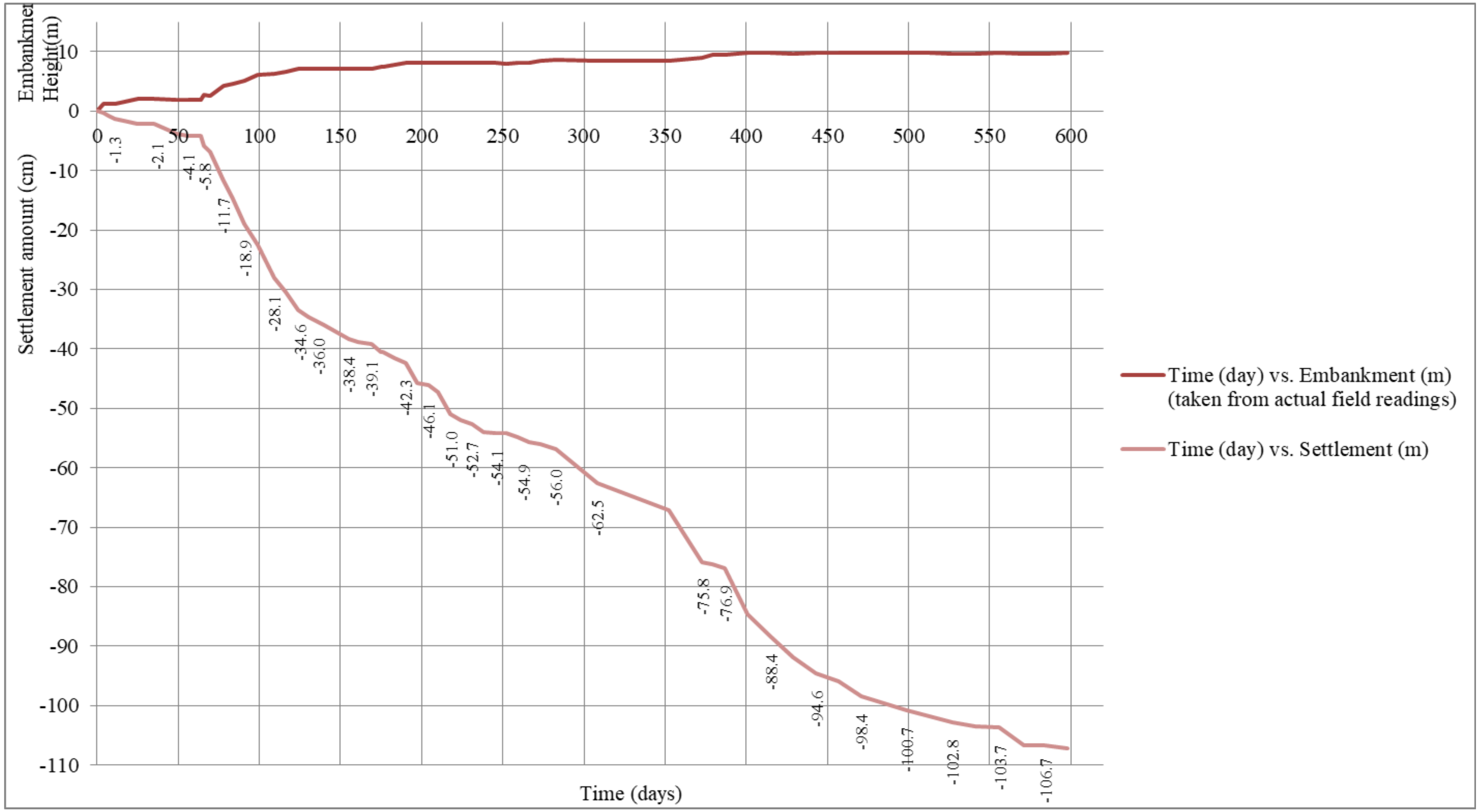

Figure 3.45. In situ Settlement (cm) vs. Time (day) behavior measured in embankment for surface settlement

3.14 KM: 150+500 Section

The soil profile of the embankment at Km: 150+500 is characterized by 20.0 m deep borehole (BSSK 685A) and BS-CPT-13 cone penetration test. The laboratory test results and SPT N graphs are presented in Appendix A and B, consolidation settlement calculations are presented in Appendix C. The soil profile consists of the layers shown in Table 3.14:

Table 3.14 A typical soil profile at Km: 150+500 section of the study area

Depth (m)	Soil Profile		SPT N (av.)	q_c (av.) (MPa)	f_s (av.) (kPa)	PI (av.) (%)	w_N (av.) (%)	c_u (kPa)
-5.00	Soft Clay (CL)		7	1.27		18	18	
-6.00	Sand (SM)		16	1.96	16.80			
-12.50	Stiff Clay (CH)		16	1.30		30	29	
-15.50	Sand (SW-SM)		42	15.60	47.80			
-46.20	Medium-Stiff Clay (CL)		12	1.51		15	28	106

The geological longitudinal section of embankment is presented in Figure 3.46. SPT results of BSSK-485 borehole and cone resistance values of BS-CPT-13 results for clay layers are presented in Figure 3.47. According to the geological longitudinal section, the embankment with 10.4 m in height is planned to be constructed on clayey soil with a thickness of more than 40.0 m, and also sand layers are defined at depths of 5.0 m – 6.0 m and 12.5 m – 15.5 m. Till to depth of 5.0 m, SPT N value is obtained as 7 whereas q_c value is obtained as 1.27 MPa in

average. According to SPT N values, it is defined as “soft clay”. On the other hand, if q_c values are considered, it is defined as “medium-stiff clay”. From depth of 6.0 m to 12.5 m, SPT N value is obtained as 16 whereas q_c value is obtained 1.30 MPa in average, which indicates “stiff clay”. From depth of 15.5 m, SPT N value is obtained as 12 whereas q_c value is obtained 1.51 MPa in average, which indicates “medium-stiff clay”. When the values of SPT N and q_c are compared, they both point out similar stiffness and also strength values for clay units defined in specified depth of intervals. The graph of In-Situ Settlement (m) vs. Time (day) behavior measured in the embankment for surface settlement plate is presented in Figure 3.48. The last measured settlement from surface settlement plate is 133.5 cm under embankment load with a maximum height of 10.4 m after 450 days of measurement.

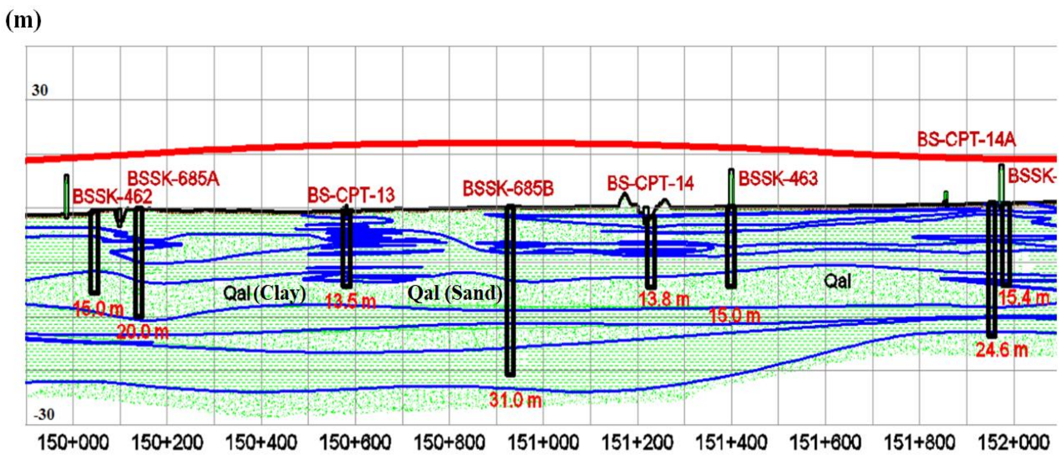

Figure 3.46. The longitudinal geological section of Km: 150+500

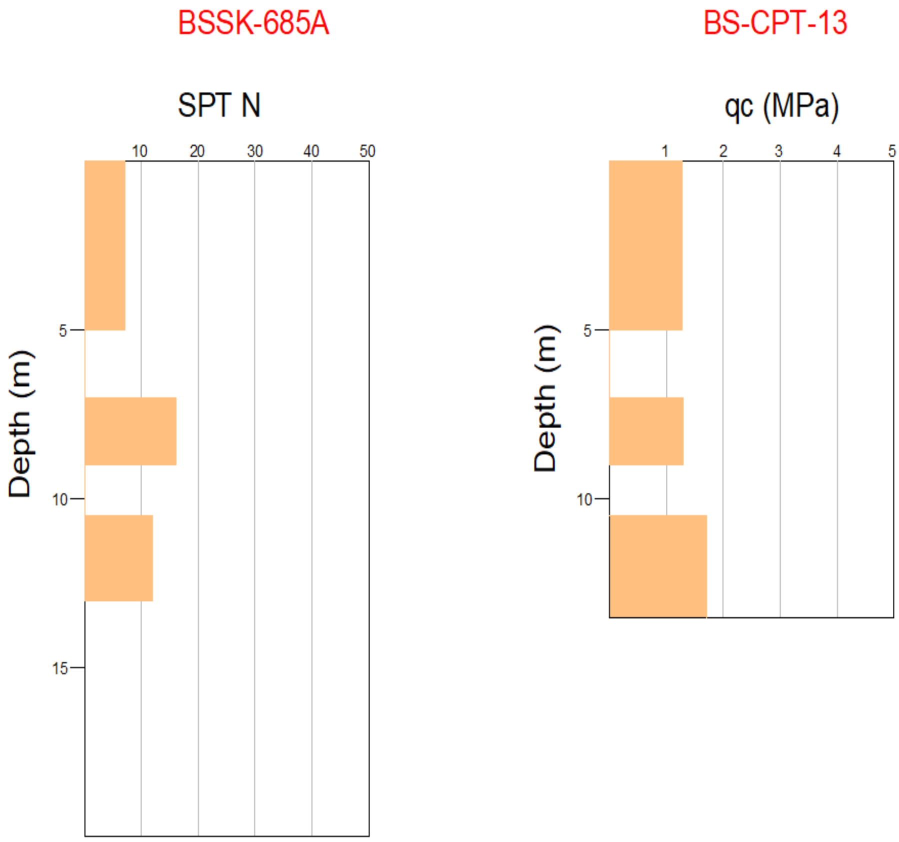

Figure 3.47. SPT N vs. Depth (m) and q_c (MPa) vs. Depth (m) graphs for clay layers

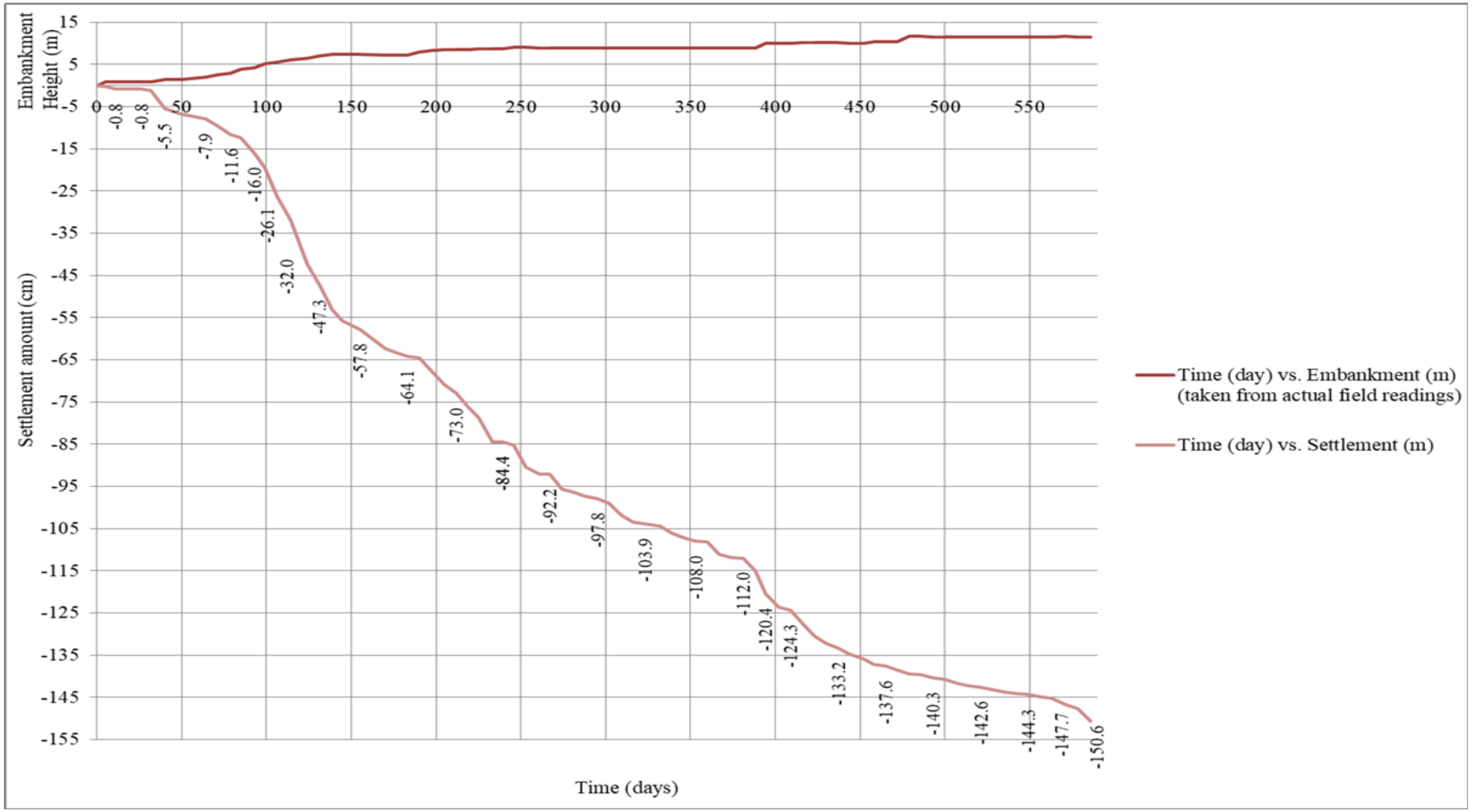

Figure 3.48. In situ Settlement (cm) vs. Time (day) behavior measured in embankment for surface settlement

3.15 KM: 151+220 Section

The soil profile of the embankment at Km: 151+220 is characterized by 15.06 m deep borehole (BSSK 463) and 13.80 m deep CPT (BS-CPT-14). The laboratory test results and SPT N graphs are presented in Appendix A and B, consolidation settlement calculations are presented in Appendix C. The soil profile consists of the layers shown in Table 3.15:

Table 3.15 A typical soil profile at Km: 151+220 section of the study area

Depth (m)	Soil Profile	SPT N (av.)	q_c (av.) (MPa)	f_s (av.) (kPa)	PI (av.) (%)	w_N (av.) (%)	c_u (kPa)
-5.00	Soft Clay (CL)	7	0.94		23	28	
-8.00	Sand (SM)	16	1.96	16.80			
-13.00	Medium-Stiff Clay (CL)	14	0.87		28	30	60
-16.00	Sand (SW-SM)	42	15.60	47.80			
-47.31	Medium-Stiff Clay (CL)		0.94				

The geological longitudinal section of embankment is presented in Figure 3.49. SPT results of BSSK-463 borehole and cone resistance values of BS-CPT-14 results for clay layers are presented in Figure 3.50. According to the geological longitudinal section, the embankment with 11.0 m in height is planned to be constructed on clayey soil with a thickness of more than 40.0 m and also sand layers are defined at depths of 5.0 m – 8.0 m and 13.0 m – 16.0 m. Till to depth of 5.0 m, SPT N value is obtained as 7 whereas q_c value is obtained as 0.94 MPa in average. According to SPT N values, it is defined as “soft clay”. On the other hand, if q_c values are considered, it is defined as “medium-stiff clay”. From depth of 8.0 m to 13.0 m, SPT N value is obtained as 14 whereas q_c value is obtained 0.87 MPa in average. The clay unit in this interval is defined as “medium-stiff clay” according to SPT N and q_c values. When the values of SPT N and q_c are compared, they both point out similar stiffness and also strength values for clay units defined in specified depth of intervals. The graph of In-Situ Settlement (m) vs. Time (day) behavior measured in embankment for surface settlement plate is presented in Figure 3.51. The last measured settlement from surface settlement plate is 171.9 cm under embankment load with a maximum height of 11.0 m after 420 days of measurement.

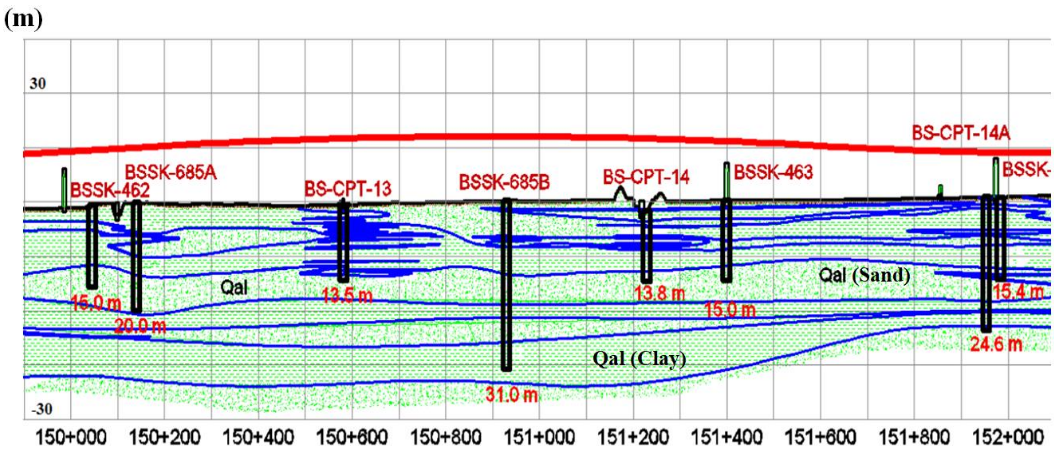

Figure 3.49. The longitudinal geological section of Km: 151+220

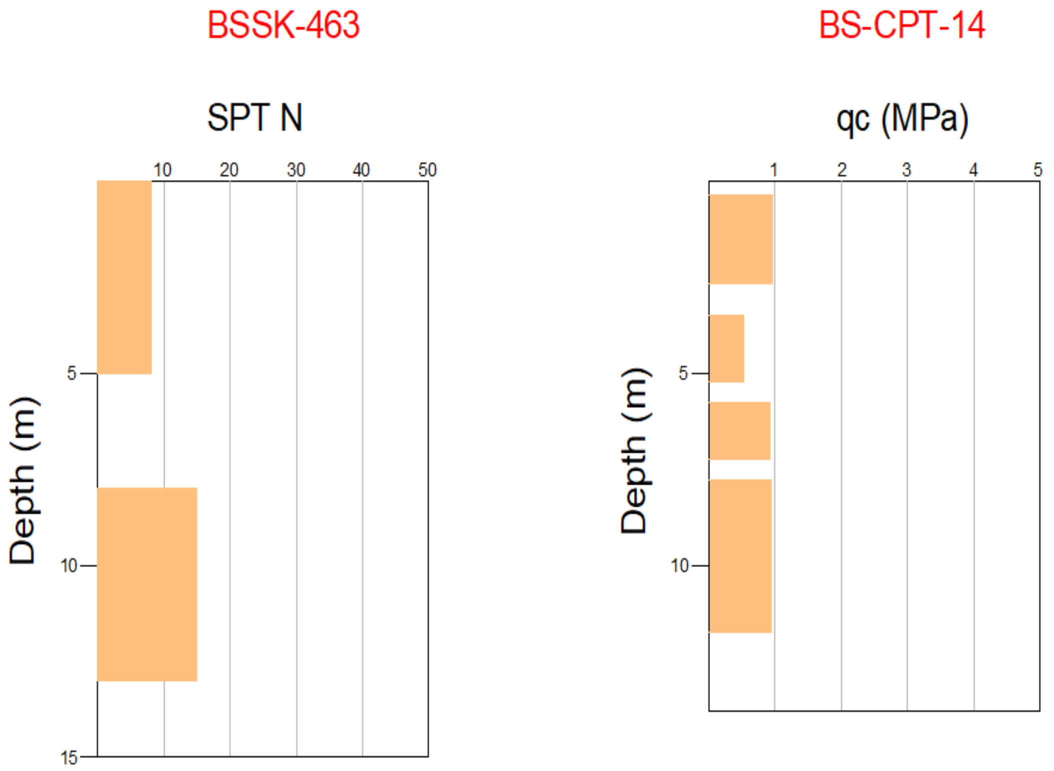

Figure 3.50. SPT N vs. Depth (m) and q_c (MPa) vs. Depth (m) graphs for clay layers

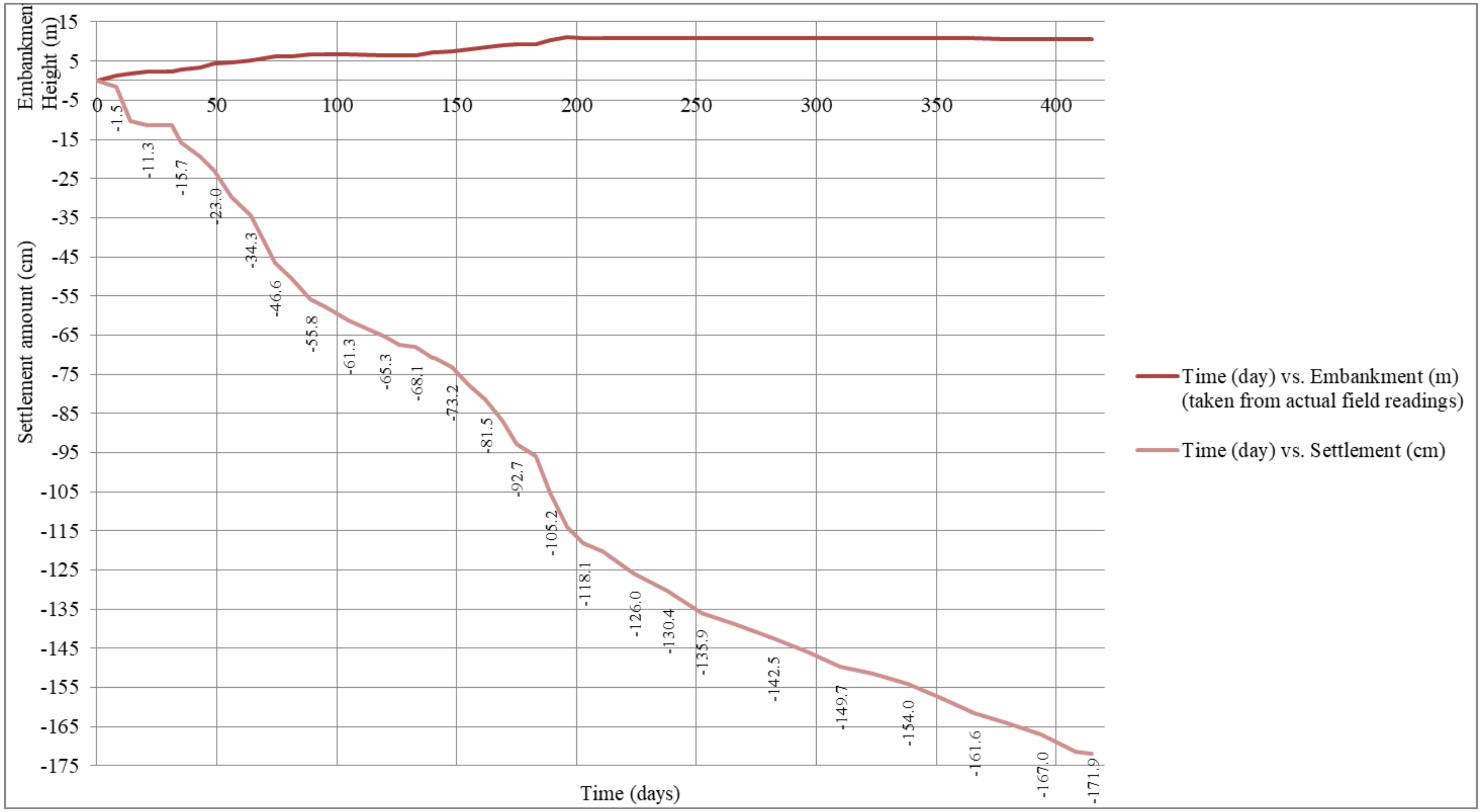

Figure 3.51. In situ Settlement (cm) vs. Time (day) behavior measured in embankment for surface settlement

3.16 KM: 151+975 Section

The soil profile of the embankment at Km: 151+975 is characterized by 15.45 m deep borehole (BSSK 464) and 24.60 m deep CPT (BS-CPT-14A). The laboratory test results and SPT N graphs are presented in Appendix A and B, consolidation settlement calculations are presented in Appendix C. The soil profile consists of the layers shown in Table 3.16:

Table 3.16 A typical soil profile at Km: 151+975 section of the study area

Depth (m)	Soil Profile	SPT N (av.)	q_c (av.) (MPa)	f_s (av.) (kPa)	PI (av.) (%)	w_N (av.) (%)	c_u (kPa)
-7.00	Medium-Stiff Clay (CL)	11	0.92		24	31	104
-9.00	Sand (ML)	13	1.96	16.80			
-13.00	Stiff Clay (CH)	18	0.94		46	32	82
-19.00	Sand (SM)	31	15.60	47.80			
-45.00	Medium-Stiff Clay (CL)		0.93				

The geological longitudinal section of embankment is presented in Figure 3.52. SPT results of BSSK-464 borehole and cone resistance values of BS-CPT-14 results for clay layers are presented in Figure 3.53. According to the geological longitudinal section, the embankment with 9.74 m in height is planned to be constructed on clayey soil with a thickness of more than 40.0 m, and also sand layers are defined at depths of 7.0 m – 9.0 m and 13.0 m – 19.0 m. Till to depth of 7.0 m, SPT N value is obtained as 11 whereas q_c value is obtained as 0.92 MPa in

average and clay unit is defined as “medium-stiff clay”. From depth of 9.0 m to 13.0 m, SPT N value is obtained as 18 whereas q_c value is obtained 0.94 MPa in average. The clay unit in this interval is defined as “stiff clay” according to SPT N values, “medium-stiff clay” according to q_c values. From depth of 19.0 m, q_c value is obtained as 0.93 MPa in average, which indicates “medium-stiff clay”. When the values of SPT N and q_c are compared, they both point out similar stiffness and also strength values for clay units defined in specified depth of intervals. The graph of In-Situ Settlement (m) vs. Time (day) behavior measured in the embankment for surface settlement plate is presented in Figure 3.54. The last measured settlement from surface settlement plate is 123.7 cm under embankment load with a maximum height of 9.74 m after 620 days of measurement.

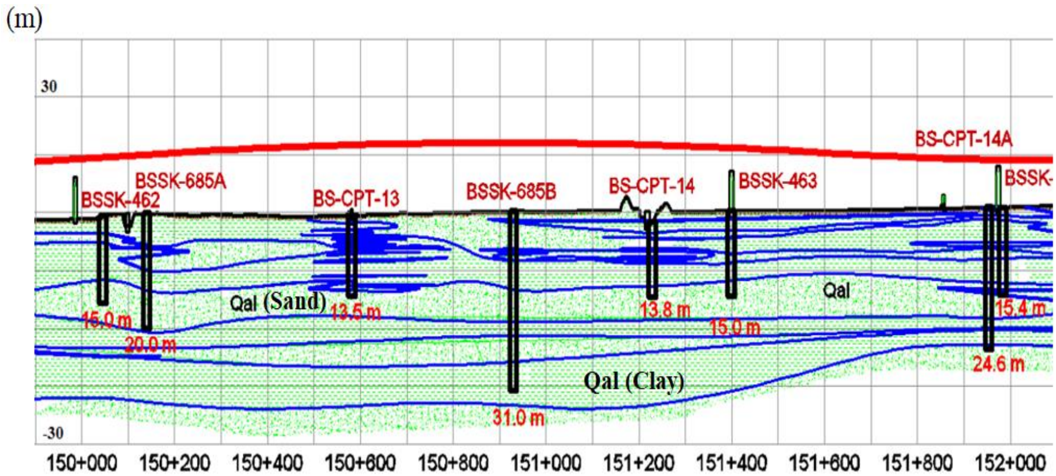

Figure 3.52. The longitudinal geological section of Km: 151+975

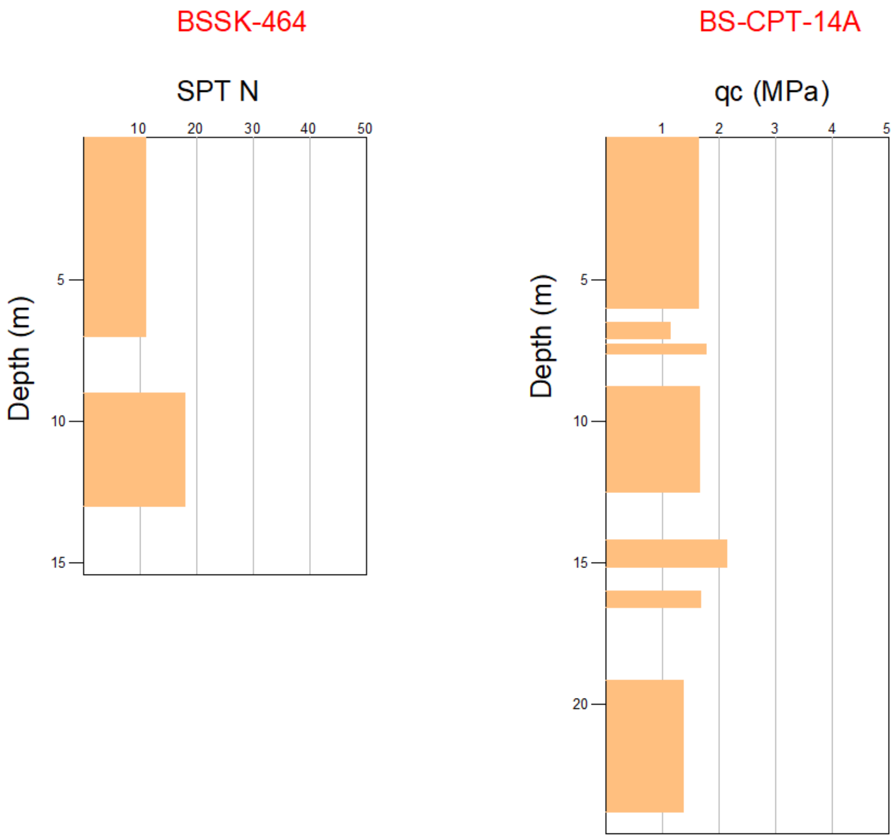

Figure 3.53. SPT N vs. Depth (m) and q_c (MPa) vs. Depth (m) graphs for clay layers

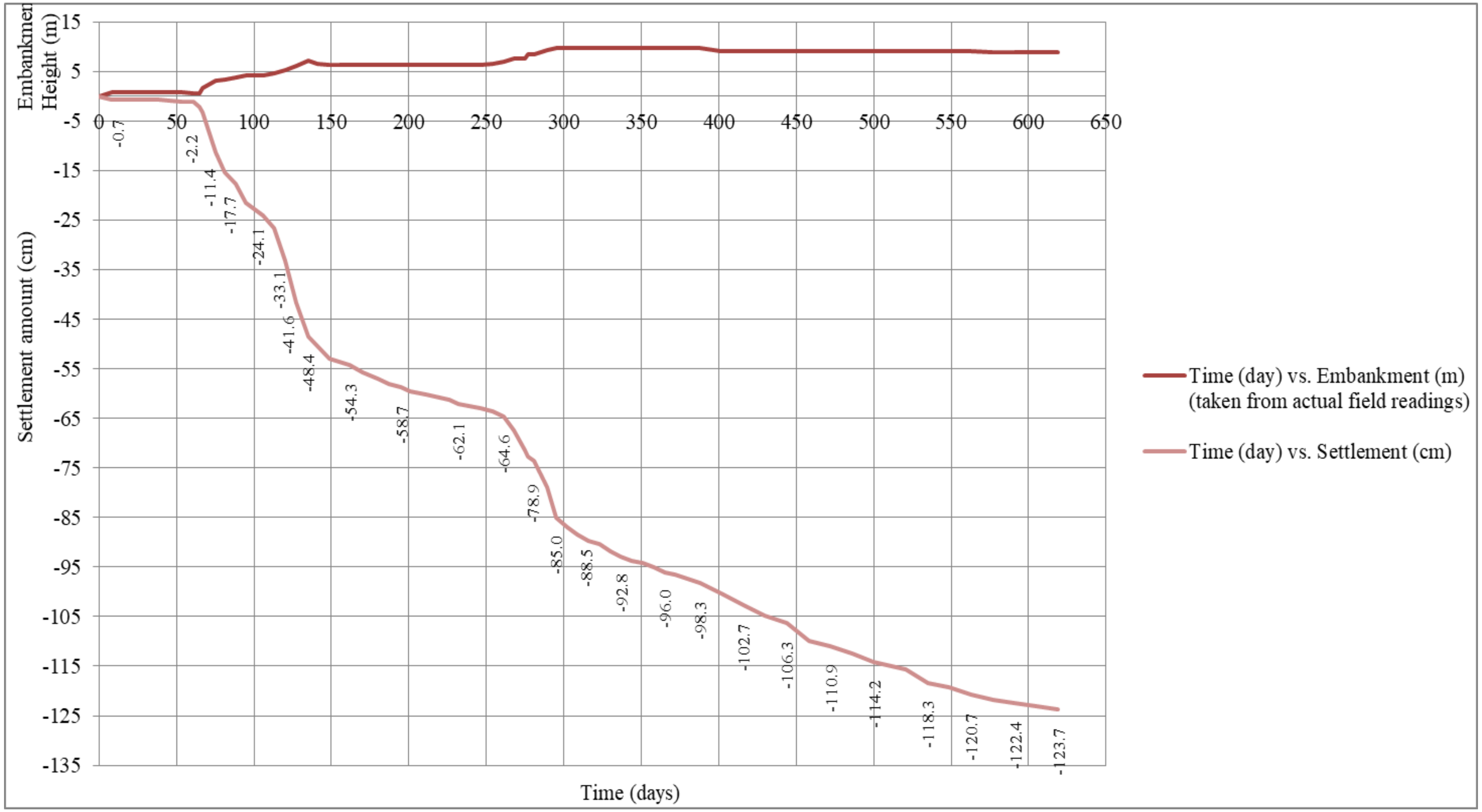

Figure 3.54. In situ Settlement (cm) vs. Time (day) behavior measured in embankment for surface settlement

3.17 KM: 152+000 Section

The soil profile of the embankment at Km: 152+000 is characterized by 15.45 m deep borehole (BSSK 464) and 24.60 m deep CPT (BS-CPT-14A). The laboratory test results and SPT N graphs are presented in Appendix A and B, consolidation settlement calculations are presented in Appendix C. The soil profile consists of the layers shown in Table 3.17:

Table 3.17 A typical soil profile at Km: 152+000 section of the study area

Depth (m)	Soil Profile	SPT N (av.)	q_c (av.) (MPa)	f_s (av.) (kPa)	PI (av.) (%)	w_N (av.) (%)	c_u (kPa)
-7.00	Medium-Stiff Clay (CL)	11	0.92		24	31	104
-9.00	Silt (ML)	13	1.96	16.80			
-13.00	Stiff Clay (CH)	18	0.94		46	32	82 115
-19.00	Sand (SM)	31	15.60	47.80			
-41.97	Medium-Stiff Clay (CL)		0.93				

The geological longitudinal section of embankment is presented in Figure 3.55. SPT results of BSSK-464 borehole and cone resistance values of BS-CPT-14 results for clay layers are presented in Figure 3.56. According to the geological longitudinal section, the embankment with 8.19 m in height is planned to be constructed on clayey soil with a thickness of more than 40.0 m, and also sand layers are defined at depths of 7.0 m – 9.0 m and 13.0 m – 19.0 m. Till to depth of 7.0 m, SPT N value is obtained as 11 whereas q_c value is obtained as 0.92 MPa in

average and clay unit is defined as “medium-stiff clay”. From depth of 9.0 m to 13.0 m, SPT N value is obtained as 18 whereas q_c value is obtained 0.94 MPa in average. The clay unit in this interval is defined as “stiff clay” according to SPT N values, “medium-stiff clay” according to q_c values. From depth of 19.0 m, q_c value is obtained as 0.93 MPa in average, which indicates “medium-stiff clay”. When the values of SPT N and q_c are compared, they both point out similar stiffness and also strength values for clay units defined in specified depth of intervals. The graph of In-Situ Settlement (m) vs. Time (day) behavior measured in the embankment for surface settlement plate is presented in Figure 3.57. The last measured settlement from surface settlement plate is 108.3 cm under embankment load with a maximum height of 8.19 m after 590 days of measurement.

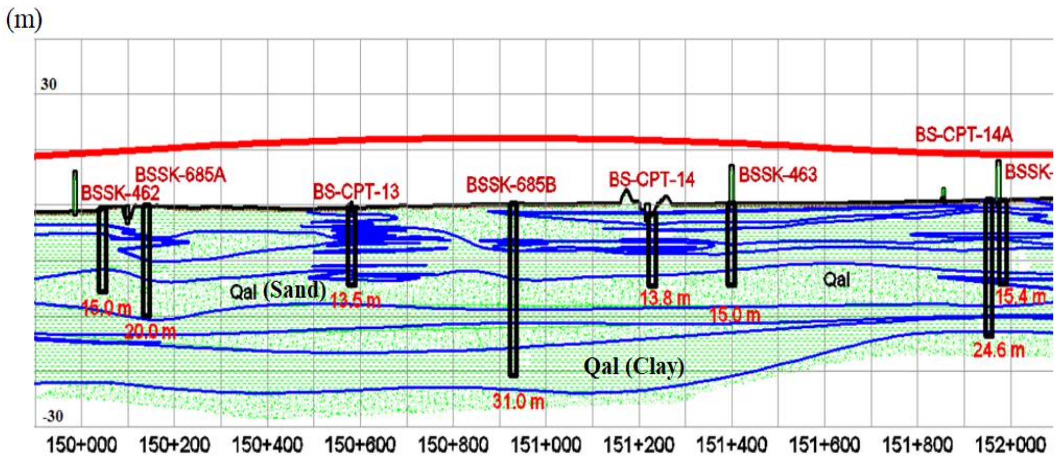

Figure 3.55. The longitudinal geological section of Km: 152+000

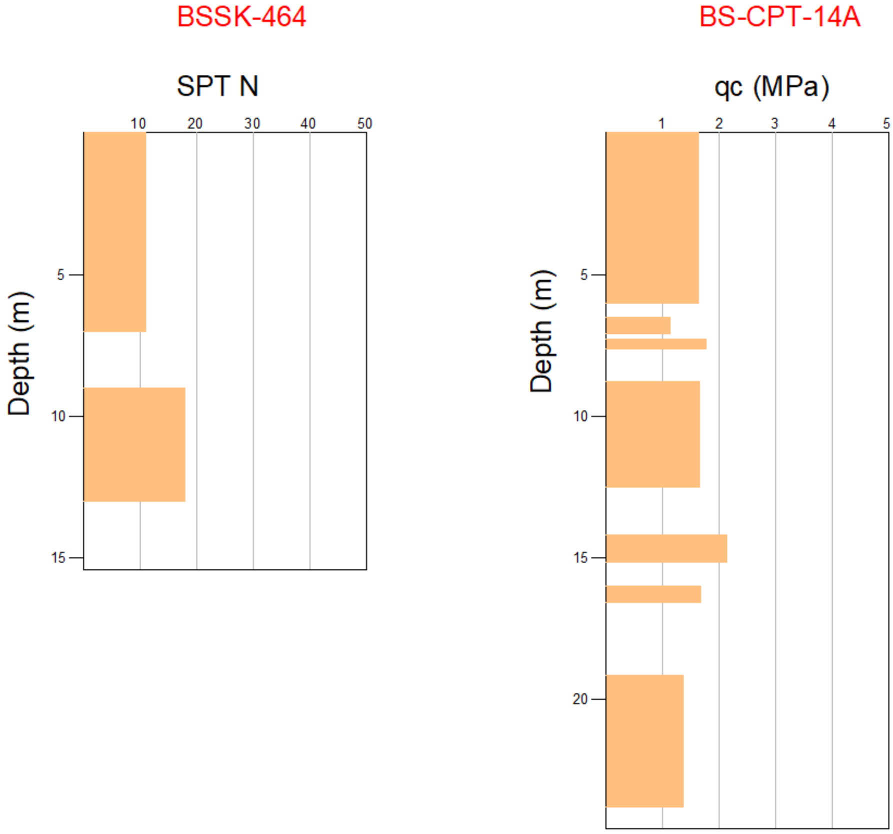

Figure 3.56. SPT N vs. Depth (m) and q_c (MPa) vs. Depth (m) graphs for clay layers

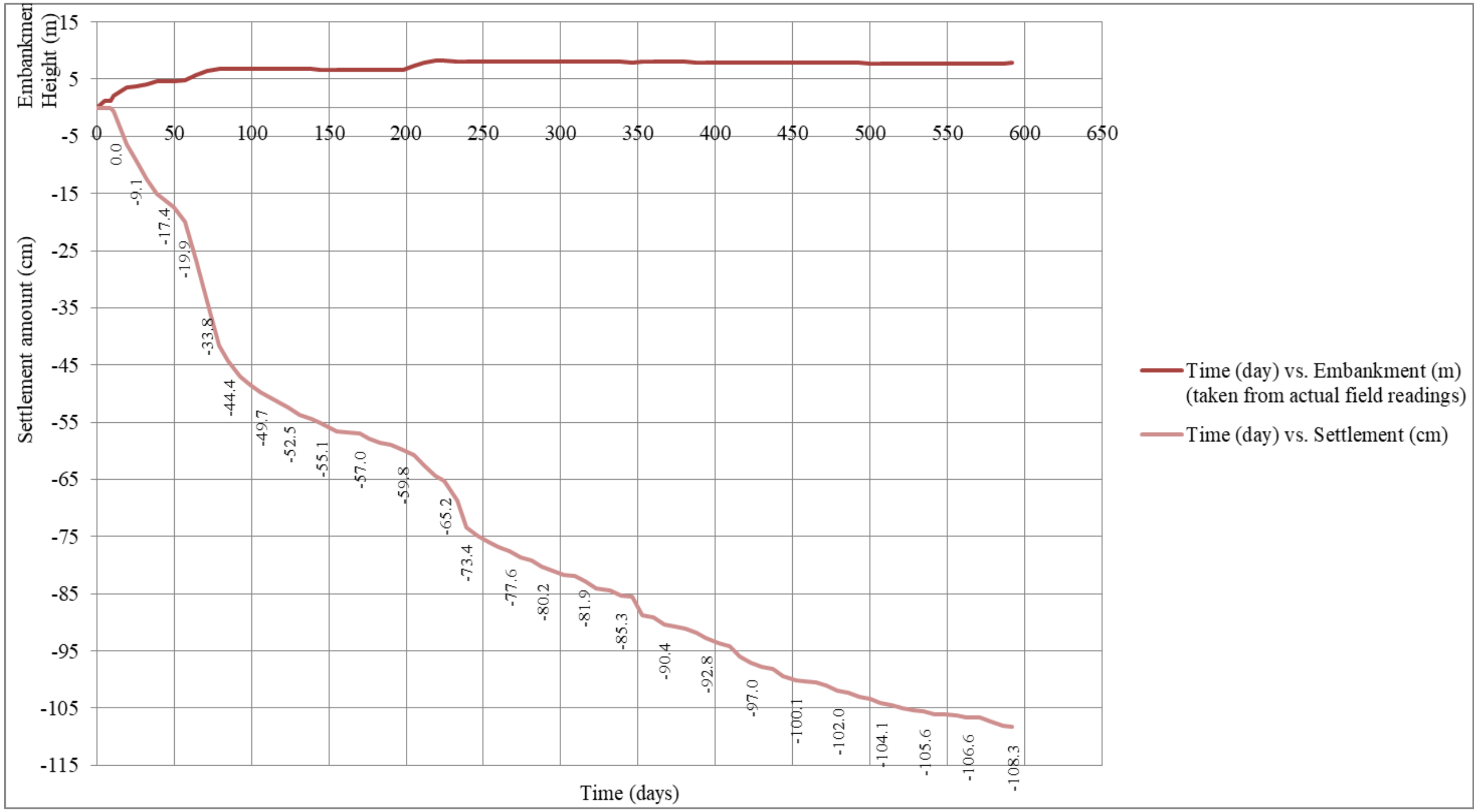

Figure 3.57. In situ Settlement (cm) vs. Time (day) behavior measured in embankment for surface settlement

3.18 KM: 154+500 Section

The soil profile of the embankment at Km: 154+500 is characterized by 15.45 m deep borehole (BSSK 468), 20.5 m deep borehole (BSSK 688), 15.06 m deep borehole (BSSK 469) and 28.10 m deep CPT (BS-CPT-17). The laboratory test results and SPT N graphs are presented in Appendix A and B, consolidation settlement calculations are presented in Appendix C. The soil profile consists of the layers shown in Table 3.18:

Table 3.18 A typical soil profile at Km: 154+500 section of the study area

Depth (m)	Soil Profile		SPT N (av.)	q_c (av.) (MPa)	f_s (av.) (kPa)	PI (av.) (%)	w_N (av.) (%)	c_u (kPa)
-6.00	Medium-Stiff Clay (CL)		13	1.62		21	35	108
-13.00	Stiff Clay (CL)		16	1.31		28	29	85 86 41
-16.00	Silt (ML)		R	6.78	60.01	NP		
-40.45	Stiff Clay (CH)		24	1.59		40	46	79 61

The geological longitudinal section of embankment is presented in Figure 3.58. SPT results of BSSK-688, BSSK-469 boreholes and cone resistance values of BS-CPT-17 results for clay layers are presented in Figure 3.59. According to the geological longitudinal section, the embankment with 7.48 m in height is planned to be constructed on clayey soil with a thickness of more than 40.0 m, and also non plastic silt layer is defined at depth of 13.0 m – 16.0 m. Till to depth of 6.0 m, SPT N value is obtained as 13 whereas q_c value is obtained as 1.62 MPa in average and clay unit is defined as “medium-stiff clay” according to SPT N values. On the other hand, if q_c values are considered, clay unit is defined as “stiff clay”. From depth of 6.0 m to 13.0 m, SPT N value is obtained as 16 whereas q_c value is obtained 1.31 MPa in average. The clay unit in this interval is defined as “stiff clay”. From depth of 16.0 m, SPT N value is obtained as 24 and q_c value is obtained as 1.59 MPa in average, which indicates “stiff clay”. When the values of SPT N and q_c are compared, they both point out similar stiffness and also strength values for clay units defined in specified depth of intervals. The graph of In-Situ Settlement (m) vs. Time (day) behavior measured in the embankment for surface settlement plate is presented in Figure 3.60. The last measured settlement from surface settlement plate is 96.1 cm under embankment load with a maximum height of 7.48 m after 640 days of measurement.

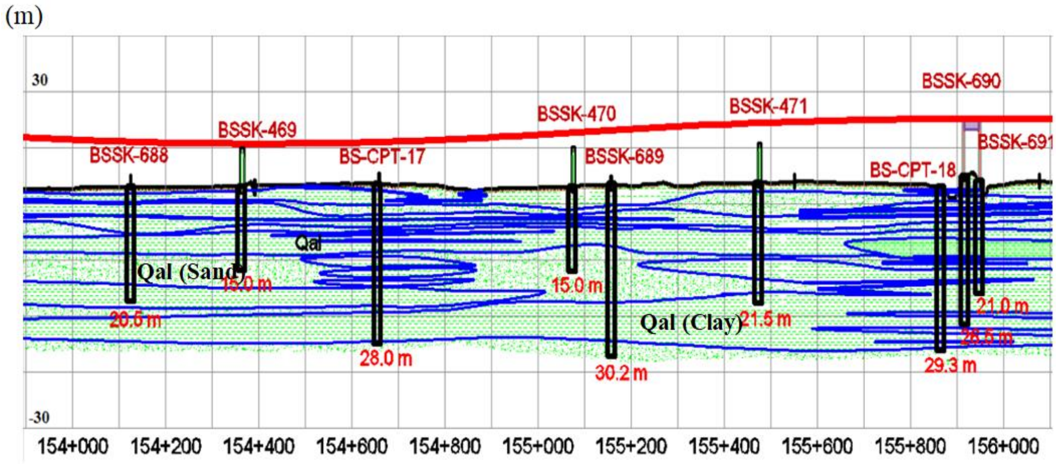

Figure 3.58. The longitudinal geological section of Km: 154+500

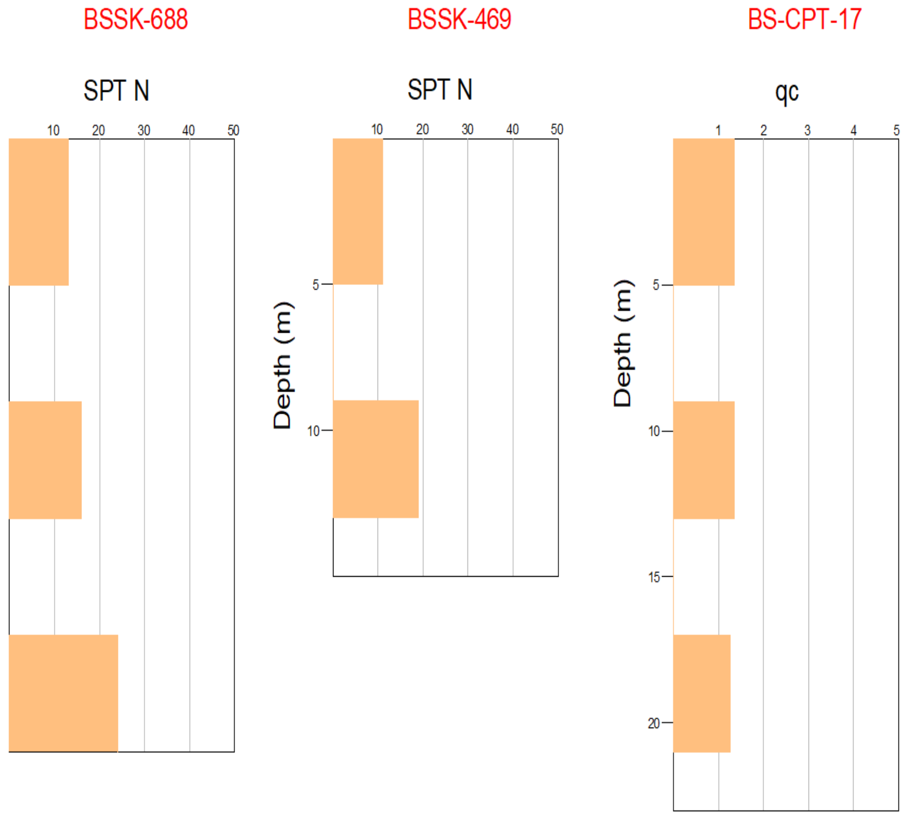

Figure 3.59. SPT N vs. Depth (m) and q_c (MPa) vs. Depth (m) graphs for clay layers

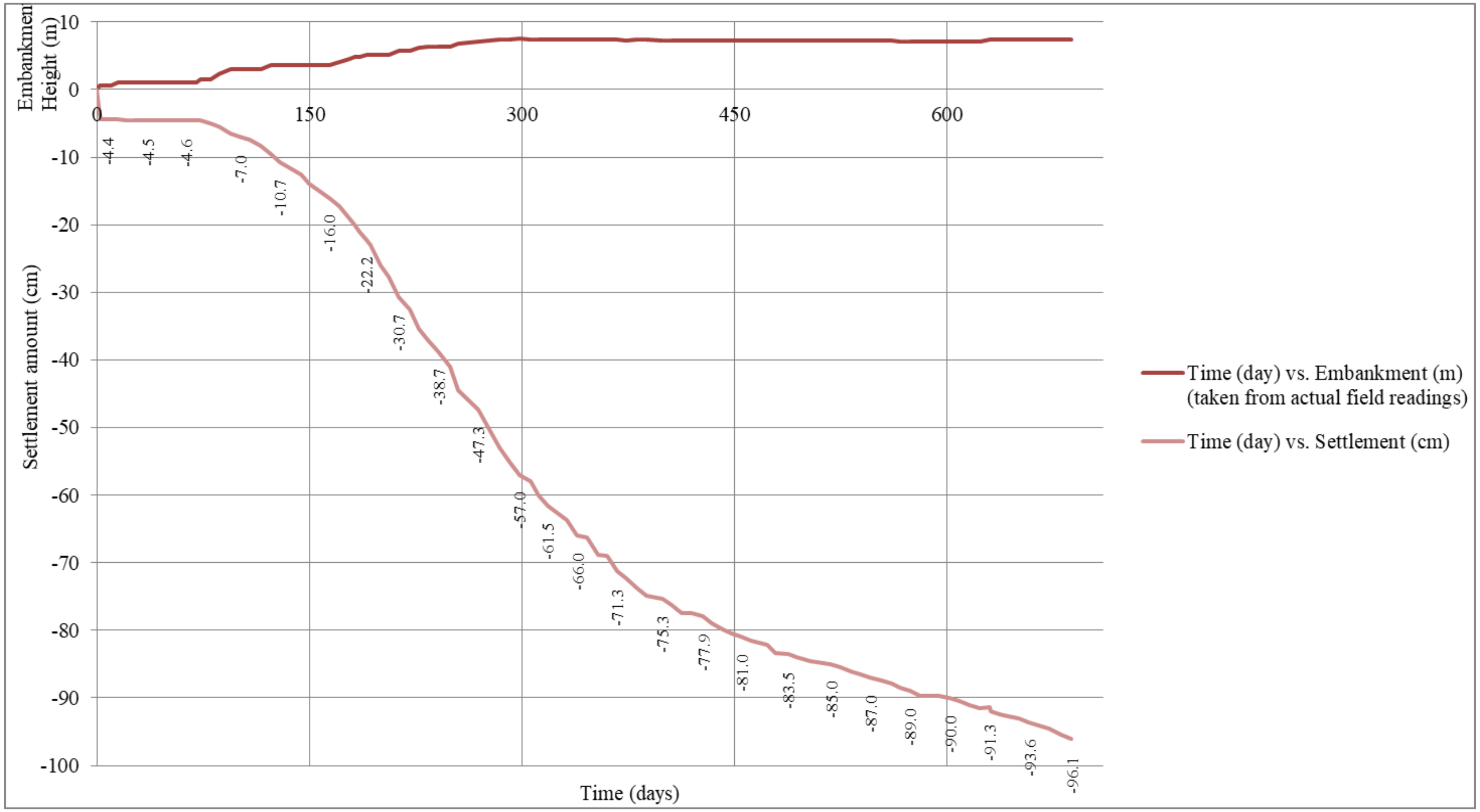

Figure 3.60. In situ Settlement (cm) vs. Time (day) behavior measured in embankment for surface settlement

3.19 KM: 155+000 Section

The soil profile of the embankment at Km: 155+000 is characterized by 30.20 m deep borehole (BSSK 689), 15.08 m deep borehole (BSSK470) and 28.10 m deep CPT (BS-CPT-17). The laboratory test results and SPT N graphs are presented in Appendix A and B, consolidation settlement calculations are presented in Appendix C. The soil profile consists of the layers shown in Table 3.19:

Table 3.19 A typical soil profile at Km: 155+000 section of the study area

Depth (m)	Soil Profile	SPT N (av.)	q_c (av.) (MPa)	f_s (av.) (kPa)	PI (av.) (%)	w_N (av.) (%)	c_u (kPa)
-3.00	Soft Clay (CL)	7	1.62		19	32	
-4.50	Sand (SC)	27	3.45	41.79	34	26	
-12.00	Stiff Clay (CL)	15	1.23		17	32	76
-20.00	Silt (ML)	R	6.78	60.01			
-28.00	Stiff Clay (CH)	24	1.59		40	46	79 61
-31.00	Sand (SM)	R	21.00	56.00			
-44.59	Stiff Clay (CH)	16	1.45		40	46	

The geological longitudinal section of embankment is presented in Figure 3.61. SPT results of BSSK-689, 470 boreholes and cone resistance values of BS-CPT-17 results for clay layers are presented in Figure 3.62. According to the geological longitudinal section, the embankment with 9.5 m in height is planned to be constructed on clayey soil with a thickness of more than 35.0 m and also sand layers are defined at depths of 3.0 m – 4.5 m, 12.0 m – 20.0 m and 28.0 m – 31.0 m. Till to depth of 3.0 m, SPT N value is obtained as 7 whereas q_c value is obtained as 1.62 MPa in average and clay unit is defined as “soft clay” according to SPT N values. On the other hand, if q_c values are considered, clay unit is defined as “stiff clay”. From depth of 4.5 m to 12.0 m, SPT N value is obtained as 15 whereas q_c value is obtained 1.23 MPa in average. The clay unit in this interval is defined as “stiff clay”. In depth of interval 20.0 m and 28.0 m, SPT N value is obtained as 24 whereas q_c value is obtained 1.59 MPa in average. The clay unit in this interval is defined as “stiff clay”. From depth of 31.0 m, SPT N value is obtained as 16 whereas q_c value is obtained 1.45 MPa in average. The clay unit in this interval is defined as “stiff clay”. When the values of SPT N and q_c are compared, except from the first layer, they both point out similar stiffness and also strength values for clay units defined in specified depth of intervals.The graph of In-Situ Settlement (m) vs. Time (day) behavior measured in the embankment for surface settlement plate is presented in Figure 3.63. The last measured settlement from surface settlement plate is 107.1 cm under embankment load with a maximum height of 9.5 m after 600 days of measurement.

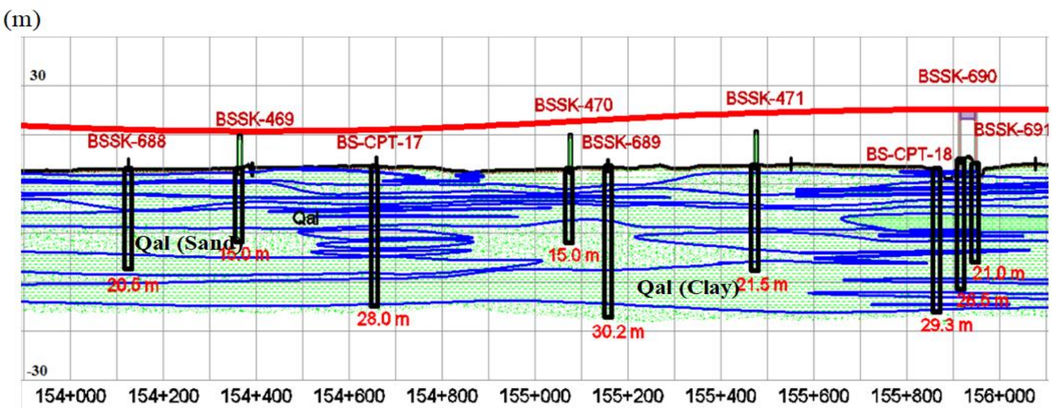

Figure 3.61. The longitudinal geological section of Km: 155+000

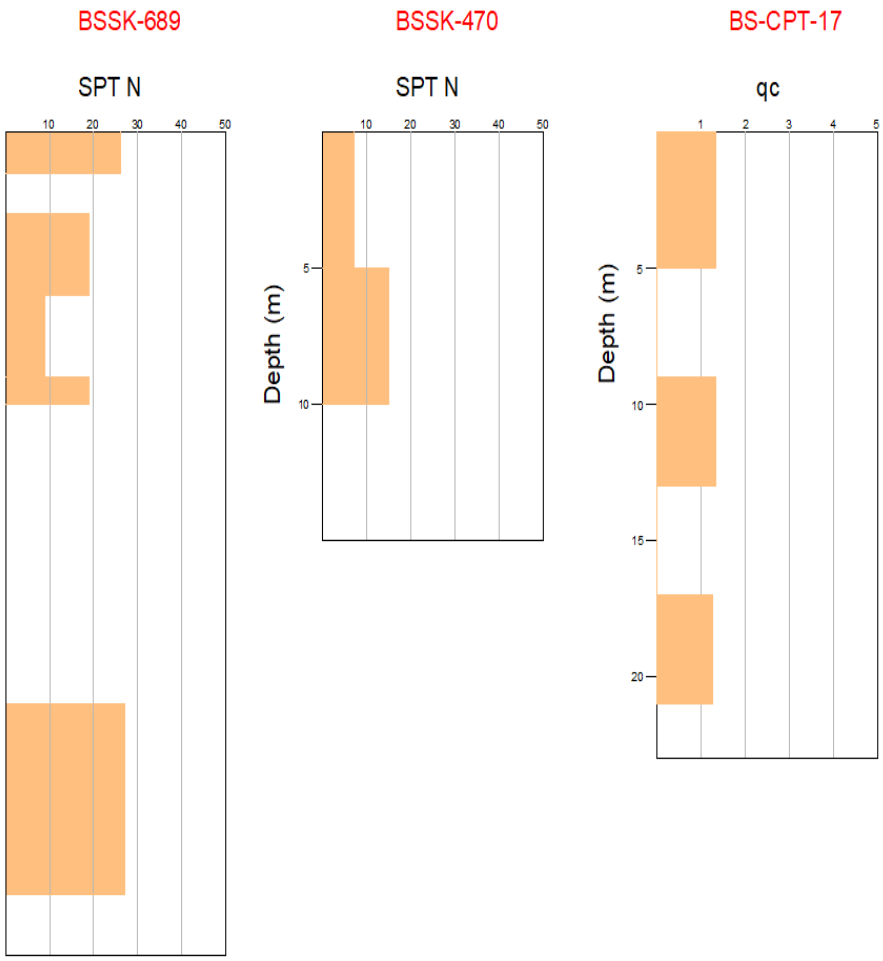

Figure 3.62. SPT N vs. Depth (m) and q_c (MPa) vs. Depth (m) graphs for clay layers

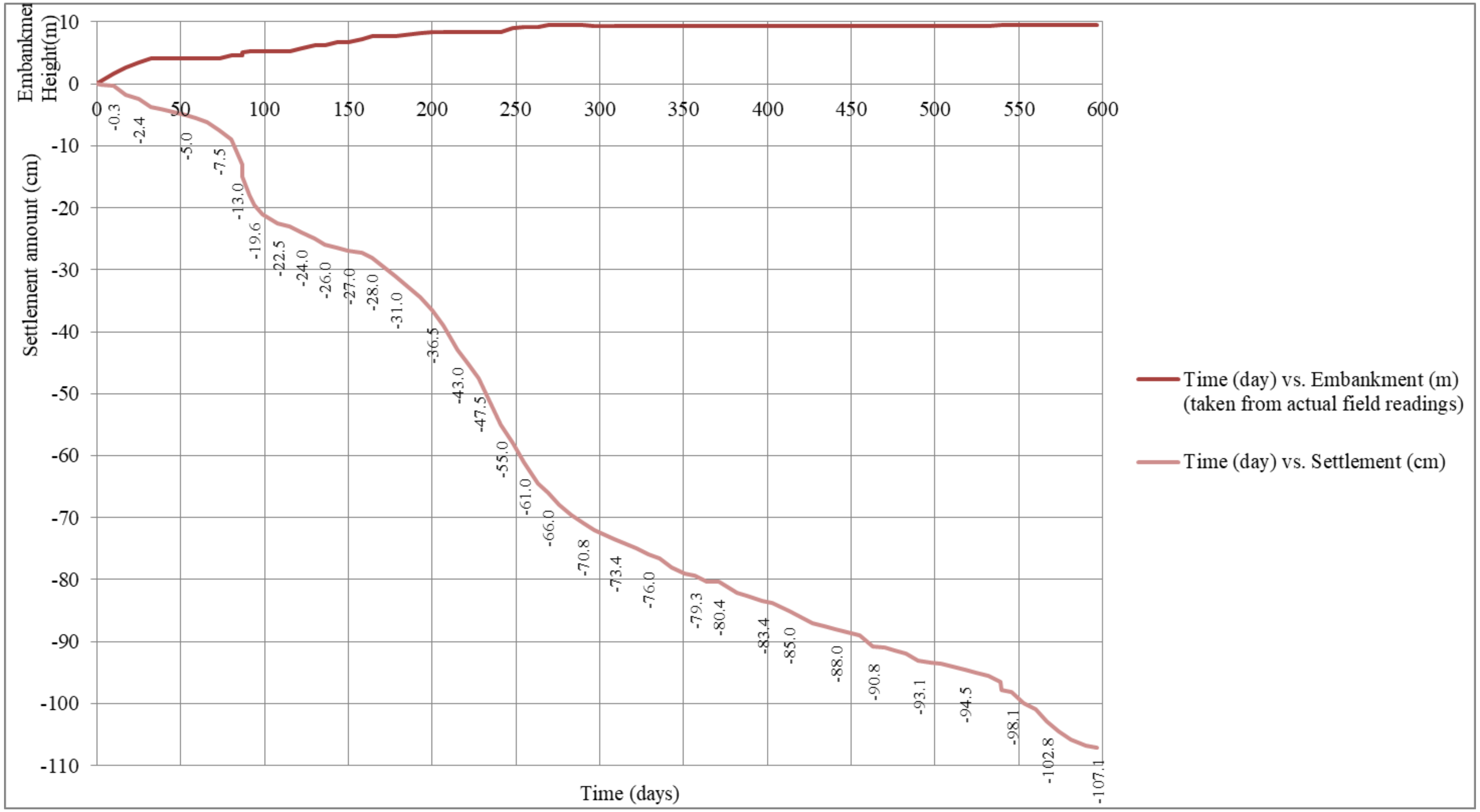

Figure 3.63. In situ Settlement (cm) vs. Time (day) behavior measured in embankment for surface settlement

3.20 KM: 155+551 Section

The soil profile of the embankment at Km: 155+551 is characterized by 21.45 m deep borehole (BSSK 471) and 29.30 m deep CPT (BS-CPT-18). The laboratory test results and SPT N graphs are presented in Appendix A and B, consolidation settlement calculations are presented in Appendix C. The soil profile consists of the layers shown in Table 3.20:

Table 3.20 A typical soil profile at Km: 155+551 section of the study area

Depth (m)	Soil Profile	SPT N (av.)	q_c (av.) (MPa)	f_s (av.) (kPa)	PI (av.) (%)	w_N (av.) (%)	c_u (kPa)
-6.00	Sand (SM)	24	5.15	49.32			
-17.00	Medium-Stiff Clay (CL)	13	1.49		38	34	85 91 100
-19.50	Sand (SM)	22	8.24	65.09			
-44.30	Stiff Clay (CH)	22	1.80		51	41	

The geological longitudinal section of embankment is presented in Figure 3.64. SPT results of BSSK-471 borehole and cone resistance values of BS-CPT-18 results for clay layers are presented in Figure 3.65. According to the geological longitudinal section, the embankment with 10.5 m in height is planned to be constructed on clayey soil with a thickness of more than 40.0 m and also sand layers are defined at depths of 0.0 m – 6.0 m and 17.0 m – 19.5 m. From depth of 6.0 m to 17.0 m, SPT N value is obtained as 13 whereas q_c value is obtained 1.49 MPa in average, which indicates “medium-stiff clay”. From depth of 19.5 m, SPT N value is obtained as 22 whereas q_c value is obtained 1.8 MPa in average, which indicates “stiff clay”. When the values of SPT N and q_c are compared, they both point out similar stiffness and also strength values for clay units defined in specified depth of intervals. The graph of In-Situ Settlement (m) vs. Time (day) behavior measured in the embankment for surface settlement plate is presented in Figure 3.66. The last measured settlement from surface settlement plate is 113.4 cm under embankment load with a maximum height of 10.5 m after 600 days of measurement.

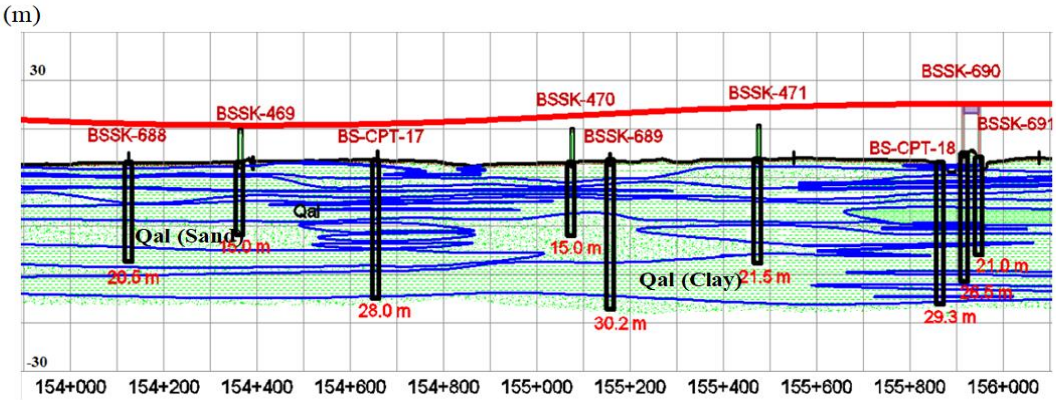

Figure 3.64. The longitudinal geological section of Km: 155+551

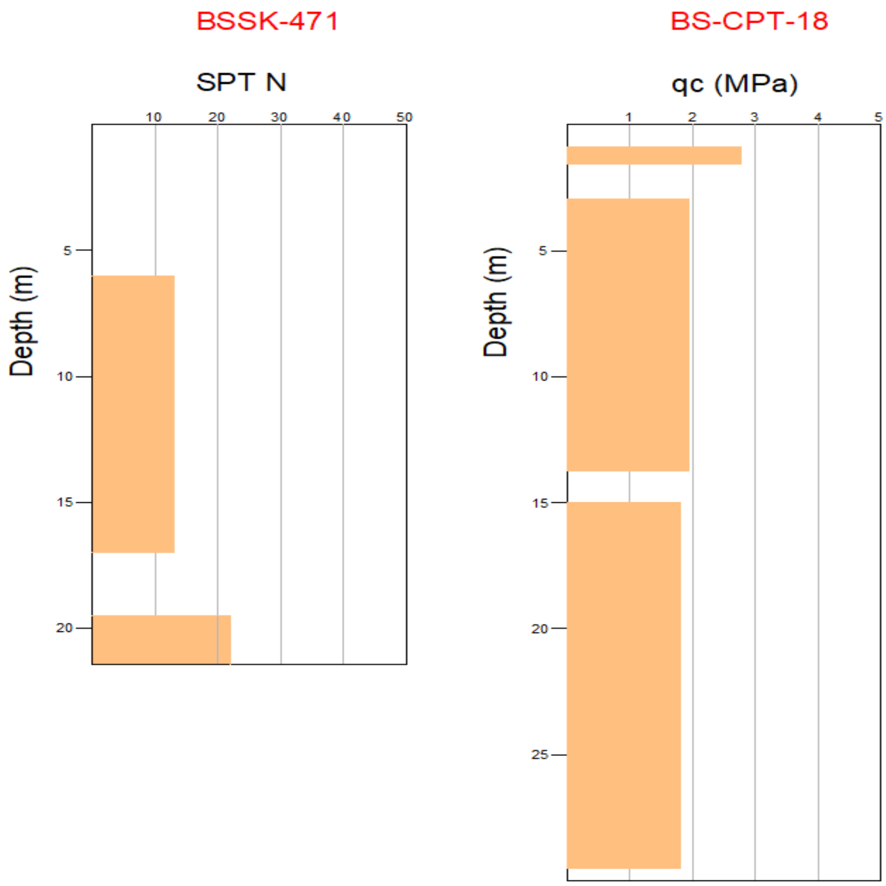

Figure 3.65. SPT N vs. Depth (m) and q_c (MPa) vs. Depth (m) graphs for clay layers

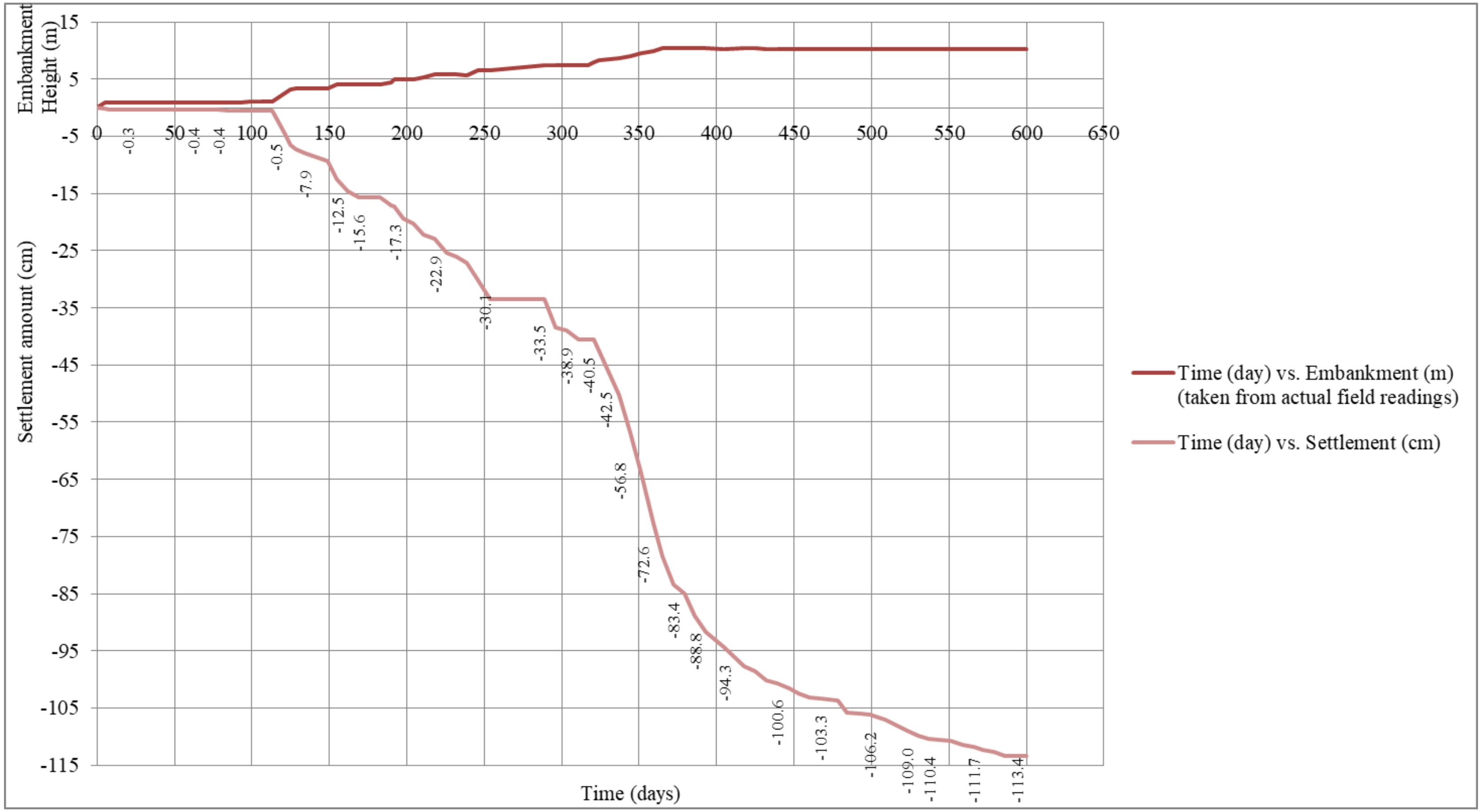

Figure 3.66. In situ Settlement (cm) vs. Time (day) behavior measured in embankment for surface settlement

3.21 KM: 157+400 Section

The soil profile of the embankment at Km: 157+400 is characterized by 25.95 m deep borehole (BSSK 474) and 29.00 m deep CPT (BS-CPT-19). The laboratory test results and SPT N graphs are presented in Appendix A and B, consolidation settlement calculations are presented in Appendix C. The soil profile consists of the layers shown in Table 3.21:

Table 3.21 A typical soil profile at Km: 157+400 section of the study area

Depth (m)	Soil Profile	SPT N (av.)	q_c (av.) (MPa)	f_s (av.) (kPa)	PI (av.) (%)	w_N (av.) (%)	c_u (kPa)
-2.00	Soft Clay (CH)	6	1.20		42	30	
-5.00	Stiff Clay (CL-ML)	14	1.41		42	33	
-7.00	Sand (SM-ML)	14	16.60	55.70	NP	25	
-42.65	Stiff Clay (CL-CH)	15	1.39		36	28	121 105

The geological longitudinal section of embankment is presented in Figure 3.67. SPT results of BSSK-474 borehole and cone resistance values of BS-CPT-19 results for clay layers are presented in Figure 3.68. According to the geological longitudinal section, the embankment with 8.5 m in height is planned to be constructed on clayey soil with a thickness of more than 40.0 m and also sand layers are defined at depth of 5.0 m – 7.0 m. Till to depth of 2.0 m, SPT N value is obtained as 6 whereas q_c value is obtained as 1.2 MPa in average. According to SPT N values, it is defined as “soft clay”. On the other hand, if q_c values are considered, it is defined as “medium-stiff clay”. From depth of 2.0 m to 5.0 m, SPT

N value is obtained as 14 whereas q_c value is obtained 1.41 MPa in average, which indicates “stiff clay”. From depth of 7.0 m, SPT N value is obtained as 15 whereas q_c value is obtained 1.39 MPa in average, which indicates “stiff clay”. When the values of SPT N and q_c are compared, except from the first layer, they both point out similar stiffness and also strength values for clay units defined in specified depth of intervals. The graph of In-Situ Settlement (m) vs. Time (day) behavior measured in the embankment for surface settlement plate is presented in Figure 3.69. The last measured settlement from surface settlement plate is 115.2 cm under embankment load with a maximum height of 8.5 m after 335 days of measurement.

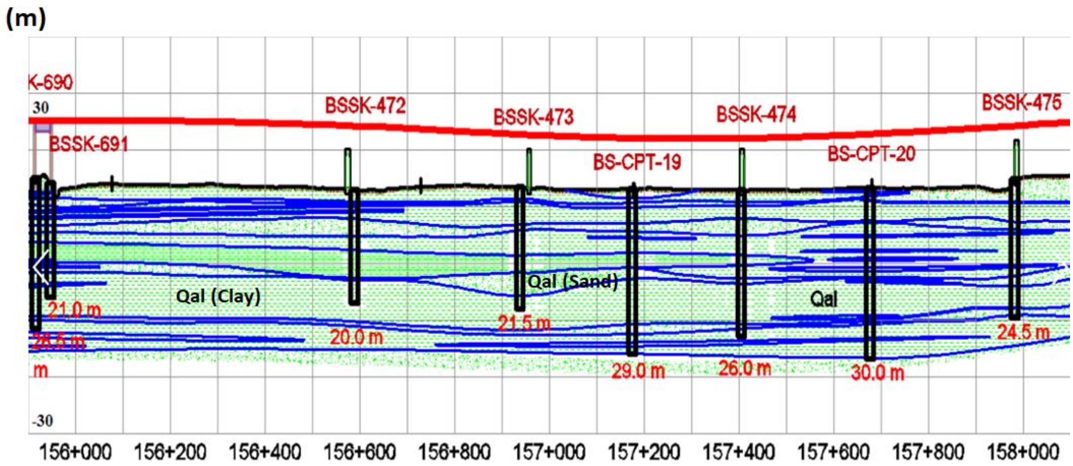

Figure 3.67. The longitudinal geological section of Km: 157+400

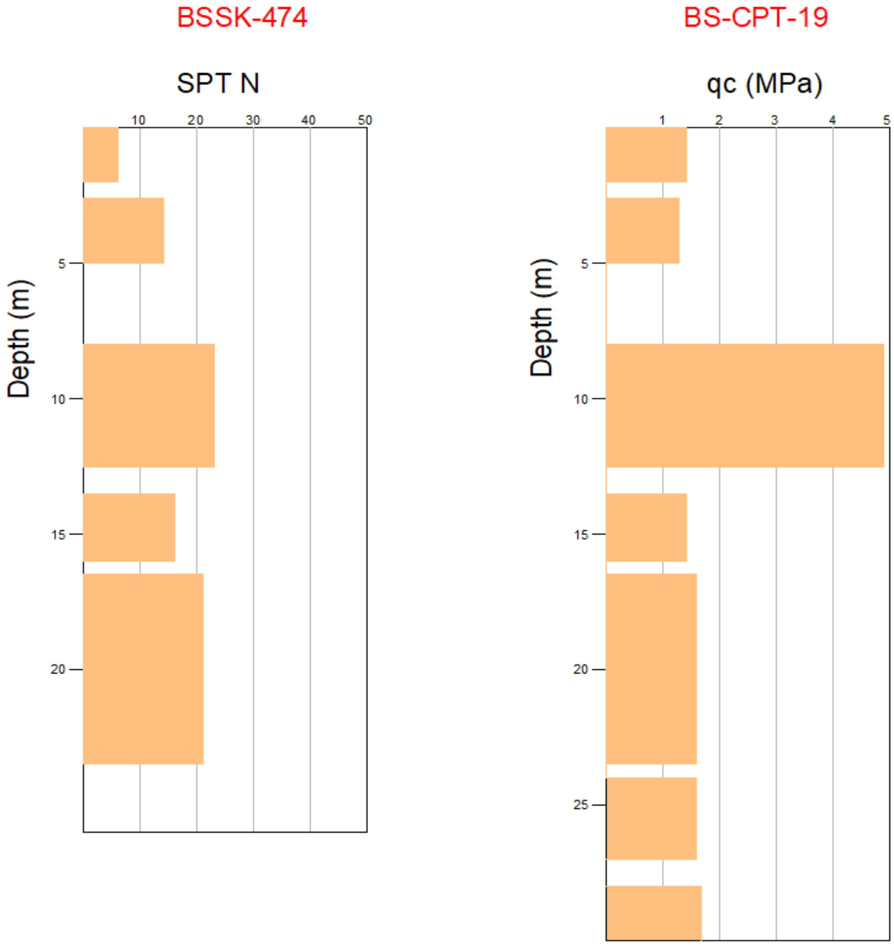

Figure 3.68. SPT N vs. Depth (m) and q_c (MPa) vs. Depth (m) graphs for clay layers

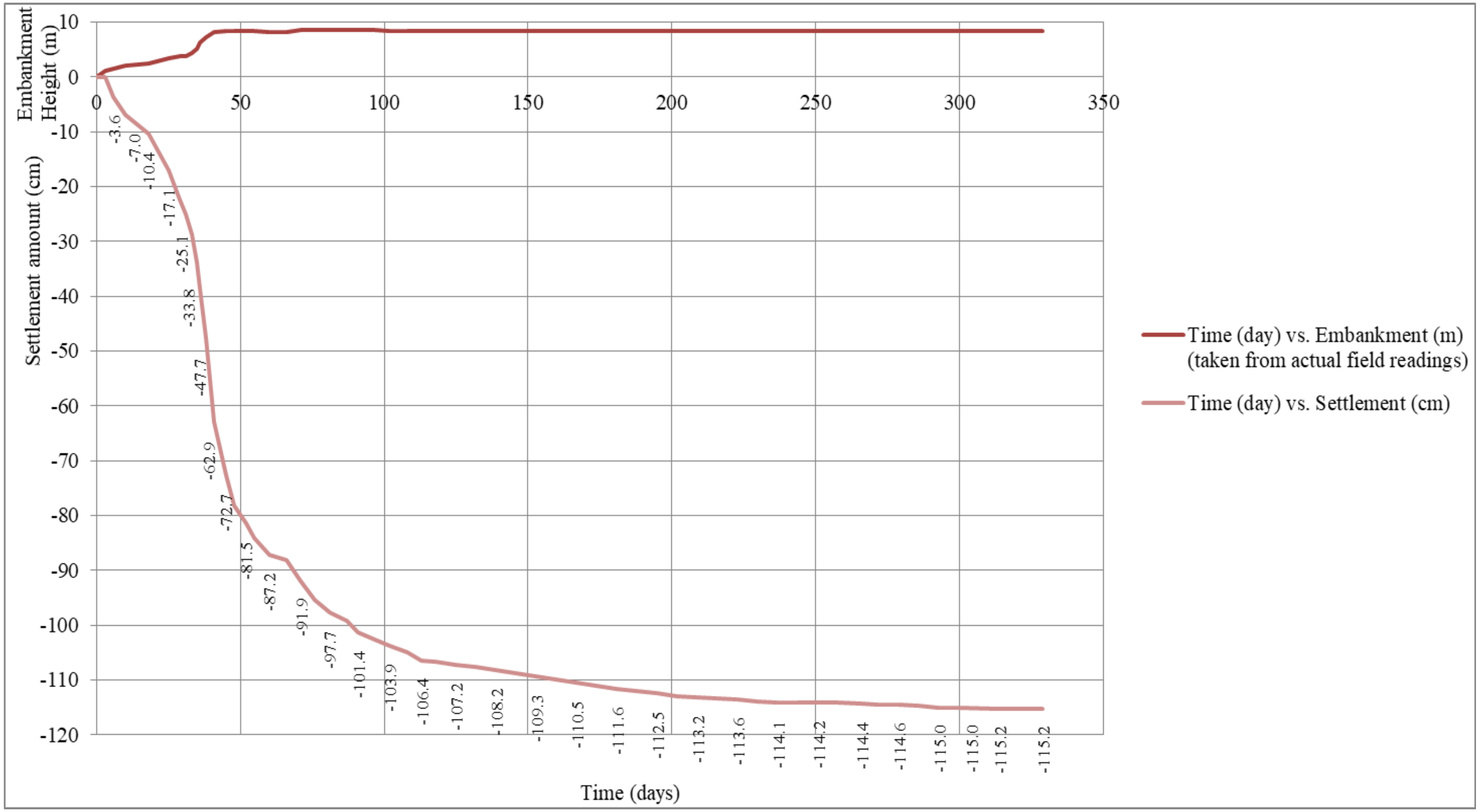

Figure 3.69. In situ Settlement (cm) vs. Time (day) behavior measured in embankment for surface settlement

3.22 KM: 158+000 Section

The soil profile of the embankment at Km: 158+000 is characterized by 24.45 m deep borehole (BSSK 475) and 29.84 m depth BS-CPT-20 test result. The laboratory test results and SPT N graphs are presented in Appendix A and B, consolidation settlement calculations are presented in Appendix C. The soil profile consists of the layers shown in Table 3.22:

Table 3.22 A typical soil profile at Km: 158+000 section of the study area

Depth (m)	Soil Profile	SPT N (av.)	q_c (av.) (MPa)	f_s (av.) (kPa)	PI (av.) (%)	w_N (av.) (%)	c_u (kPa)
-7.50	Medium-Stiff Clay (CL-ML)	11	1.15		18	23	
-9.00	Loose Sand (SM-ML)	8	5.90	32.70	NP	30	
-18.00	Stiff Clay (CH)	17	1.59		35	29	102
-19.50	Medium Dense Sand (SM)	21	1.52	80.80	NP	14	
-22.50	Stiff Clay (CH)	21	1.51		44	31	
-24.00	Medium Dense Sand (SM)	21	3.11	47.54	10	27	
-38.00	Stiff Clay (CL)	22	1.70		33	32	

The geological longitudinal section of embankment is presented in Figure 3.70. SPT results of BSSK-475 borehole and cone resistance values of BS-CPT-20 results for clay layers are presented in Figure 3.71. According to the geological longitudinal section, the embankment with 8.79 m in height is planned to be constructed on clayey soil with a thickness of more than 35.0 m, and also sand layers are defined at depths of 7.5 m – 9.0 m, 18.0 m – 19.5 m and 22.5 m – 24.0 m. Till to depth of 7.5 m, SPT N value is obtained as 11 whereas q_c value is obtained as 1.15 MPa in average and clay unit is defined as “medium-stiff clay”. From depth of 9.0 m to 18.0 m, SPT N value is obtained as 17 whereas q_c value is obtained 1.59 MPa in average, which indicates “stiff clay”. From depth of 19.5 m to 22.5 m, SPT N value is obtained as 21 whereas q_c value is obtained 1.51 MPa in average, which indicates “stiff clay”. From depth of 24.0 m, SPT N value is obtained as 22 whereas q_c value is obtained 1.70 MPa in average, which indicates “stiff clay”. When the values of SPT N and q_c are compared, they both point out similar stiffness and also strength values for clay units defined in specified depth of intervals. The graph of In-Situ Settlement (m) vs. Time (day) behavior measured in the embankment for surface settlement plate is presented in Figure 3.72. The last measured settlement from surface settlement plate is 108.1 cm under embankment load with a maximum height of 8.79 m after 440 days of measurement.

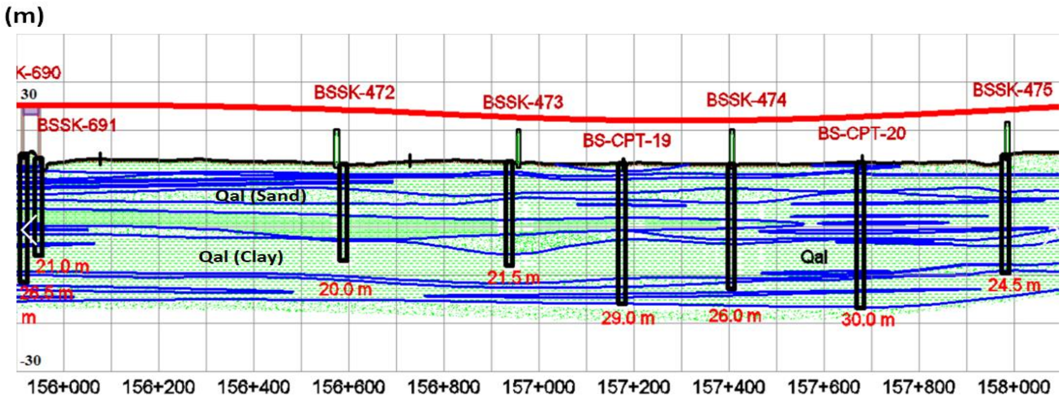

Figure 3.70. The longitudinal geological section of Km: 158+000

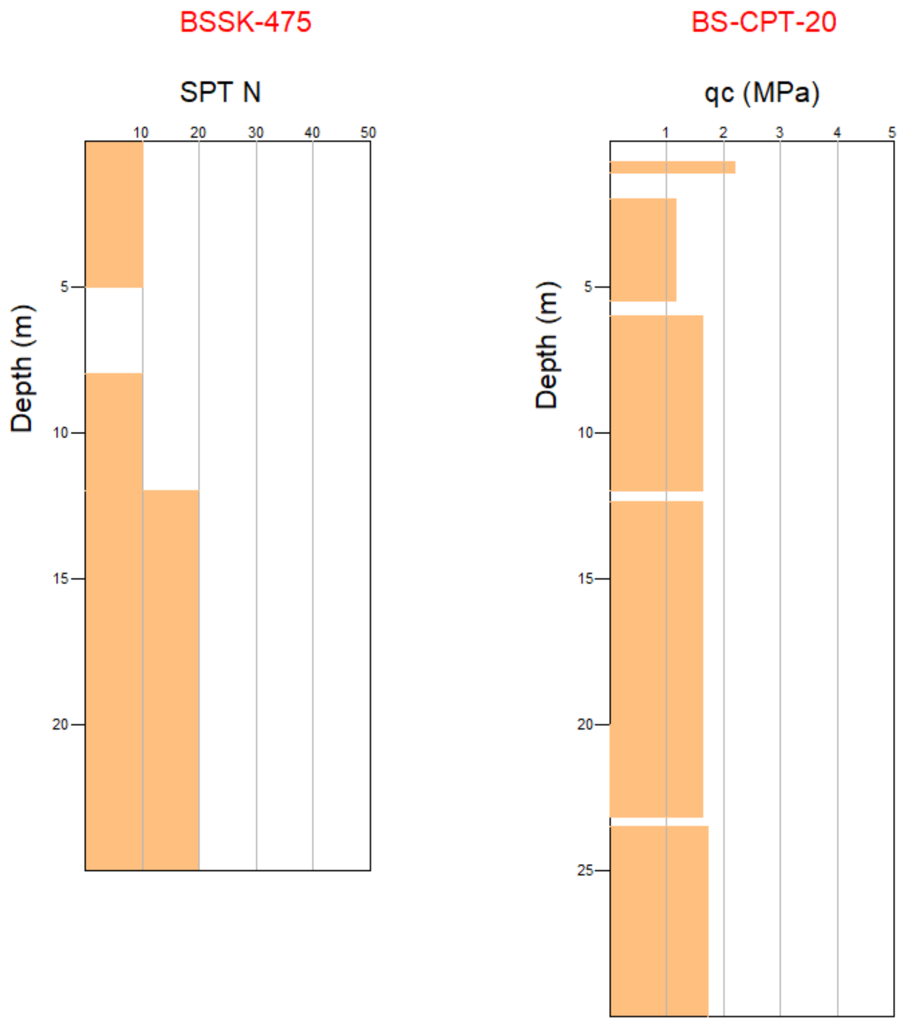

Figure 3.71. SPT N vs. Depth (m) and q_c (MPa) vs. Depth (m) graphs for clay layers

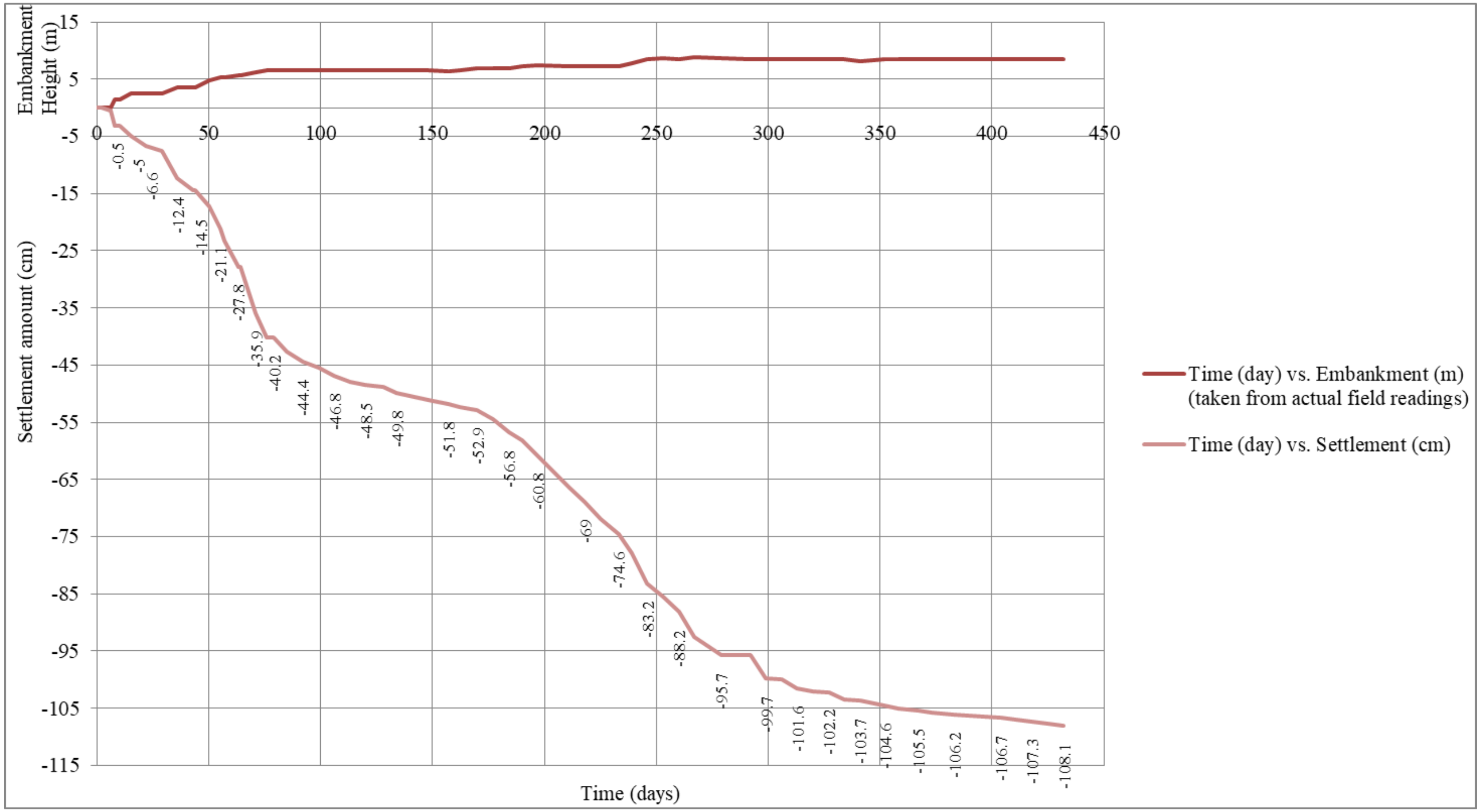

Figure 3.72. In situ Settlement (cm) vs. Time (day) behavior measured in embankment for surface settlement

3.23 KM: 159+565 Section

The soil profile of the embankment at Km: 159+565 is characterized by 21.45 m deep borehole (BSSK 477) and 31.1 m depth BS-CPT-22 test result. The laboratory test results and SPT N graphs are presented in Appendix A and B, consolidation settlement calculations are presented in Appendix C. The soil profile consists of the layers shown in Table 3.23:

Table 3.23 A typical soil profile at Km: 159+565 section of the study area

Depth (m)	Soil Profile	SPT N (av.)	q_c (av.) (MPa)	f_s (av.) (kPa)	PI (av.) (%)	w_N (av.) (%)	c_u (kPa)
-7.50	Dense Sand (SW-SM-SP)	38	14.60	57.80	NP	14	
-12.50	Medium Stiff-Stiff Clay (CL-CH)	12	1.24		23	29	84 114
-13.50	Sand		6.45	56.02			
-37.95	Stiff Clay (CL-CH-ML)	20	1.57		28	34	100

The geological longitudinal section of embankment is presented in Figure 3.73. SPT results of BSSK-477 borehole and cone resistance values of BS-CPT-22 results for clay layers are presented in Figure 3.74. According to the geological longitudinal section, the embankment with 7.2 m in height is planned to be constructed on clayey soil with a thickness of more than 35.0 m, and also sand layers are defined at depths of 0.0 m – 7.5 m and 12.5 m – 13.5 m. From depth of 7.5 m to 12.5 m, SPT N value is obtained as 12 whereas q_c value is obtained 1.24 MPa in average, which indicates “medium-stiff clay”. From depth of 13.5 m, SPT N value is obtained as 20 whereas q_c value is obtained 1.57 MPa in average, which indicates "stiff clay". When the values of SPT N and q_c are compared, they both point out similar stiffness and also strength values for clay units defined in specified depth of intervals. The graph of In-Situ Settlement (m) vs. Time (day) behavior measured in the embankment for surface settlement plate is presented in Figure 3.75. The last measured settlement from surface settlement plate is 80.5 cm under embankment load with a maximum height of 7.2 m after 480 days of measurement.

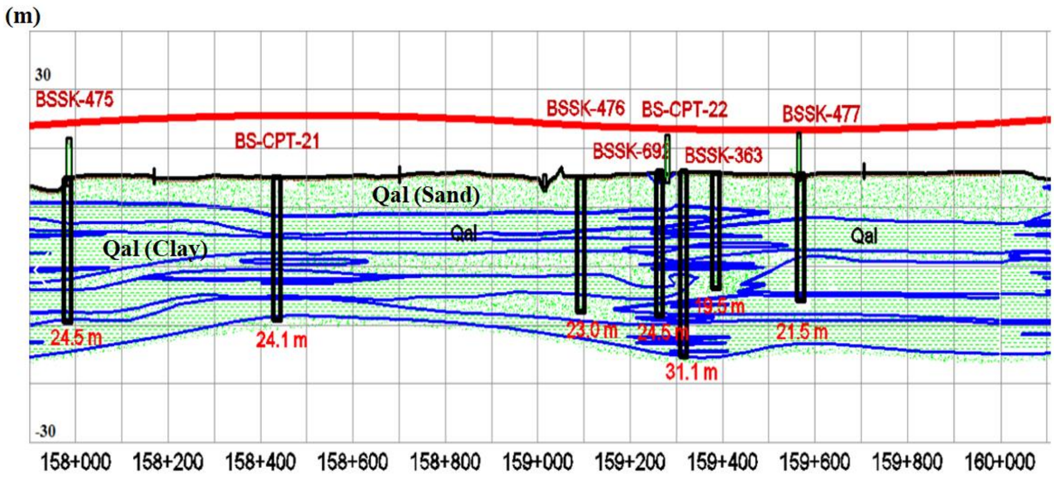

Figure 3.73. The longitudinal geological section of Km: 159+565

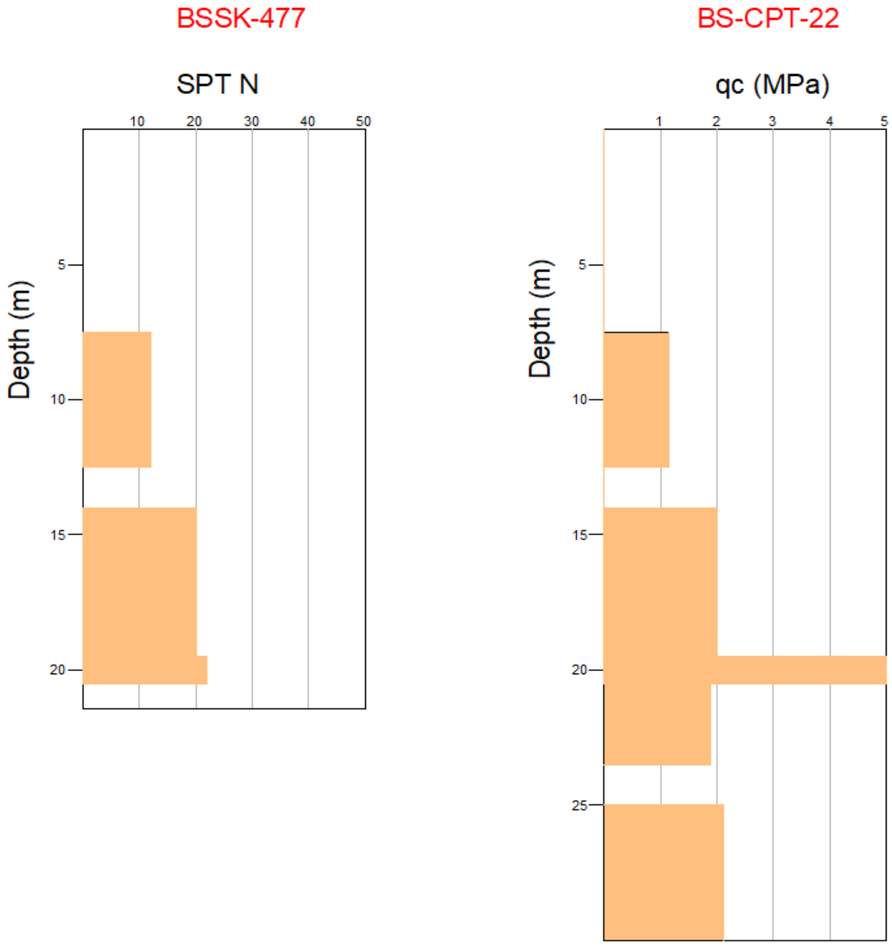

Figure 3.74. SPT N vs. Depth (m) and q_c (MPa) vs. Depth (m) graphs for clay layers

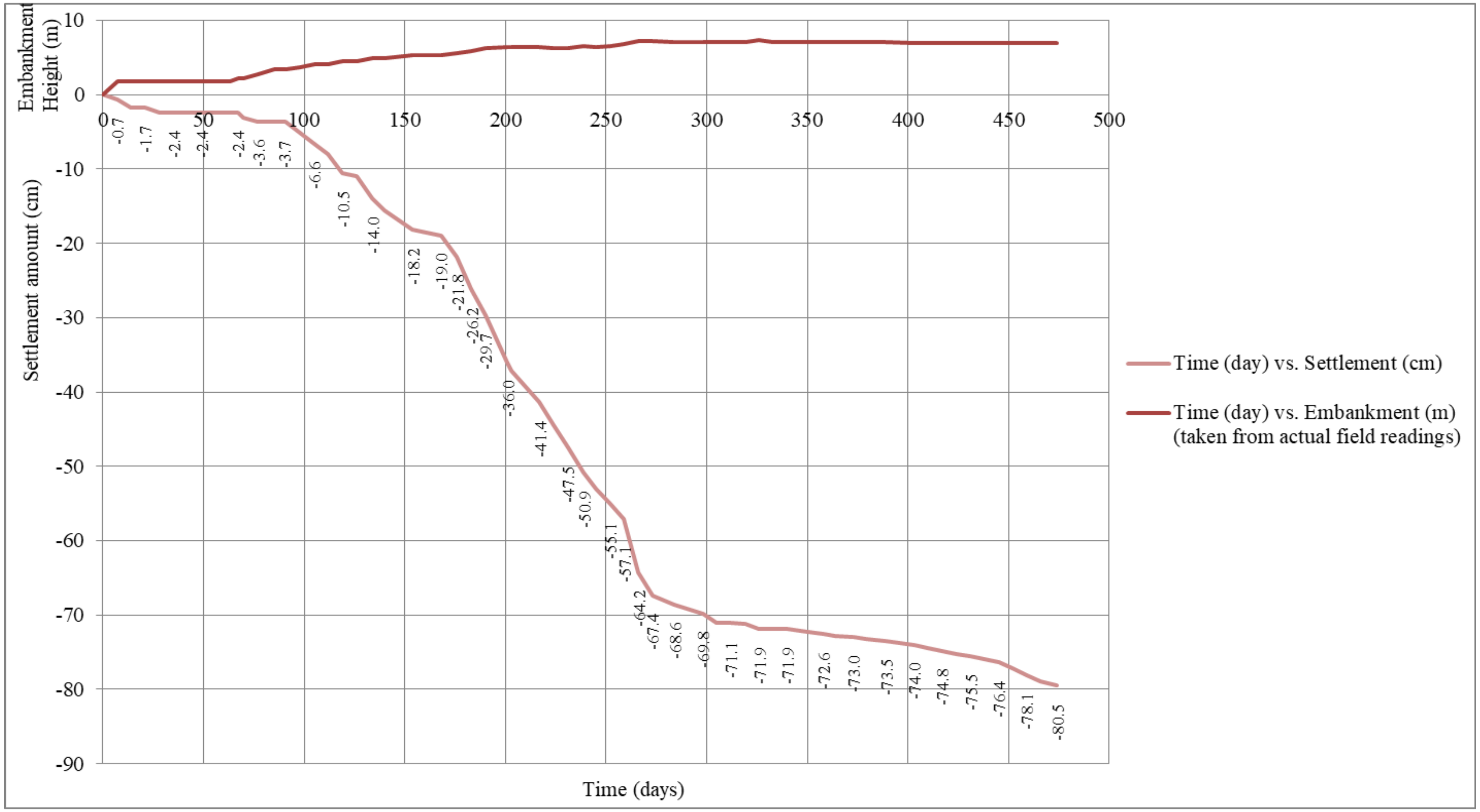

Figure 3.75. In situ Settlement (cm) vs. Time (day) behavior measured in embankment for surface settlement

3.24 KM: 161+764 Section

The soil profile of the embankment at Km: 161+764 is characterized by 18.09 m depth borehole (BSSK-480), 24.45 m depth borehole (BSSK-481) and 20.14 m depth CPT (BS-CPT-25). The laboratory test results and SPT N graphs are presented in Appendix A and B, consolidation settlement calculations are presented in Appendix C. The soil profile consists of the layers shown in Table 3.24:

Table 3.24 A typical soil profile at Km: 161+764 section of the study area

Depth (m)	Soil Profile	SPT N (av.)	q_c (av.) (MPa)	f_s (av.) (kPa)	PI (av.) (%)	w_N (av.) (%)	c_u (kPa)
-4.00	Medium Dense Sand (SM-SC)	23	4.21	39.25			
-6.00	Stiff Clay (CL)	17	0.89		12	25	
-9.00	Medium Dense Sand (SM)	21	3.93	72.87	NP	25	82
-11.00	Stiff Clay (CL)	20	1.29		25	26	
-19.00	Medium Dense Sand (SM)	R	5.30	44.76	NP	12	
-38.14	Stiff Clay (CH-CL)		1.52				

The geological longitudinal section of embankment is presented in Figure 3.76. SPT results of BSSK-480, BSSK-481 boreholes and cone resistance values of BS-CPT-24 results for clay layers are presented in Figure 3.77. According to the geological longitudinal section, the embankment with 6.5 m in height is planned to be constructed on clayey soil with a thickness of more than 35.0 m and also sand layers are defined at depths of 0.0 m – 4.0 m, 6.0 m – 9.0 m and 11.0 m – 19.0 m. From depth of 4.0 m to 6.0 m, SPT N value is obtained as 17 whereas q_c value is obtained 0.89 MPa in average. According to SPT N values, clay unit is defined as "stiff clay". On the other hand, when qc values are taken into account, it is defined as "medium-stiff clay". From depth of 9.0 m to 11.0 m, SPT N value is obtained as 20 whereas q_c value is obtained 1.29 MPa in average, which indicates "stiff clay". From depth of 19.0 m, q_c value is obtained 1.52 MPa in average, which indicates "stiff clay". When the values of SPT N and q_c are compared, they both point out similar stiffness and also strength values for clay units defined in specified depth of intervals. The graph of In-Situ Settlement (m) vs. Time (day) behavior measured in the embankment for surface settlement plate is presented in Figure 3.78. The last measured settlement from surface settlement plate is 81.9 cm under embankment load with a maximum height of 6.5 m after 590 days of measurement.

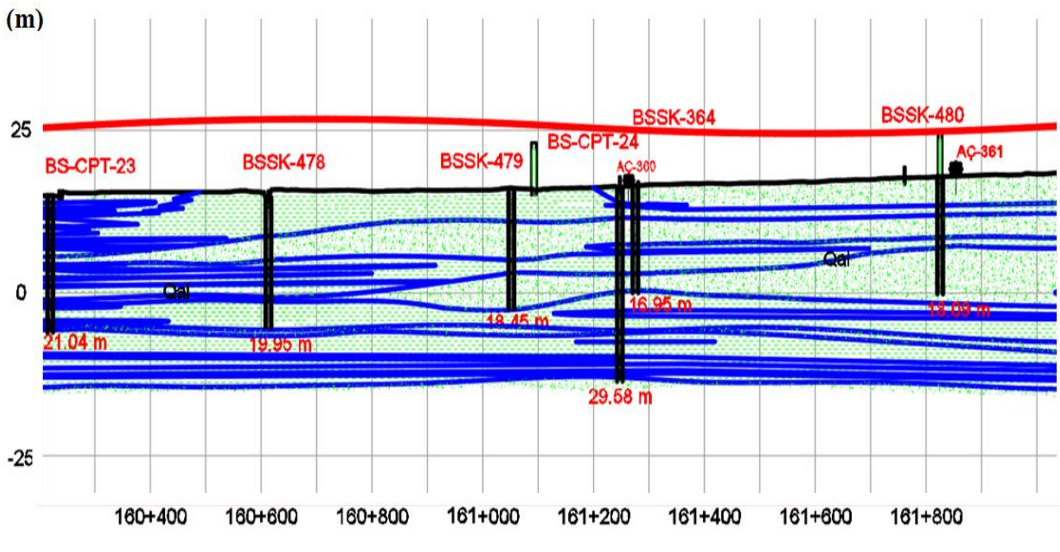

Figure 3.76. The longitudinal geological section of Km: 161+764

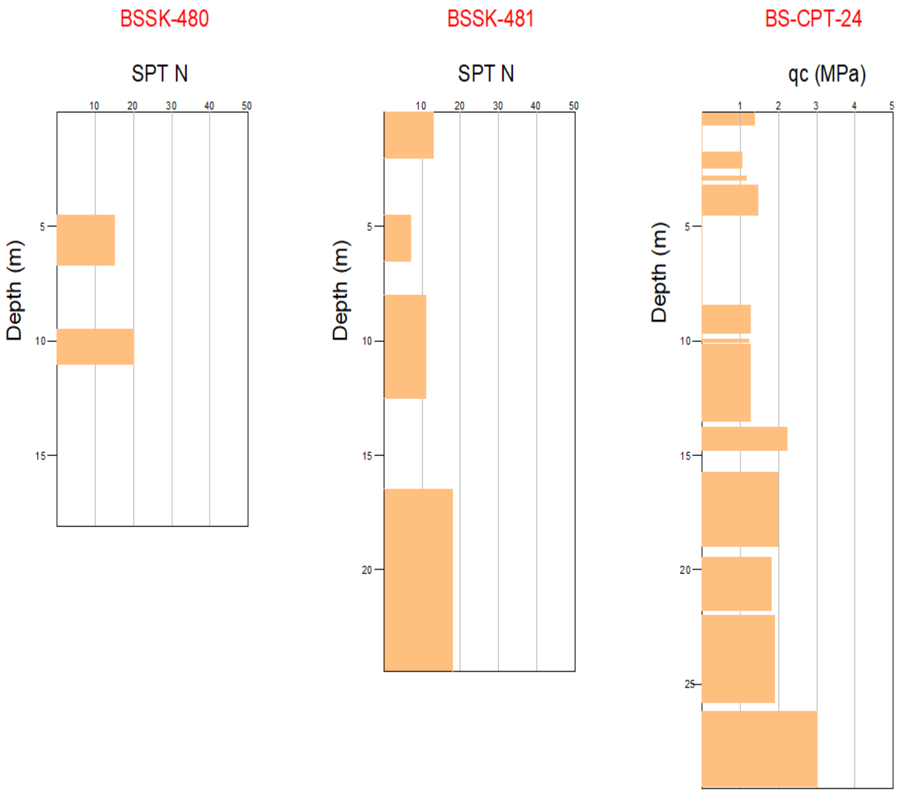

Figure 3.77. SPT N vs. Depth (m) and q_c (MPa) vs. Depth (m) graphs for clay layers

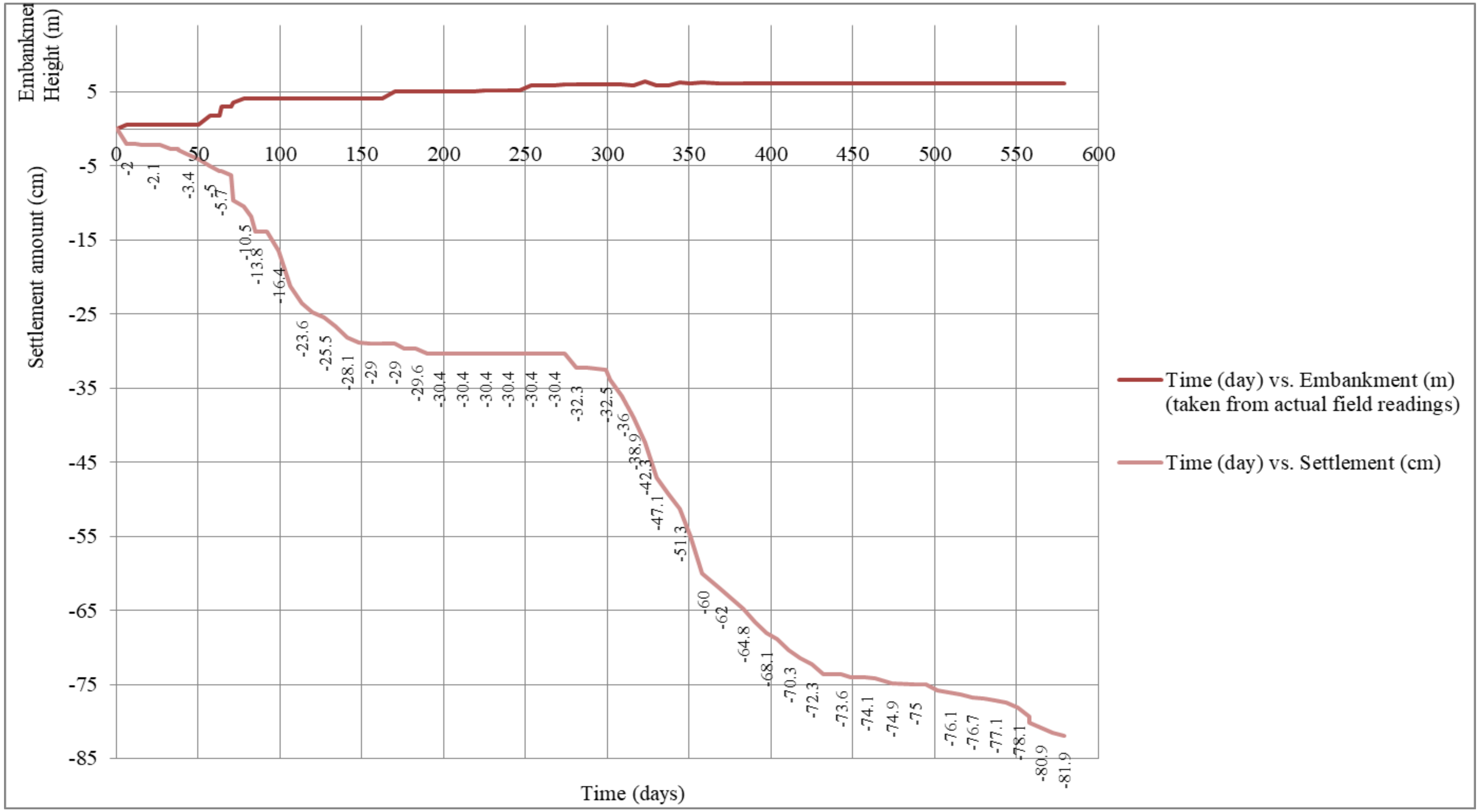

Figure 3.78. In situ Settlement (cm) vs. Time (day) behavior measured in embankment for surface settlement

3.25 KM: 162+555 Section

The soil profile of the embankment at Km: 162+555 is characterized by 24.45 m depth borehole (BSSK-481) and 20.14 m depth CPT (BS-CPT-25). The laboratory test results and SPT N graphs are presented in Appendix A and B, consolidation settlement calculations are presented in Appendix C. The soil profile consists of the layers shown in Table 3.25:

Table 3.25 A typical soil profile at Km: 162+555 section of the study area

Depth (m)	Soil Profile	SPT N (av.)	q_c (av.) (MPa)	f_s (av.) (kPa)	PI (av.) (%)	w_N (av.) (%)	c_u (kPa)
-2.00	Medium-Stiff Clay (CL)	13	0.88		17	19	
-4.50	Medium Dense Sand (SM)	21	4.21	39.25			
-6.50	Soft Clay (CL)	7	0.89		13	21	56
-8.00	Medium Dense Sand (SM)	21	3.93	72.87	NP	16	
-12.50	Medium-Stiff Clay (CL)	11	1.29		18	23	82
-16.50	Medium Dense Sand (SM)	25	5.30	44.76	NP	23	
-28.50	Medium-Stiff Clay (CL-CH)	12	1.28		36	29	

The geological longitudinal section of embankment is presented in Figure 3.79. SPT results of BSSK-481 borehole and cone resistance values of BS-CPT-25 results for clay layers are presented in Figure 3.80. According to the geological longitudinal section, the embankment with 9.2 m in height is planned to be constructed on clayey soil with a thickness of more than 25.0 m, and also sand layers are defined at depths of 2.0 m – 4.5 m, 6.5 m – 8.0 m and 12.5 m – 16.5 m. Till to depth of 2.0 m, SPT N value is obtained as 13 whereas q_c value is obtained as 0.88 MPa in average and clay unit is defined as "medium-stiff clay". From depth of 4.5 m to 6.5 m, SPT N value is obtained as 7 whereas q_c value is obtained 0.89 MPa in average, which indicates "soft clay" according to SPT N values and "medium-stiff clay" according to q_c values. From depth of 8.0 m to 12.5 m, SPT N value is obtained as 11 whereas q_c value is obtained 1.29 MPa in average, which indicates "medium-stiff clay". From depth of 16.5 m, SPT N value is obtained as 12 whereas q_c value is obtained 1.28 MPa in average, which indicates "medium-stiff clay". When the values of SPT N and q_c are compared, they both point out similar stiffness and also strength values for clay units defined in specified depth of intervals. The graph of In-Situ Settlement (m) vs. Time (day) behavior measured in the embankment for surface settlement plate is presented in Figure 3.81. The last measured settlement from surface settlement plate is 103.2 cm under embankment load with a maximum height of 9.2 m after 540 days of measurement.

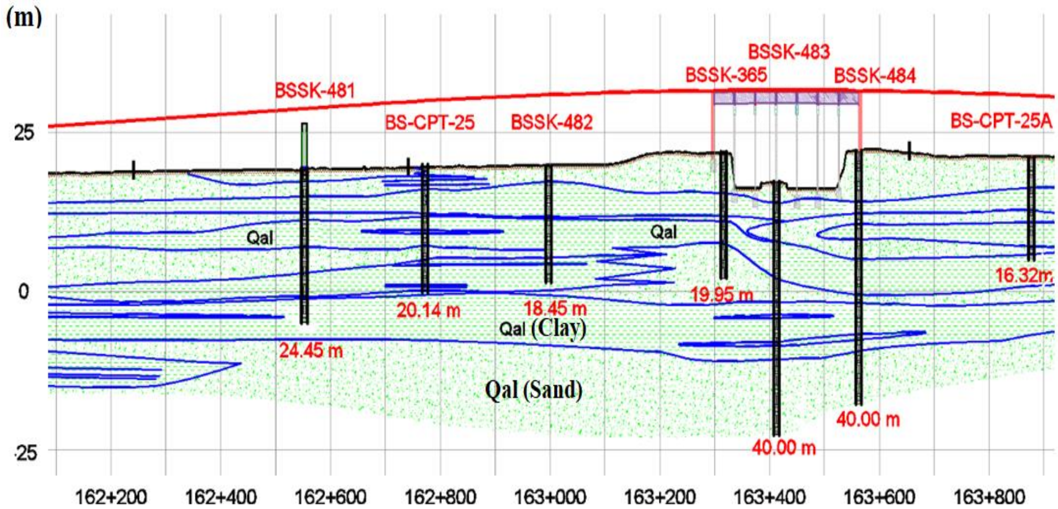

Figure 3.79. The longitudinal geological section of Km: 162+555

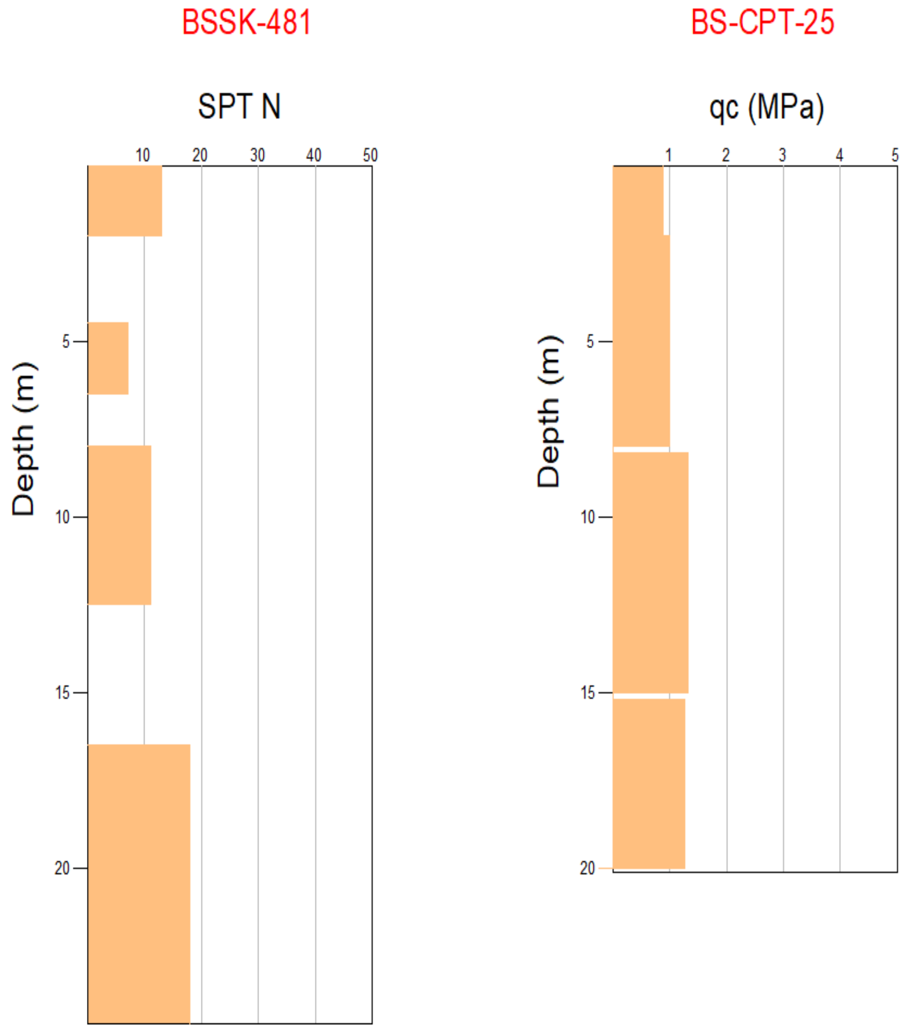

Figure 3.80. SPT N vs. Depth (m) and q_c (MPa) vs. Depth (m) graphs for clay layers

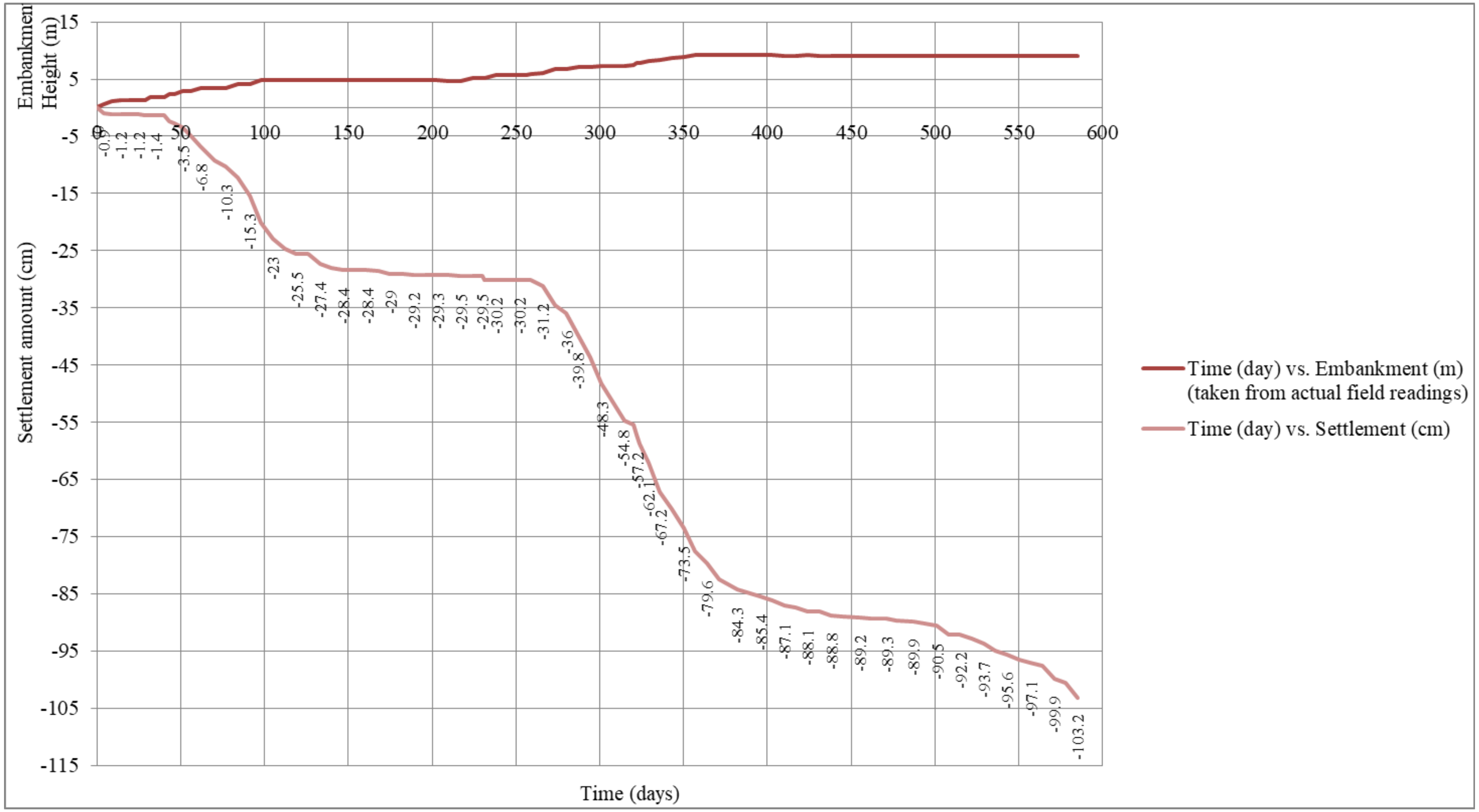

Figure 3.81. In situ Settlement (cm) vs. Time (day) behavior measured in embankment for surface settlement

3.26 KM: 163+000 Section

The soil profile of the embankment at Km: 163+000 is characterized by 18.45 m depth borehole (BSSK-482) and 20.14 m depth CPT (BS-CPT-25). The laboratory test results and SPT N graphs are presented in Appendix A and B, consolidation settlement calculations are presented in Appendix C. The soil profile consists of the layers shown in Table 3.26:

Table 3.26 A typical soil profile at Km: 163+000 section of the study area

Depth (m)	Soil Profile		SPT N (av.)	q_c (av.) (MPa)	f_s (av.) (kPa)	PI (av.) (%)	w_N (av.) (%)	c_u (kPa)
-2.00	Medium Dense Sand (SM)		19	3.32	53.67			
-13.00	Medium-Stiff Clay (CL)		9	1.16		19	35	
-28.00	Stiff Clay (CH-CL)		18	1.30		36	32	

The geological longitudinal section of embankment is presented in Figure 3.82. SPT results of BSSK-482 borehole and cone resistance values of BS-CPT-25 results for clay layers are presented in Figure 3.83. According to the geological longitudinal section, the embankment with 8.5 m in height is planned to construct on clayey soil with a thickness of 28.0 m and also sand layers are defined at depth of 0.0 m – 2.0 m. From depth of 2.0 m to 13.0 m, SPT N value is obtained as 9 whereas q_c value is obtained 1.16 MPa in average, which indicates "medium-stiff clay". From depth of 13.0 m to 28.8 m, SPT N value is obtained as 18 whereas q_c value is obtained 1.30 MPa in average, which indicates "stiff clay". When the values of SPT N and q_c are compared, they both point out similar stiffness and also strength values for clay units defined in specified depth of intervals. The graph of In-Situ Settlement (m) vs. Time (day) behavior measured in the embankment for surface settlement plate is presented in Figure 3.84. The last measured settlement from surface settlement plate is 130.7 cm under embankment load with a maximum height of 10.5 m after 1000 days of measurement.

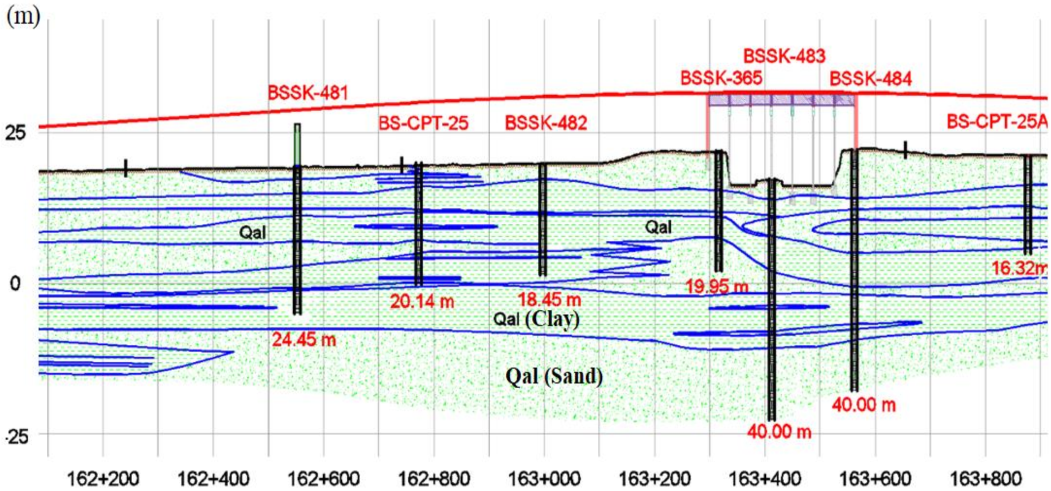

Figure 3.82. The longitudinal geological section of Km: 163+000

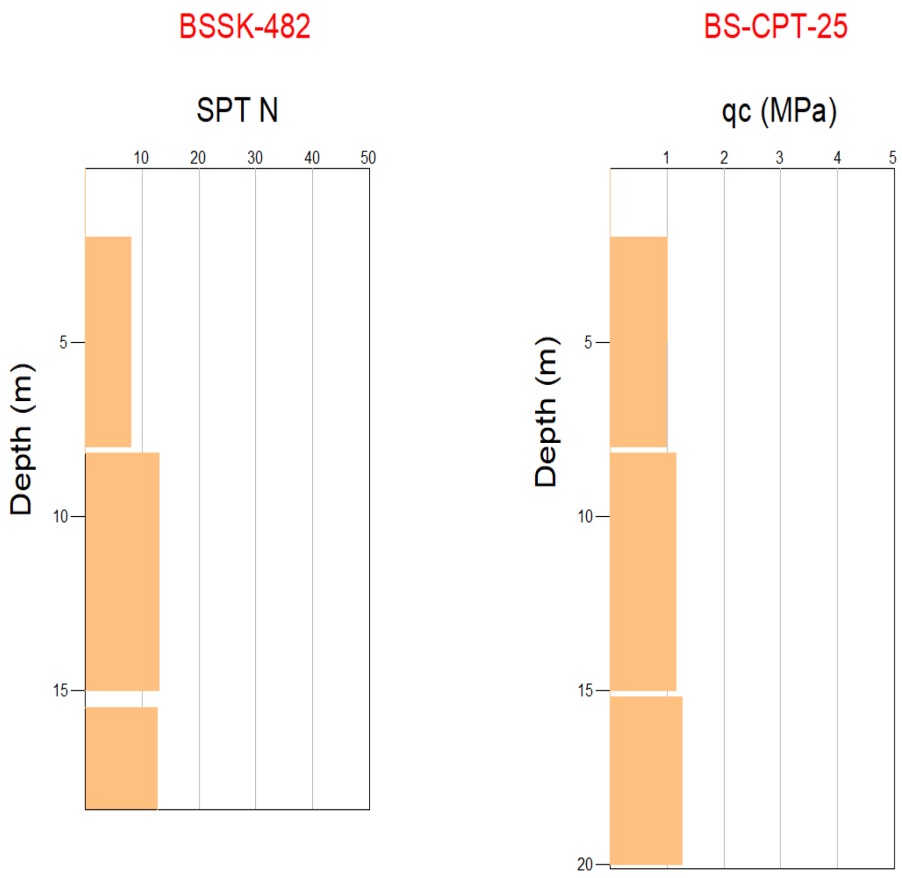

Figure 3.83. SPT N vs. Depth (m) and q_c (MPa) vs. Depth (m) graphs for clay layers

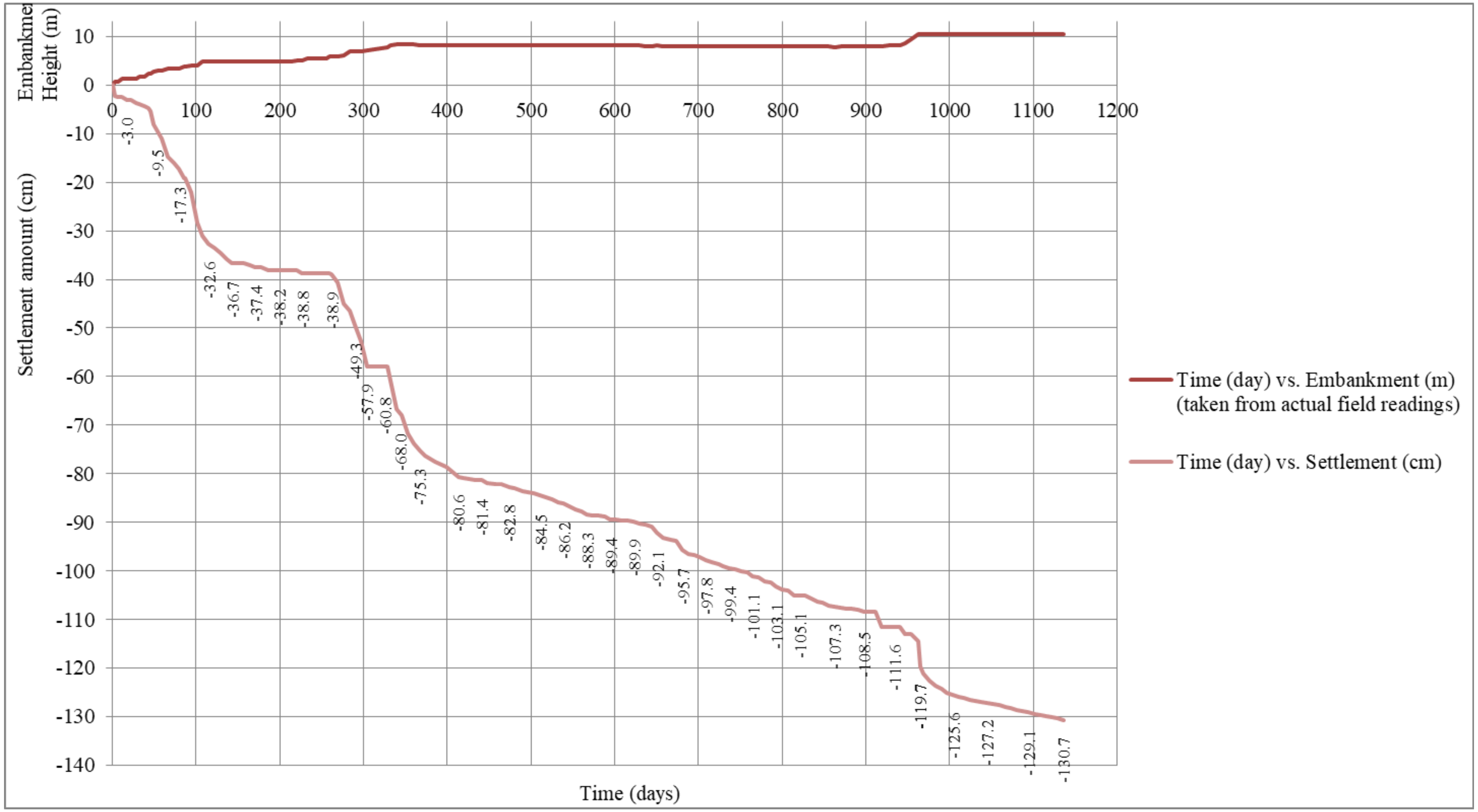

Figure 3.84. In situ Settlement (cm) vs. Time (day) behavior measured in embankment for surface settlement

The summary of description of the instrumented embankment sections are presented in Table 3.27. As presented in this table, settlement plates are located at surface except two stations which are Km: 139+764 and Km: 139+860. At Km: 139+764 and Km: 139+860, deep settlement plates are placed at depth of 24.0 m. Hence, in these station, settlement amounts till to depth of 24.0 m can be obtained by subtracting the settlement amounts read from surface settlement plate to deep settlement plate.

The maximum and minimum embankment heights are 11.18 m and 6.5 m, respectively. The average of the embankment heights is 9.0 m. As presented in this table, the maximum settlement amount is measured as 171.9 cm under the embankment with a height of 11.0 m at Km: 151+220. The minimum settlement amount is measured as 80.5 m under the embankment with a height of 7.21 m.

The thickness of sand is lower than 20% of clay thickness, in average. The ratio of sand thickness to clay thickness is lower than 10% in flood area, where it is defined in between Km: 139+000 and Km: 145+000.

SPT N values in clay units change in interval of 11 and 15 and they are defined as medium stiff clay according to SPT N values. Cone tip resistance values (q_c) mostly take place in range of 0.9 – 1.2 MPa and they are compatible to SPT N values.

Table 3.27 Summary of field description of the instrumented embankment sections

Kilometer	Settlement Plate Location	Embankment Height (m)	Final settlement measured in the plate (cm)	Total Sand Thickness (m)/Clay Thickness (m)	SPT N of clay layers (weighted av.)	qc (MPa) of clay layers (weighted av.)
KM 139+764	Depth: 0.0-24.0 m	8.8	98.2	0.011	18	1.691
	Depth>24.0 m		69.1			
KM 139+860	Depth: 0.0-24.0 m	8.8	100.2	0.011	18	1.691
	Depth>24.0 m		90.0			
KM 140+592	Surface	8.8	116.6	0.012	18	1.691
KM 141+680	Surface	10	181.2	0.163	17	1.188
KM 142+000	Surface	9.97	125.8	0.149	22	1.189
KM 142+400	Surface	8.09	105.8	0.133	17	1.191
KM 143+107	Surface	8.45	127.0	0.101	15	1.118
KM 144+000	Surface	9.98	155.4	0.095	16	1.138
KM 145+000	Surface	8.45	116.8	0.197	16	1.389
KM 146+210	Surface	11.18	108.8	0.227	14	1.122
KM 147+000	Surface	8.1	98.0	0.091	15	1.074
KM 149+000	Surface	8.2	96.0	0.246	19	1.334
KM 150+000	Surface	9.98	107.2	0.248	12	1.628
KM 150+500	Surface	10.41	150.6	0.095	12	1.449
KM 151+220	Surface	11	171.9	0.145	14	0.932
KM 151+975	Surface	9.76	123.7	0.216	15	0.929
KM 152+000	Surface	8.19	108.3	0.236	14	0.929
KM 154+500	Surface	7.49	96.1	0.080	20	1.542
KM 155+000	Surface	9.5	107.1	0.390	17	1.449
KM 155+551	Surface	10.5	113.4	0.237	19	1.705
KM 157+400	Surface	8.52	115.3	0.049	14	1.382
KM 158+000	Surface	8.79	108.1	0.134	18	1.553
KM 159+565	Surface	7.21	80.5	0.289	19	1.514
KM 161+764	Surface	6.5	81.9	0.648	16	1.446
KM 162+555	Surface	9.2	103.2	0.390	11	1.237
KM 163+000	Surface	8.5	130.7	0.077	14	1.241

CHAPTER 4

EVALUATION OF THE CALCULATED AND OBSERVED SETTLEMENTS

4.1 Introduction

In this part of the study, 26 different sections, namely; Km: 139+764, Km: 139+860, Km: 140+592, Km: 141+680, Km: 142+000, Km: 142+400, Km: 143+107, Km: 144+000, Km: 145+000, Km: 146+210, Km: 147+000, Km: 149+000, Km: 150+000, Km: 150+500, Km: 151+220, Km: 151+975, Km: 152+000, Km: 154+500, Km: 155+000, Km: 155+551, Km: 157+400, Km: 158+000, Km:159+565, Km: 161+764, Km: 162+555 and Km:163+000, were evaluated and observed settlements were divided into 3 phases; namely primary, secondary and tertiary on settlement vs. time curves.

The primary consolidation amounts, calculated and presented in Chapter 3, were compared with observed values supplied by instrumentation of test embankments and ratios of measured/calculated values were evaluated.

Asaoka's and Horn's Methods were used to predict the final settlement amounts using 70% of the monitored settlement data, and the calculated results were compared with the observed values to evaluate their applicability in engineering practice.

The compression – time relationships obtained from the field data were evaluated to define the complete time and amount of primary consolidation settlements. Secondary and tertiary compressions occurring after hydrodynamic primary period, are described by linear settlement – log time and settlement - √time curves with slopes of C_s and C_t.

Furthermore, consolidation amounts supplied by Stroud et. al. (1974) were compared with observed values. Coefficients of α_m were evaluated conducting back analysis of CPT data and compared with the approaches recommended in literature. The coefficients of secondary consolidation were calculated from settlement vs. square root (time) graphs and compared with the results of correlations proposed in literature.

Secondary and Tertiary Compression Index values (C_s-C_t) were calculated and ranges for obtaining of these index values from Compression Index (C_c) values were recommended.

In order to find correction factors between the observed and the calculated consolidation settlements (S_f/S_c), Primary and Secondary Consolidation Ratio (C_s/C_c), Primary and Tertiary Consolidation Ratio (C_t/C_c), $m_{v(field)}/m_{v(Stroud)}$ linear and nonlinear regression analysis were performed by considering LL, LI, PI, SPT N, w_N, e_0 parameters as independent variables. In order to take the geological succession into account, λ values, which are the ratios of sand thickness to clay thickness, and ψ values, the ratio of length of road platform to total clay thickness, were utilized.

4.2 Primary Consolidation Settlements

In order to determine the primary consolidation settlements occurred in the field for 26 stations under embankment loads, utilized approaches were graphical and semi-empirical methods (Asaoka's and Horn's Methods) with 70% of settlement data and compression – time relations (log (Time) vs. settlements and $\sqrt{}$(Time) vs. settlements graphs).

4.2.1 Asaoka's and Horn's Methods

Asaoka plots of surface and deep settlement plates for Station 1 (Km: 139+764) are used to predict the final settlement amount (Figure 4.1). According to Asaoka plot, final settlement amount is obtained as 145.0 cm for surface settlement plate, 55.0 cm for deep settlement plate (>24.0 m). Hence, the final predicted settlement for 0.0 m and 24.0 m is obtained as 90.0 cm.

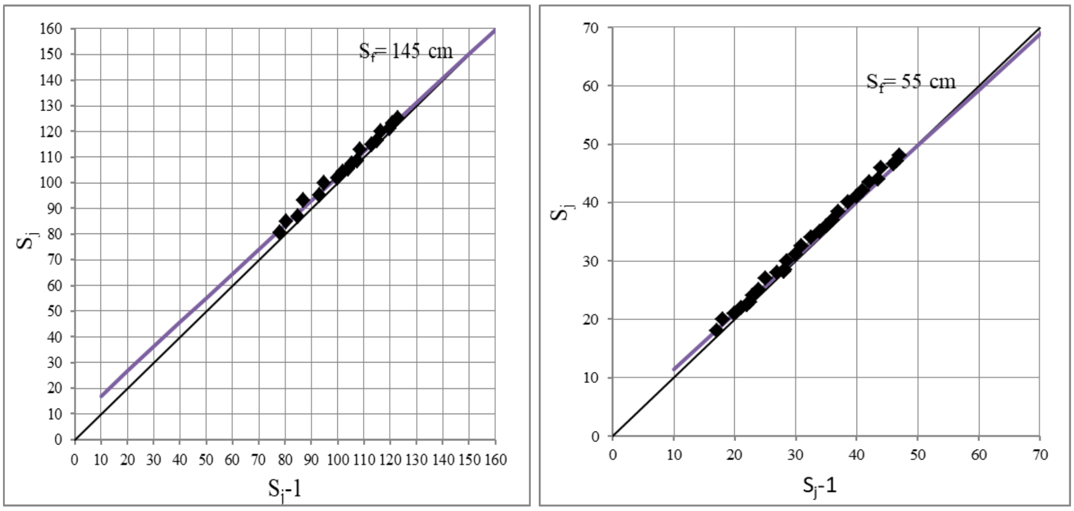

Figure 4.1. Asaoka plot for Km: 139+764 for surface and deep settlement plates

Horn plots of surface and deep settlement plates for Station 1 (Km: 139+764) are used to predict the final settlement amount (Figure 4.2). According to Horn plot, final settlement amount is obtained as 141.0 cm for surface settlement plate, 48.0 cm for deep settlement plate (>24.0 m). Hence, the final predicted settlement for 0.0 m and 24.0 m is obtained as 93.0 cm.

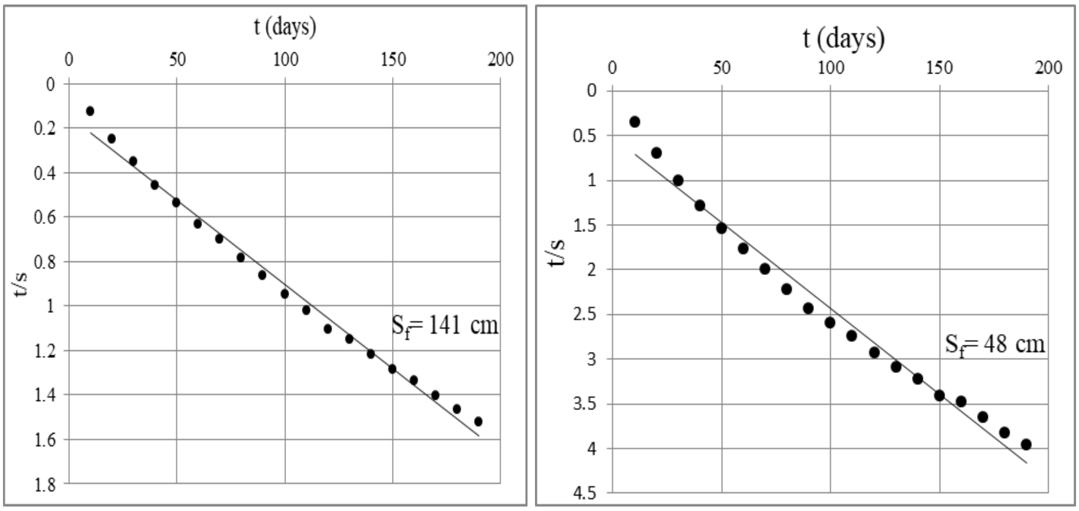

Figure 4.2. Horn plot for Km: 139+764 for surface and deep settlement plates

Asaoka plot of surface and deep settlement plates for Station 2 (Km: 139+860) are used to predict the final settlement amount (Figure 4.3). According to Asaoka plot, final settlement amount is obtained as 163.0 cm for surface settlement plate, 68.0 cm for deep settlement plate (>24.0 m). Hence, the final predicted settlement for 0.0 m and 24.0 m is obtained as 95.0 cm.

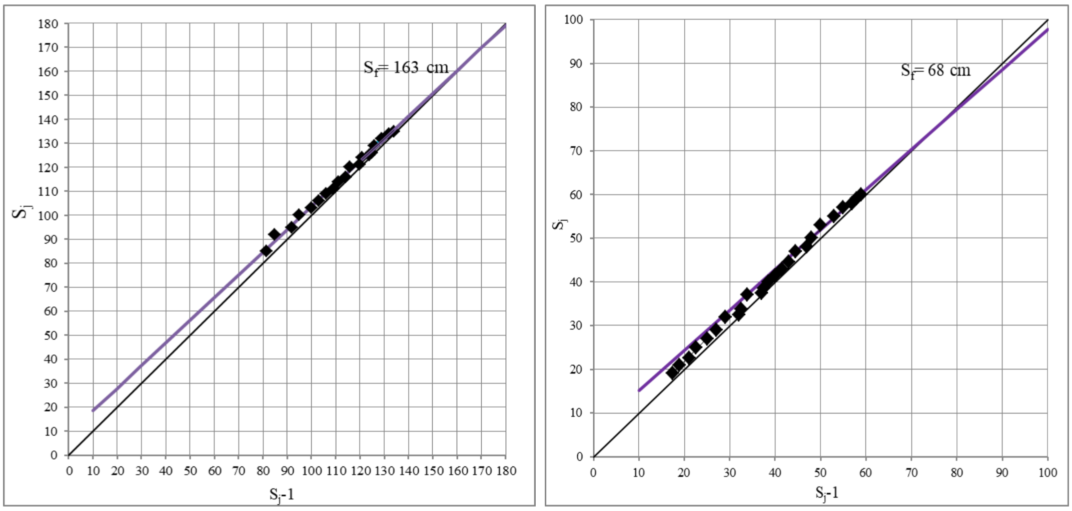

Figure 4.3. Asaoka plot for Km: 139+860 for surface and deep settlement plates

Horn plot of surface and deep settlement plates for Station 2 (Km: 139+860) are used to predict the final settlement amount (Figure 4.4). According to Horn plot, final settlement amount is obtained as 141.7 cm for surface settlement plate, 50.0 cm for deep settlement plate (>24.0 m). Hence, the final predicted settlement for 0.0 m and 24.0 m is obtained as 91.7 cm.

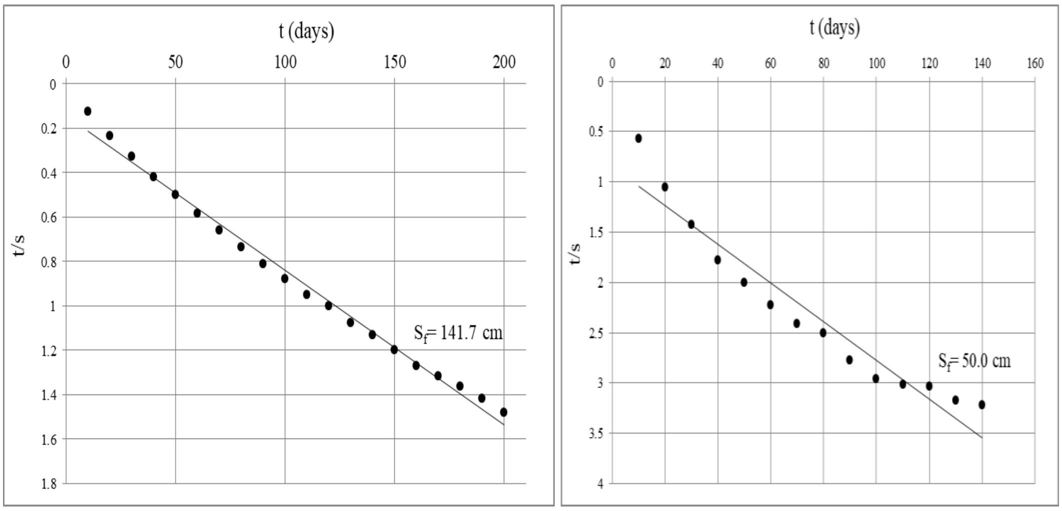

Figure 4.4. Horn plot for Km: 139+860 for surface and deep settlement plates

Asaoka plot of settlement data of surface settlement plate for Station 3 (Km: 140+592) is used to predict the final settlement amount (Figure 4.5). According to Asaoka plot, final settlement amount is obtained as 118.0 cm and according to Horn plot, final settlement amount is obtained as 111.11 cm.

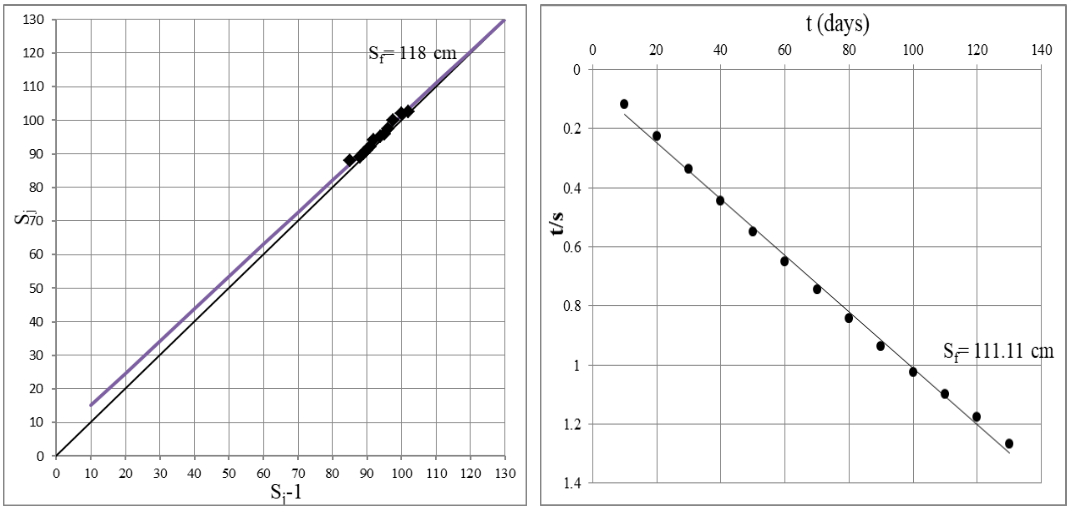

Figure 4.5. Asaoka and Horn plot for Km: 140+592 for surface settlement plates

Asaoka plot of settlement data of surface settlement plate for Station 4 (Km: 141+680) is used to predict the final settlement amount (Figure 4.6). According to Asaoka plot, final settlement amount is obtained as 170.0 cm and according to Horn plot, final settlement amount is obtained as 190.47 cm.

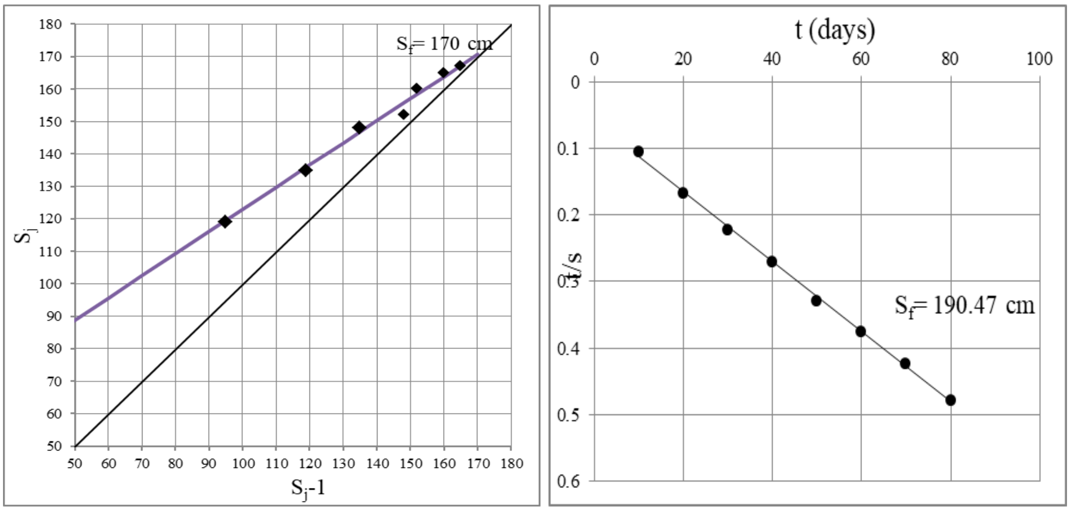

Figure 4.6. Asaoka and Horn plot for Km: 141+680 for surface settlement plates

Asaoka plot of settlement data of surface settlement plate for Station 5 (Km: 142+000) is used to predict the final settlement amount (Figure 4.7). According to Asaoka plot, final settlement amount is obtained as 119.0 cm and according to Horn plot, final settlement amount is obtained as 125.0 cm.

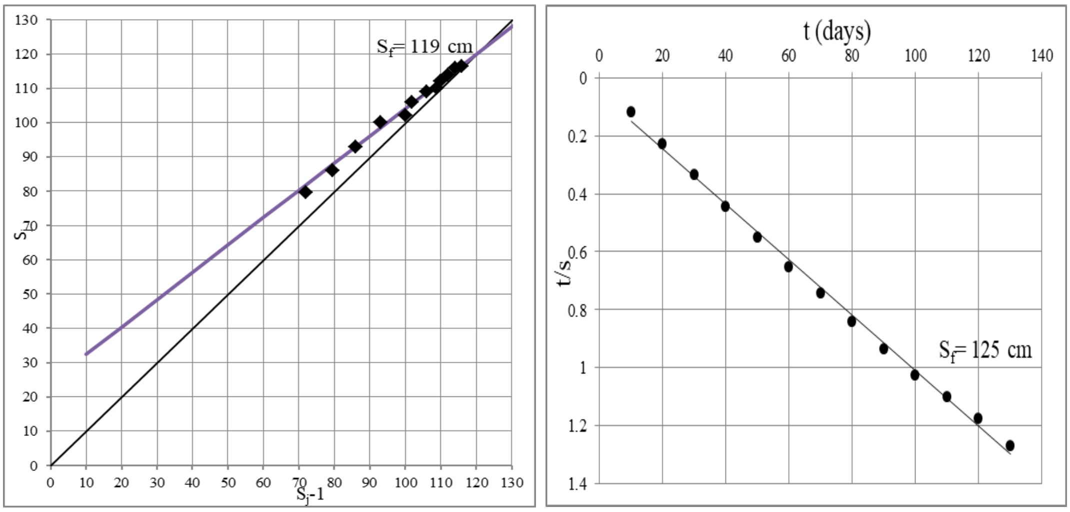

Figure 4.7. Asaoka and Horn plot for Km: 142+000 for surface settlement plates

Asaoka plot of settlement data of surface settlement plate for Station 6 (Km: 142+400) is used to predict the final settlement amount (Figure 4.8). According to Asaoka plot, final settlement amount is obtained as 118.0 cm and according to Horn plot, final settlement amount is obtained as 111.11 cm.

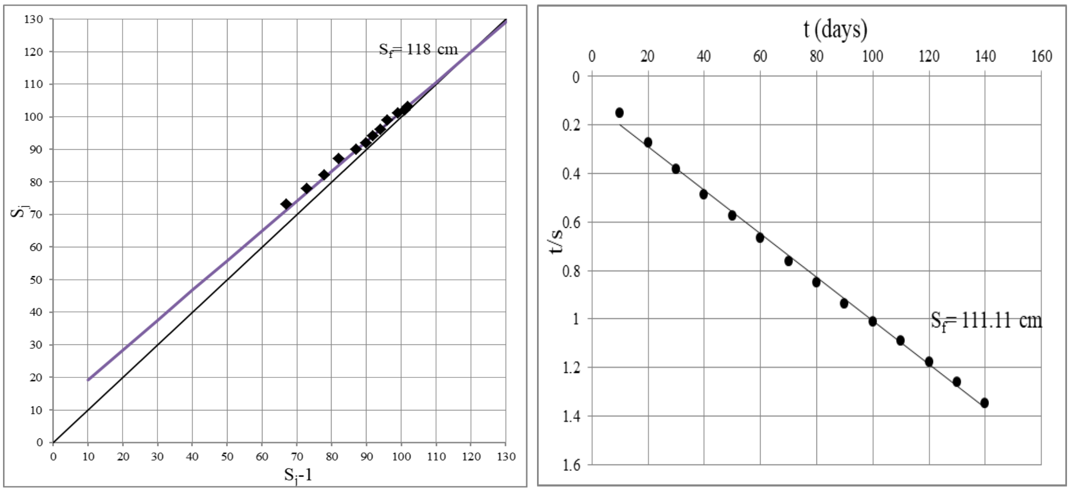

Figure 4.8. Asaoka and Horn plot for Km: 142+400 for surface settlement plates

Asaoka plot of settlement data of surface settlement plate for Station 7 (Km: 143+107) is used to predict the final settlement amount (Figure 4.9). According to Asaoka plot, final settlement amount is obtained as 114.0 cm and according to Horn plot, final settlement amount is obtained as 111.11 cm.

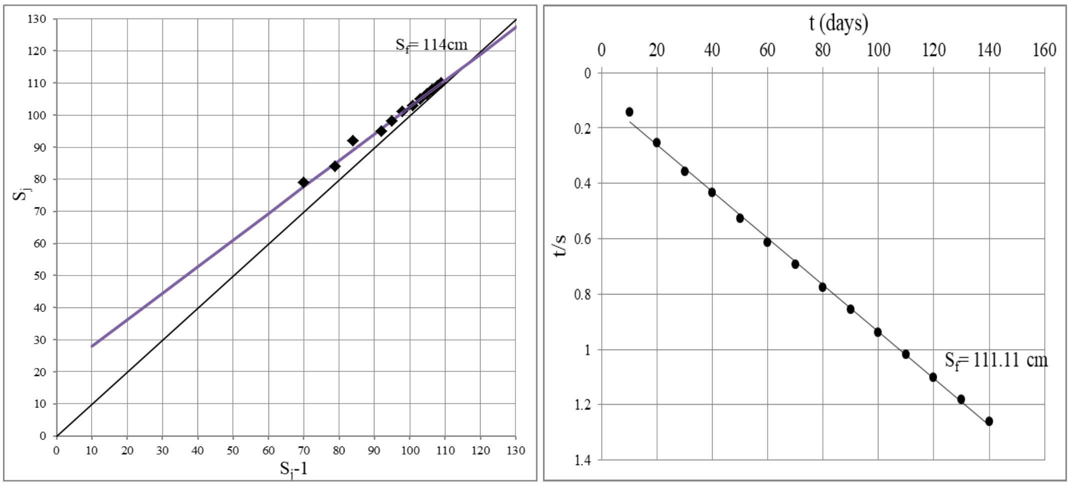

Figure 4.9. Asaoka and Horn plot for Km: 143+107 for surface settlement plates

Asaoka plot of settlement data of surface settlement plate for Station 8 (Km: 144+000) is used to predict the final settlement amount (Figure 4.10). According to Asaoka plot, final settlement amount is obtained as 114.0 cm and according to Horn plot, final settlement amount is obtained as 104 cm.

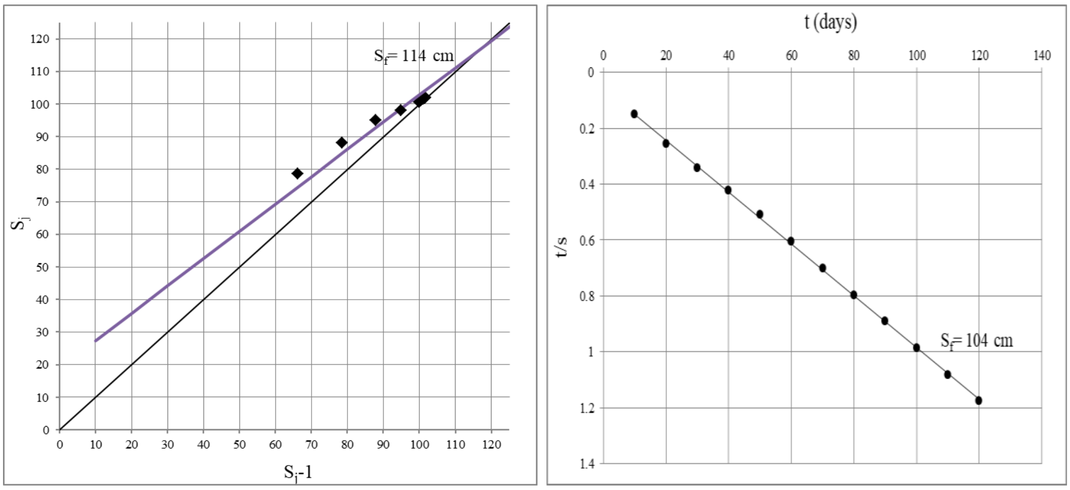

Figure 4.10. Asaoka and Horn plot for Km: 144+000 for surface settlement plates

Asaoka plot of settlement data of surface settlement plate for Station 9 (Km: 145+000) is used to predict the final settlement amount (Figure 4.11). According to Asaoka plot, final settlement amount is obtained as 124.28 cm and according to Horn plot, final settlement amount is obtained as 109.09 cm.

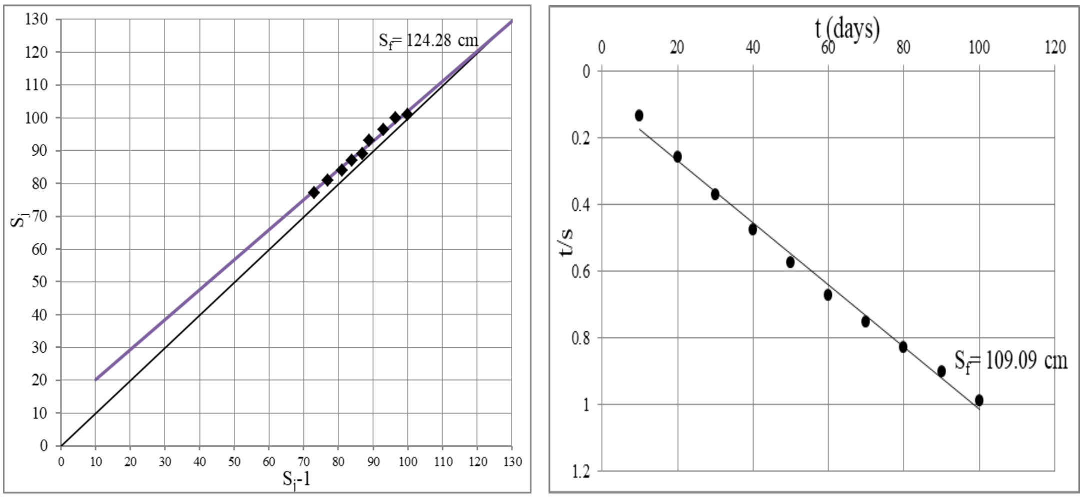

Figure 4.11. Asaoka and Horn plot for Km: 145+000 for surface settlement plates

Asaoka plot of settlement data of surface settlement plate for Station 10 (Km: 146+210) is used to predict the final settlement amount (Figure 4.12). According to Asaoka plot, final settlement amount is obtained as 114.77 cm and according to Horn plot, final settlement amount is obtained as 111.3 cm.

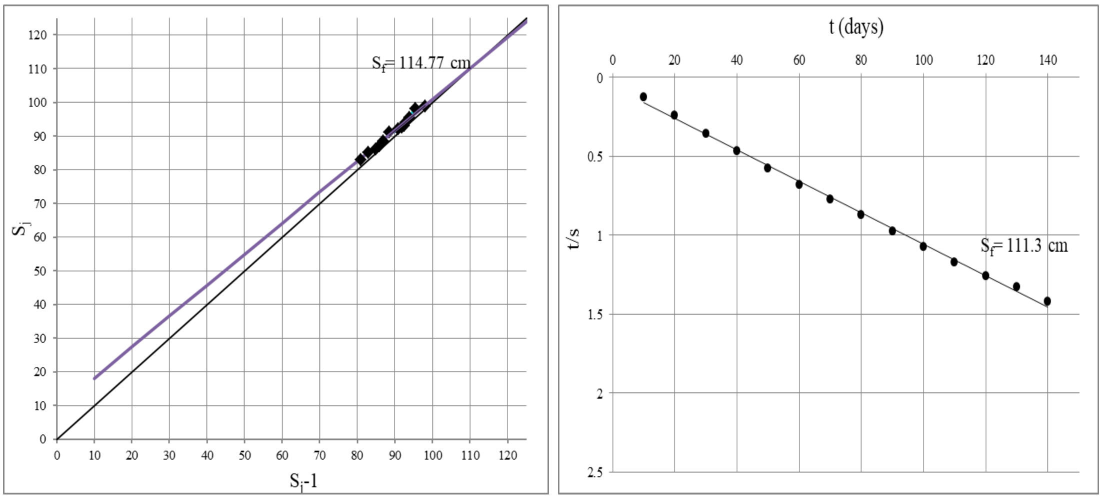

Figure 4.12. Asaoka and Horn plot for Km: 146+210 for surface settlement plates

Asaoka plot of settlement data of surface settlement plate for Station 11 (Km: 147+000) is used to predict the final settlement amount (Figure 4.13). According to Asaoka plot, final settlement amount is obtained as 83.0 cm and according to Horn plot, final settlement amount is obtained as 80.0 cm.

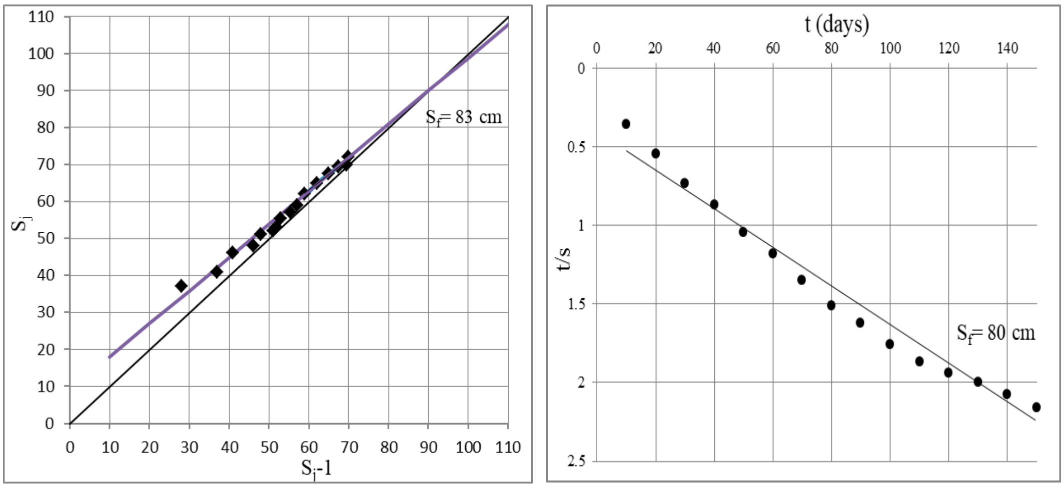

Figure 4.13. Asaoka and Horn plot for Km: 147+000 for surface settlement plates

Asaoka plot of settlement data of surface settlement plate for Station 12 (Km: 149+000) is used to predict the final settlement amount (Figure 4.14). According to Asaoka plot, final settlement amount is obtained as 72.0 cm and according to Horn plot, final settlement amount is obtained as 75.0 cm.

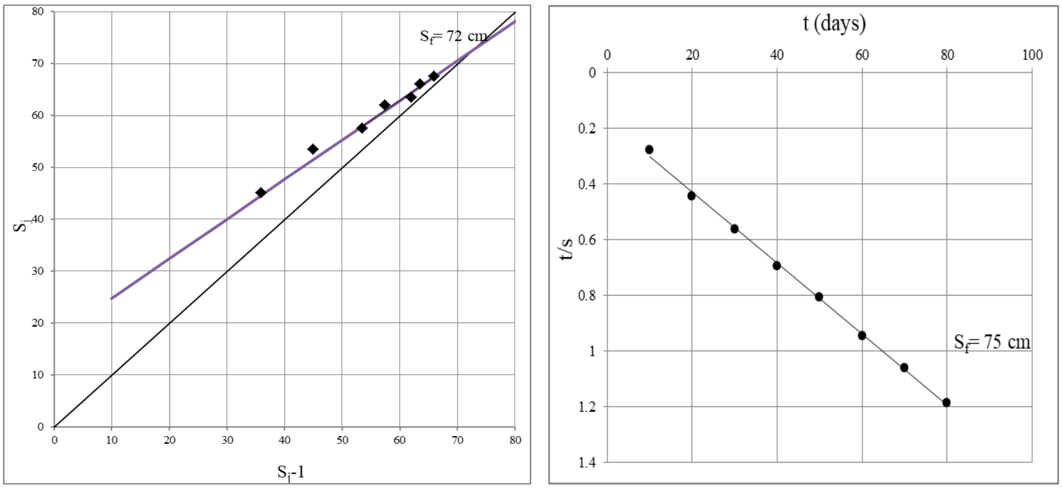

Figure 4.14. Asaoka and Horn plot for Km: 149+000 for surface settlement plates

Asaoka plot of settlement data of surface settlement plate for Station 13 (Km: 150+000) is used to predict the final settlement amount (Figure 4.15). According to Asaoka plot, final settlement amount is obtained as 109.0 cm and according to Horn plot, final settlement amount is obtained as 105.0 cm.

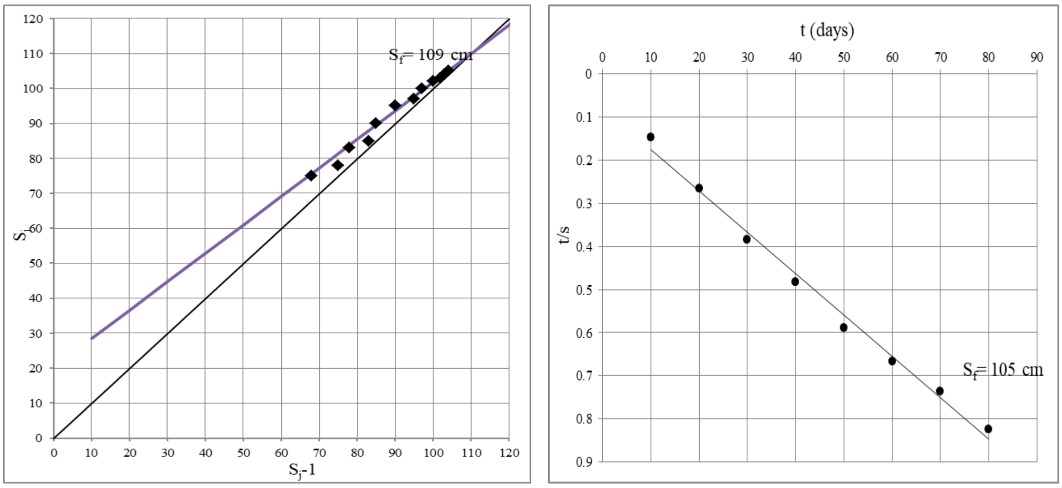

Figure 4.15. Asaoka and Horn plot for Km: 150+000 for surface settlement plates

Asaoka plot of settlement data of surface settlement plate for Station 14 (Km: 150+500) is used to predict the final settlement amount (Figure 4.16). According to Asaoka plot, final settlement amount is obtained as 124.76 cm and according to Horn plot, final settlement amount is obtained as 123.08 cm.

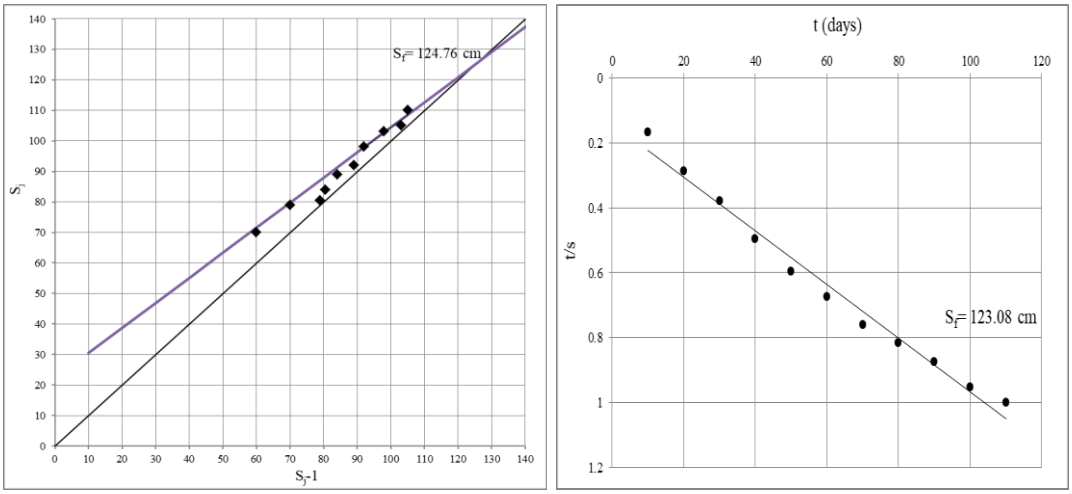

Figure 4.16. Asaoka and Horn plot for Km: 150+500 for surface settlement plates

Asaoka plot of settlement data of surface settlement plate for Station 15 (Km: 151+220) is used to predict the final settlement amount (Figure 4.17). According to Asaoka plot, final settlement amount is obtained as 159.0 cm and according to Horn plot, final settlement amount is obtained as 156.25 cm.

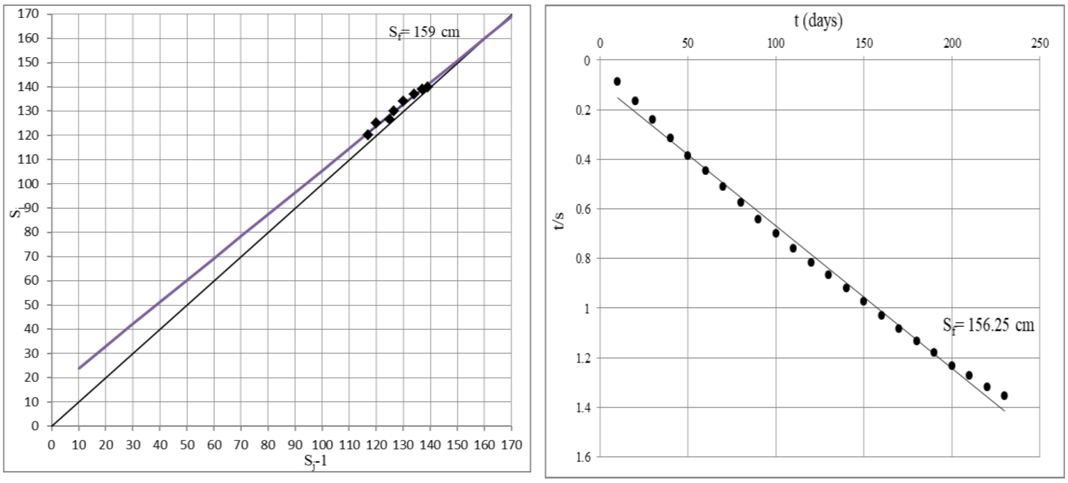

Figure 4.17. Asaoka and Horn plot for Km: 151+220 for surface settlement plates

Asaoka plot of settlement data of surface settlement plate for Station 16 (Km: 151+975) is used to predict the final settlement amount (Figure 4.18). According to Asaoka plot, final settlement amount is obtained as 127.0 cm and according to Horn plot, final settlement amount is obtained as 125.0 cm

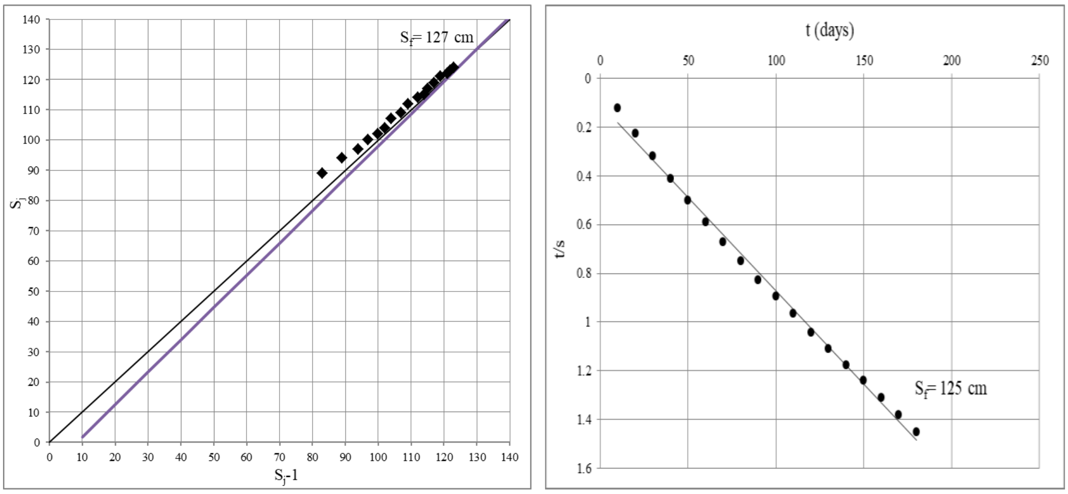

Figure 4.18. Asaoka and Horn plot for Km: 151+975 for surface settlement plates

Asaoka plot of settlement data of surface settlement plate for Station 17 (Km: 152+000) is used to predict the final settlement amount (Figure 4.19). According to Asaoka plot, final settlement amount is obtained as 110.0 cm and according to Horn plot, final settlement amount is obtained as 100.0 cm.

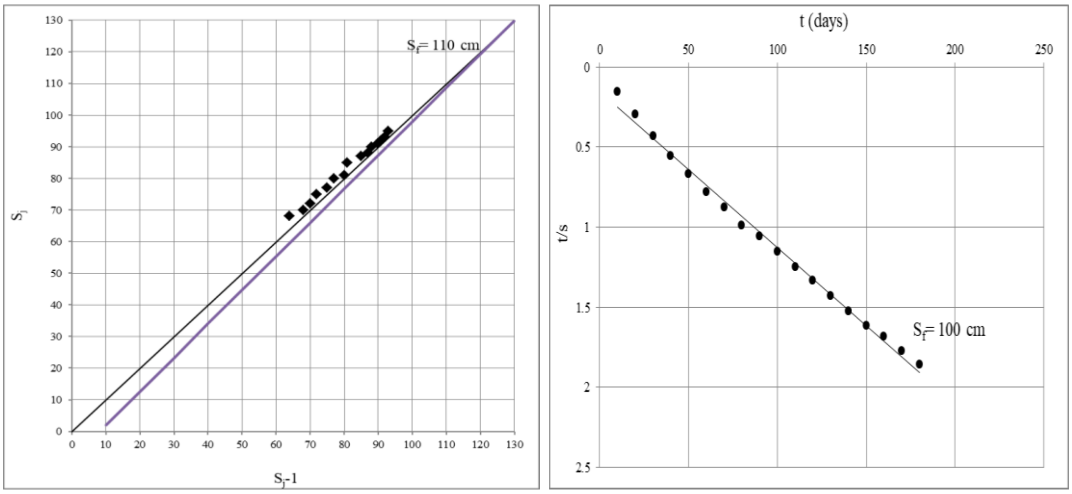

Figure 4.19. Asaoka and Horn plot for Km: 152+000 for surface settlement plates

Asaoka plot of settlement data of surface settlement plate for Station 18 (Km: 154+500) is used to predict the final settlement amount (Figure 4.20). According to Asaoka plot, final settlement amount is obtained as 83.0 cm and according to Horn plot, final settlement amount is obtained as 90.9 cm.

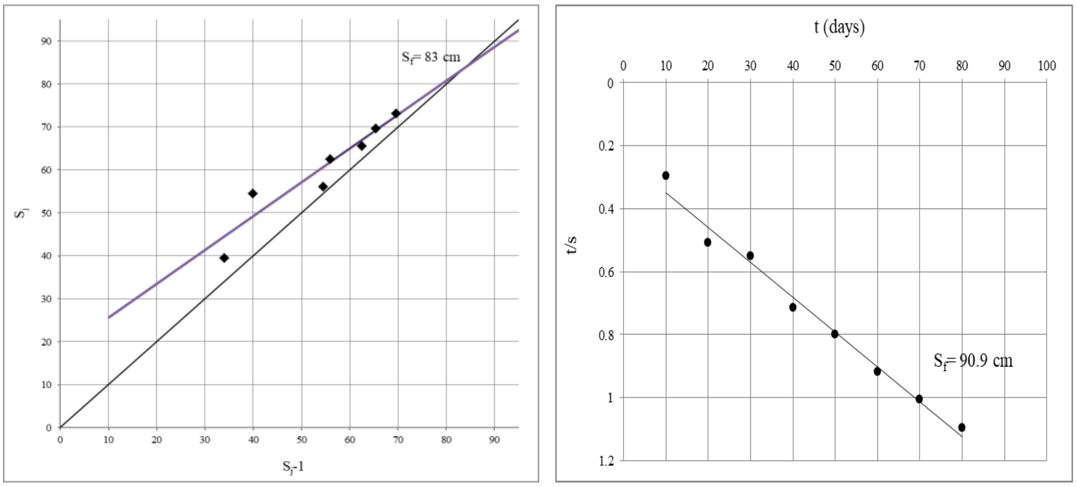

Figure 4.20. Asaoka and Horn plot for Km: 154+500 for surface settlement plates

Asaoka plot of settlement data of surface settlement plate for Station 19 (Km: 155+000) is used to predict the final settlement amount (Figure 4.21). According to Asaoka plot, final settlement amount is obtained as 85.0 cm and according to Horn plot, final settlement amount is obtained as 100.0 cm.

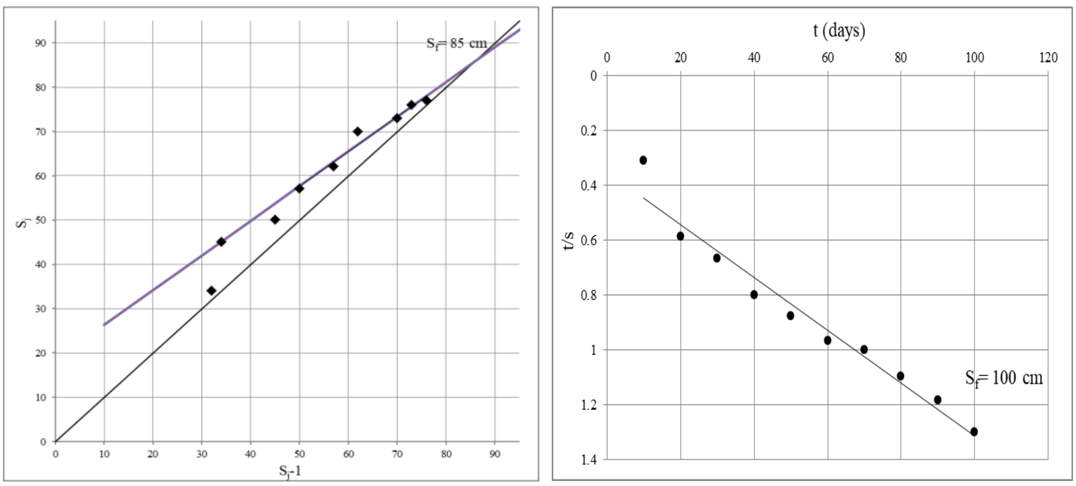

Figure 4.21. Asaoka and Horn plot for Km: 155+000 for surface settlement plates

Asaoka plot of settlement data of surface settlement plate for Station 20 (Km: 155+551) is used to predict the final settlement amount (Figure 4.22). According to Asaoka plot, final settlement amount is obtained as 117.0 cm and according to Horn plot, final settlement amount is obtained as 107.0 cm.

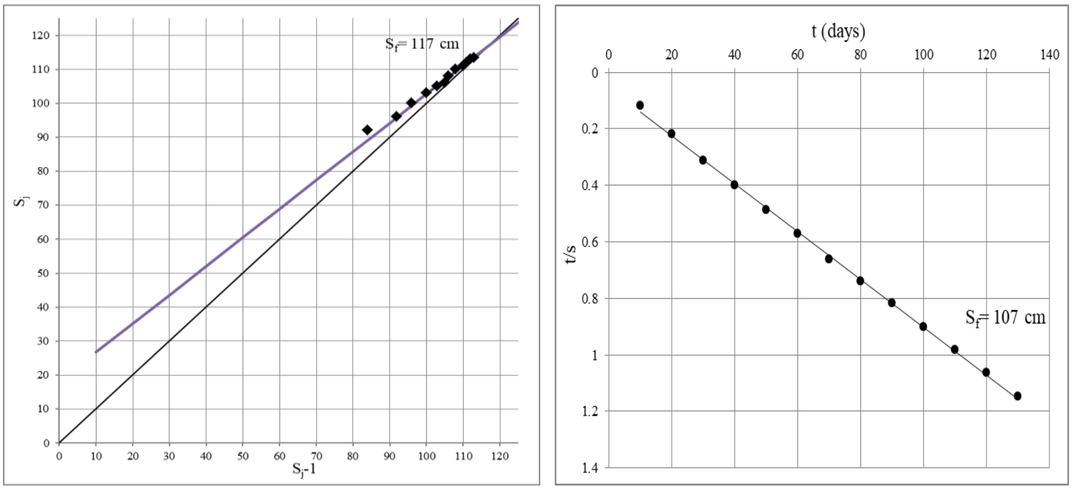

Figure 4.22. Asaoka and Horn plot for Km: 155+551 for surface settlement plates

Asaoka plot of settlement data of surface settlement plate for Station 21 (Km: 157+400) is used to predict the final settlement amount (Figure 4.23). According to Asaoka plot, final settlement amount is obtained as 115.0 cm and according to Horn plot, final settlement amount is obtained as 118.75 cm.

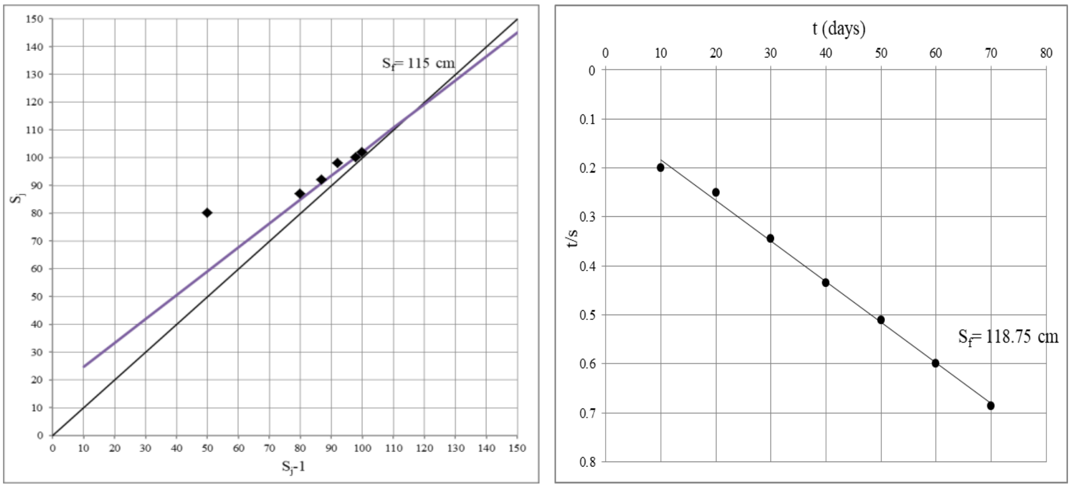

Figure 4.23. Asaoka and Horn plot for Km: 157+400 for surface settlement plates

Asaoka plot of settlement data of surface settlement plate for Station 22 (Km: 158+000) is used to predict the final settlement amount (Figure 4.24). According to Asaoka plot, final settlement amount is obtained as 115.0 cm and according to Horn plot, final settlement amount is obtained as 118.75 cm.

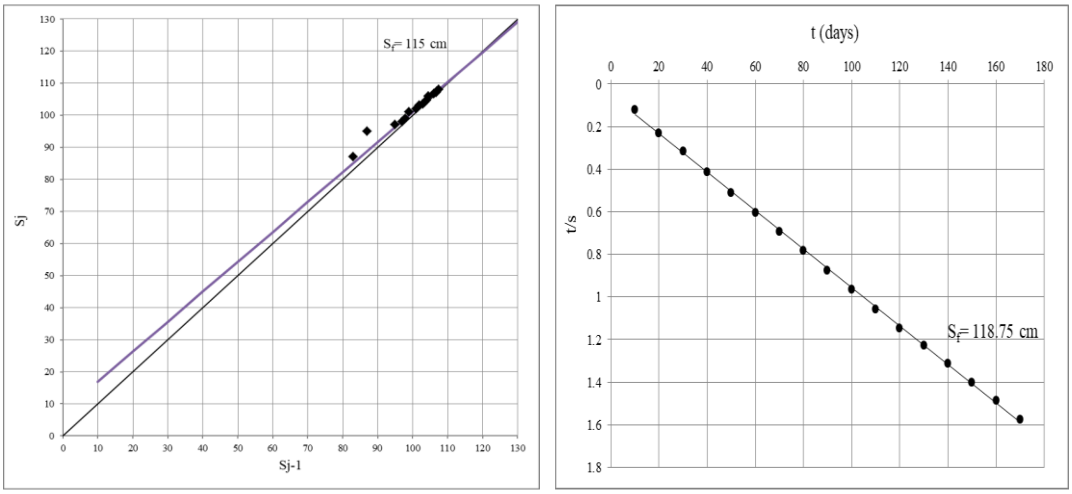

Figure 4.24. Asaoka and Horn plot for Km: 158+000 for surface settlement plates

Asaoka plot of settlement data of surface settlement plate for Station 23 (Km: 159+565) is used to predict the final settlement amount (Figure 4.25). According to Asaoka plot, final settlement amount is obtained as 66.0 cm and according to Horn plot, final settlement amount is obtained as 58.0 cm.

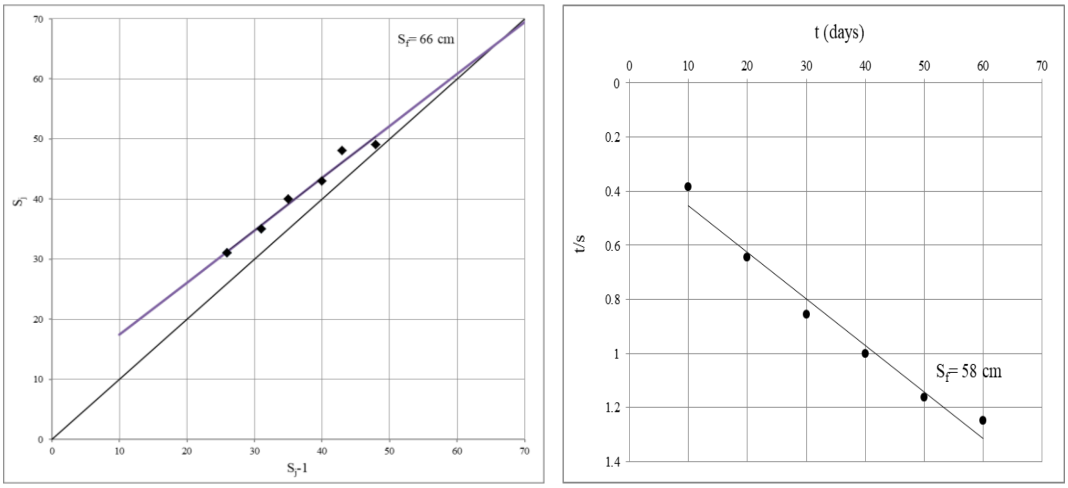

Figure 4.25. Asaoka and Horn plot for Km: 159+565 for surface settlement plates

Asaoka plot of settlement data of surface settlement plate for Station 24 (Km: 161+764) is used to predict the final settlement amount (Figure 4.26). According to Asaoka plot, final settlement amount is obtained as 73.0 cm and according to Horn plot, final settlement amount is obtained as 88.0 cm.

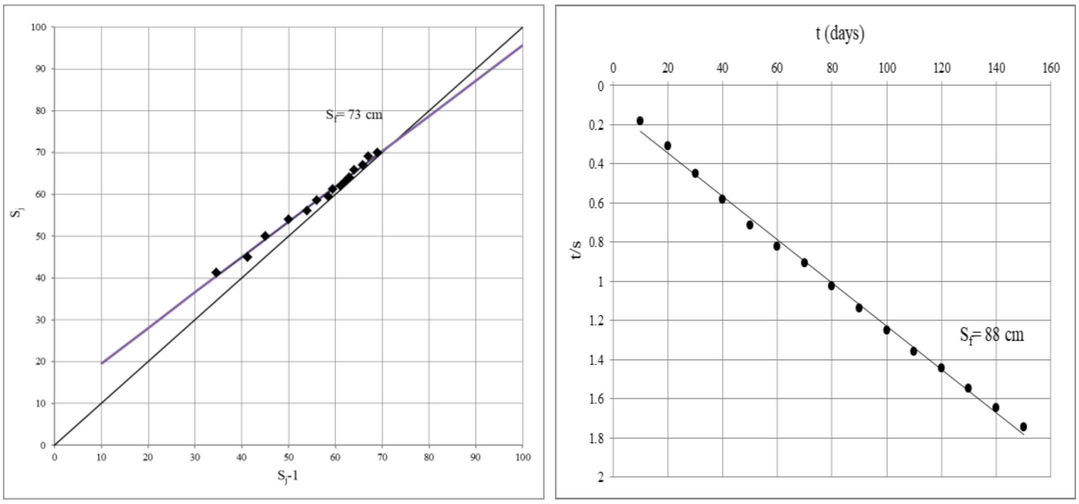

Figure 4.26. Asaoka and Horn plot for Km: 161+764 for surface settlement plates

Asaoka plot of settlement data of surface settlement plate for Station 25 (Km: 162+555) is used to predict the final settlement amount (Figure 4.27). According to Asaoka plot, final settlement amount is obtained as 100.5 cm and according to Horn plot, final settlement amount is obtained as 100.0 cm.

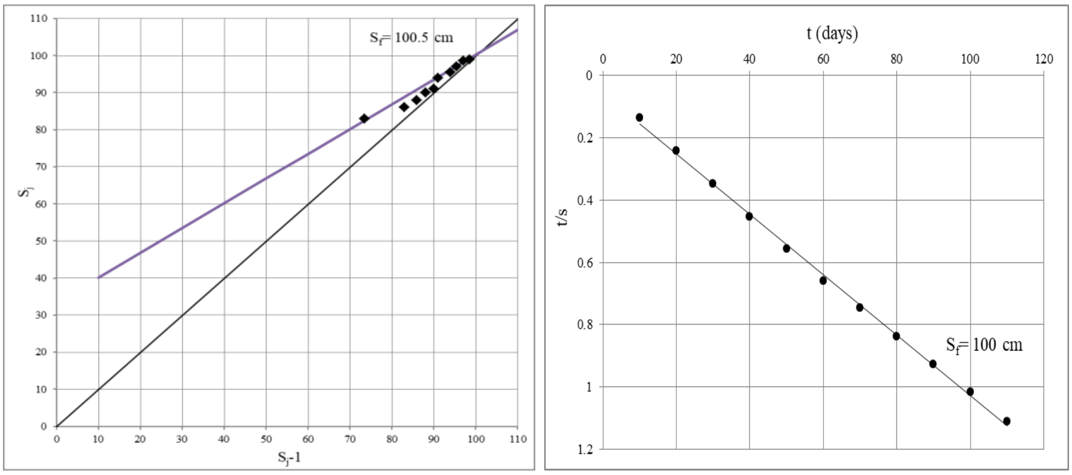

Figure 4.27. Asaoka and Horn plot for Km: 162+555 for surface settlement plates

Asaoka plot of settlement data of surface settlement plate for Station 26 (Km: 163+000) is used to predict the final settlement amount (Figure 4.28). According to Asaoka plot, final settlement amount is obtained as 85.0 cm and according to Horn plot, final settlement amount is obtained as 89.0 cm.

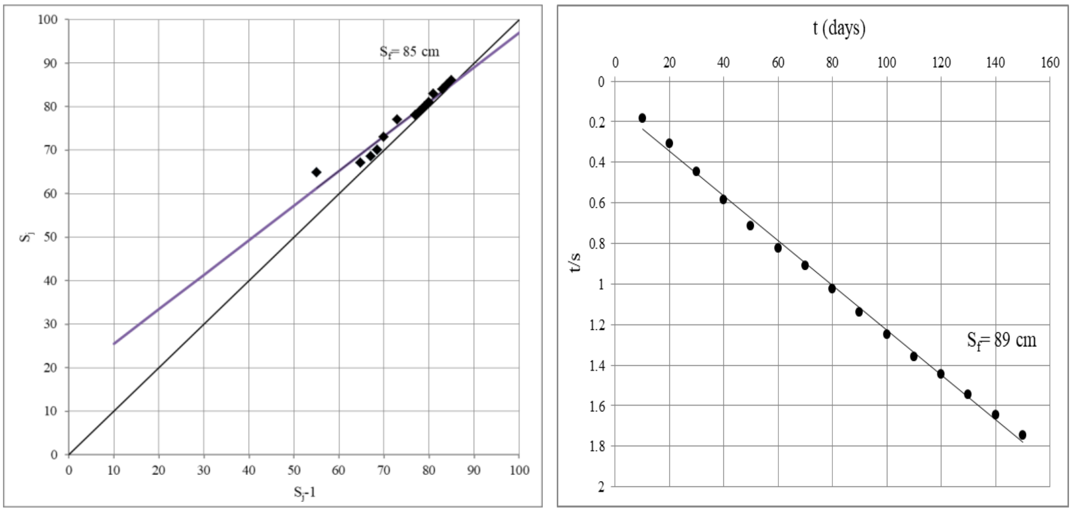

Figure 4.28. Asaoka and Horn plot for Km: 163+000 for surface settlement plates

4.2.2 Primary consolidation settlements from field settlement – time data: √t method

In Figure 4.29, completion times of the primary consolidation for Station 1 at Km: 139+764 and for Station 2 at Km: 139+860 are obtained as 146 and 125 days with final primary consolidation amounts of 91 cm and 92 cm, respectively.

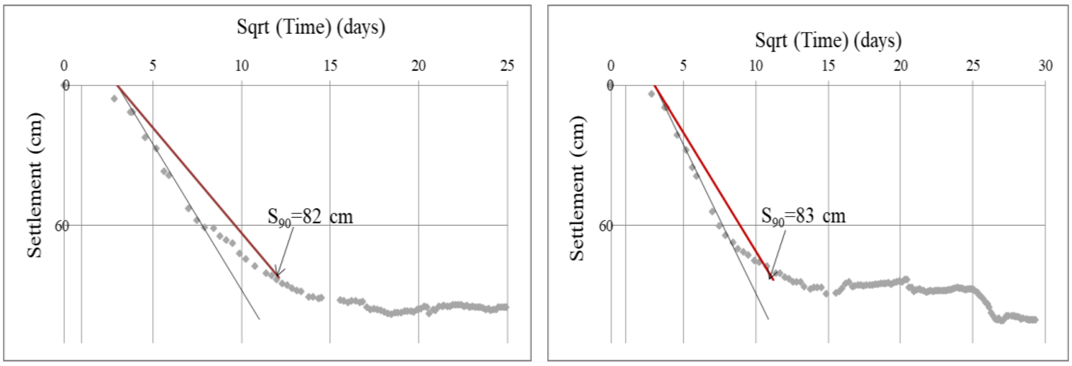

Km: 139+764 Km: 139+860

Figure 4.29. Primary consolidation settlement amounts for Station 1 at Km: 139+764 and for Station 2 at Km: 139+860

In Figure 4.30, completion times of the primary consolidation for Station 3 at Km: 140+592 and for Station 4 at Km: 141+680 are obtained as 529 and 676 days with final primary consolidation amounts of 102 cm and 185 cm, respectively.

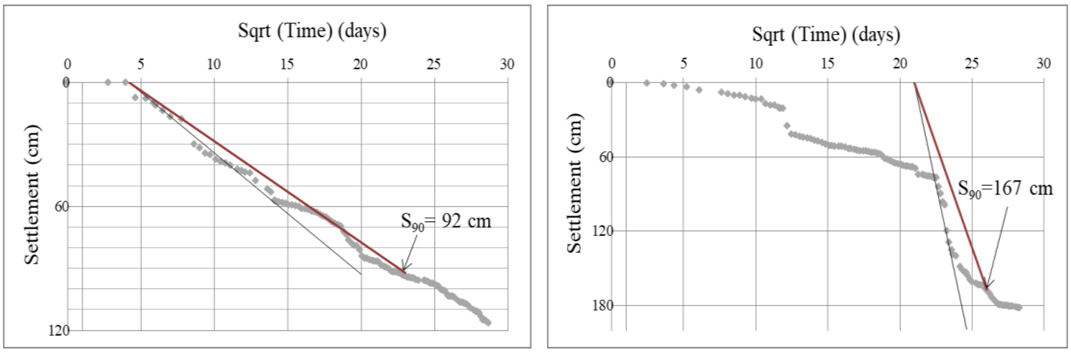

Km: 140+592 Km: 141+680

Figure 4.30. Primary consolidation settlement amounts for Station 3 at Km: 140+592 and for Station 4 at Km: 141+680

In Figure 4.31, completion times of the primary consolidation for Station 5 at Km: 142+000 and for Station 6 at Km: 142+400 are obtained as 729 days with final primary consolidation amounts of 129 cm and 120 cm, respectively.

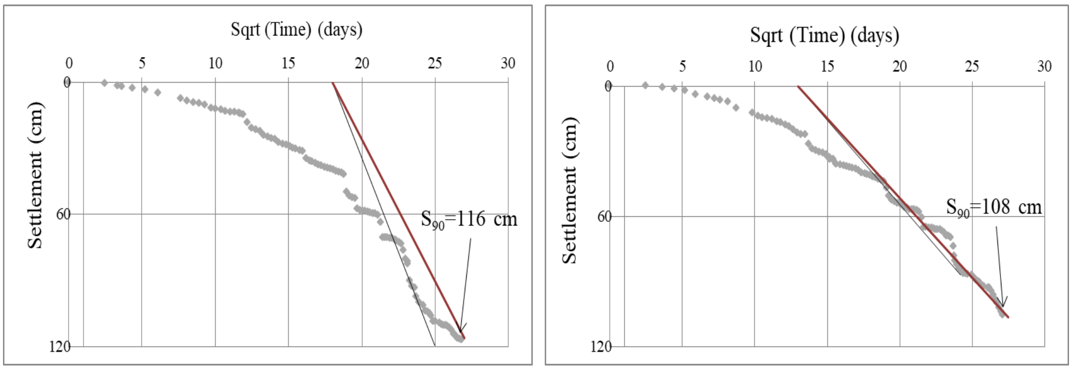

Km: 142+000

Km: 142+400

Figure 4.31. Primary consolidation settlement amounts for Station 5 at Km: 142+000 and for Station 6 at Km: 142+400

In Figure 4.32, completion times of the primary consolidation for Station 7 at Km: 143+107 and for Station 8 at Km: 144+000 are obtained as 475 and 310 days with final primary consolidation amounts of 102 cm and 112 cm, respectively.

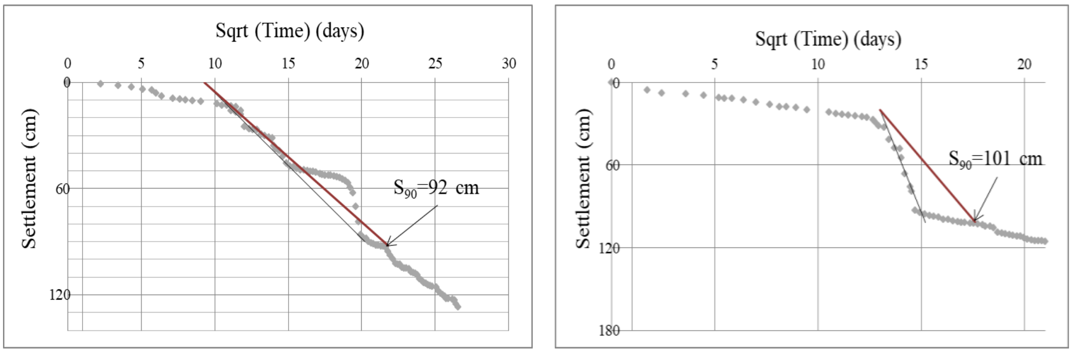

Km: 143+107

Km: 144+000

Figure 4.32. Primary consolidation settlement amounts for Station 7 at Km: 143+107 and for Station 8 at Km: 144+000

In Figure 4.33, completion times of the primary consolidation for Station 9 at Km: 145+000 and for Station 10 at Km: 146+210 are obtained as 210 and 144 days with primary consolidation amounts of 89 cm and 97 cm, respectively.

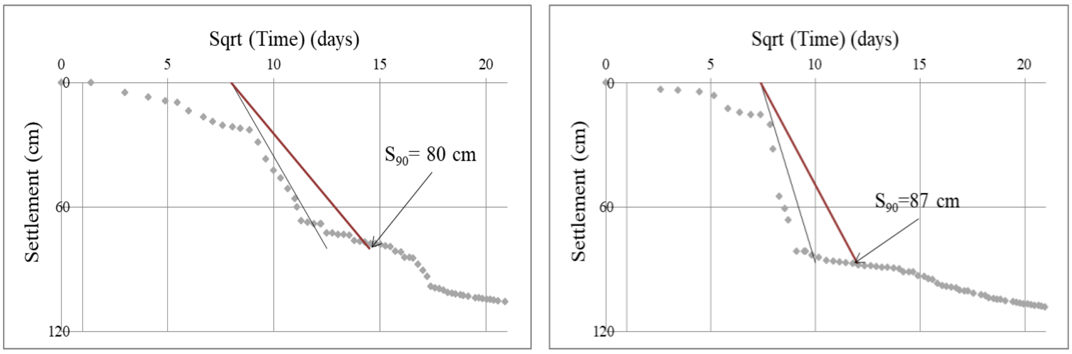

Km: 145+000

Km: 146+210

Figure 4.33. Primary consolidation settlement amounts for Station 9 at Km: 145+000 and for Station 10 at Km: 146+210

In Figure 4.34, completion times of the primary consolidation for Station 11 at Km: 147+000 and for Station 12 at Km: 149+000 are obtained as 331 and 420 days with primary consolidation amounts of 82 cm and 89 cm, respectively.

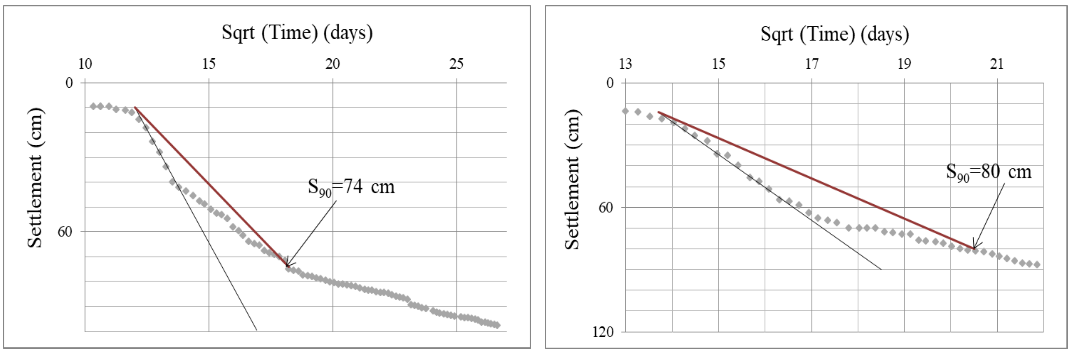

Km: 147+000

Km: 149+000

Figure 4.34. Primary consolidation settlement amounts for Station 11 at Km: 147+000 and for Station 12 at Km: 149+000

In Figure 4.35, completion times of the primary consolidation for Station 13 at Km: 150+000 and for Station 14 at Km: 150+500 are obtained as 529 and 392 days with primary consolidation amounts of 113 cm and 122 cm, respectively.

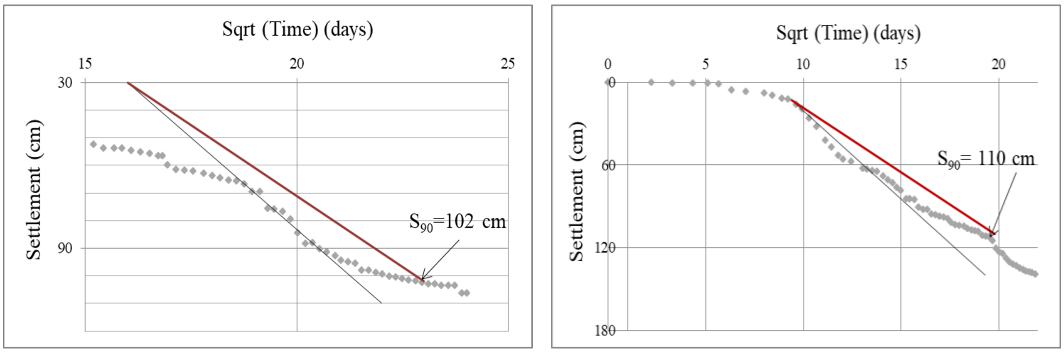

Km: 150+000 Km: 150+500

Figure 4.35. Primary consolidation settlement amounts for Station 13 at Km: 150+000 and for Station 14 at Km: 150+500

In Figure 4.36, completion times of the primary consolidation for Station 15 at Km: 151+220 and for Station 16 at Km: 151+975 are obtained as 298 and 428 days with primary consolidation amounts of 158 cm and 117 cm, respectively.

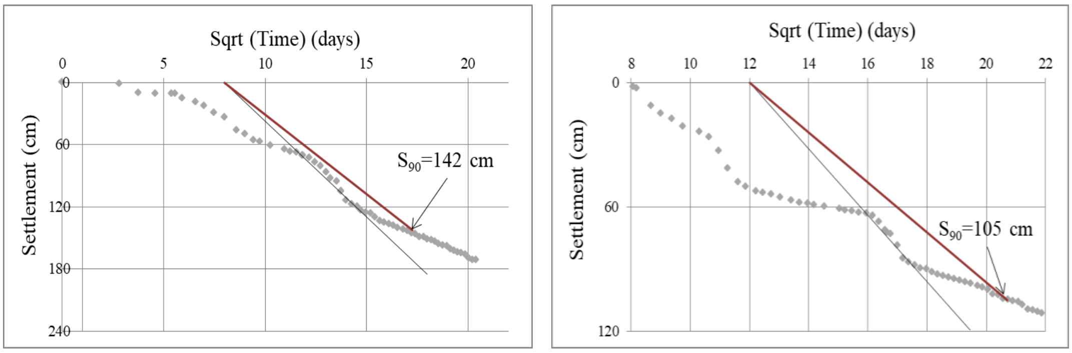

Km: 151+220 Km: 151+975

Figure 4.36. Primary consolidation settlement amounts for Station 15 at Km: 151+220 and for Station 16 at Km: 151+975

In Figure 4.37, completion times of the primary consolidation for Station 17 at Km: 152+000 and for Station 18 at Km: 154+500 are obtained as 361 and 493 days with primary consolidation amounts of 100 cm and 91 cm, respectively.

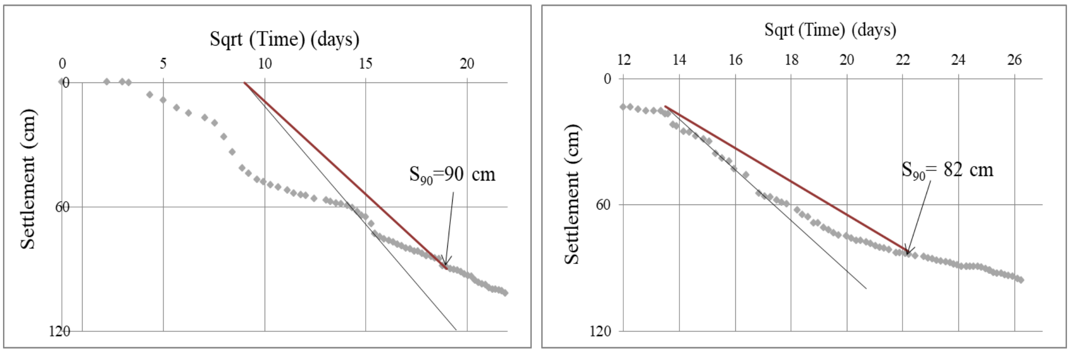

Km: 152+000 Km: 154+500

Figure 4.37. Primary consolidation settlement amounts for Station 17 at Km: 152+000 and for Station 18 at Km: 154+500

In Figure 4.38, completion times of the primary consolidation for Station 19 at Km: 155+000 and for Station 20 at Km: 155+551 are obtained as 416 and 529 days with primary consolidation amounts of 92 cm and 122 cm, respectively.

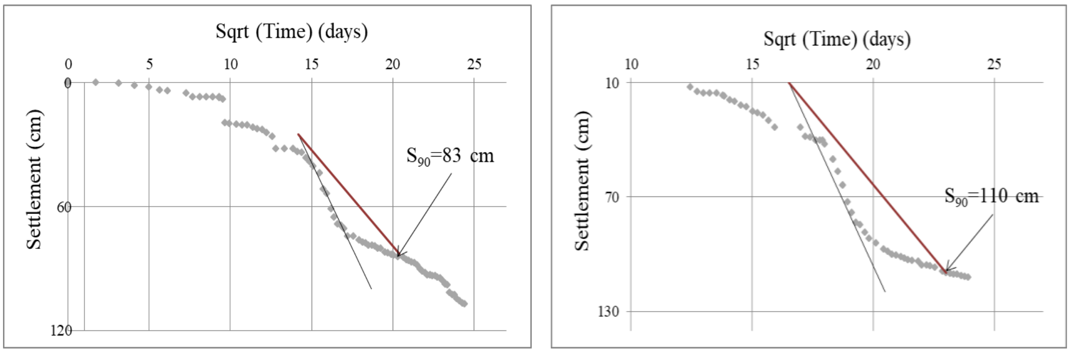

Km: 155+000 Km: 155+551

Figure 4.38. Primary consolidation settlement amounts for Station 19 at Km: 155+000 and for Station 20 at Km: 155+551

In Figure 4.39, completion times of the primary consolidation for Station 21 at Km: 157+400 and for Station 22 at Km: 158+000 are obtained as 81 and 382 days with primary consolidation amounts of 109 cm and 117 cm, respectively.

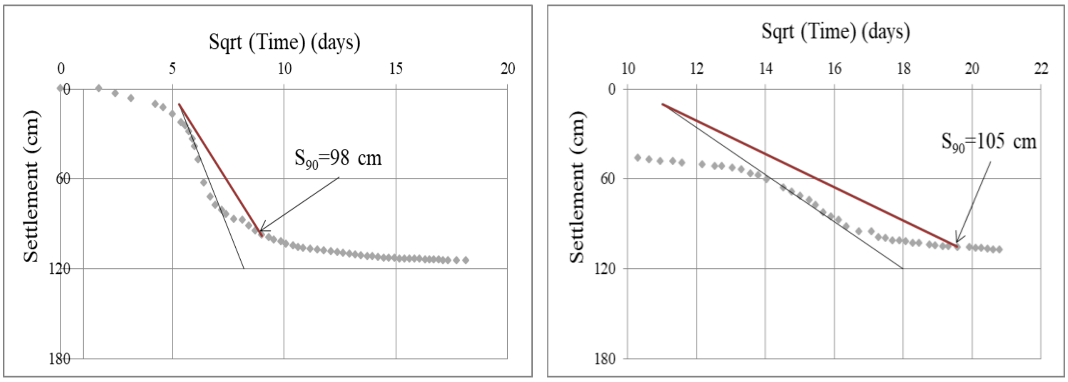

Km: 157+400 Km: 158+000

Figure 4.39. Primary consolidation settlement amounts for Station 21 at Km: 157+400 and for Station 22 at Km: 158+000

In Figure 4.40, completion times of the primary consolidation for Station 23 at Km: 159+565 and for Station 24 at Km: 161+764 are obtained as 408 and 529 days with primary consolidation amounts of 83 cm and 86 cm, respectively.

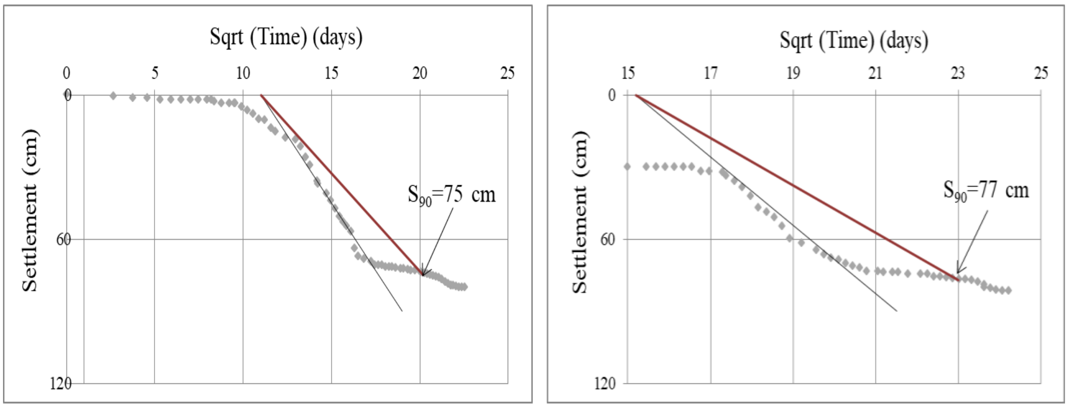

Km: 159+565 Km: 161+764

Figure 4.40. Primary consolidation settlement amounts for Station 23 at Km: 159+565 and for Station 24 at Km: 161+764

In Figure 4.41, completion times of the primary consolidation for Station 25 at Km: 162+555 and for Station 26 at Km: 163+000 are obtained as 400 and 506 days with primary consolidation amount of 94 cm.

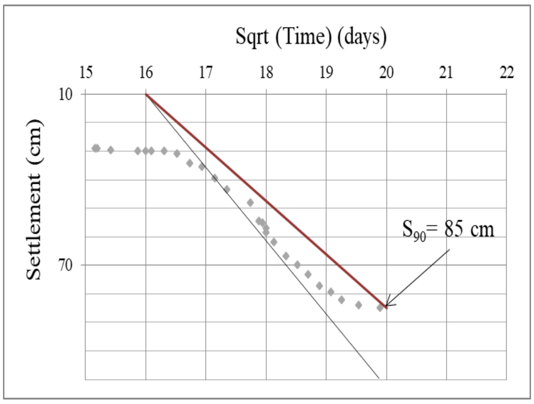

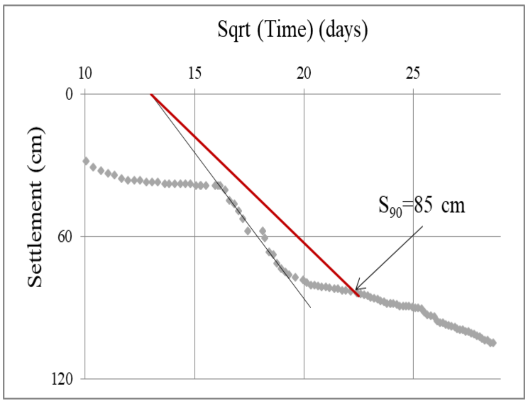

Km: 162+555 Km: 163+000

Figure 4.41. Primary consolidation settlement amounts for Station 25 at Km: 162+555 and for Station 26 at Km: 163+000

4.3 Secondary and Tertiary Consolidation Settlements from field settlement – time data: log t method

In this part of the study, secondary and tertiary consolidation settlement behaviors of the clay layers were researched. The secondary and tertiary consolidation amounts with time durations, index parameters (C_s-C_t) calculated from log (Time) vs. settlement graphs, comparisons of these index parameters with literature proposals and their relations with primary compression index (C_c) parameters were evaluated in the content of this chapter.

The graphs of log (Time) vs. settlement are presented in Figures 4.42-4.54. In these figures, the times for completion of primary consolidation settlements and the start of secondary consolidations are shown as t_{100} and C_s index values are easily determined from slopes of linear sections.

In Figure 4.42, completion times of the primary consolidation for Km: 139+764 and Km: 139+860 are obtained as 203 and 110 days with primary consolidation amounts of 93 cm and 85 cm, respectively. The coefficients of secondary consolidation index parameters are calculated from the slopes t_s-t_{100} lines as 0.00281 and 0.0017.

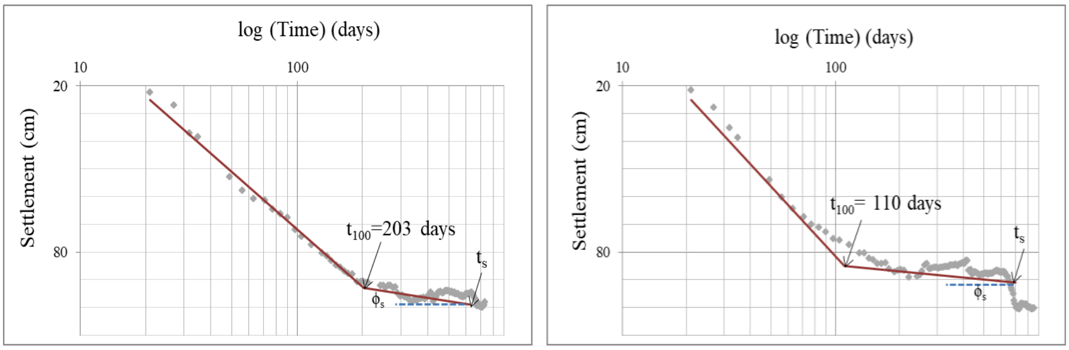

Km: 139+764 Km: 139+860

Figure 4.42. Log (Time) vs. Settlement (cm) graphs for Km: 139+764 and Km: 139+860

In Figure 4.43, completion times of the primary consolidation for Km: 140+592 and Km: 141+680 are obtained as 455 and 588 days, respectively. The primary consolidation amounts are obtained as 92 cm and 155 cm, respectively.

The coefficients of secondary consolidation index parameters are calculated from the slopes t_s-t_{100} lines as 0.0086 and 0.040. For section Km: 140+592, after 170 days from completion of the primary consolidation, the settlement curve is getting steeper, which indicates the start of tertiary consolidation. The coefficient of tertiary consolidation index is calculated as 0.038. For section Km: 141+680, after 87 days from completion of the primary consolidation, the settlement curve is getting steeper, which indicates the start of tertiary consolidation. The coefficient of tertiary consolidation index is calculated as 0.15.

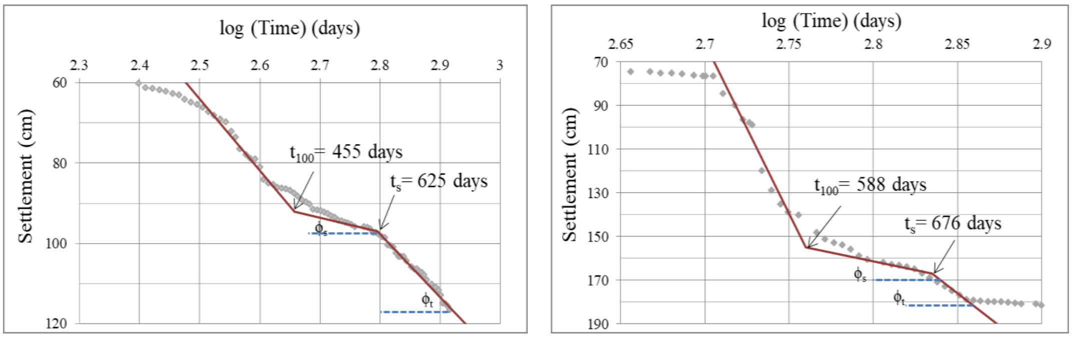

Km: 140+592

Km: 141+680

Figure 4.43. Log (Time) vs. Settlement (cm) graphs for Km: 140+592 and Km: 141+680

In Figure 4.44, completion times of the primary consolidation for Km: 142+000 and Km: 142+400 are obtained as 588 and 570 days, respectively. The primary consolidation amounts are obtained as 112 and 88 cm, respectively.

The coefficients of secondary consolidation index parameters are calculated from the slopes t_s-t_{100} lines as 0.0194 and 0.0199. For section Km: 142+400, after 114 days from completion of the primary consolidation, the settlement curve is getting steeper, which indicates the start of tertiary consolidation. The coefficient of tertiary consolidation index is calculated as 0.104.

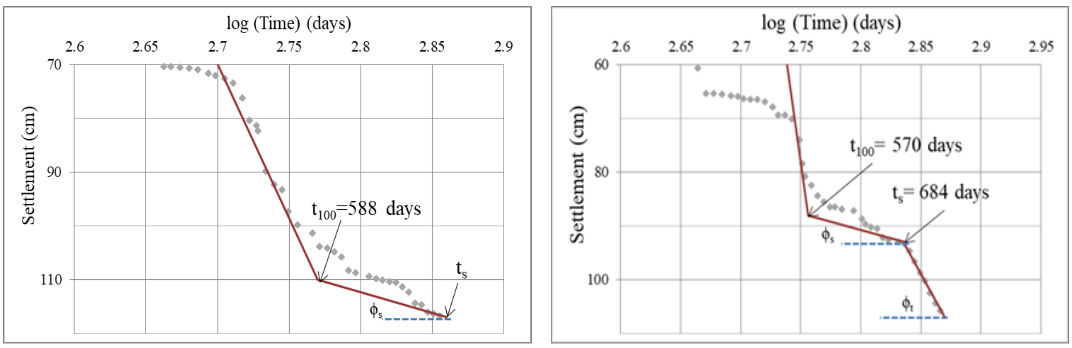

Km: 142+000

Km: 142+400

Figure 4.44. Log (Time) vs. Settlement (cm) graphs for Km: 142+000 and Km: 142+400

In Figure 4.45, completion times of the primary consolidation for Km: 143+107 and Km: 144+000 are obtained as 398 and 214 days, respectively. The primary consolidation settlement amounts are obtained as 90 and 96 cm, respectively.

The coefficients of secondary consolidation index parameters are calculated from the slopes t_s-t_{100} lines as 0.0103 and 0.0150. For section Km: 143+107, after 75 days from completion of primary consolidation, likewise, the settlement curve is getting steeper, which indicates the start of tertiary consolidation. The coefficient of tertiary consolidation index is calculated as 0.053. For section Km: 144+000, after 299 days from completion of the primary consolidation, the settlement curve is getting steeper, which indicates the start of tertiary consolidation. The coefficient of tertiary consolidation index is calculated as 0.046.

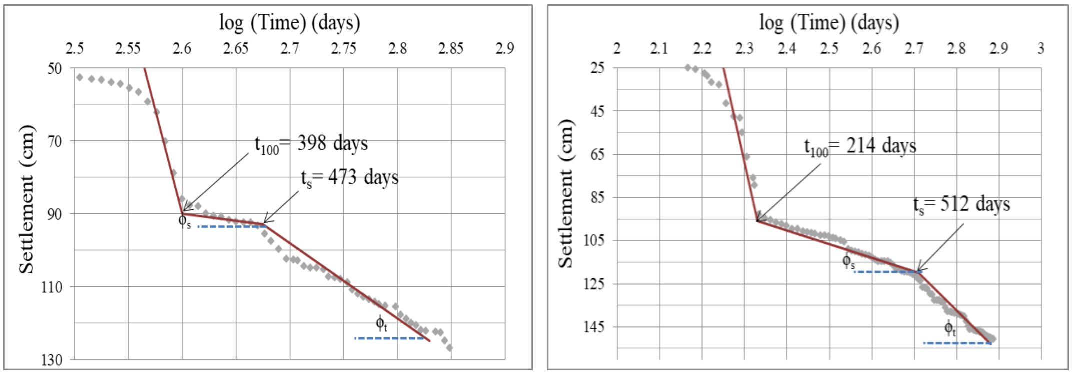

Km: 143+107 Km: 144+000

Figure 4.45. Log (Time) vs. Settlement (cm) graphs for Km: 143+107 and Km: 144+000

In Figure 4.46, completion times of the primary consolidation for Km: 145+000 and Km: 146+210 are obtained as 139 and 83 days, respectively. The primary consolidation amounts are obtained as 78 and 85 cm, respectively.

The coefficients of secondary consolidation index parameters are calculated from the slopes t_s-t_{100} lines as 0.0082 and 0.0049. For section Km: 145+000, after 123 days from completion of the primary consolidation, the settlement curve is getting steeper, which indicates the start of tertiary consolidation. The coefficient of tertiary consolidation index is calculated as 0.0657. For section Km: 146+210, after 141 days from completion of the primary consolidation, likewise, the settlement curve is getting steeper, which indicates the start of tertiary consolidation. The coefficient of tertiary consolidation index is calculated as 0.0175.

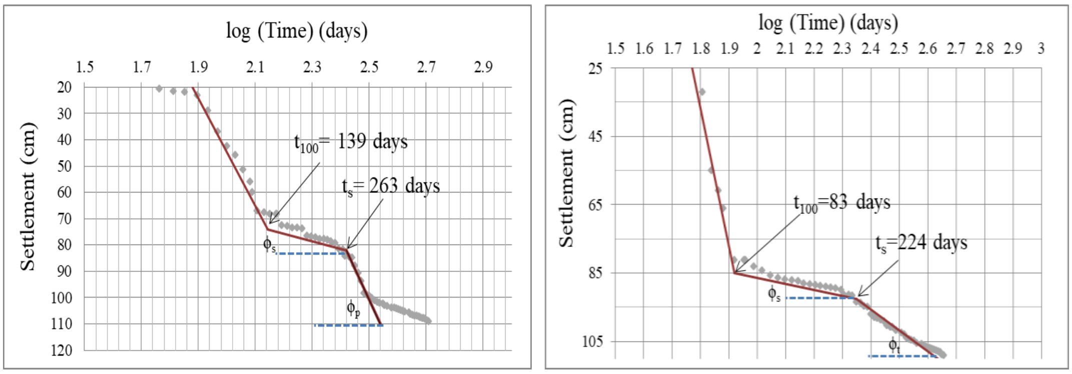

Km: 145+000

Km: 146+210

Figure 4.46. Sqrt (Time) vs. Settlement (cm) graphs for Km: 145+000 and Km: 146+210

In Figure 4.47, completion times of the primary consolidation for Km: 147+000 and Km: 149+000 are obtained as 355 and 310 days with primary consolidation amounts of 79 cm and 70 cm, respectively. The coefficients of secondary consolidation index parameters are calculated from the slopes t_s-t_{100} lines as 0.0160 and 0.0286.

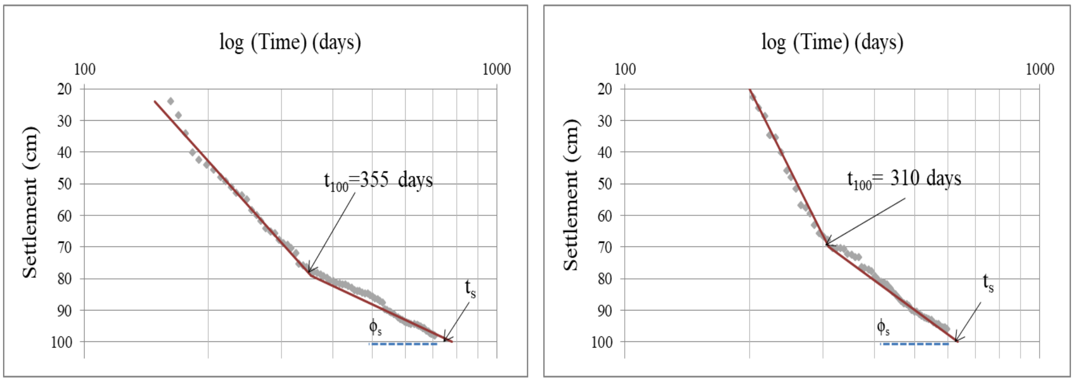

Km: 147+000 Km: 149+000

Figure 4.47. Log (Time) vs. Settlement (cm) graphs for Km: 147+000 and Km: 149+000

In Figure 4.48, completion times of the primary consolidation for Km: 150+000 and Km: 150+500 are obtained as 425 days with primary consolidation amounts of 100 cm and 132 cm, respectively. The coefficients of secondary consolidation index parameters are calculated from the slopes t_s-t_{100} lines as 0.0140 and 0.0232.

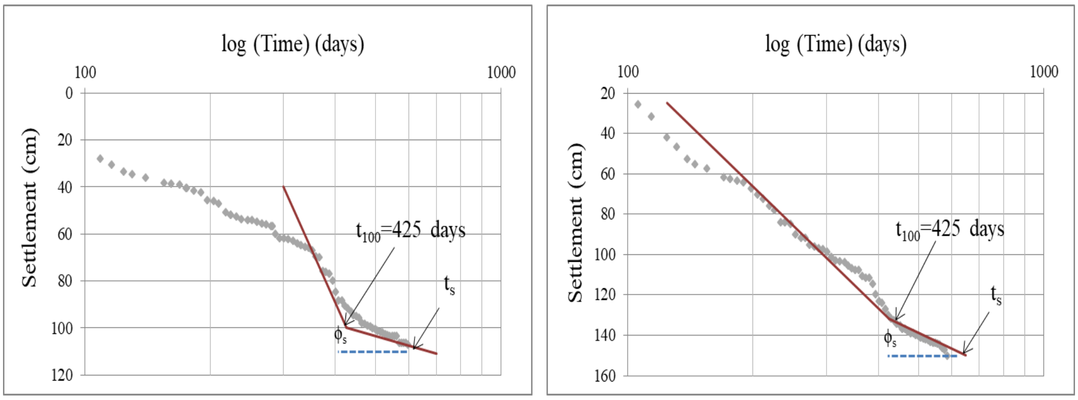

Km: 150+000 Km: 150+500

Figure 4.48. Log (Time) vs. Settlement (cm) graphs for Km: 150+000 and Km: 150+500

In Figure 4.49, completion times of the primary consolidation for Km: 151+220 and Km: 151+975 are obtained as 200 and 300 days with primary consolidation amounts of 124 cm and 92 cm, respectively. The coefficients of secondary consolidation index parameters are calculated from the slopes t_s-t_{100} lines as 0.0367 and 0.0283.

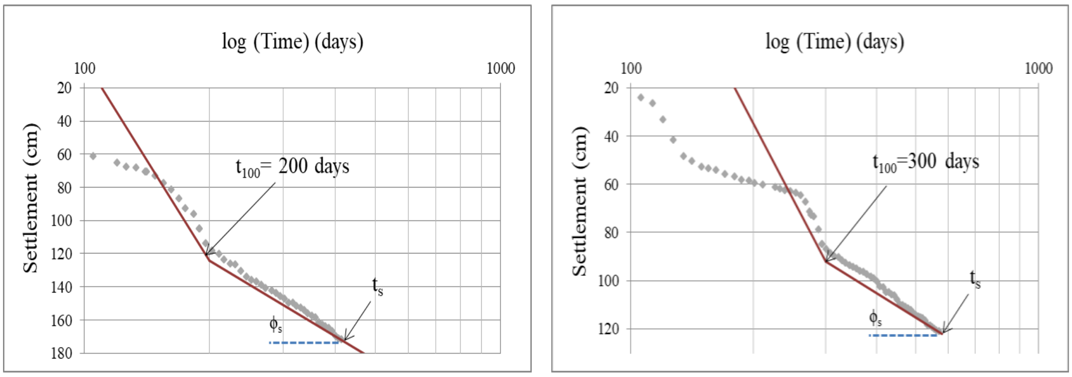

Km: 151+220 Km: 151+975

Figure 4.49. Log (Time) vs. Settlement (cm) graphs for Km: 151+220 and Km: 151+975

In Figure 4.50, completion times of the primary consolidation for Km: 152+000 and Km: 154+500 are obtained as 245 and 400 days with primary consolidation amounts of 78 cm and 80 cm, respectively. The coefficients of secondary consolidation index parameters are calculated from the slopes t_s-t_{100} lines as 0.0248 and 0.0156.

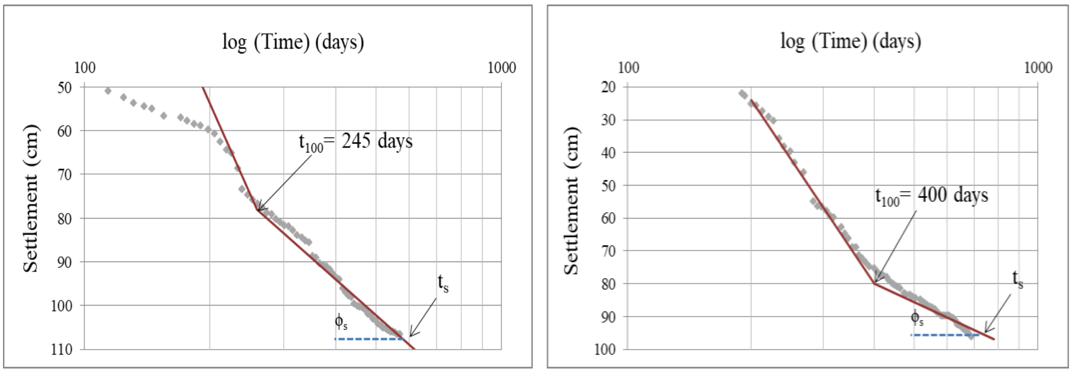

Km: 152+000 Km: 154+500

Figure 4.50. Log (Time) vs. Settlement (cm) graphs for Km: 152+000 and Km: 154+500

In Figure 4.51, completion times of the primary consolidation for Km: 155+000 and Km: 155+551 are obtained as 295 and 400 days, respectively. The primary consolidation settlement amounts are obtained as 78 and 104 cm, respectively.

The coefficients of secondary consolidation index parameters are calculated from the slopes t_s-t_{100} lines as 0.0179 and 0.0146. For section Km: 155+000, after 171 days from completion of primary consolidation, settlement curve is getting steeper, which indicates the start of tertiary consolidation. The coefficient of tertiary consolidation index is calculated as 0.0543.

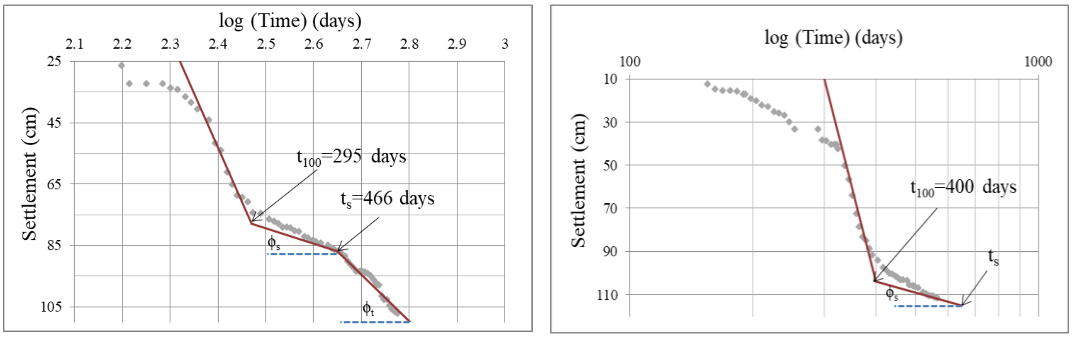

Km: 155+000 Km: 155+551

Figure 4.51. Log (Time) vs. Settlement (cm) graphs for Km: 155+000 and Km: 155+551

In Figure 4.52, completion times of the primary consolidation for Km: 157+400 and Km: 158+000 are obtained as 55 and 300 days, respectively. The primary consolidation settlement amounts are obtained as 104 and 102 cm, respectively. The coefficients of secondary consolidation index parameters are calculated from the slopes t_s-t_{100} lines as 0.0038 and 0.012.

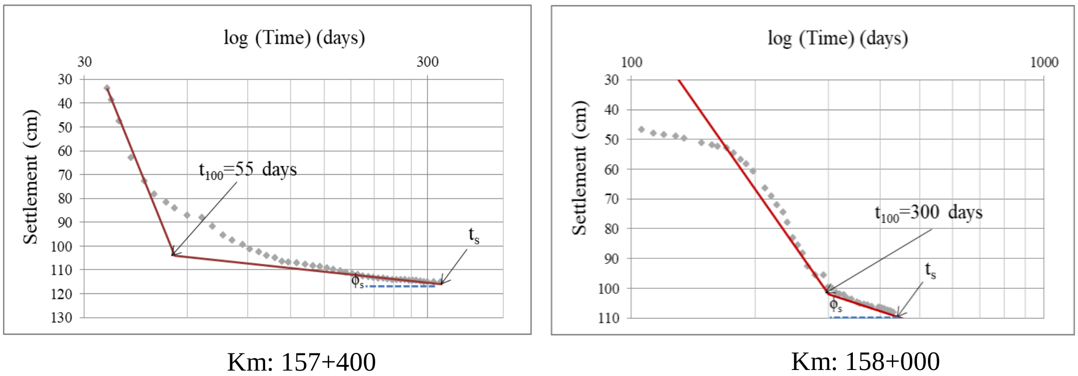

Figure 4.52. Log (Time) vs. Settlement (cm) graphs for Km: 157+400 and Km: 158+000

In Figure 4.53, completion times of the primary consolidation for Km: 159+565 and Km: 161+764 are obtained as 295 and 390 days, respectively. The primary consolidation settlement amounts are obtained as 73 cm.

The coefficients of secondary consolidation index parameters are calculated from the slopes t_s-t_{100} lines as 0.0061 and 0.0178. For section Km: 159+565, after 131 days from completion of primary consolidation, settlement curve is getting steeper, which indicates the start of tertiary consolidation. The coefficient of tertiary consolidation index is calculated as 0.0345.

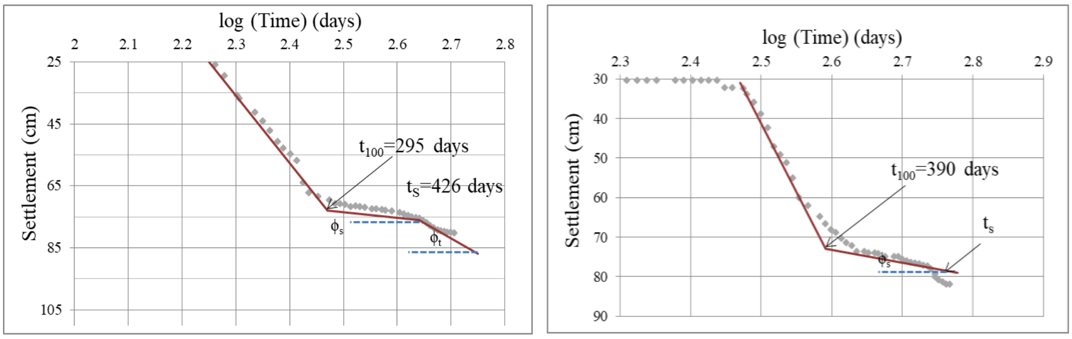

Km: 159+565 Km: 161+764

Figure 4.53. Log (Time) vs. Settlement (cm) graphs for Km: 159+565 and Km: 161+764

In Figure 4.54, completion times of the primary consolidation for Km: 162+555 and Km: 163+000 are obtained as 359 and 338 days, respectively. The primary consolidation settlement amounts are obtained as 89 and 78 cm, respectively.

The coefficients of secondary consolidation index parameters are calculated from the slopes t_s-t_{100} lines as 0.0038 and 0.0162. For section Km: 162+555, after 142 days from completion of primary consolidation, settlement curve is getting steeper, which indicates the start of tertiary consolidation. The coefficient of tertiary consolidation index is calculated as 0.045. For section Km: 163+000, after 186 days from completion of primary consolidation, settlement curve is getting steeper which indicates the start of tertiary consolidation. The coefficient of tertiary consolidation index is calculated as 0.029.

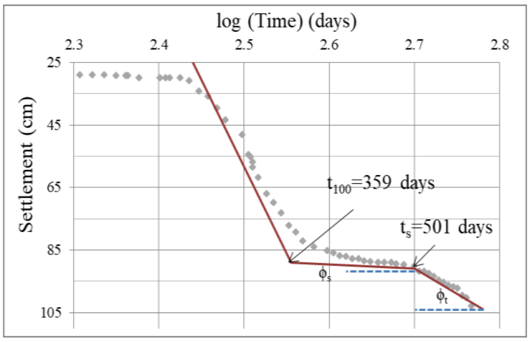

Km: 162+555

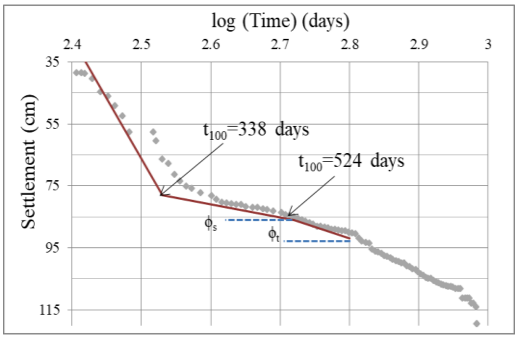

Km: 163+000

Figure 4.54. Log (Time) vs. Settlement (cm) graphs for Km: 162+555 and Km: 163+000

The summary for consolidation settlements obtained from instrumented test embankments, including primary, secondary and tertiary settlements, calculated consolidation settlements from oedometer test data, anticipated immediate settlements in the cohesionless layers are presented in Table 4.1 for each station. First of all, summary of final field settlements measured in instrumented test embankments are noted as S1. In order to subtract anticipated immediate settlements in cohesionless layer from final field settlements measured in the settlement plate, immediate settlements in the cohesionless layers are calculated and presented as S2. Primary consolidation settlements predicted from time vs. settlement graphs are presented as S3. Consolidation settlement amounts presented in Appendix C, are summarized as S4. Predicted secondary and tertiary consolidation settlement amounts from logarithm of time versus settlement graphs are presented as S5 and S6. Primary consolidation settlement amounts are considered as the settlement amounts obtained from logarithm of time versus settlement amounts graphs.

According to Table 4.1, the estimated primary consolidation settlement amounts from log (Time) graph is nearly 15% less than the consolidation settlement amounts from square root (Time) graph. The secondary consolidation amounts are 11% times of the primary consolidations, in average. The tertiary consolidation amounts are 26% times of the primary consolidations, in average.

The summary of index parameters for the primary, secondary and tertiary consolidation settlements are presented in Table 4.2 and prepared graph for C_s/C_c with a mean value of 0.084 is presented in Figure 4.55. In Figure 4.56, histogram graph is presented and it is seen that majority of C_s/C_c values fall within range of 0.02 and 0.04. The graph prepared for C_t/C_c with a mean value of 0.27 is presented in Figure 4.57. In Figure 4.58, histogram graph is presented and it is seen that majority of C_t/C_c values fall within range of 0.2 and 0.3.

The values of C_s/C_c for natural soils (modified from Mesri and Godlewski, 1977) is presented in Chapter 2 in Table 2.2. According to this table, the behavior of Karacabey Plain clay is similar to Amorphous and fibrous peat, Sensitive clay, Portland, Maine. It is also presented in Figure 4.59. According to classification of soils based on secondary compressibility (Mesri, 1973) presented in Table 2.3, soil can be defined as clay with medium to high secondary compressibility.

Table 4.1 Summary of primary, secondary, tertiary settlement amounts obtained from field data

Station No	Kilometer	Settlement Plate Location	S1	S2	S3		S4	S5	S6	S7
			(Final settlement measured in the plate) (cm)	(Anticipated immediate settlements in the cohesionless layer) (cm)	(Primary settlement from field measurements) (cm)		(Primary settlement computed from oedometer data) (cm)	(Amount of secondary settlements) (cm)	(Amount of tertiary settlement) (cm)	(Field primary consolidation settlement) (cm)
					log t	sqrt t				
Station No: 1	KM 139+764	Depth: 0.0-24.0 m)	98.2	0	93	91	90.68	5.2		93.0
		Depth>24.0 m	69.1				10.84			
Station No: 2	KM 139+860	Depth: 0.0-24.0 m)	100.2	0	85	92	90.68	15.2		85.0
		Depth>24.0 m	90.0				10.84			
Station No: 3	KM 140+592	Surface	116.6	0	92	102	101.52	5	19.6	92.0
Station No: 4	KM 141+680	Surface	181.2	5	155	185.56	140.26	12	9.2	155.0
Station No: 5	KM 142+000	Surface	125.8	3	117	128.9	111.69	5		117.8
Station No: 6	KM 142+400	Surface	105.8	2	88	120	92.44	6	9.8	88.0
Station No: 7	KM 143+107	Surface	127.0	2	90	102.2	103.09	5	30.0	90.0
Station No: 8	KM 144+000	Surface	155.4	3	96	112	103.24	16	40.4	96.0
Station No: 9	KM 145+000	Surface	116.8	3	78	80	82.75	4	31.8	78.0
Station No: 10	KM 146+210	Surface	108.8	3	85	96.67	102.04	3	17.8	85.0
Station No: 11	KM 147+000	Surface	98.0	4	79	82	69.99	15.0		79.0
Station No: 12	KM 149+000	Surface	96.0	5	70	88.9	76.48	21.0		70.0
Station No: 13	KM 150+000	Surface	107.2	4	100	113.33	98.75	3.2		100.0
Station No: 14	KM 150+500	Surface	150.6	7	132	122.22	119.41	11.6		132.0
Station No: 15	KM 151+220	Surface	171.9	6	124	157.78	127.02	41.9		124.0
Station No: 16	KM 151+975	Surface	123.7	5	92	116.67	79.88	26.7		92.0
Station No: 17	KM 152+000	Surface	108.3	2	78	100	87.42	28.3		78.0
Station No: 18	KM 154+500	Surface	96.1	1	80	91	93.14	15.1		80.0
Station No: 19	KM 155+000	Surface	107.1	2	78	92	81.9	9	18.1	78.0
Station No: 20	KM 155+551	Surface	113.4	5	104	122.22	113.06	4.4		104.0
Station No: 21	KM 157+400	Surface	115.3	1	104	108	80.73	10.3		104.0
Station No: 22	KM 158+000	Surface	108.1	3	102	116.67	72.02	3.1		102.0
Station No: 23	KM 159+565	Surface	80.5	2	73	83.33	72.79	3	2.5	73.0
Station No: 24	KM 161+764	Surface	81.9	2.5	73	85.56	58.9	6.4		73.0
Station No: 25	KM 162+555	Surface	103.2	2.3	89	94.44	80.55	3	8.9	89.0
Station No: 26	KM 163+000	Surface	130.7	1	78	94.44	82.25	3	48.7	78.0

Table 4.2 Summary of the index parameters for primary, secondary and tertiary consolidation Settlements

Station No	Kilometer	C_c	C_s	C_t	C_s/C_c	C_t/C_c
Station No: 1	KM 139+764	0.139	0.0028		0.020	
Station No: 2	KM 139+860	0.127	0.0017		0.013	
Station No: 3	KM 140+592	0.139	0.0086	0.0380	0.062	0.27
Station No: 4	KM 141+680	0.236	0.0400	0.1500	0.170	0.66
Station No: 5	KM 142+000	0.222	0.0194		0.087	
Station No: 6	KM 142+400	0.338	0.0199	0.1040	0.059	0.31
Station No: 7	KM 143+107	0.211	0.0103	0.0529	0.049	0.26
Station No: 8	KM 144+000	0.161	0.0150	0.0462	0.094	0.30
Station No: 9	KM 145+000	0.244	0.0082	0.0657	0.034	0.27
Station No: 10	KM 146+210	0.210	0.0049	0.0175	0.023	0.09
Station No: 11	KM 147+000	0.143	0.0160		0.111	
Station No: 12	KM 149+000	0.228	0.0286		0.126	
Station No: 13	KM 150+000	0.217	0.0140		0.065	
Station No: 14	KM 150+500	0.267	0.0232		0.087	
Station No: 15	KM 151+220	0.173	0.0367		0.213	
Station No: 16	KM 151+975	0.147	0.0283		0.193	
Station No: 17	KM 152+000	0.140	0.0222		0.177	
Station No: 18	KM 154+500	0.149	0.0156		0.105	
Station No: 19	KM 155+000	0.230	0.0179	0.0543	0.078	0.24
Station No: 20	KM 155+551	0.278	0.0146		0.052	
Station No: 21	KM 157+400	0.174	0.0038		0.022	
Station No: 22	KM 158+000	0.177	0.0120		0.068	
Station No: 23	KM 159+565	0.266	0.0061	0.0345	0.023	0.13
Station No: 24	KM 161+764	0.195	0.0178		0.092	
Station No: 25	KM 162+555	0.166	0.0038	0.0451	0.023	0.28
Station No: 26	KM 163+000	0.125	0.0162	0.0288	0.130	0.22

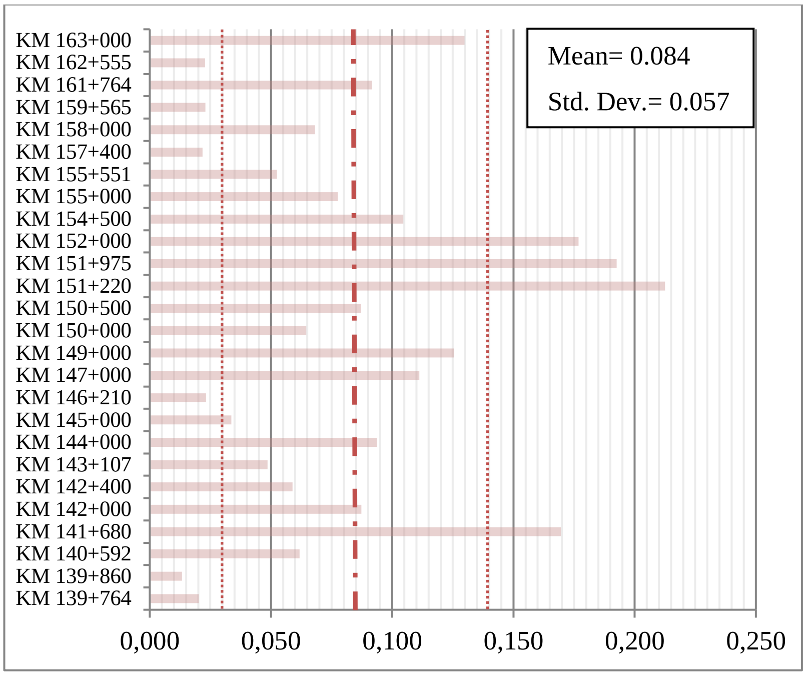

Figure 4.55. C_s/C_c graph for each station

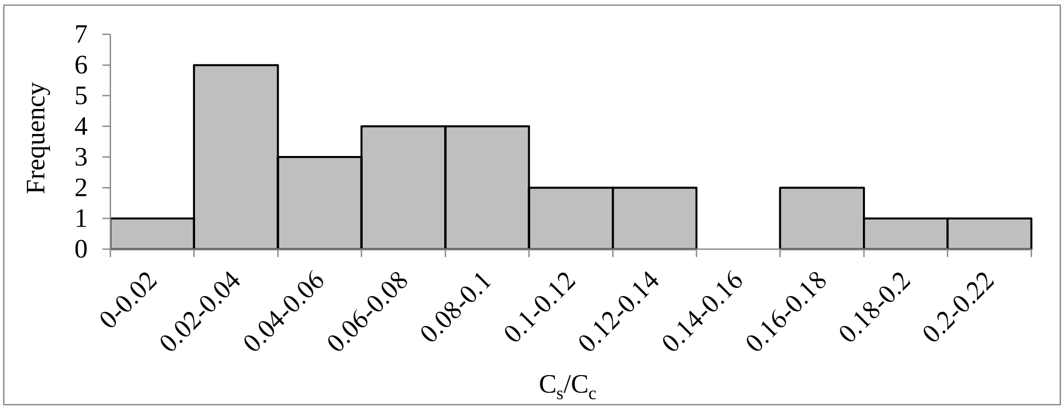

Figure 4.56. Histogram graph for C_s/C_c

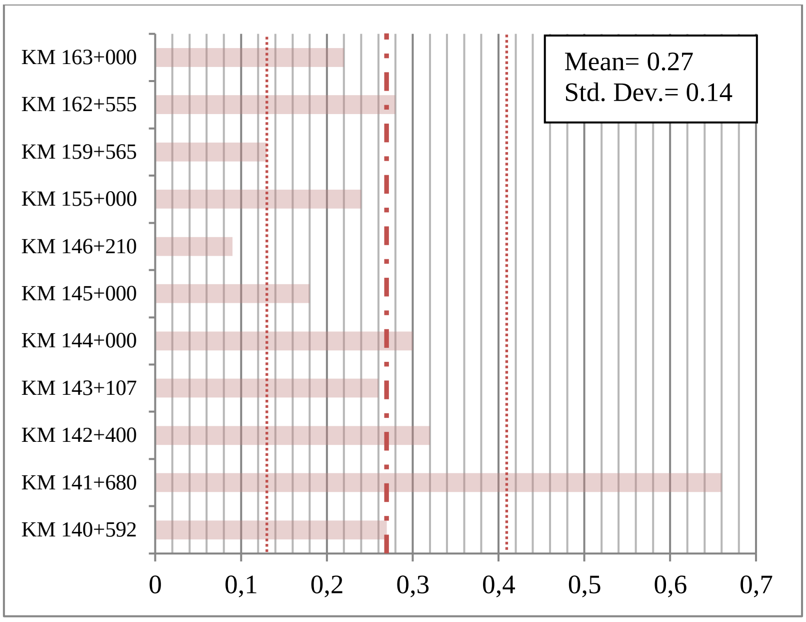

Figure 4.57. C_t/C_c graph for each station

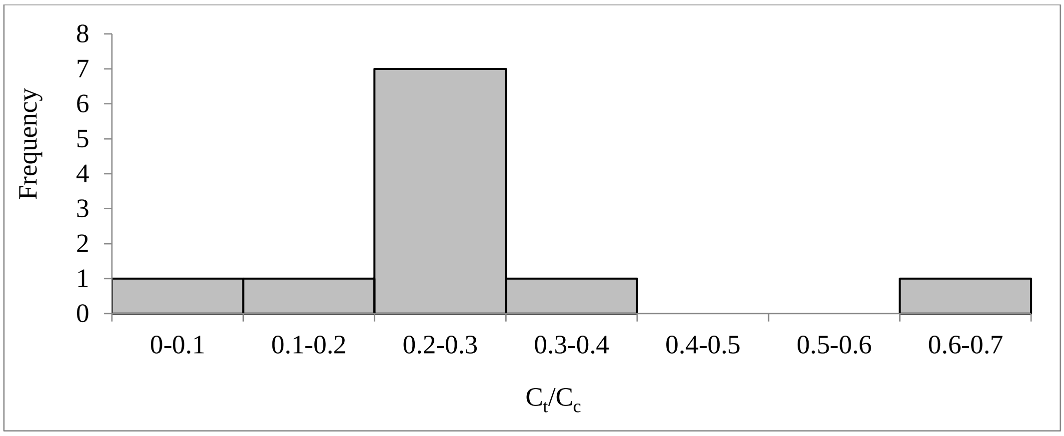

Figure 4.58. Histogram graph for C_t/C_c

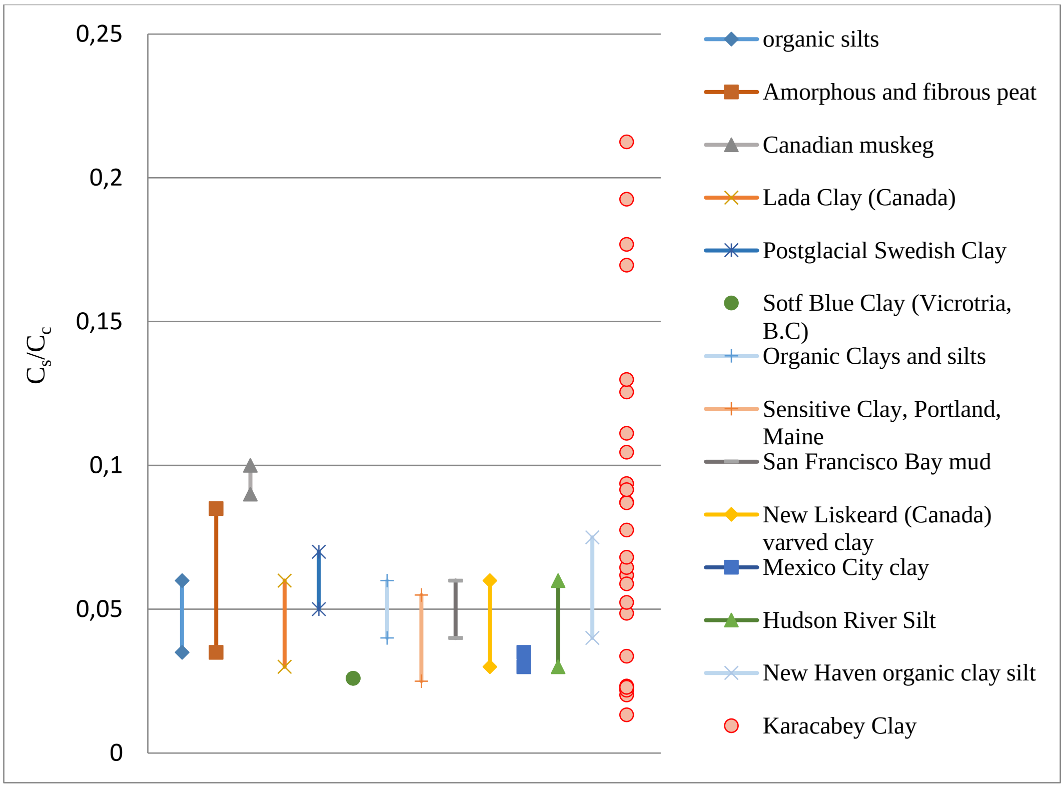

Figure 4.59. Values of C_s/C_c for natural soils (modified from Mesri and Godlewski, 1977)

4.4 Correlations of the Observed and Predicted Soil Parameters

In embankment design projects, it is very important to predict the consolidation amounts and consolidation time periods of the soil in order to follow the design time schedules. In engineering practices, engineers try to predict to the settlement amounts and durations with limited amount of laboratory test results and propose geotechnical precautions when necessary.

In this section of the study, some equations are presented to obtain the relations between the amounts of the observed settlements in field and the analytically calculated primary consolidation settlements. Also, correlations between cone tip resistance (q_c) and α_m are searched. The considered laboratory parameters are PI, LL, LI, w_N, e_0 with field parameter of SPT N and Cone tip resistance (q_c). Furthermore, to present the complex geometry of geology of the alluvial deposit of the site, λ, a parameter defined as the ratio of sand thickness to clay thickness and ψ, defined as the ratio of length of road platform to total clay thickness are also taken into account as other parameters.

The researches have revealed that the relationship between independent (SPT N, PI, LL, LI, w_N, e_0, q_c, λ, ψ) and dependent (S_o/S_p, C_t/C_c, α_m, $m_{v(field)}/m_{v(Stroud)}$) parameters are not linear. The nonlinear regression analyses are conducted to obtain correlations between independent and dependent parameters.

4.4.1 Comparisons of analytically calculated settlements from oedometer data with observed settlements

The analytically calculated primary consolidation settlements from oedometer tests, as presented in Appendix C, are compared with the data of instrumented test embankments. The graphs for calculated from laboratory values of m_v and C_c-C_r vs. observed settlement (cm) are presented in Figures 4.60 and 4.61. According to these graphs, the observed settlement amounts can be estimated by using lower and upper line equations from the calculated settlements from oedometer data.

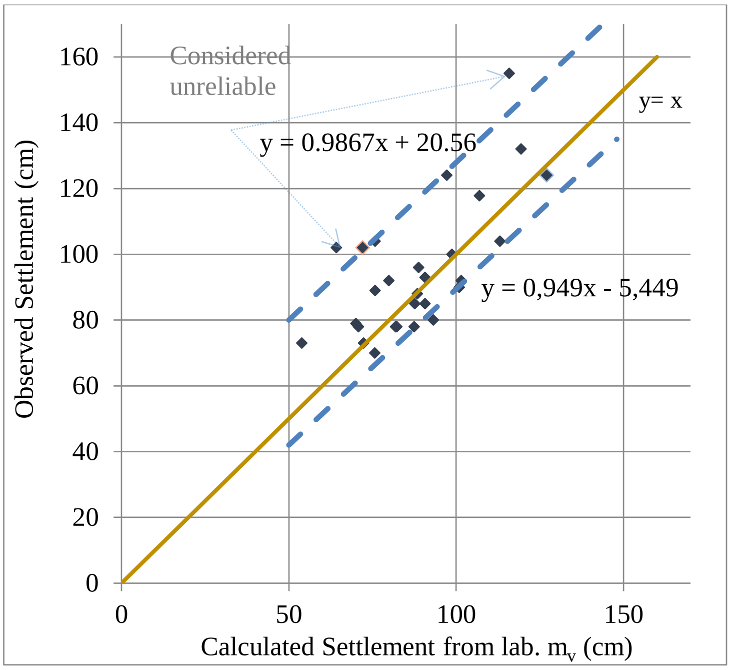

Figure 4.60. Calculated settlement (cm) from lab. m_v vs. observed settlement (cm) of the soils in the study area

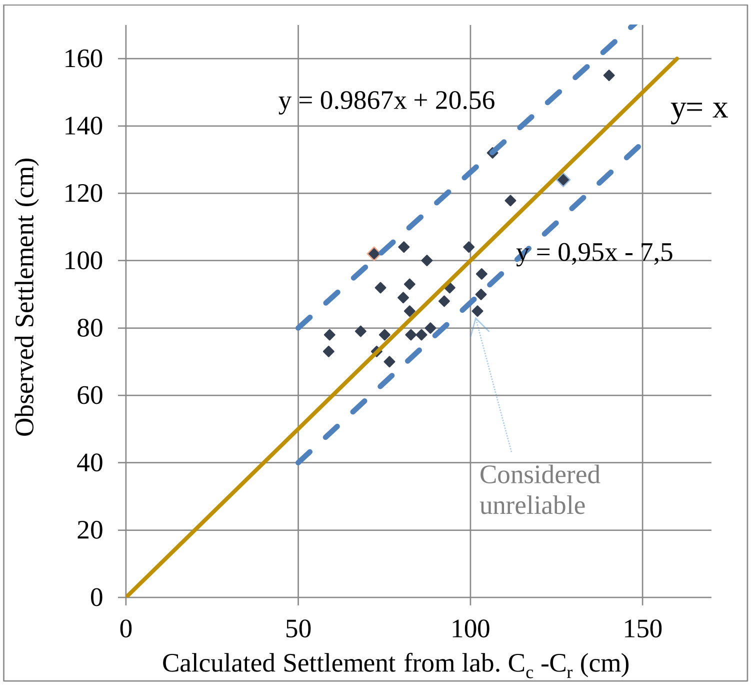

Figure 4.61. Calculated settlement (cm) from C_c-C_r vs. observed settlement (cm) of the soils in the study area

The graphs for ratio of the observed to calculated settlements from laboratory values of m_v and C_c-C_r values based on station number is presented in Figures 4.62 and 4.63. According to Figure 4.62, mean value of the ratio of the observed settlements to calculated settlements from laboratory m_v values is obtained as 1.08 with a standard deviation of 0.18. According to Figure 4.63, mean value of the ratio of the observed settlements to calculated settlements from laboratory m_v values is obtained as 1.07 with a standard deviation of 0.15.

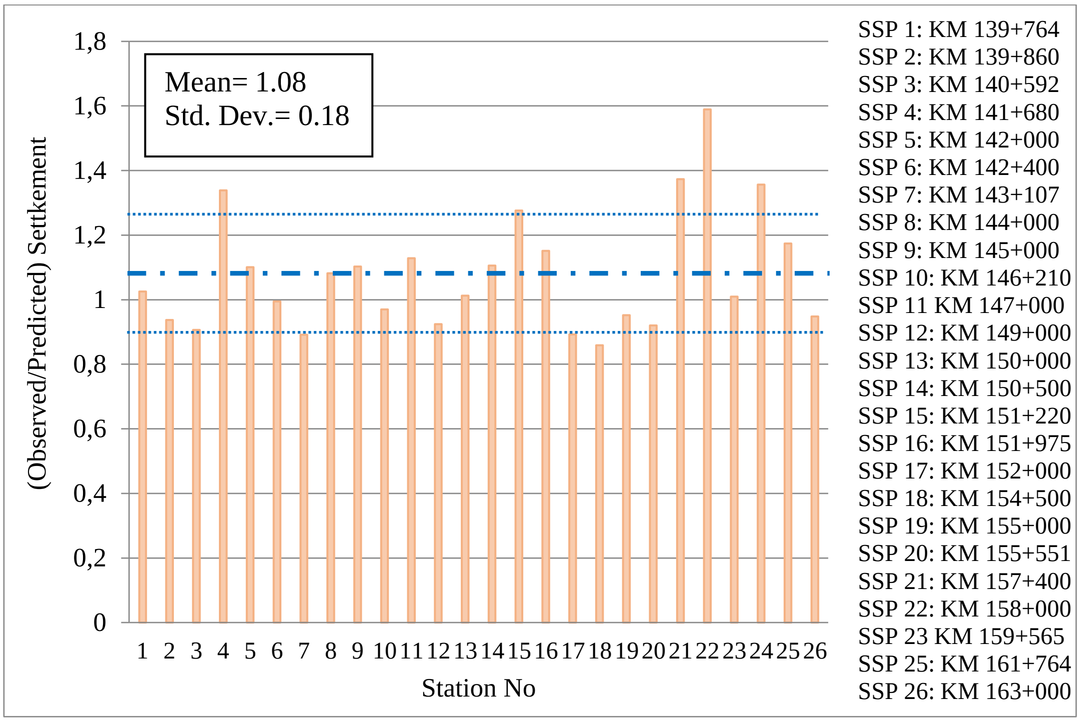

Figure 4.62. Station number vs. ratio of observed settlement to calculated settlement from lab. m_v

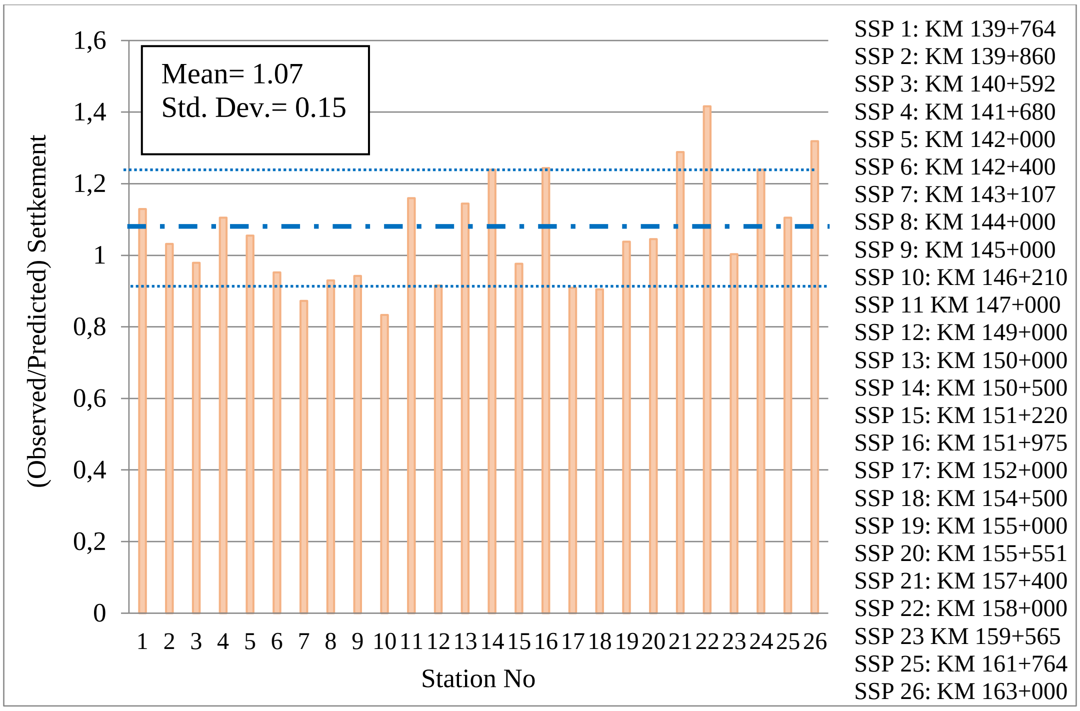

Figure 4.63. Station number vs. ratio of observed to calculated settlement from C_c-C_r

4.4.2 Comparisons of coefficient of volume compressibility values obtained from field data and Stroud approach

For each station, the coefficients of volume compressibility values were assigned from Plasticity Index and SPT N parameters by Stroud approach as presented in Figure 2.4. Plasticity Index and SPT N values were assumed as weighted average values for whole depth of each section and hence, weighted average values of coefficient of volume compressibility were obtained. The coefficients of volume compressibility values were back-calculated from magnitude of settlement of instrumented field data. In other words, the primary consolidation settlement amounts obtained from logarithm of time versus settlement graph were divided into total clay thickness and increase in vertical effective stress in the middle depth of clay layer. The graph for m_v obtained from Stroud approach versus m_v obtained from field data is presented in Figure 4.64 and histogram graph is presented in Figure 4.65. According to this graph, the coefficients of volume compressibility of field change from 0.82 to 1.47 times of Stroud approach.

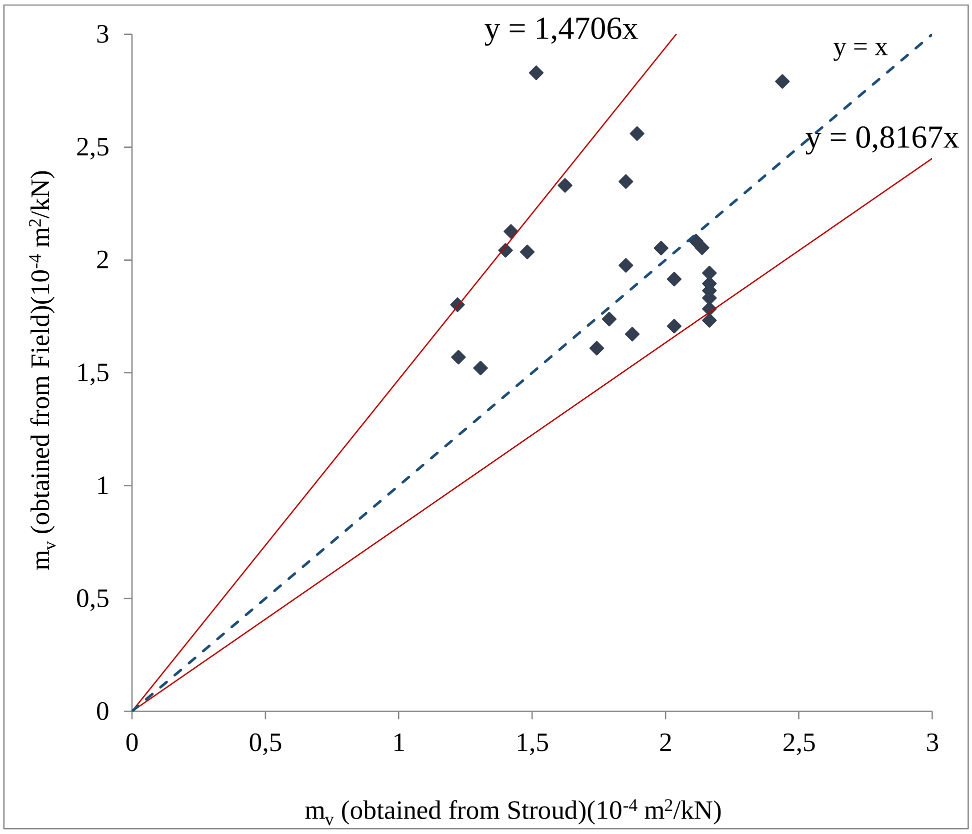

Figure 4.64. The coefficients of volume compressibility obtained from Stroud approach vs. obtained from field via back calculations from field data

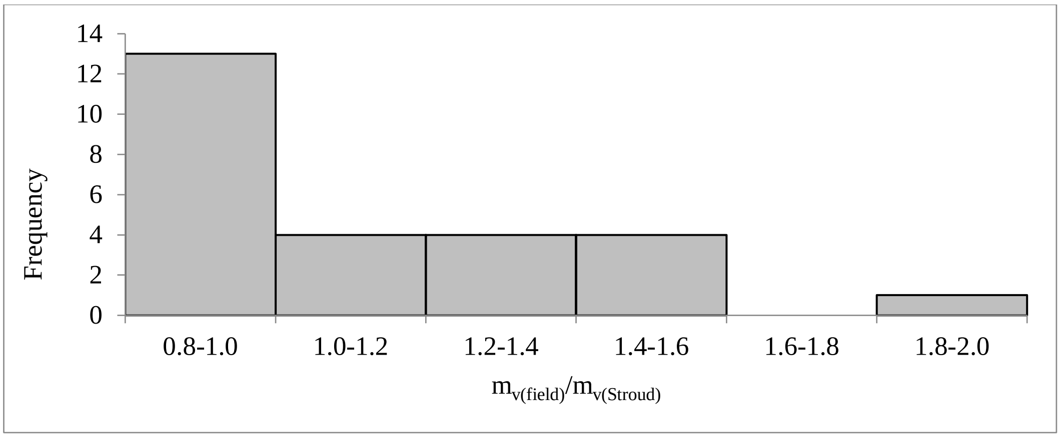

Figure 4.65. Histogram graph for $m_{v(field)}/m_{v(Stroud)}$

4.4.3 Comparisons of predicted settlements from Asaoka's and Horn's approaches with final field settlements

Asaoka and Horn's Methods were used to predict the final settlement amounts using 70% of the instrumented embankment settlement data. The graphs showing S (field)/S (Asaoka's prediction) and S (field)/S (Horn's prediction) are presented in Figures 4.66 and 4.67. Both methods predict the final primary consolidation with 11% proximity. According to this graph, mostly S (field)/S (Horn's prediction) values are closer to 1.0, which means that Horn's method estimates closer than Asaoka's method.

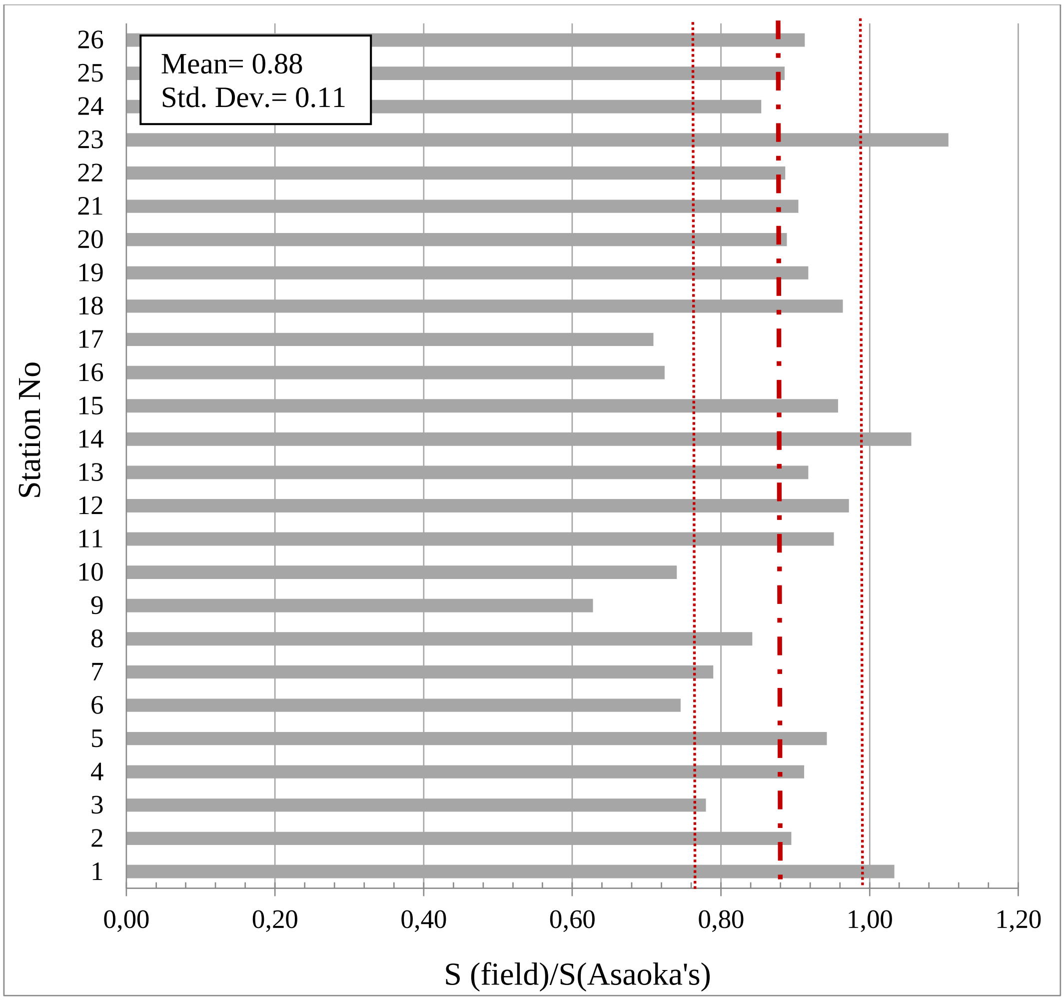

Figure 4.66. The ratio of final field settlement to predicted final settlement of Asaoka's approaches

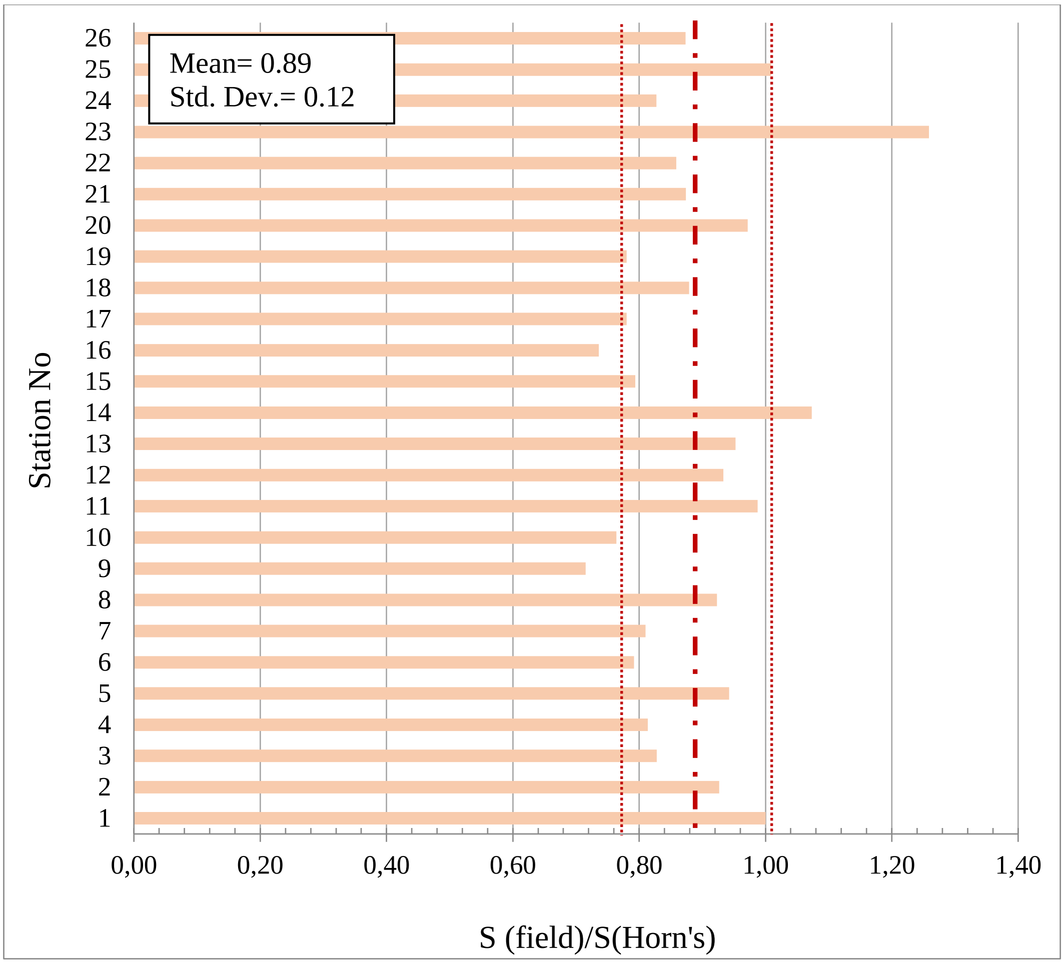

Figure 4.67. The ratio of final field settlement to predicted final settlement of Horn's approaches

4.4.4 Relation between cone tip resistance (q_c) and α_m

The relationships between cone tip resistance (q_c) and α_m coefficients are investigated and an equation for estimating α_m from cone tip resistance is achieved as presented in Figure 4.68. The variation of α_m values from cone tip resistance (q_c) recommended by Erol et al. (2004) is presented in Figure 4.69 and according to this drawing, data set of Bursa-Susurluk Highway Project is compatible to his drawing.

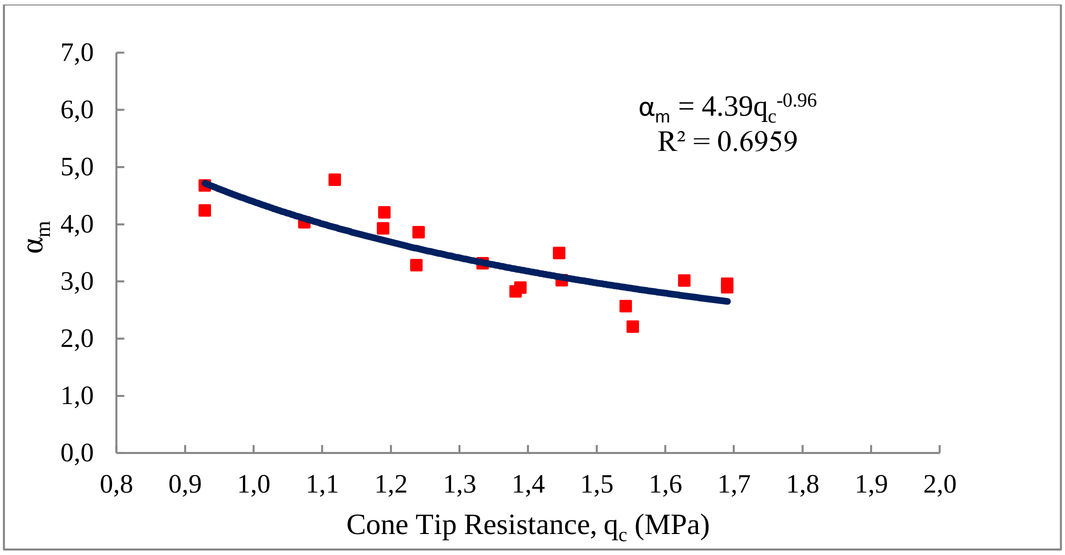

Figure 4.68. Cone tip resistance q_c (MPa) vs. α_m graph

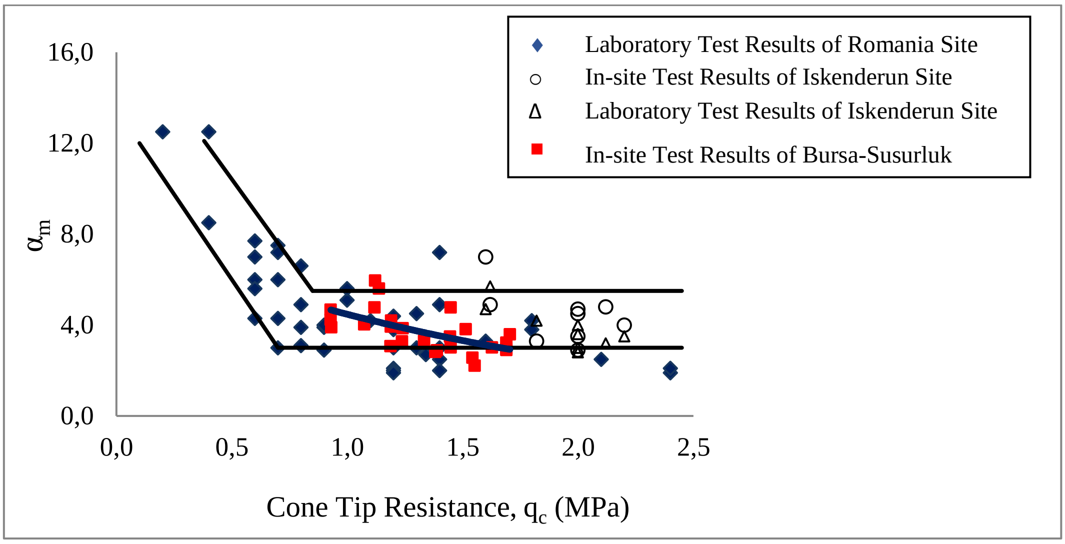

Figure 4.69. The variation of α_m values from cone tip resistance, q_c (MPa) (Erol et al., 2004)

4.4.5 A Nonlinear Regression Methodology

A Visual Basic code is built to effectively conduct nonlinear regression analyses considering different combinations of dependent and independent parameters, thus yielding different set of equations to correlate measured (observed) and calculated (analytical) results, as well as to evaluate the effect of each independent variables to the outcome of assumed statistical model.

Approach used in this study consists of three steps:

- Construction of linear regression equations with n number of independent variables by minimizing sum of squared residuals (RSE) using matrix algebra,
- Assuming a set of nonlinear equations in the form of sum of exponential components with the same n number of independent variables and linearizing the equations to apply the linear regression algorithm. Searching through multiple sets of exponent values for each independent variable to identify the combination that provides least sum of squared residuals (i.e. best fit for given data) between scanned sets of values,
- Investigation of influence of independent variables on the dependent variable by standardizing variables of the linearized final equation and performing a final linear regression

4.4.5.1 Multiple Variable Linear Regression Algorithm

Let *i* be the number of equations (i. e. number of evaluated consolidation cases), *n* be the number of independent variables (i. e. measured variables such as w_N, LL, etc.) and assume *i* number of linear equations:

$$y_1 = c_1.x_{1,1} + c_2.x_{1,2} + \cdots + c_n.x_{1,n} + I_{nt} + \varepsilon_1$$
$$y_2 = c_1.x_{2,1} + c_2.x_{2,2} + \cdots + c_n.x_{2,n} + I_{nt} + \varepsilon_2$$
$$\vdots$$
$$y_i = c_1.x_{i,1} + c_2.x_{i,2} + \cdots + c_n.x_{i,n} + I_{nt} + \varepsilon_i \qquad \text{(Eq. 4.1)}$$

where c_n is the coefficient of each independent variable, I_{nt} is the common intercept constant for all equations and ε_i is the residual (error) in respective equation i.

Writing in matrix form:

$$\begin{bmatrix} y_1 \\ y_2 \\ \vdots \\ y_i \end{bmatrix} = \begin{bmatrix} x_{1,1} & x_{1,2} & \cdots & x_{1,n} & 1 \\ x_{2,1} & x_{2,2} & \cdots & x_{2,n} & 1 \\ \vdots & \vdots & \vdots & \vdots & \vdots \\ x_{i,1} & x_{i,2} & \cdots & x_{i,n} & 1 \end{bmatrix} \begin{bmatrix} c_1 \\ c_2 \\ \vdots \\ c_n \\ I_{nt} \end{bmatrix} + \begin{bmatrix} \varepsilon_1 \\ \varepsilon_2 \\ \vdots \\ \varepsilon_i \end{bmatrix} \Longrightarrow Y = XC + \mathrm{E} \qquad \text{(Eq. 4.2)}$$

Calculating sum of squared residuals (RSE), which is a scalar:

$$E = Y - XC \qquad \text{(Eq. 4.3)}$$

$$\begin{aligned} RSE = E^T E &= (Y - XC)^T (Y - XC) \\ &= (Y^T - C^T X^T)(Y - XC) \\ &= Y^T Y - Y^T XC - C^T X^T Y + C^T X^T XC \\ &= Y^T Y - 2C^T X^T Y + C^T X^T XC \qquad \text{(Eq. 4.4)} \end{aligned}$$

To minimize RSE by taking first order derivative with respect to C and equating to 0:

$$\partial E^T E / \partial C = 0 = -2X^T Y + 2X^T XC \Longrightarrow C = (X^T X)^{-1} X^T Y \qquad \text{(Eq. 4.5)}$$

yields the solution of coefficient matrix, C for best linear regression fitting.

4.4.5.2 Multiple Variable Nonlinear Regression Algorithm

Now assuming a nonlinear form for i number of equations with n number of dependent-variables using sum of exponential components:

$$y_1 = c_1.x_{1,1}{}^{p_1} + c_2.x_{1,2}{}^{p_2} + \cdots + c_n.x_{1,n}{}^{p_n} + I_{nt} + \varepsilon_1$$

$$y_2 = c_1.x_{2,1}{}^{p_1} + c_2.x_{2,2}{}^{p_2} + \cdots + c_n.x_{2,n}{}^{p_n} + I_{nt} + \varepsilon_2$$

$$\vdots$$

$$y_i = c_1.x_{i,1}{}^{p_1} + c_2.x_{i,2}{}^{p_2} + \cdots + c_n.x_{i,n}{}^{p_n} + I_{nt} + \varepsilon_i \qquad \text{(Eq. 4.6)}$$

For an assumed set of exponents $\{p_1, p_2 \cdots p_n\}$, each independent variable, $x_{i,n}{}^{p_n}$, becomes a constant scalar, thus linearizing each equation and yielding a best-fit solution using the linear matrix algebra explained in the previous section.

The implemented algorithm in Visual Basic can be summarized as:

- Choose n number of relevant independent variables $\{c_1, c_2 \cdots c_n\}$ for the proposed equation:
  $\{\omega_N, LL, \lambda, PI \cdots etc.\}$
- Arrange the analytically calculated dependent variables $\{y_1, y_2 \cdots y_n\}$:

$\{S_O/S_P \; at \; each \; settlement \; plate\}$

- Solve for regression constants c_n assuming different sets of exponents $\{p_1, p_2 \cdots p_n\}$ and identify the set yielding minimum value of RSE to propose a sufficiently valid nonlinear equation model.

To demonstrate, let the following form of the equation to be evaluated using observed data from 26 stations:

$$S_o/S_{p_1} = c_1.w_{n_1}{}^{p_1} + c_2.e_{o_1}{}^{p_2} + c_3.\lambda_1{}^{p_3} + I_{nt} + \varepsilon_1$$

$$\vdots$$

$$S_o/S_{p_{26}} = c_1.w_{n_{23}}{}^{p_1} + c_2.e_{o_{23}}{}^{p_2} + c_3.\lambda_{23}{}^{p_3} + I_{nt} + \varepsilon_{23} \qquad \text{(Eq. 4.7)}$$

where S_o/S_p is the dependent parameter, w_N, LL and ψ are independent parameters, c_1, c_2 and c_3 are linear regression constants and p_1, p_2 and p_3 are exponential constants for each independent parameter respectively.

Software iterates through all combinations of p_1, p_2 and p_3 ranging from -3.0 to 3.0 for each exponent using an increment of 1.0, yielding 216 (6^3) combinations in total. For any combination of p_1, p_2 and p_3, set of 26 equations becomes linear and linear regression constants c_1, c_2 and c_3 and sum of squared residuals (RSE) are obtained conducting linear regression using matrix algebra.

After iteration is completed for 216 combinations, the set which yields minimum RSE among all is labeled as best fitted nonlinear regression form, e.g. :

$$S_o/S_p = \frac{5.38}{(0.1w_N(\%))^3} - 0.349\frac{LL\,(\%)}{100} + 0.0536\psi^3 + 0.934 \qquad \text{(Eq. 4.8)}$$

4.4.5.3 Influence Analysis of Independent Variables

Standardization of both independent and dependent variables in the proposed equation for each nonlinear regression analysis gives useful insight about relative influence factors for each independent variable.

In other terms, this procedure is applied to answer the question of which of the independent variables has a greater effect on the dependent variable, especially in cases where the variables have different units resulting in deviance in order of magnitudes of calculated regression coefficients.

Each variable is standardized by subtracting its mean from each of its values and then dividing these new values by the standard deviation of the variable. Standardizing all variables and applying a regression analysis yields standardized regression coefficients, making it possible to quantize the change in the dependent variable measured in standard deviations.

To demonstrate, variables of following equation were standardized and related regression coefficients are re-calculated conducting a linear regression for the standardized Equation 4.9.

First, equation is linearized by introducing new parameters as:

$x_1 = w_N(\%)^{-3}$

$x_2 = LL(\%)^1$

$x_3 = \psi^3$

$y = S_0/S_p$

Linear regression of standardized equation yields:

$$y = 0.851x_1 - 0.410x_2 + 0.243x_3 + 9.37e^{-17} \quad \text{(Eq. 4.9)}$$

A brief review indicated that; standardized terms corresponding to ${w_N}^{-3}$ and ψ^3 have similar exponents in terms of magnitude. Since standardized coefficient of ${w_N}^{-3}$ has greatest value, it can be stated that ${w_N}^{-3}$ has most correspondence and largest raw influence.

4.4.6 Results of Regression Analysis

A non-linear regression analysis was carried out using independent parameters; w_N, LL, ψ and dependent parameter; S_o/S_p. Original data set, as presented in Appendix D, consisted of 26 cases, of which 3 were deemed incompatible due to initial regression analysis and removed from set. Equation obtained from final regression analysis is given in Equation 4.10. Actual correction constant for theoretical settlement amount, i.e. S_o/S_p, was plotted against proposed values (from Equation 4.10) in Figure 4.70. Same values of S_o/S_p (i.e. actual and proposed) were also plotted for each station (test case) in Figure 4.71. Graphs (R^2= 0.728) demonstrate the conformity among proposed values and actual results. F-Test is used to check significance of the relation. F_{comp}= 53.53 and F_{crit}= 3.09 are obtained. Since $F_{comp}>F_{crit}$, the relation is said to be significant.

$$S_o/S_p = \frac{5.38}{(0.1w_N(\%))^3} - 0.349\frac{LL\,(\%)}{100} + 0.0536\psi^3 + 0.934 \quad \text{(Eq. 4.10)}$$

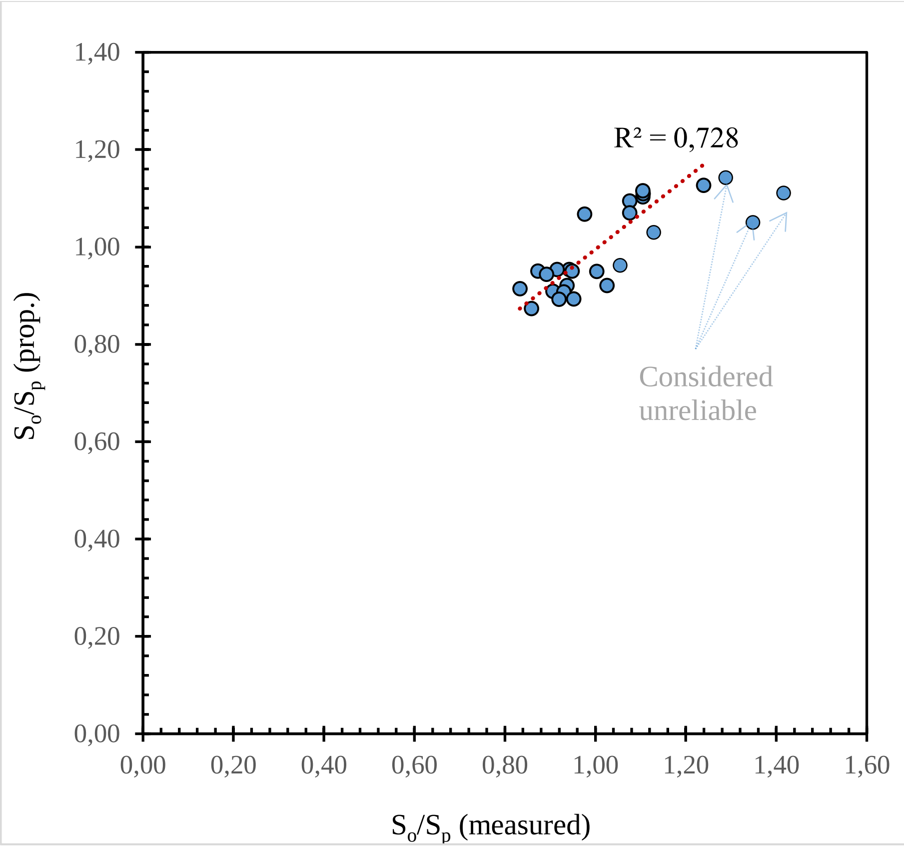

Figure 4.70. S_o/S_P (measured) vs. S_o/S_P (proposed) graph

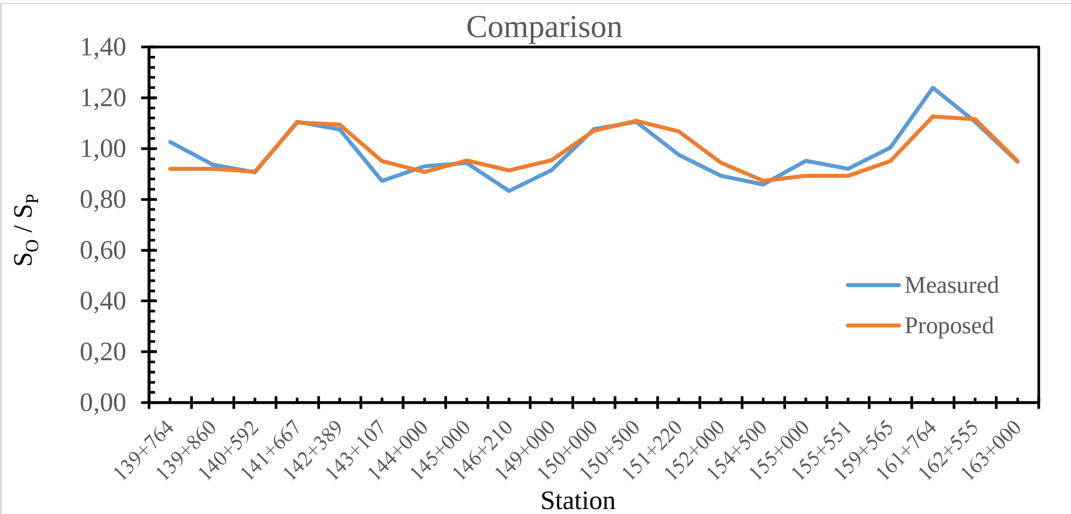

Figure 4.71. Comparison graph for the measured and proposed S_o/S_P for each station

New parameters for linearized equation:

$x_1 = w_N(\%)^{-3}$

$x_2 = LL\ (\%)^1$

$x_3 = \psi^3$

$y = S_0/S_p$

Linear regression of standardized equation for data yields:

$$y = 0.851x_1 - 0.410x_2 + 0.243x_3 + 9.37e^{-17} \qquad \text{(Eq. 4.11)}$$

A brief review indicated that; standardized terms corresponding to ${w_N}^{-3}$ and ψ^3 have similar exponents in terms of magnitudes. Since standardized coefficient of ${w_N}^{-3}$ has the greatest value, it can be stated that ${w_N}^{-3}$ has most correspondence and largest raw influence.

A non-linear regression analysis was carried out using independent parameters; w_N, λ and dependent parameter; S_o/S_p. Original data set, as presented in Appendix D, consisted of 26 cases, of which 3 were deemed incompatible due to initial regression analysis and removed from set. Equation obtained from final regression analysis is given in Equation 4.12. Actual correction constant for theoretical settlement amount, i.e. S_o/S_p, was plotted against proposed values (from Equation 4.12) in Figure 4.72. Same values of S_o/S_p (i.e. actual and proposed) were also plotted for each station (test case) in Figure 4.73. Graphs (R^2= 0.717) demonstrate the conformity among proposed values and actual results. F-Test is used to check significance of the relation. F_{comp}= 50.67 and F_{crit}= 3.09 are obtained. Since $F_{comp}>F_{crit}$, the relation is said to be significant.

$$S_o/S_p = \frac{4.20}{(0.1w_N(\%))^3} + 0.615\lambda^3 + 0.822 \qquad \text{(Eq. 4.12)}$$

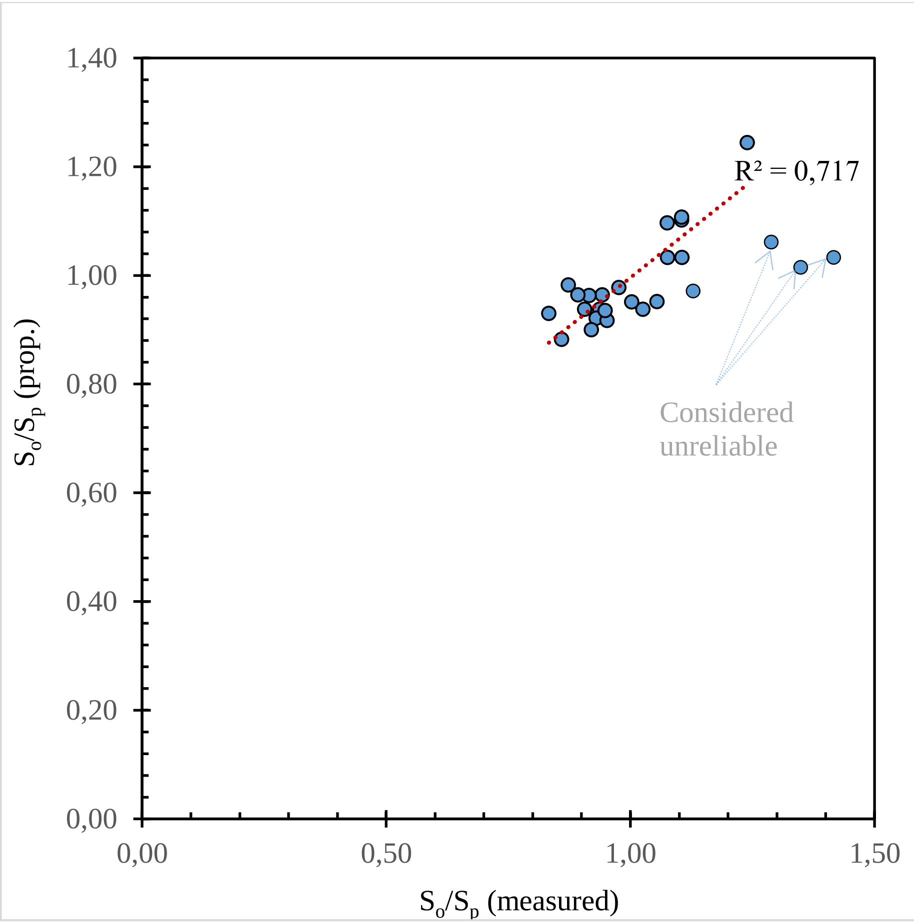

Figure 4.72. S_o/S_p (measured) vs. So/Sp (proposed) graph

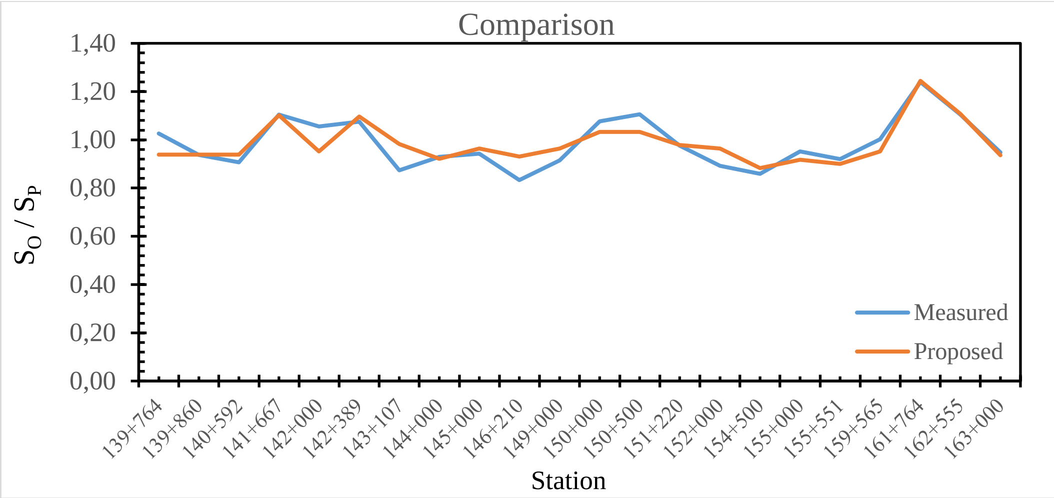

Figure 4.73. Comparison graph for the measured and proposed S_o/S_p for each station

New parameters for linearized equation:

$$x_1 = w_N^{-3}$$

$$x_2 = \lambda^3$$

$$y = S_0/S_p$$

Linear regression of standardized equation for data yields:

$$y = 0.658x_1 + 0.353x_2 + 8.78e^{-16} \quad \text{(Eq. 4.13)}$$

A brief review indicated that; standardized terms corresponding to ${w_N}^{-3}$ and λ^3 have similar exponents in terms of magnitudes. Since standardized coefficient of ${w_N}^{-3}$ has the greatest value, it can be stated that ${w_N}^{-3}$ has most correspondence and largest raw influence.

A non-linear regression analysis was carried out using independent parameters; LI and dependent parameter; C_t/C_c. Original data set, as presented in Appendix D, consisted of 11 cases. Equation obtained from final regression analysis is given in Equation 4.14. Actual values of C_t/C_c were plotted against proposed values (from Equation 4.14) in Figure 4.74. Same values of C_t/C_c (i.e. actual and proposed) were also plotted for each station (test case) in Figure 4.75. Graphs (R^2= 0.793) demonstrate the conformity among proposed values and actual results. F_{comp}= 34.48 and F_{crit}= 3.86 are obtained. Since $F_{comp}>F_{crit}$, the relation is said to be significant.

$$C_t/C_c = 0.000621LI^{-3} + 0.177 \qquad \text{(Eq. 4.14)}$$

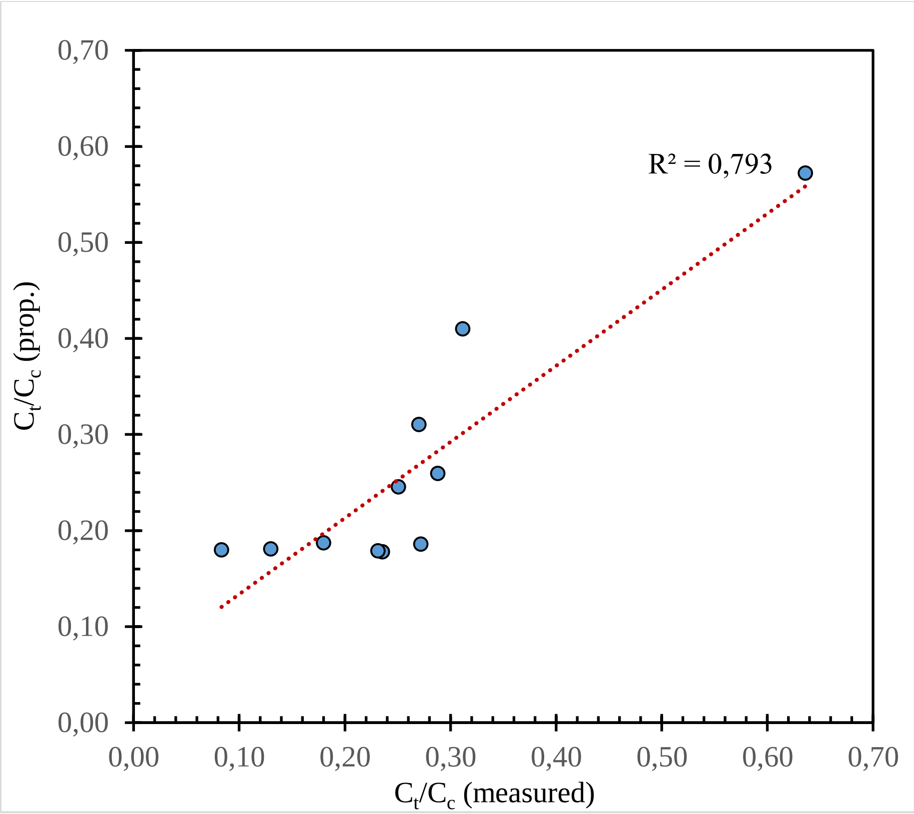

Figure 4.74. C_t/C_c (measured) vs. C_t/C_c (proposed) graph

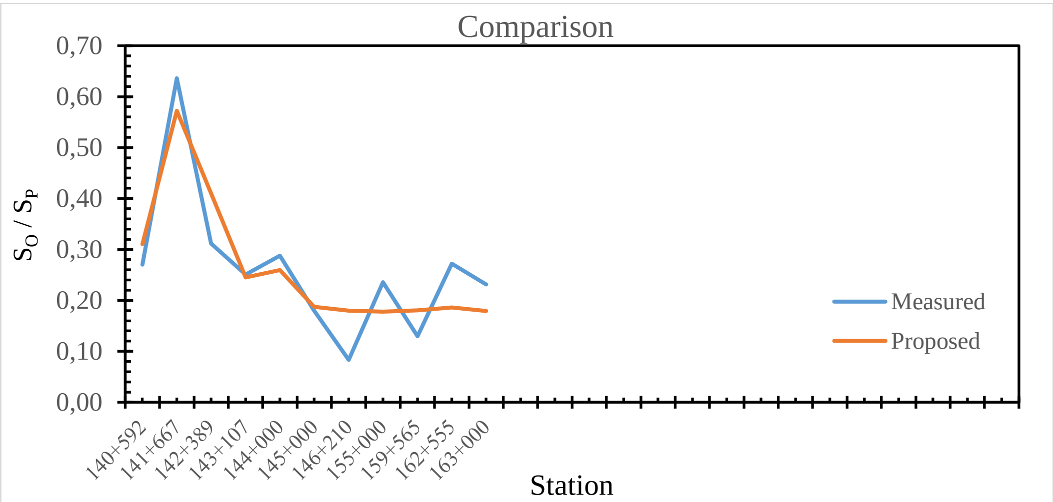

Figure 4.75. Comparison graph for Measured and Proposed C_t/C_c for each station

A non-linear regression analysis was carried out using independent parameters; SPT N, PI, w_N, LL and dependent parameter; $m_{v(field)}/m_{v(Stroud)}$. Original data set, as presented in Appendix D, consisted of 26 cases, of which 4 were deemed incompatible due to initial regression analysis and removed from set. Equation obtained from final regression analysis is given in Equation 4.15. Actual correction constant for m_v obtained from Stroud approach, i.e. $m_{v(field)}/m_{v(Stroud)}$ was plotted against proposed values (from Equation 4.15) in Figure 4.76. Same values of $m_{v(field)}/m_{v(Stroud)}$ (i.e. actual and proposed) were also plotted for each station (test case) in Figure 4.77. Graphs (R^2= 0.677) demonstrate the conformity among proposed values and actual results. F-Test is used to check significance of the relation. F_{comp}= 41.92 and F_{crit}= 2.86 are obtained. Since $F_{comp}>F_{crit}$, the relation is significant.

$$\frac{m_{v(field)}}{m_{v(Stroud)}} = 67.7\left(\frac{SPT\ N}{100}\right)^3 - 3.23\left(\frac{PI(\%)}{100}\right)^3 + 10.9\left(\frac{w_N(\%)}{10}\right)^{-3} - 0.68\left(\frac{LL(\%)}{100}\right)^3 + 0.757 \qquad \text{(Eq. 4.15)}$$

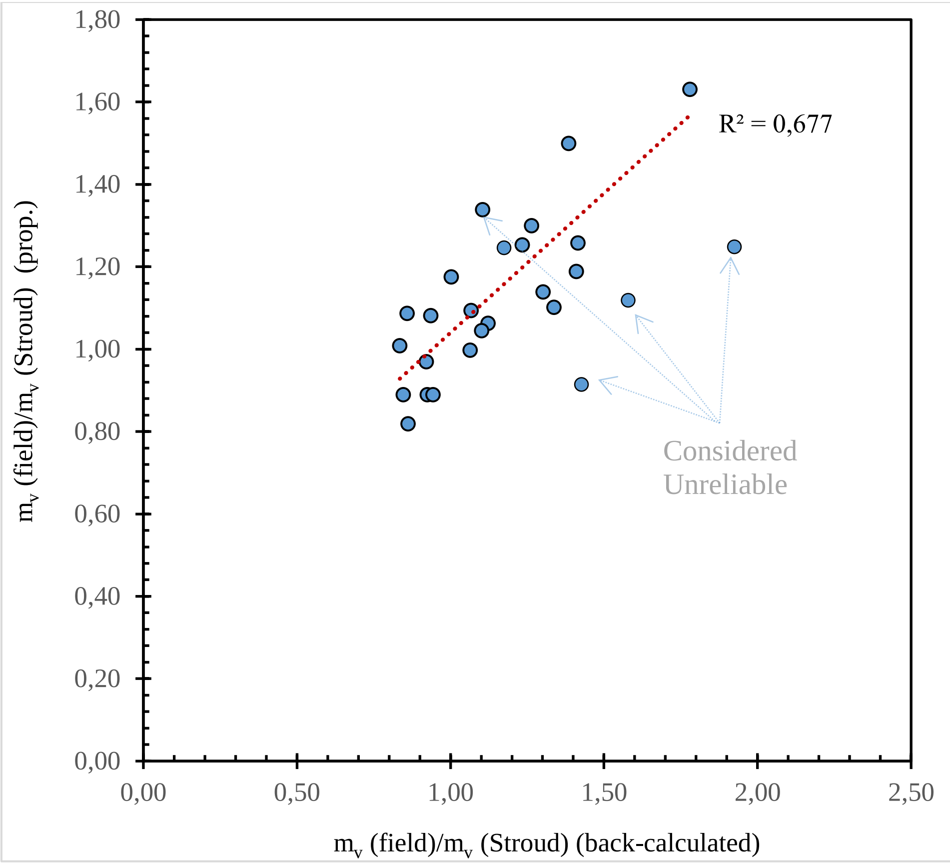

Figure 4.76 $m_{v(field)}/m_{v(Stroud)}$ (back-calculated) vs. $m_{v(field)}/m_{v(Stroud)}$ (proposed) graph

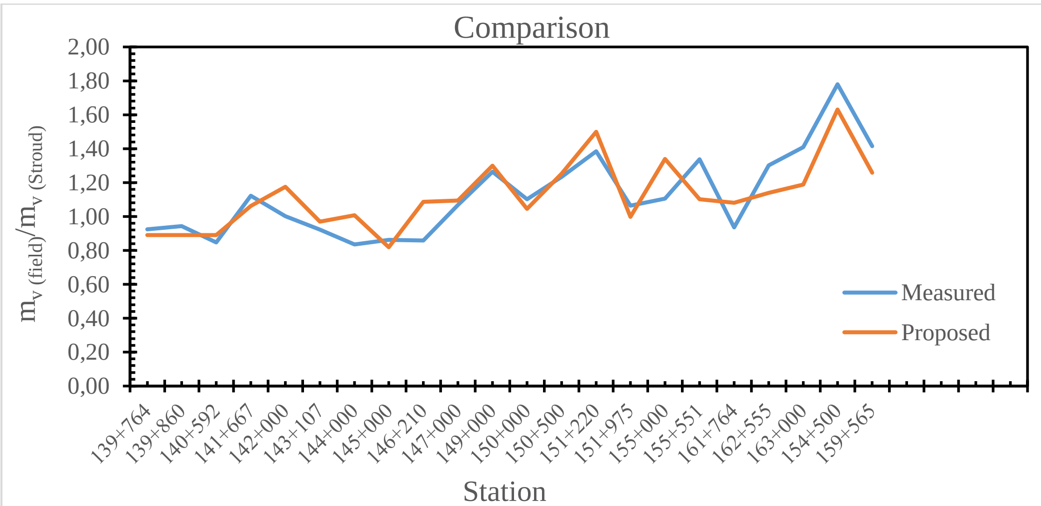

Figure 4.77 Comparison graph for the measured and proposed m_v for each station

New parameters for linearized equation:

$x_1 = SPT\ N^3$

$x_2 = PI^3$

$x_3 = w_N^{-3}$

$x_4 = LL^3$

$y = m_{v(field)}/m_{v(Stroud)}$

Linear regression of standardized equation for data yields:

$$y = 0.639x_1 - 0.658x_2 + 0.653x_3 - 0.332x_4 + 1.57e^{-15} \qquad \text{(Eq. 4.16)}$$

A brief review indicated that; standardized terms have similar exponents in terms of magnitude. Since standardized coefficient of PI has greatest value, it can be stated that PI has most correspondence and largest raw influence.

CHAPTER 5

CONCLUSIONS AND RECOMMENDATIONS

5.1 Conclusions

Field measurements of settlements in Karacabey NC clays and comparison of these measured settlements with various settlement prediction methods revealed the following conclusions:

The predicted settlements by one dimensional consolidation theory are compared with the settlement data of instrumented test embankments, the ratios of the observed settlements to predicted settlements using oedometer data change in interval of 0.80-1.20.

The coefficients of volume compressibility back calculated from field settlement records are compared with Stroud correlations. The following trend is noticed; $m_{v(field)}$ = (0.82-1.47) $m_{v(Stroud)}$.

Asaoka and Horn's extrapolation methods are utilized to estimate the magnitudes of final settlements using 70% of the monitored settlement data. Both methods predict the final consolidation settlement amounts with 11% proximity. The magnitudes of final settlement amounts predicted by Horn's method are closer than the predicted by Asaoka's method.

The correlation between tip resistance (q_c) and α_m coefficients is investigated. Sanglerat (1972) gives relationship between the constrained modulus and CPT tip resistance as $M = \alpha_m q_c$. Back analysis of field settlements reveal the α_m factor as $\alpha_m = 4.39{q_c}^{-0.96}$ (q_c is in MPa and changes in interval of 0.9-1.7, α_m is unitless).

The main contribution of this thesis is the presentation of secondary and tertiary consolidation behavior of Karacabey plain alluvium. Karacabey clays exhibit typical secondary consolidation behaviors. In 11 stations, out of 26 total stations, tertiary consolidation behaviors are observed following the secondary consolidation period. Tertiary consolidation behavior is characterized by an increase in the slope of the logarithm of time versus settlement curves.

Secondary consolidation amounts are found out from the stations, where end of the secondary consolidation is recorded. The amounts of secondary consolidation range from 3 to 30 percent of the primary consolidation settlements, and secondary consolidation amounts are 11 percent of the primary consolidation settlements on average.

C_s/C_c and C_t/C_c ranges are recommended for engineering practices to predict the secondary and tertiary consolidation amounts. The mean value of C_s/C_c is obtained as 0.084 while the mean value of C_t/C_c is obtained as 0.27. C_s/C_c values change between mostly 0.027 and 0.141 in ranges while C_t/C_c values change between mostly 0.13 and 0.41 in ranges.

The non-linear regression analysis is performed and a correlation for S_o/S_p ratio is observed statistically for 23 stations with independent parameters of w_N, LL and ψ.

$$S_o/S_p = \frac{5.38}{(0.1w_N(\%))^3} - 0.349\frac{LL\ (\%)}{100} + 0.0536\psi^3 + 0.934$$

The non-linear regression analysis is performed and a correlation for S_o/S_p is observed statistically for 23 stations with independent parameters of w_N and λ.

$$S_o/S_p = \frac{4.20}{\left(0.1w_N(\%)\right)^3} + 0.615\lambda^3 + 0.822$$

The tertiary consolidation settlement is observed in 11 stations and the non-linear regression analysis is performed and a statistical correlation for C_t/C_c ratio is observed for them with independent parameter of LI.

$$C_t/C_c = 0.000621LI^{-3} + 0.177$$

The non-linear regression analysis is performed and an equation for $m_{v(field)}/m_{v(Stroud)}$ is derived statistically from back-calculation of coefficients of volume compressibility for 22 stations with independent parameters of SPT N, PI, w_N and LL.

$$\frac{m_{v(field)}}{m_{v(Stroud)}} = 67.7(\frac{SPT\ N}{100})^3 - 3.23\left(\frac{PI}{100}\right)^3 + 10.9\left(\frac{w_n}{10}\right)^{-3} - 0.68\left(\frac{LL}{100}\right)^3 + 0.757$$

5.2 Recommendations for Future Studies

All predictions and consolidation calculations presented in this thesis are valid for the soft clays of Karacabey Plain. It is necessary to apply embankment load on soft clay with different geological characteristics and to perform instrumentation of field settlements. By this way, it is possible to determine the secondary and tertiary behavior of clays, precisely.

There are limited numbers of consolidation tests to conduct this research, especially at clay units defined in the deep. In order to achieve more exact predictions for consolidation settlement amounts, it is necessary to fulfil more laboratory consolidation settlement tests.

To be able to interpret the relationship between tertiary settlement and clay mineralogy, the quantification of clay minerals is essential by X-ray diffraction (XRD) analysis. After completion of the embankment structure, since there was no chance to get clay sample, identification of clay mineral is not performed.

REFERENCES

Abuel-Nega, H.M., 2011. Design curves of prefabricated vertical drains including smear and transitionzones effects, Geotextiles and Geomembranes J. 32, UK, pp.1-9.

Adachi T., Okano M., 1974. A constitutive equation for normally consolidated clay, Soils and Foundations, 14, (4), 55-73.

Adams, J.I., 1965. The engineering behavior of a Canadian muskeg, Proc. 6th Int. Conf. Soil Mech., Vol. 1, p.3.

Akagi, H., 1994. A physico-chemical approach to the consolidation mechanism of soft clays, Soils and Foundations, Vol. 34, No: 4, pp. 43-50.

Alexandre, G.F. et al., 2006. Creep prediction of an undisturbed sensive clay, Hal Archives-ouvertes, Rio de Janeiro, Brazil.

Al-Shamrani, M.A., 1998. Application of the C_α/C_c concept to secondary compression of sabkha soils, Canadian geotechnical journal 35 (1), 15-26.

Altınbilek, M.E., 2006. Estimation of consolidation settlements caused by groundwater drainage at Ulus-Keçiören Subway Project, M.Sc. Thesis, Geological Engineering Department, Middle East Technical University, Ankara.

Asaoka, A., 1978. Observational procedure of settlement prediction, Soils and Foundations, Vol.18, pp. 87-100.

Augustesen, A.H. et al., 2004. Evaluation of time-dependent behavior of soils, International Journal of Geomechanics 4(3).

Bagavasingam, T., 2015. Secondary consolidation and the effect of surcharge load, International Journal of Engineering Research and Technology, pp.695-699.

Barden, L., 1968. Primary and secondary consolidation of clay and peat, Geptechnique18: 1-24.

Bartlett, S.F. et al., 2017. Evaluation of secondary consolidation settlement associated with embankment construction for fast-paced transportation projects in Utah, Utah Department of Transportation Research Division, Report No. UT-17.22.

Bergado, D.T., 2000. Recent developments of ground improvement with PVD on soft Bankok clay, Seminar on Geotechnics in Kochi 2000, Japan.

Bergado, D.T. et al., 1992. Inverse analysis of geotechnic parameters on improved soft Bankok clay, Geotechnical Engineering J., Vol.118, No.7, pp. 1012-1030.

Bergado, D.T. et al., 2002. Prefabricated vertical drains (PVDs) in soft Bangkok clay: a case study of the new Bangkok International Airport project, Can. Geotech J.39, Canada, pp.304-315.

Bhosle, P. and Vaishampayan, V.V., 2009. Case study for ground improvement using PVD with preloading for coal and iron ore stackyard, Indian Geotechnical Society, pp. 506-510.

Blight, G.E., 1986. Pressures exterted by materials stored in silos: part 1, coarse materials, Geotechnique 36, No. 1, 33-46.

Bjerrum, L., 1972. Embankments on soft ground. Proceedings of the specialty conference on performance of earth and earth-supported structures, India Vol 2, 1-54.

Bowles, E.B., 1997. Foundation analysis and design, McGraw-Hill.

Brandl, H., 2018. Creeping (secondary/tertiary settlements) of highly compressible soils and sludge, Original Scientific Paper UDK: 624.131.542.

BS 5930, 1981. Code of practice for site investigation.

Buisman, A. S. K., 1936. Results of long duration settlement tests proc., Intern. Conf. on Soil Mech. and Found. Engr., Vol. 1, pp. 103-106.

Buri, P.B., 1978. Influence of secondary consolidation and overconsolidation on the behaviour of a soft alluvial clay, Ph.D. Thesis, Imperial College, University of London.

Cai, G.J. et al., 2010. Application of piezocone to evaluate consolidation and permeability properties of Taihu lacustrine clay deposits, 2nd International Symposium on Cone Penetration Testing, California.

Cao, L.F. et al., 2001. Back calculation of consolidation parameters from field measurements at a reclamation site, Can. Geotech. J., Canada, pp.755-769.

Cappa, R. et al., 2015. Settlements and excess pore pressure generation in peaty soils under embankments during cyclic loading, 6th International conference on Earthquake Geotechnical Engineering, New Zealand.

Carillo, N., 1942. Simple two and three dimensional cases in the theory of consolidation of soils. Journal of Mathematics and Physics, 21(1), 1-5.

Carter, M. and Bentley, S.P., 1991. Correlations of soil properties, Pentech Press Publishers, London, p.130.

Cascone, E. and Biondi, G., 2013. A case study on soil settlements induced by preloading and vertical drains, Geotextiles and Geomembranes J., Department of Civil Engineering, University of Messina, Italy, pp.51-67.

Cassandra, A. and Wetzel, P.E., 2014. Comparison of theoretical and actual time dependent settlement induced by fill placement, ASCE Metropolitan Section, Geo-Institute Chapter, New York City, USA.

Charles, J.A., 1996. The depth of influence of loaded areas, Geotechnique 46, No. 1.51-61.

Charles, J.A. et al., 1986. Improving the load carrying characteristics of uncompacted fills by preloading, Mun. Engr. 3, No.3 , Feb., 1-19.

Cheng, G. et al., 2019. Experimental investigation of consolidation properties of nano-bentonite mixed clayey soil, Sustainability 12, 459, doi:10.3390/su12020459.

Choy, L.E., 2018. A case study of soft ground improvement by dynamic consolidation approach, 10th Malaysian Road Conference and Exhibition, Material Science and Engineering 512.

Chu, J. et al., 2006. Improvement of ultra-soft soil using prefabricated vertical drains, Geotextiles and Geomembranes 24, School of Civil and Environmental Engineering, Nanyang Technological University, Singapore, pp. 339-348.

Chung, S.G. et al., 2009. Hyperbolic method for prediction of prefabricated vertical drains performance, Geotechnical and Geoenvironmental J., ASCE, pp. 1519-1528.

Chung, S.G. et al., 2014. Observational method for field performance of prefabricated vertical drains, Geotextiles and Geomembranes 42, Department of Civil Engineering, Dong-A University, Korea, pp. 405-416.

Craig, R.F., 1997. Soil Mechanics, Sixth edition, E and FN Spon Press, London.

Craig, R.F., 2004. Soil Mechanics, Seventh edition, Spon press, London.

Dalgıç, S. and Şimşek, O., 2002. Settlement predictions in the Anatolian Motorway, Engineering Geology 67, İstanbul University, Faculty of Engineering, İstanbul, Turkey, pp. 185-199.

Das, B.M., 1984. Principles of foundation engineering, Cole Engineering Division, California.

Das, B.M., 2008. Fundementals of geotechnical Engineering, 3rd Ed., Spain.

Das, P.P., 2015. Primary and secondary compression behavior of soft clays, M.Sc. Thesis, Rourkela, India.

TUDelft, 2014. Lecture notes: Interaction between building and foundation, Foundation Engineering, Delft University of Technology, Nederlands.

Demir, A., 2015. New computational models for better predictions of the soil-comression index, Acta geotechnica Slovenica 12(1):59-69.

Deng, Y.B., 2014. Consolidation behavior of soft deposits considering the variation of prefabricated vertical drain discharge capacity, Computers and Geotechnics J. 62, China, pp.310-316.

Den Haan, E.J., 1994. Stress-independent parameters for primary and secondary compression, Delft Geotechnicas, India.

Dey, A., 2019. Foundation engineering shallow and deep foundations, One-Day Seminar on Foundation Engineering, Siliguri Institude of Technology, Guwahati, India.

Dhowian, A.W. and Edil, T.B., 1980. Consolidation behavior of peats, Geotechnical testing journal, pp.105-114.

Dobak, P. et al., 2018. Verification of compressibility and consolidation parameters of varved clays from Radzymin (Central Poland) based on direct obsevations of settlements of road embankment, Open Geosci., pp. 911-924.

Duncan, J.M. and Bunchignani, A.L., 1976. An engineering manual for settlement studies, University of California, Berkeley.

Edil, T.B., 1997. Construction over peats and organic soils, Proceedings of conference on recent advances in soft soil engineering, Kuching, Sarawak, Malaysia, Vol. 1, pp.85-108.

Edil, T.B., 2003. Recent advances in geotechnical characterization and construction over peats and organic soils, Proceedings of the second congerence on advances in soft soil engineering and technology, Putrajaya, Malaysia, pp. 3-26.

Edil, T.B., 2016. Recent advances in construction over soft ground including peat, In: Proceedings of the soft soils 2016 conference, Bandung, Indonesia.

Elias, V. et al., 1998. Ground improvement technical summaries, Volume I, U.S. Department of Transportation Federal Highway Administration Office of Technology Application.

Ergin, S., 2014. Comparison of measured and predicted consolidation settlement in soft ground, M.Sc. Thesis, Civil Engineering Department of Middle East Technical University, Ankara.

Erol, O., 1977. Clay structure and creep behavior of clays as a rate of process, Iowa Ph.D. Thesis, Civil Engineering, Iowa State University, Ames, USA.

Erol, O., 1995. Ön yükleme dolgularının oturma-zaman ilişkilerinin belirlenmesine ilişkin yötemler, Türkiye İnşaat Mühendisliği XIII. Teknik Kongresi, Ankara.

Erol, O., 1999. Geotechnical report on coal storage area, İskenderun coal fired power plant, Middle East Technical University, Ankara.

Erol, O., 2000. Final design report on ground improvement, coal storage area, İskenderun Sugözü Power Plant, Middle East Technical University, Ankara.

Erol, O., 2000. Test embankment evaluation report, coal storage area, İskenderun Sugözü Power Plant, Middle East Technical University, Ankara.

Feda, J., 1992. Creep of soils and related phenomena, Elsevier-Academia, Amsterdam.

Fellenius, B.H. and Castonguay, N.G., 1985. The efficiency of band-shaped drains: a full scale laboratory study. Report to National Research Council and the Industrial Research Asistance Programme.

Feng, T.W., 2013. Reappraisal of surcharging to reduce secondary compression, Department of Civil Engineering, Chung Yuan Christian University, Taiwan, R.O.C.

Figueiredo, F.F.D.B. et al., 2011. What is R2 all about, Leviathan-Cadernos de Pesquisa Politica, n.3, pp. 60-68.

Flavigny, E., 1987. Proprietes visqueuses des geomateriaux. Manuel de rheology des geomateriaux. Presse de l'Ecole Nationale des Ponts et Chaussees, Paris.

Fodil, A. et al., 1997. Viscoplastic behavior of soft clay. Geotechnique 47(3); 581-591.

Fox, P.J. et al., 1992. C_α/C_c concept applied to compression of peat. Journal of Geotechnical Engineering, 118; 1256-1263.

General Directorate of Disaster Affairs, 1996. Earthquake zonning map for Turkey.

General Directorate of Highways, 2006. Technical Specifications, Ankara.

Genç, S.C., 1992. İznik-İnegöl (Bursa) arasındaki tektonik birimlerin jeolojik ve tektonik incelenmesi. Doktora Tezi, İTÜ.

Geiser, F. and Commend, S., 2012. Comparison between predicted and measured settlements on a road project. GeoMod SA, Switzerland.

Geology of Stanford University, Geol 615, 2014. Accessed: 29 October 2014. https://web.stanford.edu/~tyzhu/Documents/Some%20Useful%20Numbers.pdf.

Geotechnical and Geoenvironmental Engineering, ASCE, pp.312-322.http://www.haywardbaker.com/HB%20Wick%20Drains%20Bldg.jpg

Geo-Technics America, 2014. Accessed: 29 October 2014. http://geotechnics.com.

Giao, P.H. and Quang, N.D., 2014. Improvement of soft clay at a site in the Mekong Delta by vacuum preloading, Geotechnical and Earth Resources Engineering, Asian Institute of Technology, Pathumthani, Thailand.

Gibson, R.E, 1953. Experimental determination of true cohesion and true angle of internal friction, Proc. 3rd ICSMFE, Zurich, 126-130.

Gibson, R.E. and Lo, K.Y., 1961. A theory of consolidation for soils exhibiting secondary compression, Acta Polytech, Scand, p.296.

Gofar, N., 2006. Determination of coefficient of rate of horizontal consolidation of peat soil, Faculty of Civil Engineering Universiti Teknologi Malaysia.

Goldberg, D.T., 1965. Discussion of subsurface stabilization of organic silty clay by precompression by E. Jonas, Jour. Soil Mech. And Found. Div., ASCE, Vol. 91, No. SM3, pp. 136-140.

Google Maps, 2019. Accessed: 29 October 2019. http://maps.google.com.

Graham, J. et al., 1983. Yield states and stress-strain relationships in natural plastic clay, Can. Geotech. J. 20, 502-516.

Gray, H., 1936. Progress report on research on the consolidation of fine-grained soils, Proc. 1st Int. Conf. on Soil Mech and Found. Eng., Harvard Univ., Vol.2, p138-141.

Gundersen, A.S., et al., 2019. Characterization and engineering properties of the NGTS Onsoy soft clay site, AIMS Geosciences, 5(3), pp. 655-703.

Gündüz, B., 2010. Analysis of settlements of test embankments during 50 years-A comparison between field measurements and numerical analysis, M.Sc. Thesis, Department of Construction Sciences, Lund University, Sweden.

Gürer, Ö., Sangu, E., Özburan, M., 2005. Neotectonics of the SW Marmara region, NW Anatolia, Turkey, Geol. Mag. 143, Cambridge University Press, pp. 229-241.

Habibagahi, K.,1969. Influence of temperature on consolidation behavior of remoulded organic Paulding and inorganic Paulding soils, Ph.D. Thesis, University of Illinois.

Hadewych, V. et al., 2010. Settlement measurement optimising construction of a breakwater on soft soil, Ministry of the Flemish Community, Maritime Access Division, Coastal Division, Belgium, pp.1-14.

Haefeli, R. and Schaad, W., 1948. Time effect in connection with consolidation tests, Proc., Sec. Intern. Conf. on Soil Mech. and Found. Eng., Vol. 2, pp. 23-29.

Handy, R.L., 1985. The arch in soil arching. J. Geotech. Engng. Am. Soc. Civ. Engrs 111, No. 3, Mar, 302-318.

Hansbo, S., 1979. Consolidation of clay by band-shaped prefabricated vertical drains. Ground Engineering, 12(5), 16-25.

Hansbo, S. 1981. Consolidation of fine grained soils by prefabricated vertical drains. Proceedings of the 10th International Conference on Soil Mechanics and Foundation Engineering, 3, s. 677-682. Stocholm.

Havel, F., 2004. Creep in soft soils, Ph.D. Thesis submitted to the Faculty of Engineering, Norwegian University of Science and Technology, Norway.

Hicher, P.Y., 1985. Comportement mecanique des argiles saturees sur divers Chemins de solicitations monotones et cycliques. Application a une modelisation elastoplastique et viscoplastique. These de doctorat d'etat. Universite, Paris.

Hoefsloot, F.J.M., 2015. Long term monitoring test embankments Bloemendalerpolder-Geo-Impuls Program, Fugro GeoServices, Geotechnical Safety and Risk V, pp.621-627.

Horn, A., 1983. Determination of properties of weak soils by test embankments, International Symposium on Soil and Rock Investigations by Insitu Testing, Paris, Vol.2, pp.61-66.

Horn, H.M. and Lambe, T.W., 1964. Settlement of buildings on the MIT Campus, Jour. Of Soil Mech. and Found. Div., ASCE, Vol. 90, No. SM5, pp. 181-195.

Hsai-Yang, F., 1991. Foundation engineering hand book, second edition, Springer Science+Business Media, New York.

Indraratna, B., 2008. Recent advancement in the use of prefabricated vertical drains in soft soils, Faculty of Engineering and Information Sciences, University of Wollongong, Austrialian Geomechanics J., pp.29-46.

Indraratna, B. and Sathananthan, I., 2003. Comparison of field measurements and predicted performance beneath full scale embankments, Field Measurements in Geotechnics-Myrvoll ed., pp. 117-127.

Indraratna, B. et al., 2003. Modeling of prefabricated vertical drains in soft clay and evaluations of their effectiveness in practice, Faculty of Engineering and Information Sciences, University of Wollongong, Ground Improvement J., pp.127-138.

Indraratna, B. et al., 2007. Radial consolidation theories and numerical analysis of soft soil stabilization via prefabricated vertical drains, Faculty of Engineering and Information Sciences, University of Wollongong, International workshop on constitutive modelling, pp.155-167.

Indraratna, B. et al., 2012. Performance and prediction of surcharge and vacuum consolidation via prefabricated vertical drains with special reference to highways, railways and ports, Faculty of Engineering and Information Sciences, University of Wollongong, International Symposium on Ground Improvement, pp.29-46.

Jain, S.K. and Nanda, A., 2010. On the nature of secondary compression in soils, Indian Geotechnical Conference, GEOtrendz.

Johnson, S.J., 1970. Precompression for improving foundation soils, Soil Mechanics J. and Foundation Division, ASCE, 1:111-114.

Janssen, H.A., 1895. Verasche uber Getreidedruck in silozellen, Z. Ver. Dr. Ing. 39, 1045-1050.

Jose, B.T. et al., 1988. A study of geotechnical properties of cochin marine clays, Marine geotechnology, Vol. 7, pp. 189-209.

Kaczmarek, L. and Dobak, P., 2017. Contemporary overview of soil creep phenomenon, Contemp. Trends. Geosci., 6(1), pp.28-40.

Karim, M.R. and Lo, S.C.R., 2013. Estimation of the hydraulic conductivity of soils improved with vertical drains, School of Engineering and Information Technology, Australia, pp. 299-305.

Kazancı, N. et al., 2019. Late Quaternary landscape evalution of the southern Marmara region: paleogeographic implications for settlements, NW Turkey, Turkish J. Earth Sci., pp: 479-499.

Kellett, J.R., 1974. Terzaghi's theory of one dimensional primary consolidation of soils and its application, Department of Minerals and Energy, Australia.

Keene, P., 1964. Discussion on design of foundations for control of settlement, Proc. A.S.C.E., Evanston, Illinois.

Kemp, A. et al., 2013. The consolidation behaviour of Alluvial soft clay in Gladstone, Central Queensland, Australian Geomechanics Vol.48, No.1, pp.1-17.

Kervancıoğlu, Ö. B., 2002. Settlement behaviour of an instrumented embankment on clay, M.Sc. Thesis, Department of Civil Engineering, METU, Ankara.

Kissell, R. and Poserina, J., 2017. Chapter 2 Regression models, Optimal sports math, statistics and fantasy, pp. 39-67.

Kulhawy, F.H. and Mayne, P.W., 1990. Manual on estimating soil properties, Report EL-6800, Electric Power Res. Inst., Palo Alto.

Kurnaz, T.F. et al., 2016. Prediction of compressibility parameters of the soils using artificial neural network, SpringerPlus DOI 10.1186/s40064-016-3494-5.

Kutter, B.L. and Sathialingam, N., 1992. Elastic–viscoplastic modelling of the rate-dependent behaviour of clays, Geotechnique, 42(3): 427-441.

Lacasse, S. and Berre, T., 2005. Undrained creep susceptibility of clays, in proceeding of the 16th International Conference on Soil mechanics and Geotechnical Engineering, Osaka, Japan. Millpress, Rotterdam, Netherlands, pp. 531-536.

Ladd, C.C. and Preston, W.B., 1965. On the secondary compression of saturated clays, Vicksburg, MS, 116.

Lansivaara, T. and Nordal, S., 2000. Strain rate approach to creep evaluations, Proc. NGM-2000 Nordiska Geoteknikermotet, 13, Helsinki, June, pp.25-32.

Leroueil, S. et al., 1985. Stress-strain-strain rate relation for the compressibility of sensitive natural clays, Geotechnique, Vol 35, Issue 2, pp. 159-180.

Li, C., 2014. A simplified method for prediction of embankment settlement in clays, Journal of Rock Mechanics and Geotechnical Engineering 6, Institute of Civil Engineering, China, pp.61-66.

Liu, S. and Jing, F., 2003. Settlement prediction of embankments with stage construction on soft ground, Institute of Geotechnical Engineering, Southeast University, China, pp. 228-232.

Lo, K.Y., 1961. Stress-strain relationship and pore water pressure characteristics of a normally consolidated clay, Prc. 5th Int. Conf. on Soil Mech. And Found. Eng., Paris, Vol. 1, P219-224.

Lo, S.R. et al., 2008. Long-term performance of wide embankment on soft clay improved with prefabricated vertical drains, Can. Geotech. Journal, Canada, pp. 1073-1091.

Long, R. P., and Covo, A., 1994. Equivalent diameter of vertical drains with an oblong cross-section. Journal of Geotechnical Engineering Division, ASCE, 120(9), 1625-1630.

Long, P.V. et al., 2006. Back analyses of compressibility and flow parameters pf PVD improved soft ground in Southern Vietnam, International Conference on Geosynthetics, Netherlands.

Machine, F.M. and Too, K.A., 2013. Land reclamation using prefabricated vertical drains in part of Mombasa, Scientific Conference, Kenya.

Magnan, J. P., Pilot, G., and Queyroi, D., 1983. Back analysis of soil consolidation around vertical drains, Proc., 8th ECSMFE, Vol. 2, Balkema, Rotterdam, The Netherlands, 653–658.

Martins, I. S. M., 1992. Fundamentals of a Behavioral Model for Saturated Clayey Soils, D.Sc. thesis, COPPE/UFRJ, Rio de Janeiro, Brazil (in Portuguese).

Mehdizadeh, A. and Fakharian, K., 2015. Field instrumentation of a preloading project with prefabricated vertical drains, Australian Centre for Geomechanics, Perth, ISBN 978-0-9924810-2-5.

Mesri, G., 1973. Coefficient of secondary compression, Journal of the Soil Mechanics and Foundations Division, ASCE, Vol. 99, No. SM1, pp. 123-137.

Mesri, G. and Godlewski, P.M., 1977. Time and stress compressibility interrelationships. J. Geotech. Enging Div., ASCE, 103(GT5): 417-430.

Mesri, G., Febres‐Cordero, Shields, E., D. R., and Castro A., 1981. Shear Stress‐Strain-Time Behavior of Clays, Géotechnique, 31, 4 pp. 537‐552.

Mesri, G. and Castro, A., 1987. Cα/Cc Concept and Ko during Secondary Compression, ASCE J. Geotechnical Engineering, 113:3:230-247.

Mesri, G. and Vardhanabhuti, B., 2005. Secondary compression, Journal of Geotechnical and Geoenvironmental Engineering, 131(3), 398-401.

Moh, Z.C. et al., 1998. Improvement of soft Bankok clay by use of prefabricated vertical drain, 13th Souteast Asian Geotechnical Conference, Taiwan, pp. 369-375.

Motulsky, H., 1999. Analyzing data with graphpad prism, GraphPad Software, Inc, San Diego, USA.

MTA, 2008. Bandırma H20-C1 and Bandırma H20-C2 Maps.

Murayama, S. and Shibata, T., 1958. On the rheological characters of clay, Disaster Prevention Research Institute, Kyoto University, Bulletins, Bulletin No. 26, pp. 1-43.

Murayama, S. and Shibata, T., 1961. Rheological properties of clays, Proc. 5th ICSMFE, Vol. I, pp. 269-273.

Murayama, S., and Shibata, T., 1964. Flow and stress relaxation of clays Proceedings of I UTAM T Symposium on Rheology and Soil Mechanics, Grenoble Springer Verlag pp. 99-129.

Murthy, V.N.S., 2002. Geotechnical engineering: Principles and practices of soil mechanics and foundation engineering, Civil and Environmental Engineering, New York.

NAVFAC, DM 7.1, 1982. Soil Mechanics, Dept. of Navy.

NAVFAC, DM 7.2, 1982. Foundations and earth structures, Dept. of Navy.

NCHRP Synthesis 368 Cone penetration testing, 2007. A synthesis of highway practice Transportation. research board, Washington, D.C.

Newland, P. L. and Allely, B.H., 1960. A study of the consolidation characteristics of a clay, Geotechnique, Vol. 10, pp. 62-74.

Ofosu, B., 2013. Empirical model for estimating compression index from physical properties of weathered Birimian phyllites, Ejge vol. 18, pp. 6135-6144.

O'Kelly, 2005. Compression and consolidation anisotropy of some soft soils. Department of Civil, Structural and Environmental Engineering, University of Dublin, Ireland.

Olivares, A.M. and Forero, C.G., 2010. Goodness-of-fit testing, International encyclopedia of education 7, 190-196.

Olson, R. E., 1989. Advenced Soil Mechanics, Unit 7 Secondary Consolidation, Department of Construction Engineering, Chaoyang University of Technology.

Ottosen, N.S. and Petersson, H., 1992. Introduction to the finite element methods, Prentice Hall.

Ozcoban, S. et al., 2007. Staged construction and settlement of a dam founded on soft clay, Geotechnical and Geoenvironmental Engineering J., ASCE, pp. 1003-1016.

Ozdogan, M., Şahbaz, A., Kazancı, N., 2000. Depositional and fades properties of The Middle-Late Miocene Alluvial Fan System at South Marmara Sea, Geological Bulletin of Turkey, Vol. 43, No: I, 59-72.

Peck, R.B., Hanson, W.E. and Thornburn, T.H., 1974. Foundation engineering, John Wiley and Sons, 514p.

Peri, E. et al., 2019. How to interpret consolidation and creep in Yoldia clay, E3S Web of Conferences 92.

Phase 2 6.0, 2008. A two-dimensional elasto-plastic finite element program and its user's manual, by Rocscience Inc, Toronto-Canada.

Premalal, R.P.D.S. et al., 2013. Use of observational approach for embankment construction on organic soil deposits in Sri Lanka, University of Moratuwa, Sri Lanka.

Rahman, I., 2019. Introduction of confidence interval, Mdatascience.

Rixner, J., Kramer, S., & Smith, A., 1986. Prefabricated vertical drains, Vol.s I, II and III: Summary of Research Report: Final Report. Federal Highway Administration, Washington D.C.

Qin, A. et al., 2010. Analytical solution to one-dimensional consolidation in unsaturated soils under loading varying exponentially with time, Department of Civil Engineering, Shanghai University, China, pp. 233-238.

Quang, N.D. and Giao, P.H., 2014. Improvement of soft clay at a site in the Mekong Delta by vacuum preloading, Geomechanics and Engineering, Vol.6, No.4, Thailand, pp. 419-436.

Razak, Z. et al., 2017. Prediction of settlement by using finite element simulation 2D program at Seksyen 7, Shah Alam, AIP Conference Proceedings.

Redana, I.W., 1999. Effectiveness of vertical drains in soft clay with special reference to smear effect, Department of Civil, Mining and Environmental Engineering, University of Wollongong Thesis Collection, Australia.

Republic of Turkey Ministry of Transport, Maritime Affairs and Communications, 2006. Pavement Design Book.

Salem, M. and El-Sherbiny, R., 2013. Comparison of measured and calculated consolidation settlements of thick underconsolidated clay, Cairo University, Egypt.

Sanglerat, G., 1972. The penetrometers and soil exploration, Elsevier, Amsterdam, 488p.

Saowapakpiboon, J. et al., 2009. Measured and predicted performance of prefabricated vertical drains (PVDs) with and without vacuum preloading, Geotextiles and Geomembranes J. 28, pp. 1-11.

Sas, W., Malinowska, E., 2006. Surcharging as a method of road embankment construction on organic soils, IAEG2006 Paper number 403, The Geological Society of London.

Sathananthan, I., 2005. Modelling of vertical drains with smear installed in soft clay, Department of Civil, Mining and Environmental Engineering, University of Wollongong Thesis Collection, Australia.

Sekiguchi, H., 1984. Theory of undrained creep rupture of normally consolidated clay based on elasto- viscoplasticity, Soils and Foundations Vol. 24, No. 1, pp. 129- 147, Japanese Society of Soil Mechanics and Foundation Engineering.

Sharma, H.D. and Lewis, S.P., 1994. Waste contaminant systems, waste stabilization and landfill design and evaluation, New York, Wiley.

Shen, S.L. et al., 2005. Analysis of field performance of embankments on soft clay deposits with and without PVD improvement, Geotextile and Geomembrane J. 23, pp. 463-485.

Shrestha, S., 2015. Study of shear creep in sensitive clay, Norwegian University of Science and Technology, Geotechnical Master Degree Thesis.

Simons, N.E., 1963. The influence of stress path on triaxial test results, Proc. Symp. on lab. shear testing of soils, Ottowa, A.S.T.M. Stp 361, pp.270-278.

Singh, A. and Mitchell, J.K., 1969. Creep potential and creep rupture of soils. International Conference on Soil Mechanics and Foundation Engineering. 7, Mexico, Proceedings, pp.379-384.

Sing, W.L. et al., 2018. Compression rates of untreated and stabilized peat soils, Ejge Vol. 13, Bund. F.

Sivakugan, N. and Das, B.M., 2010. Geotechnical engineering: a practical problem solving approach. Eureka Series. J. Ross Publishing, USA.

Sivasithamparam, N. et al., 2015. Modelling creep behavior of anisotropic soft soils, Computer and Geotechnics 69, pp.46-57.

Skempton, A.W., 1944. Notes on compressibility of clays, Q.J. Geol. Soc., London, 100: 119-135.

Solanki, C.H. et al., 2008. Statistical analysis of index and consolidation properties of Alluvial deposits and new correlations, International Journal of Applied Engineering Research ISSN 0973-4562 Volume 3, Number 5, India, pp. 681-688.

Spangler, M.G., 1948. Underground conduits-an appraisal of modern research. Trans. Am. Soc. Civ. Engrs 113, 316-374.

Sridharan, A. and Jayadeva, M.S., 1982. Double layer theory and compressibility of clays, Geotechnique 32(29: 133-144.

Sridharan, A. and Rao, A.S., 1982. Mechanism controlling the secondary compression of clays, Geotechnique, 32(2): 249-260.

Stroud, M.A., 1974. The Standard Penetration Test in insensitive clays and soft rock, Proceedings of European Symposium on Penetration Resistance, National Swedish Institute for Building Research, Stockholm, Sweden, 2.2, 367-375.

Tan, T. et al., 1991. Hyperbolic Method for consolidation analysis, Geotechnical Engineering J., Vol.117, pp. 1723-1737.

Tavenas, F. et al., 1978. Creep behavior of an undisturbed lightly overconsolidated clay, Can. Geotech. J., 15, 402-423.

Taylor, D.W., 1942. Research on consolidation of clays, M.I.T. Report serial 82, Cambridge, Mass.

Tedjakusuma, B., 2012. Application of prefabricated vertical drain in soil improvement, Civil Engineering Dimension Vol.11 No.1, pp.51-56.

Terzaghi, K., 1925. Structure and volume of voids of soils, Pages of 10-13 part of Erdbaumechanik auf Bodenphysikalisher Grundlage, translated by A. Casagrande in From Theory to Practice in Soil Mechanics, New York, John Wiley and Sons, (1960) pp. 146-148.

Terzaghi, K. and Peck, R.B., 1948. Soil mechanics in engineering practice, John Wiley and Sons, New York.

Türkçebilgi, 2014. Accessed: 28 October 2014. http://www.turkcebilgi.com/bursa-otoyol -haritasi.

Tripathy, S. et al., 2010. Desorption and consolidation behavior of initially saturated clays, Geoenvironmental Research Centre, Cardiff University, Cardiff, UK.

Wahls, H.E., 1962. Analysis of primary and secondary consolidation, Proc., ASCE, Vol. 88, SM-6, pp. 207-231.

Walker, R.T., 2006. Analytical solutions for modeling soft soil consolidation by vertical drains, Department of Civil, Mining and Environmental Engineering, University of Wollongong Thesis Collection, Australia.

Walker, R.T., 2011. Vertical drain consolidation analysis in one, two and three diamensions, Faculty of Engineering and Information Sciences, University of Wollongong, Computers and Geotechnics, pp.1069-1077.

Wetzel, C.A., 2014. Comparison of theoretical and actual time dependent settlement induced by fill placement, Associate Principle, GZA GeoEnvironmental Inc., New York, USA.

White, D.J. et al., 2002. Embankment quality: Phase 3, Iowa Dot Project TR-401, Department of Civil and Construction Engineering, Iowa State University, Iowa.

Wickdrain installation, 2014. Accessed 15 November 2014.

Wu, T.H. et al., 2011. Reliability of settlement prediction-Case history, Journal of Geotechnical and Geoenvironmental Engineering, Vol. 137, Ussue 4.

Xiao, D., 2001. Consolidation of soft clay using vertical drains, Phd. Thesis, Nanyang Technological University, Singapore, p.301.

Yan, Z. et al., 2019. Study on the creep behaviors of interactive marine-terrestrial deposit soils, Hindawi advances in civil engineering, 14 p.

Yılmaz, E., 2000. Samsun Çarşamba mavi kilinin ikincil ve üçüncül sıkışma davranışı, doktora tezi, İstanbul Teknik Üniversitesi Fen Bilimleri Enstitüsü, İstanbul.

Yılmaz, E., Sağlamer, A., 2001. Secondary and tertiary compression behavior of samsun soft blue clay, 15th International conference on soil mechanics and foundation engineering, Istanbul.

Yüksel Domaniç Müh. Ltd. Şti., 2015. Gebze-Orhangazi-İzmir Highway Project, Bursa-Susurluk Section Geotechnical Report for Embankment Design. Ankara. 1246 pp.

Zainorabidin, A. et al., 2019. Settlement behavior of parit nipah peat under static embankment, International Journal of Geomate, vol.17, Issue 60, pp.151-155.

Zhao, D., 2019. Study on the creep behavior of clay under complex triaxial loading in relation to the microstructure, Phd. Thesis, University of Lorraine, France.

Zhao, J. et al., 2017. Numerical analysis of soil settlement prediction and its application in large-scale marine reclamation artificial island project, Civil Engineering Technology Research and Development Center, Dalian University, China.

APPENDICES

A. Laboratory Test Results

Plasticity and coefficient of volume compressibility charts for KM: 139+764 are presented in Figure A.1 and A.2.

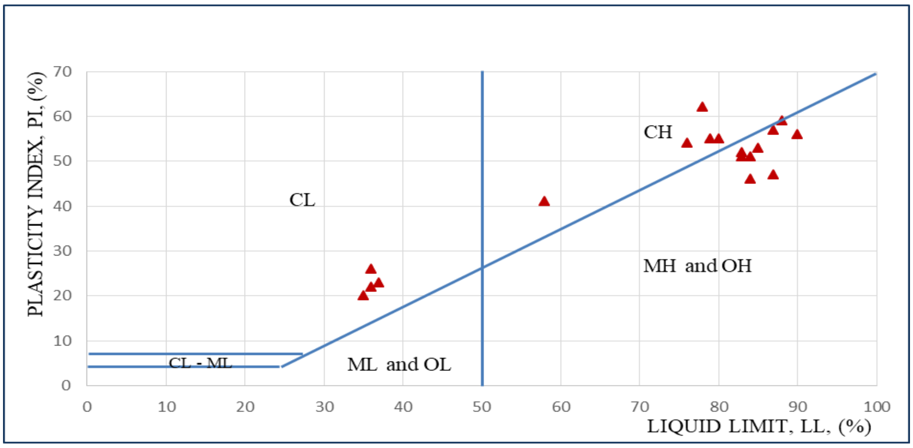

Figure A.1. Plasticity chart for BSSK-447

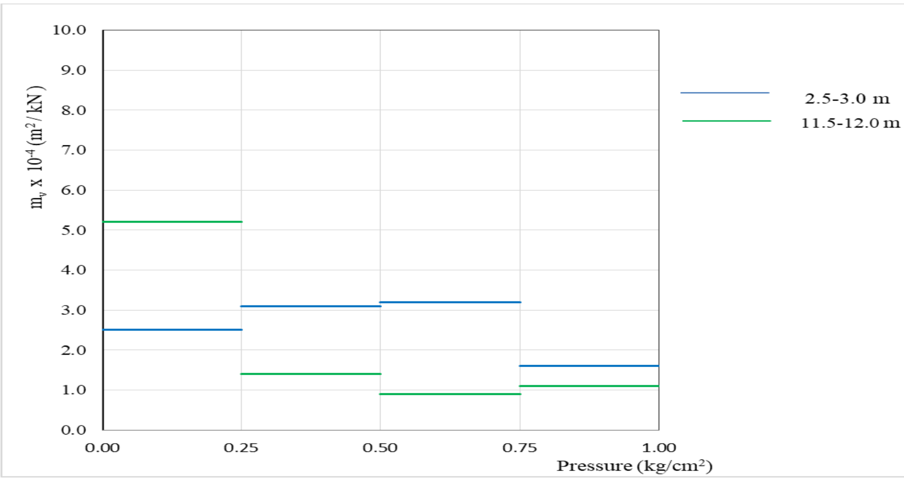

Figure A.2. The coefficient of volume compressibility (m_v) chart for BSSK-447

Plasticity and coefficient of volume compressibility charts for KM: 139+860 are presented in Figure A.3 and A.4.

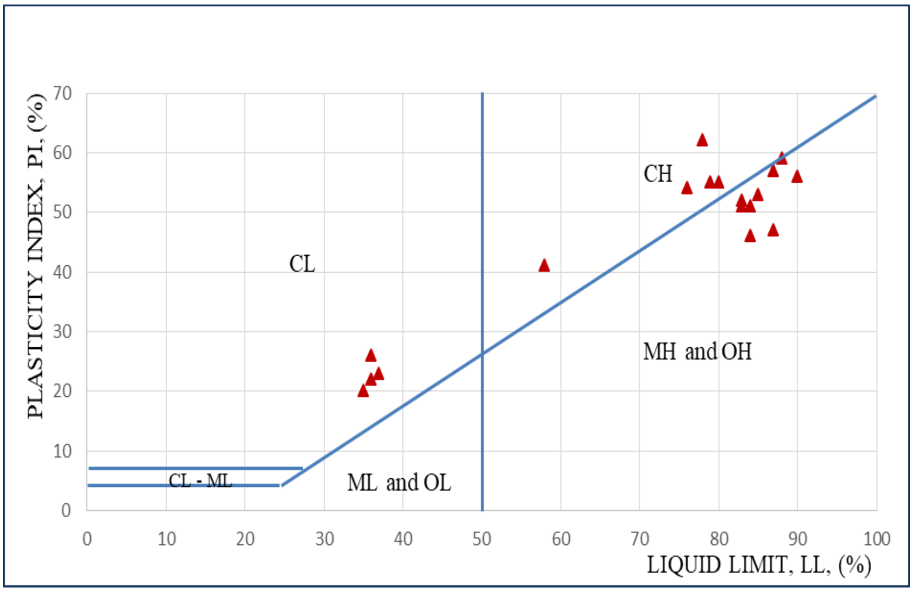

Figure A.3. Plasticity chart for BSSK-447

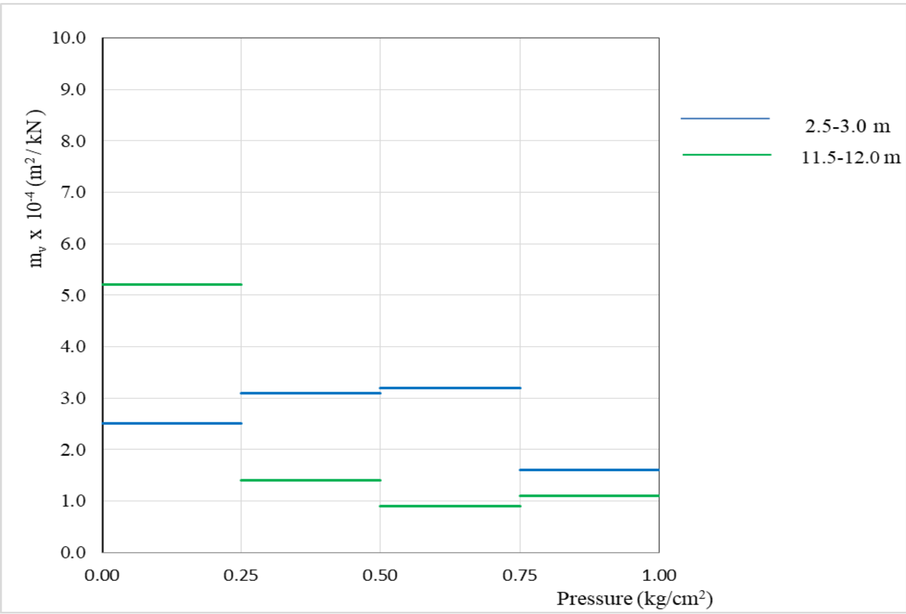

Figure A.4. The coefficient of volume compressibility (m_v) chart for BSSK-447

Plasticity and coefficient of volume compressibility charts for KM: 140+592 are presented in Figure A.5 and A.6.

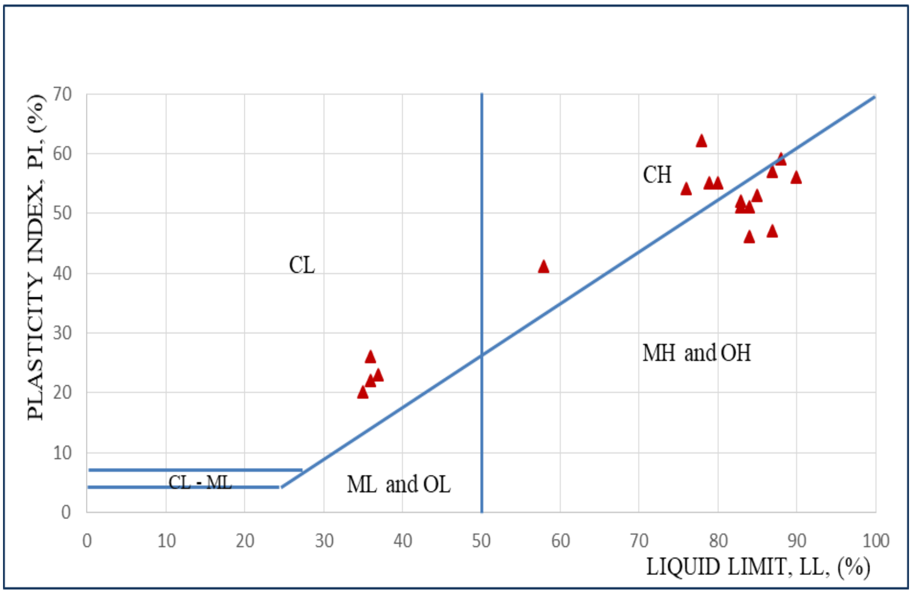

Figure A.5. Plasticity chart for BSSK-447

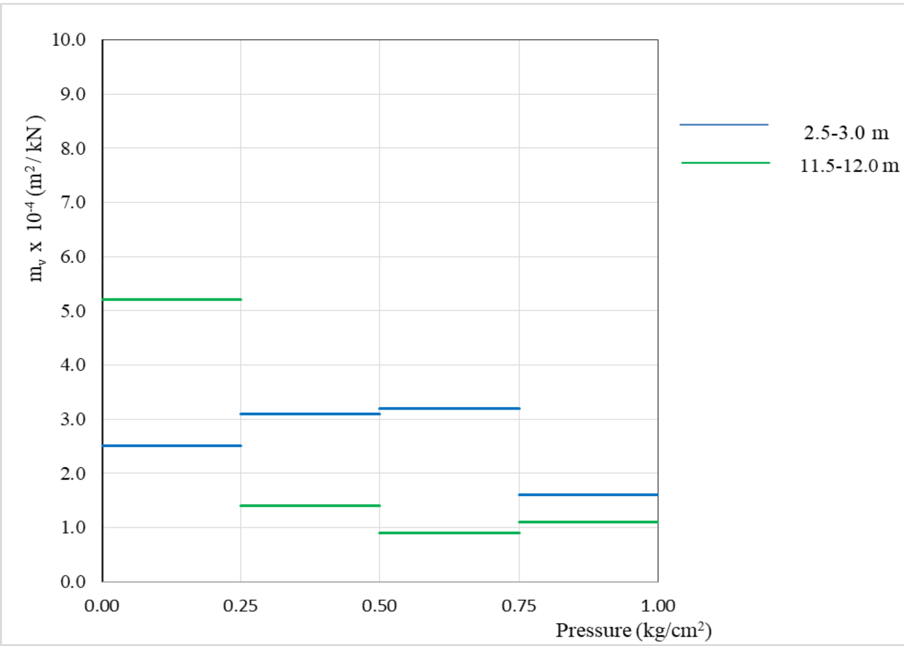

Figure A.6. The coefficient of volume compressibility (m_v) chart for BSSK-447

Plasticity and coefficient of volume compressibility charts for KM: 141+667 are presented in Figure A.7 and A.8.

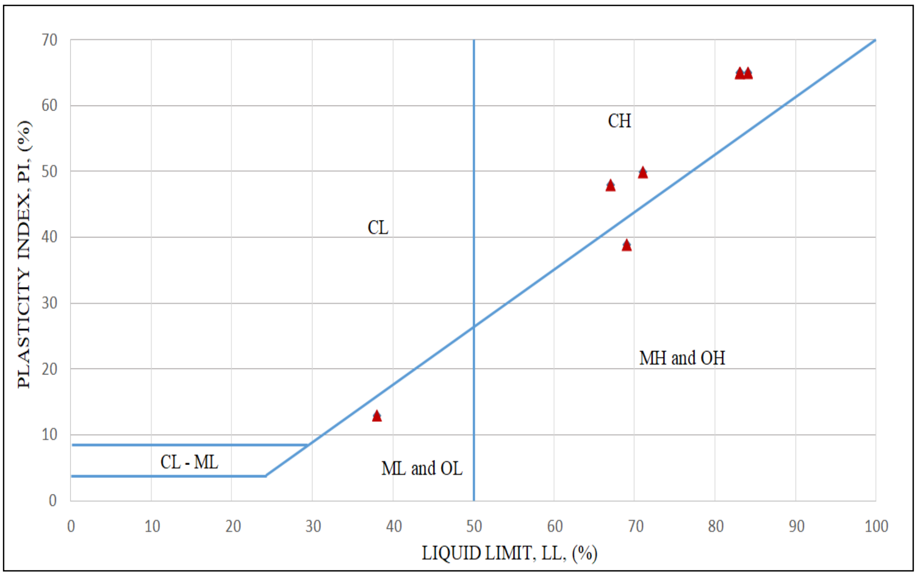

Figure A.7. Plasticity chart for BSSK-451

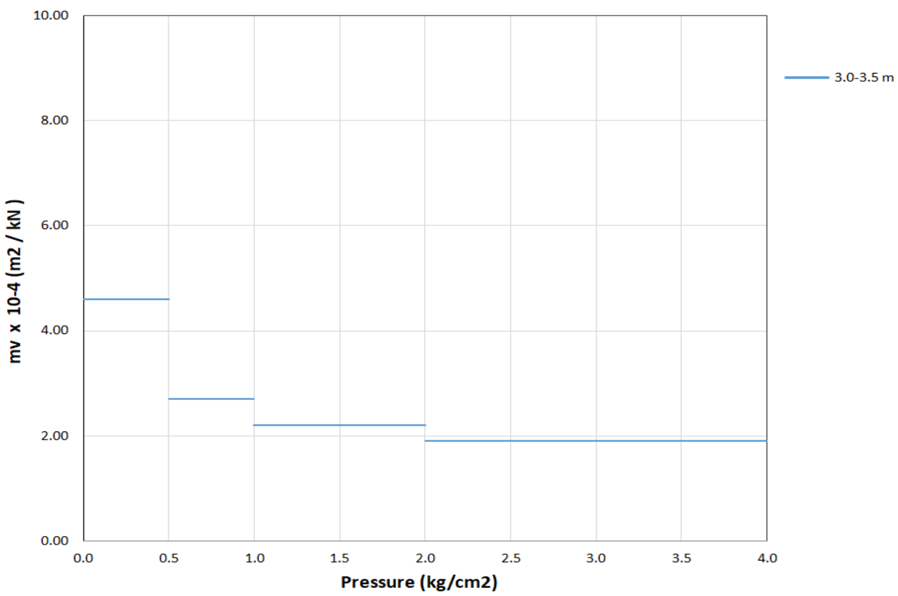

Figure A.8. The coefficient of volume compressibility (m_v) chart for BSSK-451

Plasticity and coefficient of volume compressibility charts for KM: 142+000 are presented in Figure A.9 and A.10.

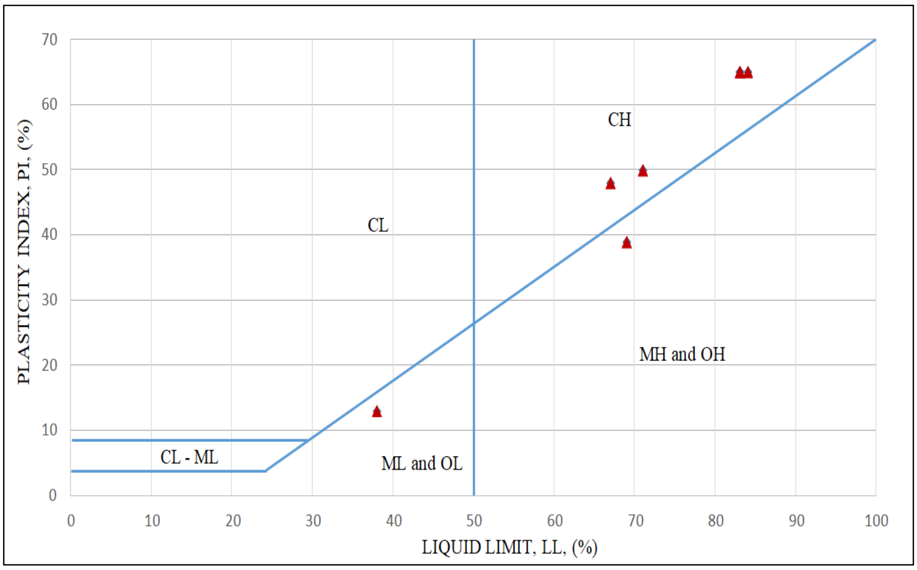

Figure A.9. Plasticity chart for BSSK-452

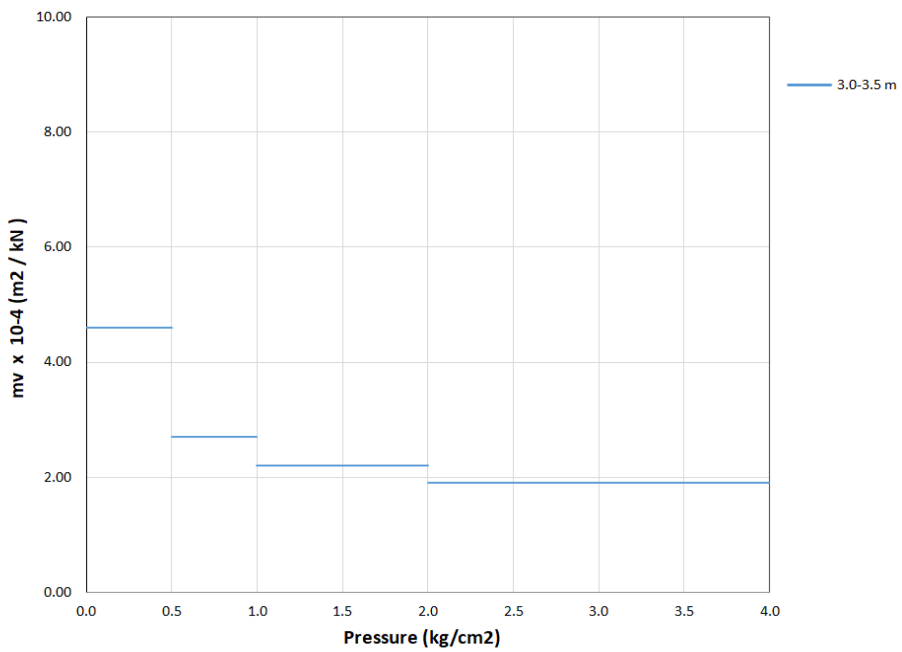

Figure A.10. The coefficient of volume compressibility (m_v) chart for BSSK-452

Plasticity and coefficient of volume compressibility charts for KM: 142+400 are presented in Figure A.11 and A.12.

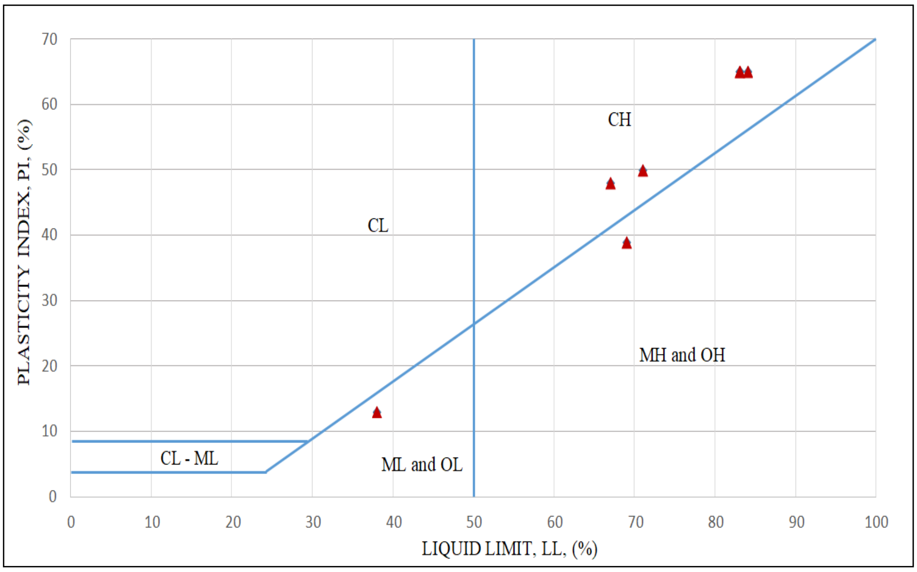

Figure A.11. Plasticity chart for BSSK-452

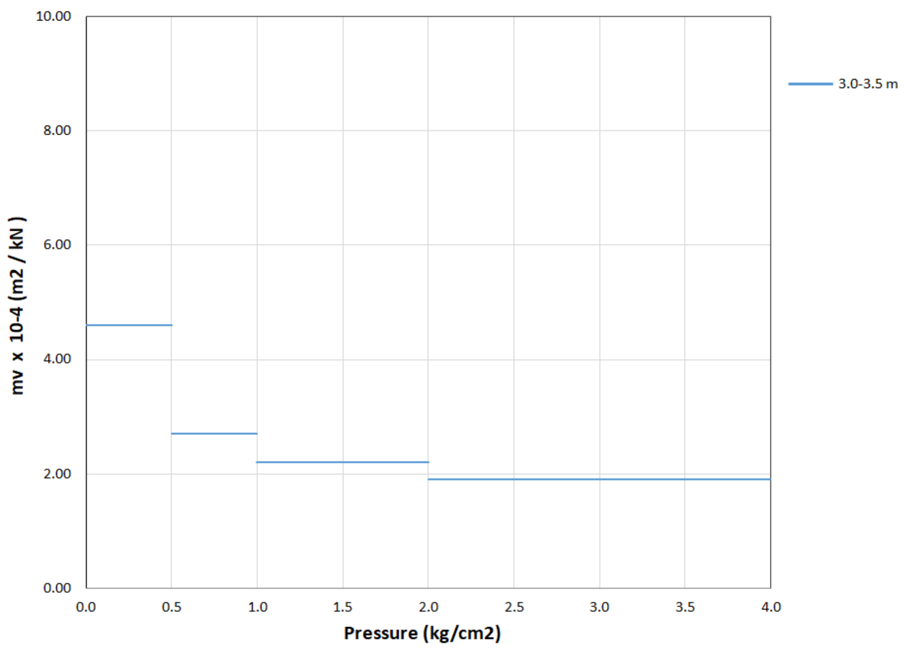

Figure A.12. The coefficient of volume compressibility (m_v) chart for BSSK-452

Plasticity and coefficient of volume compressibility charts for KM: 143+107 are presented in Figure A.13 and A.14.

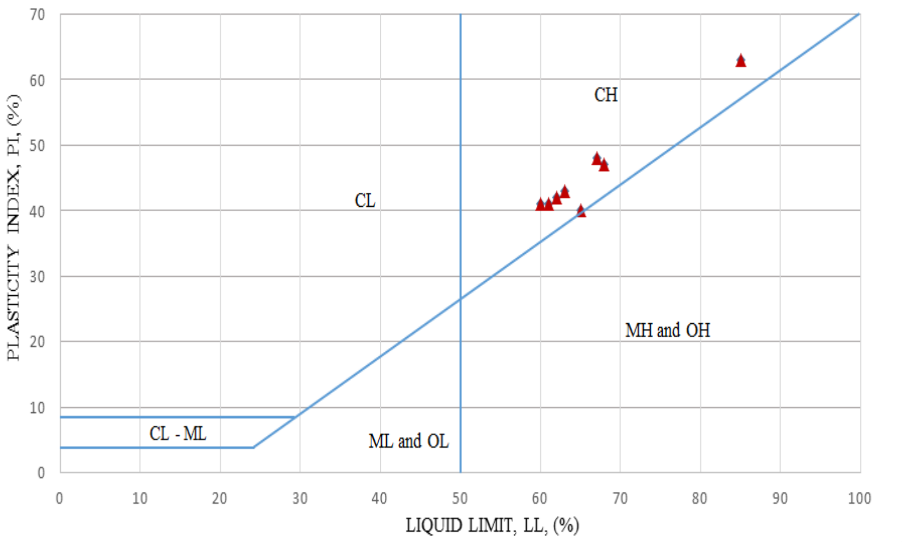

Figure A.13. Plasticity chart for BSSK-453

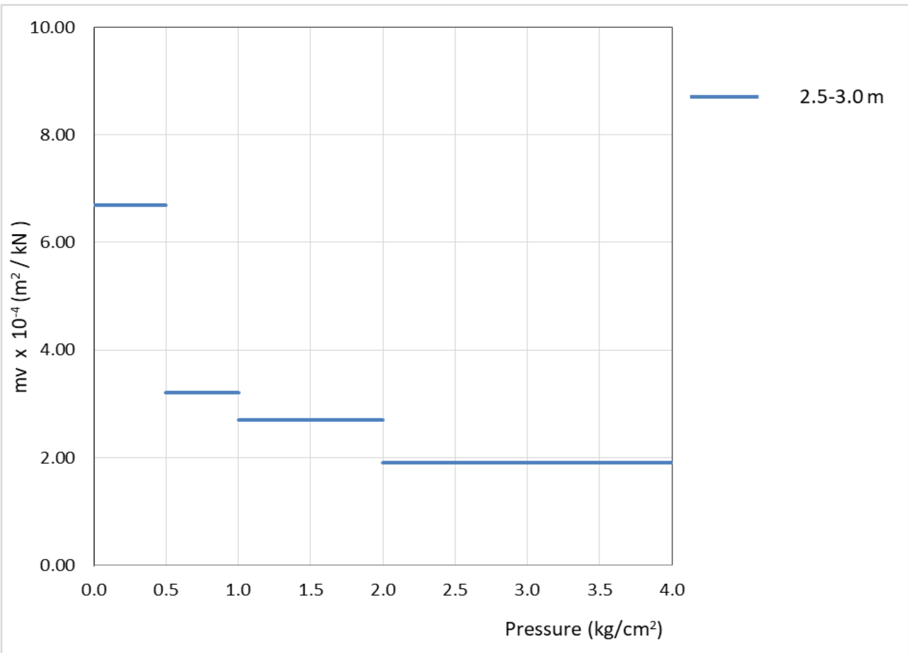

Figure A.14. The coefficient of volume compressibility (m_v) chart for BSSK-453

Plasticity and coefficient of volume compressibility charts for KM: 144+000 are presented in Figure A.15 and A.16.

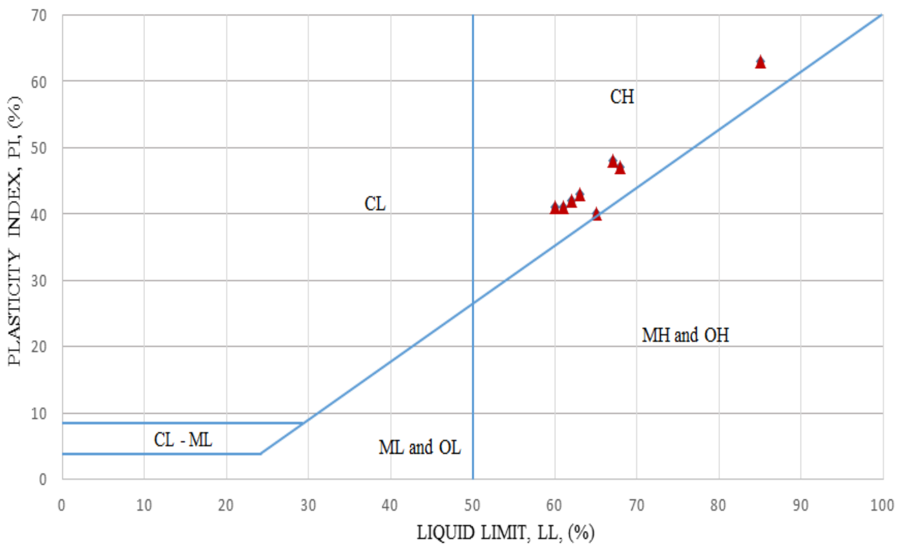

Figure A.15. Plasticity chart for BSSK-454

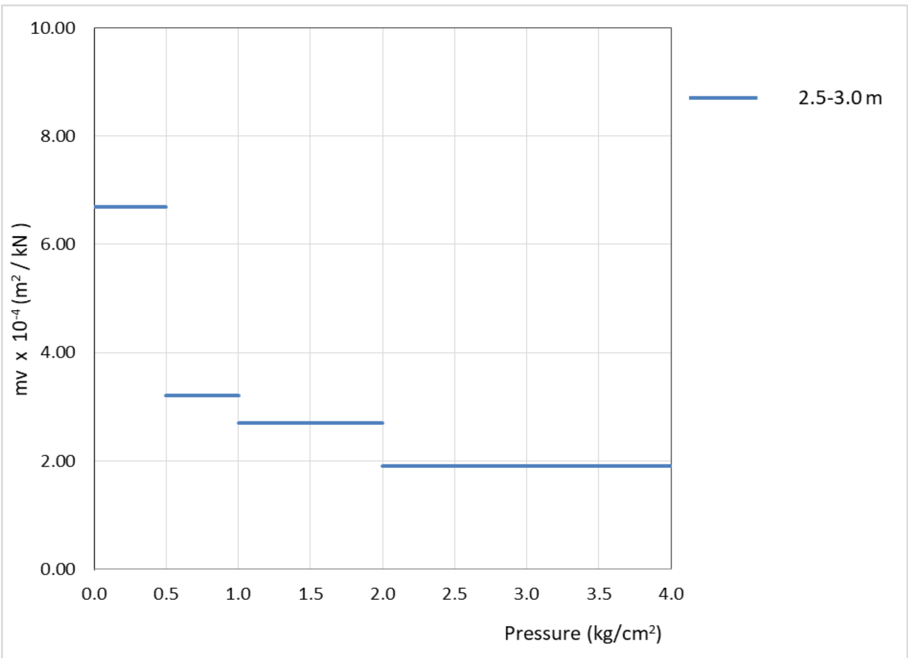

Figure A.16. The coefficient of volume compressibility (m_v) chart for BSSK-454

Plasticity and coefficient of volume compressibility charts for KM: 145+000 are presented in Figure A.17 and A.18.

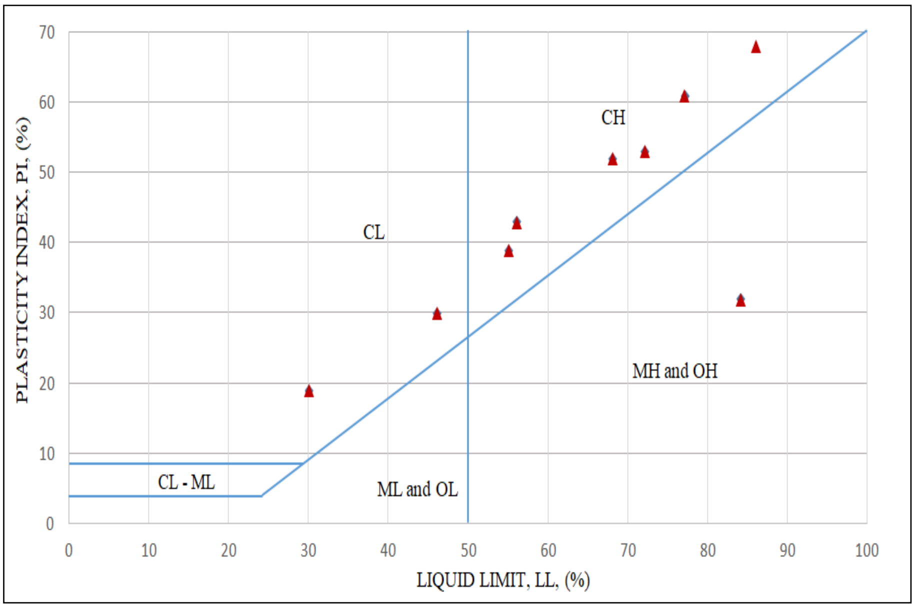

Figure A.17. Plasticity chart for BSSK-456

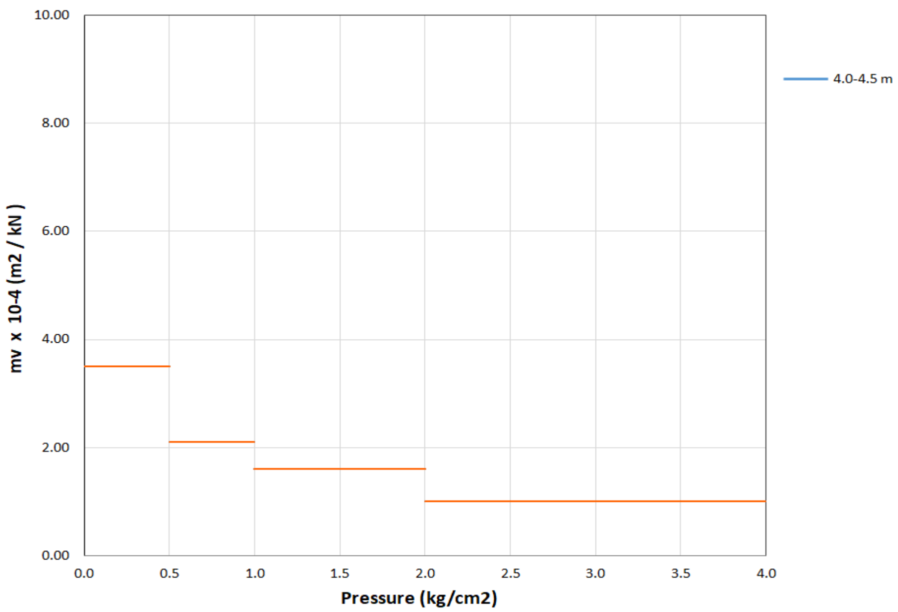

Figure A.18. The coefficient of volume compressibility (m_v) chart for BSSK-456

Plasticity and coefficient of volume compressibility charts for KM: 146+210 are presented in Figure A.19 and A.20.

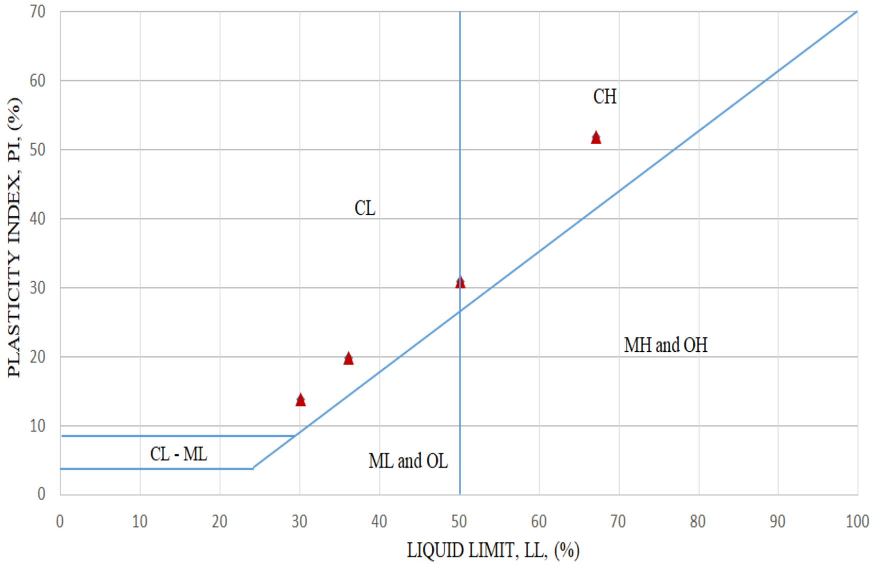

Figure A.19. Plasticity chart for BSSK-457

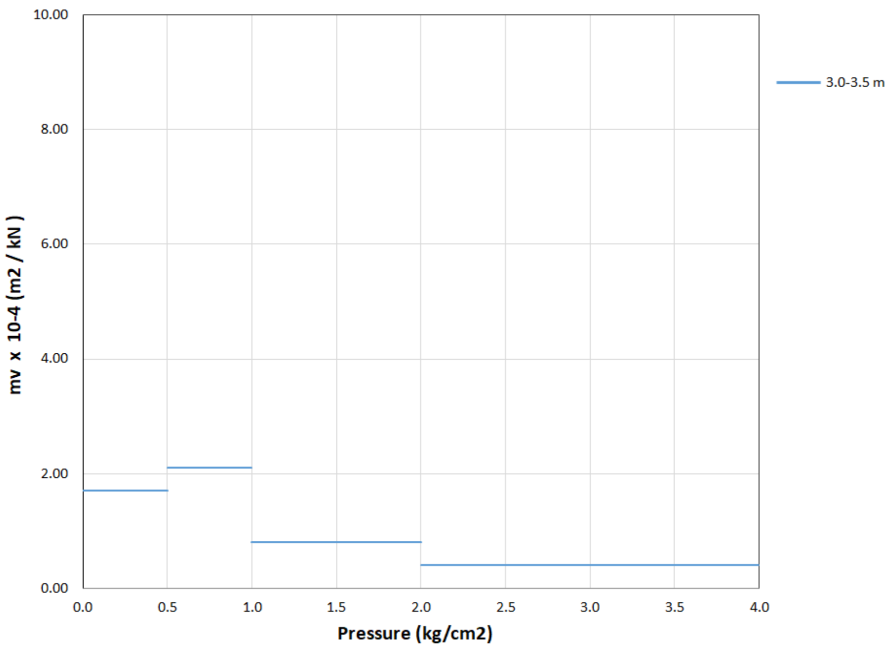

Figure A.20. The coefficient of volume compressibility (m_v) chart for BSSK-457

Plasticity and coefficient of volume compressibility charts for KM: 147+000 are presented in Figure A.21 and A.22.

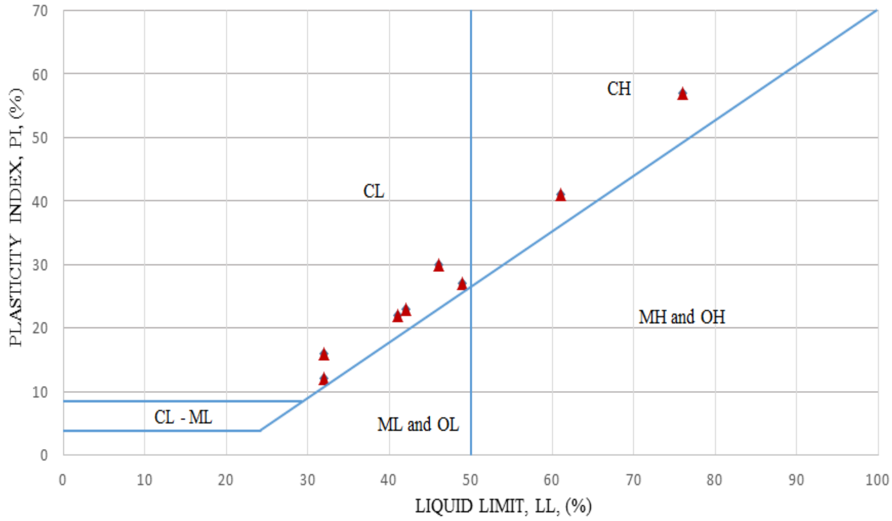

Figure A.21. Plasticity chart for BSSK-458

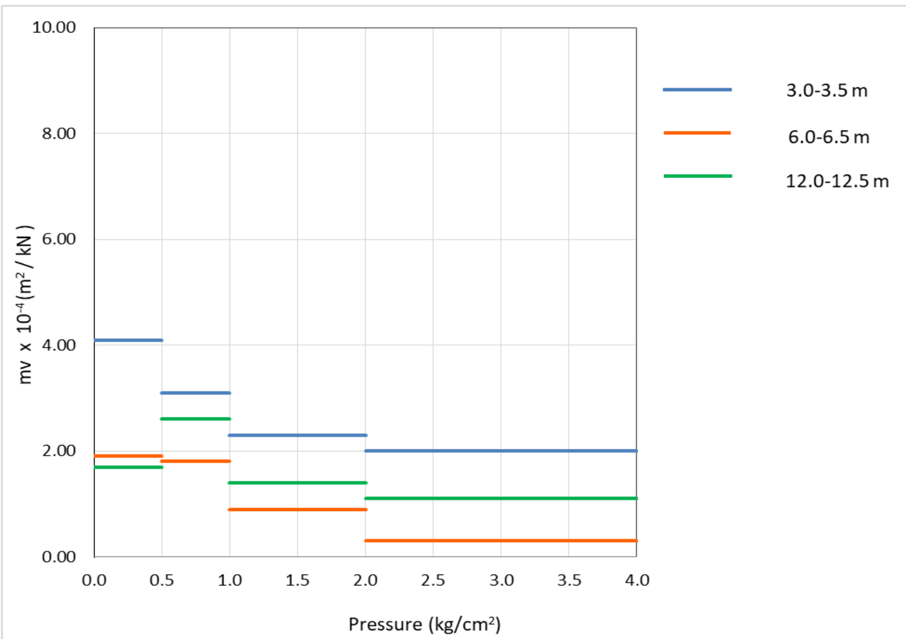

Figure A.22. The coefficient of volume compressibility (m_v) chart for BSSK-458

Plasticity and coefficient of volume compressibility charts for KM: 149+000 are presented in Figure A.23 and A.24.

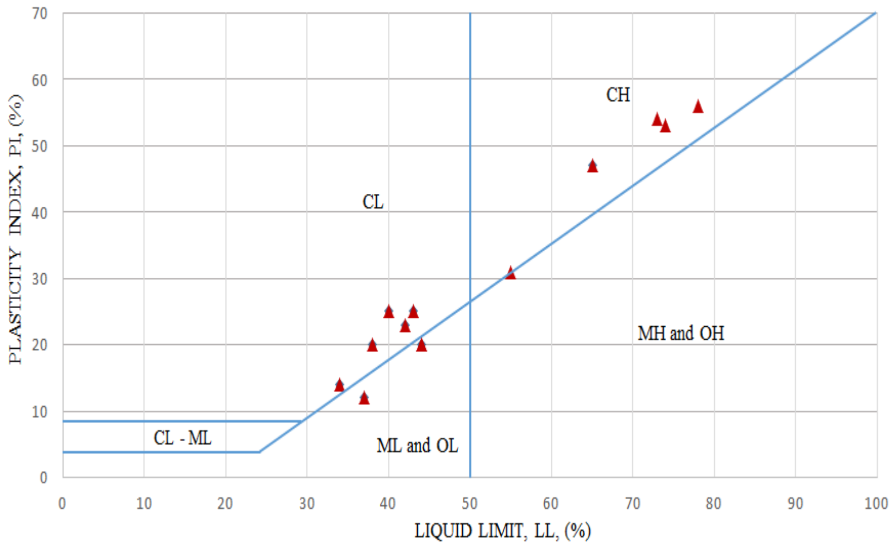

Figure A.23. Plasticity chart for BSSK-461

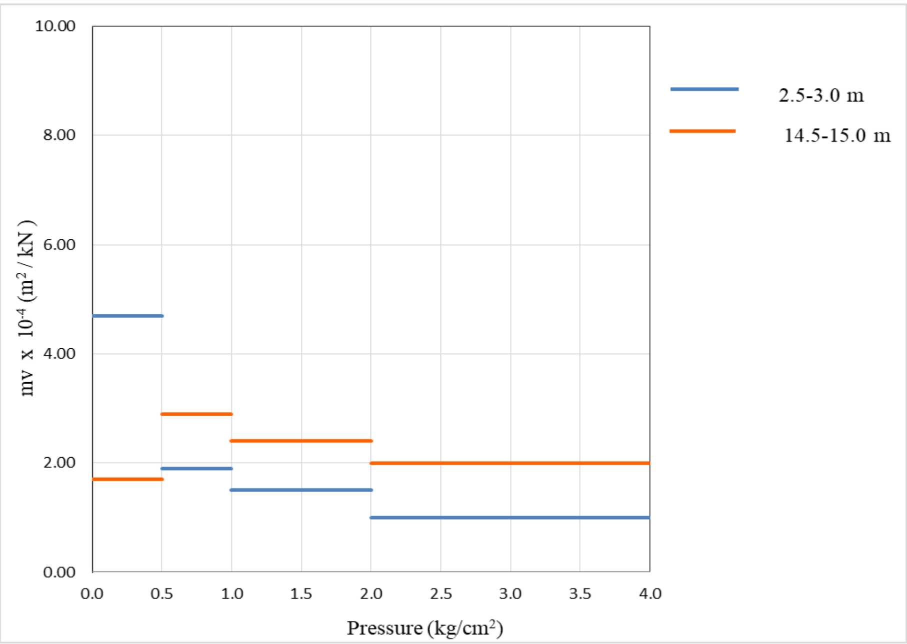

Figure A.24. The coefficient of volume compressibility (m_v) chart for BSSK-461

Plasticity and coefficient of volume compressibility charts for KM: 150+000 are presented in Figure A.25 and A.26.

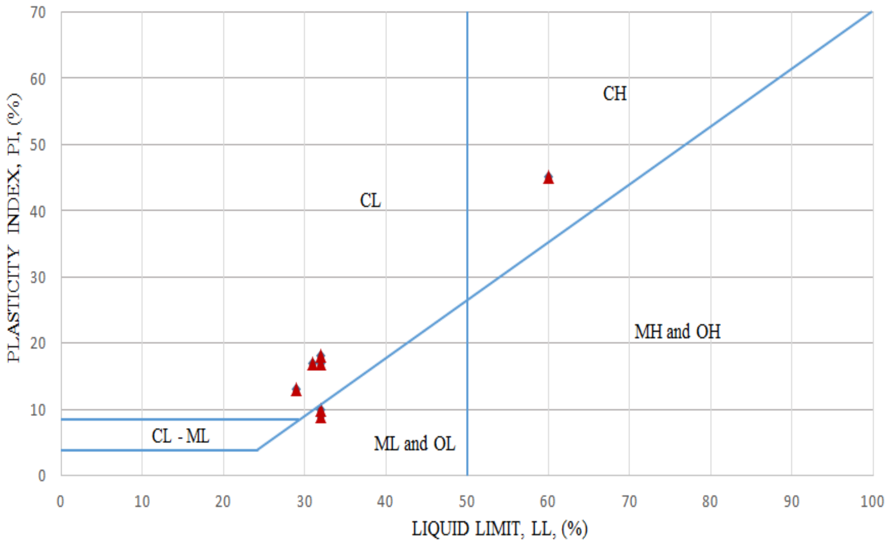

Figure A.25. Plasticity chart for BSSK-462

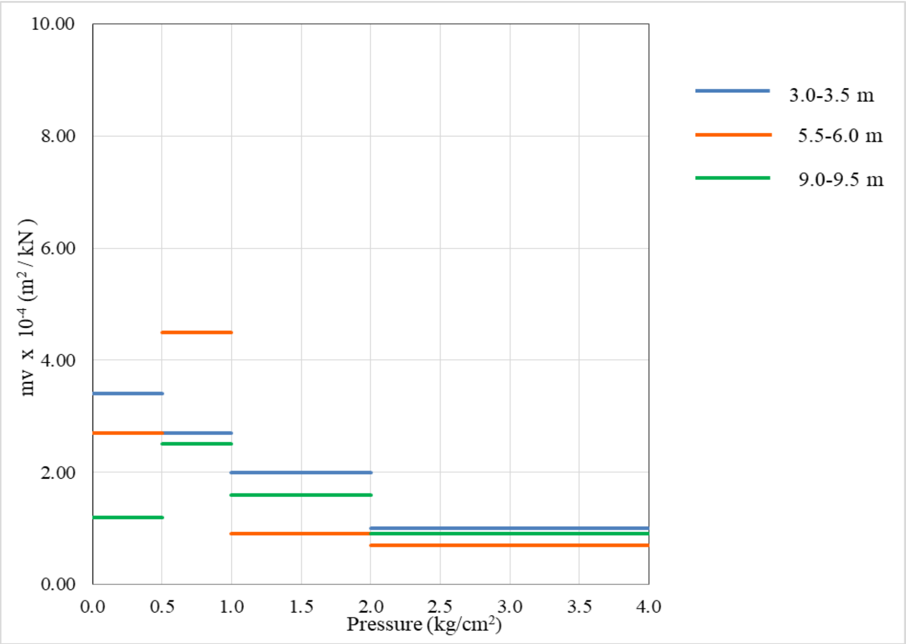

Figure A.26. The coefficient of volume compressibility (m_v) chart for BSSK-462

Plasticity and coefficient of volume compressibility charts for KM: 150+500 are presented in Figure A.27 and A.28.

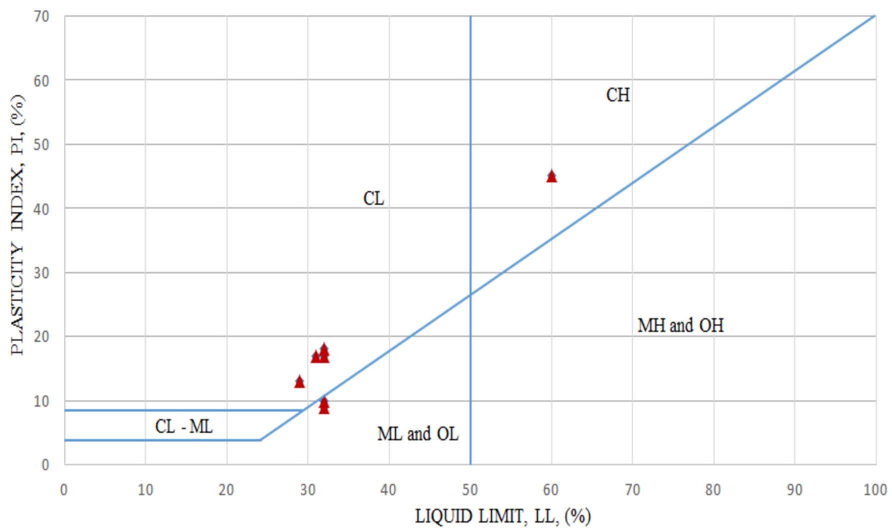

Figure A.27. Plasticity chart for BSSK-685A

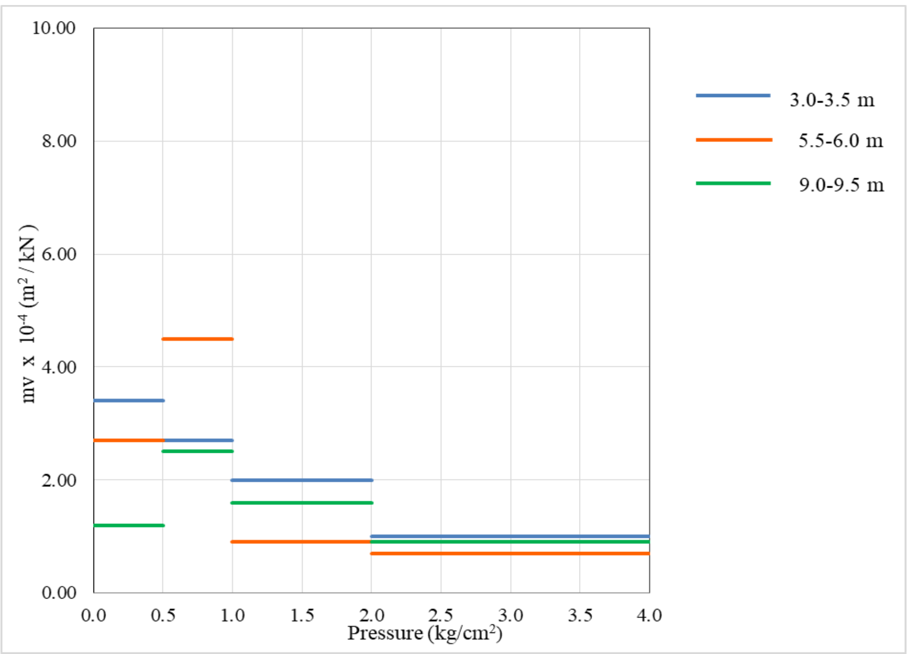

Figure A.28. The coefficient of volume compressibility (m_v) chart for BSSK-685A

Plasticity and coefficient of volume compressibility charts for KM: 151+220 are presented in Figure A.29 and A.30.

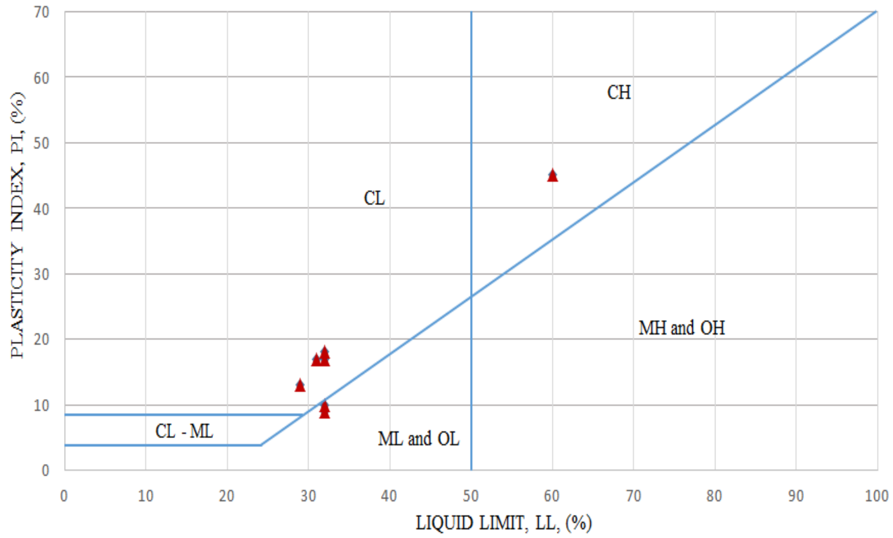

Figure A.29. Plasticity chart for BSSK-463

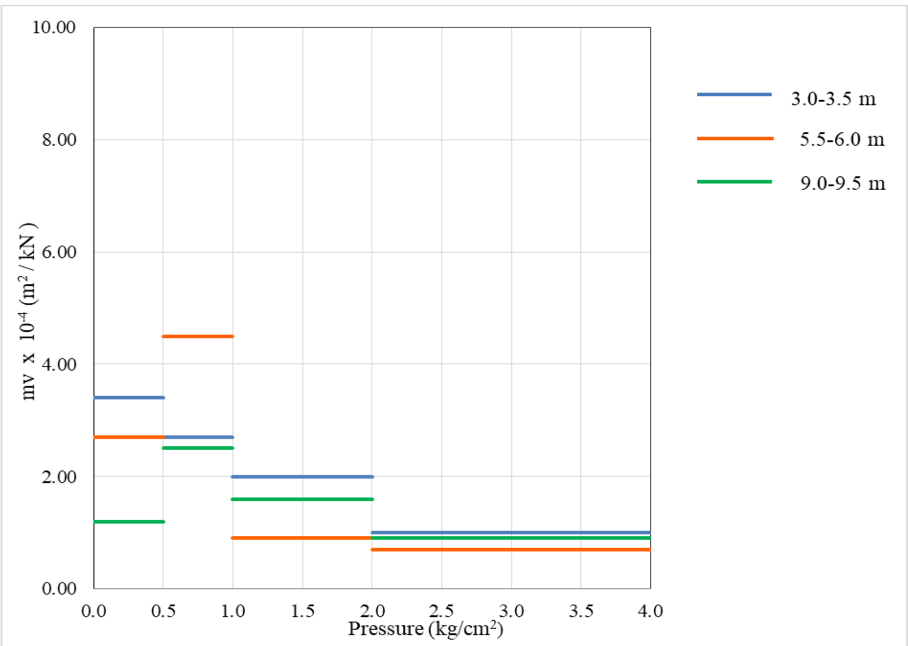

Figure A.30. The coefficient of volume compressibility (m_v) chart for BSSK-463

Plasticity and coefficient of volume compressibility charts for KM: 151+975 are presented in Figure A.31 and A.32.

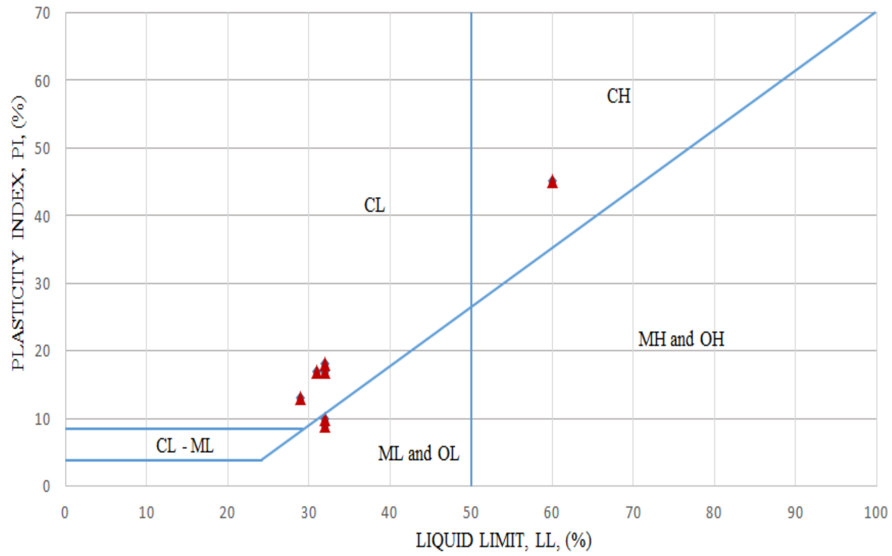

Figure A.31. Plasticity chart for BSSK-464

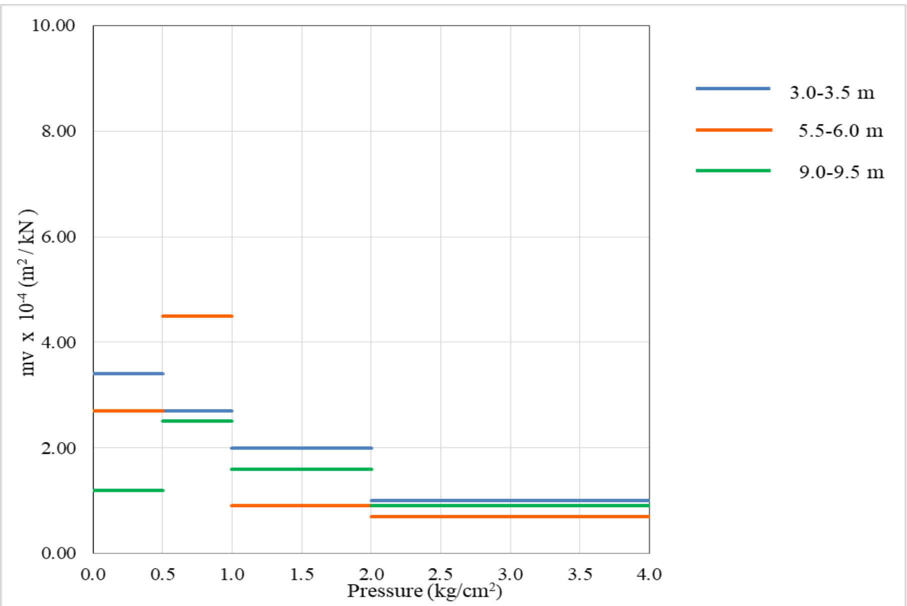

Figure A.32. The coefficient of volume compressibility (m_v) chart for BSSK-464

Plasticity and coefficient of volume compressibility charts for KM: 152+000 are presented in Figure A.33 and A.34.

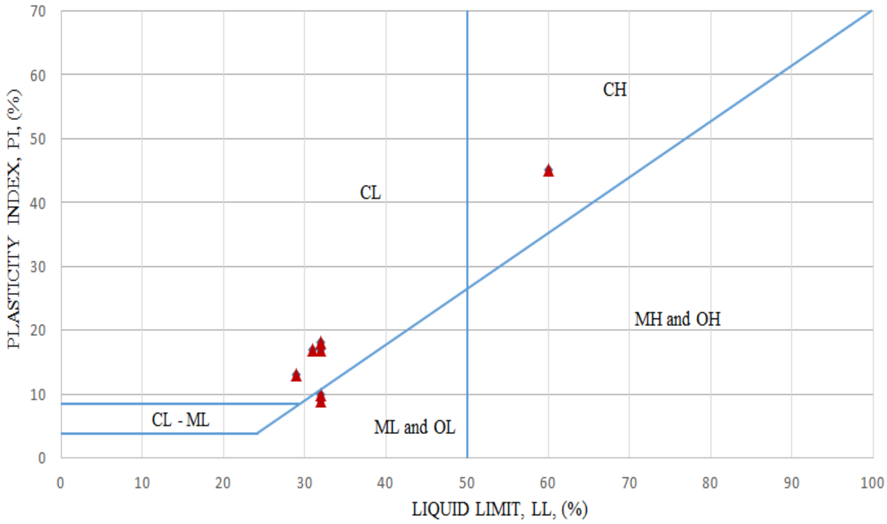

Figure A.33. Plasticity chart for BSSK-464

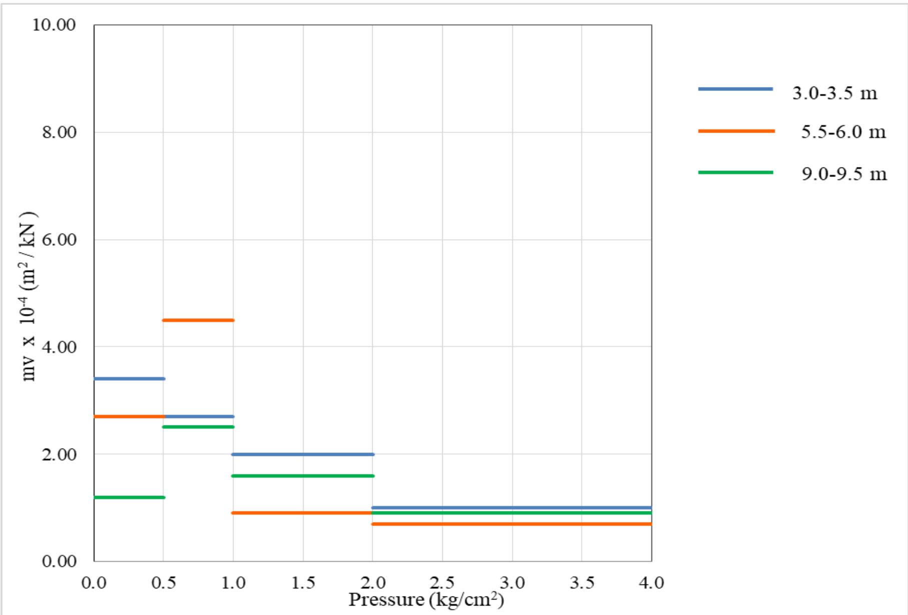

Figure A.34. The coefficient of volume compressibility (m_v) chart for BSSK-464

Plasticity and coefficient of volume compressibility charts for KM: 154+500 are presented in Figure A.35, A.36 and A.37.

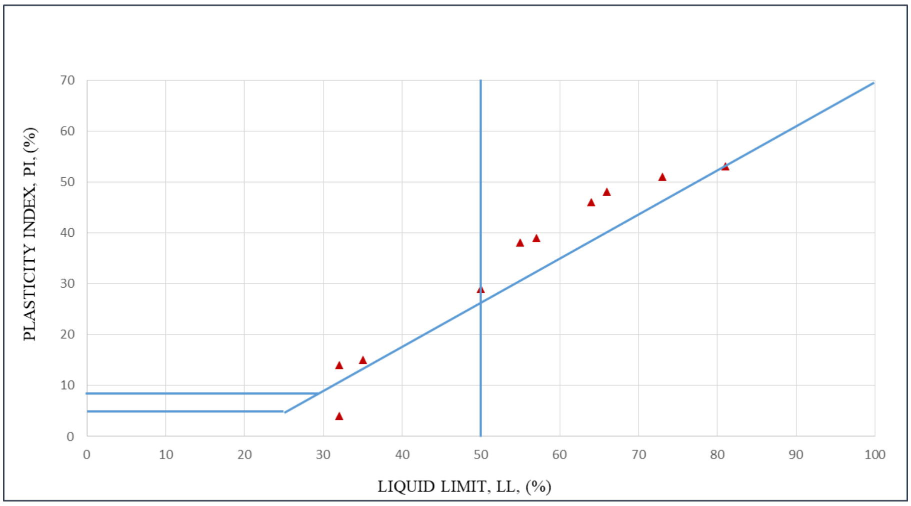

Figure A.35. Plasticity chart for BSSK-468, BSSK-469, BSSK-688

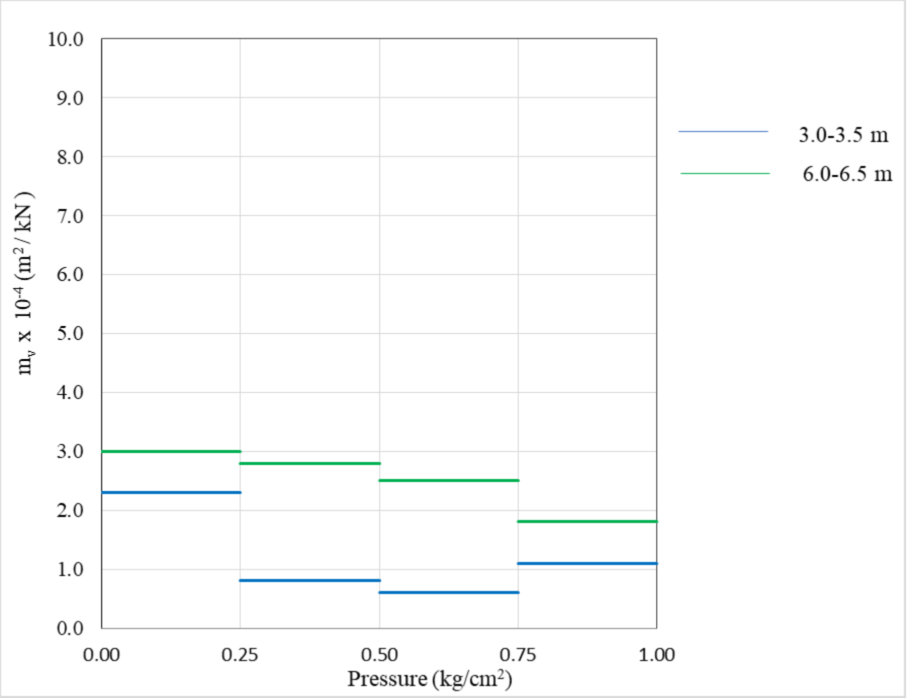

Figure A.36. The coefficient of volume compressibility (m_v) chart for BSSK-468

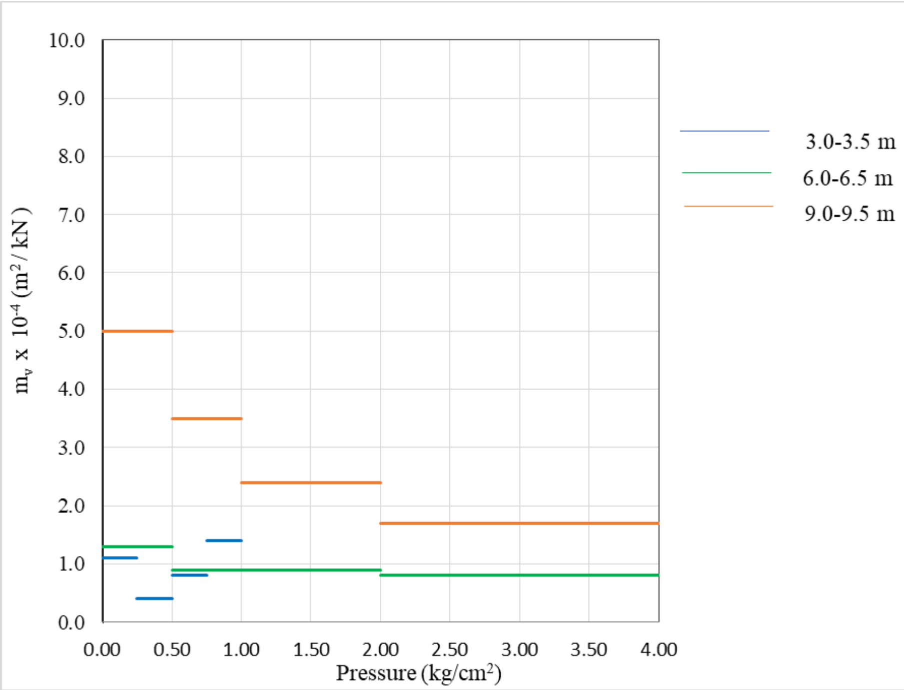

Figure A.37. The coefficient of volume compressibility (mv) chart for BSSK-469

Plasticity and coefficient of volume compressibility charts for KM: 155+000 are presented in Figure A.38 and A.39.

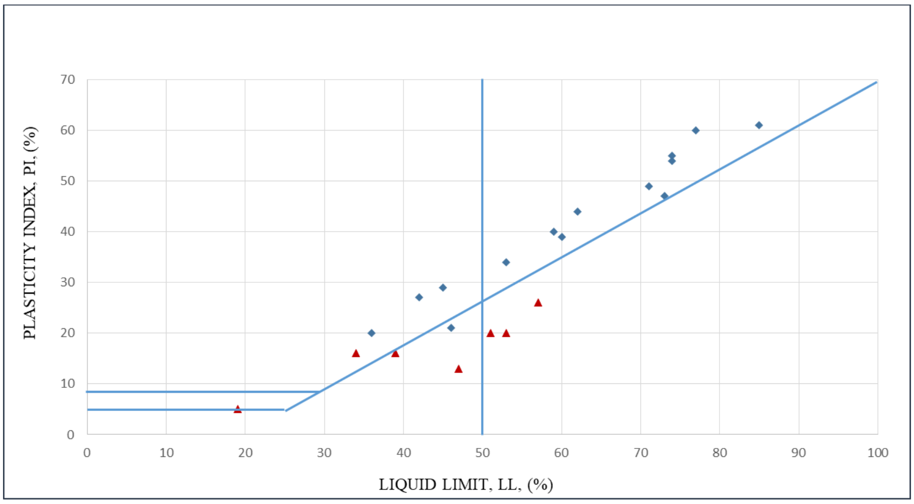

Figure A.38. Plasticity chart for BSSK-470, BSSK-689

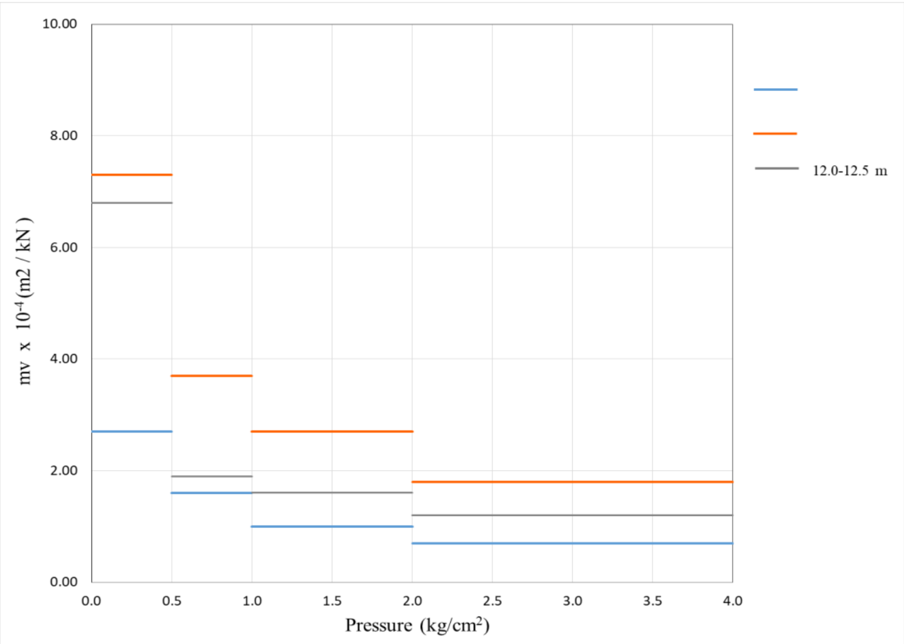

Figure A.39. The coefficient of volume compressibility (m_v) chart for BSSK-470

Plasticity and coefficient of volume compressibility charts for KM: 155+551 are presented in Figure A.40 and A.41.

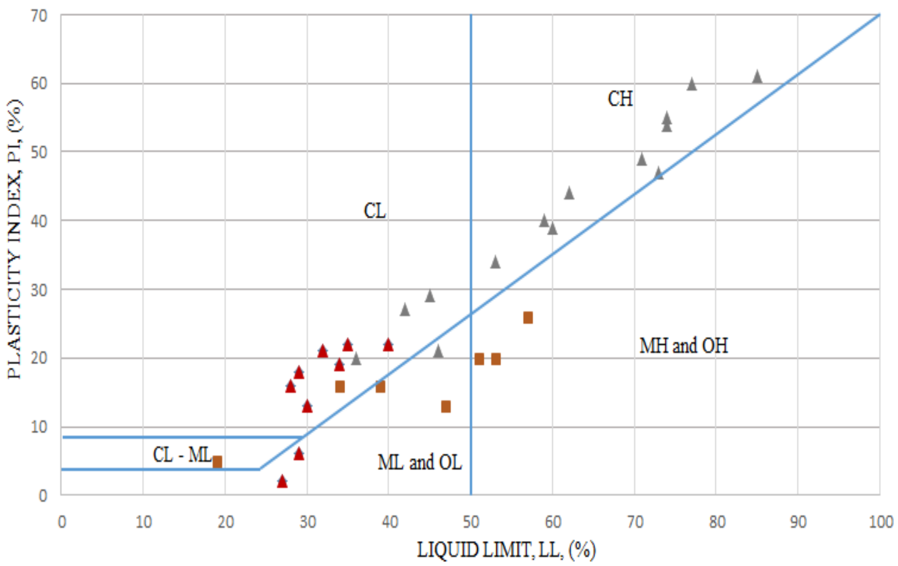

Figure A.40. Plasticity chart for BSSK-471

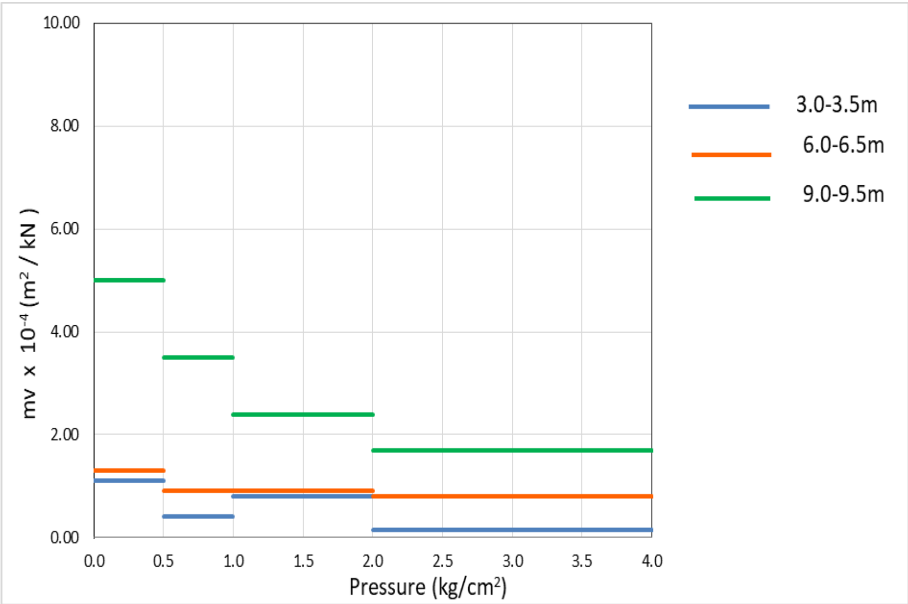

Figure A.41. The coefficient of volume compressibility (m_v) chart for BSSK-471

Plasticity and coefficient of volume compressibility charts for KM: 157+400 are presented in Figure A.42 and A.43.

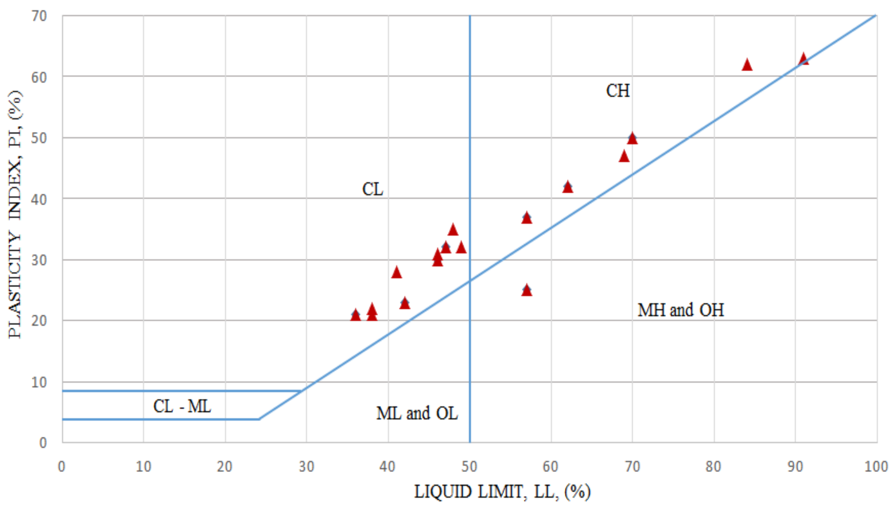

Figure A.42. Plasticity chart for BSSK-474

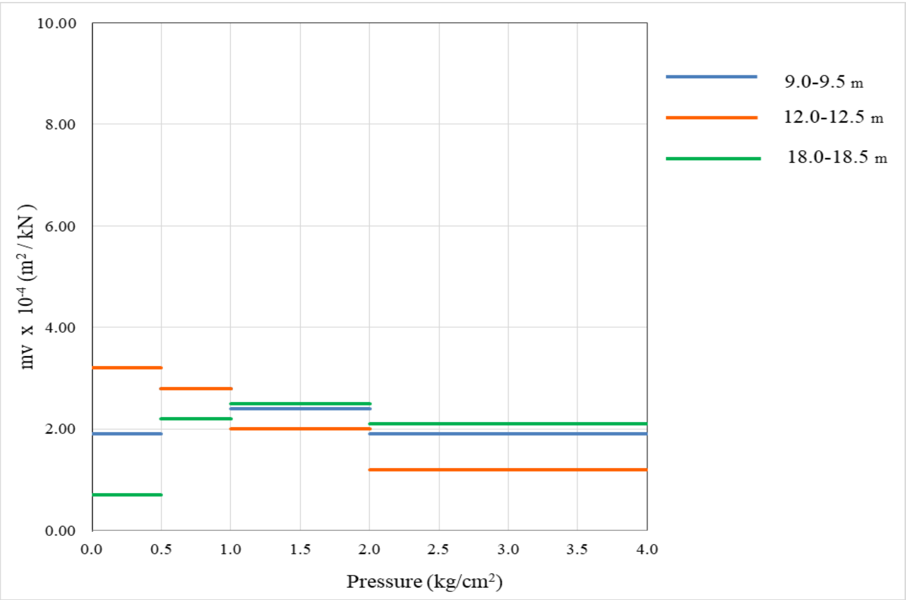

Figure A.43. The coefficient of volume compressibility (m_v) chart for BSSK-474

Plasticity and coefficient of volume compressibility charts for KM: 158+000 are presented in Figure A.44 and A.45.

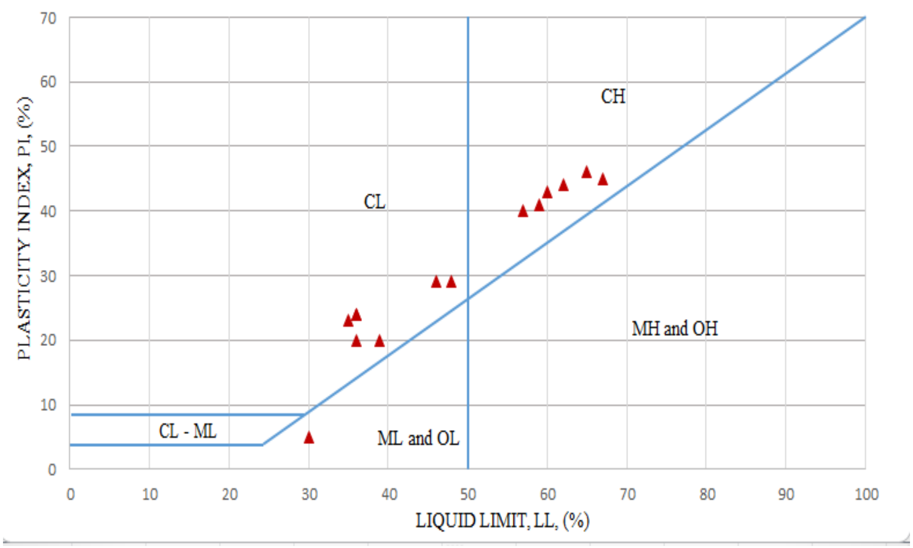

Figure A.44. Plasticity chart for BSSK-475

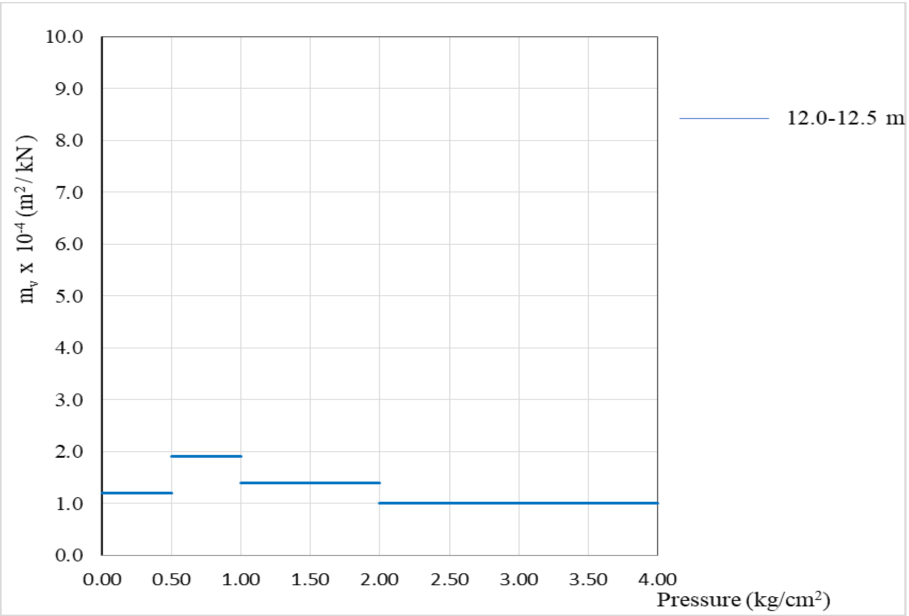

Figure A.45. The coefficient of volume compressibility (m_v) chart for BSSK-475

Plasticity and coefficient of volume compressibility charts for KM: 159+565 are presented in Figure A.46 and A.47.

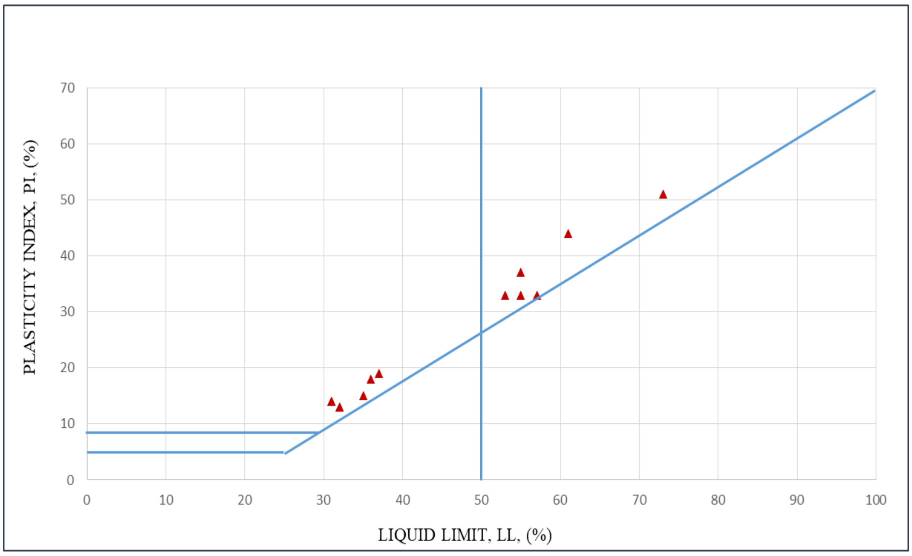

Figure A.46. Plasticity chart for BSSK-477

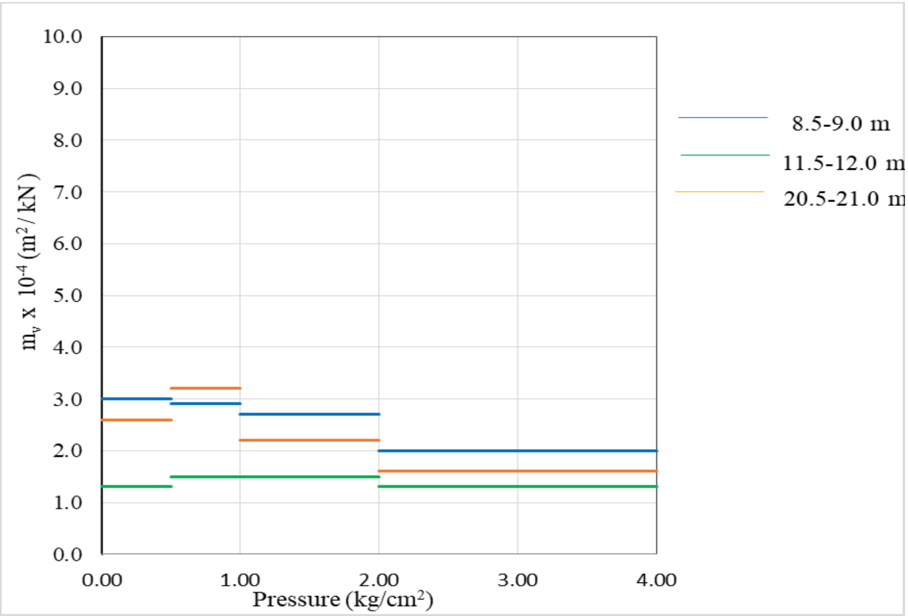

Figure A.47. The coefficient of volume compressibility (m_v) chart for BSSK-477

Plasticity and coefficient of volume compressibility charts for KM: 161+764 are presented in Figure A.48 and A.49.

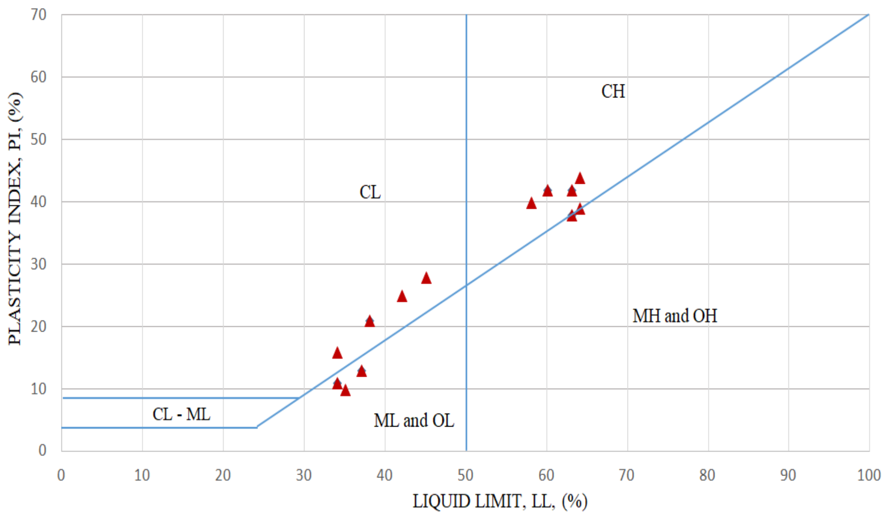

Figure A.48. Plasticity chart for BSSK-478

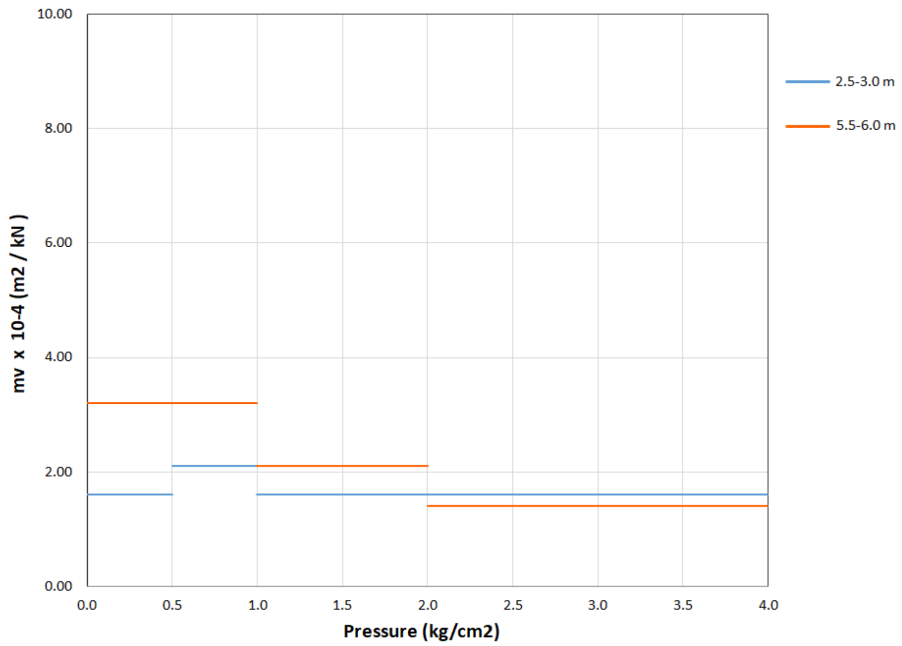

Figure A.49. The coefficient of volume compressibility (m_v) chart for BSSK-478

Plasticity and coefficient of volume compressibility charts for KM: 162+555 are presented in Figure A.50 and A.51.

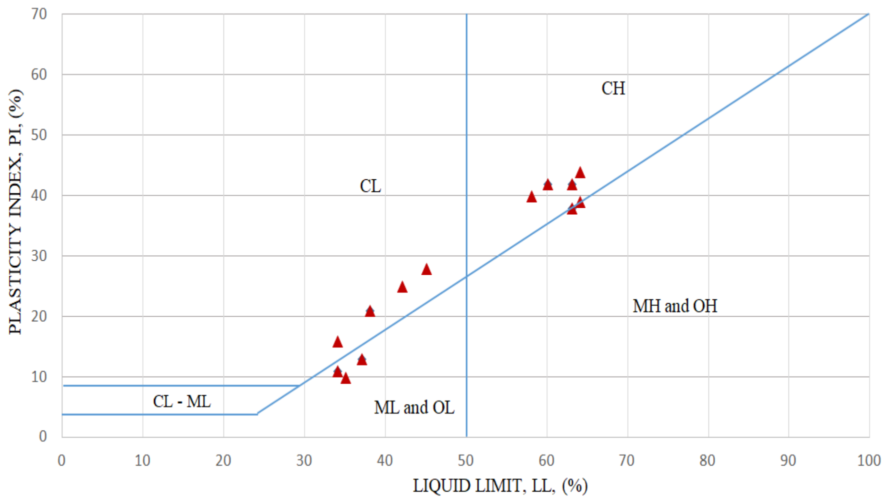

Figure A.50. Plasticity chart for BSSK-481

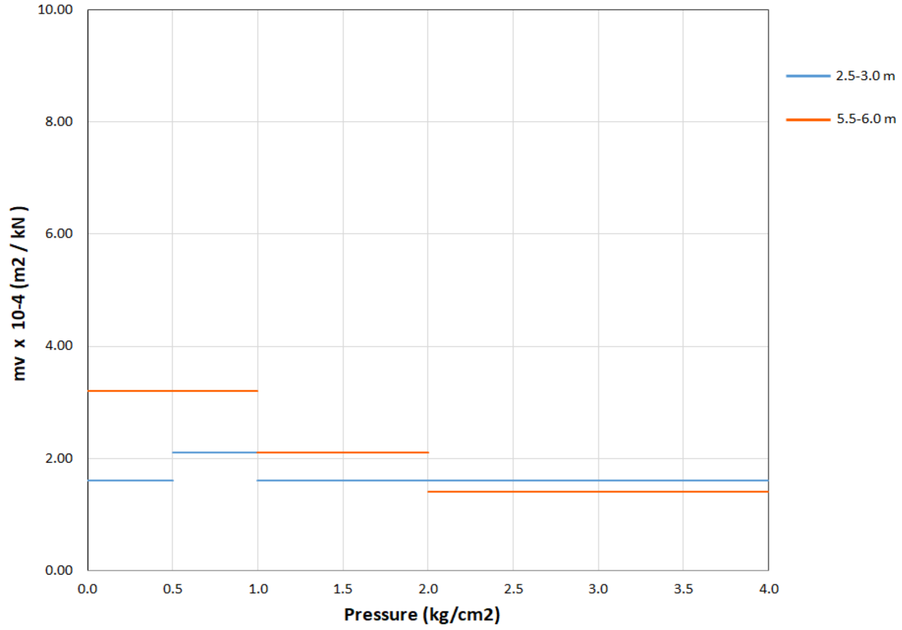

Figure A.51. The coefficient of volume compressibility (m_v) chart for BSSK-481

Plasticity and coefficient of volume compressibility charts for KM: 163+000 are presented in Figure A.52 and A.53.

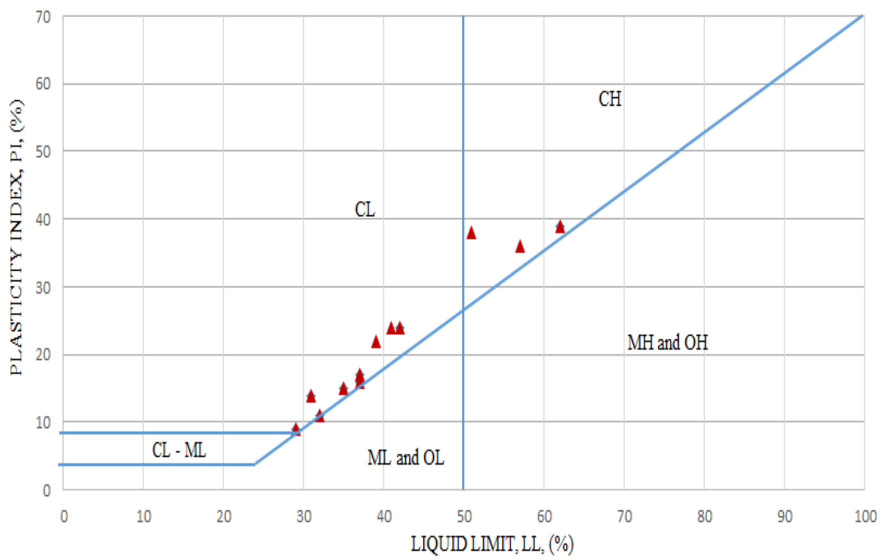

Figure A.52. Plasticity chart for BSSK-482

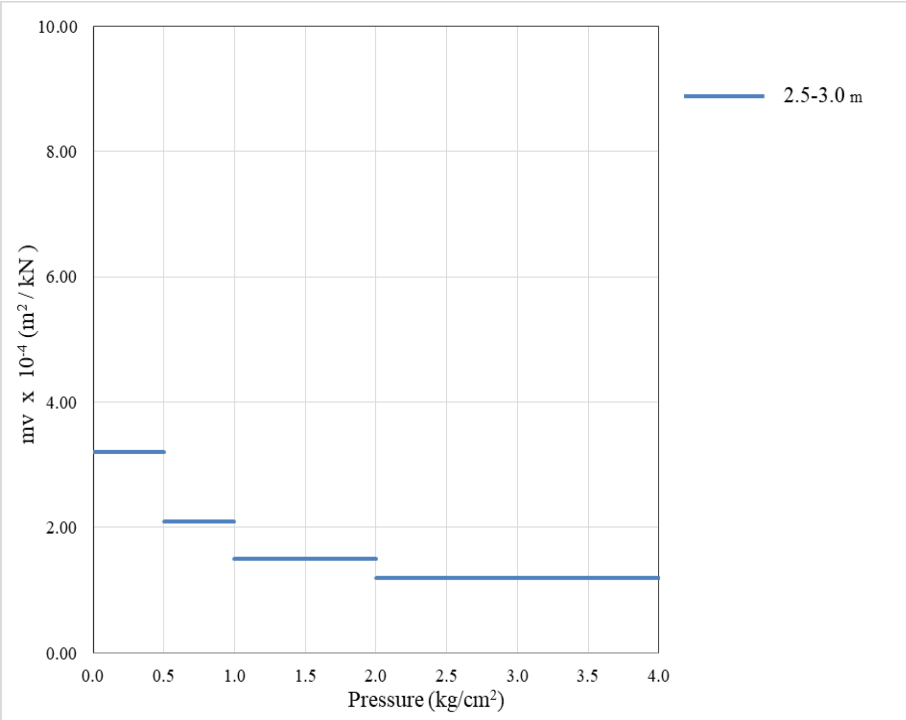

Figure A.53. The coefficient of volume compressibility (m_v) chart for BSSK-482

B. SPT N Data

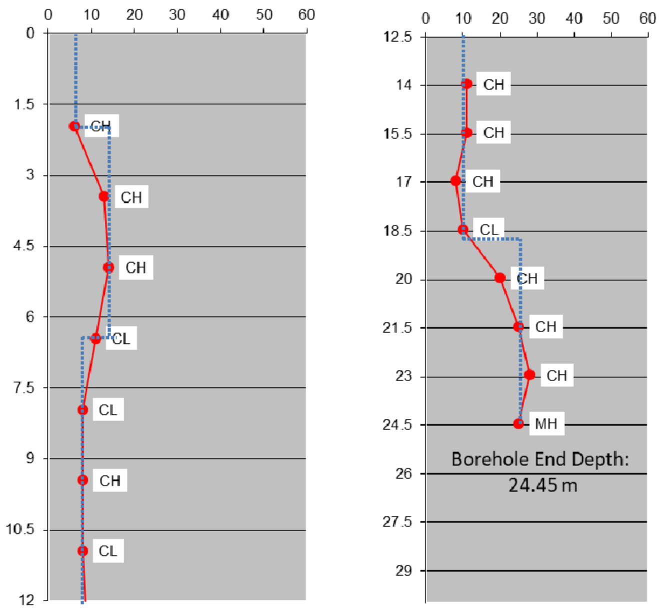

Figure B. 1. SPT N vs. Depth (m) graph for BSSK-447

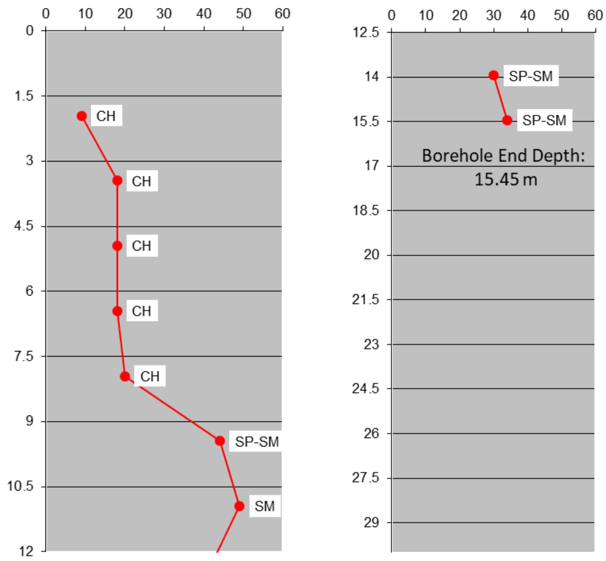

Figure B. 2. SPT N vs. Depth (m) graph for BSSK-451

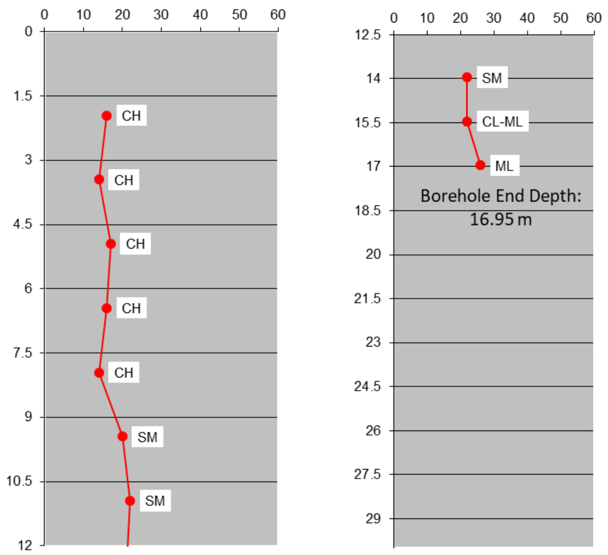

Figure B. 3. SPT N vs. Depth (m) graph for BSSK-452

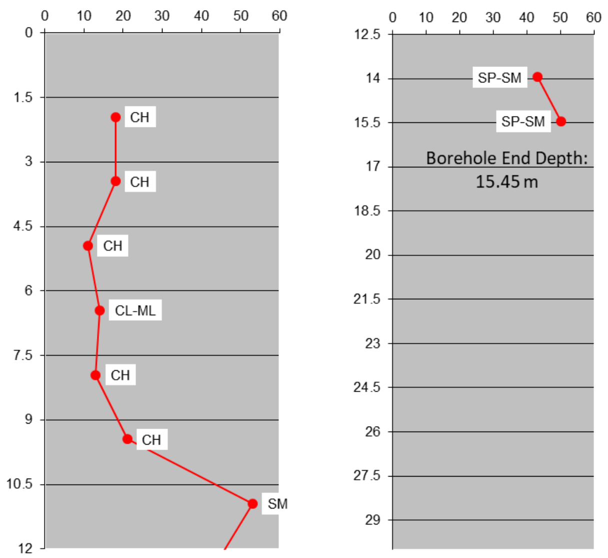

Figure B. 4. SPT N vs. Depth (m) graph for BSSK-453

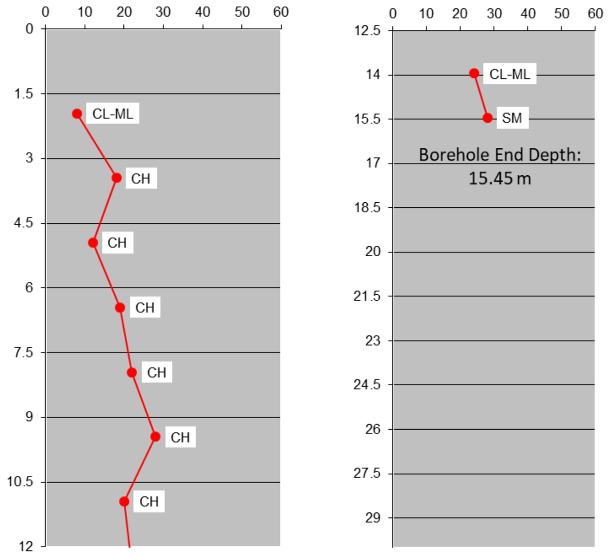

Figure B. 5. SPT N vs. Depth (m) graph for BSSK-454

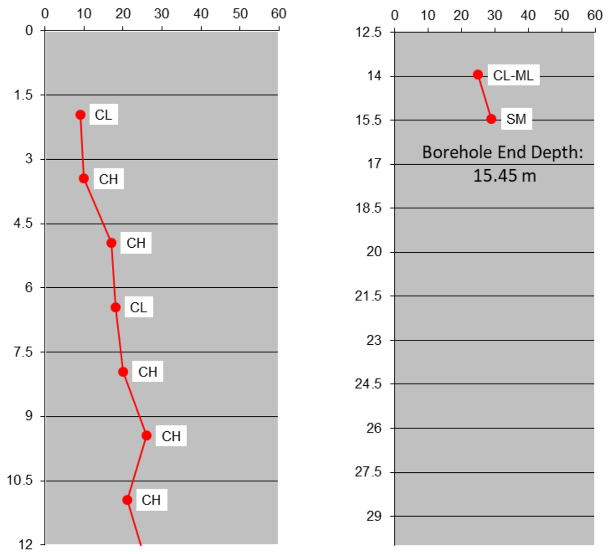

Figure B. 6. SPT N vs. Depth (m) graph for BSSK-456

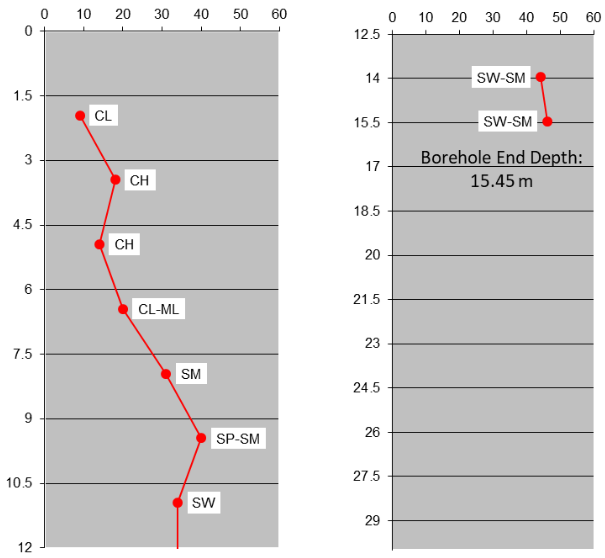

Figure B. 7. SPT N vs. Depth (m) graph for BSSK-457

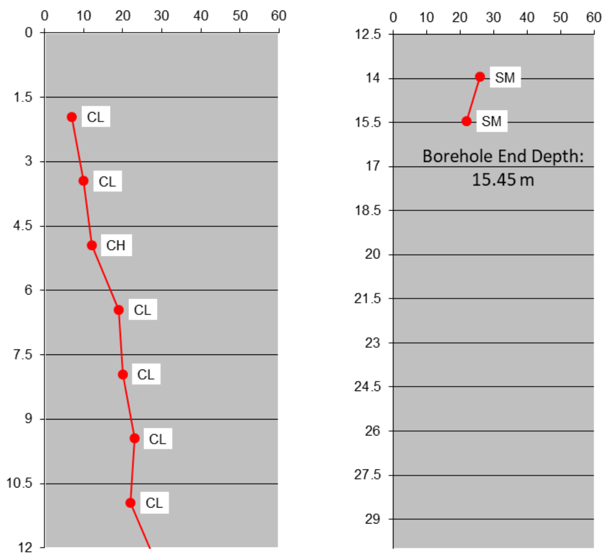

Figure B. 8. SPT N vs. Depth (m) graph for BSSK-458

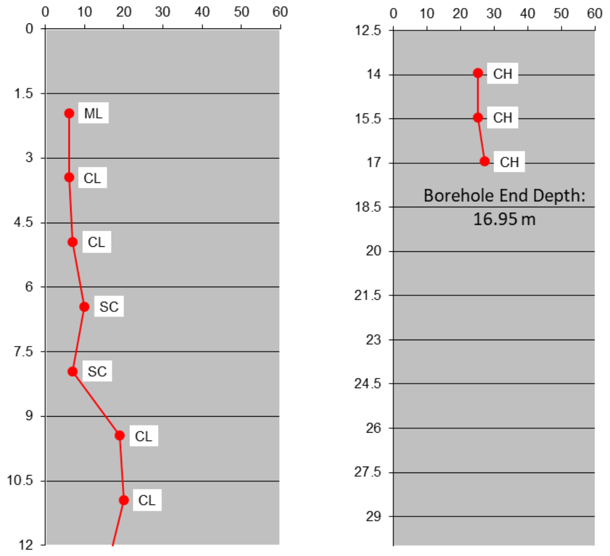

Figure B. 9. SPT N vs. Depth (m) graph for BSSK-461

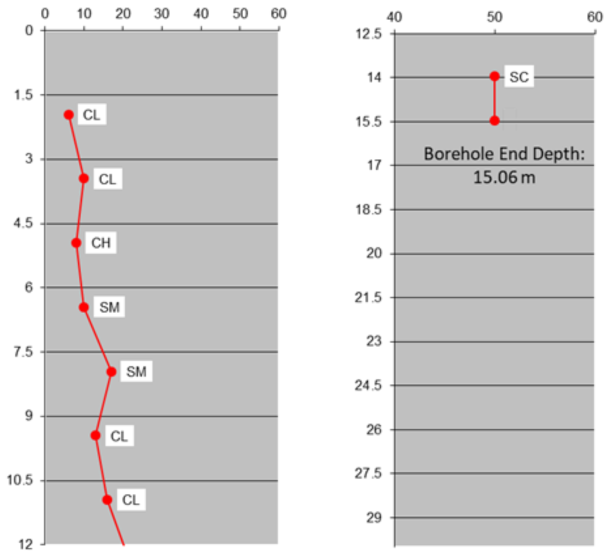

Figure B. 10. SPT N vs. Depth (m) graph for BSSK-463

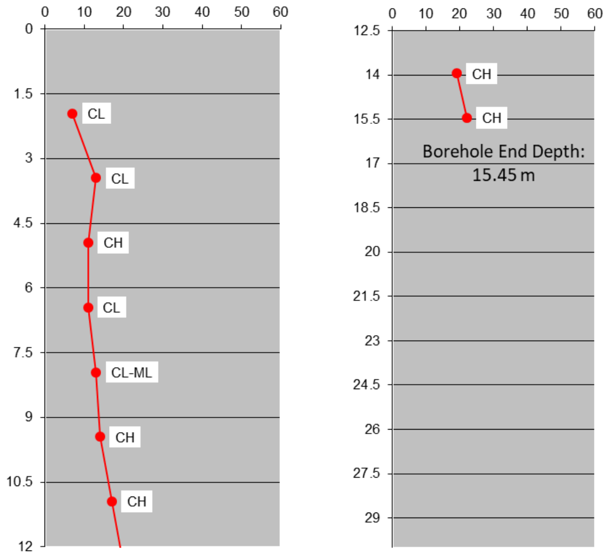

Figure B. 11. SPT N vs. Depth (m) graph for BSSK-464

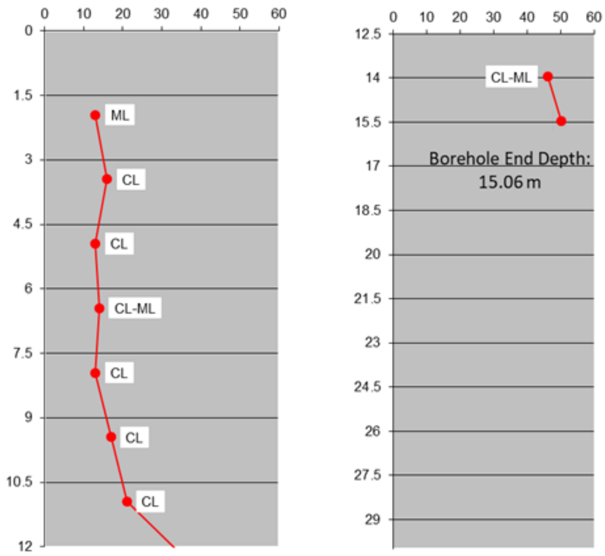

Figure B. 12. SPT N vs. Depth (m) graph for BSSK-469

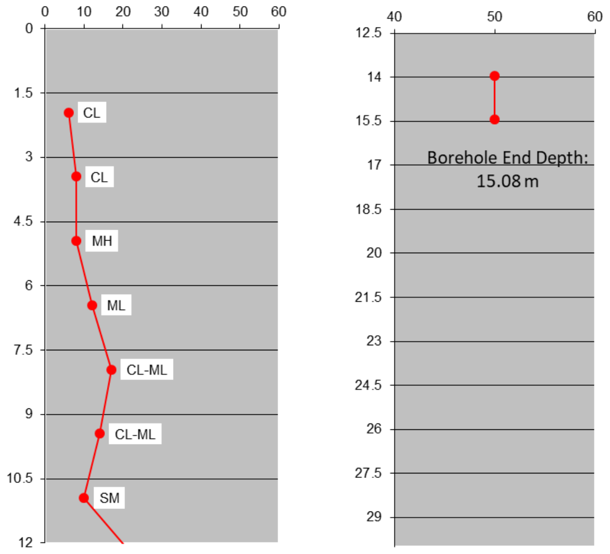

Figure B. 13. SPT N vs. Depth (m) graph for BSSK-470

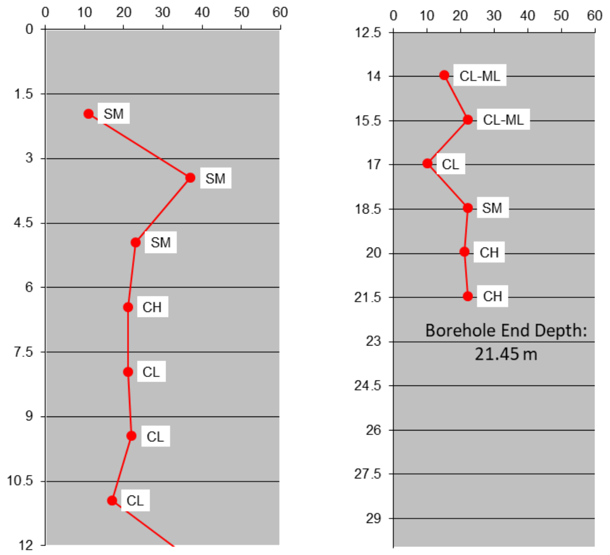

Figure B. 14. SPT N vs. Depth (m) graph for BSSK-471

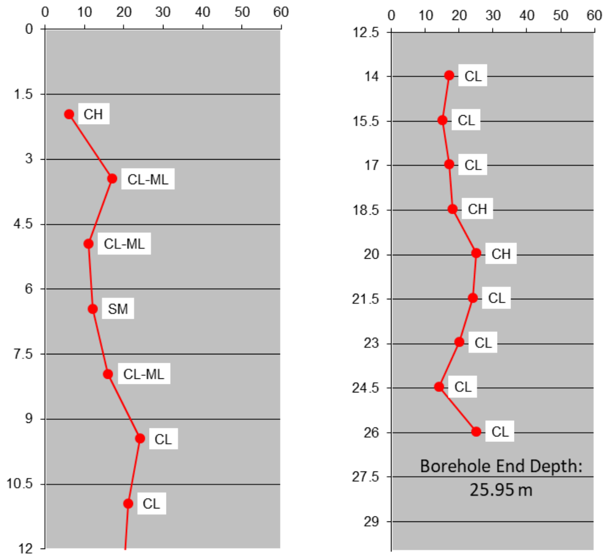

Figure B. 15. SPT N vs. Depth (m) graph for BSSK-474

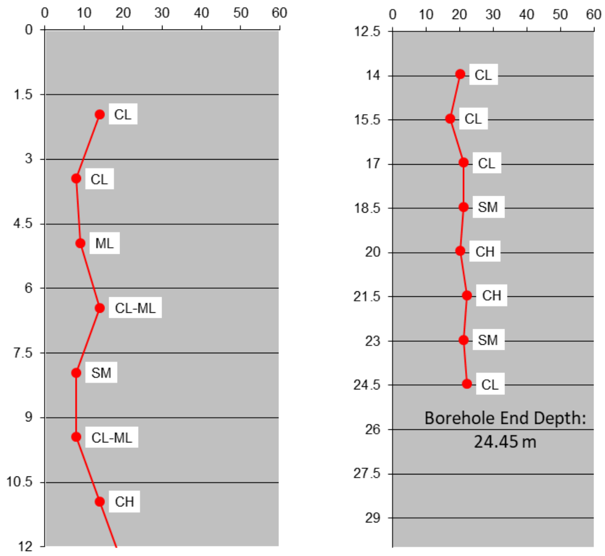

Figure B. 16. SPT N vs. Depth (m) graph for BSSK-475

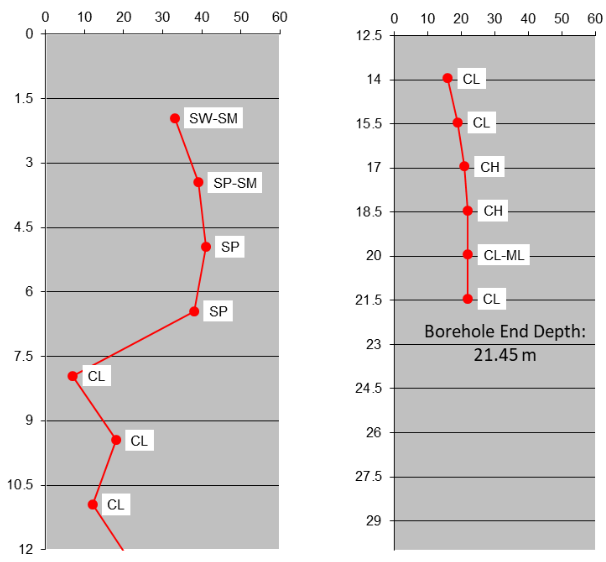

Figure B. 17. SPT N vs. Depth (m) graph for BSSK-477

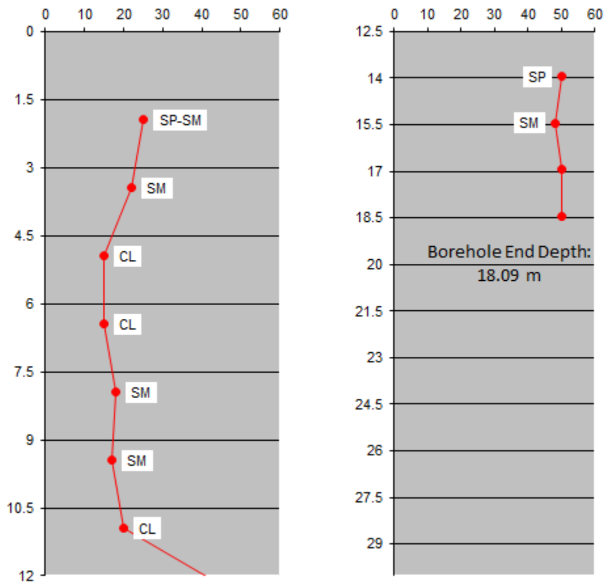

Figure B. 18. SPT N vs. Depth (m) graph for BSSK-480

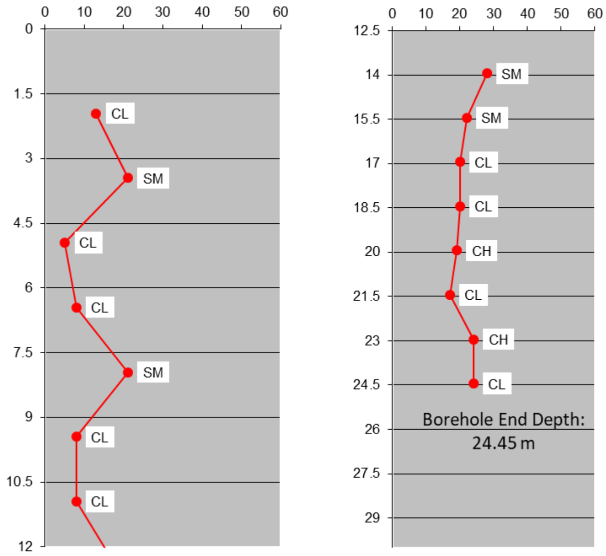

Figure B. 19. SPT N vs. Depth (m) graph for BSSK-481

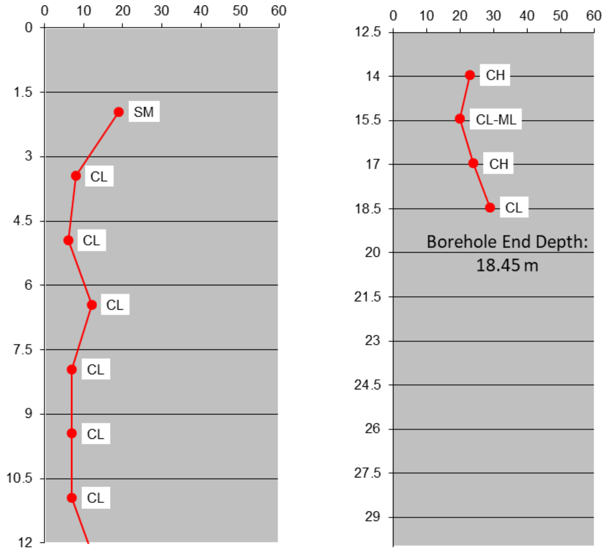

Figure B. 20. SPT N vs. Depth (m) graph for BSSK-482

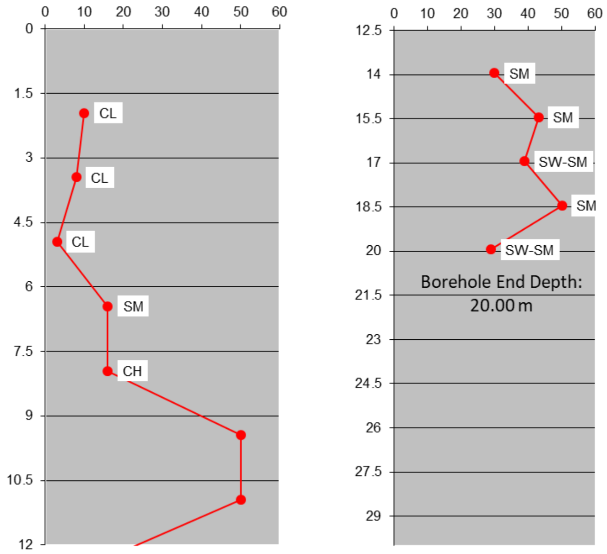

Figure B. 21. SPT N vs. Depth (m) graph for BSSK-685A

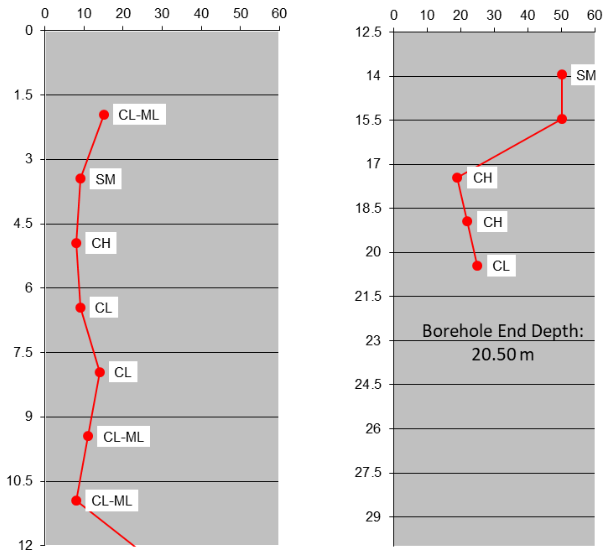

Figure B. 22. SPT N vs. Depth (m) graph for BSSK-688

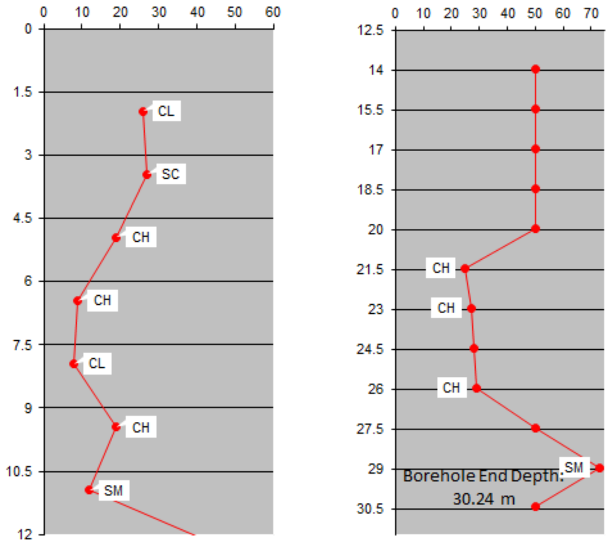

Figure B. 23. SPT N vs. Depth (m) graph for BSSK-689

C. Consolidation Calculation from Oedometer Data

C.1 KM: 139+764 Section

The embankment height: 8.8 m

Total consolidation: 101.52 cm

Table C. 1. Consolidation settlement parameters for Km: 139+764

Depth (m)	Thickness of layer (m)	z (m)	Unit weight of soil (kN/m^3)	σ_0 (kPa)	C_c (Lab. Result)	C_r (Lab. Result)	$(1+e_0)$ (Lab. Result)	m_v (m^2/kN) (Lab)	$\Delta\sigma$ (kPa)	$\sigma_1 = \sigma_0+\Delta\sigma$
2.00	2.00	1.00	18.00	8.2	0.120	0.050	1.36	0.0002932	182.2	190.4
4.00	2.00	3.00	18.00	24.6	0.120	0.050	1.36	0.0002984	176.4	201.0
6.00	2.00	5.00	18.00	41.0	0.120	0.050	1.36	0.0002954	170.3	211.2
8.00	2.00	7.00	18.00	57.3	0.120	0.050	1.36	0.0002897	163.9	221.2
10.00	2.00	9.00	18.00	73.7	0.120	0.050	1.36	0.0002802	157.2	230.9
12.00	2.00	11.00	18.00	90.1	0.120	0.050	1.36	0.0002699	150.2	240.3
14.00	2.00	13.00	18.00	106.5	0.120	0.050	1.36	0.0002585	142.9	249.4
16.00	2.00	15.00	18.00	122.9	0.120	0.050	1.36	0.0002457	135.4	258.2
18.00	2.00	17.00	18.00	139.2	0.120	0.050	1.36	0.0002313	127.6	266.8
20.00	2.00	19.00	18.00	155.6	0.120	0.050	1.36	0.0002148	119.5	275.2
22.00	2.00	21.00	18.00	172.0	0.120	0.050	1.36	0.0001957	111.3	283.2
24.00	2.00	23.00	18.00	188.4	0.120	0.050	1.36	0.0001731	102.7	291.1
26.00	2.00	25.00	18.00	204.8	0.100	0.020	1.36	0.0001055	94.0	298.7
28.00	2.00	27.00	18.00	221.1	0.100	0.020	1.36	0.0001057	85.0	306.1
30.00	2.00	29.00	18.00	237.5	0.100	0.020	1.36	0.0001059	75.8	313.3
32.00	2.00	31.00	18.00	253.9	0.100	0.020	1.36	0.0001061	66.4	320.3
34.00	2.00	33.00	18.00	270.3	0.100	0.020	1.36	0.0001062	56.8	327.1
36.00	2.00	35.00	18.00	286.7	0.100	0.020	1.36	0.0001064	47.0	333.7
38.00	2.00	37.00	18.00	303.0	0.100	0.020	1.36	0.0001066	37.0	340.0
40.00	2.00	39.00	18.00	319.4	0.100	0.020	1.36	0.0001068	26.8	346.2
42.00	2.00	41.00	18.00	335.8	0.100	0.020	1.36	0.0001070	16.5	352.2
44.00	2.00	43.00	18.00	352.2	0.100	0.020	1.36	0.0001072	5.9	358.1
44.11	1.00	44.05	18.00	360.8	0.100	0.020	1.36	0.0001073	0.3	361.1

Table C. 2. Consolidation settlement calculation for Km: 139+764

Depth (m)	Thickness of layer (m)	Consolidation settlement of layer (S) (m)	Cumulative consolidation settlement (Sc) (cm) (by C_c values)	Consolidation settlement of layer (S) (m)	Cumulative consolidation settlement (Sc) (cm) (by m_v values)
2.00	2.00	0.13 m	12.93 cm	0.11 m	10.69 cm
4.00	2.00	0.10 m	22.76 cm	0.11 m	21.21 cm
6.00	2.00	0.09 m	31.34 cm	0.10 m	31.27 cm
8.00	2.00	0.08 m	39.20 cm	0.09 m	40.77 cm
10.00	2.00	0.07 m	46.59 cm	0.09 m	49.58 cm
12.00	2.00	0.04 m	51.01 cm	0.08 m	57.68 cm
14.00	2.00	0.04 m	55.19 cm	0.07 m	65.07 cm
16.00	2.00	0.04 m	59.17 cm	0.07 m	71.72 cm
18.00	2.00	0.04 m	63.01 cm	0.06 m	77.63 cm
20.00	2.00	0.04 m	66.73 cm	0.05 m	82.76 cm
22.00	2.00	0.04 m	70.35 cm	0.04 m	87.12 cm
24.00	2.00	0.03 m	73.68 cm	0.04 m	90.68 cm
26.00	2.00	0.02 m	76.09 cm	0.02 m	92.66 cm
28.00	2.00	0.02 m	78.17 cm	0.02 m	94.46 cm
30.00	2.00	0.02 m	79.94 cm	0.02 m	96.06 cm
32.00	2.00	0.01 m	81.43 cm	0.01 m	97.47 cm
34.00	2.00	0.01 m	82.64 cm	0.01 m	98.68 cm
36.00	2.00	0.01 m	83.61 cm	0.01 m	99.68 cm
38.00	2.00	0.01 m	84.35 cm	0.01 m	100.47 cm
40.00	2.00	0.01 m	84.86 cm	0.01 m	101.04 cm
42.00	2.00	0.00 m	85.17 cm	0.00 m	101.39 cm
44.00	2.00	0.00 m	85.28 cm	0.00 m	101.52 cm
44.11	1.00	0.00 m	85.28 cm	0.00 m	101.52 cm

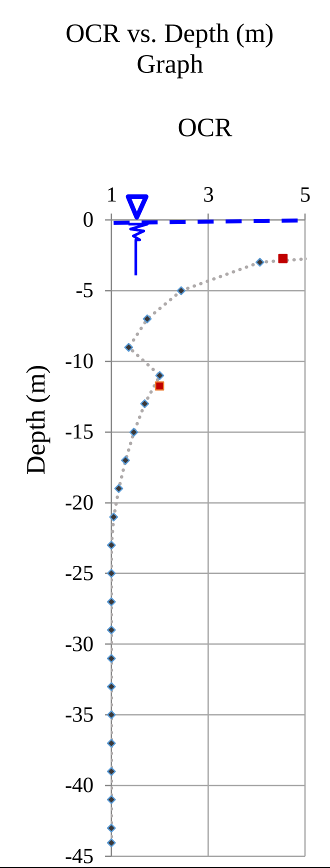

Detailed consolidation calculations of Station 1 for the depth of 0.0 m and 2.0 m:

Stress calculation in ground depth is performed by Marston Type Analysis presented by Charles (1996):

$$\frac{\sigma_v}{q} = \frac{1}{n\cdot f}\left\{1-\left[(1-n\cdot f)\exp\left(\frac{-z\cdot f}{b^*}\right)\right]\right\} \qquad \text{(Eq. C.1)}$$

where;

$$q\ (the\ vertical\ stress\ applied\ over\ the\ loaded\ area) = \gamma_s \cdot h \qquad \text{(Eq. C.2)}$$

$$n\ (load\ intensity\ ratio) = {}^{\gamma_s \cdot h}/_{\gamma' \cdot b^*} \qquad \text{(Eq. C.3)}$$

$$b^* = 2 \cdot b\ for\ strip\ footing \qquad \text{(Eq. C.4)}$$

$$f = 4 \cdot \mu \cdot K \qquad \text{(Eq. C.5)}$$

$$\mu \cdot K = tan\phi'(1 - sin\phi') \qquad \text{(Eq. C.6)}$$

$$\sigma_0 = \gamma' \cdot z \qquad \text{(Eq. C.7)}$$

$$\sigma_1 = \sigma_0 + \sigma_v \qquad \text{(Eq. C.8)}$$

γ : unit weight of the loaded soil

γ' : effective unit weight of the loaded soil

γ_s : unit weight of the fill

h : surcharge height

b : width of embankment platform

ϕ' : soil friction angle

z : vertical stress in the ground depth

Embankment height= 8.80 m (4.5 m bank constructed from rock fill and 4.3 m road fill)

$$Unit\ weight\ of\ road\ fill = 20\ {}^{kN}/_{m^3}$$

$$Unit\ weight\ of\ rock\ fill = 22\ {}^{kN}/_{m^3}$$

From Eq. C.4, b^* is calculated as:

$$b^* = 2 \cdot 37.5\ m = 75\ m$$

From Eq. C.2, weight of embankment is calculated as:

$$Weight\ of\ embankment\ fill = 4.5\ m \cdot\ 22\ {}^{kN}/_{m^3} + 4.3\ m \cdot 20\, {}^{kN}/_{m^3} = 185\ kPa$$

Load intensity ratio is calculated from Eq. C.3 as:

$$n = \frac{4.5\ m \cdot\ 22\ {}^{kN}/_{m^3} + 4.3\ m \cdot 20\, {}^{kN}/_{m^3}}{(18 - 9.81)\, {}^{kN}/_{m^3} \cdot 75\ m} = 0.301$$

From Eq. C.5, f is calculated as:

$$f = 4 \cdot tan27°(1 - sin27°) = 1.113$$

Stress at depth of 1.0 m is calculated from Eq. C.1 as:

$$\sigma_v = \frac{185}{0.301 \cdot 1.113}\left\{1 - \left[(1 - 0.301 \cdot 1.113)\exp\left(\frac{-1.0\ m \cdot 1.113}{75\ m}\right)\right]\right\} - 1\ m \cdot \left(18\ {}^{kN}/{}_{m^3} - 9.81\ {}^{kN}/{}_{m^3}\right) = 182.215\ kPa$$

Consolidation calculation in depth of interval 0.0 m and 2.0 m:

Thickness of layer: 2.0 m

Middle depth of layer (z): 1.0 m

Depth of groundwater: Surface (0.0 m)

Unit weight of soil: 18.0 kN/m^3

σ_0 and σ_1 are calculated at 1.0 m depth:

$$\sigma_0 = (18 - 9.81)\ {}^{kN}/{}_{m^3} * 1.0\ m = 8.2\ kPa$$

$$\sigma_1 = 8.2\ kPa + 182.2\ kPa = 190.4\ kPa$$

P_c is obtained from Figure C.1 as 100 kPa and coefficients of consolidation (C_c, C_r) are calculated from Eq. 2.3 as:

$$C_c = \frac{0.32-0.24}{\log(\frac{400}{90})} = 0.12, C_r = \frac{0.26-0.24}{\log(\frac{300}{100})} = 0.05$$

Since, $\sigma_0 < P_c < \sigma_0+\Delta\sigma$, Eq. 2.9 is used to calculate consolidation settlement in interval of 0.0 m and 2.0 m.

$$S = \frac{0.05*2.0\ m}{1+0.36} log \frac{100\ kPa}{8.2\ kPa} + \frac{0.12*2.0\ m}{1+0.36} log \frac{190.4\ kPa}{100\ kPa} = 0.1293\ m = 12.93\ cm$$

Coefficients of volume compressibility (m_v) is calculated from consolidation tests performed on UD1 sample. From Pressure (kPa) vs. Void Ratio (e) graph, for e_0 and e_1 are calculated for σ_0= 8.19 kPa and σ_1= 190.40 kPa as 35.89 (%) and 28.63 (%), respectively as:

$$e = \left(\frac{e_1-e_0}{\sigma_1-\sigma_0}\right)\sigma + e_0 \qquad \text{(Eq. C.9)}$$

For σ= 8.19 kPa,

$$e = \left(\frac{34.49-36.16}{49.91\ kPa-0}\right) 8.19\ kPa + 36.16 = 35.89\%$$

For σ= 190.40 kPa,

$$e = \left(\frac{28.24 - 32.41}{199.64\ kPa - 99.82\ kPa}\right)(190.40\ kPa - 99.82\ kPa) + 32.41 = 28.63\%$$

The coefficient of volume compressibility (m_v) is calculated from Eq. 2.2 as:

$$m_v = \frac{\Delta e}{\Delta\sigma(1 + e_0)} = \frac{0.3589 - 0.2863}{(190.40 - 8.19) * (1 + 0.3589)} = 0.000293 m^2/kN$$

Eq. 2.6 is used to calculate consolidation settlement from m_v for depth interval of 0.0 m and 2.0 m:

$$S_c = 0.000293\ {}^{m^2}/_{kN} * 182.215\ kPa * 2.0\ m = 0.1069\ m = 10.69\ cm$$

Table C. 3. BSSK 447 UD1 Consolidation test result of Km: 139+764

ZEMAR ZMR.COM.TR

Zemar Zemin Araştırma ve Mühendislik | Jeoloji - Jeofizik - Jeoteknik Hizmetler

KONSOLİDASYON DENEYİ SONUÇLARI / *CONSOLIDATION TEST RESULTS*

Müşteri Adı / *Customer's Name*	YÜKSEL DOMANİÇ MÜHENDİSLİK LTD.	Laboratuvar No / *Laboratory No*	13-179kon1	Num.Kabul Tarihi / *Date of Samp. Accept*	26.12.2012
Num.Alındığı Yer / *Project/Location*	Gebze-Orhangazi-İzmir (İzmit Körfez Geçişi ve Bağlantı Yolları Dahil) Otoyolu A.G.+Dolgu 24.45 m / Km: 139+670			Deney Tarihi / *Date of Test*	05.01.2013
Sondaj-Num. No / *Boring\Sample No*	BSSK447 / UD1	Derinlik (m) / *Depth*	2.50-3.00	Deney Rapor Tarihi / *Date of Test Result*	07.02.2013

Çap (cm): *Diameter*	5.00	Alan (cm^2): *Area*	19.63	Yaş Ağırlık (g): *Wet Weight*	75.85	Özgül Ağırlık: *Specific Gravity*	2.63
Boy (cm): *Lenght*	2.00	Hacim (cm^3): *Volume*	39.27	Su Muhtevası (%): *Water Content*	28.56	Ho (mm):	14.69

Basınç (σ) *Pressure (kPa)*	Oturma *Settlement* H(mm)	Hort (mm)	Boşluk Oranı *Void Ratio* e (%)	e_{ort}	Δe	Δσ	av m^2/kN	Mv m^2/kN	t90 s	Cv mm^2/s
0.00	0.00	20.00	36.16	0.36	0.00	0.00	0.00000	0.00000	0.00	0.00
49.91	0.25	19.88	34.49	0.35	0.02	49.91	0.00034	0.00025	240.00	0.35
99.82	0.55	19.60	32.41	0.33	0.02	49.91	0.00042	0.00031	6000.00	0.01
199.64	1.16	19.14	28.24	0.30	0.04	99.82	0.00042	0.00032	13500.00	0.01
399.29	1.75	18.54	24.27	0.26	0.04	199.64	0.00020	0.00016	8640.00	0.01
199.64	1.67	18.29	24.83	0.25	0.01	-199.64	-0.00003	-0.00002		
99.82	1.52	18.41	25.81	0.25	0.01	-99.82	-0.00010	-0.00008		
49.91	1.36	18.56	26.90	0.26	0.01	-49.91	-0.00022	-0.00017		

Mv=Hacimsel Sıkışma Katsayısı *Volume Change Coefficient* — av=Sıkışma Katsayısı *Compressibility Coefficient* — Cv= Konsolidasyon Katsayısı *Consolidation Coefficient* — t_{90} = Oturma Zamanı %90 *Settlement Time %90*

- Deneyler ilgili firma tarafından laboratuvarımıza teslim edilen numuneler üzerinde yapılmıştır. *Tests were done from the samples that are delivered by the related firm.*
- Bu deney TS 1900-2 standartlarına göre yapılmaktadır. *This test is being done according to the TS 1900-2 standarts.*
- Bu deney raporu Laboratuarımızın yazılı izni olmadan basılamaz ve çoğaltılamaz. *This tests results must not be reproduced in any form without the written permission of laboratory.*
- ZEMAR hologramları olmayan Deney Sonuç raporlarımız geçersizdir. Test result reports without a ZEMAR Hollogram are invalid.
- T.C.Bayındırlık ve İskan Bakanlığı logosu 16.06.2011 tarih ve 291 numaralı Laboratuvar İzin Belgesi kapsamında kullanılmaktadır. The Logo of T.R. The Ministry of Public Works and Settlement is used by Laboratory Permission Certificate dated 16.06.2011 and numbered 291.

Deneyi Yapan *Tested By*: Begüm Ağa, Jeoloji Mühendisi, Oda Sicil No: 16359

Onaylayan *Approved By*: Emre YILMAZ, Jeoloji Yük. Mühendisi, Denetçi Mühendis, Oda Sicil No.: 7733

Table C. 4. BSSK 447 UD3 Consolidation test result of Km: 139+764

ZEMAR ZMR.COM.TR

Zemar Zemin Araştırma ve Mühendislik | Jeoloji - Jeofizik - Jeoteknik Hizmetler

KONSOLİDASYON DENEYİ SONUÇLARI / *CONSOLIDATION TEST RESULTS*

Müşteri Adı / *Customer's Name*	YÜKSEL DOMANİÇ MÜHENDİSLİK LTD.	Laboratuvar No / *Laboratory No*	13-179kon2	Num.Kabul Tarihi / *Date of Samp. Accept*	26.12.2012
Num.Alındığı Yer / *Project/Location*	Gebze-Orhangazi-İzmir (İzmit Körfez Geçişi ve Bağlantı Yolları Dahil) Otoyolu A.G.+Dolgu 24.45 m / Km: 139+670			Deney Tarihi / *Date of Test*	05.01.2013
Sondaj-Num. No / *Boring\Sample No*	BSSK447 / UD3	Derinlik (m) / *Depth*	11.50-12.00	Deney Rapor Tarihi / *Date of Test Result*	07.02.2013

Çap (cm): *Diameter*	5.00	Alan (cm^2): *Area*	19.63	Yaş Ağırlık (g): *Wet Weight*	74.38	Özgül Ağırlık: *Specific Gravity*	2.57
Boy (cm): *Lenght*	2.00	Hacim (cm^3): *Volume*	39.27	Su Muhtevası (%): *Water Content*	22.52	Ho (mm):	14.74

Basınç (σ) *Pressure (kPa)*	Oturma *Settlement* H(mm)	Hort (mm)	Boşluk Oranı *Void Ratio* e (%)	e_{ort}	Δe	Δσ	av m^2/kN	Mv m^2/kN	t90 s	Cv mm^2/s
0.00	0.00	20.00	35.69	0.36	0.00	0.00	0.00000	0.00000	0.00	0.00
49.91	0.52	19.74	32.18	0.34	0.04	49.91	0.00070	0.00052	2160.00	0.04
99.82	0.65	19.42	31.28	0.32	0.01	49.91	0.00018	0.00014	240.00	0.33
199.64	0.82	19.27	30.14	0.31	0.01	99.82	0.00011	0.00009	540.00	0.15
399.29	1.22	18.98	27.40	0.29	0.03	199.64	0.00014	0.00011	6000.00	0.01
199.64	1.20	18.79	27.58	0.27	0.00	-199.64	-0.00001	-0.00001		
99.82	1.18	18.81	27.65	0.28	0.00	-99.82	-0.00001	-0.00001		
49.91	1.15	18.83	27.88	0.28	0.00	-49.91	-0.00005	-0.00004		

Mv=Hacimsel Sıkışma Katsayısı *Volume Change Coefficient* — av=Sıkışma Katsayısı *Compressibility Coefficient* — Cv= Konsolidasyon Katsayısı *Consolidation Coefficient* — t_{90} = Oturma Zamanı %90 *Settlement Time %90*

- Deneyler ilgili firma tarafından laboratuvarımıza teslim edilen numuneler üzerinde yapılmıştır. *Tests were done from the samples that are delivered by the related firm.*
- Bu deney TS 1900-2 standartlarına göre yapılmaktadır. *This test is being done according to the TS 1900-2 standarts.*
- Bu deney raporu Laboratuarımızın yazılı izni olmadan basılamaz ve çoğaltılamaz. *This tests results must not be reproduced in any form without the written permission of laboratory.*
- ZEMAR hologramları olmayan Deney Sonuç raporlarımız geçersizdir. Test result reports without a ZEMAR Hollogram are invalid.
- T.C.Bayındırlık ve İskan Bakanlığı logosu 16.06.2011 tarih ve 291 numaralı Laboratuvar İzin Belgesi kapsamında kullanılmaktadır. The Logo of T.R. The Ministry of Public Works and Settlement is used by Laboratory Permission Certificate dated 16.06.2011 and numbered 291.

Deneyi Yapan *Tested By*: Begüm Ağa, Jeoloji Mühendisi, Oda Sicil No: 16359

Onaylayan *Approved By*: Emre YILMAZ, Jeoloji Yük. Mühendisi, Denetçi Mühendis, Oda Sicil No.: 7733

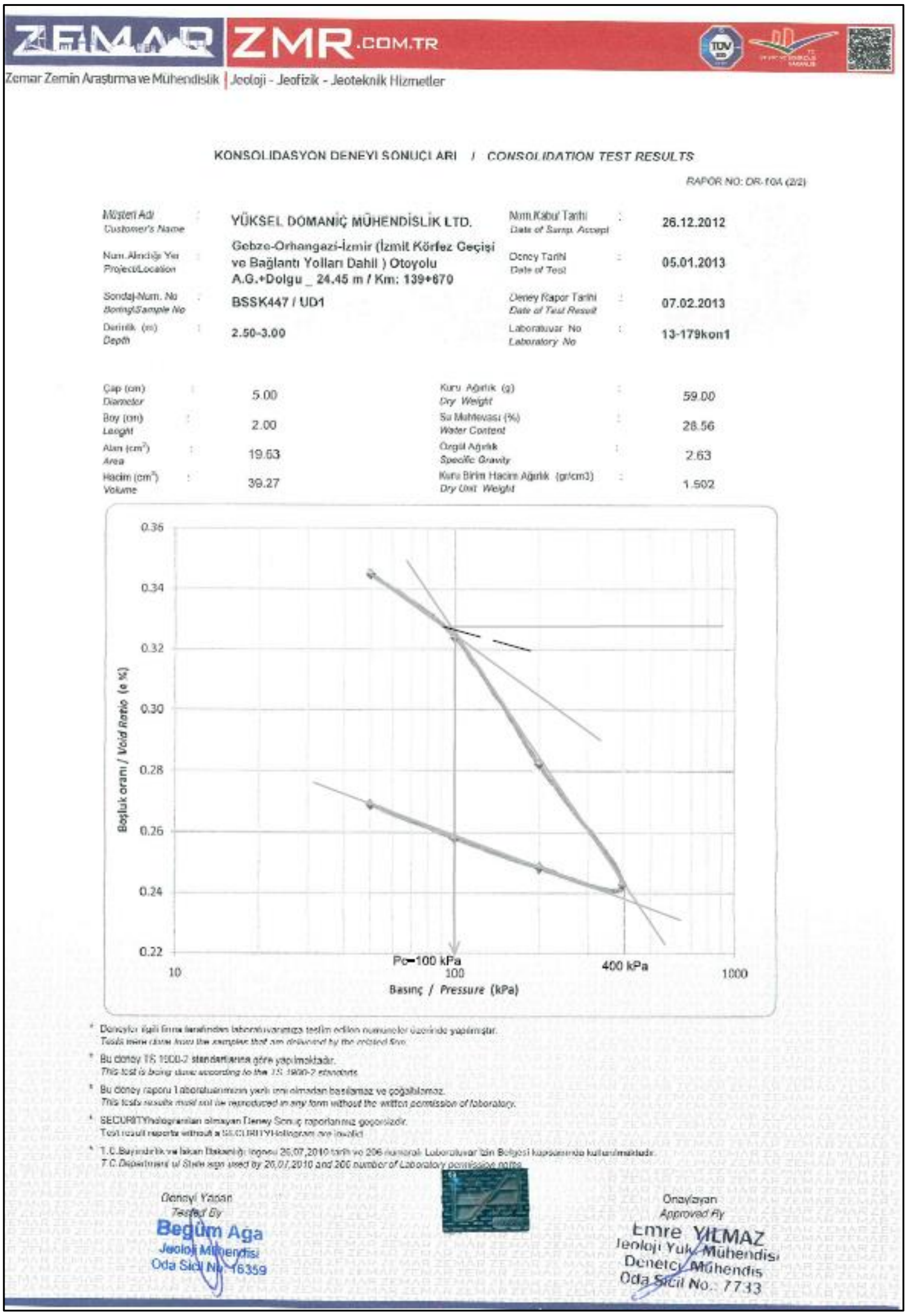
ZEMAR ZMR.COM.TR

Zemar Zemin Araştırma ve Mühendislik | Jeoloji - Jeofizik - Jeoteknik Hizmetler

KONSOLIDASYON DENEYI SONUÇLARI / CONSOLIDATION TEST RESULTS

RAPOR NO: OR-10A (2/2)

Müşteri Adı / Customer's Name	YÜKSEL DOMANİÇ MÜHENDİSLİK LTD.	Num.Kabul Tarihi / Date of Samp. Accept	26.12.2012
Num. Alındığı Yer / Project/Location	Gebze-Orhangazi-İzmir (İzmit Körfez Geçişi ve Bağlantı Yolları Dahil) Otoyolu A.G.+Dolgu _ 24.45 m / Km: 139+670	Deney Tarihi / Date of Test	05.01.2013
Sondaj-Num. No / Boring/Sample No	BSSK447 / UD1	Deney Rapor Tarihi / Date of Test Result	07.02.2013
Derinlik (m) / Depth	2.50-3.00	Laboratuvar No / Laboratory No	13-179kon1

Çap (cm) / Diameter	5.00	Kuru Ağırlık (g) / Dry Weight	59.00
Boy (cm) / Lenght	2.00	Su Muhtevası (%) / Water Content	28.56
Alan (cm^2) / Area	19.63	Özgül Ağırlık / Specific Gravity	2.63
Hacim (cm^3) / Volume	39.27	Kuru Birim Hacim Ağırlık (gr/cm3) / Dry Unit Weight	1.502

* Deneyler ilgili firma tarafından laboratuvarımıza teslim edilen numuneler üzerinde yapılmıştır.
Tests were done from the samples that are delivered by the related firm.
* Bu deney TS 1900-2 standartlarına göre yapılmaktadır.
This test is being done according to the TS 1900-2 standards.
* Bu deney raporu Laboratuarımızın yazılı izni olmadan basılamaz ve çoğaltılamaz.
This tests results must not be reproduced in any form without the written permission of laboratory.
* SECURITYhologramları olmayan Deney Sonuç raporlarımız geçersizdir.
Test result reports without a SECURITYHologram are invalid.
* T.C.Bayındırlık ve İskan Bakanlığı tarafından 26.07.2010 tarih ve 206 numaralı Laboratuvar İzin Belgesi kapsamında kullanılmaktadır.
T.C.Department of State sign used by 26.07.2010 and 206 number of Laboratory permission paper.

Deneyi Yapan / Tested By
Begüm Aga
Jeoloji Mühendisi
Oda Sicil No: 16359

Onaylayan / Approved By
Emre YILMAZ
Jeoloji Yük. Mühendisi
Denetçi Mühendis
Oda Sicil No.: 7733

Figure C. 1. Pressure vs. Void ratio graph for BSSK-447 UD1 sample

ZEMAR ZMR.COM.TR

Zemar Zemin Araştırma ve Mühendislik | Jeoloji - Jeofizik - Jeoteknik Hizmetler

KONSOLIDASYON DENEYI SONUÇLARI / *CONSOLIDATION TEST RESULTS*

RAPOR NO: DR-10A (2/2)

Müşteri Adı *Customer's Name* :	YÜKSEL DOMANİÇ MÜHENDİSLİK LTD.	Num.Kabul Tarihi *Date of Samp. Accept* :	26.12.2012
Num.Alındığı Yer *Project/Location* :	Gebze-Orhangazi-İzmir (İzmit Körfez Geçişi ve Bağlantı Yolları Dahil) Otoyolu A.G.+Dolgu _ 24.45 m / Km: 139+670	Deney Tarihi *Date of Test* :	05.01.2013
Sondaj-Num. No *Boring\Sample No* :	BSSK447 / UD3	Deney Rapor Tarihi *Date of Test Result* :	07.02.2013
Derinlik (m) *Depth* :	11.50-12.00	Laboratuvar No *Laboratory No* :	13-179kon2

Çap (cm) *Diameter* :	5.00	Kuru Ağırlık (g) *Dry Weight* :	60.71
Boy (cm) *Lenght* :	2.00	Su Muhtevası (%) *Water Content* :	22.52
Alan (cm^2) *Area* :	19.63	Özgül Ağırlık *Specific Gravity* :	2.57
Hacim (cm^3) *Volume* :	39.27	Kuru Birim Hacim Ağırlık (gr/cm3) *Dry Unit Weight* :	1.546

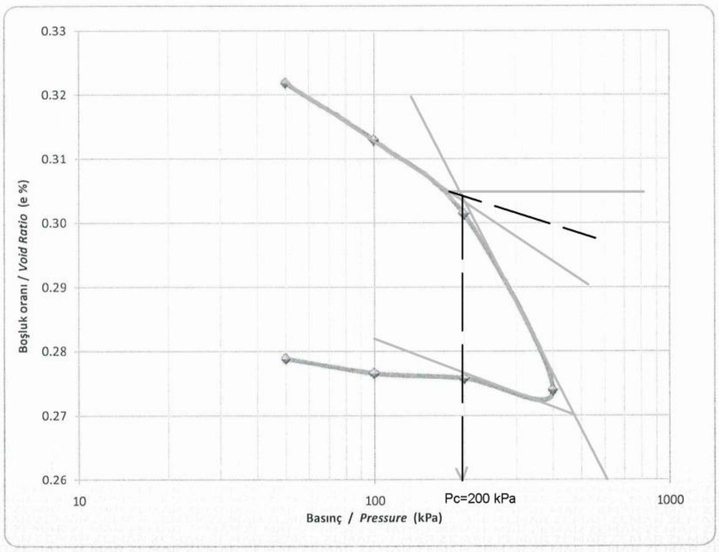

* Deneyler ilgili firma tarafından laboratuvarımıza teslim edilen numuneler üzerinde yapılmıştır.
Tests were done from the samples that are delivered by the related firm.

* Bu deney TS 1900-2 standartlarına göre yapılmaktadır.
This test is being done according to the TS 1900-2 standarts.

* Bu deney raporu Laboratuarımızın yazılı izni olmadan basılamaz ve çoğaltılamaz.
This tests results must not be reproduced in any form without the written permission of laboratory.

* SECURITYhologramları olmayan Deney Sonuç raporlarımız geçersizdir.
Test result reports without a SECURITYHollogram are invalid.

* T.C.Bayındırlık ve İskan Bakanlığı logosu 26,07,2010 tarih ve 206 numaralı Laboratuvar İzin Belgesi kapsamında kullanılmaktadır.
T.C.Department of State sign used by 26,07,2010 and 206 number of Laboratory permission notes.

Deneyi Yapan
Tested By
Jeoloji Mühendisi
Oda Sicil No: 16359

Onaylayan
Approved By
Emre YILMAZ
Jeoloji Yük. Mühendisi
Denetçi Mühendis
Oda Sicil No.: 7733

Figure C. 2. Pressure vs. Void ratio graph for BSSK-447 UD3 sample

C.2 KM: 139+860 Section

The embankment height: 8.8 m

Total consolidation: 101.52 cm

Table C. 5. Consolidation settlement parameters for Km: 139+860

Depth (m)	Thickness of layer (m)	z (m)	Unit weight of soil (kN/m^3)	σ_0 (kPa)	C_c (Lab. Result)	C_r (Lab. Result)	$(1+e_0)$ (Lab. Result)	m_v (m^2/kN) (Lab)	$\Delta\sigma$ (kPa)	$\sigma_1 = \sigma_0+\Delta\sigma$
2.00	2.00	1.00	18.00	8.2	0.120	0.050	1.36	0.000293	182.2	190.4
4.00	2.00	3.00	18.00	24.6	0.120	0.050	1.36	0.000298	176.4	201.0
6.00	2.00	5.00	18.00	41.0	0.120	0.050	1.36	0.000295	170.3	211.2
8.00	2.00	7.00	18.00	57.3	0.120	0.050	1.36	0.000290	163.9	221.2
10.00	2.00	9.00	18.00	73.7	0.120	0.050	1.36	0.000280	157.2	230.9
12.00	2.00	11.00	18.00	90.1	0.120	0.050	1.36	0.000270	150.2	240.3
14.00	2.00	13.00	18.00	106.5	0.120	0.050	1.36	0.000259	142.9	249.4
16.00	2.00	15.00	18.00	122.9	0.120	0.050	1.36	0.000246	135.4	258.2
18.00	2.00	17.00	18.00	139.2	0.120	0.050	1.36	0.000231	127.6	266.8
20.00	2.00	19.00	18.00	155.6	0.120	0.050	1.36	0.000215	119.5	275.2
22.00	2.00	21.00	18.00	172.0	0.120	0.050	1.36	0.000196	111.3	283.2
24.00	2.00	23.00	18.00	188.4	0.120	0.050	1.36	0.000173	102.7	291.1
26.00	2.00	25.00	18.00	204.8	0.100	0.020	1.36	0.000106	94.0	298.7
28.00	2.00	27.00	18.00	221.1	0.100	0.020	1.36	0.000106	85.0	306.1
30.00	2.00	29.00	18.00	237.5	0.100	0.020	1.36	0.000106	75.8	313.3
32.00	2.00	31.00	18.00	253.9	0.100	0.020	1.36	0.000106	66.4	320.3
34.00	2.00	33.00	18.00	270.3	0.100	0.020	1.36	0.000106	56.8	327.1
36.00	2.00	35.00	18.00	286.7	0.100	0.020	1.36	0.000106	47.0	333.7
38.00	2.00	37.00	18.00	303.0	0.100	0.020	1.36	0.000107	37.0	340.0
40.00	2.00	39.00	18.00	319.4	0.100	0.020	1.36	0.000107	26.8	346.2
42.00	2.00	41.00	18.00	335.8	0.100	0.020	1.36	0.000107	16.5	352.2
44.00	2.00	43.00	18.00	352.2	0.100	0.020	1.36	0.000107	5.9	358.1
44.11	1.00	44.05	18.00	360.8	0.100	0.020	1.36	0.000107	0.3	361.1

Table C. 6. Consolidation settlement calculation for Km: 139+860

Depth (m)	Thickness of layer (m)	Consolidation settlement of layer (S) (m)	Cumulative consolidation settlement (Sc) (cm) (by C_c values)	Consolidation settlement of layer (S) (m)	Cumulative consolidation settlement (Sc) (cm) (by m_v values)
2.00	2.00	0.13 m	12.93 cm	0.11 m	10.69 cm
4.00	2.00	0.10 m	22.76 cm	0.11 m	21.21 cm
6.00	2.00	0.09 m	31.34 cm	0.10 m	31.27 cm
8.00	2.00	0.08 m	39.20 cm	0.09 m	40.77 cm
10.00	2.00	0.07 m	46.59 cm	0.09 m	49.58 cm
12.00	2.00	0.04 m	51.01 cm	0.08 m	57.68 cm
14.00	2.00	0.04 m	55.19 cm	0.07 m	65.07 cm
16.00	2.00	0.04 m	59.17 cm	0.07 m	71.72 cm
18.00	2.00	0.04 m	63.01 cm	0.06 m	77.63 cm
20.00	2.00	0.04 m	66.73 cm	0.05 m	82.76 cm
22.00	2.00	0.04 m	70.35 cm	0.04 m	87.12 cm
24.00	2.00	0.03 m	73.68 cm	0.04 m	90.68 cm
26.00	2.00	0.02 m	76.09 cm	0.02 m	92.66 cm
28.00	2.00	0.02 m	78.17 cm	0.02 m	94.46 cm
30.00	2.00	0.02 m	79.94 cm	0.02 m	96.06 cm
32.00	2.00	0.01 m	81.43 cm	0.01 m	97.47 cm
34.00	2.00	0.01 m	82.64 cm	0.01 m	98.68 cm
36.00	2.00	0.01 m	83.61 cm	0.01 m	99.68 cm
38.00	2.00	0.01 m	84.35 cm	0.01 m	100.47 cm
40.00	2.00	0.01 m	84.86 cm	0.01 m	101.04 cm
42.00	2.00	0.00 m	85.17 cm	0.00 m	101.39 cm
44.00	2.00	0.00 m	85.28 cm	0.00 m	101.52 cm
44.11	1.00	0.00 m	85.28 cm	0.00 m	101.52 cm

OCR vs. Depth (m) Graph

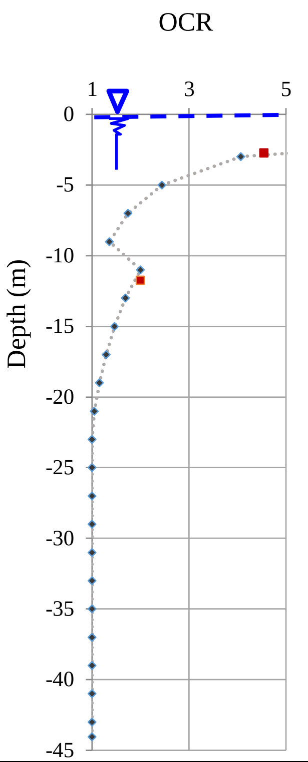

C.3 KM: 140+592 Section

The embankment height: 8.8 m

Total consolidation: 101.52 cm

Table C. 7. Consolidation settlement parameters for Km: 140+592

Depth (m)	Thickness of layer (m)	z (m)	Unit weight of soil (kN/m^3)	σ_0 (kPa)	C_c (Lab. Result)	C_r (Lab. Result)	$(1+e_0)$ (Lab. Result)	m_v (m^2/kN) (Lab)	$\Delta\sigma$ (kPa)	$\sigma_1 = \sigma_0+\Delta\sigma$
2.00	2.00	1.00	18.00	8.2	0.120	0.050	1.36	0.000293	182.2	190.4
4.00	2.00	3.00	18.00	24.6	0.120	0.050	1.36	0.000298	176.4	201.0
6.00	2.00	5.00	18.00	41.0	0.120	0.050	1.36	0.000295	170.3	211.2
8.00	2.00	7.00	18.00	57.3	0.120	0.050	1.36	0.000290	163.9	221.2
10.00	2.00	9.00	18.00	73.7	0.120	0.050	1.36	0.000280	157.2	230.9
12.00	2.00	11.00	18.00	90.1	0.120	0.050	1.36	0.000270	150.2	240.3
14.00	2.00	13.00	18.00	106.5	0.120	0.050	1.36	0.000259	142.9	249.4
16.00	2.00	15.00	18.00	122.9	0.120	0.050	1.36	0.000246	135.4	258.2
18.00	2.00	17.00	18.00	139.2	0.120	0.050	1.36	0.000231	127.6	266.8
20.00	2.00	19.00	18.00	155.6	0.120	0.050	1.36	0.000215	119.5	275.2
22.00	2.00	21.00	18.00	172.0	0.120	0.050	1.36	0.000196	111.3	283.2
24.00	2.00	23.00	18.00	188.4	0.120	0.050	1.36	0.000173	102.7	291.1
26.00	2.00	25.00	18.00	204.8	0.100	0.020	1.36	0.000106	94.0	298.7
28.00	2.00	27.00	18.00	221.1	0.100	0.020	1.36	0.000106	85.0	306.1
30.00	2.00	29.00	18.00	237.5	0.100	0.020	1.36	0.000106	75.8	313.3
32.00	2.00	31.00	18.00	253.9	0.100	0.020	1.36	0.000106	66.4	320.3
34.00	2.00	33.00	18.00	270.3	0.100	0.020	1.36	0.000106	56.8	327.1
36.00	2.00	35.00	18.00	286.7	0.100	0.020	1.36	0.000106	47.0	333.7
38.00	2.00	37.00	18.00	303.0	0.100	0.020	1.36	0.000107	37.0	340.0
40.00	2.00	39.00	18.00	319.4	0.100	0.020	1.36	0.000107	26.8	346.2
42.00	2.00	41.00	18.00	335.8	0.100	0.020	1.36	0.000107	16.5	352.2
44.00	2.00	43.00	18.00	352.2	0.100	0.020	1.36	0.000107	5.9	358.1
44.11	1.00	44.05	18.00	360.8	0.100	0.020	1.36	0.000107	0.3	361.1

Table C. 8. Consolidation settlement calculation for Km: 140+592

Depth (m)	Thickness of layer (m)	Consolidation settlement of layer (S) (m)	Cumulative consolidation settlement (Sc) (cm) (by C_c values)	Consolidation settlement of layer (S) (m)	Cumulative consolidation settlement (Sc) (cm) (by m_v values)
2.00	2.00	0.13 m	12.93 cm	0.11 m	10.69 cm
4.00	2.00	0.10 m	22.76 cm	0.11 m	21.21 cm
6.00	2.00	0.09 m	31.34 cm	0.10 m	31.27 cm
8.00	2.00	0.08 m	39.20 cm	0.09 m	40.77 cm
10.00	2.00	0.07 m	46.59 cm	0.09 m	49.58 cm
12.00	2.00	0.04 m	51.01 cm	0.08 m	57.68 cm
14.00	2.00	0.04 m	55.19 cm	0.07 m	65.07 cm
16.00	2.00	0.04 m	59.17 cm	0.07 m	71.72 cm
18.00	2.00	0.04 m	63.01 cm	0.06 m	77.63 cm
20.00	2.00	0.04 m	66.73 cm	0.05 m	82.76 cm
22.00	2.00	0.04 m	70.35 cm	0.04 m	87.12 cm
24.00	2.00	0.03 m	73.68 cm	0.04 m	90.68 cm
26.00	2.00	0.02 m	76.09 cm	0.02 m	92.66 cm
28.00	2.00	0.02 m	78.17 cm	0.02 m	94.46 cm
30.00	2.00	0.02 m	79.94 cm	0.02 m	96.06 cm
32.00	2.00	0.01 m	81.43 cm	0.01 m	97.47 cm
34.00	2.00	0.01 m	82.64 cm	0.01 m	98.68 cm
36.00	2.00	0.01 m	83.61 cm	0.01 m	99.68 cm
38.00	2.00	0.01 m	84.35 cm	0.01 m	100.47 cm
40.00	2.00	0.01 m	84.86 cm	0.01 m	101.04 cm
42.00	2.00	0.00 m	85.17 cm	0.00 m	101.39 cm
44.00	2.00	0.00 m	85.28 cm	0.00 m	101.52 cm
44.11	1.00	0.00 m	85.28 cm	0.00 m	101.52 cm

OCR vs. Depth (m) Graph

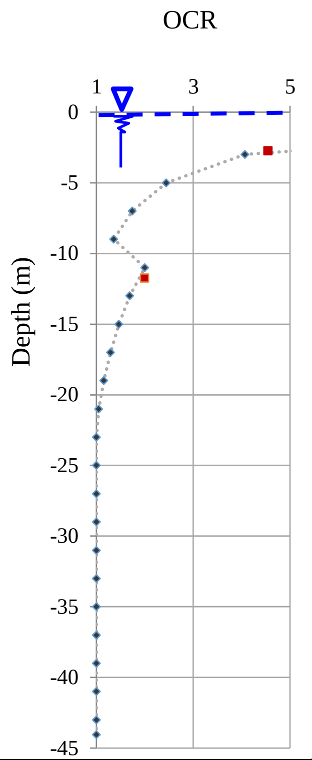

C.4 KM: 141+680 Section

The embankment height: 10.259 m

Total consolidation: 140.26 cm

Table C. 9. Consolidation calculations for Km: 141+680

Depth (m)	Thickness of layer (m)	z (m)	Unit weight of soil (kN/m^3)	σ_0 (kPa)	C_c (Lab. Result)	C_r (Lab. Result)	$(1+e_0)$ (Lab. Result)	m_v (m^2/kN) (Lab)	$\Delta\sigma$ (kPa)	$\sigma_1 = \sigma_0+\Delta\sigma$
2.00	2.00	1.00	18.00	8.2	0.125	0.030	1.48	0.000253	205.9	214.1
4.00	2.00	3.00	18.00	24.6	0.125	0.030	1.48	0.000230	199.4	223.9
6.00	2.00	5.00	18.00	41.0	0.356	0.027	1.59	0.000442	192.6	233.5
8.00	2.00	7.00	18.00	57.3	0.356	0.027	1.59	0.000425	185.5	242.8
9.00	1.00	8.50	18.00	69.6	0.356	0.027	1.59	0.000415	180.0	249.6
18.00	9.00	13.50	18.00	110.6	0.000	0.000	1.59	0.000000	160.7	271.3
20.00	2.00	19.00	18.00	155.6	0.356	0.027	1.59	0.000343	137.6	293.3
22.00	2.00	21.00	18.00	172.0	0.356	0.027	1.59	0.000325	128.8	300.8
24.00	2.00	23.00	18.00	188.4	0.356	0.027	1.59	0.000304	119.8	308.2
26.00	2.00	25.00	18.00	204.8	0.356	0.027	1.59	0.000288	110.5	315.3
28.00	2.00	27.00	18.00	221.1	0.113	0.011	1.56	0.000070	101.1	322.2
30.00	2.00	29.00	18.00	237.5	0.113	0.011	1.56	0.000071	91.4	328.9
32.00	2.00	31.00	18.00	253.9	0.338	0.054	1.56	0.000297	81.6	335.5
34.00	2.00	33.00	18.00	270.3	0.338	0.054	1.56	0.000299	71.5	341.8
36.00	2.00	35.00	18.00	286.7	0.338	0.054	1.56	0.000300	61.3	347.9
38.00	2.00	37.00	18.00	303.0	0.338	0.054	1.56	0.000302	50.9	353.9
40.00	2.00	39.00	18.00	319.4	0.338	0.054	1.56	0.000303	40.3	359.7
42.00	2.00	41.00	18.00	335.8	0.338	0.054	1.56	0.000305	29.5	365.3
44.00	2.00	43.00	18.00	352.2	0.338	0.054	1.56	0.000306	18.6	370.8
46.00	2.00	45.00	18.00	362.3	0.338	0.054	1.56	0.000308	11.8	374.1
46.34	2.00	46.17	18.00	378.1	0.338	0.054	1.56	0.000309	1.0	379.1

Table C. 10. Consolidation calculations for Km: 141+680

Depth (m)	Thickness of layer (m)	Consolidation settlement of layer (S) (m)	Cumulative consolidation settlement (Sc) (cm) (by C_c values)	Consolidation settlement of layer (S) (m)	Cumulative consolidation settlement (Sc) (cm) (by m_v values)
2.00	2.00	0.09 m	8.53 cm	0.10 m	10.42 cm
4.00	2.00	0.10 m	18.16 cm	0.09 m	19.58 cm
6.00	2.00	0.22 m	39.98 cm	0.17 m	36.62 cm
8.00	2.00	0.22 m	62.06 cm	0.16 m	52.39 cm
9.00	1.00	0.11 m	73.23 cm	0.07 m	59.86 cm
18.00	9.00	0.00 m	73.23 cm	0.00 m	59.86 cm
20.00	2.00	0.12 m	85.55 cm	0.09 m	69.29 cm
22.00	2.00	0.11 m	96.43 cm	0.08 m	77.66 cm
24.00	2.00	0.10 m	106.00 cm	0.07 m	84.95 cm
26.00	2.00	0.08 m	114.40 cm	0.06 m	91.31 cm
28.00	2.00	0.02 m	116.76 cm	0.01 m	92.73 cm
30.00	2.00	0.02 m	118.81 cm	0.01 m	94.02 cm
32.00	2.00	0.05 m	124.06 cm	0.05 m	98.87 cm
34.00	2.00	0.04 m	128.47 cm	0.04 m	103.14 cm
36.00	2.00	0.04 m	132.12 cm	0.04 m	106.82 cm
38.00	2.00	0.03 m	135.04 cm	0.03 m	109.89 cm
40.00	2.00	0.02 m	137.27 cm	0.02 m	112.33 cm
42.00	2.00	0.02 m	138.86 cm	0.02 m	114.13 cm
44.00	2.00	0.01 m	139.83 cm	0.01 m	115.27 cm
46.00	2.00	0.00 m	140.21 cm	0.00 m	115.73 cm
46.34	2.00	0.00 m	140.26 cm	0.00 m	115.79 cm

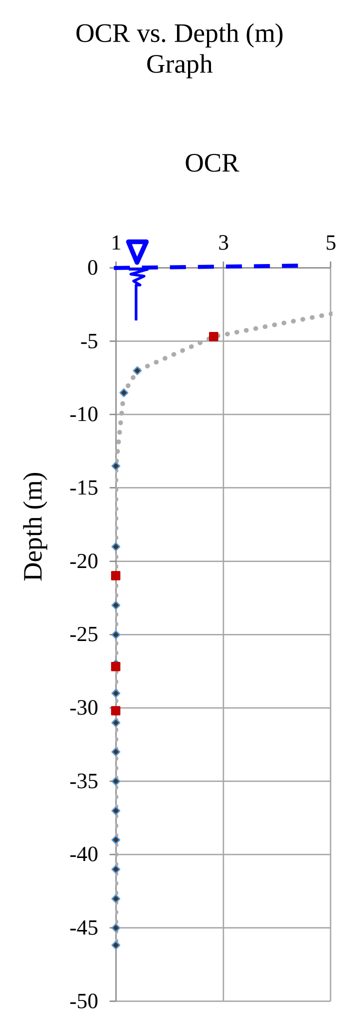

C.5 KM: 142+000 Section

The embankment height: 9.97 m

Total consolidation: 111.69 cm

Table C. 11. Consolidation settlement parameters for Km: 142+000

Depth (m)	Thickness of layer (m)	z (m)	Unit weight of soil (kN/m^3)	σ_0 (kPa)	C_c (Lab. Result)	C_r (Lab. Result)	$(1+e_0)$ (Lab. Result)	m_v (m^2/kN) (Lab)	$\Delta\sigma$ (kPa)	$\sigma_1 = \sigma_0+\Delta\sigma$
2.00	2.00	1.00	18.00	8.2	0.390	0.056	3.22	0.000272	205.2	213.4
4.00	2.00	3.00	18.00	24.6	0.390	0.056	3.22	0.000254	198.7	223.3
6.00	2.00	5.00	18.00	41.0	0.390	0.056	3.22	0.000235	192.0	232.9
8.00	2.00	7.00	18.00	57.3	0.390	0.056	3.22	0.000222	184.9	242.3
9.00	1.00	8.50	18.00	69.6	0.390	0.056	3.22	0.000218	179.5	249.1
15.00	6.00	12.00	19.00	110.3	0.000	0.000	1.63	0.000000	154.1	264.4
17.00	2.00	16.00	18.00	131.0	0.365	0.063	1.63	0.000364	149.9	281.0
19.00	2.00	18.00	18.00	147.4	0.365	0.063	1.63	0.000350	141.5	288.9
21.00	2.00	20.00	18.00	163.8	0.365	0.063	1.63	0.000334	132.8	296.6
23.00	2.00	22.00	18.00	180.2	0.365	0.063	1.63	0.000077	123.9	304.1
25.00	2.00	24.00	18.00	196.6	0.365	0.063	1.63	0.000072	114.7	311.3
27.00	2.00	26.00	18.00	212.9	0.094	0.015	1.29	0.000071	105.4	318.3
29.00	2.00	28.00	18.00	229.3	0.094	0.015	1.29	0.000295	95.9	325.2
31.00	2.00	30.00	18.00	245.7	0.094	0.015	1.29	0.000296	86.1	331.8
33.00	2.00	32.00	18.00	262.1	0.361	0.093	1.67	0.000298	76.2	338.2
35.00	2.00	34.00	18.00	278.5	0.361	0.093	1.67	0.000299	66.0	344.5
37.00	2.00	36.00	18.00	294.8	0.361	0.093	1.67	0.000301	55.7	350.6
39.00	2.00	38.00	18.00	311.2	0.361	0.093	1.67	0.000302	45.2	356.4
41.00	2.00	40.00	18.00	327.6	0.361	0.093	1.67	0.000304	34.6	362.2
43.00	2.00	42.00	18.00	344.0	0.361	0.093	1.67	0.000305	23.7	367.7
45.00	2.00	44.00	18.00	360.4	0.361	0.093	1.67	0.000307	12.7	373.1
46.28	1.28	45.64	18.00	373.8	0.361	0.093	1.67	0.000308	3.6	377.4

Table C. 12. Consolidation settlement calculation for Km: 142+000

Depth (m)	Thickness of layer (m)	Consolidation settlement of layer (S) (m)	Cumulative consolidation settlement (Sc) (cm) (by C_c values)	Consolidation settlement of layer (S) (m)	Cumulative consolidation settlement (Sc) (cm) (by m_v values)
2.00	2.00	0.09 m	9.39 cm	0.11 m	11.16 cm
4.00	2.00	0.08 m	17.60 cm	0.10 m	21.27 cm
6.00	2.00	0.08 m	25.48 cm	0.09 m	30.31 cm
8.00	2.00	0.08 m	33.27 cm	0.08 m	38.52 cm
9.00	1.00	0.04 m	37.16 cm	0.04 m	42.44 cm
15.00	6.00	0.00 m	37.16 cm	0.00 m	42.44 cm
17.00	2.00	0.09 m	46.44 cm	0.11 m	53.35 cm
19.00	2.00	0.09 m	55.88 cm	0.10 m	63.26 cm
21.00	2.00	0.12 m	67.42 cm	0.09 m	72.12 cm
23.00	2.00	0.10 m	77.60 cm	0.02 m	74.03 cm
25.00	2.00	0.09 m	86.54 cm	0.02 m	75.68 cm
27.00	2.00	0.03 m	89.09 cm	0.01 m	77.16 cm
29.00	2.00	0.02 m	91.30 cm	0.06 m	82.82 cm
31.00	2.00	0.02 m	93.20 cm	0.05 m	87.93 cm
33.00	2.00	0.05 m	97.99 cm	0.05 m	92.47 cm
35.00	2.00	0.04 m	101.99 cm	0.04 m	96.42 cm
37.00	2.00	0.03 m	105.24 cm	0.03 m	99.77 cm
39.00	2.00	0.03 m	107.78 cm	0.03 m	102.51 cm
41.00	2.00	0.02 m	109.67 cm	0.02 m	104.61 cm
43.00	2.00	0.01 m	110.92 cm	0.01 m	106.06 cm
45.00	2.00	0.01 m	111.57 cm	0.01 m	106.84 cm
46.28	1.28	0.00 m	111.69 cm	0.00 m	106.98 cm

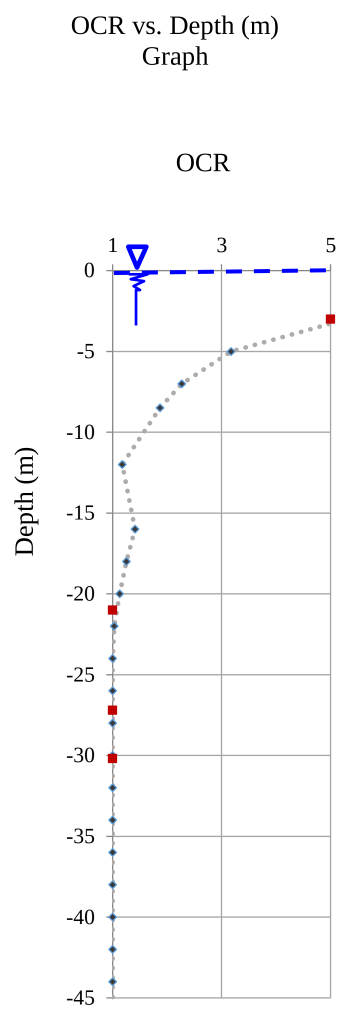

C.6 KM: 142+400 Section

The embankment height: 8.09 m

Total consolidation: 92.44 cm

Table C. 13. Consolidation settlement parameters for Km: 142+400

Depth (m)	Thickness of layer (m)	z (m)	Unit weight of soil (kN/m^3)	σ_0 (kPa)	C_c (Lab. Result)	C_r (Lab. Result)	$(1+e_0)$ (Lab. Result)	m_v (m^2/kN) (Lab)	$\Delta\sigma$ (kPa)	$\sigma_1 = \sigma_0+\Delta\sigma$
2.00	2.00	1.00	18.00	8.2	0.390	0.056	3.22	0.0002875	168.2	176.4
4.00	2.00	3.00	18.00	24.6	0.390	0.056	3.22	0.0002683	162.8	187.4
6.00	2.00	5.00	18.00	41.0	0.390	0.056	3.22	0.0002473	157.1	198.1
8.70	3.00	7.35	18.00	60.2	0.390	0.056	3.22	0.0002301	150.0	210.2
10.70	2.00	9.70	19.00	89.1	0.000	0.000	0	0.0000000	132.8	221.9
12.70	2.00	11.70	19.00	107.5	0.000	0.000	0	0.0000000	124.0	231.5
14.00	2.00	13.35	19.00	122.7	0.000	0.000	0	0.0000000	116.6	239.3
16.00	2.00	15.00	18.00	122.9	0.365	0.063	1.63	0.0003851	124.0	246.9
18.00	2.00	17.00	18.00	139.2	0.365	0.063	1.63	0.0003680	116.5	255.8
20.00	2.00	19.00	18.00	155.6	0.365	0.063	1.63	0.0003481	108.8	264.4
22.00	2.00	21.00	18.00	172.0	0.365	0.063	1.63	0.0003245	100.9	272.8
24.00	2.00	23.00	18.00	188.4	0.365	0.063	1.63	0.0000757	92.6	281.0
26.00	2.00	25.00	18.00	204.8	0.365	0.063	1.63	0.0000705	84.2	288.9
28.00	2.00	27.00	18.00	221.1	0.094	0.015	1.29	0.0000706	75.5	296.6
30.00	2.00	29.00	18.00	237.5	0.094	0.015	1.29	0.0002958	66.6	304.1
31.00	1.00	30.50	18.00	249.8	0.094	0.015	1.29	0.0002969	59.8	309.5
32.00	1.00	31.50	18.00	258.0	0.094	0.015	1.29	0.0002976	55.1	313.1
34.00	2.00	33.00	18.00	270.3	0.361	0.093	1.67	0.0002987	48.1	318.4
36.00	2.00	35.00	18.00	286.7	0.361	0.093	1.67	0.0003001	38.6	325.2
38.00	2.00	37.00	18.00	303.0	0.361	0.093	1.67	0.0003016	28.8	331.8
40.00	2.00	39.00	18.00	319.4	0.361	0.093	1.67	0.0003031	18.9	338.3
42.69	2.69	41.35	18.00	338.6	0.361	0.093	1.67	0.0003049	7.0	345.6

Table C. 14. Consolidation settlement calculation for Km: 142+400

Depth (m)	Thickness of layer (m)	Consolidation settlement of layer (S) (m)	Cumulative consolidation settlement (Sc) (cm) (by C_c values)	Consolidation settlement of layer (S) (m)	Cumulative consolidation settlement (Sc) (cm) (by m_v values)
2.00	2.00	0.07 m	7.39 cm	0.10 m	9.67 cm
4.00	2.00	0.06 m	13.75 cm	0.09 m	18.41 cm
6.00	2.00	0.06 m	19.93 cm	0.08 m	26.18 cm
8.70	3.00	0.09 m	29.25 cm	0.10 m	36.53 cm
10.70	2.00	0.00 m	29.25 cm	0.00 m	36.53 cm
12.70	2.00	0.00 m	29.25 cm	0.00 m	36.53 cm
14.00	2.00	0.00 m	29.25 cm	0.00 m	36.53 cm
16.00	2.00	0.13 m	41.91 cm	0.10 m	46.08 cm
18.00	2.00	0.07 m	49.17 cm	0.09 m	54.66 cm
20.00	2.00	0.08 m	56.70 cm	0.08 m	62.24 cm
22.00	2.00	0.08 m	64.50 cm	0.07 m	68.78 cm
24.00	2.00	0.08 m	72.28 cm	0.01 m	70.19 cm
26.00	2.00	0.07 m	78.98 cm	0.01 m	71.37 cm
28.00	2.00	0.02 m	80.84 cm	0.01 m	72.44 cm
30.00	2.00	0.02 m	82.40 cm	0.04 m	76.38 cm
31.00	1.00	0.01 m	83.08 cm	0.02 m	78.15 cm
32.00	1.00	0.01 m	83.69 cm	0.02 m	79.79 cm
34.00	2.00	0.03 m	86.77 cm	0.03 m	82.67 cm
36.00	2.00	0.02 m	89.14 cm	0.02 m	84.98 cm
38.00	2.00	0.02 m	90.84 cm	0.02 m	86.72 cm
40.00	2.00	0.01 m	91.92 cm	0.01 m	87.86 cm
42.69	2.69	0.01 m	92.44 cm	0.01 m	88.43 cm

OCR vs. Depth (m) Graph

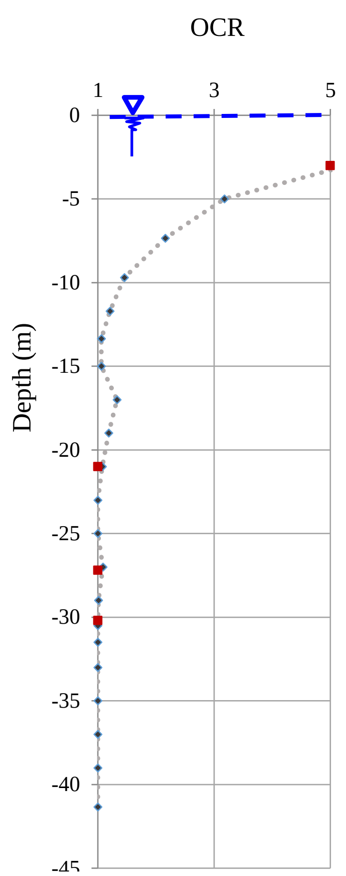

C.7 KM: 143+107 Section

The embankment height: 8.448 m

Total consolidation: 103.09 cm

Table C. 15. Consolidation settlement parameters for Km: 143+107

Depth (m)	Thickness of layer (m)	z (m)	Unit weight of soil (kN/m^3)	σ_0 (kPa)	C_c (Lab. Result)	C_r (Lab. Result)	$(1+e_0)$ (Lab. Result)	m_v (m^2/kN) (Lab)	$\Delta\sigma$ (kPa)	$\sigma_1 = \sigma_0+\Delta\sigma$
2.00	2.00	1.00	18.00	8.2	0.216	0.039	1.29	0.000358	175.3	183.5
4.00	2.00	3.00	18.00	24.6	0.216	0.039	1.29	0.000367	169.7	194.3
6.00	2.00	5.00	18.00	41.0	0.216	0.039	1.29	0.000373	163.8	204.7
7.50	1.50	6.75	19.00	62.0	0.000	0.000	1.29	0.000000	151.6	213.6
9.50	2.00	8.50	18.00	69.6	0.219	0.059	1.47	0.000293	152.7	222.3
10.50	1.00	10.00	18.00	81.9	0.219	0.059	1.47	0.000285	147.7	229.6
15.50	5.00	13.00	19.00	119.5	0.000	0.000	1.47	0.000000	124.1	243.6
17.50	2.00	16.50	18.00	135.1	0.390	0.084	1.95	0.000198	124.1	259.2
19.50	2.00	18.50	18.00	151.5	0.390	0.084	1.95	0.000190	116.3	267.8
21.50	2.00	20.50	18.00	167.9	0.279	0.057	1.61	0.000228	108.2	276.1
23.50	2.00	22.50	18.00	184.3	0.279	0.057	1.61	0.000213	99.9	284.1
25.50	2.00	24.50	18.00	200.7	0.279	0.057	1.61	0.000195	91.3	292.0
27.50	2.00	26.50	18.00	217.0	0.279	0.057	1.61	0.000196	82.5	299.6
29.50	2.00	28.50	18.00	233.4	0.279	0.057	1.61	0.000196	73.5	307.0
31.50	2.00	30.50	18.00	249.8	0.449	0.129	1.78	0.000447	64.3	314.1
34.00	2.50	32.75	18.00	268.2	0.449	0.129	1.78	0.000450	53.7	321.9
36.00	2.00	35.00	18.00	286.7	0.449	0.129	1.78	0.000454	42.8	329.5
38.00	2.00	37.00	18.00	303.0	0.449	0.129	1.78	0.000457	33.0	336.0
40.00	2.00	39.00	18.00	319.4	0.449	0.129	1.78	0.000461	22.9	342.3
42.00	2.00	41.00	18.00	335.8	0.449	0.129	1.78	0.000464	12.6	348.4
43.42	2.00	42.71	18.00	349.8	0.449	0.129	1.78	0.000467	3.7	353.5

Table C. 16. Consolidation settlement calculation for Km: 143+107

Depth (m)	Thickness of layer (m)	Consolidation settlement of layer (S) (m)	Cumulative consolidation settlement (Sc) (cm) (by C_c values)	Consolidation settlement of layer (S) (m)	Cumulative consolidation settlement (Sc) (cm) (by m_v values)
2.00	2.00	0.10 m	9.80 cm	0.13 m	12.56 cm
4.00	2.00	0.08 m	17.54 cm	0.12 m	25.00 cm
6.00	2.00	0.07 m	24.71 cm	0.12 m	37.22 cm
7.50	1.50	0.00 m	24.71 cm	0.00 m	37.22 cm
9.50	2.00	0.07 m	31.86 cm	0.09 m	46.18 cm
10.50	1.00	0.04 m	35.37 cm	0.04 m	50.38 cm
15.50	5.00	0.00 m	35.37 cm	0.00 m	50.38 cm
17.50	2.00	0.11 m	46.68 cm	0.05 m	55.29 cm
19.50	2.00	0.10 m	56.58 cm	0.04 m	59.71 cm
21.50	2.00	0.07 m	64.06 cm	0.05 m	64.65 cm
23.50	2.00	0.07 m	70.58 cm	0.04 m	68.90 cm
25.50	2.00	0.06 m	76.23 cm	0.04 m	72.46 cm
27.50	2.00	0.05 m	81.08 cm	0.03 m	75.69 cm
29.50	2.00	0.04 m	85.20 cm	0.03 m	78.57 cm
31.50	2.00	0.05 m	90.22 cm	0.06 m	84.32 cm
34.00	2.50	0.05 m	95.22 cm	0.06 m	90.37 cm
36.00	2.00	0.03 m	98.27 cm	0.04 m	94.26 cm
38.00	2.00	0.02 m	100.53 cm	0.03 m	97.27 cm
40.00	2.00	0.02 m	102.05 cm	0.02 m	99.38 cm
42.00	2.00	0.01 m	102.86 cm	0.01 m	100.56 cm
43.42	2.00	0.00 m	103.09 cm	0.00 m	100.91 cm

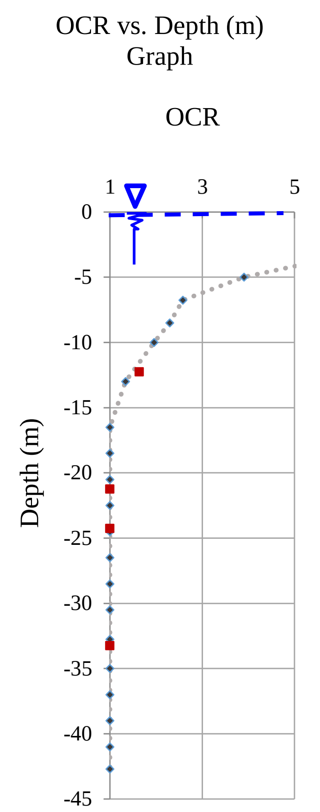

C.8 KM: 144+000 Section

The embankment height: 9.98 m

Total consolidation: 103.24 cm

Table C. 17. Consolidation settlement parameters for Km: 144+000

Depth (m)	Thickness of layer (m)	z (m)	Unit weight of soil (kN/m^3)	σ_0 (kPa)	C_c (Lab. Result)	C_r (Lab. Result)	$(1+e_0)$ (Lab. Result)	m_v (m^2/kN) (Lab)	$\Delta\sigma$ (kPa)	$\sigma_1 = \sigma_0+\Delta\sigma$
2.00	2.00	1.00	18.00	8.2	0.166	0.060	1.39	0.000346	205.5	213.7
4.00	2.00	3.00	18.00	24.6	0.166	0.060	1.39	0.000315	199.0	223.5
6.50	2.50	5.25	18.00	43.0	0.166	0.060	1.39	0.000276	191.3	234.3
7.50	1.00	7.00	18.00	64.3	0.000	0.000	0	0.000000	178.1	242.5
9.50	2.00	8.50	18.00	69.6	0.073	0.012	1.33	0.000095	179.7	249.3
11.50	2.00	10.50	18.00	86.0	0.073	0.012	1.33	0.000086	172.1	258.1
14.00	2.50	12.75	18.00	104.4	0.073	0.012	1.33	0.000076	163.4	267.8
17.00	3.00	15.50	18.00	142.4	0.000	0.000	1.39	0.000000	136.7	279.1
19.00	2.00	18.00	18.00	147.4	0.095	0.013	1.39	0.000062	141.7	289.1
21.00	2.00	20.00	18.00	163.8	0.095	0.013	1.39	0.000061	133.0	296.8
23.00	2.00	22.00	18.00	180.2	0.095	0.013	1.95	0.000060	124.1	304.2
25.00	2.00	24.00	18.00	196.6	0.095	0.013	1.95	0.000058	114.9	311.5
27.00	2.00	26.00	18.00	212.9	0.279	0.057	1.61	0.000195	105.6	318.5
29.00	2.00	28.00	18.00	229.3	0.279	0.057	1.61	0.000196	96.0	325.3
31.00	2.00	30.00	18.00	245.7	0.279	0.057	1.61	0.000197	86.3	332.0
33.00	2.00	32.00	18.00	262.1	0.279	0.057	1.61	0.000197	76.3	338.4
35.00	2.00	34.00	18.00	278.5	0.279	0.057	1.61	0.000198	66.2	344.6
37.00	2.00	36.00	18.00	294.8	0.449	0.129	1.78	0.000456	55.9	350.7
39.00	2.00	38.00	18.00	311.2	0.449	0.129	1.78	0.000459	45.4	356.6
41.00	2.00	40.00	18.00	327.6	0.449	0.129	1.78	0.000463	34.7	362.3
43.00	2.00	42.00	18.00	344.0	0.449	0.129	1.78	0.000466	23.9	367.8
45.00	2.00	44.00	18.00	360.4	0.449	0.129	1.78	0.000470	12.9	373.2
46.30	2.00	45.65	18.00	373.9	0.449	0.129	1.78	0.000473	3.7	377.6

Table C. 18. Consolidation settlement calculation for Km: 144+000

Depth (m)	Thickness of layer (m)	Consolidation settlement of layer (S) (m)	Cumulative consolidation settlement (Sc) (cm) (by C_c values)	Consolidation settlement of layer (S) (m)	Cumulative consolidation settlement (Sc) (cm) (by m_v values)
2.00	2.00	0.16 m	15.78 cm	0.14 m	14.22 cm
4.00	2.00	0.12 m	27.91 cm	0.13 m	26.74 cm
6.50	2.50	0.13 m	41.06 cm	0.13 m	39.93 cm
7.50	1.00	0.00 m	41.06 cm	0.00 m	39.93 cm
9.50	2.00	0.05 m	46.34 cm	0.03 m	43.35 cm
11.50	2.00	0.05 m	51.58 cm	0.03 m	46.29 cm
14.00	2.50	0.06 m	57.20 cm	0.03 m	49.40 cm
17.00	3.00	0.00 m	57.20 cm	0.00 m	49.40 cm
19.00	2.00	0.04 m	61.19 cm	0.02 m	51.14 cm
21.00	2.00	0.04 m	64.72 cm	0.02 m	52.76 cm
23.00	2.00	0.02 m	66.94 cm	0.01 m	54.24 cm
25.00	2.00	0.02 m	68.89 cm	0.01 m	55.58 cm
27.00	2.00	0.06 m	74.95 cm	0.04 m	59.71 cm
29.00	2.00	0.05 m	80.21 cm	0.04 m	63.47 cm
31.00	2.00	0.05 m	84.74 cm	0.03 m	66.86 cm
33.00	2.00	0.04 m	88.59 cm	0.03 m	69.87 cm
35.00	2.00	0.03 m	91.80 cm	0.03 m	72.49 cm
37.00	2.00	0.04 m	95.60 cm	0.05 m	77.58 cm
39.00	2.00	0.03 m	98.58 cm	0.04 m	81.75 cm
41.00	2.00	0.02 m	100.79 cm	0.03 m	84.96 cm
43.00	2.00	0.01 m	102.26 cm	0.02 m	87.19 cm
45.00	2.00	0.01 m	103.02 cm	0.01 m	88.40 cm
46.30	2.00	0.00 m	103.24 cm	0.00 m	88.74 cm

OCR vs. Depth (m) Graph

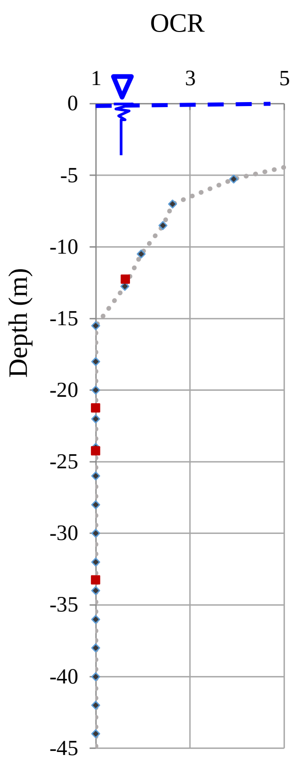

C.9 KM: 145+000 Section

The embankment height: 8.45 m

Total consolidation: 82.75 cm

Table C. 19. Consolidation settlement parameters for Km: 145+000

Depth (m)	Thickness of layer (m)	z (m)	Unit weight of soil (kN/m^3)	σ_0 (kPa)	C_c (Lab. Result)	C_r (Lab. Result)	$(1+e_0)$ (Lab. Result)	m_v (m^2/kN) (Lab)	$\Delta\sigma$ (kPa)	$\sigma_1 = \sigma_0+\Delta\sigma$
2.00	2.00	1.00	18.00	8.2	0.089	0.021	1.407	0.000221	166.5	174.6
4.00	2.00	3.00	18.00	24.6	0.089	0.021	1.407	0.000205	161.1	185.7
6.00	2.00	5.00	18.00	41.0	0.089	0.021	1.407	0.000187	155.4	196.4
8.00	2.00	7.00	18.00	57.3	0.089	0.021	1.407	0.000171	149.5	206.8
10.00	2.00	9.00	18.00	73.7	0.241	0.019	1.288	0.000162	143.2	216.9
11.00	1.00	10.50	18.00	86.0	0.241	0.019	1.288	0.000154	138.3	224.3
18.00	7.00	14.50	19.00	133.3	0.000	0.000	1.87	0.000000	109.9	243.1
20.00	2.00	19.00	18.00	155.6	0.290	0.059	2.04	0.000243	107.5	263.1
22.00	2.00	21.00	18.00	172.0	0.290	0.059	2.04	0.000238	99.5	271.5
24.00	2.00	23.00	18.00	188.4	0.290	0.059	2.04	0.000232	91.4	279.7
26.00	2.00	25.00	18.00	204.8	0.290	0.059	2.04	0.000227	82.9	287.7
28.00	2.00	27.00	18.00	221.1	0.290	0.059	2.04	0.000228	74.3	295.4
30.00	2.00	29.00	18.00	237.5	0.290	0.059	2.04	0.000229	65.4	302.9
32.00	2.00	31.00	18.00	253.9	0.646	0.090	2.56	0.000375	56.3	310.2
34.00	2.00	33.00	18.00	270.3	0.646	0.090	2.56	0.000377	47.0	317.3
36.00	2.00	35.00	18.00	286.7	0.646	0.090	2.56	0.000380	37.5	324.1
38.00	2.00	37.00	18.00	303.0	0.646	0.090	2.56	0.000382	27.8	330.8
40.00	2.00	39.00	18.00	319.4	0.646	0.090	2.56	0.000384	17.9	337.3
42.00	2.00	41.00	18.00	335.8	0.646	0.090	2.56	0.000387	7.7	343.5
42.51	0.51	42.26	18.00	346.1	0.646	0.090	2.56	0.000388	1.3	347.4

Table C. 20. Consolidation settlement calculation for Km: 145+000

Depth (m)	Thickness of layer (m)	Consolidation settlement of layer (S) (m)	Cumulative consolidation settlement (Sc) (cm) (by C_c values)	Consolidation settlement of layer (S) (m)	Cumulative consolidation settlement (Sc) (cm) (by m_v values)
2.00	2.00	0.06 m	6.31 cm	0.07 m	7.35 cm
4.00	2.00	0.05 m	11.53 cm	0.07 m	13.94 cm
6.00	2.00	0.05 m	16.39 cm	0.06 m	19.75 cm
8.00	2.00	0.05 m	21.11 cm	0.05 m	24.87 cm
10.00	2.00	0.13 m	34.08 cm	0.05 m	29.51 cm
11.00	1.00	0.07 m	40.74 cm	0.02 m	31.64 cm
18.00	7.00	0.00 m	40.74 cm	0.00 m	31.64 cm
20.00	2.00	0.06 m	47.22 cm	0.05 m	36.87 cm
22.00	2.00	0.06 m	52.86 cm	0.05 m	41.62 cm
24.00	2.00	0.05 m	57.74 cm	0.04 m	45.86 cm
26.00	2.00	0.04 m	61.94 cm	0.04 m	49.63 cm
28.00	2.00	0.04 m	65.52 cm	0.03 m	53.02 cm
30.00	2.00	0.03 m	68.52 cm	0.03 m	56.02 cm
32.00	2.00	0.04 m	72.91 cm	0.04 m	60.24 cm
34.00	2.00	0.04 m	76.43 cm	0.04 m	63.79 cm
36.00	2.00	0.03 m	79.12 cm	0.03 m	66.63 cm
38.00	2.00	0.02 m	81.04 cm	0.02 m	68.75 cm
40.00	2.00	0.01 m	82.23 cm	0.01 m	70.13 cm
42.00	2.00	0.01 m	82.73 cm	0.01 m	70.73 cm
42.51	0.51	0.00 m	82.75 cm	0.00 m	70.75 cm

OCR vs. Depth (m) Graph

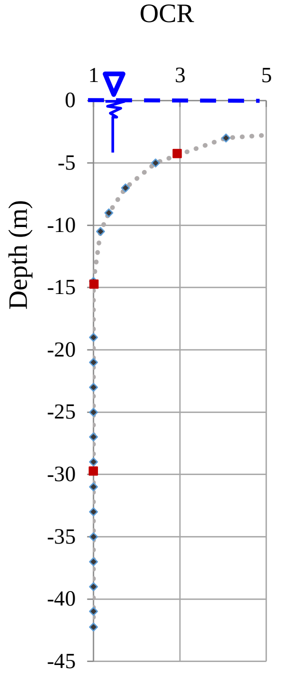

C.10 KM: 146+210 Section

The embankment height: 12.18 m

Total consolidation: 102.04 cm

Table C. 21. Consolidation settlement parameters for Km: 146+210

Depth (m)	Thickness of layer (m)	z (m)	Unit weight of soil (kN/m^3)	σ_0 (kPa)	C_c (Lab. Result)	C_r (Lab. Result)	$(1+e_0)$ (Lab. Result)	m_v (m^2/kN) (Lab)	$\Delta\sigma$ (kPa)	$\sigma_1 = \sigma_0+\Delta\sigma$
2.00	2.00	1.00	18.00	8.2	0.040	0.010	1.41	0.000189	240.0	248.1
4.00	2.00	3.00	18.00	24.6	0.040	0.100	1.41	0.000175	232.5	257.0
9.00	5.00	6.50	19.00	59.7	0.000	0.000	1.41	0.000000	212.2	272.0
11.00	2.00	10.00	18.00	81.9	0.277	0.240	2.075	0.000257	204.2	286.1
13.00	2.00	12.00	18.00	98.3	0.277	0.240	2.075	0.000243	195.6	293.9
15.00	2.00	14.00	18.00	114.7	0.277	0.240	2.075	0.000237	186.8	301.4
17.00	2.00	16.00	19.00	147.0	0.277	0.240	2.075	0.000225	161.7	308.8
19.00	2.00	18.00	18.00	147.4	0.277	0.240	2.075	0.000224	168.5	315.9
21.00	2.00	20.00	18.00	163.8	0.353	0.038	2.22	0.000245	159.0	322.8
23.00	2.00	22.00	18.00	180.2	0.353	0.038	2.22	0.000235	149.3	329.5
25.00	2.00	24.00	18.00	196.6	0.353	0.038	2.22	0.000224	139.4	336.0
27.00	2.00	26.00	18.00	212.9	0.353	0.038	2.22	0.000222	129.4	342.3

Table C. 22. Consolidation settlement calculation for Km: 146+210

Depth (m)	Thickness of layer (m)	Consolidation settlement of layer (S) (m)	Cumulative consolidation settlement (Sc) (cm) (by C_c values)	Consolidation settlement of layer (S) (m)	Cumulative consolidation settlement (Sc) (cm) (by m_v values)
2.00	2.00	0.04 m	3.78 cm	0.09 m	9.06 cm
4.00	2.00	0.11 m	14.75 cm	0.08 m	17.20 cm
9.00	5.00	0.00 m	14.75 cm	0.00 m	17.20 cm
11.00	2.00	0.14 m	29.03 cm	0.11 m	27.70 cm
13.00	2.00	0.13 m	41.73 cm	0.10 m	37.21 cm
15.00	2.00	0.11 m	52.94 cm	0.09 m	46.06 cm
17.00	2.00	0.09 m	61.54 cm	0.07 m	53.34 cm
19.00	2.00	0.09 m	70.38 cm	0.08 m	60.88 cm
21.00	2.00	0.09 m	79.75 cm	0.08 m	68.66 cm
23.00	2.00	0.08 m	88.08 cm	0.07 m	75.68 cm
25.00	2.00	0.07 m	95.49 cm	0.06 m	81.92 cm
27.00	2.00	0.07 m	102.04 cm	0.06 m	87.66 cm

OCR vs. Depth (m) Graph

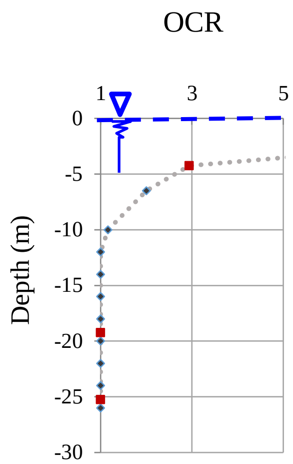

C.11 KM: 147+000 Section

The embankment height: 8.1 m

Total consolidation: 69.99 cm

Table C. 23. Consolidation settlement parameters for Km: 147+000

Depth (m)	Thickness of layer (m)	z (m)	Unit weight of soil (kN/m^3)	σ_0 (kPa)	C_c (Lab. Result)	C_r (Lab. Result)	$(1+e_0)$ (Lab. Result)	m_v (m^2/kN) (Lab)	$\Delta\sigma$ (kPa)	$\sigma_1 = \sigma_0+\Delta\sigma$
2.00	2.00	1.00	18.00	8.2	0.183	0.033	1.44	0.0002941	159.6	167.7
4.00	2.00	3.00	18.00	24.6	0.183	0.033	1.44	0.0002789	154.4	179.0
6.00	2.00	5.00	18.00	41.0	0.183	0.033	1.44	0.0002624	148.9	189.9
8.00	2.00	7.00	18.00	57.3	0.183	0.033	1.44	0.0002493	143.1	200.5
10.00	2.00	9.00	18.00	73.7	0.183	0.033	1.44	0.0002390	137.0	210.7
13.00	3.00	11.50	18.00	94.2	0.183	0.033	1.44	0.0002246	129.0	223.2
15.50	2.50	14.25	19.00	131.0	0.000	0.008	1.45	0.0000000	105.4	236.3
17.50	2.00	16.50	18.00	135.1	0.183	0.033	1.44	0.0002153	111.6	246.7
19.50	2.00	18.50	18.00	151.5	0.183	0.033	1.44	0.0002123	104.1	255.6
21.00	1.50	20.25	18.00	165.8	0.058	0.008	1.45	0.0001175	97.4	263.2
22.00	1.00	21.50	19.00	197.6	0.000	0.008	1.45	0.0001083	70.9	268.5
24.00	2.00	23.00	18.00	188.4	0.058	0.008	1.45	0.0001113	86.4	274.8
25.00	1.00	24.50	18.00	200.7	0.058	0.008	1.45	0.0001075	80.2	280.9
27.00	2.00	26.00	18.00	212.9	0.058	0.008	1.45	0.0001076	73.9	286.8
29.00	2.00	28.00	18.00	229.3	0.058	0.008	1.45	0.0001078	65.3	294.6
31.00	2.00	30.00	18.00	245.7	0.058	0.008	1.45	0.0001080	56.4	302.1
33.00	2.00	32.00	18.00	262.1	0.058	0.008	1.45	0.0001082	47.3	309.4
35.00	2.00	34.00	18.00	278.5	0.058	0.008	1.45	0.0001084	38.0	316.5
37.00	2.00	36.00	18.00	294.8	0.058	0.008	1.45	0.0001086	28.5	323.4
39.00	2.00	38.00	18.00	311.2	0.058	0.008	1.45	0.0001088	18.8	330.1
41.00	2.00	40.00	18.00	327.6	0.058	0.008	1.45	0.0001090	9.0	336.6
41.78	0.78	41.39	18.00	339.0	0.058	0.008	1.45	0.0001091	2.0	341.0

Table C. 24. Consolidation settlement calculation for Km: 147+000

Depth (m)	Thickness of layer (m)	Consolidation settlement of layer (S) (m)	Cumulative consolidation settlement (Sc) (cm) (by C_c values)	Consolidation settlement of layer (S) (m)	Cumulative consolidation settlement (Sc) (cm) (by m_v values)
2.00	2.00	0.08 m	7.65 cm	0.09 m	9.38 cm
4.00	2.00	0.06 m	13.82 cm	0.09 m	18.00 cm
6.00	2.00	0.06 m	19.63 cm	0.08 m	25.81 cm
8.00	2.00	0.09 m	28.42 cm	0.07 m	32.95 cm
10.00	2.00	0.09 m	37.25 cm	0.07 m	39.50 cm
13.00	3.00	0.14 m	51.54 cm	0.09 m	48.19 cm
15.50	2.50	0.00 m	51.54 cm	0.00 m	48.19 cm
17.50	2.00	0.05 m	56.10 cm	0.05 m	53.00 cm
19.50	2.00	0.05 m	60.83 cm	0.04 m	57.42 cm
21.00	1.50	0.01 m	61.98 cm	0.02 m	59.13 cm
22.00	1.00	0.00 m	61.98 cm	0.01 m	59.90 cm
24.00	2.00	0.01 m	63.29 cm	0.02 m	61.82 cm
25.00	1.00	0.01 m	63.88 cm	0.01 m	62.68 cm
27.00	2.00	0.01 m	64.91 cm	0.02 m	64.27 cm
29.00	2.00	0.01 m	65.78 cm	0.01 m	65.68 cm
31.00	2.00	0.01 m	66.50 cm	0.01 m	66.90 cm
33.00	2.00	0.01 m	67.08 cm	0.01 m	67.92 cm
35.00	2.00	0.00 m	67.52 cm	0.01 m	68.75 cm
37.00	2.00	0.00 m	67.84 cm	0.01 m	69.37 cm
39.00	2.00	0.00 m	68.05 cm	0.00 m	69.78 cm
41.00	2.00	0.00 m	68.14 cm	0.00 m	69.97 cm
41.78	0.78	0.00 m	68.15 cm	0.00 m	69.99 cm

OCR vs. Depth (m) Graph

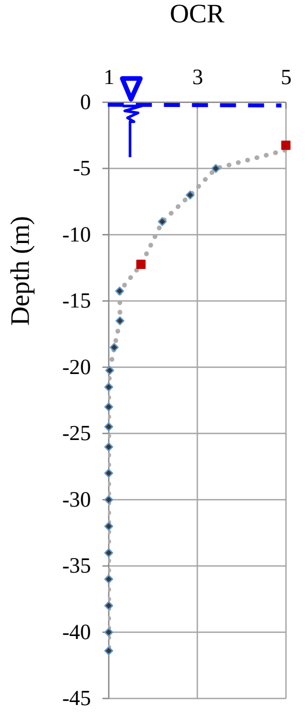

C.12 KM: 149+000 Section

The embankment height: 8.2 m

Total consolidation: 76.48 cm

Table C. 25. Consolidation settlement parameters for Km: 149+000

Depth (m)	Thickness of layer (m)	z (m)	Unit weight of soil (kN/m^3)	σ_0 (kPa)	C_c (Lab. Result)	C_r (Lab. Result)	$(1+e_0)$ (Lab. Result)	m_v (m^2/kN) (Lab)	$\Delta\sigma$ (kPa)	$\sigma_1 = \sigma_0+\Delta\sigma$
2.00	2.00	1.00	18.00	8.2	0.083	0.020	1.387	0.000240	161.5	169.7
4.00	2.00	3.00	18.00	24.6	0.083	0.020	1.387	0.000211	156.3	180.9
6.80	2.80	5.40	19.00	49.6	0.000	0.000	0	0.000000	144.2	193.9
10.00	3.20	8.40	18.00	68.8	0.183	0.017	1.41	0.000244	140.7	209.5
12.00	2.00	11.00	18.00	90.1	0.183	0.017	1.41	0.000236	132.3	222.4
14.00	2.00	13.00	18.00	106.5	0.183	0.017	1.41	0.000226	125.6	232.1
16.00	2.00	15.00	19.00	137.9	0.000	0.000	0	0.000000	103.6	241.4
17.80	1.80	16.90	18.00	138.4	0.183	0.017	1.41	0.000217	111.6	250.0
20.00	2.20	18.90	18.00	154.8	0.183	0.017	1.41	0.000213	104.1	258.9
22.00	2.00	21.00	18.00	172.0	0.646	0.091	2.558	0.000403	95.9	267.9
24.00	2.00	23.00	19.00	211.4	0.000	0.000	1.415	0.000000	64.8	276.2
27.20	3.20	25.60	18.00	209.7	0.646	0.091	2.558	0.000381	76.9	286.6
30.50	3.30	28.85	19.00	265.1	0.000	0.000	0	0.000000	34.0	299.1
32.74	2.24	31.62	18.00	259.0	0.646	0.091	2.558	0.000370	50.3	309.3
34.74	2.00	33.74	18.00	276.3	0.646	0.091	2.558	0.000372	40.5	316.8
36.74	2.00	35.74	18.00	292.7	0.646	0.091	2.558	0.000374	31.0	323.7
38.74	2.00	37.74	18.00	309.1	0.646	0.091	2.558	0.000377	21.3	330.4
40.74	2.00	39.74	18.00	325.5	0.646	0.091	2.558	0.000379	11.4	336.8
41.99	1.25	41.36	18.00	338.8	0.646	0.091	2.558	0.000381	3.2	342.0

Table C. 26. Consolidation settlement calculation for Km: 149+000

Depth (m)	Thickness of layer (m)	Consolidation settlement of layer (S) (m)	Cumulative consolidation settlement (Sc) (cm) (by C_c values)	Consolidation settlement of layer (S) (m)	Cumulative consolidation settlement (Sc) (cm) (by m_v values)
2.00	2.00	0.05 m	4.85 cm	0.08 m	7.74 cm
4.00	2.00	0.04 m	8.65 cm	0.07 m	14.33 cm
6.80	2.80	0.00 m	8.65 cm	0.00 m	14.33 cm
10.00	3.20	0.10 m	18.32 cm	0.11 m	25.32 cm
12.00	2.00	0.06 m	24.76 cm	0.06 m	31.56 cm
14.00	2.00	0.07 m	31.50 cm	0.06 m	37.23 cm
16.00	2.00	0.00 m	31.50 cm	0.00 m	37.23 cm
17.80	1.80	0.06 m	37.50 cm	0.04 m	41.59 cm
20.00	2.20	0.06 m	43.88 cm	0.05 m	46.48 cm
22.00	2.00	0.10 m	53.60 cm	0.08 m	54.22 cm
24.00	2.00	0.00 m	53.60 cm	0.00 m	54.22 cm
27.20	3.20	0.11 m	64.57 cm	0.09 m	63.59 cm
30.50	3.30	0.00 m	64.57 cm	0.00 m	63.59 cm
32.74	2.24	0.04 m	68.93 cm	0.04 m	67.75 cm
34.74	2.00	0.03 m	71.93 cm	0.03 m	70.77 cm
36.74	2.00	0.02 m	74.14 cm	0.02 m	73.09 cm
38.74	2.00	0.01 m	75.60 cm	0.02 m	74.69 cm
40.74	2.00	0.01 m	76.35 cm	0.01 m	75.55 cm
41.99	1.25	0.00 m	76.48 cm	0.00 m	75.70 cm

OCR vs. Depth (m) Graph

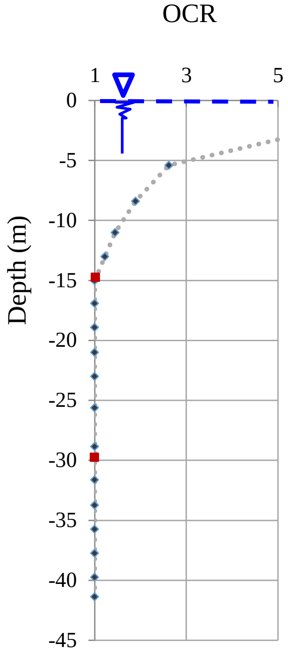

C.13 KM: 150+000 Section

The embankment height: 9.88 m

Total consolidation: 98.75 cm

Table C. 27. Consolidation settlement parameters for Km: 150+000

Depth (m)	Thickness of layer (m)	z (m)	Unit weight of soil (kN/m^3)	σ_0 (kPa)	C_c (Lab. Result)	C_r (Lab. Result)	$(1+e_0)$ (Lab. Result)	m_v (m^2/kN) (Lab)	$\Delta\sigma$ (kPa)	$\sigma_1 = \sigma_0+\Delta\sigma$
2.00	2.00	1.00	18.00	8.2	0.189	0.029	1.979	0.000314	194.6	202.8
3.00	1.00	2.50	18.00	20.5	0.189	0.029	1.979	0.000278	190.0	210.5
5.00	2.00	4.00	19.00	36.8	0.000	0.000	1.979	0.000000	181.3	218.0
7.00	2.00	6.00	18.00	49.1	0.094	0.021	1.37	0.000186	178.6	227.8
9.00	2.00	8.00	18.00	65.5	0.094	0.021	1.37	0.000156	171.7	237.3
11.00	2.00	10.00	18.00	81.9	0.094	0.021	1.37	0.000123	164.6	246.5
18.00	7.00	14.50	19.00	133.3	0.000	0.000	0	0.000000	132.9	266.2
20.00	2.00	19.00	18.00	155.6	0.083	0.017	1.39	0.000115	129.0	284.7
22.00	2.00	21.00	18.00	172.0	0.646	0.091	2.558	0.000392	120.5	292.5
24.00	2.00	23.00	18.00	188.4	0.646	0.091	2.558	0.000379	111.7	300.1
26.00	2.00	25.00	18.00	204.8	0.646	0.091	2.558	0.000369	102.7	307.4
28.00	2.00	27.00	18.00	221.1	0.646	0.091	2.558	0.000371	93.4	314.6
30.00	2.00	29.00	18.00	237.5	0.646	0.091	2.558	0.000373	84.0	321.5
32.00	2.00	31.00	18.00	253.9	0.646	0.091	2.558	0.000376	74.4	328.3
34.00	2.00	33.00	18.00	270.3	0.646	0.091	2.558	0.000378	64.5	334.8
36.00	2.00	35.00	18.00	286.7	0.646	0.091	2.558	0.000380	54.5	341.1
38.00	2.00	37.00	18.00	303.0	0.646	0.091	2.558	0.000383	44.3	347.3
40.00	2.00	39.00	18.00	319.4	0.646	0.091	2.558	0.000385	33.9	353.3
42.00	2.00	41.00	18.00	335.8	0.646	0.091	2.558	0.000387	23.3	359.1
44.00	2.00	43.00	18.00	352.2	0.646	0.091	2.558	0.000390	12.6	364.7
45.30	1.30	44.65	18.00	365.7	0.646	0.091	2.558	0.000392	3.6	369.3

Table C. 28. Consolidation settlement calculation for Km: 150+000

Depth (m)	Thickness of layer (m)	Consolidation settlement of layer (S) (m)	Cumulative consolidation settlement (Sc) (cm) (by C_c values)	Consolidation settlement of layer (S) (m)	Cumulative consolidation settlement (Sc) (cm) (by m_v values)
2.00	2.00	0.05 m	5.32 cm	0.12 m	12.21 cm
3.00	1.00	0.02 m	7.56 cm	0.05 m	17.49 cm
5.00	2.00	0.00 m	7.56 cm	0.00 m	17.49 cm
7.00	2.00	0.03 m	10.95 cm	0.07 m	24.12 cm
9.00	2.00	0.03 m	14.21 cm	0.05 m	29.48 cm
11.00	2.00	0.03 m	17.40 cm	0.04 m	33.54 cm
18.00	7.00	0.00 m	17.40 cm	0.00 m	33.54 cm
20.00	2.00	0.03 m	20.53 cm	0.03 m	36.49 cm
22.00	2.00	0.12 m	32.17 cm	0.09 m	45.94 cm
24.00	2.00	0.10 m	42.39 cm	0.08 m	54.40 cm
26.00	2.00	0.09 m	51.30 cm	0.08 m	61.97 cm
28.00	2.00	0.08 m	59.03 cm	0.07 m	68.90 cm
30.00	2.00	0.07 m	65.68 cm	0.06 m	75.18 cm
32.00	2.00	0.06 m	71.31 cm	0.06 m	80.76 cm
34.00	2.00	0.05 m	76.01 cm	0.05 m	85.64 cm
36.00	2.00	0.04 m	79.83 cm	0.04 m	89.78 cm
38.00	2.00	0.03 m	82.82 cm	0.03 m	93.17 cm
40.00	2.00	0.02 m	85.03 cm	0.03 m	95.78 cm
42.00	2.00	0.01 m	86.50 cm	0.02 m	97.59 cm
44.00	2.00	0.01 m	87.27 cm	0.01 m	98.57 cm
45.30	1.30	0.00 m	87.41 cm	0.00 m	98.75 cm

OCR vs. Depth (m) Graph

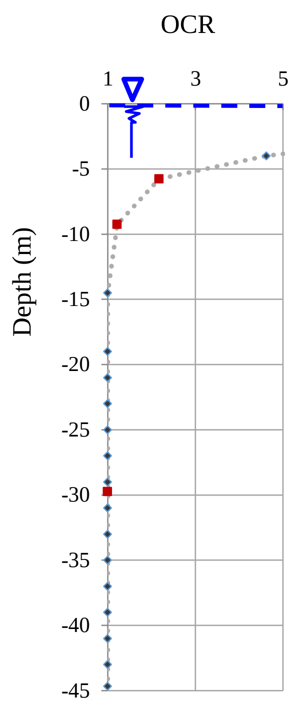

C.14 KM: 150+500 Section

The embankment height: 10.4 m

Total consolidation: 119.41 cm

Table C. 29. Consolidation settlement parameters for Km: 150+500

Depth (m)	Thickness of layer (m)	z (m)	Unit weight of soil (kN/m^3)	σ_0 (kPa)	C_c (Lab. Result)	C_r (Lab. Result)	$(1+e_0)$ (Lab. Result)	m_v (m^2/kN) (Lab)	$\Delta\sigma$ (kPa)	$\sigma_1 = \sigma_0+\Delta\sigma$
2.00	2.00	1.00	18.00	8.2	0.189	0.029	1.979	0.000304	205.1	213.3
4.00	2.00	3.00	18.00	24.6	0.189	0.029	1.979	0.000259	198.6	223.2
5.00	1.00	4.50	19.00	41.4	0.000	0.000	1.979	0.000000	189.0	230.4
6.00	1.00	5.50	18.00	45.0	0.094	0.021	1.37	0.000183	190.1	235.1
8.00	2.00	7.00	18.00	57.3	0.094	0.021	1.37	0.000166	184.8	242.1
10.00	2.00	9.00	18.00	73.7	0.094	0.021	1.37	0.000136	177.5	251.2
12.50	2.50	11.25	18.00	92.1	0.094	0.021	1.37	0.000099	168.9	261.1
15.50	3.00	14.00	19.00	128.7	0.000	0.000	1.37	0.000000	144.0	272.7
17.50	2.00	16.50	18.00	135.1	0.083	0.017	1.39	0.000121	147.7	282.9
19.50	2.00	18.50	18.00	151.5	0.083	0.017	1.39	0.000115	139.2	290.7
21.50	2.00	20.50	18.00	167.9	0.646	0.091	2.558	0.000393	130.5	298.4
23.50	2.00	22.50	18.00	184.3	0.646	0.091	2.558	0.000381	121.5	305.8
25.50	2.00	24.50	18.00	200.7	0.646	0.091	2.558	0.000368	112.3	313.0
27.50	2.00	26.50	18.00	217.0	0.646	0.091	2.558	0.000370	102.9	320.0
29.50	2.00	28.50	18.00	233.4	0.646	0.091	2.558	0.000373	93.3	326.7
31.50	2.00	30.50	18.00	249.8	0.646	0.091	2.558	0.000375	83.5	333.3
33.50	2.00	32.50	18.00	266.2	0.646	0.091	2.558	0.000377	73.6	339.7
35.50	2.00	34.50	18.00	282.6	0.646	0.091	2.558	0.000380	63.4	345.9
37.50	2.00	36.50	18.00	298.9	0.646	0.091	2.558	0.000382	53.0	352.0
39.50	2.00	38.50	18.00	315.3	0.646	0.091	2.558	0.000384	42.5	357.8
41.50	2.00	40.50	18.00	331.7	0.646	0.091	2.558	0.000387	31.8	363.5
43.50	2.00	42.50	18.00	348.1	0.646	0.091	2.558	0.000389	20.9	369.0
45.50	2.00	44.50	18.00	364.5	0.646	0.091	2.558	0.000392	9.9	374.3
46.20	0.70	45.85	18.00	375.5	0.646	0.091	2.558	0.000394	2.4	377.9

Table C. 30. Consolidation settlement calculation for Km: 150+500

Depth (m)	Thickness of layer (m)	Consolidation settlement of layer (S) (m)	Cumulative consolidation settlement (Sc) (cm) (by C_c values)	Consolidation settlement of layer (S) (m)	Cumulative consolidation settlement (Sc) (cm) (by m_v values)
2.00	2.00	0.06 m	5.74 cm	0.12 m	12.49 cm
4.00	2.00	0.05 m	10.46 cm	0.10 m	22.76 cm
5.00	1.00	0.00 m	10.46 cm	0.00 m	22.76 cm
6.00	1.00	0.02 m	12.31 cm	0.03 m	26.23 cm
8.00	2.00	0.04 m	15.87 cm	0.06 m	32.37 cm
10.00	2.00	0.03 m	19.30 cm	0.05 m	37.21 cm
12.50	2.50	0.04 m	23.52 cm	0.04 m	41.39 cm
15.50	3.00	0.00 m	23.52 cm	0.00 m	41.39 cm
17.50	2.00	0.04 m	27.35 cm	0.04 m	44.97 cm
19.50	2.00	0.03 m	30.73 cm	0.03 m	48.17 cm
21.50	2.00	0.13 m	43.34 cm	0.10 m	58.42 cm
23.50	2.00	0.11 m	54.45 cm	0.09 m	67.68 cm
25.50	2.00	0.10 m	64.20 cm	0.08 m	75.95 cm
27.50	2.00	0.09 m	72.72 cm	0.08 m	83.58 cm
29.50	2.00	0.07 m	80.09 cm	0.07 m	90.54 cm
31.50	2.00	0.06 m	86.42 cm	0.06 m	96.80 cm
33.50	2.00	0.05 m	91.77 cm	0.06 m	102.35 cm
35.50	2.00	0.04 m	96.21 cm	0.05 m	107.17 cm
37.50	2.00	0.04 m	99.80 cm	0.04 m	111.22 cm
39.50	2.00	0.03 m	102.57 cm	0.03 m	114.48 cm
41.50	2.00	0.02 m	104.58 cm	0.02 m	116.94 cm
43.50	2.00	0.01 m	105.86 cm	0.02 m	118.57 cm
45.50	2.00	0.01 m	106.44 cm	0.01 m	119.35 cm
46.20	0.70	0.00 m	106.49 cm	0.00 m	119.41 cm

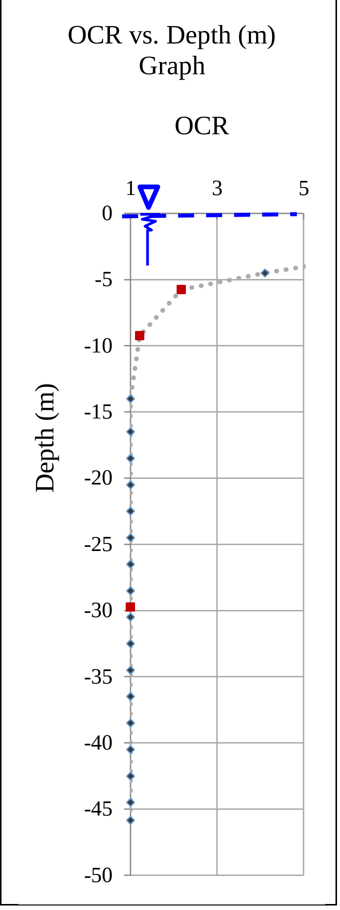

C.15 KM: 151+220 Section

The embankment height: 11.0 m

Total consolidation: 127.02 cm

Table C. 31. Consolidation settlement parameters for Km: 151+220

Depth (m)	Thickness of layer (m)	z (m)	Unit weight of soil (kN/m^3)	σ_0 (kPa)	C_c (Lab. Result)	C_r (Lab. Result)	(1+e_0) (Lab. Result)	m_v (m^2/kN) (Lab)	$\Delta\sigma$ (kPa)	$\sigma_1 = \sigma_0 + \Delta\sigma$
2.00	2.00	1.00	18.00	8.2	0.167	0.042	1.29	0.000307	216.7	224.9
4.00	2.00	3.00	18.00	24.6	0.167	0.042	1.29	0.000212	209.9	234.5
5.00	1.00	4.50	18.00	36.9	0.167	0.042	1.29	0.000132	204.6	241.4
8.00	3.00	6.50	19.00	59.7	0.000	0.000	0	0.000000	190.8	250.5
10.00	2.00	9.00	18.00	73.7	0.167	0.042	1.29	0.000036	187.8	261.5
12.00	2.00	11.00	18.00	90.1	0.167	0.042	1.29	0.000033	179.9	270.0
13.00	1.00	12.50	18.00	102.4	0.167	0.042	1.29	0.000031	173.8	276.2
16.00	3.00	14.50	19.00	133.3	0.000	0.000	0	0.000000	151.0	284.3
18.00	2.00	17.00	18.00	139.2	0.087	0.030	1.41	0.000134	154.8	294.0
20.00	2.00	19.00	18.00	155.6	0.087	0.030	1.41	0.000124	145.9	301.6
22.00	2.00	21.00	18.00	172.0	0.087	0.030	1.41	0.000114	136.9	308.9
24.00	2.00	23.00	18.00	188.4	0.087	0.030	1.41	0.000102	127.6	316.0
26.00	2.00	25.00	18.00	204.8	0.646	0.091	2.558	0.000369	118.1	322.9
28.00	2.00	27.00	18.00	221.1	0.646	0.091	2.558	0.000371	108.5	329.6
30.00	2.00	29.00	18.00	237.5	0.646	0.091	2.558	0.000373	98.6	336.1
32.00	2.00	31.00	18.00	253.9	0.646	0.091	2.558	0.000376	88.5	342.4
34.00	2.00	33.00	18.00	270.3	0.646	0.091	2.558	0.000378	78.3	348.5
36.00	2.00	35.00	18.00	286.7	0.646	0.091	2.558	0.000380	67.8	354.5
38.00	2.00	37.00	18.00	303.0	0.646	0.091	2.558	0.000383	57.2	360.2
40.00	2.00	39.00	18.00	319.4	0.646	0.091	2.558	0.000385	46.4	365.9
42.00	2.00	41.00	18.00	335.8	0.646	0.091	2.558	0.000387	35.5	371.3
44.00	2.00	43.00	18.00	352.2	0.646	0.091	2.558	0.000390	24.4	376.6
46.00	2.00	45.00	18.00	368.6	0.646	0.091	2.558	0.000392	13.2	381.7
47.31	1.31	46.65	18.00	382.1	0.646	0.091	2.558	0.000395	3.7	385.8

Table C. 32. Consolidation settlement calculation for Km: 151+220

Depth (m)	Thickness of layer (m)	Consolidation settlement of layer (S) (m)	Cumulative consolidation settlement (Sc) (cm) (by C_c values)	Consolidation settlement of layer (S) (m)	Cumulative consolidation settlement (Sc) (cm) (by m_v values)
2.00	2.00	0.15 m	15.01 cm	0.13 m	13.33 cm
4.00	2.00	0.12 m	27.39 cm	0.09 m	22.22 cm
5.00	1.00	0.06 m	33.17 cm	0.03 m	24.93 cm
8.00	3.00	0.00 m	33.17 cm	0.00 m	24.93 cm
10.00	2.00	0.10 m	43.66 cm	0.01 m	26.28 cm
12.00	2.00	0.10 m	53.95 cm	0.01 m	27.47 cm
13.00	1.00	0.05 m	59.04 cm	0.01 m	28.01 cm
16.00	3.00	0.00 m	59.04 cm	0.00 m	28.01 cm
18.00	2.00	0.04 m	63.05 cm	0.04 m	32.14 cm
20.00	2.00	0.04 m	66.59 cm	0.04 m	35.77 cm
22.00	2.00	0.03 m	69.73 cm	0.03 m	38.88 cm
24.00	2.00	0.03 m	72.50 cm	0.03 m	41.47 cm
26.00	2.00	0.10 m	82.49 cm	0.09 m	50.18 cm
28.00	2.00	0.09 m	91.25 cm	0.08 m	58.23 cm
30.00	2.00	0.08 m	98.86 cm	0.07 m	65.59 cm
32.00	2.00	0.07 m	105.42 cm	0.07 m	72.24 cm
34.00	2.00	0.06 m	111.00 cm	0.06 m	78.15 cm
36.00	2.00	0.05 m	115.66 cm	0.05 m	83.31 cm
38.00	2.00	0.04 m	119.45 cm	0.04 m	87.69 cm
40.00	2.00	0.03 m	122.43 cm	0.04 m	91.27 cm
42.00	2.00	0.02 m	124.64 cm	0.03 m	94.02 cm
44.00	2.00	0.01 m	126.11 cm	0.02 m	95.92 cm
46.00	2.00	0.01 m	126.88 cm	0.01 m	96.95 cm
47.31	1.31	0.00 m	127.02 cm	0.00 m	97.15 cm

OCR vs. Depth (m) Graph

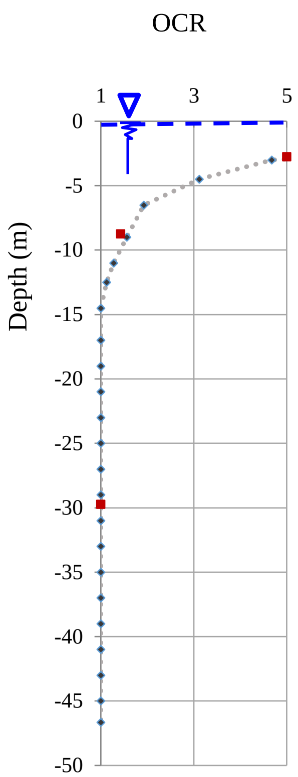

C.16 KM: 151+975 Section

The embankment height: 9.74 m

Total consolidation: 79.88 cm

Table C. 33. Consolidation settlement parameters for Km: 151+975

Depth (m)	Thickness of layer (m)	z (m)	Unit weight of soil (kN/m^3)	σ_0 (kPa)	C_c (Lab. Result)	C_r (Lab. Result)	$(1+e_0)$ (Lab. Result)	m_v (m^2/kN) (Lab)	$\Delta\sigma$ (kPa)	$\sigma_1 = \sigma_0+\Delta\sigma$
2.00	2.00	1.00	18.00	8.2	0.120	0.017	1.449	0.0002831	192.3	200.5
4.00	2.00	3.00	18.00	24.6	0.120	0.017	1.449	0.0002724	186.2	210.7
6.00	2.00	5.00	18.00	41.0	0.120	0.017	1.449	0.0002609	179.8	220.7
7.00	1.00	6.50	18.00	53.2	0.120	0.017	1.449	0.0002506	174.8	228.0
9.00	2.00	8.00	19.00	73.5	0.000	0.000	1.36	0.0000000	161.6	235.1
11.00	2.00	10.00	18.00	81.9	0.100	0.017	1.356	0.0002162	162.5	244.4
13.00	2.00	12.00	18.00	98.3	0.100	0.017	1.356	0.0001345	155.1	253.4
19.00	6.00	16.00	19.00	147.0	0.000	0.000	1.356	0.0000000	123.6	270.6
21.00	2.00	20.00	18.00	163.8	0.180	0.028	1.4	0.0001259	123.0	286.8
23.00	2.00	22.00	18.00	180.2	0.180	0.028	1.4	0.0002106	114.4	294.6
25.00	2.00	24.00	18.00	196.6	0.180	0.028	1.4	0.0002054	105.5	302.1
27.00	2.00	26.00	18.00	212.9	0.180	0.028	1.4	0.0002049	96.5	309.4
29.00	2.00	28.00	18.00	229.3	0.180	0.028	1.4	0.0002055	87.2	316.5
31.00	2.00	30.00	18.00	245.7	0.180	0.028	1.4	0.0002062	77.7	323.4
33.00	2.00	32.00	18.00	262.1	0.180	0.028	1.4	0.0002069	68.0	330.1
35.00	2.00	34.00	18.00	278.5	0.180	0.028	1.4	0.0002076	58.1	336.5
37.00	2.00	36.00	18.00	294.8	0.180	0.028	1.4	0.0002084	48.0	342.8
39.00	2.00	38.00	18.00	311.2	0.180	0.028	1.4	0.0002091	37.7	349.0
41.00	2.00	40.00	18.00	327.6	0.180	0.028	1.4	0.0002098	27.3	354.9
43.00	2.00	42.00	18.00	344.0	0.180	0.028	1.4	0.0002105	16.7	360.7
45.00	2.00	44.00	18.00	360.4	0.180	0.028	1.4	0.0002112	5.9	366.3

Table C. 34. Consolidation settlement calculation for Km: 151+975

Depth (m)	Thickness of layer (m)	Consolidation settlement of layer (S) (m)	Cumulative consolidation settlement (Sc) (cm) (by C_c values)	Consolidation settlement of layer (S) (m)	Cumulative consolidation settlement (Sc) (cm) (by m_v values)
2.00	2.00	0.08 m	7.55 cm	0.11 m	10.89 cm
4.00	2.00	0.07 m	14.35 cm	0.10 m	21.03 cm
6.00	2.00	0.07 m	20.95 cm	0.09 m	30.41 cm
7.00	1.00	0.03 m	24.24 cm	0.04 m	34.79 cm
9.00	2.00	0.00 m	24.24 cm	0.00 m	34.79 cm
11.00	2.00	0.07 m	31.24 cm	0.07 m	41.82 cm
13.00	2.00	0.06 m	37.31 cm	0.04 m	45.99 cm
19.00	6.00	0.00 m	37.31 cm	0.00 m	45.99 cm
21.00	2.00	0.06 m	43.56 cm	0.03 m	49.09 cm
23.00	2.00	0.05 m	49.05 cm	0.05 m	53.90 cm
25.00	2.00	0.05 m	53.85 cm	0.04 m	58.24 cm
27.00	2.00	0.04 m	58.02 cm	0.04 m	62.19 cm
29.00	2.00	0.04 m	61.62 cm	0.04 m	65.77 cm
31.00	2.00	0.03 m	64.69 cm	0.03 m	68.98 cm
33.00	2.00	0.03 m	67.27 cm	0.03 m	71.79 cm
35.00	2.00	0.02 m	69.38 cm	0.02 m	74.20 cm
37.00	2.00	0.02 m	71.07 cm	0.02 m	76.20 cm
39.00	2.00	0.01 m	72.34 cm	0.02 m	77.78 cm
41.00	2.00	0.01 m	73.24 cm	0.01 m	78.93 cm
43.00	2.00	0.01 m	73.77 cm	0.01 m	79.63 cm
45.00	2.00	0.00 m	73.95 cm	0.00 m	79.88 cm

OCR vs. Depth (m) Graph

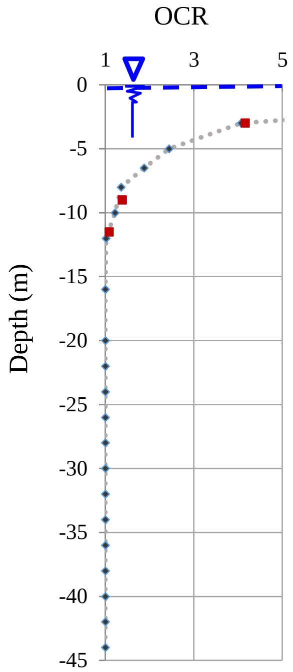

C.17 KM: 152+000 Section

The embankment height: 8.19 m

Total consolidation: 87.42 cm

Table C. 35. Consolidation settlement parameters for Km: 152+000

Depth (m)	Thickness of layer (m)	z (m)	Unit weight of soil (kN/m^3)	σ_0 (kPa)	C_c (Lab. Result)	C_r (Lab. Result)	$(1+e_0)$ (Lab. Result)	m_v (m^2/kN) (Lab)	$\Delta\sigma$ (kPa)	$\sigma_1 = \sigma_0+\Delta\sigma$
2.00	2.00	1.00	18.00	8.2	0.120	0.017	1.449	0.000297	161.3	169.5
4.00	2.00	3.00	18.00	24.6	0.120	0.017	1.449	0.000289	156.1	180.7
6.00	2.00	5.00	18.00	41.0	0.120	0.017	1.449	0.000281	150.6	191.6
7.00	1.00	6.50	18.00	53.2	0.120	0.017	1.449	0.000272	146.3	199.5
9.00	2.00	8.00	19.00	73.5	0.000	0.000	1.449	0.000000	133.7	207.2
11.00	2.00	10.00	18.00	81.9	0.180	0.028	1.4	0.000242	135.4	217.3
13.00	2.00	12.00	18.00	98.3	0.180	0.028	1.4	0.000233	128.8	227.1
19.00	6.00	16.00	19.00	147.0	0.180	0.028	1.4	0.000224	98.8	245.8
21.00	2.00	20.00	18.00	163.8	0.180	0.028	1.4	0.000218	99.7	263.5
23.00	2.00	22.00	18.00	180.2	0.180	0.028	1.4	0.000212	91.7	271.9
25.00	2.00	24.00	18.00	196.6	0.180	0.028	1.4	0.000206	83.5	280.1
27.00	2.00	26.00	18.00	212.9	0.242	0.035	1.47	0.000268	75.1	288.0
29.00	2.00	28.00	18.00	229.3	0.242	0.035	1.47	0.000270	66.4	295.8
31.00	2.00	30.00	18.00	245.7	0.242	0.035	1.47	0.000271	57.6	303.3
33.00	2.00	32.00	18.00	262.1	0.242	0.035	1.47	0.000272	48.4	310.5
35.00	2.00	34.00	18.00	278.5	0.242	0.035	1.47	0.000273	39.1	317.6
37.00	2.00	36.00	18.00	294.8	0.242	0.035	1.47	0.000274	29.6	324.4
39.00	2.00	38.00	18.00	311.2	0.242	0.035	1.47	0.000276	19.9	331.1
41.00	2.00	40.00	18.00	327.6	0.242	0.035	1.47	0.000277	10.0	337.6
41.97	0.97	41.48	18.00	339.8	0.242	0.035	1.47	0.000278	2.5	342.2

Table C. 36. Consolidation settlement calculation for Km: 152+000

Depth (m)	Thickness of layer (m)	Consolidation settlement of layer (S) (m)	Cumulative consolidation settlement (Sc) (cm) (by C_c values)	Consolidation settlement of layer (S) (m)	Cumulative consolidation settlement (Sc) (cm) (by m_v values)
2.00	2.00	0.06 m	5.76 cm	0.10 m	9.59 cm
4.00	2.00	0.05 m	10.86 cm	0.09 m	18.62 cm
6.00	2.00	0.05 m	15.85 cm	0.08 m	27.07 cm
7.00	1.00	0.03 m	18.37 cm	0.04 m	31.06 cm
9.00	2.00	0.00 m	18.37 cm	0.00 m	31.06 cm
11.00	2.00	0.09 m	27.38 cm	0.07 m	37.60 cm
13.00	2.00	0.09 m	36.73 cm	0.06 m	43.60 cm
19.00	6.00	0.17 m	53.95 cm	0.13 m	56.89 cm
21.00	2.00	0.05 m	59.26 cm	0.04 m	61.24 cm
23.00	2.00	0.05 m	63.86 cm	0.04 m	65.13 cm
25.00	2.00	0.04 m	67.81 cm	0.03 m	68.57 cm
27.00	2.00	0.04 m	72.13 cm	0.04 m	72.60 cm
29.00	2.00	0.04 m	75.77 cm	0.04 m	76.19 cm
31.00	2.00	0.03 m	78.78 cm	0.03 m	79.30 cm
33.00	2.00	0.02 m	81.21 cm	0.03 m	81.94 cm
35.00	2.00	0.02 m	83.09 cm	0.02 m	84.08 cm
37.00	2.00	0.01 m	84.45 cm	0.02 m	85.70 cm
39.00	2.00	0.01 m	85.34 cm	0.01 m	86.80 cm
41.00	2.00	0.00 m	85.77 cm	0.01 m	87.35 cm
41.97	0.97	0.00 m	85.82 cm	0.00 m	87.42 cm

OCR vs. Depth (m) Graph

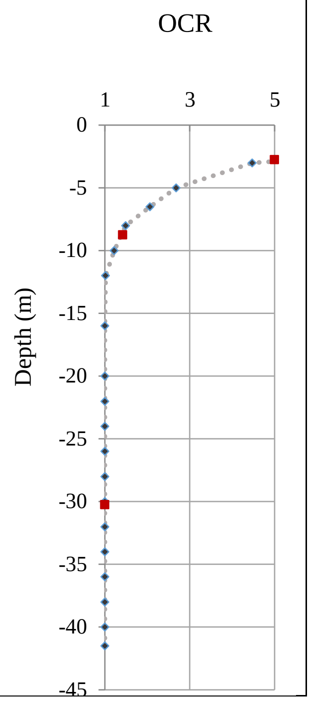

C.18 KM: 154+500 Section

The embankment height: 7.48 m

Total consolidation: 93.14 cm

Table C. 37. Consolidation settlement parameters for Km: 154+500

Depth (m)	Thickness of layer (m)	z (m)	Unit weight of soil (kN/m^3)	σ_0 (kPa)	C_c (Lab. Result)	C_r (Lab. Result)	$(1+e_0)$ (Lab. Result)	m_v (m^2/kN) (Lab)	$\Delta\sigma$ (kPa)	$\sigma_1 = \sigma_0+\Delta\sigma$
2.00	2.00	1.00	18.00	8.2	0.158	0.025	1.35	0.0003403	147.5	155.7
4.00	2.00	3.00	18.00	24.6	0.158	0.025	1.35	0.0003155	142.7	167.3
6.00	2.00	5.00	18.00	41.0	0.158	0.025	1.35	0.0002884	137.6	178.6
8.00	2.00	7.00	18.00	57.3	0.158	0.025	1.35	0.0002678	132.1	189.5
10.00	2.00	9.00	18.00	73.7	0.158	0.025	1.35	0.0002564	126.4	200.1
12.00	2.00	11.00	18.00	90.1	0.158	0.025	1.35	0.0002380	120.3	210.4
13.00	1.00	12.50	18.00	102.4	0.158	0.025	1.35	0.0002252	115.5	217.9
16.00	3.00	14.50	19.00	133.3	0.000	0.000	1.32	0.0000000	94.4	227.7
18.00	2.00	17.00	18.00	139.2	0.158	0.025	1.35	0.0002107	100.2	239.5
20.00	2.00	19.00	18.00	155.6	0.158	0.025	1.35	0.0002026	93.0	248.6
22.00	2.00	21.00	18.00	172.0	0.158	0.025	1.35	0.0004034	85.5	257.5
24.00	2.00	23.00	18.00	188.4	0.646	0.091	2.558	0.0003842	77.7	266.1
26.00	2.00	25.00	18.00	204.8	0.646	0.091	2.558	0.0003681	69.7	274.4
28.00	2.00	27.00	18.00	221.1	0.646	0.091	2.558	0.0003703	61.4	282.6
30.00	2.00	29.00	18.00	237.5	0.646	0.091	2.558	0.0003726	52.9	290.4
32.00	2.00	31.00	18.00	253.9	0.646	0.091	2.558	0.0003748	44.2	298.1
34.00	2.00	33.00	18.00	270.3	0.646	0.091	2.558	0.0003772	35.2	305.5
36.00	2.00	35.00	18.00	286.7	0.646	0.091	2.558	0.0003795	26.1	312.7
38.00	2.00	37.00	18.00	303.0	0.646	0.091	2.558	0.0003819	16.7	319.7
40.45	2.45	39.23	18.00	321.3	0.646	0.091	2.558	0.0003846	6.0	327.2

Table C. 38. Consolidation settlement calculation for Km: 154+500

Depth (m)	Thickness of layer (m)	Consolidation settlement of layer (S) (m)	Cumulative consolidation settlement (Sc) (cm) (by C_c values)	Consolidation settlement of layer (S) (m)	Cumulative consolidation settlement (Sc) (cm) (by m_v values)
2.00	2.00	0.07 m	6.97 cm	0.10 m	10.04 cm
4.00	2.00	0.06 m	12.90 cm	0.09 m	19.05 cm
6.00	2.00	0.06 m	18.67 cm	0.08 m	26.98 cm
8.00	2.00	0.06 m	24.50 cm	0.07 m	34.06 cm
10.00	2.00	0.06 m	30.48 cm	0.06 m	40.54 cm
12.00	2.00	0.06 m	36.65 cm	0.06 m	46.27 cm
13.00	1.00	0.04 m	40.49 cm	0.03 m	48.87 cm
16.00	3.00	0.00 m	40.49 cm	0.00 m	48.87 cm
18.00	2.00	0.06 m	46.00 cm	0.04 m	53.09 cm
20.00	2.00	0.05 m	50.76 cm	0.04 m	56.86 cm
22.00	2.00	0.04 m	54.86 cm	0.07 m	63.76 cm
24.00	2.00	0.08 m	62.44 cm	0.06 m	69.73 cm
26.00	2.00	0.06 m	68.86 cm	0.05 m	74.86 cm
28.00	2.00	0.05 m	74.24 cm	0.05 m	79.41 cm
30.00	2.00	0.04 m	78.65 cm	0.04 m	83.35 cm
32.00	2.00	0.04 m	82.17 cm	0.03 m	86.66 cm
34.00	2.00	0.03 m	84.86 cm	0.03 m	89.32 cm
36.00	2.00	0.02 m	86.77 cm	0.02 m	91.30 cm
38.00	2.00	0.01 m	87.94 cm	0.01 m	92.57 cm
40.45	2.45	0.00 m	88.44 cm	0.01 m	93.14 cm

OCR vs. Depth (m) Graph

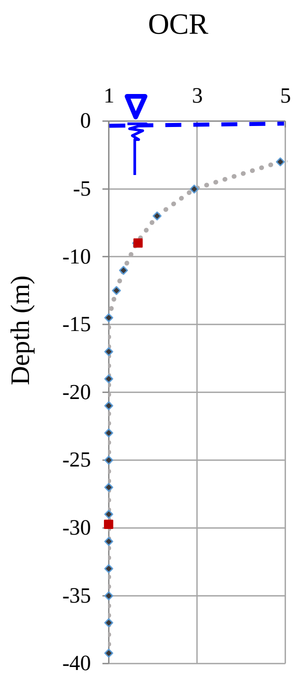

C.19 KM: 155+000 Section

The embankment height: 9.50 m

Total consolidation: 81.90 cm

Table C. 39. Consolidation settlement parameters for Km: 155+000

Depth (m)	Thickness of layer (m)	z (m)	Unit weight of soil (kN/m^3)	σ_0 (kPa)	C_c (Lab. Result)	C_r (Lab. Result)	$(1+e_0)$ (Lab. Result)	m_v (m^2/kN) (Lab)	$\Delta\sigma$ (kPa)	$\sigma_1 = \sigma_0+\Delta\sigma$
2.00	2.00	1.00	18.00	8.2	0.090	0.011	1.37	0.000186	187.1	195.3
3.00	1.00	2.50	18.00	20.5	0.090	0.011	1.37	0.000174	182.7	203.2
4.50	1.50	3.75	19.00	34.5	0.000	0.000	1.37	0.000000	175.1	209.6
6.50	2.00	5.50	18.00	45.0	0.090	0.011	1.37	0.000146	173.3	218.4
8.50	2.00	7.50	18.00	61.4	0.090	0.011	1.37	0.000139	166.7	228.1
10.00	1.50	9.25	18.00	75.8	0.090	0.011	1.37	0.000138	160.7	236.4
12.00	2.00	11.00	18.00	90.1	0.090	0.011	1.37	0.000136	154.4	244.5
20.00	8.00	16.00	19.00	147.0	0.000	0.000	1.37	0.000000	119.5	266.5
22.00	2.00	21.00	18.00	172.0	0.646	0.091	2.558	0.000393	114.9	286.9
24.00	2.00	23.00	18.00	188.4	0.646	0.091	2.558	0.000379	106.3	294.7
26.00	2.00	25.00	18.00	204.8	0.646	0.091	2.558	0.000368	97.4	302.2
28.00	2.00	27.00	18.00	221.1	0.646	0.091	2.558	0.000370	88.4	309.5
31.00	3.00	29.50	19.00	271.1	0.000	0.091	2.558	0.000377	47.2	318.3
33.00	2.00	32.00	18.00	262.1	0.646	0.091	2.558	0.000376	64.7	326.8
35.00	2.00	34.00	18.00	278.5	0.646	0.091	2.558	0.000378	54.9	333.4
37.00	2.00	36.00	18.00	294.8	0.646	0.091	2.558	0.000381	45.0	339.8
39.00	2.00	38.00	18.00	311.2	0.646	0.091	2.558	0.000383	34.8	346.0
41.00	2.00	40.00	18.00	327.6	0.646	0.091	2.558	0.000385	24.4	352.0
43.00	2.00	42.00	18.00	344.0	0.646	0.091	2.558	0.000388	13.9	357.9
44.59	1.59	43.79	18.00	358.7	0.646	0.091	2.558	0.000390	4.3	363.0

Table C. 40. Consolidation settlement calculation for Km: 155+000

Depth (m)	Thickness of layer (m)	Consolidation settlement of layer (S) (m)	Cumulative consolidation settlement (Sc) (cm) (by C_c values)	Consolidation settlement of layer (S) (m)	Cumulative consolidation settlement (Sc) (cm) (by m_v values)
2.00	2.00	0.04 m	4.45 cm	0.07 m	6.97 cm
3.00	1.00	0.02 m	6.46 cm	0.03 m	10.15 cm
4.50	1.50	0.00 m	6.46 cm	0.00 m	10.15 cm
6.50	2.00	0.04 m	10.36 cm	0.05 m	15.23 cm
8.50	2.00	0.04 m	14.29 cm	0.05 m	19.87 cm
10.00	1.50	0.03 m	17.28 cm	0.03 m	23.20 cm
12.00	2.00	0.04 m	21.33 cm	0.04 m	27.41 cm
20.00	8.00	0.00 m	21.33 cm	0.00 m	27.41 cm
22.00	2.00	0.11 m	32.56 cm	0.09 m	36.44 cm
24.00	2.00	0.10 m	42.37 cm	0.08 m	44.49 cm
26.00	2.00	0.09 m	50.91 cm	0.07 m	51.67 cm
28.00	2.00	0.07 m	58.28 cm	0.07 m	58.21 cm
31.00	3.00	0.00 m	58.28 cm	0.05 m	63.55 cm
33.00	2.00	0.05 m	63.13 cm	0.05 m	68.42 cm
35.00	2.00	0.04 m	67.08 cm	0.04 m	72.58 cm
37.00	2.00	0.03 m	70.19 cm	0.03 m	76.00 cm
39.00	2.00	0.02 m	72.51 cm	0.03 m	78.67 cm
41.00	2.00	0.02 m	74.09 cm	0.02 m	80.55 cm
43.00	2.00	0.01 m	74.96 cm	0.01 m	81.63 cm
44.59	1.59	0.00 m	75.17 cm	0.00 m	81.90 cm

OCR vs. Depth (m) Graph

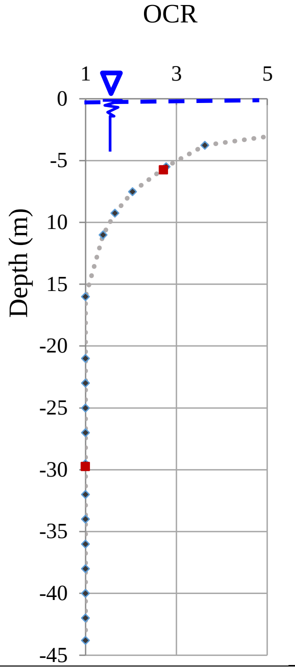

C.20 KM: 155+551 Section

The embankment height: 10.50 m

Total consolidation: 113.06 cm

Table C. 41. Consolidation setlement parameters for Km: 155+551

Depth (m)	Thickness of layer (m)	z (m)	Unit weight of soil (kN/m^3)	Effective Unit weight of soil (kN/m^3)	σ_0 (kPa)	C_c (Lab. Result)	C_r (Lab. Result)	$(1+e_0)$ (Lab. Result)	m_v (m^2/kN) (Lab)	$\Delta\sigma$ (kPa)	$\sigma_1 = \sigma_0+\Delta\sigma$
6.00	6.00	3.00	19.00	9.19	27.6	0.000	0.000	1.43	0.000000	200.3	227.8
8.00	2.00	7.00	18.00	8.19	63.3	0.141	0.035	1.43	0.000261	193.1	256.4
10.00	2.00	9.00	18.00	8.19	79.7	0.141	0.035	1.43	0.000248	187.5	267.2
12.00	2.00	11.00	18.00	8.19	96.1	0.141	0.035	1.43	0.000235	181.6	277.6
14.00	2.00	13.00	18.00	8.19	112.5	0.141	0.035	1.43	0.000224	175.3	287.8
16.00	2.00	15.00	18.00	8.19	128.9	0.141	0.035	1.43	0.000218	168.8	297.7
17.00	1.00	16.50	18.00	8.19	141.1	0.141	0.035	1.43	0.000213	163.8	304.9
19.50	2.50	18.25	19.00	9.19	156.7	0.000	0.000	1.43	0.000000	139.4	296.1
21.50	2.00	20.50	18.00	8.19	176.4	0.080	0.022	1.34	0.000127	149.5	325.9
23.50	2.00	22.50	18.00	8.19	192.8	0.080	0.022	1.34	0.000123	141.9	334.7
25.50	2.00	24.50	18.00	8.19	209.2	0.080	0.022	1.34	0.000119	134.1	343.3
27.50	2.00	26.50	18.00	8.19	225.5	0.646	0.091	2.558	0.000119	126.1	351.6
29.50	2.00	28.50	18.00	8.19	241.9	0.646	0.091	2.558	0.000372	117.8	359.7
31.50	2.00	30.50	18.00	8.19	258.3	0.646	0.091	2.558	0.000374	109.2	367.5
33.50	2.00	32.50	18.00	8.19	274.7	0.646	0.091	2.558	0.000377	100.4	375.1
35.50	2.00	34.50	18.00	8.19	291.1	0.646	0.091	2.558	0.000379	91.5	382.5
37.50	2.00	36.50	18.00	8.19	307.4	0.646	0.091	2.558	0.000381	82.3	389.7
39.50	2.00	38.50	18.00	8.19	323.8	0.646	0.091	2.558	0.000384	72.8	396.7
41.50	2.00	40.50	18.00	8.19	340.2	0.646	0.091	2.558	0.000386	63.2	403.4
43.50	2.00	42.50	18.00	8.19	356.6	0.646	0.091	2.558	0.000389	53.4	410.0
44.30	0.80	43.90	18.00	8.19	368.0	0.646	0.091	2.558	0.000390	46.4	414.5

Table C. 42. Consolidation setlement calculation for Km: 155+551

Depth (m)	Thickness of layer (m)	Consolidation settlement of layer (S) (m)	Cumulative consolidation settlement (Sc) (cm) (by C_c values)	Consolidation settlement of layer (S) (m)	Cumulative consolidation settlement (Sc) (cm) (by m_v values)
6.00	6.00	0.00 m	0.00 cm	0.00 m	0.00 cm
8.00	2.00	0.06 m	6.42 cm	0.10 m	9.87 cm
10.00	2.00	0.06 m	12.71 cm	0.09 m	18.97 cm
12.00	2.00	0.06 m	18.93 cm	0.08 m	27.28 cm
14.00	2.00	0.06 m	25.13 cm	0.08 m	35.04 cm
16.00	2.00	0.06 m	31.32 cm	0.07 m	42.29 cm
17.00	1.00	0.03 m	34.42 cm	0.03 m	45.73 cm
19.50	2.50	0.00 m	34.42 cm	0.00 m	45.73 cm
21.50	2.00	0.03 m	37.60 cm	0.04 m	49.46 cm
23.50	2.00	0.03 m	40.46 cm	0.03 m	52.89 cm
25.50	2.00	0.03 m	43.03 cm	0.03 m	56.09 cm
27.50	2.00	0.10 m	52.77 cm	0.03 m	59.11 cm
29.50	2.00	0.09 m	61.47 cm	0.09 m	67.90 cm
31.50	2.00	0.08 m	69.21 cm	0.08 m	76.10 cm
33.50	2.00	0.07 m	76.04 cm	0.08 m	83.69 cm
35.50	2.00	0.06 m	82.04 cm	0.07 m	90.64 cm
37.50	2.00	0.05 m	87.24 cm	0.06 m	96.93 cm
39.50	2.00	0.04 m	91.69 cm	0.06 m	102.54 cm
41.50	2.00	0.04 m	95.43 cm	0.05 m	107.44 cm
43.50	2.00	0.03 m	98.49 cm	0.04 m	111.60 cm
44.30	0.80	0.01 m	99.53 cm	0.01 m	113.06 cm

OCR vs. Depth (m) Graph

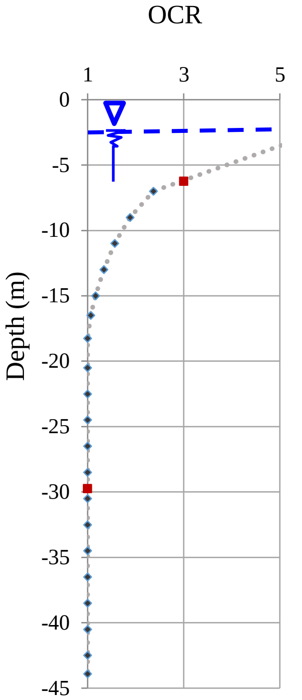

C.21 KM: 157+400 Section

The embankment height: 8.50 m

Total consolidation: 80.73 cm

Table C. 43. Consolidation settlement parameters for Km: 157+400

Depth (m)	Thickness of layer (m)	z (m)	Unit weight of soil (kN/m^3)	σ_0 (kPa)	C_c (Lab. Result)	C_r (Lab. Result)	$(1+e_0)$ (Lab. Result)	m_v (m^2/kN) (Lab)	$\Delta\sigma$ (kPa)	$\sigma_1 = \sigma_0+\Delta\sigma$
2.00	2.00	1.00	18.00	8.2	0.200	0.042	1.43	0.0002346	167.8	176.0
4.00	2.00	3.00	18.00	24.6	0.200	0.042	1.43	0.0002394	162.4	187.0
5.00	1.00	4.50	18.00	36.9	0.200	0.042	1.43	0.0002432	158.2	195.0
7.00	2.00	6.00	19.00	55.1	0.000	0.042	1.42	0.0000000	147.8	202.9
9.00	2.00	8.00	18.00	65.5	0.200	0.042	1.43	0.0002396	147.6	213.1
11.00	2.00	10.00	18.00	81.9	0.200	0.042	1.43	0.0002320	141.1	223.0
13.00	2.00	12.00	18.00	98.3	0.200	0.042	1.43	0.0002235	134.4	232.6
15.00	2.00	14.00	18.00	114.7	0.200	0.042	1.43	0.0002193	127.3	242.0
17.00	2.00	16.00	18.00	131.0	0.094	0.017	1.42	0.0001644	120.0	251.0
19.00	2.00	18.00	18.00	147.4	0.094	0.017	1.42	0.0001565	112.4	259.8
21.00	2.00	20.00	18.00	163.8	0.094	0.017	1.42	0.0001474	104.6	268.4
23.00	2.00	22.00	18.00	180.2	0.094	0.017	1.42	0.0001368	96.5	276.7
25.00	2.00	24.00	18.00	196.6	0.094	0.017	1.42	0.0001241	88.2	284.7
27.00	2.00	26.00	18.00	212.9	0.172	0.033	1.4	0.0002029	79.6	292.5
29.00	2.00	28.00	18.00	229.3	0.172	0.033	1.4	0.0002036	70.8	300.1
31.00	2.00	30.00	18.00	245.7	0.172	0.033	1.4	0.0002043	61.8	307.5
33.00	2.00	32.00	18.00	262.1	0.172	0.033	1.4	0.0002050	52.6	314.6
35.00	2.00	34.00	18.00	278.5	0.172	0.033	1.4	0.0002056	43.1	321.6
37.00	2.00	36.00	18.00	294.8	0.172	0.033	1.4	0.0002063	33.5	328.3
39.00	2.00	38.00	18.00	311.2	0.172	0.033	1.4	0.0002070	23.6	334.8
41.00	2.00	40.00	18.00	327.6	0.172	0.033	1.4	0.0002077	13.6	341.2
42.65	1.65	41.83	18.00	342.5	0.172	0.033	1.4	0.0002084	4.3	346.8

Table C. 44. Consolidation settlement calculation for Km: 157+400

Depth (m)	Thickness of layer (m)	Consolidation settlement of layer (S) (m)	Cumulative consolidation settlement (Sc) (cm) (by C_c values)	Consolidation settlement of layer (S) (m)	Cumulative consolidation settlement (Sc) (cm) (by m_v values)
2.00	2.00	0.08 m	8.16 cm	0.08 m	7.87 cm
4.00	2.00	0.06 m	14.25 cm	0.08 m	15.65 cm
5.00	1.00	0.03 m	17.04 cm	0.04 m	19.50 cm
7.00	2.00	0.00 m	17.04 cm	0.00 m	19.50 cm
9.00	2.00	0.09 m	25.56 cm	0.07 m	26.57 cm
11.00	2.00	0.09 m	34.06 cm	0.07 m	33.12 cm
13.00	2.00	0.09 m	42.61 cm	0.06 m	39.13 cm
15.00	2.00	0.09 m	51.69 cm	0.06 m	44.71 cm
17.00	2.00	0.04 m	55.42 cm	0.04 m	48.65 cm
19.00	2.00	0.03 m	58.68 cm	0.04 m	52.17 cm
21.00	2.00	0.03 m	61.52 cm	0.03 m	55.26 cm
23.00	2.00	0.02 m	63.99 cm	0.03 m	57.90 cm
25.00	2.00	0.02 m	66.12 cm	0.02 m	60.08 cm
27.00	2.00	0.03 m	69.51 cm	0.03 m	63.31 cm
29.00	2.00	0.03 m	72.38 cm	0.03 m	66.20 cm
31.00	2.00	0.02 m	74.77 cm	0.03 m	68.72 cm
33.00	2.00	0.02 m	76.72 cm	0.02 m	70.88 cm
35.00	2.00	0.02 m	78.26 cm	0.02 m	72.65 cm
37.00	2.00	0.01 m	79.41 cm	0.01 m	74.03 cm
39.00	2.00	0.01 m	80.19 cm	0.01 m	75.01 cm
41.00	2.00	0.00 m	80.62 cm	0.01 m	75.57 cm
42.65	1.65	0.00 m	80.73 cm	0.00 m	75.72 cm

OCR vs. Depth (m) Graph

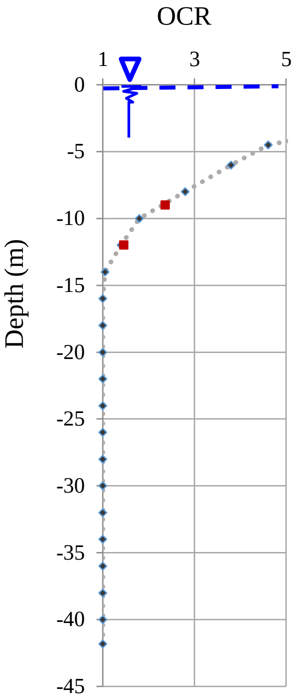

C.22 KM: 158+000 Section

The embankment height: 8.79 m

Total consolidation: 72.02 cm

Table C. 45. Consolidation settlement parameters for Km: 158+000

Depth (m)	Thickness of layer (m)	z (m)	Unit weight of soil (kN/m^3)	σ_0 (kPa)	C_c (Lab. Result)	C_r (Lab. Result)	$(1+e_0)$ (Lab. Result)	m_v (m^2/kN) (Lab)	$\Delta\sigma$ (kPa)	$\sigma_1 = \sigma_0+\Delta\sigma$
2.00	2.00	1.00	18.00	8.2	0.120	0.031	1.43	0.0001498	173.2	181.3
4.00	2.00	3.00	18.00	24.6	0.000	0.000	1.43	0.0000000	167.6	192.2
6.00	2.00	5.00	18.00	41.0	0.120	0.031	1.43	0.0001581	161.7	202.7
7.50	1.50	6.75	18.00	55.3	0.120	0.031	1.43	0.0001596	156.4	211.7
9.00	1.50	8.25	19.00	75.8	0.000	0.000	1.43	0.0000000	143.3	219.1
11.00	2.00	10.00	18.00	81.9	0.200	0.042	1.43	0.0002230	145.8	227.7
13.00	2.00	12.00	18.00	98.3	0.200	0.042	1.43	0.0002151	138.9	237.2
15.00	2.00	14.00	18.00	114.7	0.200	0.042	1.43	0.0002108	131.7	246.4
17.00	2.00	16.00	18.00	131.0	0.200	0.042	1.43	0.0002068	124.3	255.3
18.00	1.00	17.50	18.00	143.3	0.200	0.042	1.43	0.0002037	118.5	261.8
19.50	1.50	18.75	19.00	172.3	0.000	0.000	1.4	0.0000000	94.8	267.2
21.50	2.00	20.50	18.00	167.9	0.200	0.042	1.43	0.0001971	106.6	274.5
22.50	1.00	22.00	18.00	180.2	0.200	0.042	1.43	0.0001936	100.4	280.6
24.00	1.50	23.25	19.00	213.7	0.000	0.000	1.4	0.0000000	71.9	285.6
26.00	2.00	25.00	18.00	204.8	0.172	0.033	1.4	0.0001878	87.6	292.4
28.00	2.00	27.00	18.00	221.1	0.172	0.033	1.4	0.0002032	78.8	300.0
30.00	2.00	29.00	18.00	237.5	0.172	0.033	1.4	0.0002039	69.8	307.3
32.00	2.00	31.00	18.00	253.9	0.172	0.033	1.4	0.0002046	60.6	314.5
34.00	2.00	33.00	18.00	270.3	0.172	0.033	1.4	0.0002053	51.2	321.4
36.00	2.00	35.00	18.00	286.7	0.172	0.033	1.4	0.0002060	41.5	328.2
38.00	2.00	37.00	18.00	303.0	0.172	0.033	1.4	0.0002067	31.7	334.7
40.00	2.00	39.00	18.00	319.4	0.172	0.033	1.4	0.0002074	21.7	341.1
42.00	2.00	41.00	18.00	335.8	0.172	0.033	1.4	0.0002081	11.5	347.2
43.20	1.20	42.60	18.00	348.9	0.172	0.033	1.4	0.0002087	3.2	352.0

Table C. 46. Consolidation settlement calculation for Km: 158+000

Depth (m)	Thickness of layer (m)	Consolidation settlement of layer (S) (m)	Cumulative consolidation settlement (Sc) (cm) (by C_c values)	Consolidation settlement of layer (S) (m)	Cumulative consolidation settlement (Sc) (cm) (by m_v values)
2.00	2.00	0.06 m	5.87 cm	0.05 m	5.19 cm
4.00	2.00	0.00 m	5.87 cm	0.00 m	5.19 cm
6.00	2.00	0.04 m	9.53 cm	0.05 m	10.30 cm
7.50	1.50	0.03 m	12.08 cm	0.04 m	14.04 cm
9.00	1.50	0.00 m	12.08 cm	0.00 m	14.04 cm
11.00	2.00	0.07 m	19.35 cm	0.07 m	20.55 cm
13.00	2.00	0.07 m	26.66 cm	0.06 m	26.52 cm
15.00	2.00	0.07 m	34.03 cm	0.06 m	32.07 cm
17.00	2.00	0.08 m	42.14 cm	0.05 m	37.21 cm
18.00	1.00	0.04 m	45.80 cm	0.02 m	39.62 cm
19.50	1.50	0.00 m	45.80 cm	0.00 m	39.62 cm
21.50	2.00	0.06 m	51.77 cm	0.04 m	43.83 cm
22.50	1.00	0.03 m	54.46 cm	0.02 m	45.77 cm
24.00	1.50	0.00 m	54.46 cm	0.00 m	45.77 cm
26.00	2.00	0.04 m	58.26 cm	0.03 m	49.06 cm
28.00	2.00	0.03 m	61.51 cm	0.03 m	52.26 cm
30.00	2.00	0.03 m	64.26 cm	0.03 m	55.11 cm
32.00	2.00	0.02 m	66.55 cm	0.02 m	57.59 cm
34.00	2.00	0.02 m	68.40 cm	0.02 m	59.69 cm
36.00	2.00	0.01 m	69.84 cm	0.02 m	61.40 cm
38.00	2.00	0.01 m	70.90 cm	0.01 m	62.71 cm
40.00	2.00	0.01 m	71.60 cm	0.01 m	63.61 cm
42.00	2.00	0.00 m	71.96 cm	0.00 m	64.09 cm
43.20	1.20	0.00 m	72.02 cm	0.00 m	64.17 cm

OCR vs. Depth (m) Graph

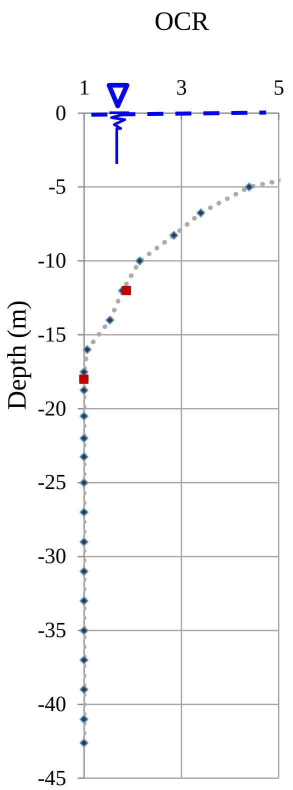

C.23 KM: 159+565 Section

The embankment height: 7.2 m

Total consolidation: 72.79 cm

Table C. 47. Consolidation settlement parameters for Km: 159+565

Depth (m)	Thickness of layer (m)	z (m)	Unit weight of soil (kN/m^3)	Effective Unit weight of soil (kN/m^3)	σ_0 (kPa)	C_c (Lab. Result)	C_r (Lab. Result)	$(1+e_0)$ (Lab. Result)	m_v (m^2/kN) (Lab)	$\Delta\sigma$ (kPa)	$\sigma_1 = \sigma_0+\Delta\sigma$
7.50	7.50	3.75	19.00	9.19	34.5	0.000	0.000	1.5	0.000000	135.5	169.9
9.50	2.00	8.50	18.00	8.19	77.1	0.166	0.040	1.5	0.000267	130.9	208.0
11.50	2.00	10.50	18.00	8.19	93.5	0.166	0.040	1.5	0.000259	126.8	220.3
12.50	1.00	12.00	18.00	8.19	105.8	0.166	0.040	1.5	0.000252	123.4	229.2
13.50	1.00	13.00	19.00	9.19	114.5	0.000	0.000	1.5	0.000000	108.1	222.6
15.50	2.00	14.50	18.00	8.19	127.3	0.220	0.017	1.42	0.000244	117.4	244.7
17.50	2.00	16.50	18.00	8.19	143.6	0.220	0.017	1.42	0.000191	112.3	255.9
19.50	2.00	18.50	18.00	8.19	160.0	0.220	0.017	1.42	0.000185	106.7	266.8
21.50	2.00	20.50	18.00	8.19	176.4	0.150	0.019	1.26	0.000177	100.9	277.3
23.50	2.00	22.50	18.00	8.19	192.8	0.150	0.019	1.26	0.000168	94.8	287.6
25.50	2.00	24.50	18.00	8.19	209.2	0.646	0.091	2.558	0.000368	88.4	297.5
27.50	2.00	26.50	18.00	8.19	225.5	0.646	0.091	2.558	0.000370	81.6	307.2
29.50	2.00	28.50	18.00	8.19	241.9	0.646	0.091	2.558	0.000372	74.6	316.6
31.50	2.00	30.50	18.00	8.19	258.3	0.646	0.091	2.558	0.000374	67.4	325.7
33.50	2.00	32.50	18.00	8.19	274.7	0.646	0.091	2.558	0.000377	59.8	334.5
35.50	2.00	34.50	18.00	8.19	291.1	0.646	0.091	2.558	0.000379	52.0	343.1
37.50	2.00	36.50	18.00	8.19	307.4	0.646	0.091	2.558	0.000381	44.0	351.4
37.95	0.45	37.73	18.00	8.19	317.5	0.646	0.091	2.558	0.000383	38.9	356.4

Table C. 48. Consolidation settlement calculation for Km: 159+565

Depth (m)	Thickness of layer (m)	Consolidation settlement of layer (S) (m)	Cumulative consolidation settlement (Sc) (cm) (by C_c values)	Consolidation settlement of layer (S) (m)	Cumulative consolidation settlement (Sc) (cm) (by m_v values)
7.50	7.50	0.00 m	0.00 cm	0.00 m	0.00 cm
9.50	2.00	0.07 m	6.95 cm	0.07 m	6.87 cm
11.50	2.00	0.07 m	14.00 cm	0.06 m	13.30 cm
12.50	1.00	0.04 m	17.57 cm	0.03 m	16.36 cm
13.50	1.00	0.00 m	17.57 cm	0.00 m	16.36 cm
15.50	2.00	0.03 m	20.75 cm	0.06 m	21.97 cm
17.50	2.00	0.04 m	24.41 cm	0.04 m	26.17 cm
19.50	2.00	0.04 m	28.52 cm	0.04 m	30.02 cm
21.50	2.00	0.04 m	32.07 cm	0.03 m	33.50 cm
23.50	2.00	0.04 m	35.87 cm	0.03 m	36.59 cm
25.50	2.00	0.08 m	43.60 cm	0.07 m	43.11 cm
27.50	2.00	0.07 m	50.38 cm	0.06 m	49.17 cm
29.50	2.00	0.06 m	56.28 cm	0.06 m	54.74 cm
31.50	2.00	0.05 m	61.36 cm	0.05 m	59.80 cm
33.50	2.00	0.04 m	65.68 cm	0.05 m	64.32 cm
35.50	2.00	0.04 m	69.29 cm	0.04 m	68.27 cm
37.50	2.00	0.03 m	72.22 cm	0.03 m	71.63 cm
37.95	0.45	0.01 m	72.79 cm	0.01 m	72.31 cm

OCR vs. Depth (m) Graph

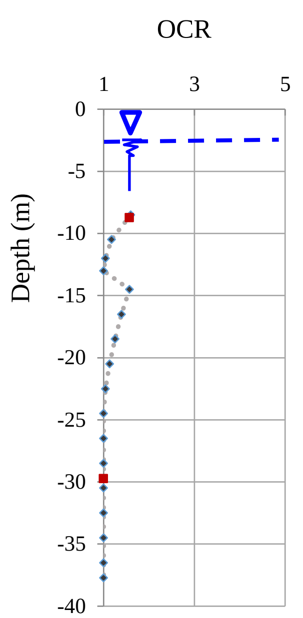

C.24 KM: 161+764 Section

The embankment height: 6.5 m

Total consolidation: 58.90 cm

Table C. 49. Consolidation settlement parameters for Km: 161+764

Depth (m)	Thickness of layer (m)	z (m)	Unit weight of soil (kN/m^3)	Effective Unit weight of soil (kN/m^3)	σ_0 (kPa)	C_c (Lab. Result)	C_r (Lab. Result)	$(1+e_0)$ (Lab. Result)	m_v (m^2/kN) (Lab)	$\Delta\sigma$ (kPa)	$\sigma_1 = \sigma_0+\Delta\sigma$
4.00	4.00	2.00	19.00	9.19	18.4	0.000	0.000	1.55	0.000000	125.9	144.3
6.00	2.00	5.00	18.00	8.19	45.0	0.116	0.016	1.55	0.000137	124.0	169.0
9.00	3.00	7.50	19.00	9.19	66.9	0.000	0.000	1.55	0.000000	112.6	179.5
11.00	2.00	10.00	18.00	8.19	88.9	0.116	0.016	1.55	0.000156	115.6	204.5
19.00	8.00	15.00	19.00	9.19	133.9	0.000	0.000	1.55	0.000000	89.8	223.6
21.00	2.00	20.00	18.00	8.19	178.8	0.646	0.091	2.558	0.000401	91.9	270.7
23.00	2.00	22.00	18.00	8.19	195.2	0.646	0.091	2.558	0.000386	86.1	281.3
25.00	2.00	24.00	18.00	8.19	211.6	0.646	0.091	2.558	0.000371	80.1	291.6
27.00	2.00	26.00	18.00	8.19	227.9	0.646	0.091	2.558	0.000369	73.7	301.6
29.00	2.00	28.00	18.00	8.19	244.3	0.646	0.091	2.558	0.000371	67.0	311.4
31.00	2.00	30.00	18.00	8.19	260.7	0.646	0.091	2.558	0.000374	60.1	320.8
33.00	2.00	32.00	18.00	8.19	277.1	0.646	0.091	2.558	0.000376	52.9	330.0
35.00	2.00	34.00	18.00	8.19	293.5	0.646	0.091	2.558	0.000378	45.4	338.9
36.34	2.00	35.67	18.00	8.19	309.8	0.646	0.091	2.558	0.000380	39.0	348.8
36.34	1.14	36.34	18.00	8.19	322.7	0.646	0.091	2.558	0.000381	36.3	359.0

Table C. 50. Consolidation settlement calculation for Km: 161+764

Depth (m)	Thickness of layer (m)	Consolidation settlement of layer (S) (m)	Cumulative consolidation settlement (Sc) (cm) (by C_c values)	Consolidation settlement of layer (S) (m)	Cumulative consolidation settlement (Sc) (cm) (by m_v values)
4.00	4.00	0.00 m	0.00 cm	0.00 m	0.00 cm
6.00	2.00	0.04 m	3.59 cm	0.03 m	3.40 cm
9.00	3.00	0.00 m	3.59 cm	0.00 m	3.40 cm
11.00	2.00	0.04 m	7.81 cm	0.04 m	7.00 cm
19.00	8.00	0.00 m	7.81 cm	0.00 m	7.00 cm
21.00	2.00	0.09 m	16.91 cm	0.07 m	14.36 cm
23.00	2.00	0.08 m	24.93 cm	0.07 m	21.01 cm
25.00	2.00	0.07 m	31.97 cm	0.06 m	26.95 cm
27.00	2.00	0.06 m	38.11 cm	0.05 m	32.39 cm
29.00	2.00	0.05 m	43.43 cm	0.05 m	37.37 cm
31.00	2.00	0.05 m	47.98 cm	0.04 m	41.87 cm
33.00	2.00	0.04 m	51.81 cm	0.04 m	45.84 cm
35.00	2.00	0.03 m	54.97 cm	0.03 m	49.28 cm
36.34	2.00	0.03 m	57.57 cm	0.03 m	52.24 cm
36.34	1.14	0.01 m	58.90 cm	0.02 m	53.82 cm

OCR vs. Depth (m) Graph

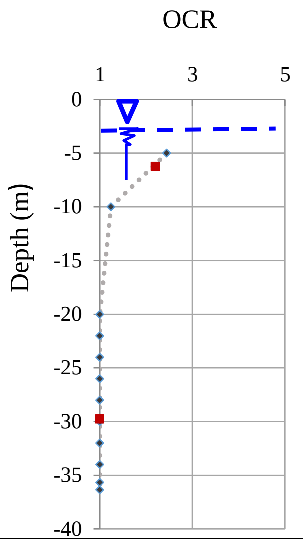

C.25 KM: 162+555 Section

The embankment height: 9.20 m

Total consolidation: 80.55 cm

Table C. 51. Consolidation settlement parameters for Km: 162+555

Depth (m)	Thickness of layer (m)	z (m)	Unit weight of soil (kN/m^3)	Effective Unit weight of soil (kN/m^3)	σ_0 (kPa)	C_c (Lab. Result)	C_r (Lab. Result)	$(1+e_0)$ (Lab. Result)	m_v (m^2/kN) (Lab)	$\Delta\sigma$ (kPa)	$\sigma_1 = \sigma_0+\Delta\sigma$
2.00	2.00	1.00	18.00	18.00	18.0	0.071	0.009	1.38	0.000240	181.2	199.2
4.50	2.50	3.25	19.00	9.19	47.5	0.000	0.000	1.38	0.000000	171.5	218.9
6.50	2.00	5.50	18.00	8.19	67.2	0.071	0.009	1.38	0.000164	167.8	235.0
8.00	1.50	7.25	19.00	9.19	82.2	0.000	0.000	1.38	0.000000	154.9	237.2
10.00	2.00	9.00	18.00	8.19	97.3	0.175	0.017	1.45	0.000271	156.3	253.6
12.50	2.50	11.25	18.00	8.19	115.8	0.175	0.017	1.45	0.000251	148.4	264.2
16.50	4.00	14.50	19.00	9.19	144.4	0.000	0.000	1.45	0.000000	122.0	266.4
18.50	2.00	17.50	18.00	8.19	170.9	0.646	0.091	2.558	0.000399	124.8	295.8
20.50	2.00	19.50	18.00	8.19	187.3	0.646	0.091	2.558	0.000390	116.7	304.1
22.50	2.00	21.50	18.00	8.19	203.7	0.646	0.091	2.558	0.000382	108.4	312.1
24.50	2.00	23.50	18.00	8.19	220.1	0.646	0.091	2.558	0.000372	99.9	319.9
26.50	2.00	25.50	18.00	8.19	236.5	0.646	0.091	2.558	0.000369	91.1	327.5
28.50	2.00	27.50	18.00	8.19	252.8	0.646	0.091	2.558	0.000371	82.1	334.9

Table C. 52. Consolidation settlement calculation for Km: 162+555

Depth (m)	Thickness of layer (m)	Consolidation settlement of layer (S) (m)	Cumulative consolidation settlement (Sc) (cm) (by C_c values)	Consolidation settlement of layer (S) (m)	Cumulative consolidation settlement (Sc) (cm) (by m_v values)
2.00	2.00	0.04 m	3.66 cm	0.08 m	8.05 cm
4.50	2.50	0.00 m	3.66 cm	0.00 m	8.05 cm
6.50	2.00	0.04 m	7.32 cm	0.05 m	12.80 cm
8.00	1.50	0.00 m	7.32 cm	0.00 m	12.80 cm
10.00	2.00	0.09 m	16.20 cm	0.08 m	20.44 cm
12.50	2.50	0.11 m	27.02 cm	0.09 m	29.18 cm
16.50	4.00	0.00 m	27.02 cm	0.00 m	29.18 cm
18.50	2.00	0.12 m	39.04 cm	0.10 m	38.76 cm
20.50	2.00	0.11 m	49.67 cm	0.09 m	47.51 cm
22.50	2.00	0.09 m	59.03 cm	0.08 m	55.49 cm
24.50	2.00	0.08 m	67.23 cm	0.07 m	62.88 cm
26.50	2.00	0.07 m	74.38 cm	0.07 m	69.66 cm
28.50	2.00	0.06 m	80.55 cm	0.06 m	75.81 cm

OCR vs. Depth (m) Graph

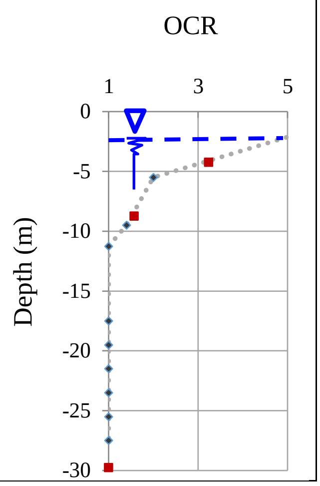

C.26 KM: 163+000 Section

The embankment height: 8.50 m

Total consolidation: 82.25 cm

Table C. 53. Consolidation settlement parameters for Km: 163+000

Depth (m)	Thickness of layer (m)	z (m)	Unit weight of soil (kN/m^3)	Effective Unit weight of soil (kN/m^3)	σ_0 (kPa)	C_c (Lab. Result)	C_r (Lab. Result)	$(1+e_0)$ (Lab. Result)	m_v (m^2/kN) (Lab)	$\Delta\sigma$ (kPa)	$\sigma_1 = \sigma_0+\Delta\sigma$
2.00	2.00	1.00	19.00	19.00	19.0	0.000	0.000	1.39	0.000000	167.4	186.4
4.00	2.00	3.00	18.00	8.19	46.2	0.108	0.009	1.39	0.000228	165.0	211.2
6.00	2.00	5.00	18.00	8.19	62.6	0.108	0.009	1.39	0.000239	161.2	223.8
8.00	2.00	7.00	18.00	8.19	79.0	0.108	0.009	1.39	0.000236	157.0	236.0
10.00	2.00	9.00	18.00	8.19	95.3	0.108	0.009	1.39	0.000222	152.5	247.8
12.00	2.00	11.00	18.00	8.19	111.7	0.108	0.009	1.39	0.000207	147.6	259.3
14.00	2.00	13.00	18.00	8.19	128.1	0.214	0.022	1.43	0.000474	142.4	270.5
16.00	2.00	15.00	18.00	8.19	144.5	0.214	0.022	1.43	0.000468	136.8	281.3
18.00	2.00	17.00	18.00	8.19	160.9	0.137	0.014	1.38	0.000192	131.0	291.8
20.00	2.00	19.00	18.00	8.19	177.2	0.137	0.014	1.38	0.000185	124.8	302.0
22.00	2.00	21.00	18.00	8.19	193.6	0.137	0.014	1.38	0.000177	118.3	311.9
24.00	2.00	23.00	18.00	8.19	210.0	0.137	0.014	1.38	0.000168	111.6	321.5
26.00	2.00	25.00	18.00	8.19	226.4	0.137	0.014	1.38	0.000161	104.5	330.9
28.00	2.00	27.00	18.00	8.19	242.8	0.137	0.014	1.38	0.000162	97.2	340.0

Table C. 54. Consolidation settlement calculation for Km: 163+000

Depth (m)	Thickness of layer (m)	Consolidation settlement of layer (S) (m)	Cumulative consolidation settlement (Sc) (cm) (by C_c values)	Consolidation settlement of layer (S) (m)	Cumulative consolidation settlement (Sc) (cm) (by m_v values)
2.00	2.00	0.00 m	0.00 cm	0.00 m	0.00 cm
4.00	2.00	0.03 m	2.97 cm	0.08 m	7.83 cm
6.00	2.00	0.03 m	6.16 cm	0.07 m	15.17 cm
8.00	2.00	0.03 m	9.58 cm	0.07 m	21.88 cm
10.00	2.00	0.04 m	13.22 cm	0.06 m	27.94 cm
12.00	2.00	0.04 m	17.08 cm	0.06 m	33.47 cm
14.00	2.00	0.10 m	26.80 cm	0.13 m	46.67 cm
16.00	2.00	0.09 m	35.46 cm	0.13 m	59.17 cm
18.00	2.00	0.05 m	40.59 cm	0.05 m	63.91 cm
20.00	2.00	0.05 m	45.19 cm	0.04 m	68.23 cm
22.00	2.00	0.04 m	49.30 cm	0.04 m	72.12 cm
24.00	2.00	0.04 m	52.98 cm	0.04 m	75.72 cm
26.00	2.00	0.03 m	56.25 cm	0.03 m	79.10 cm
28.00	2.00	0.03 m	59.15 cm	0.03 m	82.25 cm

OCR vs. Depth (m) Graph

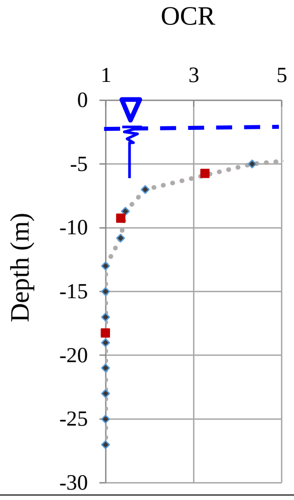

D. Non-Linear Regression Anaysis Data Set

Table D. 1 Data set for non-linear regression analysis

Station No	KM	SPT N	PI (%)	wn (%)	e_0	LL (%)	LI	λ (S/C)	ψ (H/B)	So (cm)/Sp (cm)	C_t/C_c	mv (Field)/mv (Stroud)
1	139+764	18	46.05	33.08	0.36	71.44	0.1669924	0.0113353	1.1762667	1.025584473		0.925
2	139+860	18	46.05	33.08	0.36	71.44	0.1669924	0.0113353	1.1762667	0.937362153		0.944
3	140+592	18	46.05	33.08	0.36	71.44	0.1669924	0.0119048	1.12	0.906225374	0.270	0.847
4	141+667	17	53.49	24.73	0.48	72	0.1162834	0.1631526	1.0624	1.105090546	0.636	1.123
5	142+000	22	55	32	2.22	71	0.2909091	0.1489573	1.0741333	1.054704987		1.002
6	142+389	17	52.41	24.86	2.22	70	0.138714	0.1326612	1.0050667	1.075565945	0.311	0.922
7	143+107	15	53.43	29.73	1.038	72	0.2088714	0.1014713	1.0512	0.873023572	0.251	0.835
8	144+000	16	38.73	34.87	0.65	66	0.1962303	0.0945626	1.128	0.929872143	0.288	0.862
9	145+000	16	44.11	31.26	1.04	58	0.3937883	0.1971276	0.9469333	0.942598187	0.180	0.859
10	146+210	14	29.25	34.63	1.11	46	0.6112821	0.2272727	0.5866667	0.833006664	0.083	1.068
11	147+000	15	30.17	35.44	0.45	47	0.6168379	0.0914316	1.0208	1.128732676		1.264
12	149+000	19	31	31.69	0.387	54	0.2803226	0.2463639	0.8984	0.915271967		1.101
13	150+000	12	27.23	27.51	0.979	49	0.2107969	0.2479339	0.968	1.075964347		1.234
14	150+500	12	27.23	27.12	0.979	49	0.1964745	0.0947867	1.1253333	1.105435056		1.385
15	151+220	14	23.19	30.09	1.558	39	0.6157827	0.1452433	1.1016	0.976224217		1.064
16	151+975	15	41.53	31.57	0.449	58	0.3635926	0.2162162	0.9866667	1.348407681		1.105
17	152+000	14	41.53	31.5	0.449	58	0.3619071	0.2355019	0.9058667	0.892244338		1.337
18	154+500	20	34.69	41.12	0.42	55	0.5998847	0.0801068	0.9986667	0.858922053		0.936
19	155+000	17	32.57	41.53	1.558	43	0.9548664	0.3895294	0.8557333	0.952380952	0.236	1.302
20	155+551	19	46.91	39.17	0.456	51	0.747815	0.2374302	0.9546667	0.919865558		1.410
21	157+400	14	36.39	28.52	0.43	54.18	0.2948612	0.0492005	1.084	1.288244767		1.780
22	158+000	18	31.28	30.15	0.43	48	0.4293478	0.1343284	0.8933333	1.416273257		1.415
23	159+565	19	26.76	33.22	0.5	45	0.5597907	0.2886248	0.7853333	1.002885012	0.130	1.426
24	161+764	16	23.88	25.45	0.55	42.08	0.3036013	0.6482282	0.6170667	1.239388795		1.174
25	162+555	11	27.95	25.65	0.38	42	0.4150268	0.3902439	0.5466667	1.104903786	0.272	1.925
26	163+000	14	28.81	33.37	0.39	42	0.7004512	0.0769231	0.6933333	0.948328267	0.231	1.579

CURRICULUM VITAE

PERSONAL INFORMATION

Surname, Name: Çelik, Gözde
Nationality: Turkish (TC)
Date and Place of Birth: 14 October 1984, Nevşehir
Marital Status: Single
Phone: +90 312 235 98 53
Fax: +90 312 235 94 65
email: gozdecelik@hotmail.com

EDUCATION

Degree	Institution	Year of Graduation
PHD	METU Geological Engineering	2020
MS	METU Geological Engineering	2011
BS	METU Geological Engineering	2007
High School	Nevşehir Anadolu High School, Nevşehir	2002

WORK EXPERIENCE

Year	Place	Enrollment
2007-Present	Yüksel Domaniç Ltd. Şti.	Geological/Geotechnical/Tunnel Design Engineer
2006 July	SRK Consulting	Intern Eng. Student
2005 August	T.P.A.O.	Intern Eng. Student

PARTICIPATED DESIGNS AND PROJECTS

Year	Project Name	Explanation
Present	Van Bahçesaray Highway	Geotechnical-Tunnel Design Engineer
Present	Tomarza-Tufanbeyli Highway	Geotechnical Engineer
Present	Eskişehir-Afyon High Speed Railway	Geological-Geotechnical Engineer

Year	**Project Name**	**Explanation**
Present	Adıyaman Freeway	Geotechnical Engineer
Present	Eskişehir Mihalgazi State Highway	Geotechnical Engineer
March 2020	Narince-Gerger State Highway	Geological-Geotechnical Engineer
Fabruary 2018	Delice-Çorum High Speed Railway	Geological-Geotechnical Engineer
March 2017	Aksaray-Ulukışla High Speed Railway	Geological Engineer
September 2015	Gebze-İzmir Motorway – Bursa-Susurluk Section	Geotechnical Engineer
August 2015	Manavgat-Akseki State Highway	Geotechnical Engineer
August 2015	Ardahan-Posof-Türkgözü State Highway	Geotechnical Engineer
March 2015	Karaman-Ayrancı-Ereğli State Highway	Geotechnical Engineer
May 2013	Gebze-İzmir Motorway-Selçukgazi Tunnel Project	Geological-Tunnel Design Engineer
January 2011	Gebze-İzmir Motorway-Belkahve Tunnel Project	Geological-Tunnel Design Engineer
April 2011	Antalya-Kayseri Railway	Geological-Geotechnical Engineer
January 2011	Gebze-İzmir Motorway-Samanlı Tunnel Project	Geotechnical-Tunnel Design Engineer
October 2010	Adapazarı-Karasu-Bartın Railway	Geological Engineer

Year	Project Name	Explanation
October 2009	Gebze-İzmir Motorway – Gebze-Orhangazi Section	Geological-Geotechnical Engineer
February 2009	Kırşehir-Yerköy Railway	Geological Engineer
October 2008	Ankara-Kırıkkale-Delice Motorway	Geological and Tunnel Design Engineer
August 2008	Karaman-Bucakkışla-Ermenek State Highway	Geological-Geotechnical Engineer
September 2007	Kars-Tiflis Railway	Geological Engineer

THESIS AND DISSERTION

Çelik, G., 2011. Verification of Empirically Determined Support Systems of the Kılıçlar Highway Tunnel by Numerical Modelling. M.Sc. thesis, Department of Geological Engineering, Middle East Technical University, Ankara, 263 pages. (Supervisor: Prof. Dr. Tamer Topal)

PUBLICATIONS

Çelik, G., Köse, A., Akbulut, A., 2015.Improvement of Soft Clays in Bursa-Susurluk Section of the Gebze-İzmir Project Using Prefabricated Vertical Drains, Mühjeo’2015 National Symposium on Engineering Geology, Trabzon, 538 pages.

HONORS AND AWARDS

Year	Honors	University
June 2007	High Honor Student	Middle East Technical University
June 2006	Honor Student	Middle East Technical University

FOREIGN LANGUAGES

English : Advanced level

French : Beginner level

COMPUTER SKILLS

Microsoft Office Programs: Word, Excel and Powerpoint

AutoCad

FLAC

RocScience Software: Slide, Phase, Dips, RocPlane, Swedge

MEMBERSHIPS

Union of Chambers of Turkish Engineers and Architects-Chamber of Geological Engineers, Member ID No: 12237

METU Alumni Association

HOBBIES

Plates, Travelling, Diving, Guitar Playing